Dissertation zur Erlangung des Doktorgrades

der Fakultät für Chemie und Pharmazie

der Ludwig-Maximilians-Universität München

Reactivity Selectivity Relationships in Reactions of Carbocations with Nucleophiles

M. Eng. (Master of Engineering) Shinya Minegishi

aus

Saitama (Japan)

2004

Dissertation zur Erlangung des Doktorgrades

der Fakultät für Chemie und Pharmazie

der Ludwig-Maximilians-Universität München

Reactivity Selectivity Relationships in Reactions of Carbocations with Nucleophiles

M. Eng. (Master of Engineering) Shinya Minegishi

aus

Saitama (Japan)

2004

Erklärung

Diese Dissertation wurde im Sinne von § 13 Abs. 3 bzw. 4 der Promotionsordnung vom 29. Januar 1998 von Prof. Dr. Herbert Mayr betreut.

Ehrenwörtliche Versicherung

Diese Dissertation wurde selbständig, ohne unerlaubte Hilfe erarbeitet.

München, am 7. 2. 2004

……………………………………

Shinya Minegishi

Dissertation eingereicht am 7. 2. 2004

1. Gutachter: Prof. Dr. H. Mayr

2. Gutachter: Prof. Dr. H. R. Pfaendler

Mündliche Prüfung am 4. 3. 2004

Acknowledgment

This thesis presents the studies which the author carried out from 2001 to 2004 at the Department Chemie, Ludwig-Maximilians-Universität München under the guidance of Professor Dr. H. Mayr. I would like to express my sincere gratitude to Professor Dr. H. Mayr.

I am also grateful to Professor Dr. S. Kobayashi, Professor Dr. M. Mishima, Professor Dr. M. Fujio, Dr. M. Kotani who supported my research from Oct. to Dec. 2002 during my stay at Kyushu University, Japan and to Dr. A. Ofial for their encouragement and helpful suggestions. Great thanks go to Dr. P. T. Binh, F. Brotzel, Dr. T. Bug, B. Janker, Dr. B. Kempf, Dr. T. Lemek, Dr. R. Loos, N. Hampel, Dr. G. Remennikov, C. Schlierf, M. Sakamoto, and Dr. T. Tokuyasu.

I thank Frau C. Dubler and Herrn Dr. Stephenson for the measurement of NMR spectra, and Herrn Dr. W. Spahl and Frau E. Okazaki for the measurement of Mass spectra.

Finally, I sincerely wish to thank my family and friends for their continuous encouragement and support throughout the present studies.

Parts of this Dissertation have been published in:

First Direct Observation of the Two Distinct Steps in an S_N1 Reaction.
H. Mayr, S. Minegishi, *Angew. Chem.* **2002**, *114*, 4674-4676; *Angew. Chem. Int. Ed.* **2002**, *41*, 4493-4495.

How Constant are Ritchie's "Constant Selectivity Relationships"?– A General Reactivity Scale for n-, π-, and σ-Nucleophiles.
S. Minegishi, H. Mayr, *J. Am. Chem. Soc.* **2003**, *125*, 286-295.

Autopsy of S_N1 Reactions
B. Denegri, S. Minegishi, O. Kronja, H. Mayr, *Angew. Chem.* **2004**, in print.

Solvent Nucleophilicity
S. Minegishi, S. Kobayashi, H. Mayr, *J. Am. Chem. Soc.* **2004**, in print.

Table of contents

0. Summary

0.1 General

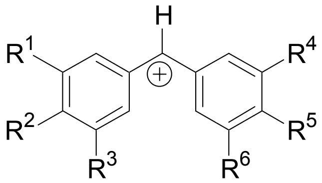

for R^1 – R^6, see page 11

Benzhydrylium ions, which have previously been characterized as reference electrophiles in the Mayr group, have been employed for the construction of general nucleophilicity and electrophilicity scales using the correlation equation 0.1.

$$\log k\ (20\ °\mathrm{C}) = s\,(N + E) \tag{0.1}$$

s = nucleophile-specific parameter

N = nucleophilicity parameter

E = electrophilicity parameter

0.2 The kinetics of the reactions of benzhydrylium ions with 15 n-nucleophiles in water and DMSO were measured to yield the N- and s-parameters listed in Table 0.1. Table 0.1 shows that all nucleophiles except water (s = 0.89) and $^{-}SCH_2CO_2^{-}$ (s = 0.43) have closely similar slope parameters ($0.52 < s < 0.71$) indicating that the reactions of most n-nucleophiles approximately follow Ritchie's constant selectivity relationship (s = constant). The different slope parameter for water is recognized as the main reason for the deviations from the Ritchie relationship reported in 1986.

Table 0.1: Nucleophilicity (N) and slope (s) parameters for fifteen Ritchie-type nucleophiles.

Nucleophile (Solvent)	N	s	Nucleophile (Solvent)	N	s
H_2O (Water)	5.11	0.89	$H_2NCH_2CO_2Et$ (DMSO)	14.30	0.67
OH^{-} (50AN)	10.19	0.62	HOO^{-} (Water)	15.40	0.55
OH^{-} (Water)	10.47	0.61	n-$PrNH_2$ (DMSO)	15.70	0.64
$H_2NNHCONH_2$ (Water)	11.05	0.52	SO_3^{2-} (Water)	16.83	0.56
$HONH_2$ (Water)	11.41	0.55	Morpholine (DMSO)	16.96	0.67
$CF_3CH_2NH_2$ (DMSO)	12.15	0.65	Piperidine (DMSO)	17.19	0.71
$CF_3CH_2O^{-}$ (Water)	12.66	0.59	$^{-}SCH_2CO_2^{-}$ (Water)	22.62	0.43
n-$PrNH_2$ (Water)	13.33	0.56			

The *N*- and *s*-parameters of the n-nucleophiles derived from their reactions with benzhydrylium ions (Table 1.1) were combined with literature data for the reactions of these nucleophiles with other carbocations to yield electrophilicity parameters *E* for tritylium, tropylium, and xanthylium ions (Scheme 0.1).

Scheme 0.1: Electrophilicity parameters *E* for Ritchie's electrophiles compared with electrophilicity parameters for benzhydrylium ions.

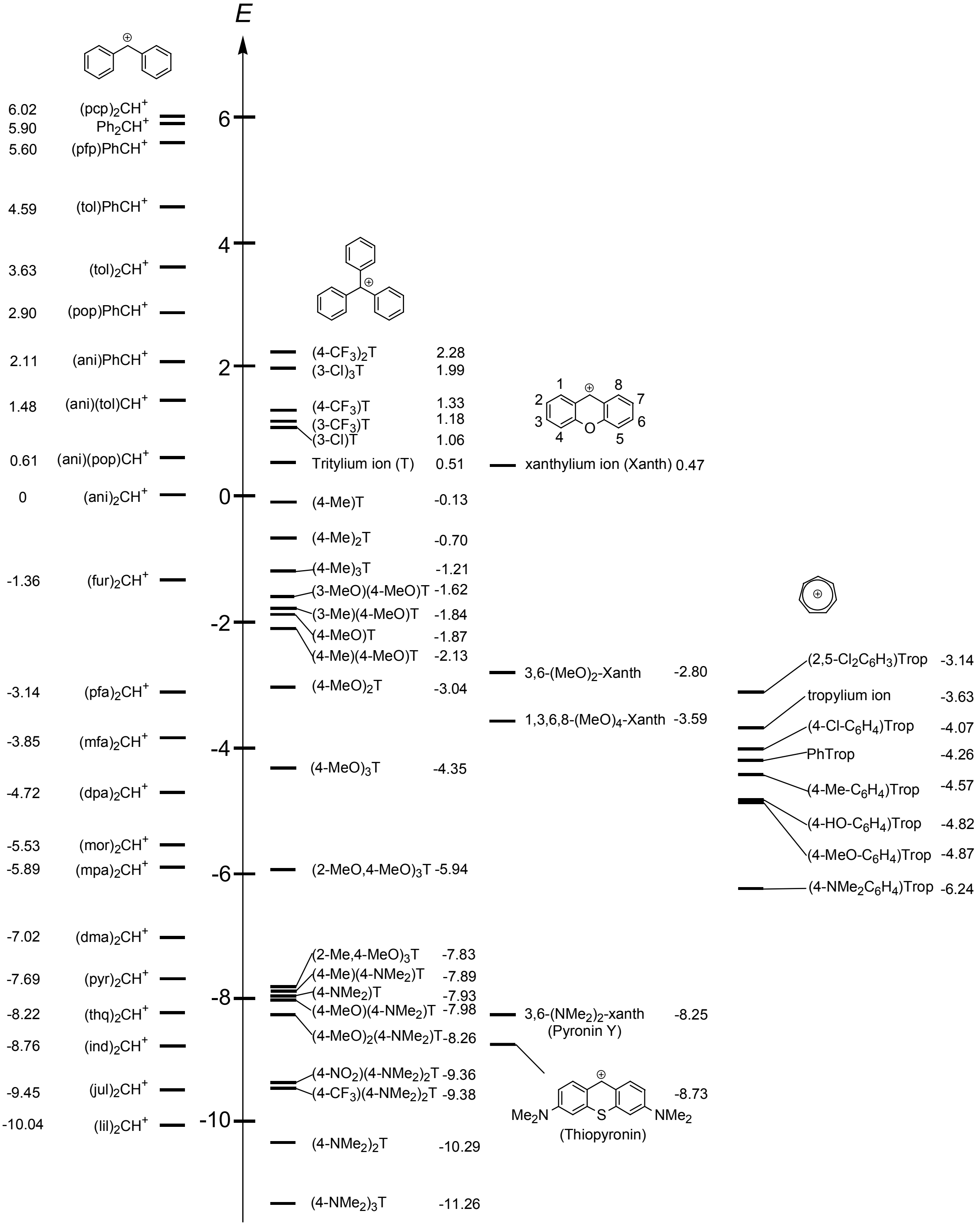

While the *E*-parameters for tropylium and xanthylium ions appear to be generally applicable, it is demonstrated that the *E*-parameters of tritylium ions can be used to predict reactivities toward n-nucleophiles as well as hydride transfer rate constants but not rates for the reactions of tritylium ions with π-nucleophiles. It is now possible to merge the large data sets determined by Ritchie and others with our kinetic data and present a nucleophilicity scale comprising n- (e.g. amines), π- (e.g. alkenes and arenes), and σ-nucleophiles (e.g. hydrides) (Scheme 0.2)

Scheme 0.2: Comparison of the nucleophilic reactivities of n-nucleophiles with typical π-nucleophiles, hydride donors, and carbanions.

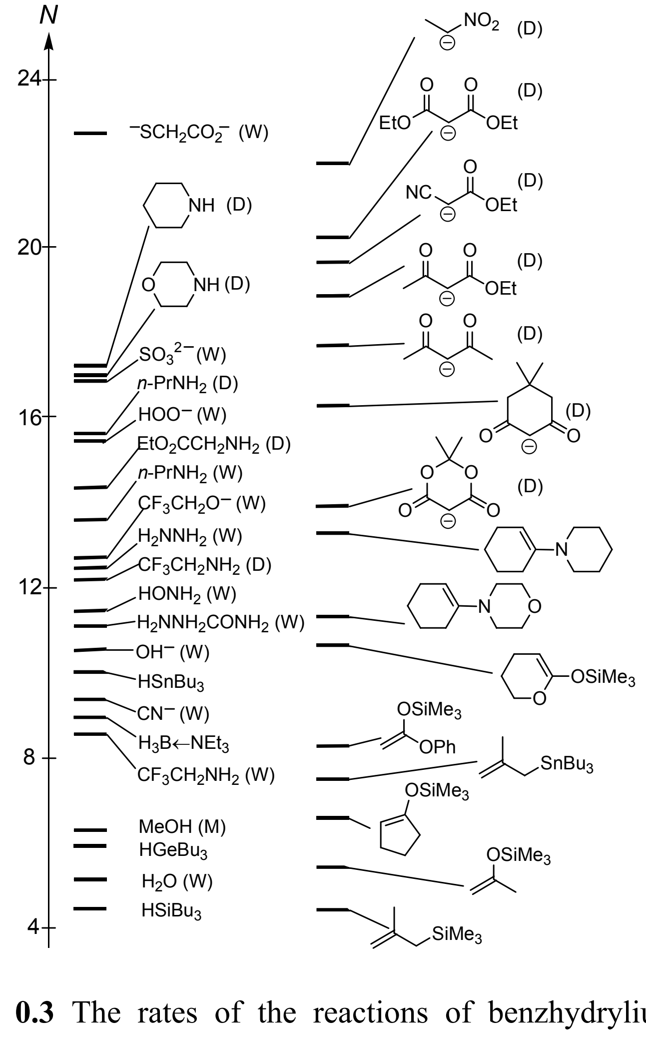

0.3 The rates of the reactions of benzhydrylium ions with solvent mixtures of variable composition (water/acetonitrile, methanol/acetonitrile, ethanol/acetonitrile, ethanol/water, and trifluoroethanol/water) have been determined photometrically by conventional UV-Vis spectroscopy, stopped-flow methods, and laser flash techniques. From plots of the first-order rate constants (log *k*) versus *E* of the benzhydrylium ions, the solvent nucleophilicity parameters *s* and *N* are derived, the latter of which are designated as N_1 to emphasize that their use in the quoted correlation equation gives rise to first order rate constants. Because the

N_1 values are directly comparable to the previously reported nucleophilicity parameters N for π-systems, the systematic design of Friedel-Crafts reactions with solvolytically generated carbocations becomes possible (Scheme 0.3).

Scheme 0.3: Comparison of the nucleophilicity parameters N_1 of solvents with the N parameters of typical π-systems and hydride donors.

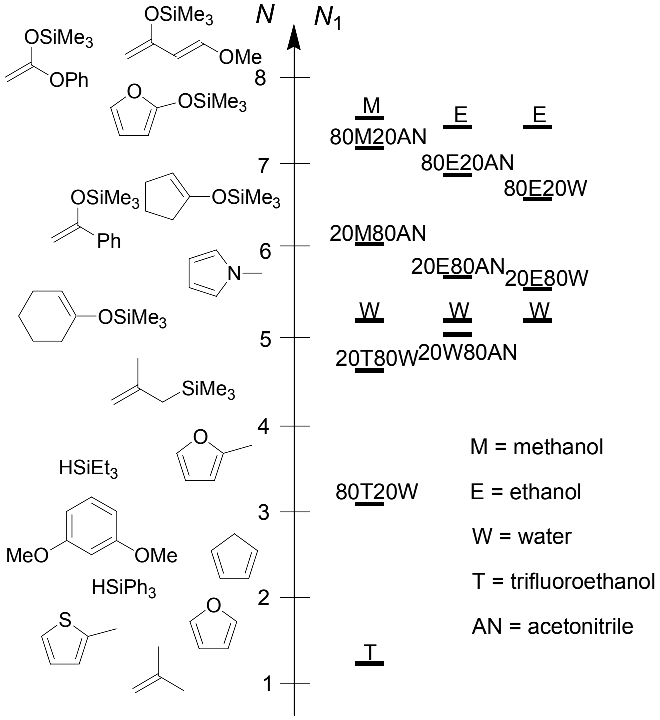

A linear correlation between N_1 and Kevill's solvent nucleophilicity N_T based on *S*-methyldibenzothiophenium ions was found, which allows us to interconvert the two sets of data (Figure 0.1)

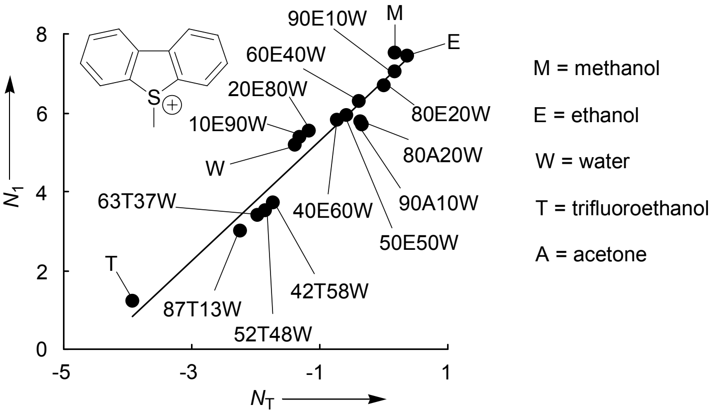

Figure 0.1: Relationship between nucleophilicity parameters N_1 and N_T from reactions with benzhydrylium ions (this work) and the *S*-methyldibenzothiophenium ion (Kevill), respectively.

0.4 Rate constants for the reactions of laser flash photolytically or solvolytically generated carbocations with solvents of characterized N_1 and s parameters (Chapter 3) have been collected in literatures. By substituting log k, N_1, and s into eq. 0.1, electrophilicity parameters of a large variety of carbocations have been derived. Some of the carbocations thus characterized are shown in Schemes 0.4 and 0.5.

Scheme 0.4: Comparison of the electrophilicity parameters E of 1-arylethyl cations, cumyl cations, and benzhydrylium ions.

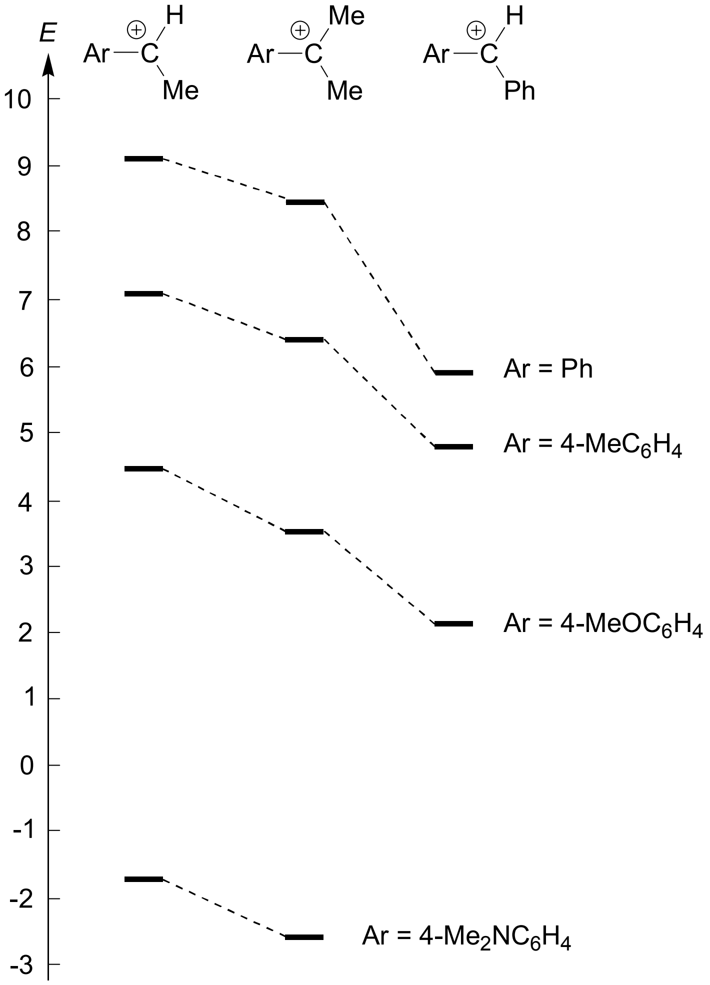

Scheme 0.5: Comparison of the electrophilicity parameters *E* of various 4-methoxy α-substituted benzyl cations.

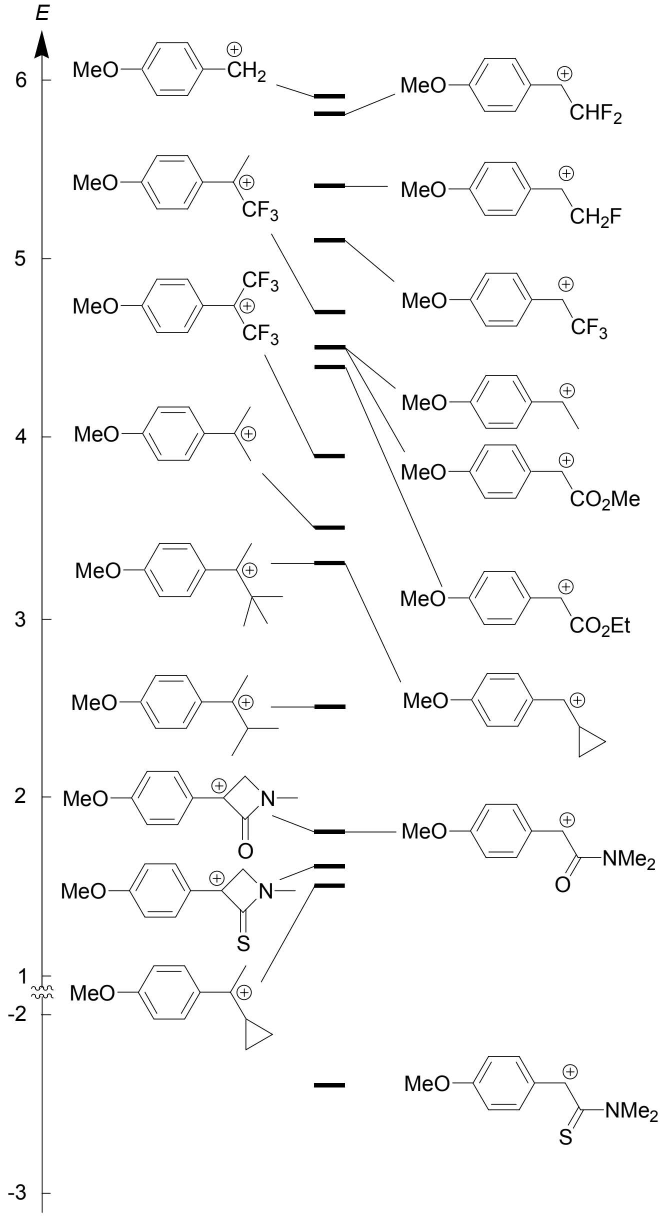

0.5 Rate constants for the reactions of laser flash photolytically generated benzhydrylium ions with chloride and bromide anions have been determined in various solvents and compared with literature data. In accord with previous literature results, the bromide anion is generally more nucleophilic than the chloride anion, and in aqueous acetonitrile mixtures, halide nucleophilicities increase with decreasing water content of the solvent mixtures (Figure 0.2)

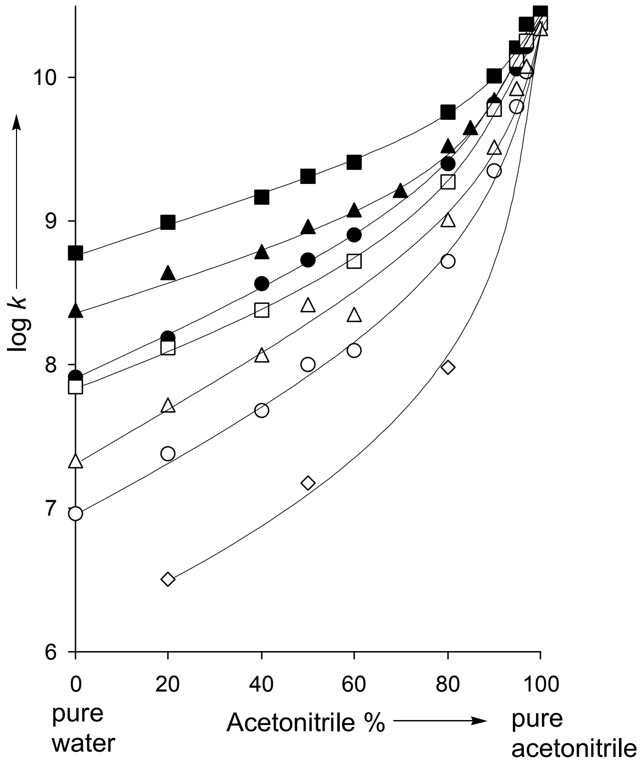

Figure 0.2: Variations in rate constants for the combinations of bromide anion and chloride anion with benzhydrylium ions in aqueous acetonitrile.

The linear correlation with negative slope between nucleophilicity *N* of chloride in different solvents and solvent ionizing power *Y* (Figure 0.3) indicates that the same interactions between solvents and chloride anions are responsible for the ionization of RCl and for the combination of R^+ with Cl^-.

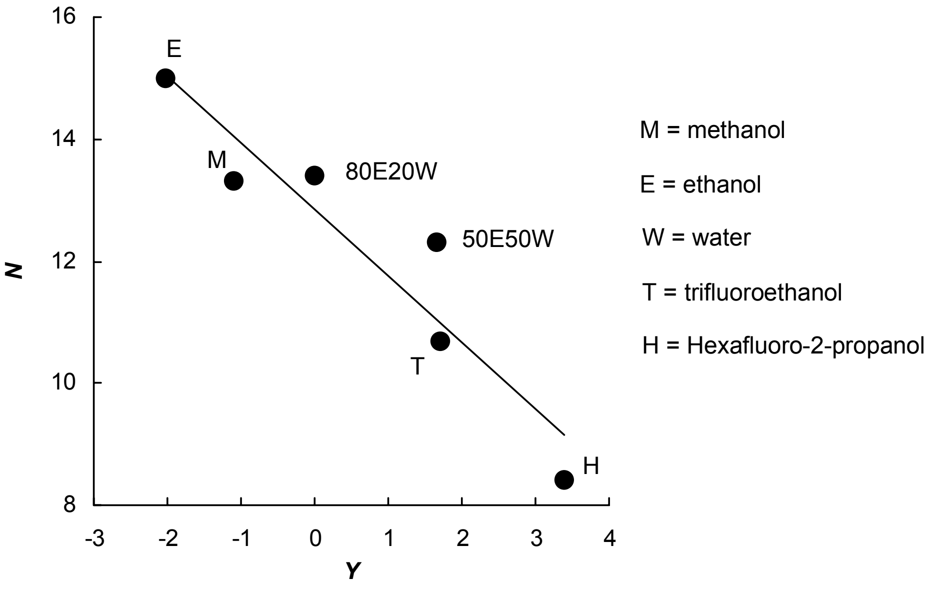

Figure 0.3: Correlation of *N*-parameters of Cl^- in several solvents with solvent ionizing power *Y*

0.6 The rate constants for the ionization of benzhydryl halides and for the reactions of benzhydrylium ions with halide anions and with solvent are combined to give complete free energy profiles for solvolysis reactions as shown for the trifluoroethanolysis of benzhydryl chlorides in Figure 0.4.

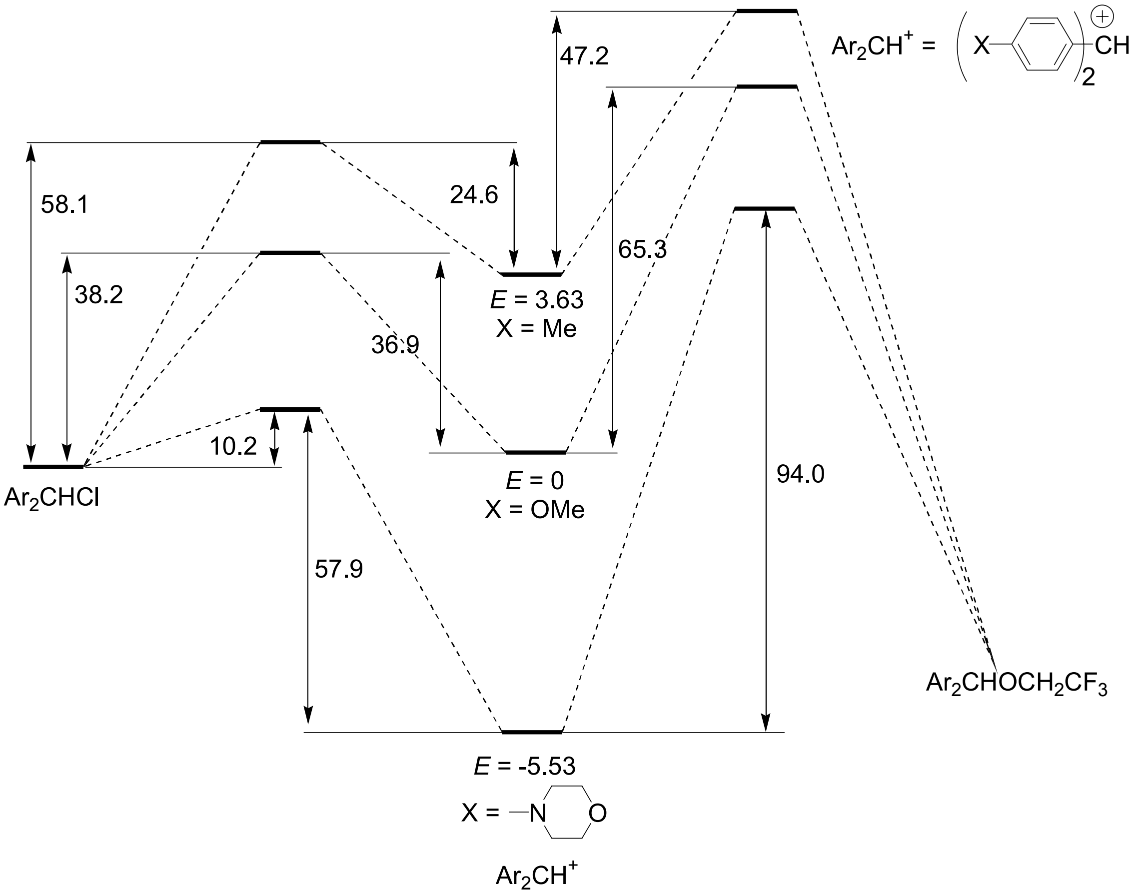

Figure 0.4: Free energy profiles for the solvolysis of various benzhydryl chlorides in TFE at 20°C (for ionization at 25°C). Unit is kJ mol^{-1}.

0.7 The predicted accumulation of the dianisylcarbenium ion during the trifluoroethanolysis of (ani)$_2$CHCl is UV-Vis spectroscopically observed, and we reported the first S$_N$1 reaction, where ionization and trapping of the carbocation by the solvent could directly be observed (Figure 0.5)

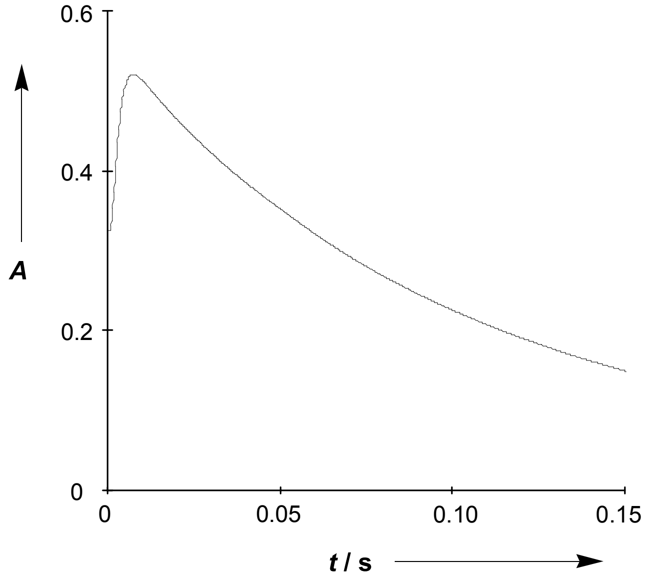

Figure 0.5: Generation and decay of the dianisylcarbenium ion ($(\text{ani})_2\text{CH}^+$) observed after dissolving chloro-bis(4-methoxyphenyl)methane ($(\text{ani})_2\text{CHCl}$) in 20/80 (v/v) TFE/$CH_3CN$ containing 1.0 M of $LiClO_4$ (at 20°C).

1. Introduction

Kinetic investigations played a crucial role for the elucidation of reaction mechanisms and the development of the electronic theory of Organic Chemistry.[1] For numerous classes of reactions, structure reactivity relationships have been investigated, and it became clear that the majority of organic reactions proceed via combinations of electrophiles with nucleophiles.[2] As discussed previously, generally applicable electrophilicity and nucleophilicity scales cannot exist for several reasons.[3]

However, comprehensive nucleophilicity as well as electrophilicity scales can be constructed with respect to structurally related reaction partners. Thus, just before my arrival in München, the Mayr group had established a series of benzhydrylium ions as reference electrophiles (Table 1.1) which can be used for directly comparing nucleophiles of wide structural variety.[4]

It was the goal of this work to employ the reference electrophiles listed in Table 1.1 for characterizing the nucleophilic reactivities of simple anions as well as of amines, alcohols and water, or mixtures of these solvents. By comparing nucleophiles of different functionality, new insights into reaction mechanisms were expected, and it will be shown how these data can be employed for developing novel synthetic methods and for developing a general electrophilicity scale for carbenium ions.

Since the major parts of this thesis have already been published in a series of papers, individual introductions, will be given at the beginning of each chapter.

Table 1.1: Abbreviations and electrophilicity parameters *E* of benzhydrylium ions.

	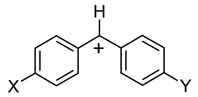 X	Y	E [4d]
$(pcp)_2CH^+$	Cl	Cl	6.02
Ph_2CH^+	H	H	5.90
$(pfp)PhCH^+$	F	H	5.60
$(tol)PhCH^+$	CH_3	H	4.59
$(tol)_2CH^+$	CH_3	CH_3	3.63
$(pop)PhCH^+$	OPh	H	2.90
$(ani)PhCH^+$	OCH_3	H	2.11
$(ani)(tol)CH^+$	OCH_3	CH_3	1.48
$(ani)(pop)CH^+$	OCH_3	OPh	0.61
$(ani)_2CH^+$	OCH_3	OCH_3	0.00
$(fur)_2CH^+$	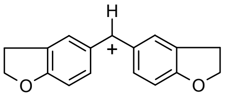		–1.36
$(pfa)_2CH^+$	$N(Ph)CH_2CF_3$	$N(Ph)CH_2CF_3$	–3.14
$(mfa)_2CH^+$	$N(CH_3)CH_2CF_3$	$N(CH_3)CH_2CF_3$	–3.85
$(dpa)_2CH^+$	NPh_2	NPh_2	–4.72
$(mor)_2CH^+$	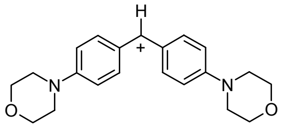		–5.53
$(mpa)_2CH^+$	$N(Ph)CH_3$	$N(Ph)CH_3$	–5.89
$(dma)_2CH^+$	$N(CH_3)_2$	$N(CH_3)_2$	–7.02
$(pyr)_2CH^+$	$N(CH_2)_4$	$N(CH_2)_4$	–7.69
$(thq)_2CH^+$	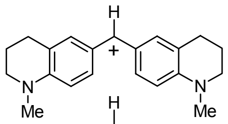		–8.22
$(ind)_2CH^+$	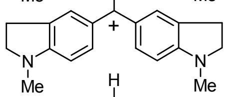		–8.76
$(jul)_2CH^+$	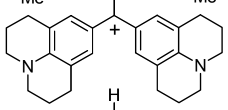		–9.45
$(lil)_2CH^+$	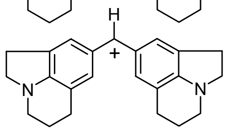		–10.04

1.2 References

(1) (a) Hine, J. *Structural Effects on Equilibria in Organic Chemistry*; Robert, E. Krieger Publishing Company: Huntington, New York, 1981. (b) Carpenter, B. K. *Determination of Organic Reaction Mechanisms*; Wiley-Interscience: New York, 1984. (c) Maskill H. *The Physical Basis of Organic Chemistry*; Oxford University Press: New York, 1985. (d) *Investigations of Rates and Mechanisms of Reactions, Techniques in Chemistry*; Bernasconi, C., Ed.; Wiley: NewYork, 1986; Vol. 6, 4/E, Part 1 and 2. (e) Ritchie, C. D. *Physical Organic Chemistry*, 2nd ed.; Marcel Dekker: New York, 1990. (f) Espenson, J. H. *Chemical Kinetics and Reaction Mechanisms*, 2nd ed.; McGraw-Hill: New York, 1995. (g) Pross, A. *Theoretical and Physical Principles of Organic Reactivity*; John Wiley & Sons: New York, 1995. (h) Logan, S. R. *Grundlagen der Chemischen Kinetik*; Wiley-VCH: Weinheim, 1997.

(2) (a) Ingold, C. K. *Structure and Mechanism in Organic Chemistry*, 2nd ed;, Cornell Univ. Press, Ithaca, New York, 1969. (b) Carey, F. A. *Organic Chemistry*, 2nd Ed.; McGraw-Hill: New York, 1996. (c) Smith, M. B.; March, J. *Advanced Organic Chemistry*, 5th ed.; Wiley: New York, 2001.

(3) (a) Pearson, R. G.; Sobel, H. R.; Songstad, J. *J. Am. Chem. Soc.* **1968**, *90*, 319–326 (b) Ritchie, C. D. *Can. J. Chem.* **1986**, *64*, 2239–2250.

(4) (a) Mayr, H.; Patz, M. *Angew. Chem.* **1994**, *106*, 990–1010; *Angew. Chem., Int. Ed. Engl.* **1994**, *33*, 938–957. (b) Mayr, H.; Kuhn, O.; Gotta, M. F.; Patz, M. *J. Phys. Org. Chem.* **1998**, *11*, 642–654. (c) Mayr, H.; Patz, M.; Gotta, M. F.; Ofial, A. R. *Pure Appl. Chem.* **1998**, *70*, 1993–2000. (d) Mayr, H.; Bug, T.; Gotta, M. F.; Hering, N.; Irrgang, B.; Janker, B.; Kempf, B.; Loos, R.; Ofial, A. R.; Remennikov, G.; Schimmel, H. *J. Am. Chem. Soc.* **2001**, *123*, 9500–9512. (e) Mayr, H.; Kempf, B.; Ofial, A. R. *Acc. Chem. Res.* **2003**, *36*, 66–77.

2. How constant are Ritchie's "constant selectivity relationships"?– a general reactivity scale for n-, π-, and σ-nucleophiles

2.1 Introduction

Ritchie's discovery that the rates of the reactions of stabilized carbocations and diazonium ions with water, alcohols, and several anions can be described by eq. 2.1 marked a change of paradigm in Physical Organic Chemistry.[1]

$$\log (k/k_0) = N_+ \qquad (2.1)$$

$$\log k = N_+ + \log k_0 \qquad (2.1a)$$

$\log k_0$ = electrophile dependent parameter

N_+ = nucleophile dependent parameter

Eq. 2.1 implies that the relative reactivities of two nucleophiles are given by the differences of their N_+ values, which are independent of the electrophilicities of the reaction partners. It thus contradicts the previously accepted reactivity-selectivity principle, which postulates a decrease of selectivity with increasing reactivity.[2] The so-called "constant selectivity relationship" (2.1) found wide acceptance, but in 1986 Ritchie replaced the electrophile-independent parameters N_+ by several sets of N_+-values, which actually are relative reactivities toward malachite green, tris(4-methoxy)tritylium, pyronin-Y, or the 4-(dimethylamino)-phenyltropylium ion. Since then many authors have either been using the "largest revised set of N_+ parameters" which effectively are reactivities toward malachite green (or tris-4-methoxytritylium ion)[3] or have been referring to Ritchie's original parameters,[1] when analyzing new reactivity data.[4]

Rearranging eq. 2.1 leads to eq. 2.1a which emphasizes that $\log k_0$ in the Ritchie equation corresponds to a nucleophile–independent electrophilicity parameter which was initially defined as the rate constant for the reaction of an electrophile with water. During the past 15 years, the Mayr group has been studying reactions of carbocations with π-nucleophiles,[5–8] carbanions,[9] and hydride donors[10–12] and demonstrated that the rates of these reactions can be described by eq. 2.2.

$$\log k\ (20\ °\mathrm{C}) = s\,(N + E) \tag{2.2}$$

s = nucleophile-specific parameter

N = nucleophilicity parameter

E = electrophilicity parameter

Eq. 2.2 differs from eq. 2.1/2.1a by the use of an additional nucleophile-specific slope parameter s. This parameter, which was set to $s = 1$ for 2-methyl-1-pentene,[5,8] represents a correction term which improves the fit of data compared to eq. 2.1. A theoretical interpretation of the physical meaning of s has recently been published.[13] The Ritchie equation (eq. 2.1/2.1a) can be considered as a special case of eq. 2.2 which holds for reactions with groups of nucleophiles that have identical slope parameters s.

It was the goal of this work to investigate Ritchie-type reactions (carbocations + n-nucleophiles) with our methodology and to identify domains which can sufficiently be described by Ritchie's eq. 2.1. In this way it should become possible to search for relationships between the reactivity parameters of eqs 2.1 and 2.2, and to create a common reactivity scale for n-, π-, and σ-nucleophiles.

2.2 Method

Recently, the Mayr group has recommended 22 differently substituted benzhydrylium ions as reference electrophiles for quantifying the reactivities of various types of nucleophiles.[7,8] (Table 1.1)

It was demonstrated that the same electrophilicity parameters E can be used for describing the reactions of benzhydryl cations with alkenes, arenes, allylsilanes, allylstannanes, enol ethers, ketene acetals, enamines,[7] carbanions,[9] and hydride donors.[10–12] We have now investigated the kinetics of the reactions of benzhydrylium ions with n-nucleophiles (Ritchie-type nucleophiles), and analyzed the observed second-order rate constants by eqs 2.1 and 2.2.

2.3 Kinetic Measurement

The combination of a benzhydrylium salt with more than ten equivalents of a nucleophile usually resulted in an exponential decay of the carbocation absorption, from which the pseudo-first-order rate constant $k_{1\Psi}$ was derived. As shown for the reaction of $(lil)_2CH^+$ with OH^- in Figure 2.1, $k_{1\Psi}$ increases linearly with the concentration of the nucleophile, and the slope of this correlation corresponds to the second-order rate constant (k_2). All second-order rate constants reported in this chapter have analogously been derived from $k_{1\Psi}$ vs. [nucleophile]$_0$ plots, as explicitly shown in the Experimental Part.

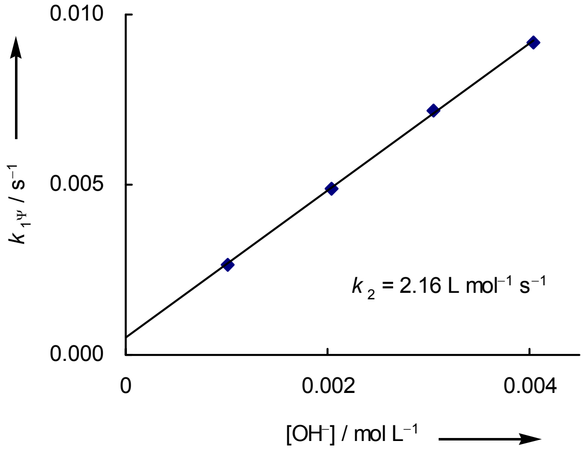

Figure 2.1: Determination of the second-order rate constant for the reaction of $(lil)_2CH^+$ with OH^- in water (20 °C).

In some cases, a bathochromic shift of the absorption maximum up to 5 nm was observed in the final stages of the reactions, when the carbocation concentrations became small (> 95% conversion). Since the reason of this shift is not known, we have not evaluated the late stages of such reactions.

The rates of cation-anion combinations are known to depend on ionic strength (I).[14] However, Ritchie reported that for aqueous solutions, changes of ionic strength are negligible when $I < 0.1$ mol L^{-1}.[15] In accord with this report, the second-order rate constant for the reaction of $(lil)_2CH^+BF_4^-$ with OH^- remained almost unchanged when $NaBF_4$ was added to realize a constant ionic strength of $I = 0.005$ or 0.01 mol L^{-1} instead of $I = 0.001$–0.004 mol L^{-1} in the absence of the inert salt (Table 2.1). Only when the ionic strength was set to $I = 0.05$ mol L^{-1} by the addition of $NaBF_4$, the second-order rate constant decreased to 50% of the value observed in the absence of an inert salt (Table 2.1). Since all reactions studied in this investigation were carried out at $I < 0.01$ mol L^{-1}, we did not enforce constant ionic strength by adding inert salts.

Table 2.1: Influence of ionic strength on the rate constant of the reaction of $(lil)_2CH^+BF_4^-$ (1×10^{-5} mol L^{-1}) + OH^- in water.

[KOH], mol L^{-1}	[NaBF$_4$], mol L^{-1}	I, mol L^{-1}	k_2, L mol^{-1} s^{-1}
0.001–0.004	–	0.001–0.004	2.16
0.001–0.004	0.004–0.001	0.005	2.24
0.001–0.004	0.009–0.006	0.01	1.93
0.002–0.008	0.048–0.042	0.05	1.18

To examine the influence of the co-solvents (trifluoroethanol or acetonitrile) on the rate constants in water, we have studied the reactivity of OH^- in water/acetonitrile mixtures of different composition. As shown in Figure 2.2, the second-order rate constants for the reaction of hydroxide with $(lil)_2CH^+$ decrease from 2.16 to 1.03 L mol^{-1} s^{-1} when the acetonitrile content in water is increased from 0.4% to 50%.

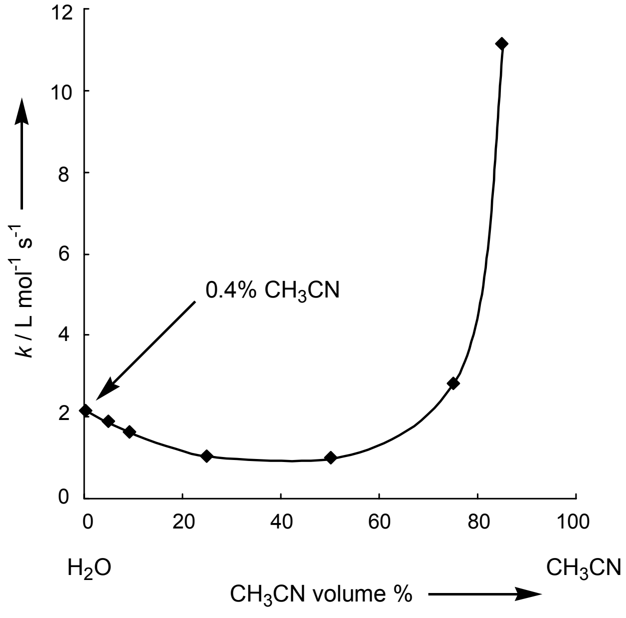

Figure 2.2: Solvent effect on the second-order rate constant of the reaction of $(lil)_2CH^+$ with OH^- in acetonitrile–water mixtures (individual rate constants are given in Experimental Part). Because of the poor solubility of $(lil)_2CH^+BF_4^-$, the rate constant in pure water cannot be measured.

A dramatic enhancement of reactivity is observed, when the acetonitrile content exceeds 75% (v/v) (11.2 L mol^{-1} s^{-1} for 15/85 (v/v) H_2O/CH_3CN). An analogous solvent dependence has been reported for the reaction of malachite green with hydroxide ion[16] and for the hydroxide induced hydrolysis of 4-nitrophenyl acetate in acetonitrile/water mixtures.[17] The small curvature of the graph in the water-rich section on the left of Figure 2.2 suggests an insignificant difference of reactivity in water and in 99.6/0.4 (v/v) H_2O/CH_3CN. In accord with this interpretation, the rate constants measured for the reactions of benzhydrylium ions with semicarbazide, sulfite, hydroxylamine, or thiolatoacetate in aqueous solutions containing 0.4% of acetonitrile agreed with those determined in aqueous solutions containing 0.4% TFE within a standard deviation of 3% (Table 2.2). For that reason, the presence of 0.4% of co-solvents in water will be neglected in the following discussion.

Table 2.2: Kinetics of the reactions of n-nucleophiles with benzhydrylium tetrafluoroborates at 20 ºC.

Nucleophile	Electrophile	k_2 / L mol^{-1} s^{-1}	Solvent ^{a}
H_2O	$(thq)_2CH^+$	$2.20 \times 10^{-3\,b}$	99.6/0.4 W/AN
	$(pyr)_2CH^+$	$5.57 \times 10^{-3\,b}$	99.6/0.4 W/AN
	$(dma)_2CH^+$	$2.6 \times 10^{-2\,b,c}$	W
	$(mor)_2CH^+$	$3.31 \times 10^{-1\,b}$	50/50 W/AN
	$(mfa)_2CH^+$	$3.78^{\,b}$	50/50 W/AN
	$(ani)_2CH^+$	$1.3 \times 10^{5\,b,c}$	67/33 W/AN
	$ani(tol)CH^+$	$9.1 \times 10^{5\,b,c}$	67/33 W/AN
	$ani(Ph)CH^+$	$2.1 \times 10^{6\,b,c}$	67/33 W/AN
	$(tol)_2CH^+$	$3.2 \times 10^{7\,b,c}$	67/33 W/AN
OH^-	$(lil)_2CH^+$	2.16	99.6/0.4 W/AN
		1.90	95/5 W/AN
		1.65	91/9 W/AN
		1.05	80/20 W/AN
		1.03	50/50 W/AN
		2.81	25/75 W/AN

Table 2.2: Continued

Nucleophile	Electrophile	k_2 / L mol^{-1} s^{-1}	Solvent^{a}
OH^{-}	$(lil)_2CH^+$	1.12×10^1	15/85 W/AN
	$(jul)_2CH^+$	3.44	99.6/0.4 W/AN
	$(ind)_2CH^+$	1.08×10^1	99.6/0.4 W/AN
		8.56	50/50 W/AN
	$(pyr)_2CH^+$	4.85×10^1	99.6/0.4 W/AN
	$(dma)_2CH^+$	1.31×10^2	99.6/0.4 W/AN
		9.83×10^1	50/50 W/AN
	$(mor)_2CH^+$	1.06×10^3	50/50 W/AN
	$(mfa)_2CH^+$	6.67×10^3	50/50 W/AN
$H_2NNHCONH_2$	$(lil)_2CH^+$	3.32	99.6/0.4 W/TFE
	$(thq)_2CH^+$	2.86×10^1	99.6/0.4 W/TFE
	$(pyr)_2CH^+$	5.56×10^1	99.6/0.4 W/TFE
	$(dma)_2CH^+$	1.20×10^2	99.6/0.4 W/TFE
		1.20×10^2	99.6/0.4 W/AN
$HONH_2$	$(lil)_2CH^+$	6.59	99.6/0.4 W/TFE
		6.37	99.6/0.4 W/AN
	$(jul)_2CH^+$	9.58	99.6/0.4 W/TFE
	$(ind)_2CH^+$	2.94×10^1	99.6/0.4 W/TFE
	$(pyr)_2CH^+$	1.24×10^2	99.6/0.4 W/TFE
	$(dma)_2CH^+$	2.52×10^2	99.6/0.4 W/TFE
$CF_3CH_2NH_2$	$(lil)_2CH^+$	2.26×10^1	DMSO
	$(ind)_2CH^+$	1.44×10^2	DMSO
	$(dma)_2CH^+$	3.09×10^3	DMSO
	$(mor)_2CH^+$	1.65×10^4	DMSO
$CF_3CH_2O^{-}$	$(lil)_2CH^+$	3.79×10^1	99.6/0.4 W/TFE
	$(jul)_2CH^+$	7.06×10^1	99.6/0.4 W/TFE
	$(thq)_2CH^+$	4.35×10^2	99.6/0.4 W/TFE
	$(dma)_2CH^+$	2.14×10^3	99.6/0.4 W/TFE
n-$PrNH_2$	$(lil)_2CH^+$	7.89×10^1	99.6/0.4 W/AN
	$(ind)_2CH^+$	3.07×10^2	99.6/0.4 W/AN

Table 2.2: Continued

Nucleophile	Electrophile	k_2 / L mol^{-1} s^{-1}	Solvent ^{a}
n-PrNH$_2$	(pyr)$_2$CH$^+$	1.23×10^3	99.6/0.4 W/AN
	(dma)$_2$CH$^+$	3.12×10^3	99.6/0.4 W/AN
	(mor)$_2$CH$^+$	2.44×10^4	91/9 W/AN
	(pfa)$_2$CH$^+$	1.87×10^5	91/9 W/AN
$H_2NCH_2CO_2Et$	(lil)$_2$CH$^+$	7.78×10^2	DMSO
	(jul)$_2$CH$^+$	2.05×10^3	DMSO
	(ind)$_2$CH$^+$	3.99×10^3	DMSO
	(thq)$_2$CH$^+$	1.33×10^4	DMSO
	(dma)$_2$CH$^+$	8.43×10^4	DMSO
HOO$^-$	(lil)$_2$CH$^+$	9.43×10^2	99.6/0.4 W/AN
	(ind)$_2$CH$^+$	4.22×10^3	99.6/0.4 W/AN
	(dma)$_2$CH$^+$	4.31×10^4	99.6/0.4 W/AN
n-PrNH$_2$	(lil)$_2$CH$^+$	3.93×10^3	DMSO
	(jul)$_2$CH$^+$	1.12×10^4	DMSO
	(ind)$_2$CH$^+$	2.06×10^4	DMSO
	(thq)$_2$CH$^+$	6.61×10^4	DMSO
SO_3^{2-}	(lil)$_2$CH$^+$	7.72×10^3	99.6/0.4 W/TFE
		7.50×10^3	99.6/0.4 W/AN
	(jul)$_2$CH$^+$	1.20×10^4	99.6/0.4 W/TFE
	(ind)$_2$CH$^+$	3.83×10^4	99.6/0.4 W/TFE
	(thq)$_2$CH$^+$	7.06×10^4	99.6/0.4 W/TFE
	(pyr)$_2$CH$^+$	1.50×10^5	99.6/0.4 W/TFE
Morpholine	(lil)$_2$CH$^+$	4.62×10^4	DMSO
	(jul)$_2$CH$^+$	1.17×10^5	DMSO
	(ind)$_2$CH$^+$	3.23×10^5	DMSO
	(thq)$_2$CH$^+$	7.94×10^5	DMSO
Piperidine	(lil)$_2$CH$^+$	1.13×10^5	DMSO
	(jul)$_2$CH$^+$	3.19×10^5	DMSO
	(ind)$_2$CH$^+$	6.67×10^5	DMSO
	(thq)$_2$CH$^+$	2.51×10^6	DMSO

Table 2.2: Continued

Nucleophile	Electrophile	k_2 / L mol^{-1} s^{-1}	Solvent [a]
$^{-}SCH_2CO_2^{-}$	$(lil)_2CH^+$	2.88×10^5	99.6/0.4 W/TFE
		3.09×10^5	99.6/0.4 W/AN
	$(jul)_2CH^+$	3.87×10^5	99.6/0.4 W/TFE
	$(ind)_2CH^+$	9.67×10^5	99.6/0.4 W/TFE
	$(thq)_2CH^+$	1.61×10^6	99.6/0.4 W/TFE
N_3^{-}	$(lil)_2CH^+$	1.68×10^6	DMSO
	$(jul)_2CH^+$	$> 2 \times 10^6$	DMSO

[a] Mixtures of solvents are given as (v/v), solvents: W = water, AN = acetonitrile, TFE = trifluoroethanol. [b] Unit is s^{-1}. [c] Counter ion is 4-cyanophenolate or acetate[18].

In the reactions of benzhydrylium ions with *n*-propylamine, hydrogen peroxide anion, or 2,2,2-trifluoroethoxide in water, competition of hydroxide with these nucleophiles has to be considered. As explicitly described for the reaction of $(lil)_2CH^+$ with *n*-propylamine in water (Table 2.3), the pseudo-first order rate constant reflects the reaction of the carbocation with *n*-propylamine and with OH^{-} (eq. 2.3).

$$k_{1\Psi} = k_{2,\mathrm{OH}^-}[\mathrm{OH}^-] + k_{2,n\text{-PrNH2}}[n\text{-PrNH}_2]_{\mathrm{eff}} \tag{2.3}$$

Table 2.3. Competing reaction of *n*-propylamine and OH^{-} with $(lil)_2CH^+$ (7.39×10^{-6} mol L^{-1}) in water at 20 °C.

$[n\text{-PrNH}_2]_0$, mol L^{-1}	$k_{1\Psi}$, s^{-1}	$[\mathrm{OH}^-]_{\mathrm{eff}}$,[a] mol L^{-1}	$[n\text{-PrNH}_2]_{\mathrm{eff}}$, mol L^{-1}	$k_{2,\mathrm{OH}^-}[\mathrm{OH}^-]_{\mathrm{eff}}$, s^{-1}	$k_{2,n\text{-PrNH}_2}[n\text{-PrNH}_2]_{\mathrm{eff}}$, s^{-1}
1.29×10^{-3}	5.63×10^{-2}	5.96×10^{-4}	6.93×10^{-4}	1.30×10^{-3}	5.50×10^{-2}
2.15×10^{-3}	1.05×10^{-1}	8.24×10^{-4}	1.32×10^{-3}	1.78×10^{-3}	1.03×10^{-1}
3.01×10^{-3}	1.59×10^{-1}	1.01×10^{-3}	2.00×10^{-3}	2.19×10^{-3}	1.57×10^{-1}
4.30×10^{-3}	2.39×10^{-1}	1.25×10^{-3}	3.05×10^{-3}	2.70×10^{-3}	2.36×10^{-1}
5.16×10^{-3}	3.02×10^{-1}	1.39×10^{-3}	3.77×10^{-3}	3.01×10^{-3}	2.99×10^{-1}

[a] Calculated from pK_a ($n\text{-PrNH}_3^+$ = 10.7); ref. 19a.

Since the concentrations of *n*-propylamine and hydroxide ion can be calculated from the known pK_a values,[19a] and the second-order rate constant for the reaction with OH^- has independently been determined in this work, one can easily derive the contribution of $k_{2,n\text{-PrNH2}}$ to the observed pseudo-first-order rate constant. Table 2.3 shows that the corrections due to the contribution of OH^- are marginal (< 2%), and $k_{2,n\text{-PrNH2}}$ can again be derived from a plot of $k_{1\Psi,\, n\text{-PrNH2}}$ vs. [*n*-$PrNH_2$]$_{eff}$.

Analogously, the observed pseudo-first-order rate constants for the reactions of benzhydrylium ions with trifluoroethoxide (pK_a = 12.4)[3] and the anion of hydrogen peroxide (pK_a =11.8)[19b] are only slightly affected by the competing reaction with hydroxide. In accord with this interpretation, the reaction of (dma)$_2CH^+BF_4^-$ with 99.6/0.4 (v/v) H_2O/TFE in presence of OH^- gave preferentially the trifluoroethyl ether.

In several cases, the equilibrium constant for product formation was relatively small, and the carbocation absorbance disappeared not or only partially upon addition of the nucleophile. Thus, the reaction of (lil)$_2CH^+$ with semicarbazide required a relatively large concentration of semicarbazide (1.4×10^{-3} mol L^{-1}) to achieve 90% of conversion.

When (lil)$_2CH^+$ or (jul)$_2CH^+$ were combined with N_3^- in water,[20] the carbocation absorbances decreased by less than 5%. The reactions of (thq)$_2CH^+$ and (dma)$_2CH^+$ with N_3^- were also incomplete in water,[21] but proceeded so fast that we were not able to determine the rate constants. Only for the reaction of (lil)$_2CH^+$ with N_3^- in DMSO, which proceeded with 6 % conversion at $[N_3^-]_0 = 2.6 \times 10^{-5}$ mol L^{-1}, the combination rate constant could be determined (Table 2.2).

In previous work by McClelland and co-workers[18] it has been shown that the first-order decay of benzhydrylium ions in acetonitrile/water mixtures increases with [H_2O] at low water concentrations but remained almost constant for mixtures containing more than 20% water. In agreement with this report, we have found the pseudo-first-order rate constants for the consumption of (mfa)$_2CH^+$ to increase by less than 16% when the solvent mixture was changed from 91/9 to 50/50 (v/v) H_2O/CH_3CN (Chapter 3). For that reason, the first-order rate constants for the reactions with water in Table 2.2

referring to different water/acetonitrile mixtures can directly be compared with each other.

2.4 Discussion

Figure 2.3 shows that the rate constants of the reactions of n-nucleophiles with benzhydrylium ions correlate linearly with the electrophilicity parameters *E*, which have been derived from the reactions of these benzhydrylium ions with a set of π-nucleophiles.[8]

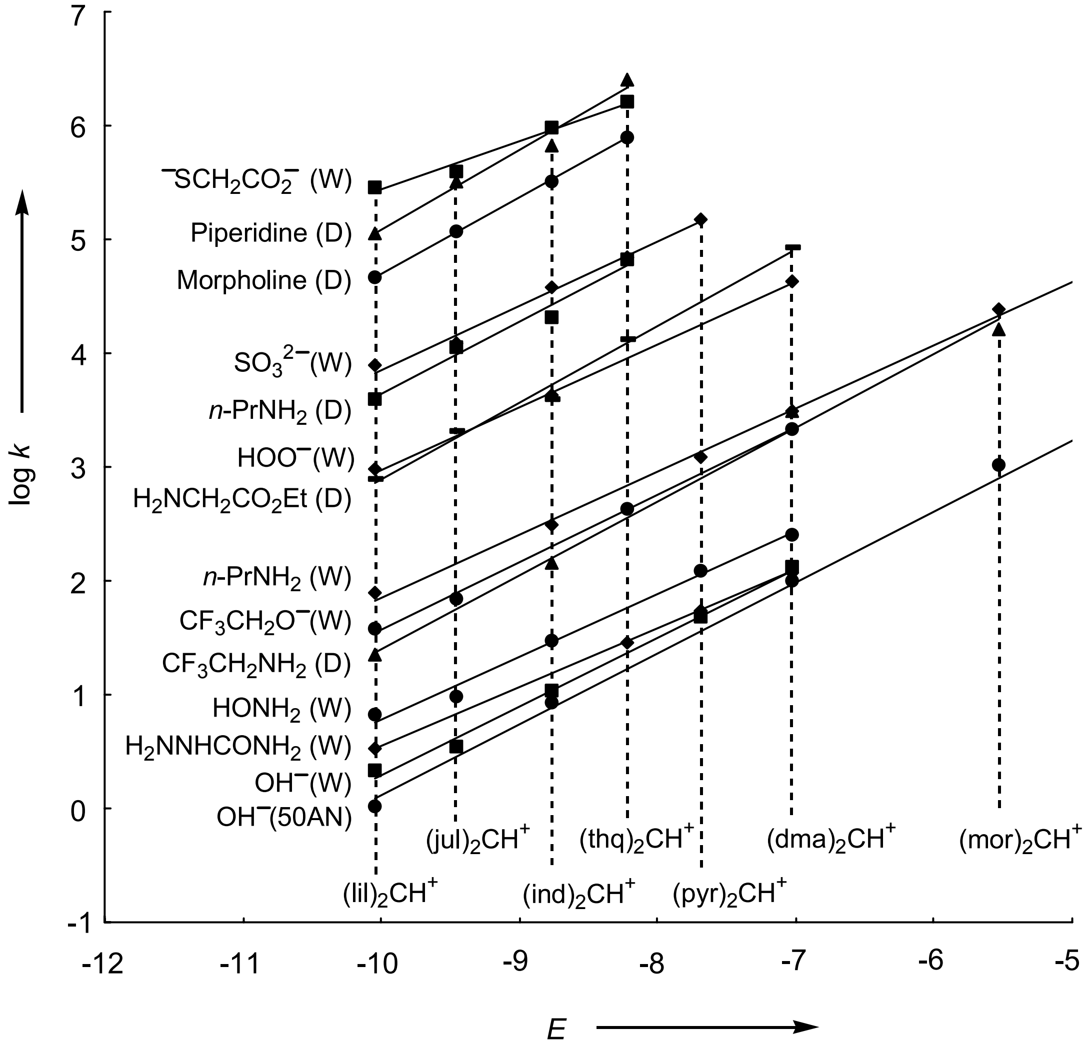

Figure 2.3: Correlation of the rate constants (20 °C) for the reactions of n-nucleophiles with benzhydrylium ions (Ar_2CH^+) towards the electrophilicity parameters *E*. Solvents: W = water, D = DMSO, 50AN = 50/50 (v/v) H_2O/CH_3CN. Data from Table 2.2.

It was, therefore, possible to derive *N* and *s* parameters for n-nucleophiles from the rate constants given in Table 2.2 and the previously published *E*-parameters[8] by linear regressions on the basis of eq. 2.2 (Table 2.4).

Table 2.4: Nucleophilicity (*N*) and slope (*s*) parameters for fifteen Ritchie-type nucleophile solvent systems.

Nucleophile (Solvent)	*N*	*s*	Nucleophile (Solvent)	*N*	*s*
H_2O (Water)	5.11 [a]	0.89 [a]	$H_2NCH_2CO_2Et$ (DMSO)	14.30	0.67
OH^- (50AN) [b]	10.19	0.62	HOO^- (Water)	15.40	0.55
OH^- (Water)	10.47	0.61	n-$PrNH_2$ (DMSO)	15.70	0.64
$H_2NNHCONH_2$ (Water)	11.05	0.52	SO_3^{2-} (Water)	16.83	0.56
$HONH_2$ (Water)	11.41	0.55	Morpholine (DMSO)	16.96	0.67
$CF_3CH_2NH_2$ (DMSO)	12.15	0.65	Piperidine (DMSO)	17.19	0.71
$CF_3CH_2O^-$ (Water)	12.66	0.59	$^-SCH_2CO_2^-$ (Water)	22.62	0.43
n-$PrNH_2$ (Water)	13.33	0.56			

[a] From first-order rate constant, correlation not shown in Figure 2.3. [b] 50/50 (v/v) H_2O/CH_3CN.

The small value of the standard deviation (factor 1.14) between experimental rate constants and those calculated by eq. 2.2 from *E* [8] and the *N* and *s* values given in Table 2.4 corroborates the suitability of the previously published electrophilicity parameters *E* [8] for characterizing also n-nucleophiles.

Table 2.4 shows that with the exception of water (s = 0.89) and 2-thiolatoacetate in water (s = 0.43) all nucleophiles investigated in this work have slope parameters of $0.52 < s < 0.71$, indicating that most carbocation nucleophile combinations follow almost constant selectivity relationships: For constant values of *s*, eq. 2.2 transforms into eq. 2.1/1a. The exceptionally high value of *s* for water given in Table 2.4 is consistent with Ritchie's report that in reactions of tritylium ions the ratio k_{OH^-}/k_{H_2O} decreases as the electrophilicities of the tritylium ions increase.[3]

The narrow range which embraces most *s*-parameters in Table 2.4 suggests evaluating the rate constants of Table 2.2 by the Ritchie equation (eq. 2.1/1a, Figure 2.4). When water with the different *s*-parameter is excluded, the standard deviation between calculated (eq. 2.1) and experimental rate constants is somewhat larger (factor 1.20) than that obtained by employing eq. 2.2 (factor 1.14), despite the fact that the linear regression according to eq. 2.2 uses the fixed *E*-parameters from ref. 8, while the log k_0 parameters in eq. 2.1 are fully optimized for the data of this investigation.

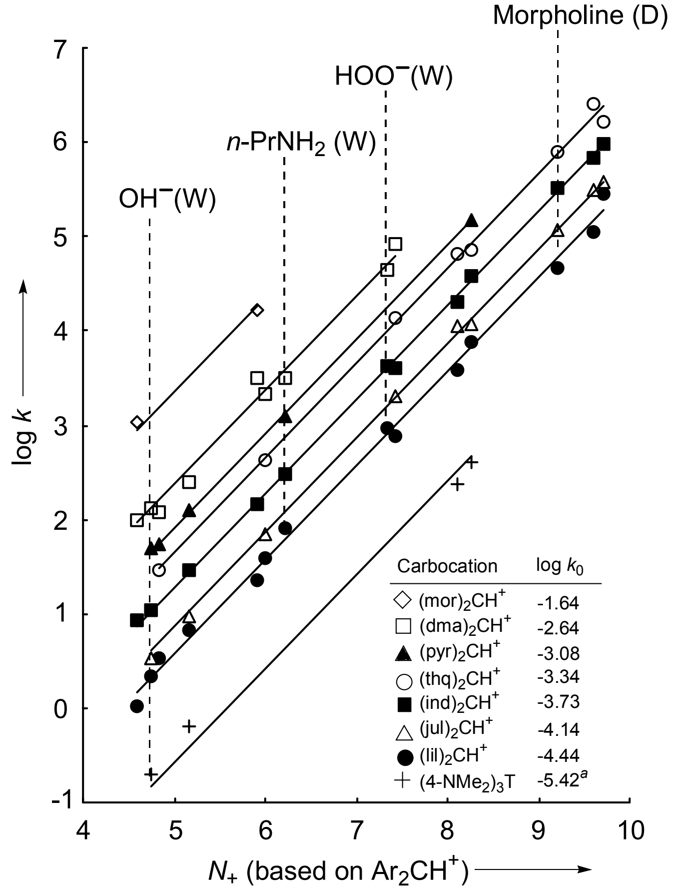

Figure 2.4: Analysis of the rate constants for the reactions of benzhydrylium ions with n-nucleophiles (20 °C) in water (W) or dimethylsulfoxide (D) according to the Ritchie formalism (eq. 2.1/1a) compared with crystal violet (4-NMe$_2$)$_3$T. [a] Data for (4-NMe$_2$)$_3$T from refs 3 and 22, all other data from Table 2.2.

As expected, the N_+ values thus derived from the reactions of the n-nucleophiles with benzhydrylium ions differ only slightly from those reported by Ritchie (Table 2.5). Since the different N_+ values given in Ritchie's 1986 paper[3] for reactions with tritylium ions, tropylium ions, and pyronines are not based on rate constants for series of reactions but refer to only a single electrophile of each class, we will not attempt an interpretation of the differences of N_+ from different sources.

Table 2.5: Comparison of N_+ values for n-nucleophiles with respect to different series of electrophiles.

Nucleophile (Solvent)	Ar_2CH^+ [a]	Ar_3C^+ [b]	Pyronin-Y [c]	Ar-Trop [d]
OH^- (Water)	= 4.75 (5)	= 4.75	= 4.75	= 4.75
OH^- (50AN) [e]	4.60 (4)			
$H_2NNHCONH_2$ (Water)	4.83 (4)	3.73		3.42
$HONH_2$ (Water)	5.16 (5)	5.05		3.82
$CF_3CH_2NH_2$ (DMSO)	5.92 (4)	4.86	4.70	
$CF_3CH_2O^-$ (Water)	5.99 (4)	5.06		5.66
n-$PrNH_2$ (Water)	6.22 (4)			
HOO^- (Water)	7.35 (3)	8.52	7.33	7.20
$H_2NCH_2CO_2Et$ (DMSO)	7.43 (5)	6.54		
n-$PrNH_2$ (DMSO)	8.11 (4)	7.88	8.40	
SO_3^{2-} (Water)	8.26 (5)	8.01	7.91	7.50
Morpholine (DMSO)	9.20 (4)		9.17	
Piperidine (DMSO)	9.61 (4)		9.32	
$^-SCH_2CO_2^-$ (Water)	9.72 (4)	9.09		

[a] This work; least-squares fit; number of reactions given in parentheses. [b] From ref. 3, relative reactivities toward malachite green. [c] From ref. 3. [d] From ref. 3, relative reactivities toward the 4-(dimethylamino)-phenyltropylium ion. [e] Solvent mixture, 50/50 (v/v) H_2O/CH_3CN.

Evaluation of the kinetic data in Table 2.2 by the Ritchie equation eq. 2.1/1a also provides log k_0 values for benzhydrylium ions (Figure 2.4), which allow us to compare the benzhydrylium ions studied in this work with those electrophiles previously investigated by Ritchie.

However, because of the much wider applicability of eq. 2.2 compared to eq. 2.1 (in contrast to eq. 2.1, eq. 2.2. also holds for reactions with π-systems) it is more advantageous not to employ log k_0 (Figure 2.4) but to use the electrophilicity parameters *E* as defined by eq. 2.2 for comparing electrophiles of different type. Therefore, the previously reported rate constants for the reactions of tritylium, tropylium, and xanthylium ions with the fifteen nucleophile-systems characterized in this work (Table 2.4) were subjected to a correlation analysis on the basis of eq. 2.2. When calculating the *E* parameters of these electrophiles by a least squares minimization of the deviations between observed and calculated rate constants, the *N* and *s* values of Table 2.4, which were derived from reactions with reference electrophiles, were kept as fixed parameters. In Scheme 2.1 only those *E*-parameters are listed which could be derived from kinetics at an ionic strength of $I < 0.1$.

Scheme 2.1: Electrophilicity parameters *E* (according to eq. 2.2) for Ritchie's electrophiles from reactions with n-nucleophiles (at $I < 0.1$) compared with electrophilicity parameters for benzhydrylium ions. Note: The *E*-parameters for tritylium ions given in this Scheme must not be used for predicting reactivities toward π-systems (see text).

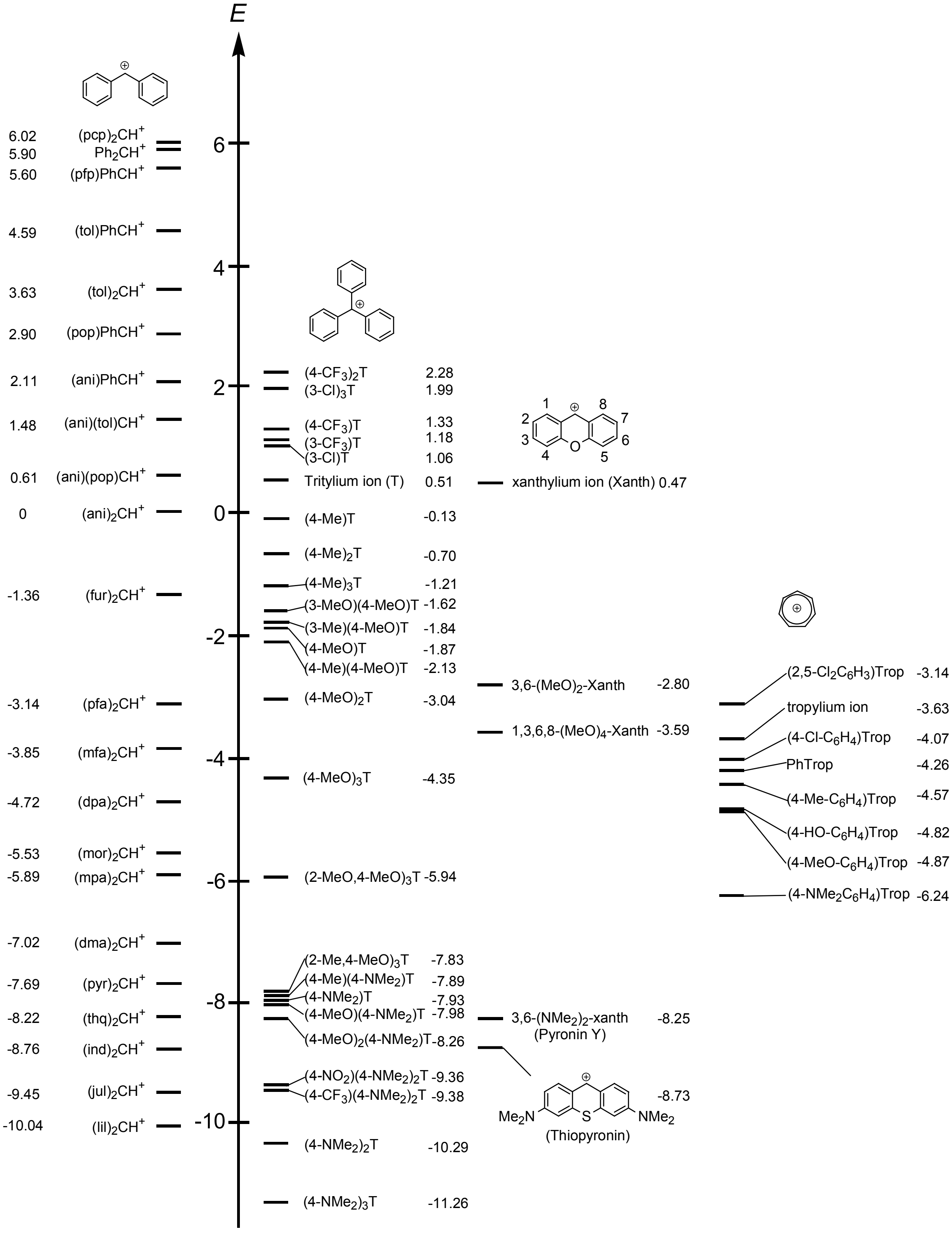

Though calculated and experimental rate constants for reactions with tropylium ions often differ by one order of magnitude, the *E*-parameter derived for the parent tropylium ion from reactions with n-nucleophiles (-3.63, Scheme 2.1) differs only slightly from that derived from the reactions of this electrophile with the reference π-nucleophiles (-3.72).[8] One can, therefore, expect that all *E*-parameters for tropylium ions given in Scheme 2.1 can be used for calculating reactivities of these electrophiles toward all types of nucleophiles, i.e., also for reactions with alkenes, arenes, or hydrides.

The applicability of the *E*-parameters of tritylium ions is more limited, however, since the sensitivity of bulky reagents towards variation of the steric requirements of the reaction partner will be large. Because our approach, like Ritchie's, does not explicitly treat steric effects, we have recommended that reactions of bulky reagents should not be treated with eq. 2.2.[5,8] The satisfactory agreement between calculated (eq. 2.2) and experimental rate constants indicates, however, that reactivities of tritylium ions toward n-nucleophiles can generally be reproduced by eq. 2.2, in accord with Ritchie's previous work.

When the *E*-parameters of tritylium ions given in Scheme 2.1 are used to calculate rate constants of hydride abstractions, however, k_{calc} is usually somewhat larger than k_{obs}, indicating that the transition states of hydride transfer reactions have higher steric requirements than the reactions of carbocations with n-nucleophiles (Table 2.6). This result is surprising in view of the almost linear C-H-X arrangement in the corresponding transition states.[27] However, since the deviation between k_{calc} and k_{obs} in Table 2.6 rarely exceeds one order of magnitude, it is possible to combine all *E*-parameters presented in Scheme 2.1 with the *N*- and *s*-parameters of hydride donors[8,12] for estimating the rates of hydride transfer reactions.

Table 2.6: Comparison between calculated and experimental rate constants for the reactions of tritylium ions with hydride donors.

Electrophile (*E*) [a]	Nucleophile (*N*, *s*) [b]	k_{calc} (20 °C),[c] L mol^{-1} s^{-1}	k_{exp}, L mol^{-1} s^{-1}
$(4\text{-MeO})_3$T (-4.35)	cycloheptatriene (0.52, 0.97)	1.9×10^{-4}	1.6×10^{-3} [d] (80 °C, CH_3CN)
$(4\text{-MeO})_2$T (-3.04)	cycloheptatriene (0.52, 0.97)	3.6×10^{-3}	1.1×10^{-3} [d] (23 °C, CH_3CN)
(4-MeO)T (-1.87)	cycloheptatriene (0.52, 0.97)	4.9×10^{-2}	2.0×10^{-2} [d] (23 °C, CH_3CN)
$(4\text{-Me})_3$T (-1.21)	cycloheptatriene (0.52, 0.97)	2.1×10^{-1}	2.7×10^{-2} [d] (23 °C, CH_3CN)
T (0.51)	1,4-cyclohexadiene (0.09, 0.98)	3.9	3.2×10^{-1} [e] (20 °C, CH_2Cl_2)
	1,4-dihydronaphthalene (-0.07, 1.03)	2.8	8.2×10^{-2} [e] (20 °C, CH_2Cl_2)
	9,10-dihydroanthracene (-0.86, 0.92)	4.8×10^{-1}	1.4×10^{-2} [e] (20 °C, CH_2Cl_2)
	cycloheptatriene (0.52, 0.97)	1.0×10^{1}	1.8 [f] (20 °C, CH_2Cl_2)
	$HSiEt_3$ (3.64, 0.65)	5.0×10^{2}	1.2×10^{2} [g] (20 °C, CH_2Cl_2)
	$HSiMe_2Ph$ (3.27, 0.73)	5.7×10^{2}	2.1×10^{2} [g] (25 °C, CH_2Cl_2)
	$HSiBu_3$ (4.45, 0.64)	1.5×10^{3}	2.4×10^{2} [g] (20 °C, CH_2Cl_2)
(3-Cl)T (1.06)	1,4-cyclohexadiene (0.09, 0.98)	1.3×10^{1}	2.3 [e] (20 °C, CH_2Cl_2)
$(3\text{-Cl})_3$T (1.99)	1,4-cyclohexadiene (0.09, 0.98)	1.1×10^{2}	5.4×10^{1} [e] (20 °C, CH_2Cl_2)
	H_3SiPh (0.25, 0.67)	3.2×10^{1}	4.6 [e] (20 °C, CH_2Cl_2)

[a] Scheme 2.1. [b] From ref. 8 or 12. [c] Calculated according to eq. 2.2. [d] From ref. 23. [e] From ref. 24. [f] From ref. 25. [g] From ref. 26, for $HSiEt_3$: $\Delta H^{\ddagger} = 29.3$ kJ mol^{-1}, $\Delta S^{\ddagger} = -105$ J K^{-1} mol^{-1}; for $HSiBu_3$: $\Delta H^{\ddagger} = 26.4$ kJ mol^{-1}, $\Delta S^{\ddagger} = -109$ J K^{-1} mol^{-1}.

As expected, the reactions of π-nucleophiles with tritylium ions are considerably slower than predicted by eq. 2.2. For the reactions of tritylium ions with 1-methoxy-2-methyl-1-(trimethylsiloxy)propene ($N = 9.00$, $s = 0.98$),[8] the rate constants calculated by eq. 2.2 are 4 to 6 orders of magnitude higher than experimentally observed by Fukuzumi (Table 2.7).[28] Since the large steric demand of both reagents enforces a reaction at the *p*-position of a phenyl group at tritylium, the steric effect for attack at the tertiary carbenium center is even larger than derived from the ratio $k_{\text{calc}}/k_{\text{obs}}$. Furthermore, Fukuzumi[28] reported rate constants for the reactions of 1-ethoxy-1-(triethylsiloxy)ethene and *t*-butyldimethylsiloxy-1-ethoxyethene which are two orders of magnitude smaller than the prediction of eq. 2.2 for reactions of tritylium ions with the less nucleophilic 1-phenoxy-1-(trimethylsiloxy)ethene ($N = 8.23$, $s = 0.81$).[8] These examples demonstrate that reactions of tritylium ions with π-nucleophiles cannot be described by eq. 2.2, and we explicitly advise not using the *E*-parameters of tritylium ions listed in Scheme 2.1 for calculating reactivities toward π-nucleophiles.

Table 2.7: Comparison between calculated (eq. 2.2) and observed rate constants for the reactions of tritylium ions with π-nucleophiles.

Nucleophile	N	s	Tritylium ion[a]	E	k_{calc}, L mol^{-1} s^{-1}	k_{exp},[b] L mol^{-1} s^{-1}	
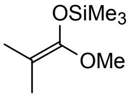	9.00	0.98	T	0.51	2.1×10^{9}[c]	4.2×10^{4}	
			(4-MeO)T	-1.87	9.7×10^{6}	3.3×10^{3}	
			(4-MeO)$_2$T	-3.04	6.9×10^{5}	7.9	
			(4-MeO)$_3$T	-4.35	3.6×10^{4}	6.1×10^{-2}	
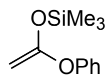	8.23	0.81	(4-MeO)$_2$T	-3.04	1.6×10^{4}	5.0×10^{2}	k_{exp} refers to 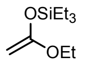
			(4-MeO)$_3$T	-4.35	1.4×10^{3}	1.9×10^{1}	
			T	0.51	1.2×10^{7}	3.4×10^{4}	k_{exp} refers to 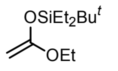
			(4-MeO)$_3$T	-4.35	1.4×10^{3}	2.1×10^{1}	

[a] T = tritylium ion. [b] From ref 28. [c] Calculated from eq. 2.2, though its limitation is 10^{8} L mol^{-1} s^{-1}.

The previously mentioned suitability of the N and s parameters for the n-nucleophiles in Table 2.4 for calculating their reactivities toward benzhydrylium, tritylium, tropylium, and xanthylium ions indicates that differential steric effects are not important in the reactions of O-, S-, and N-nucleophiles with these carbocations. The nucleophilicity parameters N and s of many additional n-nucleophiles (and hydride donors) can, therefore, be derived from the published rate constants of their reactions with tritylium, tropylium, and xanthylium ions and the corresponding *E*-parameters given in Scheme 2.1. The *N* and *s* parameters of 23 of these nucleophiles for which rate constants over more than three log *k* units were available, have been listed in Table 2.8.

Table 2.8: Approximate nucleophilicity parameters *N* and *s* of nucleophiles from reactions with Ritchie's electrophiles (Scheme 2.1).[a]

Nucleophile (Solvent [b])	*N*	*s*	Nucleophile (Solvent [b])	*N*	*s*
MeOH (M)	6.02 [c]	1.01 [c]	*n*-$BuNH_2$ (W)	11.69	0.65
$CF_3CH_2NH_2$ (W)	8.70	0.68	$MeOCH_2CH_2NH_2$ (W)	11.81	0.57
CN^- (W)	9.19	0.60	BH_4^- (W)	12.23	0.78
NH_3 (W)	9.26	0.66	$EtNH_2$ (W)	12.24	0.61
CH_3ONH_2 (W)	9.81	0.63	H_2NNH_2 (W)	12.45	0.61
$H_2NCH_2CONHCH_2CO_2^-$ (W)	10.28	0.77	*N*-Benzyldihydronicotinamide (W)	12.48	0.66
$H_2NCH_2CO_2Et$ (W)	10.28	0.70	$Me_3N^+CH_2CH_2O^-$ (W)	12.66	0.56
$NCCH_2CH_2NH_2$ (W)	10.33	0.63	$HC\equiv CCH_2O^-$ (W)	12.77	0.57
$H_2NCH_2CH_2NH_2$ (W)	10.37	0.82	CH_3O^- (M)	13.59	0.90
$PhNHNH_2$ (W)	10.83	0.64	$HOCH_2CH_2S^-$ (W)	15.62	0.78
BH_3CN^- (W)	11.02	0.59	$MeO_2CCH_2CH_2S^-$ (W)	15.82	0.81
$H_2NCH_2CO_2^-$ (W)	11.15	0.74			

[a] These *N* and *s* parameters are less accurate than those in Table 2.4 because of the indirect evaluation. [b] M = methanol, W = water. [c] Based on first-order rate constants.

Readers not familiar with our recent papers[7,8,12] may be wondering, why the stepwise procedure summarized in Scheme 2.2 has been used to determine the electrophilicity parameters of Scheme 2.1 and the nucleophilicity parameters of Table 2.8 instead of subjecting all available rate constants for the reactions of nucleophiles with carbocations to a single correlation analysis.

Scheme 2.2

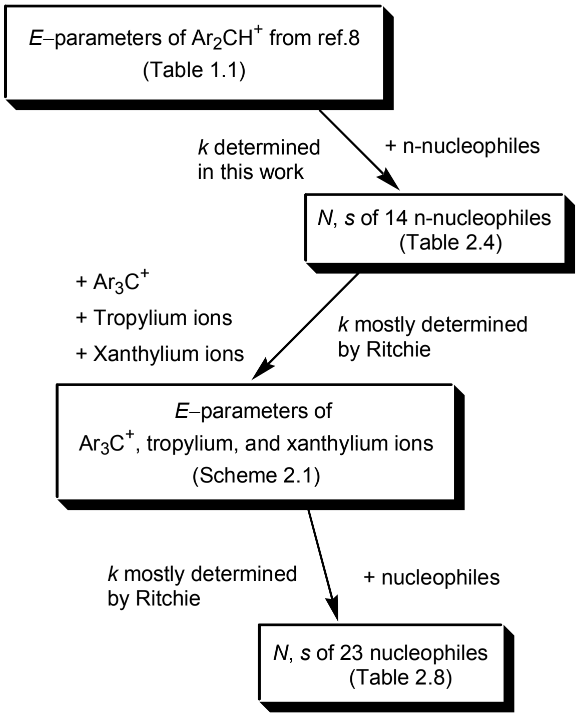

As previously discussed in detail,[8] only the unequal treatment of data from different sources allows us to systematically extend our reactivity scales without the necessity to continuously revise the entire sets of electrophilicity and nucleophilicity parameters. It is thus possible to employ preliminary numbers in some cases, which can be replaced by more reliable data at a later stage without affecting the "established" parameters. This procedure also allows us to define reactivity parameters which can only be used for certain types of reactions (e.g., *E*-parameters of Ar_3C^+ for their reactions with n-nucleophiles and hydride donors) which would be impossible if all reactions would be treated equally. Inclusion of reactivity data for more reactive carbocations is in progress.[29]

2.5 Conclusion

We have demonstrated that the problem with "constant selectivity relationships" reported by Ritchie in 1986 is predominately caused by the widely deviating slope parameter *s* of water. By employing eq. 2.2 instead of eq. 2.1, we can describe all reactions of tritylium, tropylium, and xanthylium ions with n-nucleophiles with a single set of parameters. Since eq. 2.2 has previously been demonstrated to hold for the reactions of carbocations with π- and σ-nucleophiles, it has now become possible to combine kinetic data from different sources and create a nucleophilicity scale that directly compares n-, π-, and σ-nucleophiles (Scheme 2.3).

Scheme 2.3: Comparison of the nucleophilic reactivities of n-nucleophiles with typical π-nucleophiles, hydride donors, and carbanions from refs 8 or 9. Solvents: CH_2Cl_2 if not otherwise mentioned, H_2O (W), DMSO (D), methanol (M). [a] From Table 2.4. [b] From Table 2.8.

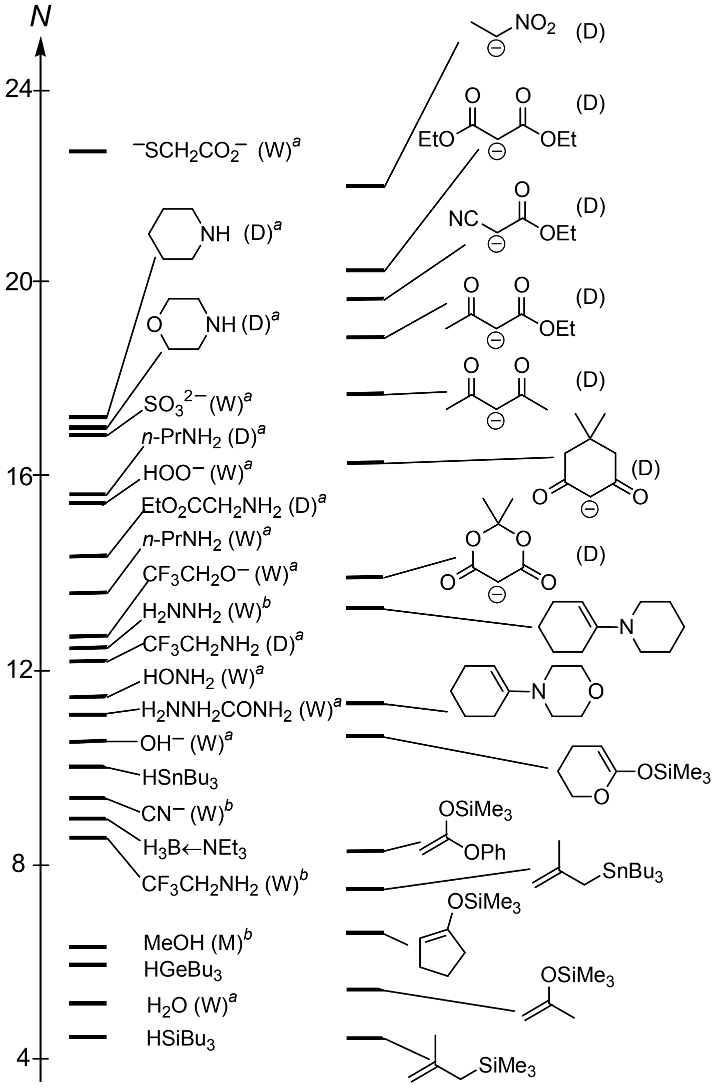

Though the data of Table 2.4 indicate a fair correlation between *N* and *s* for n-nucleophiles, the situation becomes more complicated when π-nucleophiles and hydride donors are included. It is evident that most π-nucleophiles are characterized by higher values of *s* than n-nucleophiles, even when compounds of similar *N*-values are compared. As a consequence, more reactive carbocations (harder electrophiles) will show a relative preference for π-nucleophiles over n-nucleophiles compared to less reactive carbocations (softer electrophiles). Since alkoxides and amines are considered as hard bases in contrast to alkenes and arenes (soft bases) we must conclude that the Hard Soft Acid Base Principle[30] is not useful for describing our correlations.

According to a recent theoretical analysis,[13] slope parameters of 0.67, as found for most nucleophiles in this investigation, are indicative of constant intrinsic barriers within a reaction series. A more detailed analysis considering absolute intrinsic barriers of these reactions[4b,31] is now needed to reveal the physical background of these correlations.

2.6 References

(1) (a) Ritchie, C. D. *Acc. Chem. Res.* **1972**, *5*, 348–354. (b) Ritchie, C. D. *J. Am. Chem. Soc.* **1975**, *97*, 1170–1179.

(2) Analyses of reactivity selectivity relationships: (a) Stock, L. M.; Brown, H. C. *Adv. Phys. Org. Chem.* **1963**, *1*, 35–154. (b) Leffler, J. E.; Grunwald, E. *Rates and Equilibria of Chemical Reactions*; Wiley: New York, 1963; pp 162–168. (c) Johnson, C. D. *Chem. Rev.* **1975**, *75*, 755–765. (d) Giese, B. *Angew. Chem.* **1977**, *89*, 162–173; *Angew. Chem., Int. Ed. Engl.* **1977**, *16*, 125–136. (e) Pross, A. *Adv. Phys. Org. Chem.* **1977**, *14*, 69–132. (f) Young, P. R.; Jencks, W. P. *J. Am. Chem. Soc.* **1979**, *101*, 3288–3294. (g) Ta-Shma, R.; Rappoport, Z. *J. Am. Chem. Soc.* **1983**, *105*, 6082–6095. (h) Richard, J. P.; Jencks, W. P. *J. Am. Chem. Soc.* **1984**, *106,* 1373–1383. (i) Arnett, E. M.; Molter, K. E. *Acc. Chem. Res.* **1985**, *18*, 339–346. (j) Jencks, W. P. *Chem. Rev.* **1985**, *85*, 511–527. (k) Argile, A.; Carey, A. R. E.; Fukata, G.; Harcourt, M.; More O'Ferrall, R. A.; Murphy, M. G. *Isr. J. Chem.* **1985**, *26*, 303–312. (l) Buncel, E.; Wilson, H. *J. Chem. Educ.* **1987**, *64*, 475–480. (m) Formosinho, S. J. *J. Chem. Soc., Perkin Trans. 2* **1988**, 839–846. (n) Johnson, C. D.; Stratton, B. *J. Chem. Soc., Perkin Trans. 2* **1988**, 1903–1907. (o) Exner, O. *Correlation Analysis of Chemical Data*; Plenum Press: New York, SNTL, Prague, 1988. (p) Lee, I. *Chem. Soc. Rev.* **1990**, *19*, 317–333. (q) Exner, O. *J. Chem. Soc., Perkin Trans. 2* **1993**, 973–979.

(3) Ritchie, C. D. *Can. J. Chem.* **1986**, *64*, 2239–2250.

(4) (a) Richard, J. P.; Amyes, T. L.; Vontor, T. *J. Am. Chem. Soc.* **1992**, *114*, 5626–5636. (b) Richard, J. P. *Tetrahedron* **1995**, *51*, 1535–1573. (c) Richard, J. P.; Toteva, M. M.; Crugeiras, J. *J. Am. Chem. Soc.* **2000**, *122*, 1664–1674. (d) Okuyama, T.; Haga, N.; Takane, S.; Ueno, K.; Fueno, T. *Bull. Chem. Soc. Jpn.* **1991**, *64*, 2751–2756. (e) Heo, C. K. M.; Bunting, J. W. *J. Chem. Soc., Perkin. Trans. 2* **1994**, 2279–2290. (f) Vigroux, A.; Kresge, A. J.; Fishbein, J. C. *J. Am. Chem. Soc.* **1995**, *117*, 4433–4434. (g) Dalby, K. N.; Jencks, W. P. *J. Am. Chem.*

Soc. **1997,** *119,* 7271–7280. (h) de Lucas, N. C.; Netto-Ferreira, J. C.; Andraos, J.; Scaiano, J. C. *J. Org. Chem.* **2001,** *66,* 5016–5021.

(5) Mayr, H.; Patz, M. *Angew. Chem.* **1994**, *106*, 990–1010; *Angew. Chem., Int. Ed. Engl.* **1994**, *33*, 938–957.

(6) (a) Mayr, H.; Kuhn, O.; Gotta, M. F.; Patz, M. *J. Phys. Org. Chem.* **1998**, *11*, 642–654. (b) Mayr, H.; Patz, M.; Gotta, M. F.; Ofial, A. R. *Pure Appl. Chem.* **1998**, *70*, 1993–2000.

(7) (a) Mayr, H.; Kempf, B.; Ofial, A. R. *Acc. Chem. Res.* **2003**, *36*, 66–77. (b) Kempf, B.; Hampel, N.; Ofial, A. R.; Mayr, H. *Chem. Eur. J.* **2003**, *9*, 2209–2218.

(8) Mayr, H.; Bug, T.; Gotta, M. F.; Hering, N.; Irrgang, B.; Janker, B.; Kempf, B.; Loos, R.; Ofial, A. R.; Remennikov, G.; Schimmel, H. *J. Am. Chem. Soc.* **2001**, *123*, 9500–9512.

(9) (a) Lucius, R.; Mayr, H. *Angew. Chem.* **2000**, *112*, 2086–2089; *Angew. Chem., Int. Ed.* **2000**, *39*, 1995–1997. (b) Lucius, R.; Loos, R.; Mayr, H. *Angew. Chem.* **2002**, *114*, 97–102; *Angew. Chem., Int. Ed.* **2002**, *41*, 91–95.

(10) (a) Mayr, H.; Basso, N.; Hagen, G. *J. Am. Chem. Soc.* **1992**, *114*, 3060–3066. (b) Mayr, H.; Basso, N. *Angew. Chem.* **1992**, *104*, 1103-1105; *Angew. Chem. Int. Ed. Engl.* **1992**, *31*, 1046–1048.

(11) Funke, M.-A.; Mayr, H. *Chem. Eur. J.* **1997**, *3*, 1214–1222.

(12) Mayr, H.; Lang, G.; Ofial, A. R. *J. Am. Chem. Soc.* **2002**, *124*, 4076–4083.

(13) Schindele, C.; Houk, K. N.; Mayr, H. *J. Am. Chem. Soc.* **2002**, *124*, 11208–11214.

(14) (a) Ritchie, C. D.; Skinner, G. A.; Badding, V. G. *J. Am. Chem. Soc.* **1967**, *89*, 2063–2071. (b) Bunton, C. A.; Huang, S. K. *J. Am. Chem. Soc.* **1972**, *94*, 3536–3544.

(15) Ritchie, C. D.; Minasz, R. J.; Kamego. A. A.; Sawada, M. *J. Am. Chem. Soc.* **1977**, *99*, 3747–3753.

(16) Bunton, C. A.; Huang, S. K.; Paik, C. H. *Tetrahedron Lett.* **1976**, *18*, 1445–1448.

(17) Um, I.; Lee, G. J.; Yoon, H. W; Kwon, D. S. *Tetrahedron Lett.* **1992**, *33*, 2023–2026.

(18) McClelland, R. A.; Kanagasabapathy, V. M.; Banait, N. S.; Steenken, S. *J. Am. Chem. Soc.* **1989**, *111*, 3966–3972.

(19) (a) Evans, A.G.; Hamann, S. D. *Trans. Faraday Soc.* **1951**, *47,* 34–40. (b) Evans, M. G.; Uri, N. *Trans. Faraday. Soc.* **1949**, *45*, 224–230.

(20) (a) $[(\text{lil})_2\text{CH}^+]_0 = 1.5 \times 10^{-5}$ mol L^{-1}; $[\text{N}_3^-]_0 = (1–4) \times 10^{-3}$ mol L^{-1}. (b) $[(\text{jul})_2\text{CH}^+]_0 = 2.2 \times 10^{-5}$ mol L^{-1}; $[\text{N}_3^-]_0 = (0.4–1.4) \times 10^{-3}$ mol L^{-1}mol L^{-1}.

(21) (a) $[(\text{thq})_2\text{CH}^+]_0 = 1.2 \times 10^{-5}$ mol L^{-1}; $[\text{N}_3^-]_0 = (1–4) \times 10^{-3}$ mol L^{-1}. (b) $[(\text{dma})_2\text{CH}^+]_0 = 1.4 \times 10^{-5}$ mol L^{-1}; $[\text{N}_3^-]_0 = (0.4–1.4) \times 10^{-3}$ mol L^{-1}.

(22) (a) Ritchie, C. D.; Virtanen, P. O. I. *J. Am. Chem. Soc.* **1973**, *95*, 1882–1889. (b) Ritchie, C. D.; Wright, D. J.; Huang, D.-S.; Kamego, A. A. *J. Am. Chem. Soc.* **1975**, *97*, 1163–1170. (c) Hillier, K.; Scott, J. M. W.; Barnes, D. J.; Steele, F. J. P. *Can. J. Chem.* **1976**, *54*, 3312–3314. (d) Ritchie, C. D.; VanVerth, J. E.; Virtanen, P. O. I. *J. Am. Chem. Soc.* **1982**, *104*, 3491–3497.

(23) McDonough, L. M. *PhD Thesis*, University of Washington, Seattle WA, 1960.

(24) Lang, G. *Dissertation*, Ludwig-Maximilians-Universität München, 1998.

(25) Müller, K.-H. *Dissertation*, Technische Hochschule Darmstadt, 1997.

(26) Chojnowski, J.; Fortuniak, W.; Stańczyk, W. *J. Am. Chem. Soc.* **1987**, *109*, 7776–7781.

(27) Würthwein, E.-U.; Lang, G.; Schappele, L. H.; Mayr, H. *J. Am. Chem. Soc.* **2002**, *124*, 4084–4092.

(28) Fukuzumi, S.; Otera, J.; Ohkubo, K. *J. Org. Chem.* **2001**, *66,* 1450–1454.

(29) (a) Cozens, F. L.; Mathivanan, N.; McClelland, R. A.; Steenken, S. *J. Chem. Soc., Perkin. Trans. 2* **1992**, 2083–2090. (b) McClelland, R. A. *Tetrahedron* **1996**, *52*, 6823–6858. (c) Cozens, F. L.; Kanagasabapathy, V. M.; McClelland, R. A.; Steenken, S. *Can. J. Chem.* **1999**, *77*, 2069–2082. (d) Pezacki, J. P.; Shukla, D.; Lusztyk, J.; Warkentin, J. *J. Am. Chem. Soc.* **1999**, *121,* 6589–6598.

(30) Pearson, R. G. *Chemical Hardness*; Wiley-VCH: Weinheim, **1997**.

(31) Richard, J. P.; Amyes, T. L.; Toteva, M. M. *Acc. Chem. Res.* **2001**, *34*, 981–988.

3. Solvent nucleophilicity

3.1 Introduction

The development of quantitative scales of solvent nucleophilicity has intrigued chemists for several decades.[1,2] Such scales are important for the theory of nucleophilic substitutions and for designing syntheses where the solvent may compete with other nucleophiles for the electrophile under consideration.

In 1948, Grunwald and Winstein presented the relationship (3.1), which expresses the rates of S_N1 solvolyses of substrates RX by a substrate-specific parameter m ($m = 1$ for *tert*-butyl chloride) and a solvent-specific parameter, the solvent-ionizing power Y ($Y = 0$ for 80% aqueous ethanol).[3]

$$\log (k/k_0)_{25°\mathrm{C}} = mY \qquad (3.1)$$

where k and k_0 are the first-order rate constants for the solvolysis of RX in a given solvent and the standard solvent 80% aqueous ethanol (v/v), respectively, at 25°C. Equation (3.1) holds for S_N1 reactions with a rate-determining ionization step where nucleophilic solvent participation is absent.[4]

Three years later, Winstein, Grunwald, and Jones reported that S_N2 reactions proceed considerably faster in aqueous alcohols than in mixtures of acetic acid and formic acid of equal ionizing power Y and assigned these differences to the higher nucleophilicities of alcohols.[5] In the extended Grunwald-Winstein equation (3.2)[6] the electrophilic term mY of eq. (3.1) is accompanied by the nucleophilic term lN, where l is the sensitivity toward changes in solvent nucleophilicity N.

$$\log (k/k_0)_{\mathrm{RX}} = mY + lN \qquad (3.2)$$

While the solvent ionizing power Y can easily be determined by investigating substrates which solvolyze without nucleophilic solvent participation (limiting S_N1, $l = 0$), it is difficult to find reactions which are entirely controlled by the nucleophilic term, i.e., substitutions with $m = 0$.

Peterson and Waller[7] derived a scale of nucleophilicities of solvent molecules from the rates of reactions of solvent molecules with tetramethylenehalonium ions in liquid sulfur dioxide (Scheme 3.1).

Scheme 3.1

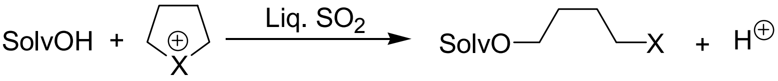

More widely employed is the N_{OTs} scale. Schadt, Bentley, and Schleyer defined the sensitivity of solvolysis rates of methyl tosylate on solvent nucleophilicity as $l = 1$.[8] With the assumption of equal nucleophilicities of acetic and formic acid, as derived from Peterson's and Waller's work, Bentley and Schleyer concluded that the sensitivity of methyl tosylate solvolyses on solvent ionizing power is $m = 0.3$. Substitution of this value into eq. (3.2) yields eq. (3.3) which has widely been used for the determination of solvent nucleophilicities.[8]

$$N_{\mathrm{OTs}} = \log (k/k_0)_{\mathrm{MeOTs}} - 0.3Y_{\mathrm{OTs}} \qquad (3.3)$$

k = rate constant for the solvolysis of methyl tosylate in the solvent under consideration,

k_0 = rate constant for the solvolysis of methyl tosylate in 80% aqueous ethanol (v/v).

While the choice of $m = 0.3$ for methyl tosylate solvolyses was still being debated and other factors, e.g. $m = 0.55$, had been proposed,[9] Kevill recognized that substrates with neutral leaving groups provide a superior tool for determining solvent nucleophilicity. In analogy to earlier studies by Swain,[10] the solvolysis rates of 1-adamantyldimethylsulfonium triflate were found to be affected by solvent variation by less than a factor of seven, while the solvolysis rates of 1-adamantyl tosylate varied by 7 powers of ten within the same group of solvents. Consequently, it was concluded that in solvolyses of oxonium and sulfonium ions, i.e., substrates with neutral leaving groups, the contribution of solvent ionizing power can be neglected, and Kevill employed the solvolysis rates of the *S*-methyldibenzothiophenium ion (S_N2 reactions) as the basis of the solvent nucleophilicity scale N_T (eq. 3.4).[11]

$$N_T = \log (k/k_0)_{\mathrm{MeDBTh}^+} \qquad (3.4)$$

k = rate constant for the solvolysis of the *S*-methyldibenzothiophenium ion (MeDBTh^+) in the solvent under consideration.

k_0 = rate constant for the solvolysis of the *S*-methyldibenzothiophenium ion (MeDBTh^+) in 80% aqueous ethanol (v/v).

Though the solvent nucleophilicity parameters N_{OTs} and N_{T} defined by eqs (3.3) and (3.4) show fairly good correlations with each other as well as with solvent nucleophilicities derived from solvolyses of other methylsulfonium or triethyloxonium ions,[2] they are relative parameters, which are not linked to other scales of nucleophilicity. The ongoing controversy on the role of nucleophilic solvent participation is highlighted by the title of a recent JACS article: "Is the *tert*-Butyl Chloride Solvolysis the Most Misunderstood Reaction in Organic Chemistry?".[12]

The development of fast kinetic methods provides a possibility for the direct measurement of solvent nucleophilicity. Thus, carbocations have been generated by laser flash induced heterolysis of suitable precursors, and the rate of decay of these carbocations in various solvents reflects solvent nucleophilicity, decoupled from solvent ionizing power.[13] Similar information has also been obtained with Jencks' and Richard's azide clock method which derives solvent nucleophilicity from the ability of solvents to compete with azide ions for solvolytically generated carbocations.[14]

Mayr and co-workers have recently suggested the employment of benzhydrylium ions as reference electrophiles (Table 1.1) for the quantitative comparison of nucleophiles of widely differing structures and reactivities.[15] As described in detail in refs 15 and 16, nucleophilicity parameters N and s, as defined by eq. 3.5, can be obtained by plotting log k(20°C) for the reactions of a certain nucleophile with a series of electrophiles of Table 1.1 versus the corresponding electrophilicity parameters, E.

$$\log k(20\ ^\circ\mathrm{C}) = s\,(N + E) \qquad (3.5)$$

We have now used this method for characterizing the nucleophilic reactivities of a series of common solvents and solvent mixtures, and we will compare the solvent nucleophilicities thus obtained with the nucleophilicities of other n-, π-, and σ-nucleophiles.

3.2 Method

For the sake of clarity, nucleophilicity parameters of solvents and solvent mixtures which refer to first-order rate constants (k_1) are designated as N_1. For solvent mixtures where only one component of the solvent is acting as the nucleophile, they may be converted into ordinary N values (referring to second-order rate constants) by subtraction of the logarithm of the molarity (log [Nuc]) of the nucleophilic component. For the solvent mixtures investigated in this work, [Nuc] = 2 – 55 mol L^{-1}, i.e., the N values referring to second-order rate constants are 0.3 to 1.7 units smaller than N_1.

Scheme 3.2

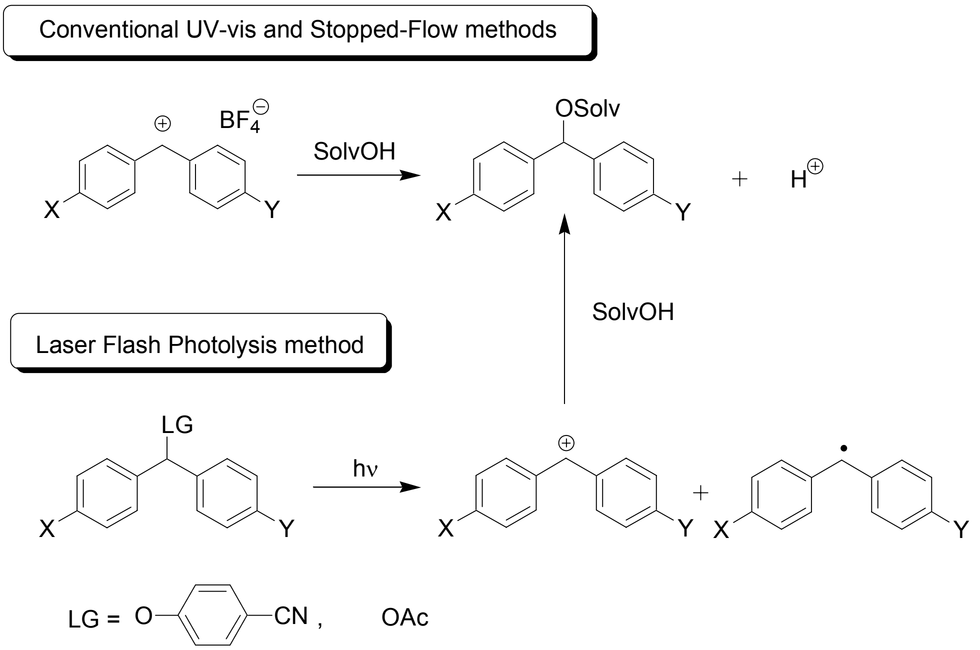

Most solvent nucleophilicity parameters N_1 and s presented in this work are based on the UV-Vis photometric detection of the decay of the benzhydrylium ion concentrations[15,19,20] with three independent kinetic methods (Scheme 3.2): Conventional UV-Vis spectrometry ($\tau_{1/2}$ > 10 s),[20-22] stopped flow (10 s > $\tau_{1/2}$ > 10^{-3} s),[15,20,23] and laser flash techniques (10^{-3} s > $\tau_{1/2}$ > 10^{-7} s).[13,17,18] The mutual agreement of the rate constants determined by using these three methods corroborates the reliability of the present data.

3.3 Results

When the benzhydrylium ions were exposed to the aqueous or alcoholic solvent mixtures specified in Tables 3.1-3.7, an exponential decay of the benzhydrylium absorbances was observed. Only the reactions of $(dpa)_2CH^+$ and of $(pfa)_2CH^+$ with trifluoroethanol/water = 20/80 or 10/90, and $(dpa)_2CH^+$ with water/acetonitrile = 91/9, 80/20, or 67/33 could not be described by a single exponential, and rate constants for these reactions are not given in Table 3.4.

Laser flash photolysis of the benzhydryl 4-cyanophenolates or acetates[24] results in heterolytic or homolytic cleavage of the Ar_2CH-O bond as shown in Scheme 3.2. Since the absorption maxima of the benzhydryl radicals are at considerably lower wavelengths than those of the benzhydryl cations,[19] the concomitant formation of both species does not affect the observation of the exponential decay of the benzhydryl cation absorbances during the reactions with the nucleophilic solvent.

As described for acetonitrile/water mixtures in Tables 3.1 and 3.2, and for many other solvents and solvent mixtures in Tables 3.3-3.7, the solvent nucleophilicities were examined with benzhydrylium ions of widely differing reactivity. Generally, rate constants covering a range of 7 to 10 powers of ten were employed for characterizing each of the solvent systems.

Rate constants for the reactions of acetonitrile/water mixtures with the weak electrophiles $(thq)_2CH^+$ (E = -8.22) and $(pyr)_2CH^+$ (E = -7.69) were obtained with a conventional UV-Vis spectrometer by injecting concentrated solutions of the corresponding benzhydrylium tetrafluoroborates in acetonitrile into the solvent mixtures under consideration. Table 3.1 shows that the rate constants for the first-order decay of $(thq)_2CH^+$ in 50W50AN mixtures are independent of the concentrations of DABCO/DABCO-H^+ buffer additives.

Table 3.1: Independence of the first-order decay of $(thq)_2CH^+$ in 50W50AN of the concentration of DABCO/H^+-DABCO BF_4^- (1/1) buffer additive.

$[(thq)_2CH^+]$, mol L^{-1}	[DABCO], [DABCO-H^+], mol L^{-1}	k_{obs}, s^{-1}
6.84×10^{-6}	9.44×10^{-4}	1.24×10^{-3}
8.57×10^{-6}	2.37×10^{-3}	1.22×10^{-3}
8.06×10^{-6}	3.33×10^{-3}	1.21×10^{-3}
7.84×10^{-6}	4.33×10^{-3}	1.22×10^{-3}
8.39×10^{-6}	5.79×10^{-3}	1.22×10^{-3}

Average $k = 1.22 \times 10^{-3}$ s^{-1}

Since an analogous behavior has been observed for the consumption of $(pyr)_2CH^+$ in acetonitrile/water and of $(ind)_2CH^+$ and $(thq)_2CH^+$ in ethanol/water mixtures (see Experimental section), it is concluded that the reaction of the benzhydrylium ion with the solvent molecule and not the successive proton transfer is rate-determining (Scheme 3.3). This conclusion is in accord with Ritchie's report that the reaction of crystal violet (E = -11.3)[20] with H_2O and D_2O does not show a kinetic isotope effect.[25]

Scheme 3.3

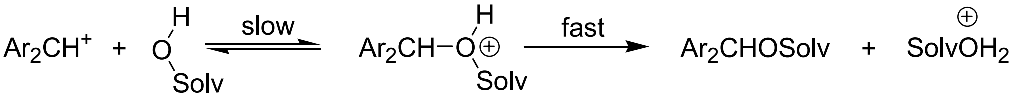

If more electrophilic benzhydrylium ions are employed, the rates of deprotonation of the oxonium ions in Scheme 3.3 can be assumed to remain almost unaffected while the reverse reactions, i.e., the regeneration of the benzhydrylium ions, must become slower. Consequently, we can conclude that all reactions monitored by stopped-flow and laser flash techniques in this work proceed via rate-determining attack of the solvent nucleophiles at the benzhydrylium ions.

The reactions of benzhydrylium ions of electrophilicity $-6 < E < -1$ with acetonitrile-water mixtures were determined with stopped-flow techniques by combining solutions of benzhydrylium tetrafluoroborates in acetonitrile with water or acetonitrile/water mixtures to yield the solvent mixtures listed in Table 3.2. Since the stopped-flow instrument used in this work does not allow us to employ mixing ratios > 10:1, we were unable to study solvent mixtures with water or alcohol contents > 91%.

Benzhydrylium ions of $E \geq 0$ have been generated by 20-ns laser pulses in the corresponding solvent mixtures, and their decay has been followed by UV-Vis spectroscopy. Some of these data were already available in the literature as indicated in Table 3.2.

Table 3.2: First-Order Rate Constants (s^{-1}) for the Reactions of Water-Acetonitrile Mixtures with Benzhydrylium Ions at 20 ºC.[a]

Cation	*E*	W	91W9AN	80W20AN	67W33AN	50W50AN	33W67AN	20W80AN	10W90AN
Ph_2CH^+	5.90					1.33×10^{9} [b]			
$(tol)_2CH^+$	3.63			3.2×10^{7} [c]	3.2×10^{7} [c]	3.28×10^{7}	3.47×10^{7}	3.06×10^{7}	2.37×10^{7}
$(ani)PhCH^+$	2.11	1.9×10^{6} [d]		2.0×10^{6} [c]	2.1×10^{6} [c]	1.84×10^{6}	1.91×10^{6}	1.87×10^{6}	1.83×10^{6}
$(ani)(tol)CH^+$	1.48	7.8×10^{5} [d]	7.99×10^{5}	8.2×10^{5} [c]	9.1×10^{5} [c]	8.55×10^{5}	8.95×10^{5}	8.29×10^{5}	6.81×10^{5}
$(ani)_2CH^+$	0.00	9.44×10^{4}	9.55×10^{4}	1.0×10^{5} [c]	1.3×10^{5} [c]	1.04×10^{5}	1.01×10^{5}	9.82×10^{4}	9.87×10^{4}
$(fur)_2CH^+$	-1.36								7.11×10^{2}
$(pfa)_2CH^+$	-3.14		9.36×10^{1}	4.93×10^{1}	4.96×10^{1}	3.62×10^{1}	3.39×10^{1}	3.32×10^{1}	1.42×10^{1}
$(mfa)_2CH^+$	-3.85		4.39	3.98	4.47	3.78 [e]	3.58	3.62	1.57
$(dpa)_2CH^+$	-4.72					4.44	4.12	3.97	1.56
$(mor)_2CH^+$	-5.53		6.73×10^{-1}	4.93×10^{-1}	4.13×10^{-1}	3.31×10^{-1} [e]	2.85×10^{-1}	2.51×10^{-1}	8.03×10^{-2}
$(mpa)_2CH^+$	-5.89		3.31×10^{-1}	2.84×10^{-1}	2.83×10^{-1}	2.52×10^{-1}	2.24×10^{-1}	2.17×10^{-1}	8.08×10^{-2}
$(dma)_2CH^+$	-7.02	2.06×10^{-2}							
$(pyr)_2CH^+$	-7.69	5.57×10^{-3} [e]	4.29×10^{-3}	3.77×10^{-3}	4.05×10^{-3}	4.33×10^{-3}			
$(thq)_2CH^+$	-8.22	2.20×10^{-3} [e]	1.66×10^{-3}	1.23×10^{-3}	1.17×10^{-3}	1.22×10^{-3}	1.28×10^{-3}		

[a] Compositions of solvents are given as (v/v); W = water, AN = acetonitrile. [b] Ref. 13d, because of the proximity of the diffusion limit, this value was not used for the correlation. [c] Ref. 13c. [d] From ref. 17 at 25 ºC. [e] Ref. 20.

Table 3.3: First-order rate constants (s^{-1}) of the reactions of water-ethanol mixtures with benzhydrylium ions at 20 ºC.[a]

Cation	*E*	90E10W	80E20W	60E40W	50E50W	40E60W	20E80W	10E90W
$(ani)PhCH^+$	2.11	*7.04×10^{6}* [b]	1.22×10^{7}	1.06×10^{7}	7.91×10^{6}	6.62×10^{6}		
$(ani)(tol)CH^+$	1.48	9.47×10^{6}	7.88×10^{6}	6.55×10^{6}	3.86×10^{6}	3.38×10^{6}	2.72×10^{6}	9.54×10^{5}
$(ani)_2CH^+$	0.00	2.53×10^{6}	1.51×10^{6}	7.13×10^{5}	4.96×10^{5}	3.68×10^{5}	2.20×10^{5}	1.38×10^{5}
$(dma)_2CH^+$	-7.02	8.33×10^{-1}	4.05×10^{-1}	1.70×10^{-1}	7.43×10^{-2}	5.71×10^{-2}		
$(pyr)_2CH^+$	-7.69	3.02×10^{-1}	1.40×10^{-1}	5.28×10^{-2}				
$(thq)_2CH^+$	-8.22						2.91×10^{-3}	2.43×10^{-3}
$(ind)_2CH^+$	-8.76	2.78×10^{-2}	1.45×10^{-2}	5.84×10^{-3}	3.84×10^{-3}	2.61×10^{-3}		
$(lil)_2CH^+$	-10.04	3.03×10^{-3}	1.65×10^{-3}	7.16×10^{-4}				

[a] Compositions of solvents are given as (v/v); E = ethanol, W = water. [b] Not included in the correlation.

Table 3.4: First-order rate constants (s^{-1}) of the reactions of water-trifluoroethanol mixtures with benzhydrylium ions at 20 ºC.[a]

Cation	*E*	TFE	90T10W	80T20W	60T40W	50T50W	40T60W	20T80W	10T90W
Ph_2CH^+	5.90	3.2×10^{6} [b]				*2.8×10^{8}* [c]			
$(tol)PhCH^+$	4.59	2.7×10^{5} [b]	2.45×10^{6}	4.19×10^{6}	6.95×10^{6}	8.20×10^{6}	1.07×10^{7}	1.92×10^{7}	
$(tol)_2CH^+$	3.63	2.4×10^{4} [b]	4.32×10^{5}	9.11×10^{5}	1.24×10^{6}	1.39×10^{6}	1.41×10^{6}	5.57×10^{6}	
$(ani)PhCH^+$	2.11	1.2×10^{3} [b]	4.01×10^{4}	3.45×10^{4}	1.27×10^{5}	1.66×10^{5}	2.26×10^{5}	1.20×10^{6}	2.59×10^{6}
$(ani)(tol)CH^+$	1.48	2.8×10^{2} [b]	1.28×10^{4}	2.35×10^{4}	5.46×10^{4}	7.15×10^{4}	1.02×10^{5}	3.25×10^{5}	5.78×10^{5}
$(ani)_2CH^+$	0.00	1.4×10^{1} [b]	6.50×10^{2}	2.55×10^{3}	6.04×10^{3}	7.03×10^{3}	9.95×10^{3}	4.05×10^{4}	7.95×10^{4}
$(pfa)_2CH^+$	-3.14		3.01×10^{-1}	5.55×10^{-1}	9.37×10^{-1}	1.34	1.79		
$(mfa)_2CH^+$	-3.85		1.23×10^{-1}	1.53×10^{-1}	1.90×10^{-1}	2.57×10^{-1}	3.27×10^{-1}	1.48	3.80
$(dpa)_2CH^+$	-4.72		3.76×10^{-2}	6.59×10^{-2}	7.96×10^{-2}	1.12×10^{-1}	1.20×10^{-1}		
$(mor)_2CH^+$	-5.53						4.79×10^{-2}	2.69×10^{-1}	7.09×10^{-1}

[a] Compositions of solvents are given as (v/v); W = water, T = trifluoroethanol. [b] Ref. 13b. [c] Ref. 14g, not included in the correlation.

Table 3.5: First-order rate constants (s^{-1}) of the reactions of ethanol-acetonitrile mixtures with benzhydrylium ions at 20 ºC.[a]

Cation	*E*	EtOH	91E9AN	80E20AN	67E33AN	50E50AN	33E67AN	20E80AN	10E90AN
(ani)PhCH$^+$	2.11	9.56×10^{6} [b]	9.04×10^{6} [b]	8.98×10^{6} [b]	1.07×10^{7} [b]	1.10×10^{7} [b]	1.18×10^{7}	9.41×10^{6}	4.80×10^{6}
(ani)(tol)CH$^+$	1.48	8.68×10^{6} [b]	1.05×10^{7} [b]	1.08×10^{7} [b]	1.23×10^{7}	1.21×10^{7}	8.48×10^{6}	5.99×10^{6}	2.44×10^{6}
(ani)$_2$CH$^+$	0.00	5.5×10^{6} [c]	4.33×10^{6}	3.02×10^{6}	2.30×10^{6}	1.41×10^{6}	8.77×10^{5}	5.33×10^{5}	3.06×10^{5}
(pfa)$_2$CH$^+$	-3.14					4.05×10^{2}	3.11×10^{2}	1.72×10^{2}	5.86×10^{1}
(mfa)$_2$CH$^+$	-3.85		2.55×10^{2}	2.07×10^{2}	1.53×10^{2}	5.23×10^{1}	4.05×10^{1}	2.24×10^{1}	7.07
(dpa)$_2$CH$^+$	-4.72		2.60×10^{2}	2.22×10^{2}	1.65×10^{2}	5.39×10^{1}	4.03×10^{1}	2.18×10^{1}	7.28
(mor)$_2$CH$^+$	-5.53		1.38×10^{1}	1.07×10^{1}	7.60		1.68	9.05×10^{-1}	2.96×10^{-1}
(mpa)$_2$CH$^+$	-5.89		1.45×10^{1}	1.14×10^{1}	7.92	2.49	1.63	9.54×10^{-1}	2.87×10^{-1}
(dma)$_2$CH$^+$	-7.02		9.24×10^{-1}	6.78×10^{-1}	4.51×10^{-1}	2.46×10^{-1}	1.40×10^{-1}		
(pyr)$_2$CH$^+$	-7.69		2.72×10^{-1}	2.27×10^{-1}	1.39×10^{-1}	7.04×10^{-2}	3.67×10^{-2}	1.78×10^{-2}	
(thq)$_2$CH$^+$	-8.22	1.63×10^{-1}				2.32×10^{-2}			
(ind)$_2$CH$^+$	-8.76	5.75×10^{-2}	3.82×10^{-2}	2.40×10^{-2}	1.46×10^{-2}	7.95×10^{-3}	3.97×10^{-3}	2.32×10^{-3}	
(jul)$_2$CH$^+$	-9.45	1.52×10^{-2}							
(lil)$_2$CH$^+$	-10.04	5.70×10^{-3}	3.52×10^{-3}	2.12×10^{-3}	1.26×10^{-3}	6.65×10^{-4}			

[a] Compositions of solvents are given as (v/v); E = ethanol, AN = acetonitrile. [b] Not included in the correlation. [c] Ref. 13h.

Table 3.6: First-order rate constants (s^{-1}) of the reactions of methanol-acetonitrile mixtures with benzhydrylium ions at 20 ºC.[a]

Cation	*E*	MeOH	91M9AN	80M20AN	67M33AN	50M50AN	33M67AN	20M80AN	10M90AN
(ani)PhCH$^+$	2.11	*1.15×10^{7}* [b]	*9.88×10^{6}* [b]	*8.55×10^{6}* [b]	*8.87×10^{6}* [b]	*9.16×10^{6}* [b]	*1.00×10^{7}* [b]	*1.07×10^{7}* [b]	*7.47×10^{6}* [b]
(ani)(tol)CH$^+$	1.48	*1.33×10^{7}* [b]	*1.39×10^{7}* [b]	*1.20×10^{7}* [b]	*1.24×10^{7}* [b]	1.47×10^{7}	1.33×10^{7}	9.91×10^{6}	6.22×10^{6}
(ani)$_2$CH$^+$	0.00	8.6×10^{6} [c]	4.95×10^{6}	4.12×10^{6}	3.48×10^{6}	2.33×10^{6}	1.54×10^{6}	8.58×10^{5}	4.20×10^{5}
(pfa)$_2$CH$^+$	-3.14						4.85×10^{2}	3.58×10^{2}	1.60×10^{2}
(mfa)$_2$CH$^+$	-3.85		4.02×10^{2}	3.11×10^{2}	2.42×10^{2}	1.22×10^{2}	8.46×10^{1}	4.81×10^{1}	1.64×10^{1}
(dpa)$_2$CH$^+$	-4.72		3.60×10^{2}	2.89×10^{2}	2.23×10^{2}	9.52×10^{1}	8.87×10^{1}	5.43×10^{1}	1.78×10^{1}
(mor)$_2$CH$^+$	-5.53		2.65×10^{1}	1.82×10^{1}	1.28×10^{1}		3.51	1.96	6.83×10^{-1}
(mpa)$_2$CH$^+$	-5.89		2.79×10^{1}	1.85×10^{1}	1.32×10^{1}	4.81	3.85	2.15	7.21×10^{-1}
(dma)$_2$CH$^+$	-7.02		2.31	1.30	8.82×10^{-1}	4.36×10^{-1}	2.62×10^{-1}	1.22×10^{-1}	3.93×10^{-2}
(pyr)$_2$CH$^+$	-7.69		9.32×10^{-1}	4.64×10^{-1}	3.27×10^{-1}				7.07×10^{-3}
(thq)$_2$CH$^+$	-8.22		2.17×10^{-1}					6.55×10^{-3}	
(ind)$_2$CH$^+$	-8.76	6.00×10^{-2}				1.34×10^{-2}	5.80×10^{-3}	3.09×10^{-3}	7.72×10^{-4}
(jul)$_2$CH$^+$	-9.45								
(lil)$_2$CH$^+$	-10.04	6.23×10^{-3}	6.14×10^{-3}	3.49×10^{-3}	1.99×10^{-3}	1.17×10^{-3}	5.96×10^{-4}		

[a] Compositions of solvents are given as (v/v); M = methanol, AN = acetonitrile. [b] Not included in the correlation. [c] Ref. 13b.

Table 3.7: First-order rate constants (s^{-1}) of the reactions of water-acetone mixtures with benzhydrylium ions at 20 ºC.[a]

Cation	*E*	20W80A	10W90A
$(pfa)_2CH^+$	–3.14	1.90×10^{2}	1.37×10^{2}
$(mfa)_2CH^+$	–3.85	1.90×10^{1}	1.78×10^{1}
$(dpa)_2CH^+$	–4.72	3.07×10^{1}	2.47×10^{1}
$(mor)_2CH^+$	–5.53	9.34×10^{-1}	7.75×10^{-1}
$(mpa)_2CH^+$	–5.89	1.20	9.40×10^{-1}
$(ind)_2CH^+$	–8.76	2.08×10^{-3}	1.84×10^{-3}
$(lil)_2CH^+$	–10.04	1.89×10^{-4}	2.21×10^{-4}

[a] Mixtures of solvents are given as (v/v), solvents: W = water, A = acetone.

Figure 3.1 shows that plots of rate constants (log k_1) determined by the three different methods versus the empirical electrophilicity parameters *E* give linear correlations. This proves the consistency of the data obtained by the independent methods as well as the applicability of eq. 3.5 for describing the reactions of carbocations with these solvents. The fact that some of the data depicted in Figure 3.1 as well as in 35 analogous correlations have been taken from the literature is an additional confirmation for the reliability of our data, and vice versa.

Slopes and intercepts of the correlations in Figure 3.1 and the analogous correlations yield the nucleophilicity parameters N_1 and *s* given in Table 3.8. In some cases, carbocations of different electrophilicity were found to react with equal rates, corresponding to $k = 10^7$ s^{-1}. Since this value appeared to be the limit of the instrumentation employed, these rate constants were not used for the calculation of the correlation equations.

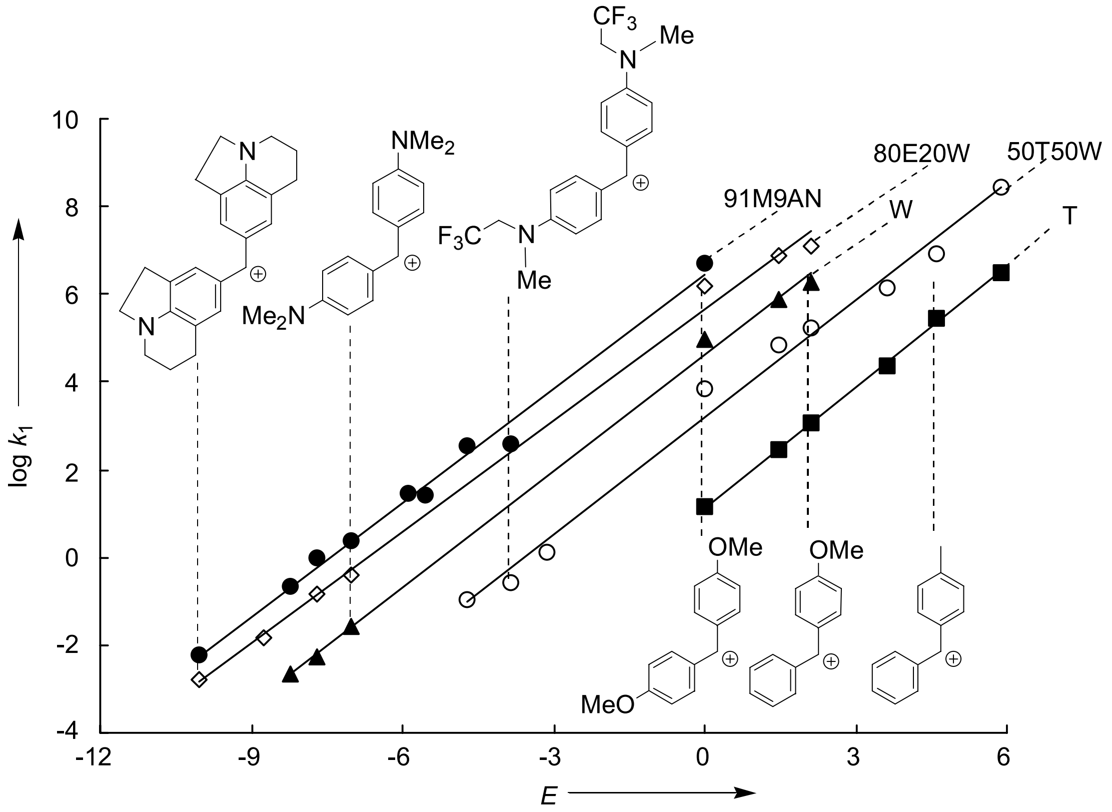

Figure 3.1: Plots of log k_1 for the decay of benzhydrylium ions in several solvents versus the electrophilicity parameters E of the benzhydrylium ions (20 °C). Mixtures of solvents are given as (v/v), solvents: M = methanol, E = ethanol, W = water, T = trifluoroethanol, AN = acetonitrile.

The nucleophilicity parameter for methanol listed in Table 3.8 can be compared with those derived from Ritchie's rate constants for the reactions of methanol with tritylium ions and tropylium ions, $N_1 = 6.02$ and $s = 1.01$.[20] These values, which have explicitly been labeled as "Approximate Parameters" in Table 2.8 can now be revised. It should be noted, however, that our previous guess[20] was able to reproduce the rate constants for the reactions of benzhydrylium ions with methanol reported here, with an accuracy of a factor of 50. The rate constants given in Table 3.2-3.7 can be reproduced by the reactivity parameters in Table 3.8 with a standard deviation of a factor of 1.82.

Table 3.8: Nucleophilicity (N_1) and slope (s) parameters for solvents.

Solvent [a]	N_1	s	Solvent [a]	N_1	s	Solvent [a]	N_1	s
W	5.20	0.89	20T80W	4.78	0.83	50E50AN	6.37	0.90
91W9AN	5.16	0.91	10T90W	5.04	0.90	33E67AN	6.06	0.90
80W20AN	5.04	0.89	E	7.44	0.90	20E80AN	5.77	0.92
67W33AN	5.05	0.90	90E10W	7.03	0.86	10E90AN	5.19	0.96
50W50AN	5.05	0.89	80E20W	6.68	0.85	M	7.54	0.92
33W67AN	5.02	0.90	60E40W	6.28	0.87	91M9AN	7.45	0.87
20W80AN	5.02	0.89	50E50W	5.96	0.89	80M20AN	7.20	0.89
10W90AN	4.56	0.94	40E60W	5.81	0.90	67M33AN	7.01	0.91
T	1.23	0.92	20E80W	5.54	0.94	50M50AN	6.67	0.90
90T10W	2.93	0.88	10E90W	5.38	0.91	33M67AN	6.38	0.92
80T20W	3.20	0.88	10E90W	5.38	0.91	20M80AN	6.04	0.94
60T40W	3.42	0.90	91E9AN	7.10	0.90	10M90AN	5.55	0.97
50T50W	3.57	0.89	80E20AN	6.94	0.90	20W80A	5.77	0.87
40T60W	3.77	0.88	67E33AN	6.74	0.89	10W90A	5.70	0.85

[a] Mixtures of solvents are given as (v/v), solvents: M = methanol, E = ethanol, W = water, T = trifluoroethanol, A = acetone, AN = acetonitrile.

3.4 Discussion

The close similarity of all s parameters in Table 3.8 implies that the relative nucleophilicities of these solvents and solvent mixtures are fairly independent of the carbocation electrophilicities. As a consequence, the data set reported in this work might also be described by constant selectivity relationships of the Ritchie type.[26] However, because the s parameters in Table 3.8 are considerably larger than those of most other nucleophiles investigated by Ritchie ($s \approx 0.6$ for amines, alkoxides, etc.),[20] it is not possible to treat the whole set of nucleophilicity parameters by Ritchie's equation.[26] We, therefore, base the following discussion on the nucleophilicity parameters N_1 and s as derived from eq. 3.5.

In agreement with a previous report by McClelland,[13c] the nucleophilicities of acetonitrile/water mixtures remain almost constant when the extent of water exceeds 20% (v/v, Figure 3.2).

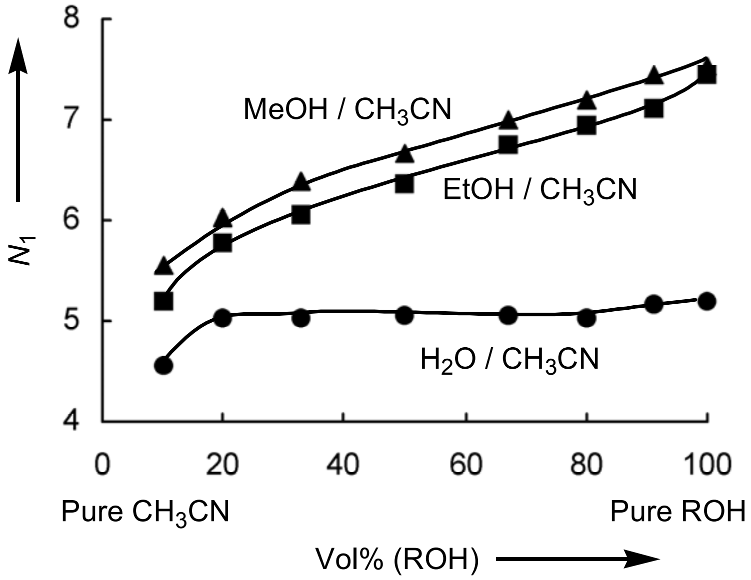

Figure 3.2: Dependence of the nucleophilicity N_1 on the composition of mixtures of acetonitrile with water, methanol, or ethanol.

In contrast, the nucleophilicities of methanol/acetonitrile and of ethanol/acetonitrile mixtures increase steadily with the amount of alcohol. While pure methanol and pure ethanol possess approximately the same nucleophilicity, methanol/acetonitrile mixtures are more nucleophilic (by ca. 0.3 logarithmic units) than the corresponding ethanol/acetonitrile mixtures. Figure 3.2 shows a remarkable increase of nucleophilicity from 90% ethanol/10% acetonitrile to pure ethanol, consistent with the almost equal reactivities of pure methanol and pure ethanol. Since variation of solvent composition over such wide ranges causes significant medium effects, we will not discuss the formal second-order rate constants.

Figure 3.3 shows that the nucleophilicity of ethanol/water mixtures grows with increasing content of alcohol while the nucleophilicity of trifluoroethanol/water mixtures decreases with increasing content of alcohol. The steep decrease from 90% trifluoroethanol to pure trifluoroethanol is particularly obvious.

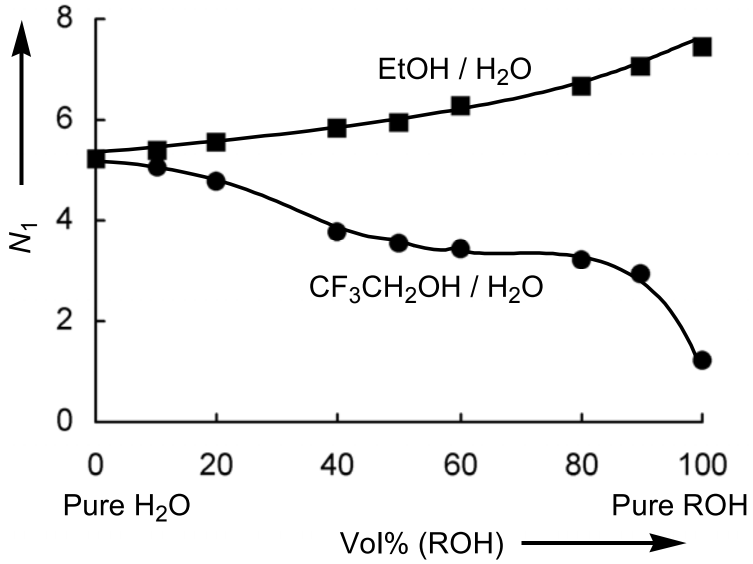

Figure 3.3: Dependence of the nucleophilicity N_1 on the composition of water-alcohol mixtures

Product ratios obtained from solvolytically generated carbocations in alcohol/water mixtures (Scheme 3.4) have been the topic of extensive investigations,[27] and have been reviewed by Ta-Shma and Rappoport[27r].

Scheme 3.4: Selectivities of carbocations in alcohol/water mixtures

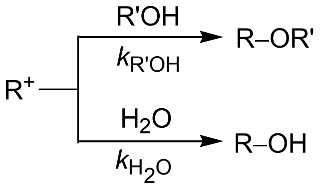

It has been found that the ratio $k_{R'OH}/k_{H_2O}$ derived from product analysis depends on solvent polarity and generally decreases slightly from 50% aqueous alcohols to pure alcohols.[27r] Combination of the absolute rate constants for the decay of Laser-flash solvolytically generated benzhydrylium ions $(ani)_2CH^+$ with the product ratios yields the individual rate constants $k_{R'OH}$ and k_{H_2O} as defined in Scheme 3.4. For ethanol/water mixtures it has been shown, for example, that both individual rate constants, k_{EtOH} and k_{H_2O}, grow by a factor of approximately 10^2 when 5% ethanol/95% water was gradually replaced by 95% ethanol/5% water.[27r] The rate constants do not increase uniformly, however: While the ratio k_{EtOH}/k_{H_2O} was close to 1 in 95% ethanol as well as in 95% water, k_{EtOH}/k_{H_2O} reached a broad maximum of 4.6 in 15-50% aqueous ethanol. Because of the reported dependence of the selectivities $k_{R'OH}/k_{H_2O}$ on the medium,[27r] we have not calculated individual rate constants in this work.

How do the solvent nucleophilicities N_1 derived from the reactions with benzhydrylium ions (Table 3.8) compare with the solvent nucleophilicities[2] previously derived from S_N2 reactions of methyl sulfonium ions and methyl tosylate? The good correlation shown in Figure 3.4 demonstrates that nucleophilicities towards carbocations and towards methyl sulfonium ions (S_N2 reactions)[2] are closely related, which justifies Kevill's choice of methyl sulfonium ions as substrates for determining nucleophilic solvent participation in S_N1 reactions. Correlation equation (3.6) indicates that nucleophile variation has a considerably stronger influence on the reactivities towards carbocations than towards methyl sulfonium ions.

$$N_1 = 1.51 N_T + 6.79,\ n = 17,\ R^2 = 0.948 \qquad (3.6)$$

An analogous conclusion has previously been drawn by Bunting, who found a linear correlation between the aminolysis rates of methyl 4-nitrobenzenesulfonate (S_N2 reaction) and the corresponding rates of amine additions to the 1-methyl-4-vinylpyridinium ion with a slope of 2.27 (= 1/0.44).[28] Bunting's and Richard's reports of a linear correlation between Ritchie's N_+-parameters (nucleophilicities towards carbocations)[26] and Swain's and Scott's n-parameters (nucleophilicities towards CH_3Br)[29] with a slope of 2 also indicate that variations of nucleophiles affect reactivities towards electrophilic C_{sp^2} centers to a larger extent than towards electrophilic C_{sp^3} centers.[28,30] In accordance with these findings, l-values (according to eq. (3.2)) greater than 1 have been found for solvolyses of chloroformate when nucleophilic addition to the carbonyl group was rate-determining.[31,32]

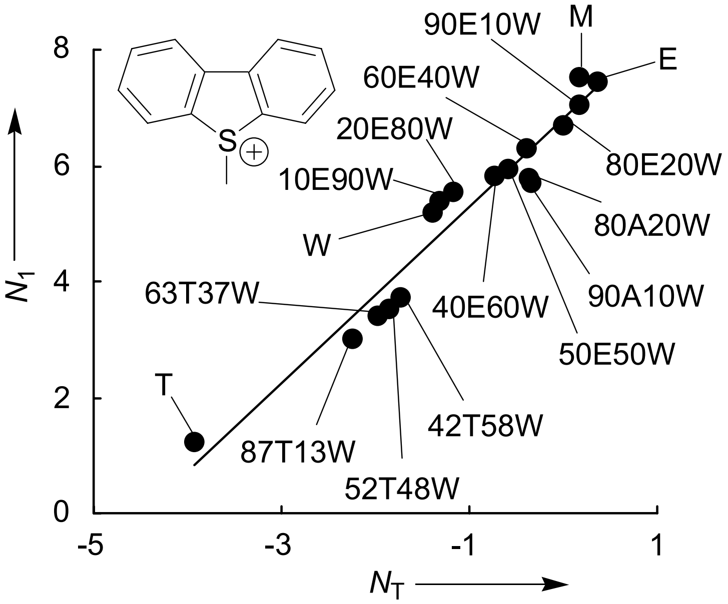

Figure 3.4: Relationship between nucleophilicity parameters N_1 and N_T from reactions with benzhydrylium ions and the *S*-methyldibenzothiophenium ion, respectively. Mixtures of solvents are given as (v/v), solvents: M = methanol, E = ethanol, W = water, T = trifluoroethanol, A = acetone. Details are shown in Table 3.9.

Since linear correlations between N_T, N'_T, N_{OTs}, and N'_{OTs} have previously been reported,[2] it is not surprising that the nucleophilicity parameters N_1 derived from reactions with benzhydrylium ions in this work also correlate with N'_T, N_{OTs}, and N'_{OTs} [33] (Figures 3.5–3.7).

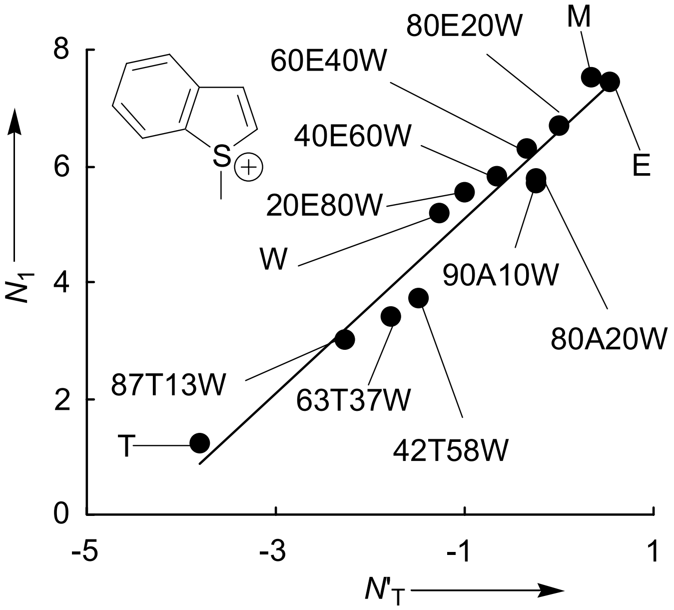

Figure 3.5: Relationship between nucleophilicity parameters N_1 and N'_T from *S*-methylbenzothiophenium ion. Mixtures of solvents are given as (v/v), solvents: M = methanol, E = ethanol, W = water, T = trifluoroethanol, A = acetone. Details are shown in Table 3.9.

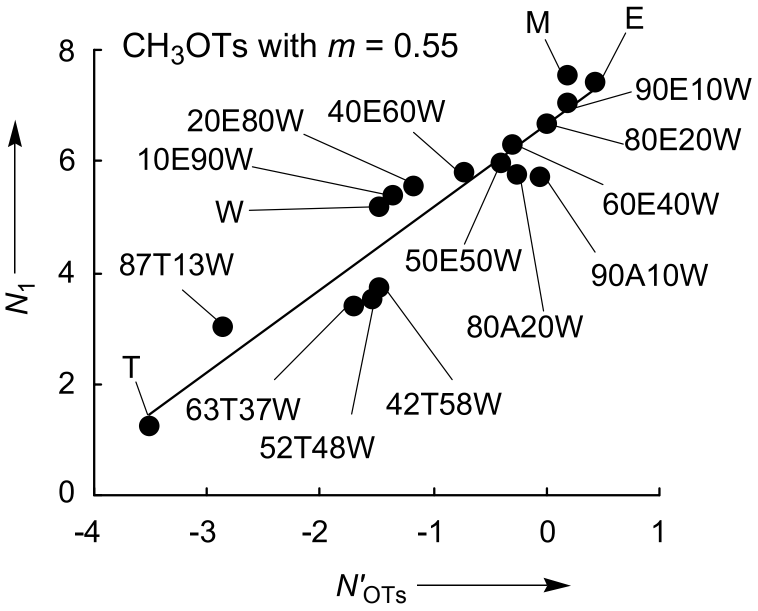

Figure 3.6: Relationship between nucleophilicity parameters N_1 and N'_{OTs} from methyl tosylate. Mixtures of solvents are given as (v/v), solvents: M = methanol, E = ethanol, W = water, T = trifluoroethanol, A = acetone. Details are shown in Table 3.9.

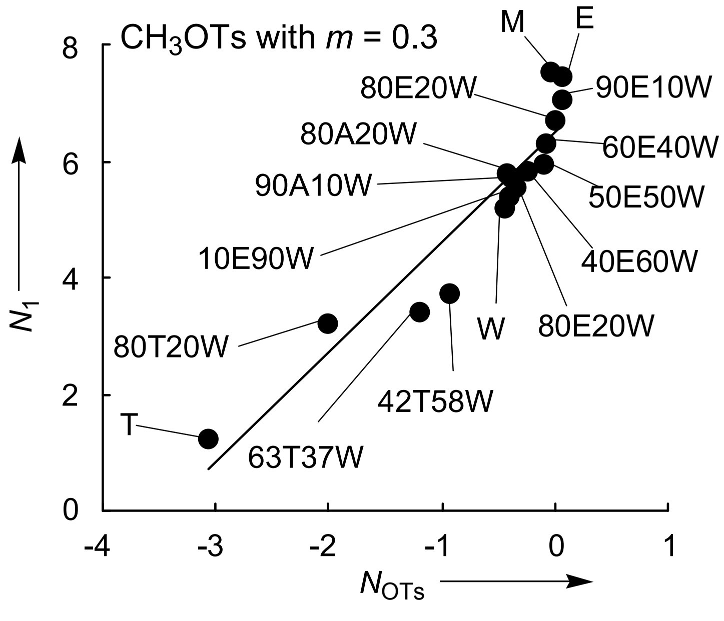

Figure 3.7: Relationship between nucleophilicity parameters N_1 and N_{OTs} from methyl tosylate. Mixtures of solvents are given as (v/v), solvents: M = methanol, E = ethanol, W = water, T = trifluoroethanol, A = acetone. Details are shown in Table 3.9.

Table 3.9: The relationship of N_T, N'_T, N'_{OTs}, and N_{OTs} with nucleophilicity parameters N_1 of solvents derived from the reactions with benzhydrylium ions.

Solvents [a]	N_1	N_T [b]	N'_T [c]	N'_{OTs} [d]	N_{OTs} [e]
M	7.54	0.17	0.33	0.19	-0.04
E	7.44	0.37	0.54	0.43	0.06
90E10W	7.03	0.16		0.19	0.07
80E20W	6.68	0.00	0.00	0.00	0.00
60E40W	6.28	-0.39	-0.35	-0.31	-0.08
50E50W	5.96	-0.58		-0.41	-0.09
40E60W	5.81	-0.74	-0.65	-0.72	-0.23
20E80W	5.54	-1.16	-1.01	-1.17	-0.34
10E90W	5.38	-1.31		-1.36	-0.41
W	5.20	-1.38	-1.26	-1.47	-0.44
80A20W	5.77	-0.37	-0.25	-0.27	-0.42
90A10W	5.70	-0.35	-0.25	-0.05	-0.39
42T58W (50T50W w/w)	3.73 [f]	-1.73	-1.49	-1.47	-0.93
52T48W (60T40W w/w)	3.54 [f]	-1.85		-1.54	
63T37W (70T30W w/w)	3.39 [f]	-1.98	-1.77	-1.70	-1.20
80T20W (85T15W w/w)	3.20				-2.01
87T13W (90T10W w/w)	3.01 [f]	-2.25	-2.28	-2.87	
T	1.23	-3.93	-3.80	-3.51	-3.07

[a] Mixtures of solvents are given as (v/v), solvents: W = water, E = ethanol, M = methanol, T = trifluoroethanol, A = acetone [b] Based on *S*-methyldibenzothiophenium ion [c] Based on *S*-methylbenzothiophenium ion [d] Based on methyltosylate with m = 0.55, [e] Based on methyltosylate with m = 0.3. [f] Interpolated value.

Because of the good correlation between N_1 and N_T shown in Figure 3.4, we suggest the employment of eq. 3.6 for estimating N_1 of further solvent mixtures from reported N_T values (Table 3.10). Though the data obtained in this way have to be considered as approximate, they are most useful for designing syntheses in these solvents.

Table 3.10: Approximate Solvent Nucleophilicity Parameters (N_1) for Solvent Mixtures Calculated by Equation 3.5.

Solvent [a]	N_T [b]	N_1 [c]	Solvent [a]	N_T [b]	N_1 [c]	Solvent [a]	N_T [b]	N_1 [c]
70E30W	-0.20	6.48 [d]	80D20W	-0.46	6.10	50T50E	-0.64	5.82
30E70W	-0.93	5.68 [d]	70D30W	-0.37	6.23	40T60E	-0.34	6.28
95A5W	-0.49	6.05	60D40W	-0.54	5.97	20T80E	0.08	6.91
70A30W	-0.42	6.16	50D50W	-0.66	5.79	97H3W [e]	-5.26	-1.15
60A40W	-0.52	6.00	40D60W	-0.84	5.52	90H10W [e]	-3.84	0.99
50A50W	-0.70	5.73	20D80W	-1.12	5.10	70H30W [e]	-2.94	2.35
40A60W	-0.83	5.54	97T3W [e]	-3.30	1.81	50H50W [e]	-2.49	3.03
30A70W	-0.96	5.34	80T20W [e]	-2.19	3.48	HCO_2H	-2.44	3.11
20A80W	-1.11	5.11	80T20E	-1.76	4.13	CH_3CO_2H	-1.78	4.10
10A90W	-1.23	4.93	60T40E	-0.94	5.37			

[a] Unless otherwise stated mixtures of solvents are given as (v/v), solvents: M = methanol, E = ethanol, W = water, T = trifluoroethanol, A = acetone, D = dioxane, H = hexafluoro-2-propanol. [b] From ref. 2. [c] A slope parameter of $s = 0.9$ is recommended for these solvents (compare s parameters in Table 3.8). [d] Not by using eq 3.6, but by interpolating data for aqueous ethanol from Table 3.8. [e] Mixtures of solvents are given as (w/w).

The linear correlation shown in Figure 3.4 implies that the solvent nucleophilicities N_1 toward carbocations reported in this work are controlled by the same factors as the solvent nucleophilicity N_T towards methylsulfonium ions. A major advantage of the new parameters N_1 is that they can be combined with the electrophilicity parameters E of carbocations, using eq. (3.5), so as to estimate absolute lifetimes of carbocations which are produced solvolytically in aqueous or alcoholic solutions (see Appendix).

Because $s \approx 0.9$ for all solvents investigated (Table 3.8), eq. (3.5) predicts that carbocations have a half-life $\tau_{1/2} > 10^{-10}$ s^{-1} if $E + N_1 > 11$. As 10^{-10} s^{-1} is the time needed for solvent reorganization, one can conclude that in 80% aqueous ethanol ($N_1 = 6.68$), carbocations with $E < 4.5$ will be thermally equilibrated, while in trifluoroethanol ($N_1 = 1.23$) thermal equilibration will already be reached for carbocations of $E < 10$. Typical E values for carbocations are ca. 8.5 (for $(CH_3)_3C^+$),[34] 5.9 (for Ph_2CH^+),[15] and 0.5 (Ph_3C^+).[20] It should be noted, however, that eq. (3.5) has been reported to be limited to second-order rate constants

$< 10^8$ L mol^{-1} s^{-1}.[15,35] For faster reactions, the magnitude of the rate constants will be overestimated because of the flattening of the correlation curves.[34] As a consequence one may expect thermal equilibration of the intermediate carbocations also if the sum (E + N_1) is slightly less than 11.

The flattening of the log k versus E correlations for $k > 10^8$ L mol^{-1} s^{-1} also prevents the calculation of the exact point, where the enforced change from S_N1 to S_N2 mechanisms is taking place. According to Jencks, this point is related to the lifetimes of intermediates, which cannot be shorter than the duration of a bond vibration (ca. 10^{-13} s).[36] Having in mind the flattening of the correlation lines for $s(E + N) > 8$,[34] one can only derive a lower limit and conclude that solvolysis with $s(E + N) < 13$ will not proceed via enforced S_N2 type mechanisms.

A further advantage of the N_1 parameters quoted in Table 3.8 is their direct comparability with the previously published N parameters of π-systems[15,16,35,37–39] and hydride donors.[15,40–43] Thus it becomes possible to predict nucleophiles which can intercept solvolytically generated carbocations in alcoholic or aqueous solutions as previously determined for one example by Richard.[44] If the nucleophiles on the left side of Figure 3.8 are employed in concentrations of [Nuc] = 1 mol L^{-1}, the calculated second-order rate constants become numerically identical to the pseudo-first-order rate constants ($k_{1\Psi} = k_2$[Nuc]) with the consequence that the N and N_1 parameters on both sides of Figure 3.8 become directly comparable.

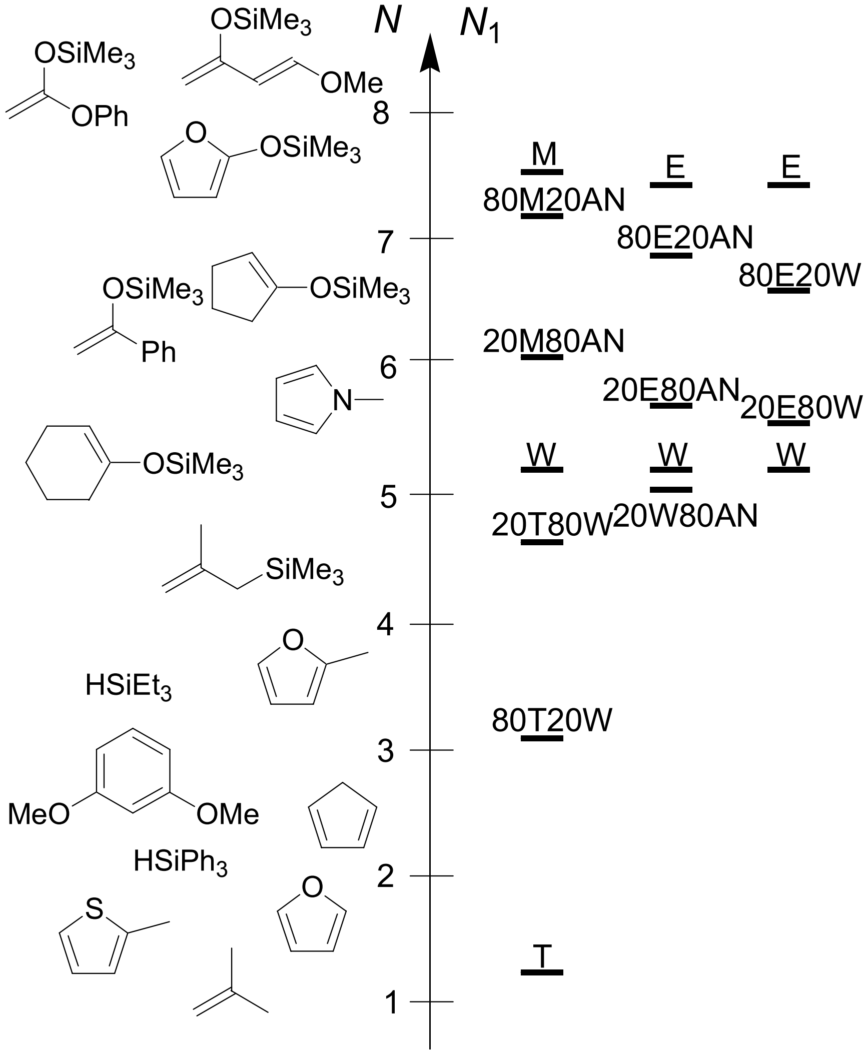

Figure 3.8: Comparison of the nucleophilicity parameters N_1 of solvents with the N parameters of typical π-systems and hydride donors. Mixtures of solvents are given as (v/v), solvents: M = methanol, E = ethanol, W = water, T = trifluoroethanol, AN = acetonitrile.

If the *s* parameters are neglected in a first approximation, 1 mol L^{-1} solutions of the nucleophiles on the left of Figure 3.8 may be expected to react equally fast with carbocations as the solvents on the right of Figure 3.8. As a consequence, carbocations may be trapped by 1 M solutions of nucleophiles of $N > 1.2$ if trifluoroethanol is used as the solvent and by nucleophiles of $N > 7.5$ if they are generated in methanol. This analysis is not perfectly correct, however, since it neglects the solvent dependence of the N parameters. Though the Mayr group has shown that the rates of the reactions of carbocations with neutral π-nucleophiles and neutral hydride donors only slightly depend on solvent polarity (chloroform, dichloromethane, acetonitrile, nitromethane)[21,35,40,45] there is evidence that π-nucleophilicity increases somewhat in protic solvents.[44] As a consequence, it is not only possible to trap carbocations by π-nucleophiles and hydride donors which are located above the corresponding reaction media in Figure 3.8 but also by those located slightly below the corresponding solvents. In agreement with this conclusion, Richard had previously reported that carbocations which are solvolytically generated in 50% aqueous acetonitrile ($N_1 = 5.05$) can be trapped by π-nucleophiles which possess N parameters greater than 6 even when they are used in lower concentrations (0.01-0.1 mol L^{-1}).[44] Kitagawa's trapping of fullerenyl cations (E ca. 7-8)[46] by anisol ($N = -1.18$, $s = 1.20$)[16] in 9/1 (v/v) anisol/CF_3CH_2OH must be due to the high s parameter of this π-nucleophile which becomes important in fast reactions.

As in previous papers dealing with the application of eq. (3.5), it should be reminded that the rate constants predicted by eq. (3.5) are usually accurate within a factor of 10-100 if systems with strong steric shielding (e.g., tritylium ions) or systems which may be perturbed by anomeric effects (e.g., reactions of alkoxycarbenium ions with alcohols) are excluded. With these exceptions in mind, Figure 3.8 is a useful guide for designing syntheses via solvolytically generated carbocations. Synthetic investigation in the Mayr group have been shown that it is possible to base acid free Friedel-Crafts chemistry on Figure 3.8.[47]

3.5 References

(1) Bentley, T. W.; Llewellyn, G. *Prog. Phys. Org. Chem.* **1990**, *17*, 121–159.

(2) Kevill, D. N. *Advances in Quantitative Structure-Property Relationships*; Charton, M. Ed., JAI Press, Greenwich, CT, **1996**, Vol. 1, pp 81–115.

(3) Grunwald, E.; Winstein, S. *J. Am. Chem. Soc.* **1948**, *70*, 846–854.

(4) More exactly: Eq. 3.1 would hold for any situation where nucleophilic solvent participation is of equal in both the substrate under condition and the standard *t*-butyl chloride.

(5) Winstein, S.; Grunwald, E.; Jones, H. W. *J. Am. Chem. Soc.* **1951**, *73*, 2700–2707.

(6) Winstein, S.; Fainberg, A. H.; Grunwald, E. *J. Am. Chem. Soc.* **1957**, *79*, 4146–4155.

(7) Peterson, P. E.; Waller, F. J. *J. Am. Chem. Soc.* **1972**, *94*, 991–992.

(8) Schadt, F. L.; Bentley, T. W.; Schleyer, P. v. R. *J. Am. Chem. Soc.* **1976**, *98*, 7667–7675.

(9) Kevill, D. N.; Rissmann, T. J. *J. Org. Chem.* **1985**, *50*, 3062–3064.

(10) Swain, C. G.; Kaiser, L. E.; Knee, T. E. C. *J. Am. Chem. Soc.* **1958**, *80*, 4092–4094.

(11) Kevill, D. N.; Anderson, S. W. *J. Org. Chem.* **1991**, *56*, 1845–1850.

(12) Gajewski, J. J. *J. Am. Chem. Soc.* **2001,** *123,* 10877-10883.

(13) (a) McClelland, R. A.; Banait, N.; Steenken, S. *J. Am. Chem. Soc.* **1986**, *108*, 7023–7027. (b) McClelland, R. A; Kanagasabapathy, V. M.; Steenken, S. *J. Am. Chem. Soc.* **1988**, *110*, 6913–6914. (c) McClelland, R. A.; Kanagasabapathy, V. M.; Banait, N. S.; Steenken, S. *J. Am. Chem. Soc.* **1989**, *111*, 3966–3972. (d) Chateauneuf, J. E. *J. Chem. Soc., Chem. Commun.* **1991**, 1437–1438. (e) Das, P. K. *Chem. Rev.* **1993**, *93*, 119–144. (f) Kirmse, W.; Krzossa, B.; Steenken, S. *J. Am. Chem. Soc.* **1996**, *118*, 7473–7477. (g) Kirmse, W.; Guth, M.; Steenken, S. *J. Am. Chem. Soc.* **1996**, *118*, 10838–10849. (h) McClelland, R. A. *Tetrahedron* **1996**, *52*, 6823–6858.

(14) (a) Richard, J . P.; Jencks, W. P. *J. Am. Chem. Soc.* **1982**, *104,* 4689–4691. (b) Richard, J . P.; Jencks, W. P. *J. Am. Chem. Soc.* **1982**, *104*, 4691–4692. (c) Richard, J . P.; Jencks, W. P. *J. Am. Chem. Soc.* **1984**, *106*, 1373–1383. (d) Richard, J . P.; Jencks, W. P. *J. Am. Chem. Soc.* **1984**, *106*, 1383–1396. (e) Richard, J . P.; Jencks, W. P. *J. Am. Chem. Soc.* **1984**, *106*, 1396–1401. (f) Ta-Shma, R.; Jencks, W. P. *J. Am. Chem. Soc.* **1986**, *108*, 8041–8050. (g) Amyes, T. L.; Richard, J. P.; Novak, M. *J. Am. Chem. Soc.* **1992**, *114*, 8032–

8041. (h) Richard, J. P.; Amyes, T. L.; Lin, S.-S.; O'Donoghue, A. C.; Toteva, M. M.; Tsuji, Y.; Williams, K. B. *Adv. Phys. Org. Chem.* **2000**, *35*, 67–116.

(15) Mayr, H.; Bug, T.; Gotta, M. F.; Hering, N.; Irrgang, B.; Janker, B.; Kempf, B.; Loos, R.; Ofial, A. R.; Remennikov, G.; Schimmel, H. *J. Am. Chem. Soc.* **2001**, *123*, 9500–9512.

(16) Mayr, H.; Kempf, B.; Ofial, A. R. *Acc. Chem. Res.* **2003**, *36*, 66–77.

(17) Pham, T. V.; McClelland, R. A. *Can. J. Chem.* **2001**, *79*, 1887–1897.

(18) (a) Kirmse, W.; Kilian, J.; Steenken, S. *J. Am. Chem. Soc.* **1990**, *112*, 6399–6400. (b) Belt, S. T.; Bohne, C.; Charette, G.; Sugamori, S.E.; Sciano, J. C. *J. Am. Chem. Soc.* **1993**, *115*, 2200–2205. (c) Faria, J. L.; McClelland, R. A.; Steenken, S. *Chem. Eur. J.* **1998**, *4*, 1275–1280.

(19) Bartl, J.; Steenken, S.; Mayr, H.; McClelland, R. A. *J. Am. Chem. Soc.* **1990**, *112*, 6918–6928.

(20) Minegishi, S.; Mayr, H. *J. Am. Chem. Soc.* **2003**, *125*, 286–295.

(21) Mayr, H.; Schneider, R.; Schade, C.; Bartl, J.; Bederke, R. *J. Am. Chem. Soc.* **1990**, *112*, 4446–4454.

(22) Dilman, A. D.; Ioffe, S. L.: Mayr, H. *J. Org. Chem.* **2001**, *66*, 3196–3200.

(23) Mayr, H.; Ofial, A. R. *Einsichten - Forschung an der LMU München* **2001**, *20*, 30–33.

(24) Most experiments were performed with 4-cyanophenolates; benzhydrylium acetates were used in highly aqueous solutions, where the solubility of the benzhydryl 4-cyanophenolates is low, or in solvents of low nucleophilicity, where the recombination of the benzhydrylium ions with 4-cyanophenolate anion is fast compared to the reaction of Ar_2CH^+ with the solvent.

(25) Ritchie, C. D.; Skinner, G. A.; Badding, V. G. *J. Am. Chem. Soc.* **1967**, *89*, 2063–2071.

(26) (a) Ritchie, C. D. *Acc. Chem. Res.* **1972**, *5*, 348–354. (b) Ritchie, C. D. *J. Am. Chem. Soc.* **1975**, *97*, 1170–1179. (c) Ritchie, C. D. *Can. J. Chem.* **1986**, *64*, 2239–2250.

(27) (a) Harris, J. M.; Becker, A.; Clark, D. C.; Fagen, J. F.; Kennan, S. L. *Tetrahedron Lett.* **1973**, *14*, 3813–3816. (b) Pross, A.; Koren, R. *Tetrahedron Lett.* **1975**, *16*, 3613–3616. (c) Ando, T.; Tsukamoto, S. *Tetrahedron Lett.* **1977**, *18*, 2775–2778. (d) Bentley, T. W.; Harris, H. C *J. Org. Chem.* **1988**, *53*, 724–728. (e) Bentley, T. W.; Koo, I. S. *J. Chem. Soc., Perkin Trans. 2* **1989**, 1385–1392. (f) Kevill, D. N.; Kyong, J. B.; Weitl, F. L. *J. Org. Chem.* **1990**, *55*, 4304–4311. (g) Bentley, T. W.;

Koo, I. S.; Norman, S. J. *J. Org. Chem.* **1991**, *56*, 1604–1609. (h) Shimizu, N.; Osajima, E.; Tsuno, Y. *Bull. Chem. Soc. Jpn.* **1991**, *64*, 1145–1152. (i) Bentley, T. W.; Shim, C. S. *J. Chem. Soc., Perkin Trans. 2* **1993**, 1659–1663. (j) Bentley, T. W.; Christl, M.; Kemmer, R.; Llewellyn, G.; Oakley, J. E. *J. Chem. Soc., Perkin Trans. 2* **1994**, 2531–2518. (k) D'Souza, M. J.; Kevill, D. N.; Bentley, T. W.; Devaney, A. C. *J. Org. Chem.* **1995**, *60*, 1632–1637. (l) Kevill, D. N.; Casamassa, A. J.; D'Souza, M. J. *J. Chem. Res. (S)* **1996**, 472–473. (m) Kevill, D. N.; Anderson, S. W.; Ismail, N. H. J *J. Org. Chem.* **1996**, *61*, 7256–7262. (n) Bentley, T. W.; Llewellyn, G.; McAlister, J. A. *J. Org. Chem.* **1996**, *61*, 7927–7932. (o) Bentley, T. W.; Ebdon, D.; Llewellyn, G.; Abduljaber, M. H.; Miller, B. Kevill, D. N. *J. Chem. Soc., Dalton Trans.* **1997**, 3819–3825. (p) Koo, I. S.; Yang, K.; Kang, K.; Lee, I.; Bentley, T. W. *J. Chem. Soc., Perkin Trans. 2* **1998**, 1179–1184. (q) Bentley, T. W.; Llewellyn, G.; Zoon, H. R. *J. Org. Chem.* **1998**, *63*, 4654–4659. (r) Ta-Shma, R.; Rappoport, Z. *Adv. Phys. Org. Chem*. **1992**, *27*, 239–291, and references cited there in.

(28) Bunting, J. W.; Mason, J. M.; Heo, C. K. M. *J. Chem. Soc., Perkin Trans. 2* **1994**, 2291–2230.

(29) Swain, C. G.; Scott, C. B. *J. Am. Chem. Soc.* **1953**, *75*, 141–147.

(30) Richard, J. P.; Toteva, M. M.; Crugeiras, J. *J. Am. Chem. Soc.* **2000**, *122*, 1664–1674.

(31) Kevill, D. N.; D'Souza, M. J. *J. Chem. Soc., Perkin Trans. 2* **1997**, 1721–1724.

(32) Kevill, D. N.; D'Souza, M. J. *Can. J. Chem.* **1999**, *77*, 1118–1122.

(33) (a) $N_1 = 1.51N'_T + 6.60$, $n = 13$, $R^2 = 0.950$. (b) $N_1 = 1.48N'_{OTs} + 6.65$, $n = 17$, $R^2 = 0.892$. (c) $N_1 = 1.87N_{OTs} + 6.48$ $n = 16$, $R^2 = 0.885$.

(34) Roth, M.; Mayr, H. *Angew. Chem.* **1995**, *107*, 2428–2430; *Angew. Chem., Int. Ed. Engl.* **1995**, *34*, 2250–2252.

(35) Mayr, H.; Patz, M. *Angew. Chem.* **1994**, *106*, 990–1010; *Angew. Chem., Int. Ed. Engl.* **1994**, *33*, 938–957.

(36) Jencks, W. P. *Acc. Chem. Res.* **1980**, *13*, 161–169. (b) Jencks, W. P. *Chem. Soc. Rev.* **1981**, *10*, 345–375 (c) Jencks, W. P. *Chem. Rev.* **1985**, *85*, 511–527.

(37) Mayr, H.; Kuhn, O.; Gotta, M. F.; Patz, M. *J. Phys. Org. Chem.* **1998**, *11*, 642–654.

(38) Mayr, H.; Patz, M.; Gotta, M. F.; Ofial, A. R. *Pure Appl. Chem.* **1998**, *70*, 1993–2000.

(39) (a) Kempf, B.; Hampel, N.; Ofial, A. R.; Mayr, H. *Chem. Eur. J.* **2003**, *9*, 2209–2218. (b) Bug, T.; Hartnagel, M.; Schlierf, C.; Mayr, H. *Chem. Eur. J.* **2003**, *9*, 4068–4076.

(40) Mayr, H.; Basso, N.; Hagen, G. *J. Am. Chem. Soc.* **1992**, *114*, 3060–3066.

(41) Mayr, H.; Basso, N. *Angew. Chem.* **1992**, *104*, 1103-1105; *Angew. Chem., Int. Ed. Engl.* **1992**, *31*, 1046–1048.

(42) Funke, M.-A.; Mayr, H. *Chem. Eur. J.* **1997**, *3*, 1214–1222.

(43) Mayr, H.; Lang, G.; Ofial, A. R. *J. Am. Chem. Soc.* **2002**, *124*, 4076–4083.

(44) Richard, J. P.; Szymanski, P.; Williams, K. B. *J. Am. Chem. Soc.* **1998**, *120*, 10372–10378.

(45) (a) Kane-Maguire, L. A. P.; Mansfield, C. A. *J. Chem. Soc., Dalton Trans.* **1976**, 2192–2196. (b) John, G. R.; Mansfield, C. A.; Kane-Maguire, L. A. P. *J. Chem. Soc., Dalton Trans.* **1977**, 574–578. (c) John, G. R.; Kane-Maguire, L. A. P. *J. Chem. Soc., Dalton Trans.* **1979**, 873–878. (d) John, G. R.; Kane-Maguire, L. A. P. *Inorg. Chim. Acta.* **1981**, *48*, 179–183.

(46) Kitagawa, T.; Lee, Y.; Hanamura, M.; Sakamoto, H.; Konno, H.; Takeuchi, K.; Komatsu, K. *Chem. Commun*. **2002**, 3062–3063.

(47) Hofmann, M.; Hampel, N.; Mayr, H. Unpublished results.

4. Carbocation electrophilicities derived from rates of reactions of carbocations with solvents

4.1 Introduction

In previous work,[1] it was suggested that carbocation electrophilicities should generally be derived from the rates of reactions of the corresponding carbocations with those π_{CC}-systems that had been selected as reference nucleophiles. If this recommendation were strictly obeyed, one could not take advantage of a large set of kinetic data on the reactions of carbocations with solvents which are available in the literature. Since Chapter 3 reports N_1 and s parameters for typical solvents, I will now use these parameters for determining electrophilicity parameters E of carbocations and, if possible, compare them with E-parameters derived from reactions of the same carbocations with reference nucleophiles.

4.2 Treatment of data

E parameters of carbocations were evaluated by a least-squares minimization procedure from eq. 4.1 using the solvent nucleophilicity parameters listed in chapter 3 and the rate constants for the reactions of the corresponding carbocations with solvents determined by clock methods or by laser flash photolysis.

$$\log k\,(20\ °\mathrm{C}) = s\,(N + E) \qquad (4.1)$$

In the case of alkoxycarbenium ions, rate constants have also been measured in sulfuric acid by monitoring the decay of alkoxycarbenium ions, which are formed as observable intermediates in the acid induced hydrolyses of acetals and ortho esters. When deviating rate constants have been obtained with different methods, I usually considered the directly measured data. However, when the directly measured rate constants referred to sulfuric acid solution, data obtained by clock-methods were preferentially used, because the evaluation of the kinetic data in sulfuric acid requires knowledge of the exact value of the activity of water. In most cases, the rate constants determined by clock methods showed excellent agreement with directly measured ones. As discussed previously, eq. 4.1 is only valid for $k < 10^8$ L mol^{-1} s^{-1} because the linear correlation lines flatten when the diffusion limit is approached.[2a] For that reason, only pseudo-first order rate constants with $k < 10^9$ s^{-1} were used for the calculation of E-parameters of carbocations in this chapter. For several systems an increase of ionic strength from 0 to 0.5 mol L^{-1} causes a reduction of the rate constants for the reactions with water in water or aqueous solutions by a factor of two.[2b] Because this deviation is within the error limits of our approach (eq. 4.1), we have not explicitly treated the influence of ionic strength. Data which have not been used for the calculation of electrophilicity parameters are indicated by italic printing in the following Tables.

4.3 1-Arylethyl cations

1-Arylethyl cations have extensively been studied by direct kinetic measurements as well as by the azide clock method. Table 4.1 shows that these data are generally in good agreement. Only in the case of the 4-dimethylamino-substituted 1-phenylethyl cation, the rate constant derived from the decay of laser flash photolytically generated carbocations in 50% aqueous trifluoroethanol was 50 times smaller than that determined by the sulfide clock method under the same conditions. As discussed below, the rate constant determined by laser flash photolysis is in better agreement with the data for the corresponding cumyl cations. Therefore, we consider the value determined by the sulfide clock method to be erroneous.

The *E*-parameter for the 1-(4-methoxyphenyl)ethyl cation given in Table 4.1 is similar to that derived from reactions of this carbocation with reference π-nucleophiles (E = 4.8).[3] As a consequence, we conclude that the *E*-parameters listed in Table 4.1 and Scheme 4.1 can also be employed for calculating reactions of these carbocations with other types of nucleophiles.

Table 4.1: Rate constants for the reactions of 1-arylethyl cations with solvents and electrophilicity parameters derived therefrom.

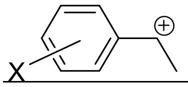

X	E	Solvent[a]	N_1	s	T, °C	I,[b]	k_{exp} s^{-1}	k_{calc} s^{-1}	$\Delta^2 \log k$	Method[c]	Ref.
4-NO$_2$		*50T50W*	*3.57*	*0.89*	*22*	*0.5*	1.0×10^{13}			*Azide*	*4*
4-CN		*50T50W*	*3.57*	*0.89*	*22*	*0.5*	6.0×10^{12}			*Azide*	*4*
3-Br		*50T50W*	*3.57*	*0.89*	*22*	*0.5*	1.2×10^{12}			*Azide*	*4*
3-MeO		*50T50W*	*3.57*	*0.89*	*22*	*0.5*	2.0×10^{11}			*Azide*	*4*
H		*50T50W*	*3.57*	*0.89*	*22*	*0.5*	1.0×10^{11}			*Azide*	*4*
4-F		*50T50W*	*3.57*	*0.89*	*22*	*0.5*	2.0×10^{10}			*Azide*	*4*
4-Me		*50T50W*	*3.57*	*0.89*	*22*	*0.5*	4.0×10^{9}			*Azide*	*4*
3-Br,4-(OMe)	6.1	50T50W	3.57	0.89	22	*0.5*	4.0×10^{8}	4.0×10^{8}		Azide	4
4-OPh	6.0	50T50W	3.57	0.89	25	*0.5*	3.0×10^{8}	3.0×10^{8}		Azide	4
4-SMe	5.2	50T50W	3.57	0.89	25	*0.5*	6.0×10^{7}	6.0×10^{7}		Azide	5
3,4-(OMe)$_2$	4.8	T	1.23	0.92	20	–	4.0×10^{7}	2.6×10^{7}	3.4×10^{-2}	LF	6
		50T50W	3.57	0.89	25	*0.5*	2.1×10^{5}	3.2×10^{5}	3.7×10^{-2}	Azide	4
4-OMe	4.4	T	1.23	0.92	20	–	3.9×10^{5}	1.8×10^{5}	1.1×10^{-1}	LF	7
		T	*1.23*	*0.92*	*20*	–	3.5×10^{5}	1.8×10^{5}	8.3×10^{-2}	*LF*	*8*
		T	*1.23*	*0.92*	*20*	–	3.7×10^{5}	1.8×10^{5}	9.8×10^{-2}	*LF*	*8*
		T	*1.23*	*0.92*	*?*	–	3.9×10^{5}	1.8×10^{5}	1.1×10^{-1}	*LF*	*9*
		T	*1.23*	*0.92*	*20*	–	3.9×10^{5}	1.8×10^{5}	1.1×10^{-1}	*LF*	*10*
		90T10W	2.93	0.88	20	–	3.6×10^{6}	3.4×10^{6}	7.7×10^{-4}	LF	6
		80T20W	3.20	0.88	20	–	6.3×10^{6}	5.8×10^{6}	1.1×10^{-3}	LF	6
		60T40W	3.42	0.90	20	–	1.3×10^{7}	1.3×10^{7}	1.5×10^{-5}	LF	6
		50T50W	3.57	0.89	20	–	2.5×10^{7}	1.5×10^{7}	5.1×10^{-2}	LF	10
		50T50W	*3.57*	*0.89*	*22*	*0.5*	5.0×10^{7}	1.5×10^{7}	2.7×10^{-1}	*Azide*	*4*
		50T50W	*3.57*	*0.89*	*25*	*0.5*	5.0×10^{7}	1.5×10^{7}	2.7×10^{-1}	*Azide*	*11*
		50T50W	*3.57*	*0.89*	*25*	*0.5*	4.8×10^{7}	1.5×10^{7}	2.6×10^{-1}	*Azide*	*12*
		W	5.20	0.89	22	*0.5*	1.0×10^{8}	4.2×10^{8}	3.9×10^{-1}	Azide	4
		50W50AN	5.05	0.89	22	*0.5*	1.6×10^{8}	2.5×10^{8}	3.7×10^{-2}	Azide	4
		50E50W	5.96	0.89	22	*0.5*	6.7×10^{8}	1.6×10^{9}	1.4×10^{-1}	Azide	4
2-OH	3.4		5.20	0.89	25	0.1	4.4×10^{7}	4.4×10^{7}		LF	13
4-OMe,2,3-benzo	3.0	T	1.23	0.92	20	–	7.5×10^{3}	7.5×10^{3}		LF	6
4-NMe$_2$	-1.8	50T50W	3.57	0.89	20	–	4.0×10^{1}	4.0×10^{1}		LF	6
		50T50W	*3.57*	*0.89*	*22*	*0.5*	2.0×10^{3}	4.0×10^{1}	*2.9*	*RS¯*	*4*

[a] Mixtures of solvents are given as (v/v), solvents: W = water, T = trifluoroethanol, AN = acetonitrile. [b] Ionic strength maintained with NaClO$_4$. [c] LF = laser flash photolysis, Azide = azide clock, RS¯ = MeOC(O)CH$_2$S¯ clock.

Scheme 4.1: Comparison of the electrophilicity parameters *E* of various 1-arylethyl cations.

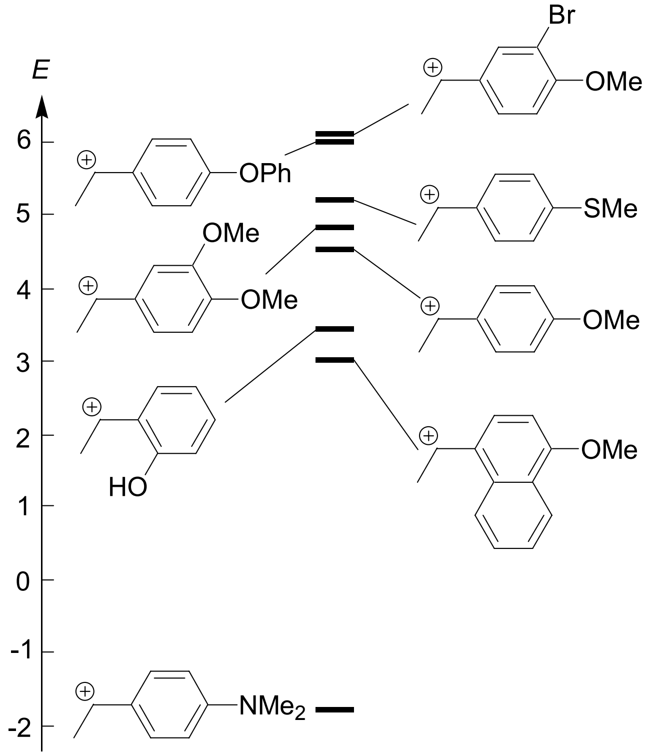

Figure 4.1 shows a linear correlation of *E* versus σ^+ with a slope of 6.22 which is slightly smaller than the corresponding slope in the symmetric benzhydrylium series (7.46).[1]

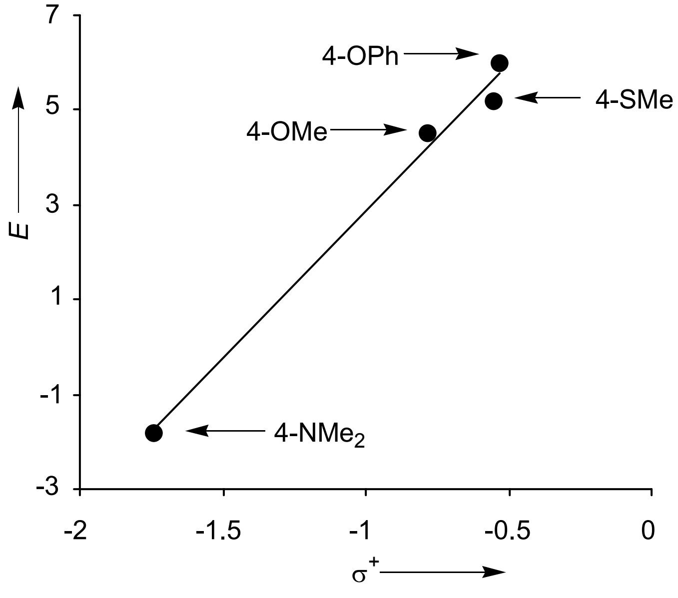

Figure 4.1: Correlation of the electrophilicity parameters *E* of 4-substituted 1-phenylethyl cations with the Hammett σ^+-parameters.[14a] $E = 6.22\sigma^+ + 9.07$, n = 4, $R^2 = 0.991$.

4.4 Cumyl cations

For most cumyl cations, only rate constants for reactions with a single solvent were available. However, the 4-methoxy substituted cumyl cation has been investigated in three different solvents with widely varying nucleophilicity, yielding an averaged electrophilicity E of 3.5. The good agreement between experimental and calculated rate constants in Table 4.2 corroborates the applicability of eq. 4.1 as well as of the solvent nucleophilicities N_1 and s for describing these reactions.

Table 4.2: Rate constants for the reactions of cumyl cations with solvents and electrophilicity parameters derived therefrom.

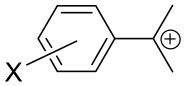

X	E	Solvent [a]	N_1	s	T, °C	I,[b]	k_{exp}, s^{-1}	k_{calc}, s^{-1}	$\Delta^2 \log k$	Method [c]	Ref.
H		*50T50W*	*3.57*	*0.89*	*25*	*0.5*	1.7×10^{10}			*Azide*	*15*
4-Me	6.4	T	1.23	0.92	20	–	1.0×10^{7}	1.0×10^{7}		LF	7
		50T50W	*3.57*	*0.89*	*25*	0.5	1.0×10^{9}	7.2×10^{8}		*Azide*	*16*
2,4,6-(Me)$_3$	4.5	50T50W	3.57	0.89	25	0.5	1.4×10^{7}	1.4×10^{7}		Azide	17
4-OMe	3.5	67W33AN	5.05	0.90	20	–	4.0×10^{7}	4.9×10^{7}	7.5×10^{-3}	LF	6
		50T50W	3.57	0.89	20	–	3.3×10^{6}	1.9×10^{6}	5.4×10^{-2}	LF	10
		50T50W	*3.57*	*0.89*	*25*	0.5	1.3×10^{7}	1.9×10^{6}	7.0×10^{-1}	*Azide*	*12*
		T	1.23	0.92	20	–	1.6×10^{4}	2.2×10^{4}	2.0×10^{-2}	LF	7
		T	*1.23*	*0.92*	*20*	–	1.6×10^{4}	2.2×10^{4}	2.0×10^{-2}	*LF*	*10*
4-NMe$_2$	-2.6	67W33AN	5.05	0.90	20	–	1.5×10^{2}	1.5×10^{2}		LF	6

[a] Mixtures of solvents are given as (v/v), solvents: W = water, T = trifluoroethanol, AN = acetonitrile. [b] Ionic strength maintained with NaClO$_4$. [c] LF = laser flash photolysis, Azide = azide clock.

Table 4.2 and Scheme 4.2 indicate the 2,4,6-trimethylcumyl cation being less electrophilic than the 4-methylcumyl cation. Obviously the electronic stabilization of the cumyl cation by the ortho-methyl groups is larger than the effect of disturbed conjugation of the phenyl ring with the carbenium center caused by the steric effect of these substituents.

Scheme 4.2: Comparison of the electrophilicity parameters *E* of various cumyl cations.

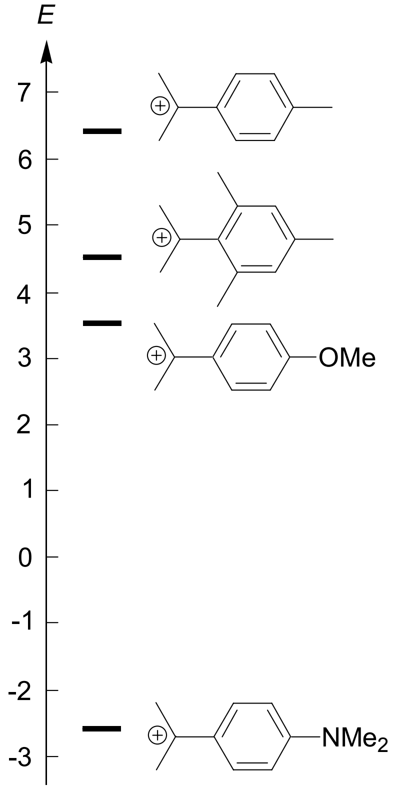

Though only three entries are available for the correlation of *E* versus σ^+ (Figure 4.2), it is remarkable that the slope is almost the same as in the 1-arylethyl cation series.

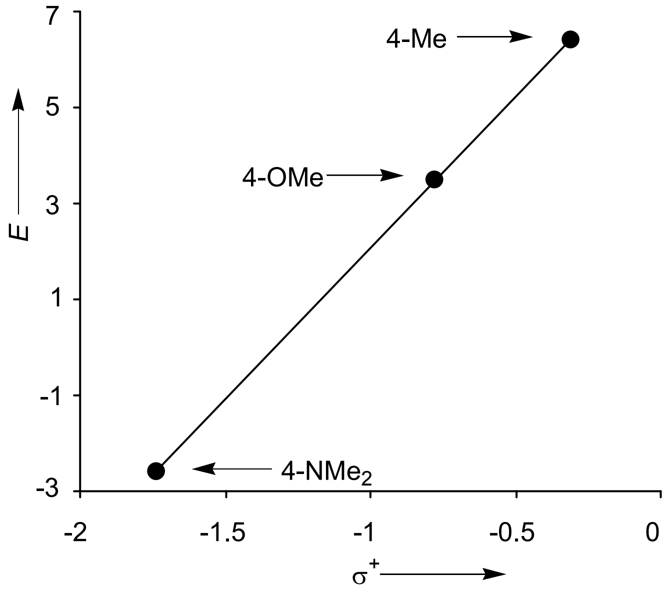

Figure 4.2: Correlation of the electrophilicity parameters *E* of 4-substituted cumyl cations with the Hammett σ^+-parameters.[14a] $E = 6.30\sigma^+ + 8.38$, n = 3, $R^2 = 1.000$.

Scheme 4.3 illustrates the decrease of electrophilicity from 1-arylethyl cations to cumyl and benzhydrylium ions.

Scheme 4.3: Comparison of the electrophilicity parameters *E* of 1-arylethyl cations, cumyl cations, and benzhydrylium ions.

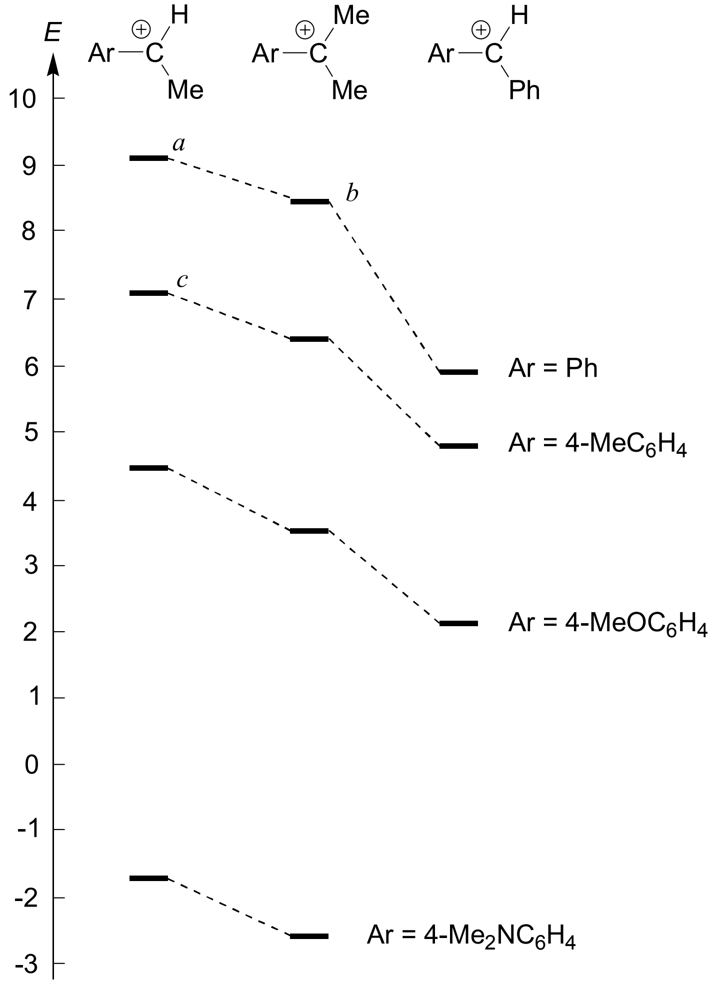

[a] E = 9.1 estimated from correlation in Figure 4.1. [b] E = 8.4 estimated from correlation in Figure 4.2. [c] E = 7.1 estimated from correlation in Figure 4.1.

4.5 Various 4-methoxy α-substituted benzyl cations

Table 4.3: Rate constants for the reactions of various 4-methoxy α-substituted benzyl cations with solvents and electrophilicity parameters derived therefrom.

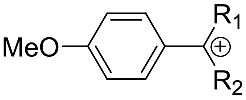

R^1	R^2	*E*	Solvent [a]	N_1	*s*	*T*, °C	*I*,[b]	k_{exp}, s^{-1}	k_{calc}, s^{-1}	$\Delta^2 \log k$	Method [c]	Ref.
H	H	5.9	T	1.23	0.92	20	–	4.3×10^{6}	3.4×10^{6}	9.9×10^{-3}	LF	7
			T	*1.23*	*0.92*	*20*	–	*4.3×10^{6}*	*3.4×10^{6}*	*9.9×10^{-3}*	*LF*	*10*
			50T50W	3.57	0.89	25	0.5	2.0×10^{8}	2.5×10^{8}	1.1×10^{-2}	Azide	12
			80A20W	*5.77*	*0.87*	*25*	*0.5*	*6.0×10^{8}* [d]	*1.3×10^{10}*	*1.8*	*Azide*	*17*
H	CHF_2	5.8	50T50W	3.57	0.89	25	0.5	1.0×10^{8}	2.0×10^{8}	9.7×10^{-2}	Azide	12
			T	1.23	0.92	20	–	5.5×10^{6}	2.7×10^{6}	9.1×10^{-2}	LF	10
H	CH_2F	5.4	50T50W	3.57	0.89	25	0.5	1.0×10^{8}	1.0×10^{8}	2.1×10^{-4}	Azide	12
			T	1.23	0.92	20	–	1.4×10^{6}	1.4×10^{6}	2.0×10^{-4}	LF	10
H	CF_3	5.1	50T50W	3.57	0.89	20	–	3.0×10^{7}	4.7×10^{7}	3.8×10^{-2}	LF	10
			50T50W	*3.57*	*0.89*	*25*	*0.5*	*5.0×10^{7}*	*4.7×10^{7}*	*7.2×10^{-4}*	*Azide*	*11*
						25	0.5				*Azide*	12
			T	1.23	0.92	20	–	9.3×10^{5}	6.0×10^{5}	3.6×10^{-2}	LF	10
Me	CF_3	4.7	50T50W	3.57	0.89	25	0.5	2.5×10^{7}	2.5×10^{7}		Azide	12
H	Me	4.5	From Table 4.1									
H	CO_2Et	4.5	50T50W	3.57	0.89	25	0.5	1.4×10^{7}	1.4×10^{7}		Azide	12
H	CO_2Me	4.4	T	1.23	0.92	20	–	1.7×10^{5}	1.7×10^{5}	1.0×10^{-3}	LF	18
			50T50W	3.57	0.89	20	–	1.2×10^{7}	1.2×10^{7}	1.1×10^{-3}	LF	18
			W	*5.20*	*0.89*	*20*	–	*2.0×10^{7}*	*3.9×10^{8}*	*1.6*	*LF*	*18*
CF_3	CF_3	3.9	50T50W	3.57	0.89	20	–	3.0×10^{6}	4.1×10^{6}	1.9×10^{-2}	LF	10
			50T50W	*3.57*	*0.89*	*22*	0.5	*4.5×10^{6}*	*4.1×10^{6}*	*1.6×10^{-3}*	*Azide*	*19*
			T	1.23	0.92	20	–	6.6×10^{4}	4.8×10^{4}	1.8×10^{-2}	LF	10
Me	Me	3.5	From Table 4.2									
Me	*t*-Bu	3.3	T	1.23	0.92	20	–	1.6×10^{4}	1.6×10^{4}		LF	6
H	*c*-Pr	3.3	T	1.23	0.92	?	–	1.4×10^{4}	1.4×10^{4}		LF	20
Me	*i*-Pr	2.5	T	1.23	0.92	20	–	3.0×10^{3}	3.0×10^{3}		LF	6

Table 4.3: Continued

R^1	R^2	E	Solvent [a]	N_1	s	T, °C	I,[b]	k_{exp}, s^{-1}	k_{calc}, s^{-1}	$\Delta^2 \log k$	Method [c]	Ref.
H	$C(O)NMe_2$	1.8	60W40AN[e]	5.05	0.90	20	–	1.6×10^6	1.6×10^6		LF	21
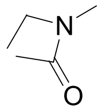		1.8	M	7.54	0.92	25	0.2	3.9×10^{8}[f]	3.9×10^8		Azide	22
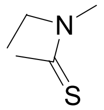		1.6	M	7.54	0.92	25	0.2	2.5×10^{8}[f]	2.5×10^8		Azide	22
Me	*c*-Pr	1.5	T	1.23	0.92	20	–	3.3×10^2	3.3×10^2		LF	6
H	$C(S)NMe_2$	-2.6	60W40AN [e]	5.05	0.90	20	–	1.5×10^2	1.7×10^2	2.7×10^{-3}	LF	21
			50W50AN	5.05	0.89	25	0.5	1.8×10^2	1.6×10^2	2.7×10^{-3}	LF	23

[a] Mixtures of solvents are given as (v/v), solvents: M = methanol, W = water, T = trifluoroethanol, A = acetone, AN = acetonitrile. [b] Ionic strength, $NaClO_4$. [c] LF = laser flash photolysis, Azide = azide clock. [d] The reaction of azide ion is S_N2 mechanism. [e] N_1 and s parameters of 67W33AN were used for calculation. [f] Calculated from $k_{AZ} = 5 \times 10^9$ L mol^{-1} s^{-1}.

A more general comparison of the effect of α-substitution in benzyl cations includes acceptor substituents (Table 4.3). Many carbocations listed in Scheme 4.4 have been investigated in solvents that differ considerably in nucleophilicity, e.g., trifluoroethanol and 50% aqueous trifluoroethanol. Despite the different medium for trapping and despite the fact that some of the data have been determined with the laser flash method while others have been obtained with the azide clock, the maximum deviation between calculated and experimental rate constants is a factor of 2.

Only for the reaction of $[(4\text{-}MeOC_6H_4)CHCO_2Me]^+$ with water, calculated and experimental rate constants deviated by a factor of 20; probably because k_{exp} reflects the rate-limit of the detecting unit.

Scheme 4.4: Comparison of the electrophilicity parameters E of various 4-methoxy α-substituted benzyl cations.

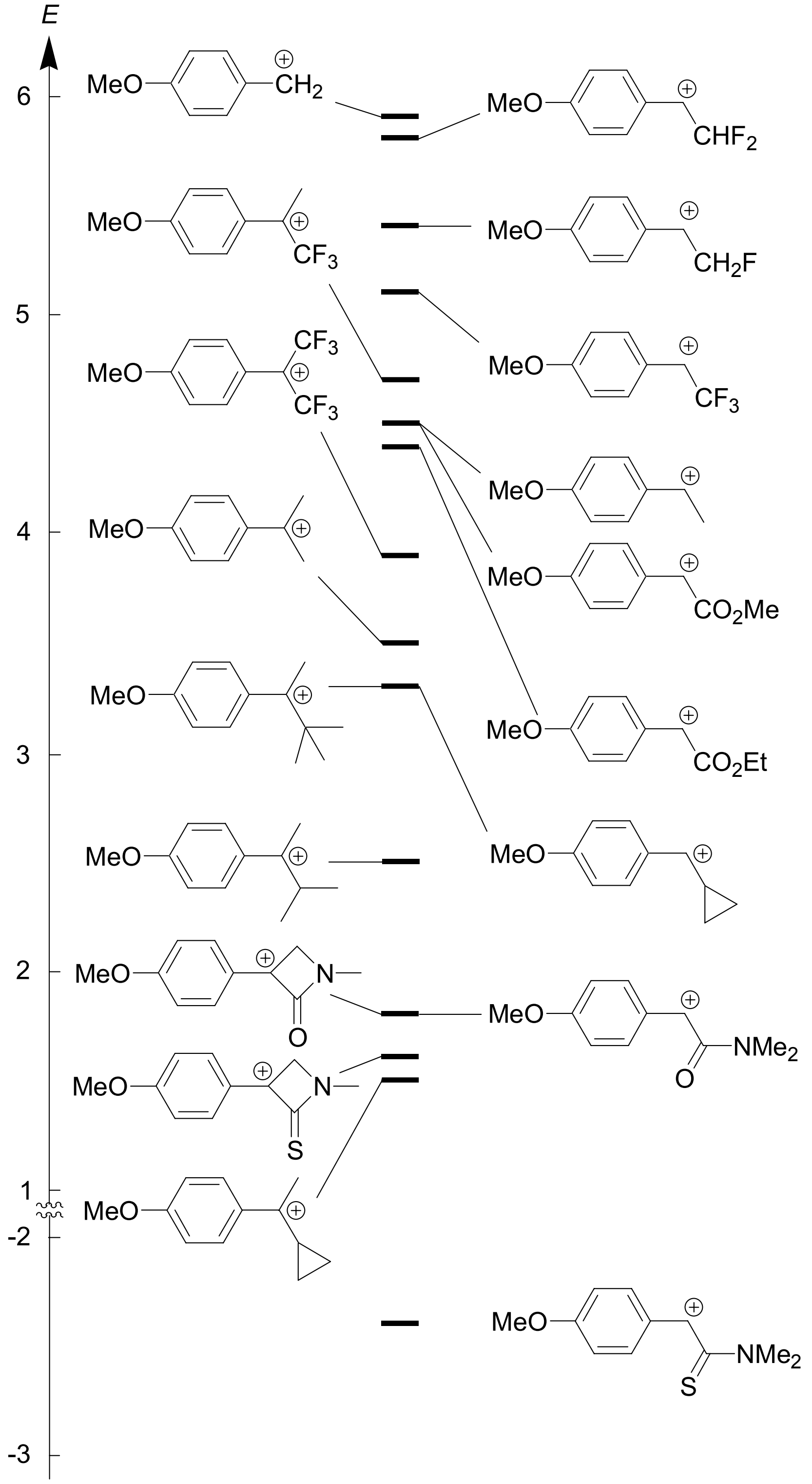

Richard has already discussed that the electrophilicities of 4-methoxybenzyl cations are quite insensitive to variation of the α-substituents.[12,19,23–27] Thus the electrophilicities of 4-$MeOC_6H_4CH^+R$ are similar for R = Me and CF_3, the CO_2R substituent has a slightly larger kinetic stabilizing effect, and the stabilization by a cyclopropyl group is as effective as by a phenyl group. For these systems there is no simple relationship between rate and equilibrium constants for the reaction with solvent. It was explained that the addition of electron-withdrawing α-substituents to the 4-methoxybenzyl cation enhances resonance electron donation from the aromatic ring. Therefore, positive charge is separated from the variable substituent which results in a reduction of the substituent's destabilizing interaction.[27] The situation is further complicated by the fact that $MeOC_6H_4C^+MeCF_3$ and $MeOC_6H_4C^+(CF_3)_2$ react with H_2O not only at the benzyl position but also at the 4-position of the aromatic ring.[10]

When α-Me and α-CF_3 substituted benzylic cations are compared, the activation energies of the reactions with solvents are similar, but the stabilities of products are different as depicted in Figure 4.3 (path a: α- CF_3, path b: α-Me). From this relationship, one can derive that the intrinsic barrier for the addition of a nucleophile to an α-CF_3 substituted carbocation is greater than that for the addition of a nucleophile to an α-Me substituted carbocation.[28]

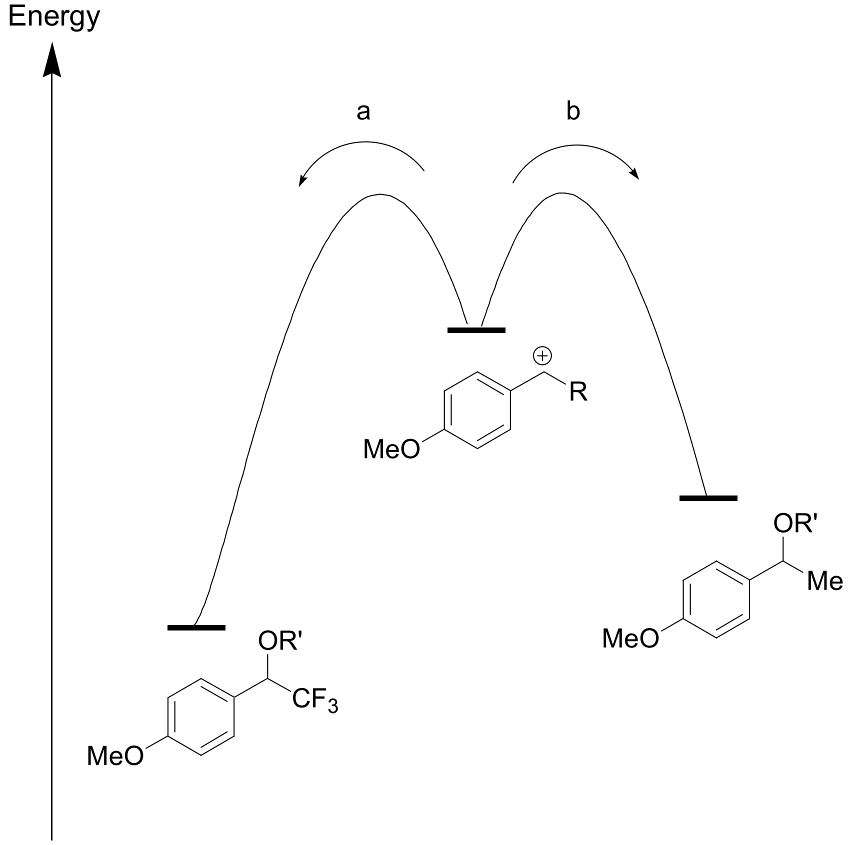

Figure 4.3: Reaction profiles for the addition of nucleophiles to α-methyl and α-trifluoromethyl substituted carbocations.

4.6 α-Cyclopropyl substituted benzyl cations

Only laser flash experiments in trifluoroethanol have been employed to determine the electrophilic reactivities of α-cyclopropyl substituted benzyl cations (Table 4.4).[20]

Table 4.4: Rate constants for the reactions of α-cyclopropyl substituted benzyl cations with solvents and electrophilicity parameters derived therefrom (temperature not given in ref. 20).

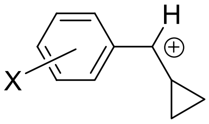

X	E	Solvent [a]	N_1	s	k_{exp}, s^{-1}	Method [b]	Ref.
4-H	5.5	T	1.23	0.92	1.6×10^{6}	LF	20
4-Me	4.6	T	1.23	0.92	2.2×10^{5}	LF	20
4-Ph	4.6	T	1.23	0.92	2.2×10^{5}	LF	20
4-(1-naphthyl)	4.5	T	1.23	0.92	1.9×10^{5}	LF	20
4-OMe	3.3	T	1.23	0.92	1.4×10^{4}	LF	20

[a] T = trifluoroethanol. [b] LF = laser flash photolysis.

Scheme 4.5 compares the calculated electrophilicities with those of analogously substituted benzhydrylium ions. One can see that α-cyclopropyl and α-phenyl substituted species have equal electrophilicity for X = 4-Me. In the case of the unsubstituted systems (X = H), the electrophilicity of the cyclopropyl substituted compound is lower, while in the case of the X = OMe, the electrophilicity of the cyclopropyl substituted compound is higher than that of the corresponding phenyl analogue.

Scheme 4.5: Comparison of the electrophilicity parameters *E* of α-cyclopropyl substituted benzyl cations and of the corresponding benzhydrylium ions.

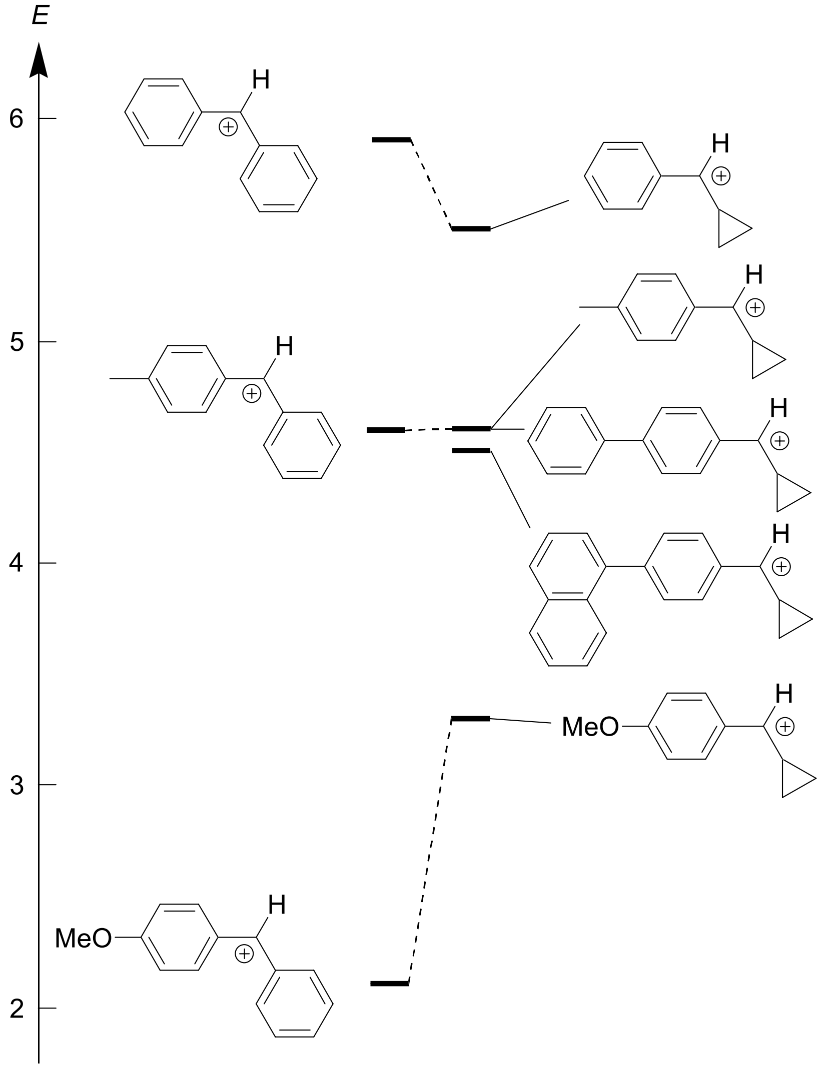

This observation is in accord with previous reports that cyclopropyl and phenyl possess comparable electron-donating abilities for stabilizing positive charge and that their relative abilities depend on the nature of the corresponding carbocation.[29] As a consequence of these different effects, the slope of the *E* versus σ^+ correlation ($\rho = 2.71$) is considerably smaller than in the benzhydrylium series ($\rho = 5.11$, Figure 4.4).

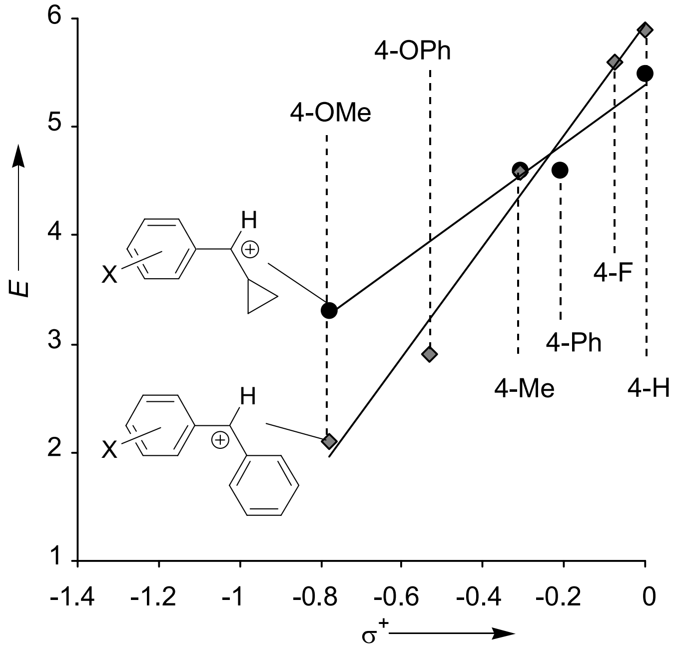

Figure 4.4: Correlation of the electrophilicity parameters E of α-cyclopropyl substituted benzyl cations and of the corresponding benzhydrylium ions with the Hammett σ^+-parameters.[14a] (α-cyclopropyl substituted benzyl cations: $E = 2.71\sigma^+ + 5.38$, n = 4, $R^2 = 0.974$; benzhydrylium ions: $E = 5.11\sigma^+ + 5.95$, n = 5, $R^2 = 0.983$).

4.7 Miscellaneous benzyl cations

Table 4.5: Rate constants for the reactions of 4-amino-α-(1-hydroxybenzyl) substituted benzyl cations with solvents at 20 °C, I = 0.5 ($NaClO_4$) and electrophilicity parameters derived therefrom.

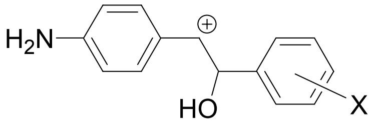

X	E	Solvent [a]	N_1	s	k_{exp}, s^{-1}	Method [b]	Ref.
4-Br	-2.3	80W20AN	5.04	0.89	2.5×10^2	LF	30
H	-2.3	80W20AN	5.04	0.89	2.5×10^2	LF	30
3-Me	-2.3	80W20AN	5.04	0.89	2.5×10^2	LF	30
4-Me	-2.3	80W20AN	5.04	0.89	2.5×10^2	LF	30
4-OMe	-2.3	80W20AN	5.04	0.89	2.5×10^2	LF	30
4-NMeAc	-2.3	80W20AN	5.04	0.89	2.5×10^2	LF	30

[a] Mixtures of solvents are given as (v/v), solvents: W = water, AN = acetonitrile. [b] LF = laser flash photolysis.

As expected for para- and ortho-amino substituted benzyl cations, the compounds listed in Tables 4.5 and 4.6 possess relatively low electrophilicity. Table 4.5 shows that the substituents X at the non-conjugated phenyl ring of this benzyl cation do not affect electrophilicity. As described in Scheme 4.6, this cation has been generated via hydration of a nitrenium ion.[30]

Scheme 4.6

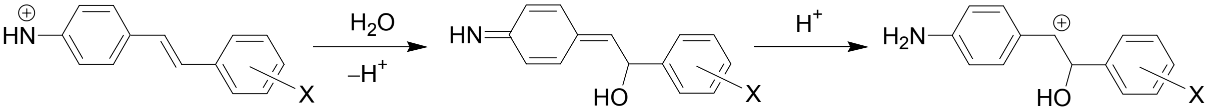

In the hydroquinolinium ions depicted in Table 4.6, the substituents R^1 and R^2 are not located at positions with partial positive charge and, therefore, have little influence on electrophilicity.

Table 4.6: Rate constants for the reactions of tetrahydroquinolinium ions with solvents at 20 °C and electrophilicity parameters derived therefrom.

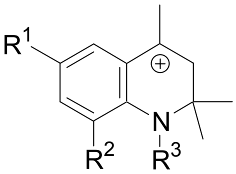

R^1	R^2	R^3	E	Solvent [a]	N_1	s	k_{exp}, s^{-1}	k_{calc}, s^{-1}	$\Delta^2 \log k$	Method [b]	Ref.
H	OMe	H	-3.6	M	7.54	0.92	1.8×10^{3}	4.3×10^{3}	1.4×10^{-1}	LF	31
				W	5.20	0.89	6.5×10^{1}	2.7×10^{1}	1.5×10^{-1}	LF	31
Me	H	Me	-4.4	M	7.54	0.92	7.9×10^{2}	7.9×10^{2}		LF	31
Me	H	H	-4.5	M	7.54	0.92	6.0×10^{2}	6.0×10^{2}		LF	31

[a] M = methanol, W = water. [b] LF = laser flash photolysis.

Table 4.7: Rate constants for the reactions of miscellaneous benzyl cations with solvents and electrophilicity parameters derived therefrom.

Carbocation	E	Solvent [a]	N_1	s	T, °C	I	k_{exp}, s^{-1}	k_{calc}, s^{-1}	$\Delta^2 \log k$	Method [b]	Ref.
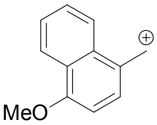	4.5	T	1.23	0.92	20	–	1.8×10^5	1.8×10^5		LF	6
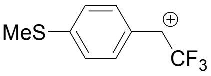	4.4	50T50W	3.57	0.89	22	0.5 [c]	1.2×10^7	1.2×10^7		Azide	23
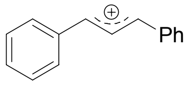	3.5	T	1.23	0.92	?	–	2.1×10^4	2.1×10^4		LF	32
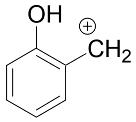	3.4	W	5.20	0.89	25	0.1 [c]	4.4×10^7	4.4×10^7		LF	33
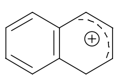	2.8	75W25AN [d]	5.04	0.89	25	1.0 [e]	1.0×10^7	1.0×10^7		Azide	34
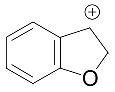	2.7	W	5.20	0.89	25	0.5 [e]	1.1×10^7	1.1×10^7		Azide	35
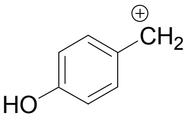	2.4	W	5.20	0.89	25	0.1 [c]	5.8×10^6	5.8×10^6		LF	33
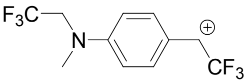	0.6	50T50W	3.57	0.89	22	0.5 [c]	3.3×10^4	1.2×10^5	3.0×10^{-1}	Azide	36
		80W20AN	5.04	0.89	22	0.8 [c]	2.0×10^4	5.7×10^3	3.0×10^{-1}	Azide	36
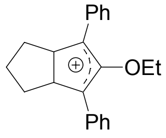	-2.5	M	7.54	0.92	20	–	4.3×10^3	4.3×10^3		LF	37

[a] Mixtures of solvents are given as (v/v), solvents: M = methanol, W = water, T = trifluoroethanol, AN = acetonitrile. [b] LF = laser flash photolysis, Azide = azide clock. [c] Ionic strength maintained with NaClO$_4$. [d] N_1 and s parameters of 80W20AN were used for calculation. [e] Ionic strength maintained with NaCl.

The 1,3-diphenylallyl cation listed in Table 4.7, which can be considered as a vinylogous benzhydryl cation, turned out to be 2.4 units less electrophilic than the parent benzhydrylium ion.

Because the 2-hydro-benzo[*b*]furanium ion is structurally analogous to 2-oxyphenylethyl cations, one can explain why its electrophilicity parameter (*E* = 2.7) differs by less than one unit from that of the 1-(2-hydroxyphenyl)ethyl cation (Table 4.1).

4.8 Xanthylium ions

Table 4.8: Rate constants for the reactions of xanthylium ions with solvents at 25 °C and electrophilicity parameters derived therefrom.

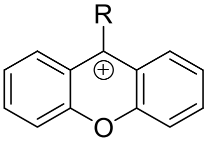

R	E	Solvent [a]	N_1	s	k_{exp}, s^{-1}	k_{calc}, s^{-1}	$\Delta^2 \log k$	Method [b]	Ref.
H	-0.4	80W20AN	5.04	0.89	2.3×10^{4} [c]	1.5×10^{4}	3.8×10^{-2}	LF	38
	-0.4	W	5.20	0.89	1.3×10^{4} [c]	2.0×10^{4}	3.8×10^{-2}	LF	8
4-$CF_3C_6H_4$	-3.3	80W20AN	5.04	0.89	3.4×10^{1}	3.4×10^{1}		LF	38
4-ClC_6H_4	-3.4	80W20AN	5.04	0.89	2.7×10^{1}	2.7×10^{1}		LF	38
Ph	-3.5	80W20AN	5.04	0.89	2.3×10^{1}	2.3×10^{1}		LF	38
3-$MeOC_6H_4$	-3.5	80W20AN	5.04	0.89	2.2×10^{1}	2.2×10^{1}		LF	38
4-FC_6H_4	-3.6	80W20AN	5.04	0.89	2.1×10^{1}	2.1×10^{1}		LF	38
3-MeC_6H_4	-3.6	80W20AN	5.04	0.89	1.9×10^{1}	1.9×10^{1}		LF	38
4-MeC_6H_4	-3.7	80W20AN	5.04	0.89	1.6×10^{1}	1.6×10^{1}		LF	38
4-$MeOC_6H_4$	-3.9	80W20AN	5.04	0.89	1.1×10^{1}	9.6	3.6×10^{-3}	LF	38
		50E50W	5.96	0.89	5.5×10^{1} [d]	6.3×10^{1}	3.6×10^{-3}	LF	39

[a] Mixtures of solvents are given as (v/v), solvents: E = ethanol, W = water, AN = acetonitrile. [b] LF = laser flash photolysis. [c] T = 20°C. [d] I = 0.1 ($NaClO_4$).

Scheme 4.7: Comparison of the electrophilicity parameters *E* of xanthylium ions.

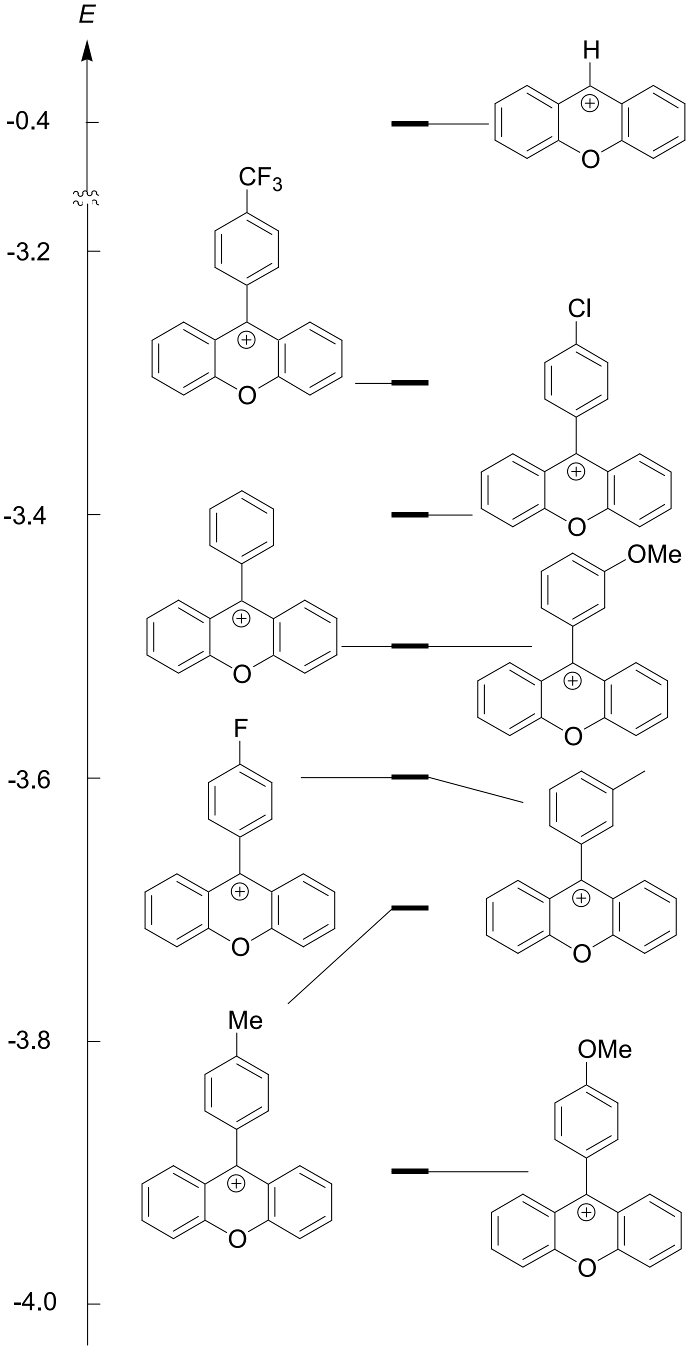

The parent xanthylium ion has previously been investigated with allyltrimethylsilane, one of our selected reference π-nucleophiles.[40] The *E* parameter derived from this experiment (E = -0.51) was proven to be suitable for calculating the rate constants for the reactions of the xanthylium ion with (triisopropylsiloxy)ethene and tributylsilane.[40] Table 4.8 shows that this *E* parameter also reproduces the reactivities toward water and 80% water/20% acetonitrile, but predicts smaller reactivities toward OH^- ($k_{calc} = 4.7 \times 10^6$ L mol^{-1} s^{-1}, $k_{obs} = 3.5 \times 10^7$ L mol^{-1} s^{-1}) and n-PrNH$_2$ ($k_{calc} = 2.8 \times 10^7$ L mol^{-1} s^{-1}, $k_{obs} = 2.8 \times 10^7$ L mol^{-1} s^{-1}) than experimentally observed.[41]

Variation of the aryl substituents in 9-arylxanthylium ions has little influence on the electrophilicity of these ions, as demonstrated by the small value of the slope (= 0.46) in the correlation depicted in Figure 4.5.

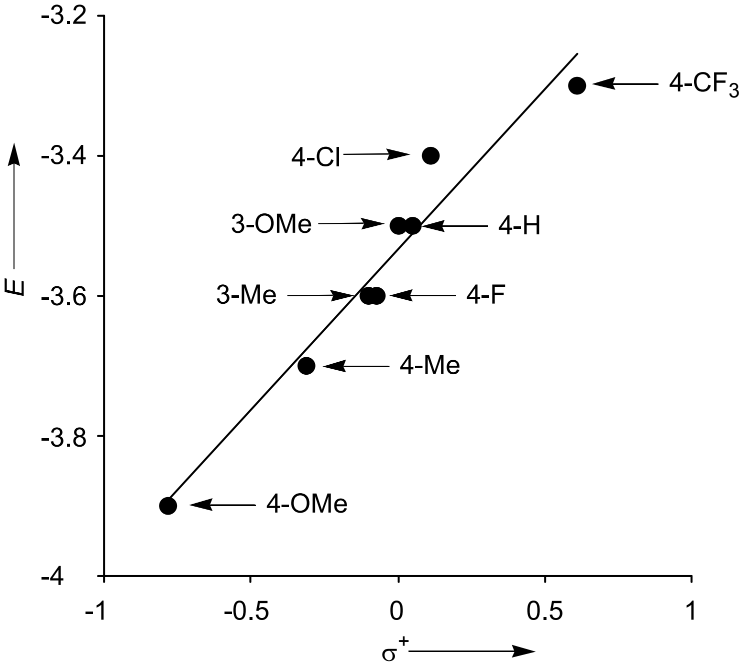

Figure 4.5: Correlation of the electrophilicity parameters *E* of 9-arylxanthylium ions with the Hammett σ^+-parameters.[14a] $E = 0.46\sigma^+ - 3.53$, n = 8, $R^2 = 0.950$.

The electrophilicities *E* of the 9-arylxanthylium ions derived from the reactions with solvents, particularly 80% water/20% acetonitrile, range between –3 and –4. Thus, they are approximately two units larger than *E* parameters derived from reactions with reference π-nucleophiles (*E* = -5.7 for 9-phenylxanthylim ion).[40] As discussed previously, such deviations are common in reactions of triarylcarbenium ions because of the greater steric demand of π-nucleophiles. Table 4.9 shows, however, that the *E*-parameters listed in Table 4.8 are suitable for calculating the rate constants of the reactions of 9-arylxanthylium ions with *n*-propylamine, hydroxide ion, and sulfite ion in aqueous acetonitrile.

Table 4.9: The reaction of 9-aryl-xanthylium ions with n-nucleophiles in 80W20AN at 25 °C.[38]

Ar	E	Nucleophile	N_1	s	k_{exp}, L mol $^{-1}$ s^{-1}	k_{calc}, L mol $^{-1}$ s^{-1}
4-$CF_3C_6H_4$	-3.3	n-$PrNH_2$	13.33	0.56	3.2×10^5	4.1×10^5
		SO_3^{2-}	16.83	0.56	2.5×10^7	3.8×10^7
		N_3^-	–	–	4.5×10^8	–
4-ClC_6H_4	-3.4	OH^-	10.47	0.61	7.2×10^4	2.1×10^4
		n-$PrNH_2$	13.33	0.56	2.5×10^5	3.6×10^5
		SO_3^{2-}	16.83	0.56	2.0×10^7	3.3×10^7
		N_3^-	–	–	3.0×10^8	–
Ph	-3.5	OH^-	10.47	0.61	3.5×10^4	1.8×10^4
		n-$PrNH_2$	13.33	0.56	1.7×10^5	3.2×10^5
		SO_3^{2-}	16.83	0.56	1.4×10^7	2.9×10^7
		N_3^-	–	–	1.7×10^8	–
3-$MeOC_6H_4$	-3.5	OH^-	10.47	0.61	3.6×10^4	1.8×10^4
		n-$PrNH_2$	13.33	0.56	1.8×10^5	3.2×10^5
		SO_3^{2-}	16.83	0.56	1.3×10^7	2.9×10^7
		N_3^-	–	–	1.8×10^8	–
4-FC_6H_4	-3.6	OH^-	10.47	0.61	3.4×10^4	1.6×10^4
		n-$PrNH_2$	13.33	0.56	2.1×10^5	2.8×10^5
		SO_3^{2-}	16.83	0.56	2.1×10^7	2.6×10^7
		N_3^-	–	–	2.2×10^8	–
3-MeC_6H_4	-3.6	OH^-	10.47	0.61	3.4×10^4	1.6×10^4
		n-$PrNH_2$	13.33	0.56	1.8×10^5	2.8×10^5
		SO_3^{2-}	16.83	0.56	1.0×10^7	2.6×10^7
4-MeC_6H_4	-3.7	OH^-	10.47	0.61	3.0×10^4	1.3×10^4
		n-$PrNH_2$	13.33	0.56	1.9×10^5	2.5×10^5
		SO_3^{2-}	16.83	0.56	8.5×10^6	2.3×10^7
		N_3^-	–	–	1.4×10^7	–
4-$MeOC_6H_4$	-3.9	OH^-	10.47	0.61	2.6×10^4	1.0×10^4
		n-$PrNH_2$	13.33	0.56	1.6×10^5	1.9×10^5
		SO_3^{2-}	16.83	0.56	8.9×10^6	1.7×10^7
		N_3^-	–	–	8.8×10^7	–

4.9 Miscellaneous benzhydryl cations

In Chapter 3 the rate constants of the reactions of reference benzhydrylium ions with solvents have been employed for determining solvent nucleophilicity parameters. Table 4.10 lists rate constants for the reactions of solvents with benzhydrylium ions which have not been used in Chapter 3.

For the 4-hydroxy-4'-methoxybenzhydrylium ion, an E value (0.1) almost identical to that of the bis(4-methoxy)benzhydrylium ion is calculated. It should be noted, however, that a direct comparison of rate constants would lead to a different result. Thus the bis(4-methoxy)benzhydrylium ion reacts two times faster with water than the 4-hydroxy-4'-methoxybenzhydrylium ion. This example again demonstrates that small differences in E are not significant, if they refer to reactions with different reference nucleophiles.

The comparison of the last and the third-last entries in Table 4.10 shows that 4-hydroxy-substitution reduces electrophilicity by one order of magnitude more than 2-hydroxy substitution. It should be noted, however, that part of this difference is due to the difference of ionic strength in the two experiments.

The first two entries show that 1-naphthyl stabilizes the carbocation better than 2-naphthyl, in accord with the relative magnitude of the corresponding σ^+ arene parameters.[14a]

Table 4.10: Rate constants for the reactions of miscellaneous benzhydrylium ions with solvents and electrophilicity parameters derived therefrom.

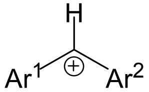

Ar^1	Ar^2	*E*	Solvent [a]	N_1	*s*	*T*, °C	*I*,[b]	k_{exp}, s^{-1}	k_{calc}, s^{-1}	$\Delta^2 \log k$	Method [c]	Ref.
Ph	2-naphthyl	5.7	T	1.23	0.92	RT	–	2.2×10^6	2.2×10^6		LF	42
Ph	1-naphthyl	4.6	T	1.23	0.92	?	–	2.3×10^5	2.3×10^5		LF	20
Ph	4-PhC_6H_4	4.6	T	1.23	0.92	?	–	2.2×10^5	2.2×10^5		LF	20
Ph	2-Fluorenyl	2.9	W	5.20	0.89	20	–	1.5×10^7	1.5×10^7		LF	43
Ph	2-HOC_6H_4	2.4	W	5.20	0.89	25	0.1	5.6×10^6	5.6×10^6		LF	13
4-$MeOC_6H_4$	4-$CF_3C_6H_4$	2.4	80W20AN	5.04	0.89	25	–	4.0×10^6	4.4×10^6	2.1×10^{-3}	LF	44a
			10W90AN	4.56	0.94	25	–	4.1×10^6	3.7×10^6	1.9×10^{-3}	LF	44a
4-$MeOC_6H_4$	2-naphthyl	1.2	95W5AN[d]	5.16	0.91	RT	–	1.4×10^6	6.2×10^5	1.2×10^{-1}	LF	42
			M	7.54	0.92	RT	–	5.0×10^7	1.1×10^8	1.2×10^{-1}	LF	42
4-$MeOC_6H_4$	2-HOC_6H_4	1.2	W	5.20	0.89	25	0.1	5.2×10^5	5.2×10^5		LF	13
Ph	(4-MeO-1-naphthyl)	0.4	90W10AN	5.16	0.91	RT	–	1.4×10^5	1.2×10^5	5.7×10^{-3}	LF	42
			M	7.54	0.92	RT	–	9.5×10^6	2.1×10^7	1.2×10^{-1}	LF	42
			20T80W	4.78	0.83	RT	–	4.0×10^4	2.0×10^4	8.6×10^{-2}	LF	42
4-$MeOC_6H_4$	4-HOC_6H_4	0.1	W	5.20	0.89	20	1.0	5.4×10^4	5.4×10^4		LF	44b

[a] Mixtures of solvents are given as (v/v), solvents: M = methanol, W = water, T = trifluoroethanol, AN = acetonitrile. [b] Ionic strength maintained with $NaClO_4$ [c] LF = laser flash photolysis. [d] N_1 and *s* parameters of 91W9AN were used for calculation.

4.10 1,1-Diarylethyl cations and 9,10-dihydroanthracene-9-ylium ions

Because 1,1-diarylethyl cations and 9,10-dihydroanthracene-9-ylium ions may undergo different types of reactions with nucleophiles, as shown in Scheme 4.8 the interpretation of the data is problematic.

Scheme 4.8: Reaction of 1,1-diarylethyl cations with nucleophiles

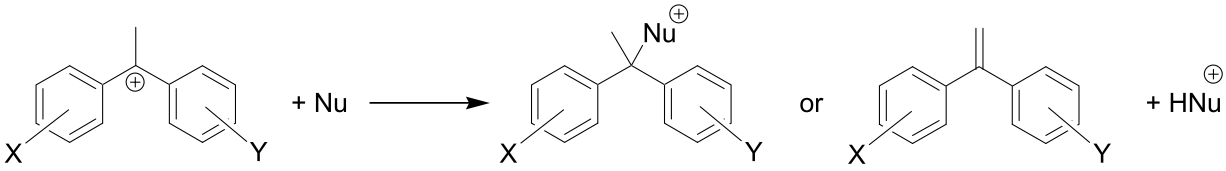

While a reduction of electrophilicity from the parent benzhydrylium ion (E = 5.9)[1] to the 1,1-diphenylethyl cation (E = 4.8) is in line with expectations, the increase of electrophilicity from bis(4-methoxy)benzhydrylium ion (E = 0.0)[1] to the 1,1-bis(4-methoxyphenyl)ethylium ion (E = 1.1) may be due to the fact that the two carbocations react differently (Tables 4.11 and 4.12): bis(4-methoxy)benzhydrylium ion as a Lewis acid and 1,1-bis(4-methoxyphenyl)ethylium ions a Brønsted acid (Scheme 4.8).

Table 4.11: Rate constants for the reactions of 1,1-diarylethyl cations with solvents and electrophilicity parameters derived therefrom.

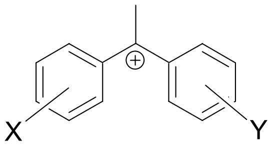

X	Y	E	Solvent [a]	N_1	s	T, °C	I,	k_{exp}, s^{-1}	k_{calc}, s^{-1}	$\Delta^2 \log k$	Method [b]	Ref.
H	H	(4.8)	T	1.23	0.92	20	–	1.5×10^{5}	3.5×10^{5}	1.4×10^{-1}	LF	6
			50T50W	3.57	0.89	25	0.5 [c]	6.8×10^{7}	2.8×10^{7}	1.5×10^{-1}	Azide	15
H	4-MeO	(1.7)	T	1.23	0.92	20	–	5.1×10^{2}	5.1×10^{2}		LF	6
4-MeO	4-MeO	(1.1)	T	1.23	0.92	20	–	1.3×10^{2}	1.3×10^{2}		LF	6

[a] Mixtures of solvents are given as (v/v), solvents: W = water, T = trifluoroethanol. [b] LF = laser flash photolysis, Azide = azide clock. [c] Ionic strength is maintained with $NaClO_4$.

On the other hand, both 9,10-dihydroanthracene-9-ylium ions listed in Table 4.12 have been found to undergo addition reactions exclusively, and we cannot explain, why the methyl substituted derivative is considerably more electrophilic (E = 4.3) than the parent cation (E = 2.8). For that reason, a reexamination of the kinetic data is suggested.

Table 4.12: Rate constants for the reactions of 9,10-dihydroanthracene-9-ylium ions with solvents and electrophilicity parameters derived therefrom.

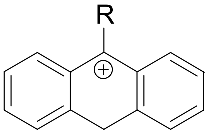

R	E	Solvent [a]	N_1	s	T, °C	I,	k_{exp}, s^{-1}	Method [b]	Ref.
H	2.8	W	5.20	0.89	25		1.3×10^7	Azide	35
Me	4.3	50W50AN	5.05	0.89	25	0.1-0.5	2.2×10^8	Azide	45

[a] Mixtures of solvents are given as (v/v), solvents: W = water, AN = acetonitrile. [b] Azide = azide clock.

4.11 9-Fluorenyl cations

Because of the presence of an antiaromatic five-membered ring, 9-fluorenyl cations are strong electrophiles (Table 4.13 and Scheme 4.9), and the calculated E-parameter of 8.4 for the parent 9-fluorenyl cation may even be too small because it is derived from a first-order rate constant of 8.0×10^8 s^{-1} for its reaction with trifluoroethanol.

Unlike in the 4-methoxybenzyl series (Scheme 4.3), the *N,N*-dimethylthiocarbamoyl group has a relatively weak stabilizing effect on the fluorenyl cation (ΔE = -3.8, Table 4.13), and the origin for this discrepancy is not yet clear.

Table 4.13: Rate constants for the reactions of 9-fluorenyl cations with solvents at 20 °C and electrophilicity parameters derived therefrom.

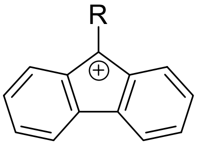

R	E	Solvent [a]	N_1	s	k_{exp}, s^{-1}	k_{calc}, s^{-1}	$\Delta^2 \log k$	Method [b]	Ref.
H	8.4	T	1.23	0.92	8.0×10^8	8.0×10^8		LF	46
Me	6.4	50T50W	3.57	0.89	$7.7\times10^{8\,c}$	7.7×10^8		Azide	15
C(S)NMe$_2$	4.6	T	1.23	0.92	2.4×10^5	2.4×10^5		LF	47
4-CF$_3$C$_6$H$_4$	4.2	T	1.23	0.92	1.0×10^5	1.0×10^5		LF	48
3-CF$_3$C$_6$H$_4$	4.1	T	1.23	0.92	8.2×10^4	8.2×10^4		LF	48
3-ClC$_6$H$_4$	3.6	T	1.23	0.92	4.2×10^4	2.9×10^4	2.5×10^{-2}	LF	48
		80W20AN	5.05	0.89	3.6×10^7	5.2×10^7	2.7×10^{-2}	LF	48
4-ClC$_6$H$_4$	3.2	T	1.23	0.92	1.6×10^4	1.3×10^4	1.1×10^{-2}	LF	48
		80W20AN	5.05	0.89	1.8×10^7	2.3×10^7	1.2×10^{-2}	LF	48
3-MeOC$_6$H$_4$	3.2	T	1.23	0.92	1.6×10^4	1.2×10^4	1.7×10^{-2}	LF	48
		80W20AN	5.05	0.89	1.6×10^7	2.2×10^7	1.8×10^{-2}	LF	48
Ph	3.2	T	1.23	0.92	1.5×10^4	1.1×10^4	1.7×10^{-2}	LF	48
		80W20AN	5.05	0.89	1.5×10^7	2.1×10^7	1.9×10^{-2}	LF	48
3-MeC$_6$H$_4$	3.0	T	1.23	0.92	9.5×10^3	7.5×10^3	1.1×10^{-2}	LF	48
		80W20AN	5.05	0.89	1.1×10^7	1.4×10^7	1.1×10^{-2}	LF	48
4-MeC$_6$H$_4$	2.6	T	1.23	0.92	4.1×10^3	3.1×10^3	1.6×10^{-2}	LF	48
		80W20AN	5.05	0.89	4.4×10^6	5.9×10^6	1.7×10^{-2}	LF	48
4-MeOC$_6$H$_4$	1.0	T	1.23	0.92	1.8×10^2	1.2×10^2	3.1×10^{-2}	LF	48
		80W20AN	5.05	0.89	1.7×10^5	2.6×10^5	3.3×10^{-2}	LF	48

[a] Mixtures of solvents are given as (v/v), solvents: W = water, T = trifluoroethanol, AN = acetonitrile. [b] LF = laser flash photolysis, Azide = azide clock. [c] 25°C, I = 0.5 (NaClO$_4$).

Scheme 4.9: Comparison of the electrophilicity parameters *E* of 9-fluorenyl cations.

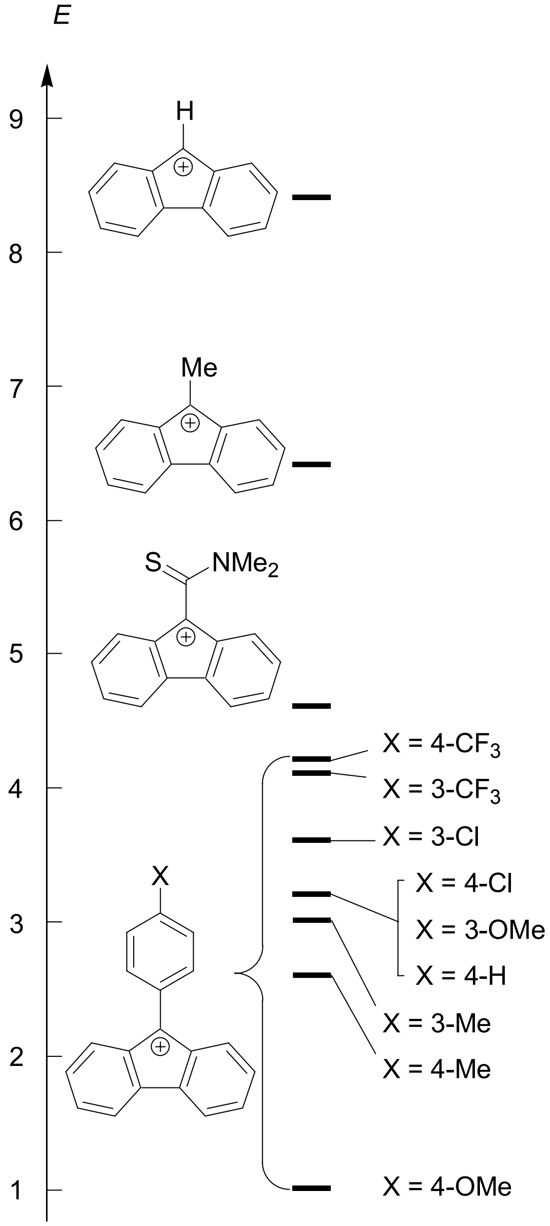

Many of the *E*-parameters of the 9-aryl substituted fluorenyl cations are based on the kinetics of their reactions with solvents of significantly different nucleophilicity. The good agreement between calculated and experimental values demonstrates the reliability of the calculated *E*-parameters. Because of the larger electron-deficiency of the fluorenyl system compared with the 4-methoxybenzyl system, replacement of 9-H by methyl or phenyl has a somewhat greater influence on electrophilicity than in the 4-methoxybenzyl series (Scheme 4.10).

Scheme 4.10: Comparison of the electrophilicity parameters *E* of 9-fluorenyl cations and 4-methoxybenzyl cations.

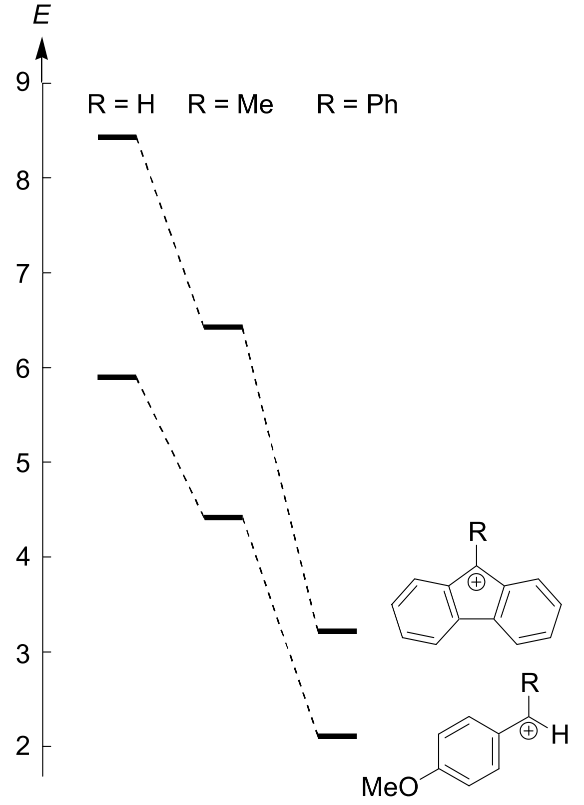

The moderate Hammett correlation in Figure 4.6 has a higher slope than in the 9-arylxanthylium series but a smaller slope than in the 1-arylethyl and cumyl series which reflects the relative electron demand in the four series (Table 4.14).

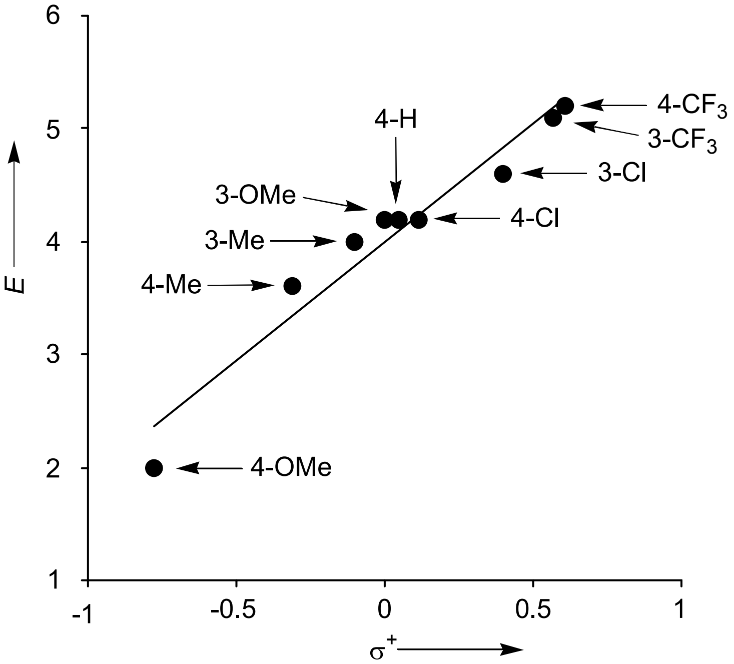

Figure 4.6: Correlation of the electrophilicity parameters *E* of 9-arylfluorenyl cations with the Hammett σ^+-parameters.[14a] $E = 2.10\sigma^+ + 2.99$, n = 9, $R^2 = 0.950$.

Table 4.14: Caparison of slopes of correlations between *E* and Hammett σ^+ for 1-arylethyl cations, cumyl cations, 9-arylfluorenyl cations, and 9-arylxanthylium ions.

	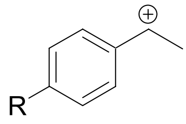	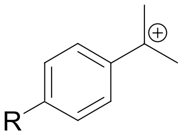	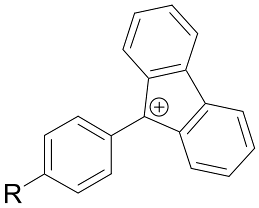	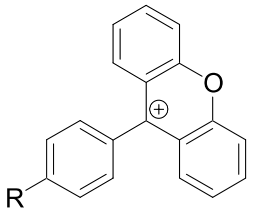
E (R = OMe)	4.4	3.5	1.0	-3.9
Slope	6.2	6.3	2.1	0.5

4.12 Vinyl cations

Numerous kinetic investigations have dealt with the reactions of vinyl cations with small concentrations of alcohols in acetonitrile solution.[49] The second-order rate constants derived from these experiments have already indicated relatively low electrophilicities of vinyl cations.

Correspondingly, the 4-methoxyphenyl substituted vinyl cations shown in Table 4.15 show electrophilicities comparable to those of 4-methoxy-cumyl cations and 1-(4-methoxyphenyl)ethyl cations (Scheme 4.11). This behavior is remarkable in view of the extremely slow formation of vinyl cations in S_N1 type reactions. One has to conclude, therefore, that additions of nucleophiles to sp-hybridized carbocations have significantly larger intrinsic barriers than the corresponding additions to sp^2-hybridized carbocations.

Table 4.15: Rate constants for the reactions of vinyl cations with solvents and electrophilicity parameters derived therefrom.

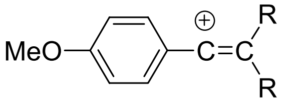

R	*E*	Solvent [a]	N_1	*s*	*T*, °C	k_{exp}, s^{-1}	Method [b]	Ref.
H	5.4	T	1.23	0.92	?	1.3×10^6	LF	9
Me	4.6	T	1.23	0.92	20	2.3×10^5	LF	6
Ph	3.3	T	1.23	0.92	20	1.4×10^4	LF	6
9-Fluorenylidene	1.1	E	7.44	0.90	20	5.0×10^7	LF	50

[a] E = ethanol, T = trifluoroethanol. [b] LF = laser flash photolysis.

Scheme 4.11: Comparison of the electrophilicity parameters *E* of vinyl cations with analogously substituted benzyl cations.

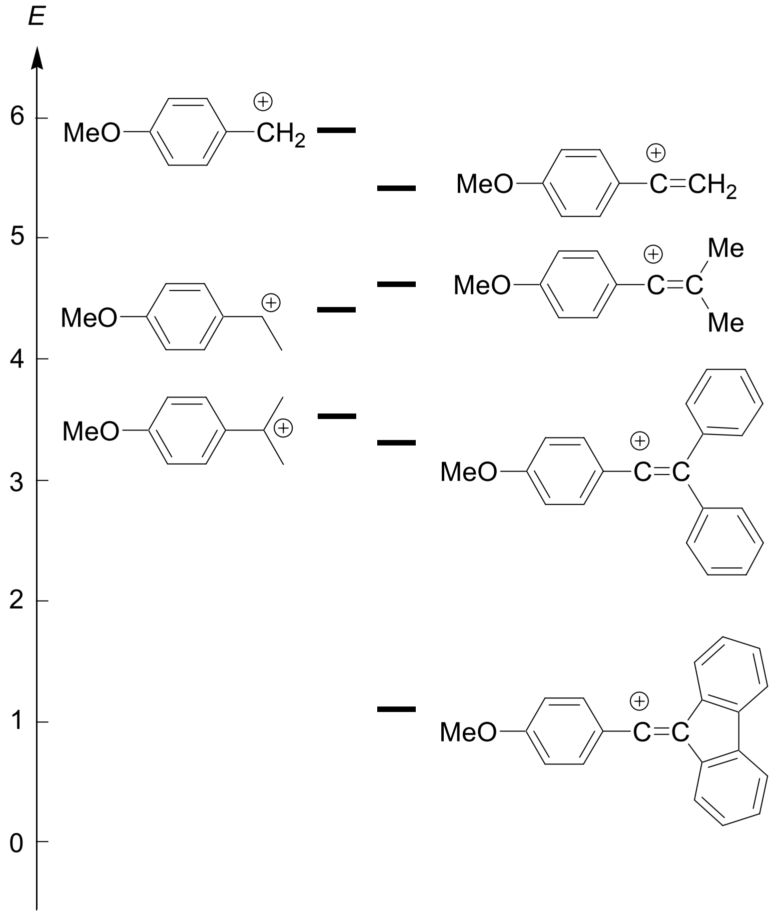

Bromide ions in trifluoroethanol even react faster with the 1-(4-methoxyphenyl)ethyl cation (4.5 × 10^9 L mol^{-1} s^{-1})[6] than with the structurally analogous vinyl cations, 1-(4-methoxyphenyl)vinyl cation (2.3 × 10^9 L mol^{-1} s^{-1})[6] and 1-(4-methoxyphenyl)-2,2-dimethyl-vinyl cation (2.2 × 10^8 L mol^{-1} s^{-1}), [6] again emphasizing the large intrinsic barriers for sp/sp^2 rehybridizations.

4.13 Alkoxy and siloxycarbenium ions

While the E-parameters derived in the preceding sections appeared to be applicable to reactions of different types of nucleophiles, the limited validity of the E-parameters of carboxonium ions is obvious. While reactions with π_{CC}-nucleophiles yielded an electrophilicity parameter of $E = 0.14$ for the α,4-dimethoxybenzyl cation,[1] Table 4.16 shows that a considerably higher reactivity ($E = 4.8$) is derived from its reactions with aqueous trifluoroethanol. This strong discrepancy can be explained by the high stability of the products obtained by addition of O-nucleophiles to alkoxy-carbenium ions. The anomeric stabilization of the resulting acetals is already realized in the transition states of the additions of O-nucleophiles to alkoxy-carbenium ions.

Table 4.16: Rate constants for the reactions of alkoxy and siloxycarbenium ions with solvents and electrophilicity parameters derived therefrom.

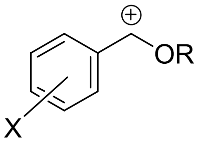

X	R	E	Solvent [a]	N_1	s	T, °C	I,[b]	k_{exp}, s^{-1}	Method [c]	Ref.
H	*Me*		*W*	*5.20*	*0.89*	*25*	2.0	2.0×10^{9}	*Azide*	*51*
4-OMe	CH_2CF_3	6.5	50T50W	3.57	0.89	25	0.5	8.3×10^{8}	Azide	52
H	$SiMe_3$	6.4	T	1.23	0.92	20	–	1.0×10^{7}	LF	53
2-naphthyl	$SiMe_3$	5.9	T	1.23	0.92	20	–	4.0×10^{6}	LF	53
4-Me	$SiMe_3$	5.6	T	1.23	0.92	20	–	2.0×10^{6}	LF	53
4-OMe	Me	4.8	50T50W	3.57	0.89	25	0.5	3.0×10^{7}	Azide	54
4-OMe	$SiMe_3$	4.5	T	1.23	0.92	20	–	2.0×10^{5}	LF	53

[a] Mixtures of solvents are given as (v/v), solvents: W = water, T = trifluoroethanol, AN = acetonitrile. [b] Ionic strength maintained with $NaClO_4$ [c] LF = laser flash photolysis, Azide = azide clock.

α-Trimethylsiloxybenzyl cations have been obtained by irradiation of α-trimethylsilylketones. As shown in Scheme 4.12, the intermediate aryl(trimethylsiloxy)carbenes are protonated by the solvent trifluoroethanol to give the corresponding carbenium ions.[53]

Scheme 4.12

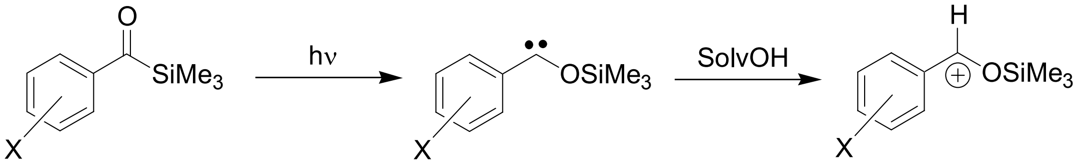

Their reactivity towards alcohols is comparable to that of analogous methoxy substituted carbocations (last two entries in Table 4.16), indicating a comparable carbenium-stabilizing effect of trimethylsiloxy and methoxy. A similar conclusion has previously been drawn from the similar nucleophilicities of trimethylsiloxy- and alkoxy-substituted ethenes.[55]

The small reaction parameter $\rho = 2.43$, i.e., the slope of the Hammett correlation in Figure 4.7 indicates a small electron-demand of the carbocationic centers, in agreement with the small *E*-value for the α,4-dimethoxybenzyl cation (0.14) derived from its reactions with π-nucleophiles (cf. Table 4.14).

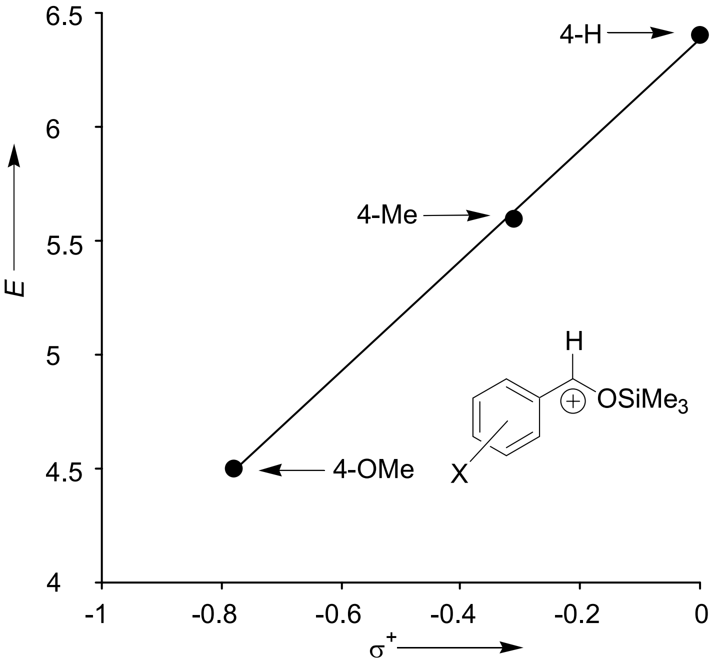

Figure 4.7: Correlation of the electrophilicity parameters *E* of 1-trimethylsiloxy-1-arylmethyl cations with the Hammett σ^+-parameters.[14a] $E = 2.43\sigma^+ + 6.38$, n = 3, $R^2 = 0.999$.

Taking account of a comparable carbenium-stabilizing effect of trimethylsiloxy and methoxy, α-methoxyarylethyl cations are less electrophilic than the corresponding α-methoxybenzyl cations approximately 2 units in *E* (Table 4.17).

Table 4.17: Rate constants for the reactions of α-methoxyarylethyl cations with solvents at 25°C and electrophilicity parameters derived therefrom.

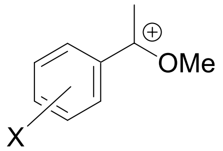

X	E	Solvent [a]	N_1	s	I,	k_{exp}, s^{-1}	k_{calc}, s^{-1}	Method [b]	Ref.
4-Br	4.3	W	5.20	0.89	1.0 [c]	3.0×10^{8}	3.0×10^{8}	Sulfite	56
4-Cl	4.2	W	5.20	0.89	1.0 [c]	2.1×10^{8}	2.1×10^{8}	Sulfite	56
					–	*1.3×10^{8}*	*2.1×10^{8}*	*Hydrolysis in H_2SO_4*	*57*
H	3.8	W	5.20	0.89	1.0 [c]	9.5×10^{7}	9.5×10^{7}	Sulfite	56
					0.5 [d]	*5.0×10^{7}*	*9.5×10^{7}*	*Azide*	*51*
					–	*5.0×10^{7}*	*9.5×10^{7}*	*Hydrolysis in H_2SO_4*	*57*
4-Me	3.5	W	5.20	0.89	1.0 [c]	5.0×10^{7}	5.0×10^{7}	Sulfite	56
					–	*1.0×10^{7}*	*5.0×10^{7}*	*Hydrolysis in H_2SO_4*	*57*
4-OMe	2.5	W	5.20	0.89	1.0 [c]	7.0×10^{6}	7.0×10^{6}	Sulfite	56
					–	*1.4×10^{6}*	*7.0×10^{6}*	*Hydrolysis in H_2SO_4*	*57*

[a] W = water. [b] Sulfite = sulfite clock, Azide = azide clock. [c] Ionic strength maintained with KCl [d] Ionic strength maintained with $NaClO_4$.

In view of the low reactivity difference between cumyl and 1-phenylethyl cations, the interaction of an α-methyl group in an α-methoxybenzyl cation appears to be relatively high (Scheme 4.13).

Scheme 4.13

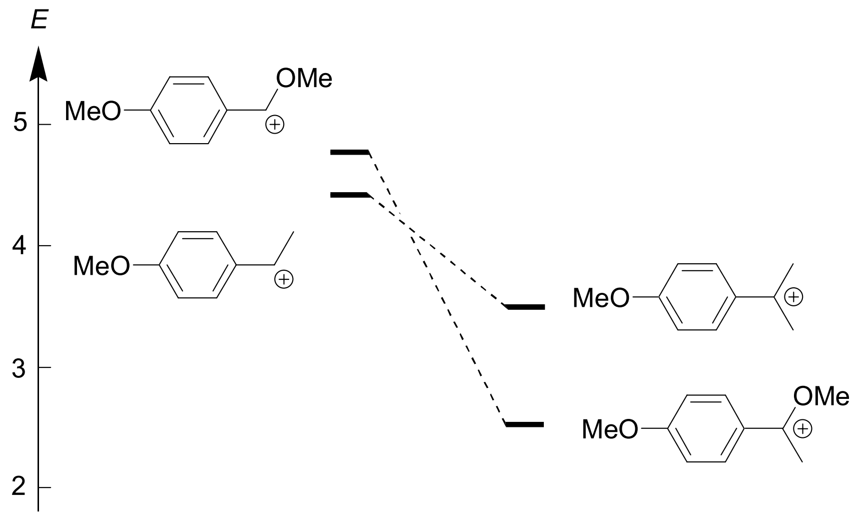

In agreement with the reduced electron demand due to the extra methyl group, the slope of the Hammett correlation in Figure 4.8 is even smaller than that in Figure 4.7.

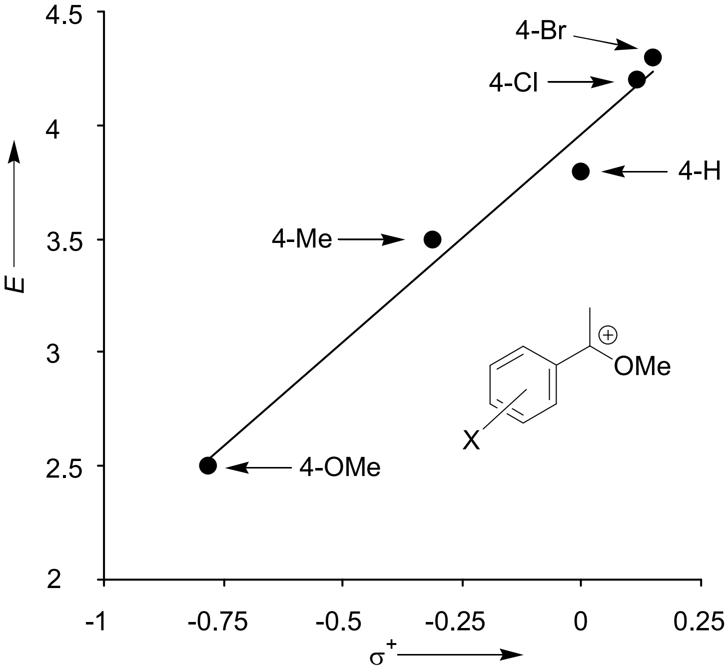

Figure 4.8: Correlation of the electrophilicity parameters E of 1-methoxy-1-arylethyl cations with the Hammett σ^+-parameters.[14a] $E = 1.84\sigma^+ + 3.96$, n = 5, $R^2 = 0.979$.

Exchange of the methyl group in the carboxonium ions of Table 4.17 by α-methoxy yields α,α-dimethoxybenzyl cations, which reduces electrophilicities by approximately 3 units (Table 4.18).

Remarkably, dimethoxycarbenium ions with a phenyl or methyl group as the third substituent possess almost identical electrophilicities. The slightly higher electrophilicity of the *t*-butyl-dimethoxycarbenium ion compared with that of the methyl-dimethoxycarbenium ion may be explained by disturbed resonance stabilization of the *t*-butyl substituted carbocation.

Table 4.18: Rate constants for the reactions of α,α-dimethoxycarbenium ions with solvents and electrophilicity parameters derived therefrom.

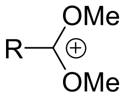

R	*E*	Solvent [a]	N_1	*s*	*T*, °C	k_{exp}, s^{-1}	k_{calc}, s^{-1}	$\Delta^2 \log k$	Method [b]	Ref.
$4\text{-}NO_2C_6H_4$	2.8	W	5.20	0.89	25	1.3×10^{7}	1.3×10^{7}		Hydrolysis in H_2SO_4	57
$3\text{-}ClC_6H_4$	1.6	W	5.20	0.89	25	1.0×10^{6}	1.0×10^{6}		Hydrolysis in H_2SO_4	57
i-Pr	1.5	W	5.20	0.89	20	7.6×10^{5}	8.3×10^{5}	1.6×10^{-3}	LF	58
		67W33AN [c]	5.05	0.90	20	7.8×10^{5}	7.1×10^{5}	1.6×10^{-3}	LF	59
t-Bu	1.3	W	5.20	0.89	20	6.2×10^{5}	6.2×10^{5}		LF	58
s-Bu	1.3	W	5.20	0.89	20	6.0×10^{5}	6.0×10^{5}		LF	58
$4\text{-}ClC_6H_4$	1.1	W	5.20	0.89	25	4.5×10^{5}	4.5×10^{5}		Hydrolysis in H_2SO_4	57
i-Bu	0.7	W	5.20	0.89	20	1.9×10^{5}	1.9×10^{5}		LF	58
Me	0.7	W	5.20	0.89	20	1.3×10^{5}	1.7×10^{5}	1.1×10^{-2}	LF	58
		67W33AN [c]	5.12	0.89	20	1.8×10^{5}	1.4×10^{5}	1.1×10^{-2}	LF	59
n-Bu	0.6	W	5.20	0.89	20	1.6×10^{5}	1.6×10^{5}		LF	58
Et	0.6	W	5.20	0.89	20	1.5×10^{5}	1.5×10^{5}		LF	58
n-Pr	0.5	W	5.20	0.89	20	1.2×10^{5}	1.2×10^{5}		LF	58
Ph	0.5	60W40AN [d]	5.05	0.90	20	1.3×10^{5}	1.0×10^{5}	9.1×10^{-3}	LF	59
		W	5.20	0.89	20	1.0×10^{5}	1.2×10^{5}	9.3×10^{-3}	LF	59
		W	*5.20*	*0.89*	*25*	$\mathit{1.1\times10^{5}}$	$\mathit{1.2\times10^{5}}$	1.4×10^{-3}	*Hydrolysis in* H_2SO_4	*57*
$4\text{-}MeC_6H_4$	-0.1	W	5.20	0.89	25	3.5×10^{4}	3.5×10^{4}		Hydrolysis in H_2SO_4	57
$4\text{-}MeOC_6H_4$	-0.5	W	5.20	0.89	25	1.7×10^{4}	1.7×10^{4}		Hydrolysis in H_2SO_4	57

[a] Mixtures of solvents are given as (v/v), solvents: W = water, AN = acetonitrile. [b] LF = laser flash photolysis. [c] Precise water content of the aqueous acetonitrile (50-80% water) is not given in the literature. [d] N_1 and *s* parameters of 67W33AN were used for calculation.

The close slope of the *E* versus σ^+ lot in Figure 4.9 indicates a similar electron demand of α,α-dimethoxybenzyl cations to that of α-methoxy- α-methyl benzyl cations (Figure 4.8).

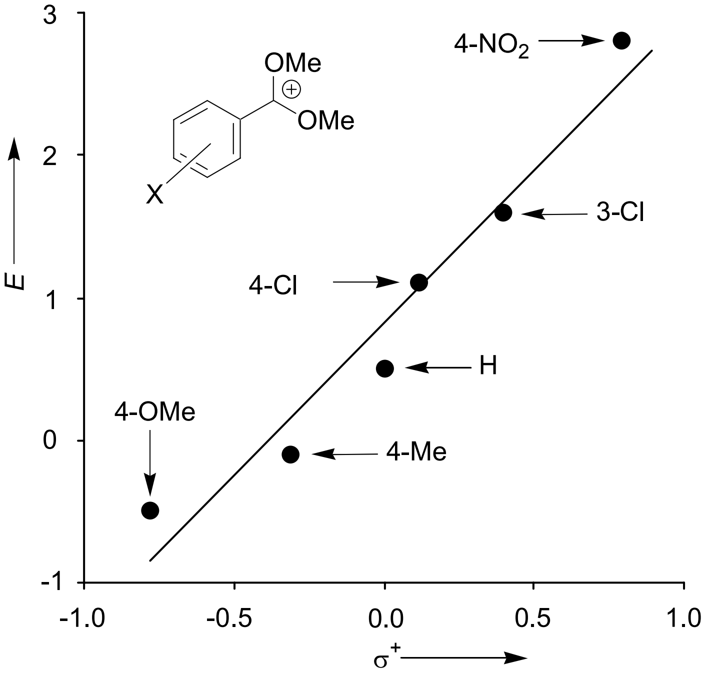

Figure 4.9: Correlation of the electrophilicity parameters E of α,α-dimethoxycarbenium ions with the Hammett σ^{+}-parameters.[14a] $E = 2.15\sigma^{+} + 0.82$, n = 6, $R^2 = 0.948$.

Generally, α,α-diethoxycarbenium ions are less electrophilic than the corresponding α,α-dimethoxycarbenium ions by 0.5-1 units in E (Table 4.19). Their reactivities are closely similar to those of 2-alkoxy-tetrahydrofuran-2-ylium ions (Table 4.20).

Table 4.19: Rate constants for the reactions of α,α-diethoxycarbenium ions with solvents and electrophilicity parameters derived therefrom.

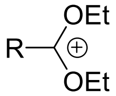

R	E	Solvent [a]	N_1	s	T, °C	k_{exp}, s^{-1}	k_{calc}, s^{-1}	$\Delta^2 \log k$	Method [b]	Ref.
H	3.1	67W33AN[c]	5.05	0.90	20	2.0×10^{7}	2.0×10^{7}		LF	59
i-Pr	0.2	W	5.20	0.89	20	6.7×10^{4}	6.7×10^{4}		LF	58
t-Bu	0.2	W	5.20	0.89	20	6.5×10^{4}	6.5×10^{4}		LF	58
Ph	0.1	67W33AN[c]	5.05	0.90	20	4.3×10^{4}	4.3×10^{4}		LF	59
Me	-0.1	W	5.20	0.89	20	2.8×10^{4}	3.1×10^{4}	2.5×10^{-3}	LF	58
		67W33AN[c]	5.05	0.90	20	2.9×10^{4}	2.6×10^{4}	2.5×10^{-3}	LF	59
Et	-0.2	W	5.20	0.89	20	2.8×10^{4}	2.8×10^{4}		LF	58

Table 4.19: Continued

R	*E*	Solvent [a]	N_1	*s*	*T*, °C	k_{exp}, s^{-1}	k_{calc}, s^{-1}	$\Delta^2 \log k$	Method [b]	Ref.
n-Pr	-0.3	W	5.20	0.89	20	2.3×10^4	2.3×10^4		LF	58
4-MeOC$_6$H$_4$	-1.8	W	5.20	0.89	25	1.1×10^3	1.1×10^3		Hydrolysis in H_2SO_4	57

[a] Mixtures of solvents are given as (v/v), solvents: W = water, AN = acetonitrile. [b] LF = laser flash photolysis. [c] Precise water content of the aqueous acetonitrile (50-80% water) is not given in the literature.

Table 4.20: Rate constants for the reactions of 2-alkoxy-tetrahydrofuran-2-ylium ions with solvents at 20 °C and electrophilicity parameters derived therefrom.

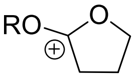

R	*E*	Solvent [a]	N_1	*s*	k_{exp}, s^{-1}	Method [b]	Ref.
Me	0.5	W	5.20	0.89	1.2×10^5	LF	58
Et	0.0	W	5.20	0.89	4.0×10^4	LF	58
i-Pr	-0.8	W	5.20	0.89	8.8×10^3	LF	58

[a] W = water. [b] LF = laser flash photolysis.

The electrophilicity of 2-alkoxy-oxan-2-ylium ions are almost the same as those of the corresponding five-membered ring dialkoxycarbenium ions (Table 4.21)

Table 4.21: Rate constants for the reactions of 2-alkoxy-oxan-2-ylium ions with solvents at 20 °C and electrophilicity parameters derived therefrom.

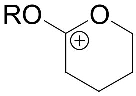

R	*E*	Solvent [a]	N_1	*s*	k_{exp}, s^{-1}	Method [b]	Ref.
Me	0.5	W	5.20	0.89	1.3×10^5	LF	58
Et	0.2	W	5.20	0.89	6.4×10^4	LF	58
i-Pr	-0.3	W	5.20	0.89	2.4×10^4	LF	58

[a] W = water. [b] LF = laser flash photolysis.

As shown in Table 4.22, a further reduction of electrophilicity by approximately one unit (relative to 1,1-diethoxy-carbenium ions) is found in α,α-diisopropoxycarbenium ions.

Table 4.22: Rate constants for the reactions of α,α-diisopropoxycarbenium ions with solvents at 20 °C and electrophilicity parameters derived therefrom.

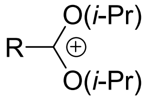

R	E	Solvent [a]	N_1	s	k_{exp}, s^{-1}	Method [b]	Ref.
H	2.0	67W33AN[c]	5.05	0.90	2.2×10^6	LF	59
Me	-1.5	W	5.20	0.89	2.0×10^3	LF	58

[a] Mixtures of solvents are given as (v/v), solvents: W = water, AN = acetonitrile. [b] LF = laser flash photolysis. [c] Precise water content of the aqueous acetonitrile (50-80% water) is not given in the literature.

Dialkoxycarbenium ions, where both oxygens are within a six-membered ring (1,3-dioxan-2-ylium ions) possess similar electrophilicities as acyclic α,α-diethoxycarbenium ions, but now, the phenyl substituted compound is less electrophilic than the alkyl substituted analogs which are closely similar to each other.

Table 4.23: Rate constants for the reactions of 1,3-dioxan-2-ylium ions with solvents at 20 °C and electrophilicity parameters derived therefrom.

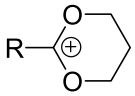

R	E	Solvent [a]	N_1	s	k_{exp}, s^{-1}	k_{calc}, s^{-1}	$\Delta^2 \log k$	Method [b]	Ref.
Me	0.7	W	5.20	0.89	1.4×10^5	1.7×10^5	8.7×10^{-3}	LF	58
		67W33AN[c]	5.05	0.90	1.8×10^5	1.5×10^5	8.5×10^{-3}	LF	59
i-Pr	0.6	W	5.20	0.89	1.6×10^5	1.6×10^5		LF	58
Et	0.6	W	5.20	0.89	1.4×10^5	1.4×10^5		LF	58
t-Bu	0.4	W	5.20	0.89	9.3×10^4	9.3×10^4		LF	58
Ph	-1.1	W	5.20	0.89	4.7×10^3	4.7×10^3		LF	59

[a] Mixtures of solvents are given as (v/v), solvents: W = water, AN = acetonitrile. [b] LF = laser flash photolysis. [c] Precise water content of the aqueous acetonitrile (50-80% water) is not given in the literature.

When both oxygen atoms are within a five-membered ring (1,3-dioxolan-2-ylium ions), electrophilicity increases by approximately one unit in *E* compared to six-membered ring compounds, but again, unlike in acyclic dialkoxycarbenium ions, the phenyl substituted compound is considerably less electrophilic than the alkyl substituted analogues, because in cyclic systems, coplanarity of the phenyl ring can be achieved.

Table 4.24: Rate constants for the reactions of 1,3-dioxolan-2-ylium ions with solvents and electrophilicity parameters derived therefrom.

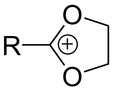

R	*E*	Solvent [a]	N_1	*s*	*T*, °C	*I*,	k_{exp}, s^{-1}	k_{calc}, s^{-1}	$\Delta^2 \log k$	Method [b]	Ref.
i-Pr	1.9	67W33AN[c]	5.05	0.90	20	–	1.8×10^6	1.8×10^6		LF	59
t-Bu	1.8	W	5.20	0.89	20	–	1.5×10^6	1.6×10^6	1.1×10^{-3}	LF	58
		67W33AN[c]	5.05	0.90	20	–	1.5×10^6	1.4×10^6	1.1×10^{-3}	LF	59
n-Bu	1.8	67W33AN[c]	5.05	0.90	20	–	1.4×10^6	1.4×10^6		LF	59
Et	1.8	67W33AN[c]	5.05	0.90	20	–	1.4×10^6	1.4×10^6		LF	59
Me	1.7	W	5.20	0.89	20	–	1.4×10^6	1.5×10^6	1.1×10^{-3}	LF	58
		67W33AN[c]	5.05	0.90	20	–	1.4×10^6	1.3×10^6	1.1×10^{-3}	LF	59
n-Pr	1.7	67W33AN[c]	5.05	0.90	20	–	1.3×10^6	1.3×10^6		LF	59
s-Bu	1.7	67W33AN[c]	5.05	0.90	20	–	1.2×10^6	1.2×10^6		LF	59
Ph	0.1	67W33AN[c]	5.05	0.90	20	–	4.0×10^4	4.0×10^4		LF	59
4-$MeOC_6H_4$	-1.8	W	5.20	0.89	25	0.1	1.2×10^3	1.2×10^3		?	60

[a] Mixtures of solvents are given as (v/v), solvents: W = water, AN = acetonitrile. [b] LF = laser flash photolysis. [c] Precise water content of the aqueous acetonitrile (50-80% water) is not given in the literature.

Table 4.25 shows that the steric effect of the four methyl groups in the pinacol derivatives reduces the electrophilicities of the 1,3-dioxolanium ion by 1.5-2.0 units in *E* (comparison with Table 4.24).

Table 4.25: Rate constants for the reactions of 1,3-dioxolan-4,5-tetramethyl-2-ylium ions with solvents at 20 °C and electrophilicity parameters derived therefrom.

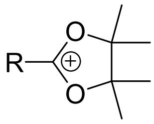

R	E	Solvent [a]	N_1	s	k_{exp}, s^{-1}	k_{calc}, s^{-1}	$\Delta^2 \log k$	Method [b]	Ref.
H	3.5	67W33AN[c]	5.05	0.90	4.6×10^{7}	4.6×10^{7}		LF	59
i-Pr	0.2	W	5.20	0.89	5.9×10^{4}	5.9×10^{4}		LF	58
Et	0.1	W	5.20	0.89	5.1×10^{4}	5.1×10^{4}		LF	58
Me	0.0	W	5.20	0.89	3.5×10^{4}	4.0×10^{4}	3.6×10^{-3}	LF	58
		67W33AN[c]	5.05	0.90	3.8×10^{4}	3.3×10^{4}	3.5×10^{-3}	LF	59
t-Bu	-0.1	W	5.20	0.89	3.7×10^{4}	3.7×10^{4}		LF	58
Ph	-1.9	W	5.20	0.89	8.6×10^{2}	8.6×10^{2}		LF	59

[a] Mixtures of solvents are given as (v/v), solvents: W = water, AN = acetonitrile. [b] LF = laser flash photolysis. [c] Precise water content of the aqueous acetonitrile (50-80% water) is not given in the literature.

In the series of acyclic trialkoxycarbenium ions (Table 4.26), again the reactivity order $(MeO)_3C^+ > (EtO)_3C^+ > (i\text{-}PrO)_3C^+$ is found comparable to that of the dialkoxycarbenium ions.

Table 4.26: Rate constants for the reactions of trialkoxycarbenium ions with solvents at 20 °C and electrophilicity parameters derived therefrom.

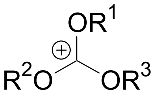

R^1	R^2	R^3	E	Solvent [a]	N_1	s	I,[b]	k_{exp}, s^{-1}	Method [c]	Ref.
Et	Et	CF_3CH_2	-0.7	W	5.20	0.89	–	1.0×10^{4}	LF	58
Me	Me	Me	-1.7	W	5.20	0.89	2×10^{-4}–1×10^{-2}	1.4×10^{3}	LF	61
Me	Me	Et	-2.3	W	5.20	0.89	–	4.0×10^{2}	LF	58
Me	Me	*i*-Pr	-3.0	W	5.20	0.89	–	9.8×10^{1}	LF	58
Et	Et	Et	-3.2	W	5.20	0.89	2×10^{-4}–1×10^{-2}	5.9×10^{1}	LF	61
i-Pr	*i*-Pr	*i*-Pr	-5.2	W	5.20	0.89	2×10^{-4}–1×10^{-2}	1.0	LF	61

[a] W = water. [b] Ionic strength maintained with $NaClO_4$. [c] LF = laser flash photolysis.

The slightly higher electrophilicity of 1,3-dioxolan-2-ylium ions compared to 1,3-dioxan-2-ylium ions is also observed, when the third substituent at the carbocation center is a methoxy group (Table 4.27).

Table 4.27: Rate constants for the reactions of cyclic trialkoxycarbenium ions with solvents at 20 °C, $I = 2\times10^{-4}$–1×10^{-2} ($NaClO_4$) and electrophilicity parameters derived therefrom.

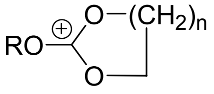

R	n	E	Solvent [a]	N_1	s	k_{exp}, s^{-1}	Method [b]	Ref.
Me	1	-0.2	W	5.20	0.89	2.7×10^4	LF	61
Me	2	-1.0	W	5.20	0.89	5.4×10^3	LF	61
i-Pr	1	-1.0	W	5.20	0.89	5.3×10^3	LF	61

[a] W = water. [b] LF = laser flash photolysis.

Scheme 4.14 shows that replacement of a methyl group in 1,1-dialkoxy-ethyl cations by an alkoxy group reduces electrophilicities by ca. 3 units.

Scheme 4.14

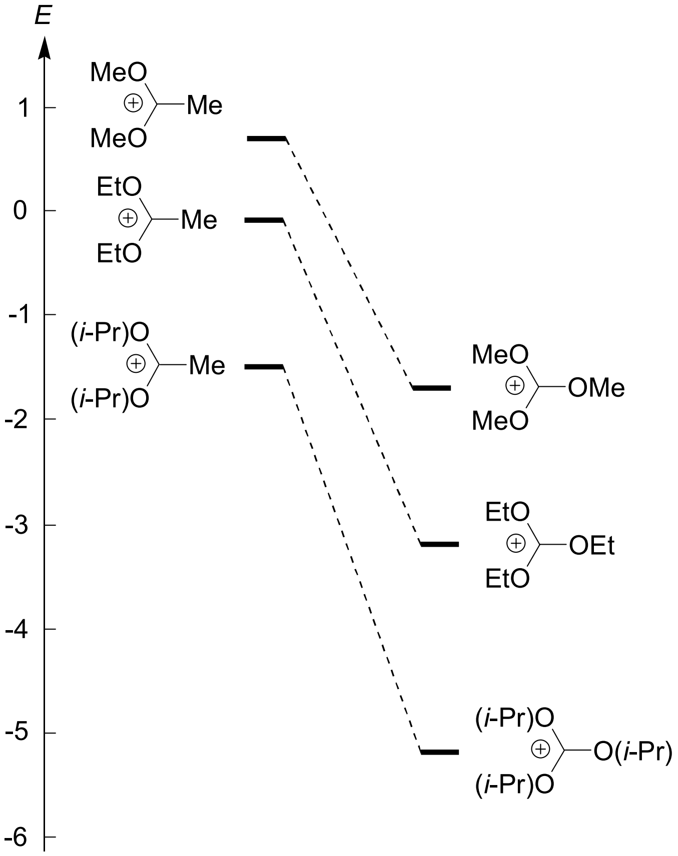

Slightly smaller reductions in electrophilicities are observed, when cyclic dialkoxy- and trialkoxycarbenium ions are compared (Scheme 4.15).

Scheme 4.15

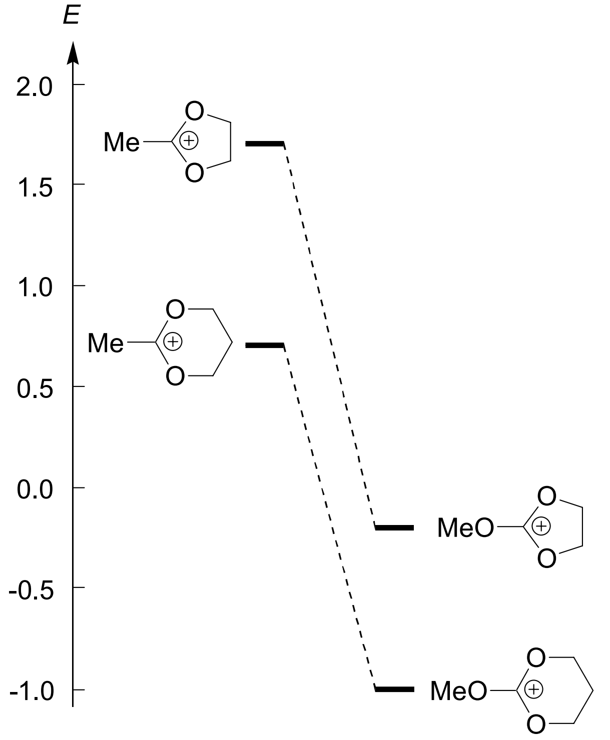

As mentioned at the beginning of this section, the *E* parameters for alkoxy substituted carbenium ions listed in Table 4.16-4.27 cannot be used to predict reactivities toward π-nucleophiles, because these reactions will be considerably slower due to the missing anomeric effect. On the other hand, Table 4.28 shows that the rate constants observed for the reactions of di- and trialkoxycarbenium ions with hydroxide ion are generally 10^2 times faster than calculated from the *E*-parameters listed in Tables 4.16-4.27. Obviously, the anomeric stabilization in reactions of alkoxycarbenium ions with OH^- is even higher than in reactions with neutral O-nucleophiles.

Table 4.28: Comparison of experimental and calculated rate constants for the reactions of oxocarbenium ions with hydroxide ions in water at 20 °C.[a]

Electrophile	*E*	Nucleophile	k_{exp}, L mol^{-1} s^{-1}	k_{calc}, L mol^{-1} s^{-1}	Ref.
$(MeO)_2C^+Me$	0.7	OH^-	3.7×10^8	6.5×10^6	58
$(MeO)_2C^+Et$	0.6	OH^-	2.7×10^8	5.7×10^6	58
$(MeO)_2C^+Ph$	0.5	OH^-	2.8×10^8	4.9×10^6	59
$(EtO)_2C^+$*i*-Pr	0.2	OH^-	1.3×10^8	3.2×10^6	58
$(EtO)_2C^+Ph$	0.1	OH^-	2.0×10^8 [b]	2.8×10^6	59
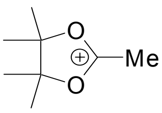	0.0	OH^-	5.1×10^7	2.4×10^6	58
$(EtO)_2C^+Me$	-0.1	OH^-	9.2×10^7	2.1×10^6	58
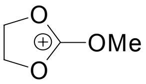	-0.2	OH^-	2.8×10^8 [c]	1.8×10^6	61
$(EtO)_2C^+Et$	-0.2	OH^-	1.2×10^8	1.8×10^6	58
$(MeO)_2C^+OCH_2CF_3$	-0.7	OH^-	1.5×10^8	9.1×10^5	58
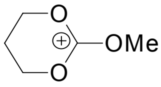	-1.0	OH^-	7.9×10^7 [c]	6.0×10^5	61
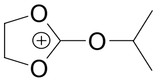	-1.0	OH^-	2.8×10^7 [c]	6.0×10^5	61
(*i*-PrO)$_2C^+Me$	-1.5	OH^-	1.8×10^7	3.0×10^5	58
$(MeO)_3C^+$	-1.7	OH^-	5.7×10^7 [c]	2.2×10^5	61
$(MeO)_2C^+OEt$	-2.3	OH^-	1.8×10^7	9.6×10^4	58
$(MeO)_2C^+O$*i*-Pr	-3.0	OH^-	5.7×10^7	3.6×10^4	58
$(EtO)_3C^+$	-3.2	OH^-	9.6×10^6 [c]	2.7×10^4	61

[a] By laser flash photolysis. [b] Precise water content of the aqueous acetonitrile (50-80% water) is not given in the literature. [c] $I = 2\times10^{-4}$–1×10^{-2} ($NaClO_4$).

4.14 Thio-substituted carbenium ions

Kinetic measurements of the reactions of the 2-phenyl-1,3-dithiolan-2-ylium ion with π-nucleophiles gave an electrophilicity parameter of E = -5.91.[62] This parameter can be combined with the N_1 and *s* parameters of 50% aqueous ethanol and 50% aqueous acetonitrile to calculate rate constants for the decay of this carbocation in the corresponding solvents [63] (Table 4.29).

Table 4.29: The calculated rate constants with E derived from the reactions with π-nucleophiles and observed rate constants for reactions of 2-phenyl-1,3-dithiolan-2-ylium ion with solvents at 25 °C, I = 0.1 (KCl).

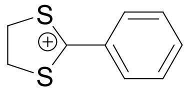	Solvent [a]	N_1	s	k_{exp} / s^{-1}	k_{calc} / s^{-1}
	50E50W	5.96	0.89	3.83	1.11
E = -5.91 [62]	50W50AN	5.05	0.89	0.56	0.17

[a] Mixtures of solvents are given as (v/v), solvents: E = ethanol, W = water, AN = acetonitrile.

Table 4.29 shows that the experimental values, obtained with flash photolytically generated dithiolan-2-ylium ions are only 3-4 times larger than the calculated values. It can be concluded, therefore, that the same E parameters can be employed for reactions of thiosubstituted carbenium ions with C- and O-nucleophiles, in accord with quantum chemical calculations which show that the geminal interaction of SR and OR is much less stabilizing than the geminal interaction of two alkoxy groups.[64]

For that reason, the low electrophilicities of the 1,3-dithiolan-2-ylium ions listed in Table 4.30 will also be representative for their reactions with carbon nucleophiles. The lower electrophilicities of the dithiolanium ions listed in Table 4.30 compared to 1,3-dioxolan-2-ylium ions (ΔE = -2) must be considered to be specific for reactions with water or related nucleophiles. Comparison of E-parameters of 1,3-dioxolan-2-ylium ions and 1,3-dithiolan-2-ylium ions is shown in Scheme 4.16.

Table 4.30: Rate constants for the reactions of dithiolan-2-ylium ions with solvents at 25°C and electrophilicity parameters derived therefrom.

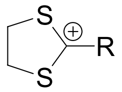

R	E	Solvent [a]	I,	N_1	s	k_{exp}, s^{-1}	Method [b]	Ref.
CH_2Ph	-3.4	W	0.5 (KCl)	5.20	0.89	3.9×10^{1}	UV-vis	65
i-Pr	-3.5	W	0.5 (KCl)	5.20	0.89	3.2×10^{1}	UV-vis	65
Et	-3.6	W	0.5 (KCl)	5.20	0.89	2.4×10^{1}	UV-vis	65
Me	-3.7	W	0.5 (KCl)	5.20	0.89	2.1×10^{1}	UV-vis	65
4-MeOC$_6$H$_4$	*(-6.5)*	*90W10AN* [c]	*0.45*	*5.16*	*0.91*	6.1×10^{-2} [d]	UV-vis	*66*

[a] Mixtures of solvents are given as (v/v), solvents: W = water, AN = acetonitrile [b] UV-vis = conventional UV-vis spectroscopy. [c] N_1 and s parameters of 91W9AN were used for calculation. [d] T = 30°C.

Scheme 4.16

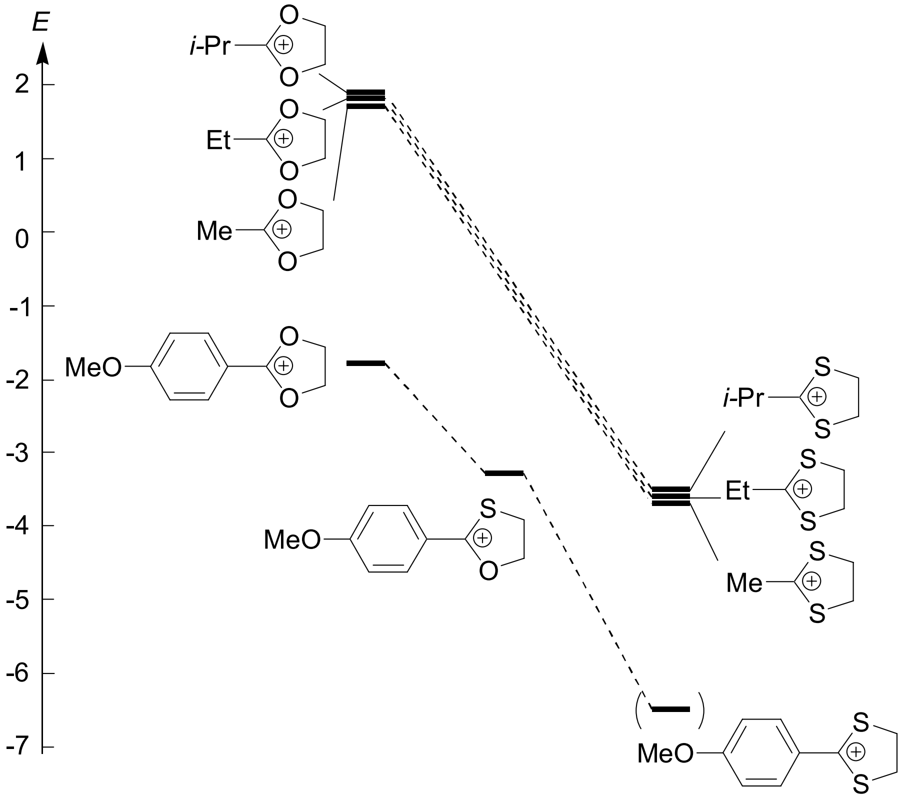

Comparison of entries 1 and 2 as well as of 3 and 4 in Table 4.31 also indicates that alkoxy substituted carbenium ions are significantly more electrophilic towards water and 50% aqueous TFE than the mercapto substituted analogues. Because of the previously mentioned anomeric effects, one has to expect, however, that these differences will almost disappear in reactions with C-nucleophiles.

Table 4.31: Rate constants for the reactions of α-oxocarbenium ions and α-thiocarbenium ions with solvents at 25 °C and electrophilicity parameters derived therefrom.

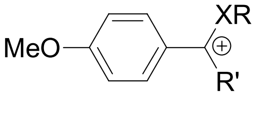

XR	R'	E	Solvent [a]	N_1	s	I, [b]	k_{exp}, s^{-1}	Method [c]	Ref.
OCH_2CF_3	H	4.8	50T50W	3.57	0.89	0.5	3.0×10^7	Azide	52
SCH_2CF_3	H	1.9	50T50W	3.57	0.89	0.5	7.0×10^4	Azide	52
OCH_3	4-$MeOC_6H_4$	-0.3	W	5.20	0.89	–	2.3×10^4	Hydrolysis in H_2SO_4	57
SCH_3	4-$MeOC_6H_4$	-4.5	W	5.20	0.89	–	4.6	Hydrolysis in H_2SO_4	57

[a] Mixtures of solvents are given as (v/v), solvents: W = water, T = trifluoroethanol. [b] Ionic strength maintained with $NaClO_4$. [c] Azide = azide clock.

Table 4.32: Rate constants for the reactions of α-oxocyclopropenyl cations with solvents at 25°C and electrophilicity parameters derived therefrom.

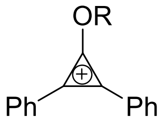

R	*E*	Solvent [a]	N_1	*s*	k_{exp}, s^{-1}	Method	Ref.
Me	-2.9	W	5.20	0.89	1.2×10^{2}	Hydrolysis in H_2SO_4	57
Et	-3.4	W	5.20	0.89	4.4×10^{1}	Hydrolysis in H_2SO_4	57

[a] W = water.

4.15 Iminium ions

The high electron-donating ability of nitrogen is responsible for the high stability of iminium ions and their extensive use in organic synthesis. Table 4.33 compares the electrophilicities of *N*-aryl-*N*-methyliminium ions, for which *E*-parameters between 2 and 4 are obtained.

Table 4.33: Rate constants for the reactions of *N*-aryl-*N*-methyliminium ions with solvents at 25 °C, *I* = 0.5 (NaCl) and electrophilicity parameters derived therefrom.

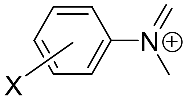

X	*E*	Solvent [a]	N_1	*s*	k_{exp}, s^{-1}	Method [b]	Ref.
4-NO_2	3.8	W	5.20	0.89	1.0×10^{8}	ArS^-	67
4-CN	3.2	W	5.20	0.89	3.1×10^{7}	ArS^-	67
3-NO_2	3.2	W	5.20	0.89	3.0×10^{7}	ArS^-	67
3-Cl	2.4	W	5.20	0.89	5.5×10^{6}	ArS^-	67
4-CO_2^-	2.3	W	5.20	0.89	4.5×10^{6}	ArS^-	67
4-Cl	2.1	W	5.20	0.89	3.1×10^{6}	ArS^-	67
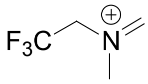	3.0	W	5.20	0.89	1.8×10^{7}	ArS^-	68

[a] W = water. [b] ArS^- = $^-SC_6H_4$-2-CO_2^- clock

Amazingly, the correlation of *E* with σ^- (R^2 = 0.95) is better than with σ (R^2 = 0.80) indicating that the direct conjugation between the nitrogen lone-pair in the developing tertiary amine and the 4-aryl substituent can already be recognized in the transition states (Figures 4.10 and 4.11)

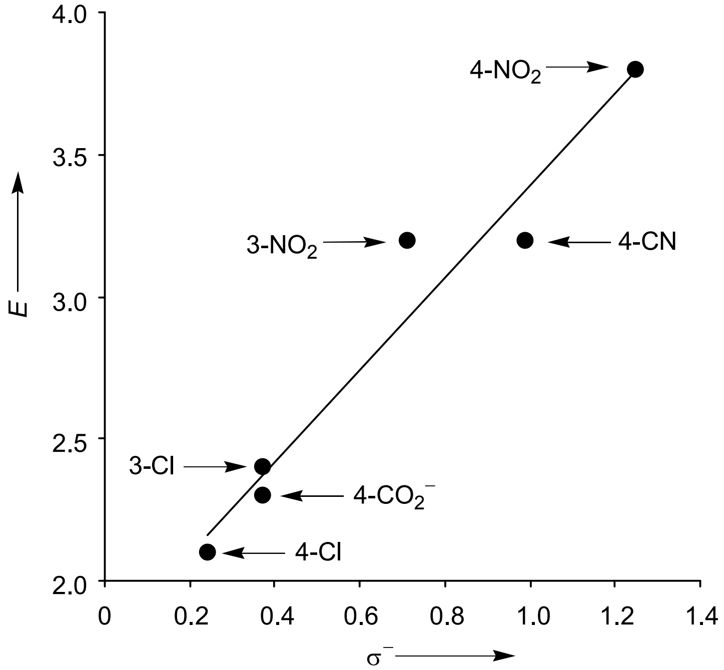

Figure 4.10: Correlation of the electrophilicity parameters *E* of *N*-aryl-*N*-methyliminium ions with the Hammett σ^--parameters.[14b] $E = 1.61\sigma^- + 1.78$, n = 6, R^2 = 0.947.

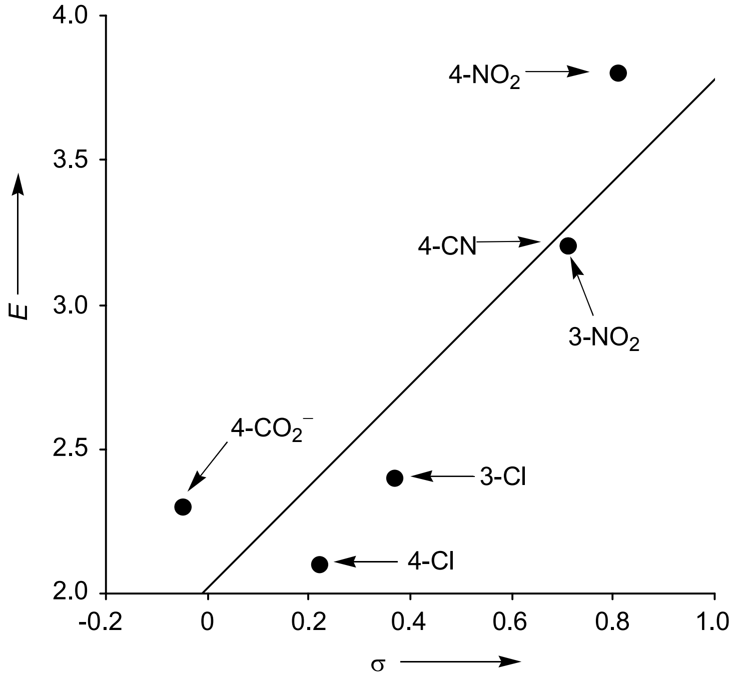

Figure 4.11: Correlation of the electrophilicity parameters *E* of *N*-aryl-*N*-methyliminium ions with the Hammett σ-parameters.[14b] $E = 1.76\sigma + 2.02$, n = 6, R^2 = 0.802.

According to Table 4.34, the dialkylamino-benzylidenenammonium ions are considerably less electrophilic than the iminium ions described in Table 4.33, as expected for more highly substituted carbenium ions. There seems to be some inconsistency in the data, however, since *E*-parameters differing by 2.5 units have been obtained for the structurally closely related species $[PhCH{=}NMe_2]^+$ and $[PhCH{=}NMeBu]^+$. Because of this discrepancy, it is problematic to derive the importance of the anomeric effect in reactions of iminium ions with O-nucleophiles from these data. The reduction of electrophilicity by 7 units when introducing a methoxy group into a highly stabilized carbenium ion (last entry of Table 4.34) is also surprising and should only be discussed after confirming the experimental data.

Table 4.34: Rate constants for the reactions of *N*-aryl-*N*-methyliminium ions with solvents and electrophilicity parameters derived therefrom.

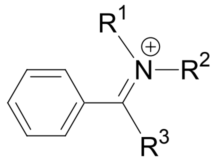

R^1	R^2	R^3	E	Solvent [a]	N_1	s	T, °C	I, [b]	k_{exp}, s^{-1}	k_{calc}, s^{-1}	$\Delta^2 \log k$	Method [c]	Ref.
Me	NO	H	1.4	W	5.20	0.89	25	0.5	7.6×10^5	7.8×10^5	1.5×10^{-4}	LF	69
				90W10AN [d]	5.16	0.91	25	0.1	1.0×10^6	9.7×10^5	1.5×10^{-4}	LF	69
Me	Bu	H	-2.5	M	7.54	0.92	?	–	4.5×10^4	4.5×10^4		LF	70
Bn	Bu	H	-3.1	M	7.54	0.92	?	–	1.1×10^4	1.1×10^4		LF	70
Me	Me	H	-5.0	50W50AN	5.05	0.89	20	–	1.16	1.16		Stopped-flow	71
H	H	OMe	-9.4	W	5.20	0.89	25	–	1.7×10^{-4}	1.7×10^{-4}		Hydrolysis in H_2SO_4	57

[a] Mixtures of solvents are given as (v/v), solvents: M = methanol, W = water, AN = acetonitrile. [b] Ionic strength maintained with $NaClO_4$. [c] LF = laser flash photolysis. [d] N_1 and s parameters of 91W9AN were used for calculation.

4.16 Imidinium ions

Imidinium ions, which were generated in aqueous solution by the solvolysis of fluoro- and chloroformamidines, are considerably more electrophilic than ordinary iminium ions due to the presence of the strained heterocumulene system (Table 4.35).

Table 4.35: Rate constants for the reactions of imidinium ions with solvents at 25 °C, *I* = 1.0 (KCl) and electrophilicity parameters derived therefrom.

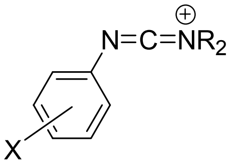

X	NR₂	*E*	Solvent [a]	N_1	*s*	k_{exp}, s^{-1}	Method [b]	Ref.
3-NO_2	Morpholino	1.8	W	5.20	0.89	1.8×10^{6}	AcS¯	69
4-CN	Morpholino	1.8	W	5.20	0.89	1.6×10^{6}	AcS¯	69
3-CN	Morpholino	1.7	W	5.20	0.89	1.5×10^{6}	AcS¯	69
4-Cl	Morpholino	1.3	W	5.20	0.89	5.8×10^{5}	AcS¯	69
H	Morpholino	1.0	W	5.20	0.89	3.6×10^{5}	AcS¯	69
H	Pyrrolidino	1.0	W	5.20	0.89	3.1×10^{5}	Azide, AcS¯	69
H	N-Methylpiperazino	0.8	W	5.20	0.89	2.0×10^{5}	Azide, AcS¯	69
4-NO_2	NMeOMe	3.2	W	5.20	0.89	3.1×10^{7}	Azide	69
H	NMeOMe	2.1	W	5.20	0.89	3.4×10^{6}	Azide	69

[a] W = water. [b] AcS¯ = CH_3COS^- clock, Azide = azide clock.

Replacement of an alkyl group by methoxy at the formally positively charged nitrogen increases electrophilicity by approximately one unit, indicating that the inductive effect of methoxy is more important than its mesomeric electron donating effect (α-effect).

When the *E* values derived in Table 4.35 are employed to calculate rate constants for the reactions of imidinium ions with other n-nucleophiles, agreement within a factor of 35 has been obtained (Table 4.36).

Table 4.36: Comparison of experimental and calculated rate constants for the reactions of 4-$ClC_6H_4N{=}C{=}N^+(CH_2CH_2)_2O$ (E = 1.3) with n-nucleophiles in water at 25 °C (k_{exp} for ionic strength I = 1.0, KCl)

Nucleophile	N_1	s	k_{exp}, L mol^{-1} s^{-1}	k_{calc}, L mol^{-1} s^{-1}
OH^-	10.47	0.61	5.2×10^8	1.5×10^7
$EtNH_2$ [a]	13.33	0.56	5.8×10^7	1.6×10^8
SO_3^{2-}	16.83	0.56	5.1×10^8	(1.4×10^{10})
$^-SCH_2CO_2^-$	22.62	0.43	5.0×10^9	(1.1×10^{10})

[a] N and s parameters of n-$PrNH_2$ were used for calculation.

4.17 α-Azidocarbenium ions

Formally, α-azidocarbenium ions can be considered as iminium ions, in which the alkyl groups at nitrogen are replaced by an N_2 unit (Scheme 4.17).

Scheme 4.17

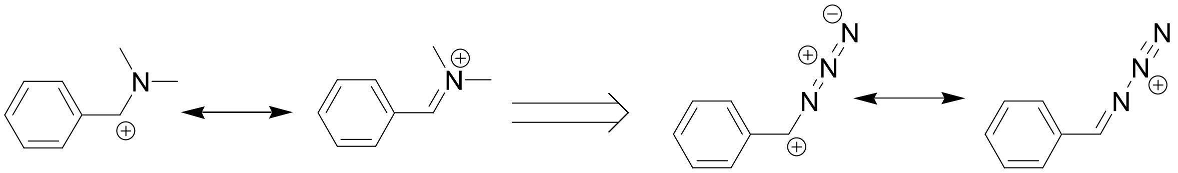

Even when the uncertainties noted in Table 4.34 are taken into account, comparison with Table 4.37 shows that α-azido benzyl cations are more electrophilic than the corresponding iminium ions by at least six units of E. It is not clear why 4-methoxy-α-azidobenzyl cations show similar rates of decay in 100% water and in 50% aqueous trifluoroethanol, two solvents of significantly different nucleophilicity, and only part of the observed reactivity difference can be due to the different ionic strength used in these two experiments.

Table 4.37: Rate constants for the reactions of α-azidocarbenium ions with solvents at 25 °C, $I = 2.0$ ($NaClO_4$) and electrophilicity parameters derived therefrom.

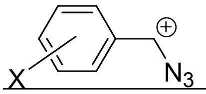

X	E	Solvent [a]	N_1	s	k_{exp}, s^{-1}	k_{calc}, s^{-1}	$\Delta^2 \log k$	Method [b]	Ref.
4-NO_2	4.8	W	5.20	0.89	8.6×10^{8}	8.6×10^{8}		Azide	72
3-F	4.3	W	5.20	0.89	3.1×10^{8}	3.1×10^{8}		Azide	72
3-MeO	3.6	W	5.20	0.89	6.4×10^{7}	6.4×10^{7}		Azide	72
H	3.5	W	5.20	0.89	5.8×10^{7}	5.8×10^{7}		Azide	72
4-F	3.2	W	5.20	0.89	2.9×10^{7}	2.9×10^{7}		Azide	72
4-Me	2.7	W	5.20	0.89	1.1×10^{7}	1.1×10^{7}		Azide	72
4-MeO	2.0	W	5.20	0.89	5.8×10^{5}	2.3×10^{6}	3.6×10^{-1}	Azide	72
		50T50W	3.57	0.89	3.3×10^{5} [c]	8.2×10^{4}	3.6×10^{-1}	Azide	12
4-MeS	1.7	W	5.20	0.89	1.4×10^{6}	1.4×10^{6}		Azide	72

[a] Mixtures of solvents are given as (v/v), solvents: W = water, T = trifluoroethanol. [b] Azide = azide clock. [c] $I = 0.5$ ($NaClO_4$).

Comparison of the slope of the Hammett correlation in Figure 4.12 with the corresponding values in Table 4.14 shows that the electron demand of the carbocationic center in α-azidobenzyl cations is similar to that in 9-arylfluorenyl cations. Correspondingly, the 4-methoxy-α-azido benzyl cation (E = 2.0) and the 9-(4-methoxyphenyl)fluorenyl cation (E = 1.0) possess similar electrophilicities.

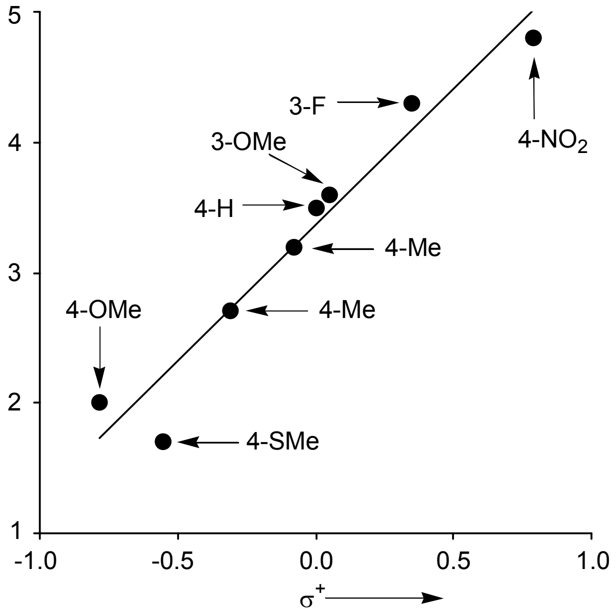

Figure 4.12: Correlation of the electrophilicity parameters E of α-azidocarbenium ions with the Hammett σ^+-parameters.[14a] $E = 2.08\sigma^+ + 3.36$, n = 8, $R^2 = 0.942$.

4.18 Nitrilium ions

Preliminary investigations of the reactions of *N*-methylbenzonitrilium ions with π-nucleophiles yielded an electrophilicity parameter of E = -4.5,[73] considerably smaller than that derived for the *N*-isopropylbenzonitrilium ion from its reaction with water (last entry, Table 4.38), again indicating the importance of geminal interactions in the transition states.

Table 4.38: Rate constants for the reactions of *N*-aryl and *N*-alkylbenzonitrilium ions with solvents at 20 °C, I = 0.1 ($NaClO_4$) and electrophilicity parameters derived therefrom.

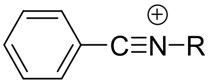

R	E	Solvent[a]	N	s	k_{exp}, s^{-1}	Method[b]	Ref.
4-$CF_3C_6H_4$	0.8	80W20AN	5.04	0.89	1.6×10^5	LF	74
3-$CF_3C_6H_4$	0.5	80W20AN	5.04	0.89	8.9×10^4	LF	74
3-ClC_6H_4	0.4	80W20AN	5.04	0.89	7.1×10^4	LF	74
4-ClC_6H_4	0.3	80W20AN	5.04	0.89	5.3×10^4	LF	74
Ph	-0.2	80W20AN	5.04	0.89	2.1×10^4	LF	74
3-MeC_6H_4	-0.2	80W20AN	5.04	0.89	1.9×10^4	LF	74
4-$PhOC_6H_4$	-0.3	80W20AN	5.04	0.89	1.7×10^4	LF	74
4-MeC_6H_4	-0.4	80W20AN	5.04	0.89	1.5×10^4	LF	74
4-$MeOC_6H_4$	-0.5	80W20AN	5.04	0.89	1.0×10^4	LF	74
i-Pr	-2.3	W	5.20	0.89	4.0×10^2	LF	74

[a] Mixtures of solvents are given as (v/v), solvents: W = water, AN = acetonitrile. [b] LF = laser flash photolysis.

As in the corresponding iminium series, E correlates somewhat better with σ^- than with σ (Figures 4.13 and 4.14).

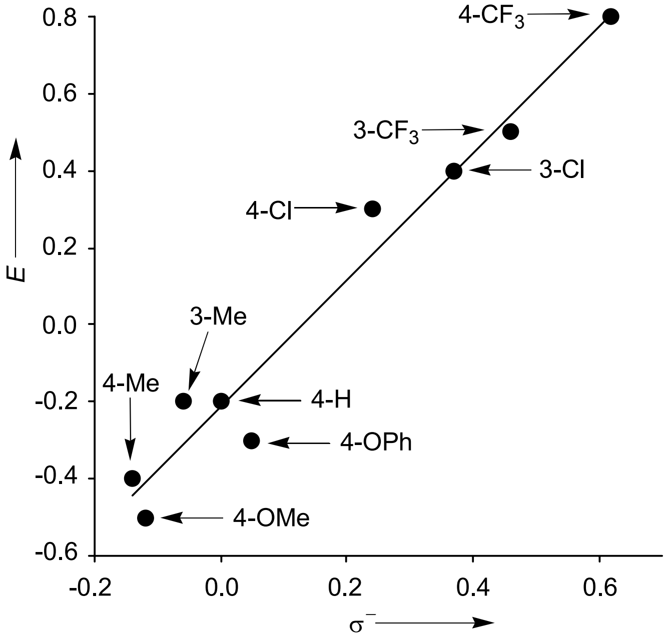

Figure 4.13: Correlation of the electrophilicity parameters E of *N*-arylbenzonitrilium ions cations with the Hammett σ^--parameters.[14b] $E = 1.64\sigma^- - 0.21$, n = 9, $R^2 = 0.961$.

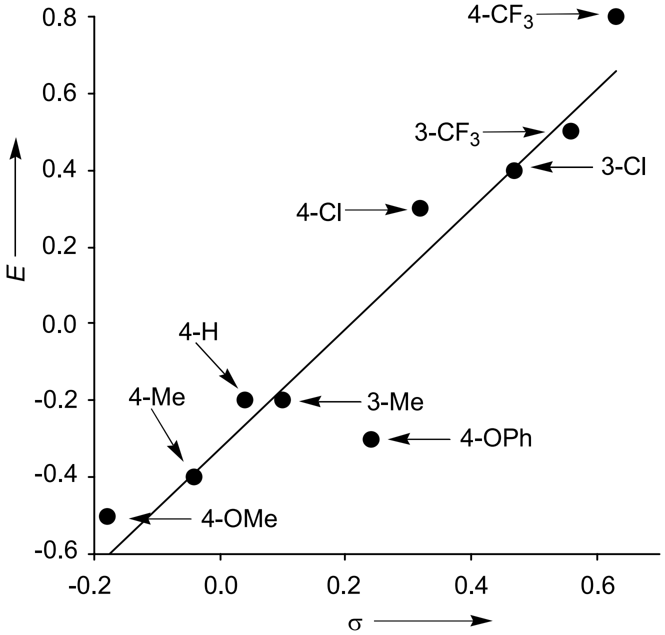

Figure 4.14: Correlation of the electrophilicity parameters E of *N*-arylbenzonitrilium ions cations with the Hammett σ-parameters.[14b] $E = 1.56\sigma - 0.17$, n = 9, $R^2 = 0.896$.

A much better Hammett correlation is obtained for *N*-phenylbenzonitrilium ions (Table 4.39), where substituent variation at the phenyl ring attached to carbon is considered (Figure 4.15). It can generally be concluded that diarylnitrilium ions have E parameters around 0, which are only slightly affected by variation of the substituents. The frequently applied rule that the slopes of E/σ^+ correlations are associated with the electron demand at the carbenium center and with the electrophilicity (Table 4.14) does not seem to be applicable here.

Table 4.39: Rate constants for the reactions of *N*-phenylbenzonitrilium ions with solvents at 20 °C, $I = 0.1$ ($NaClO_4$) and electrophilicity parameters derived therefrom.

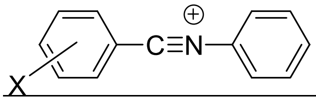

X	*E*	Solvent[a]	*N*	*s*	k_{exp}, s^{-1}	Method[b]	Ref.
4-CF_3	0.2	80W20AN	5.04	0.89	5.1×10^4	LF	74
3-CF_3	0.2	80W20AN	5.04	0.89	4.3×10^4	LF	74
3-Cl	0.0	80W20AN	5.04	0.89	3.2×10^4	LF	74
3-MeO	-0.1	80W20AN	5.04	0.89	2.6×10^4	LF	74
4-Cl	-0.1	80W20AN	5.04	0.89	2.4×10^4	LF	74
H	-0.2	80W20AN	5.04	0.89	2.1×10^4	LF	74
3-Me	-0.2	80W20AN	5.04	0.89	2.0×10^4	LF	74
4-Me	-0.3	80W20AN	5.04	0.89	1.6×10^4	LF	74
4-PhO	-0.5	80W20AN	5.04	0.89	1.1×10^4	LF	74
4-MeO	-0.7	80W20AN	5.04	0.89	6.7×10^3	LF	74

[a] Mixtures of solvents are given as (v/v), solvents: W = water, AN = acetonitrile.
[b] LF = laser flash photolysis.

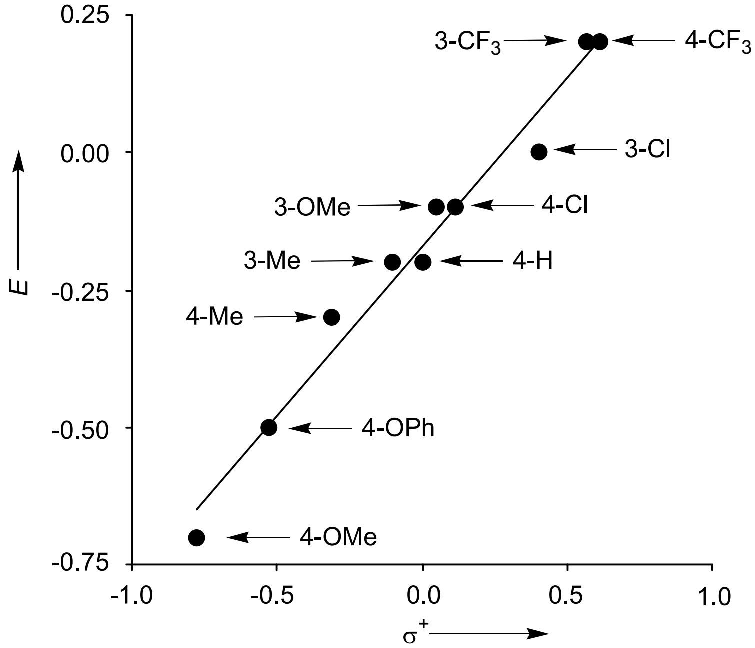

Figure 4.15: Correlation of the electrophilicity parameters *E* of *N*-phenylbenzonitrilium ions cations with the Hammett σ^+-parameters.[14a] $E = 0.62\sigma^+ - 0.17$, n = 10, $R^2 = 0.978$.

When the *E* parameters of nitrilium ions are employed to calculate rate constants for the reactions with OH^-, again systematic deviations are observed, and the calculated rate constants are generally 50 times smaller than the experimental numbers (Table 4.40). It is assumed that geminal interactions again account for these deviations, like in the reactions with oxocarbenium ions, which also reacted faster with OH^- and more slowly with π-nucleophiles than expected on the basis of *E*-parameters that were derived from reactions with water or alcohols.

Table 4.40: Comparison of calculated and experimental rate constants for the reactions of hydroxide ion and azide ion with nitrilium ions in 80W20AN, $I = 0.1$ ($NaClO_4$) at 20 °C.[74]

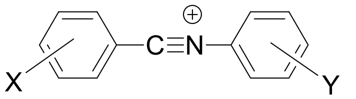

X	Y	*E*	Nucleophile	k_{exp}, L mol^{-1} s^{-1}	k_{calc}, L mol^{-1} s^{-1}
4-CF_3	H	0.2	N_3^-	5.8×10^8	–
3-CF_3	H	0.2	N_3^-	4.5×10^8	–
3-Cl	H	0.0	OH^-	1.2×10^8	2.4×10^6
			N_3^-	4.5×10^8	–
3-MeO	H	-0.1	N_3^-	2.8×10^8	–
4-Cl	H	-0.1	OH^-	1.0×10^8	2.4×10^6
			N_3^-	3.2×10^8	–
H	H	-0.2	OH^-	6.4×10^7	1.8×10^6
			N_3^-	2.6×10^8	–
3-Me	H	-0.2	N_3^-	2.4×10^8	–
4-Me	H	-0.3	OH^-	4.4×10^7	1.6×10^6
			N_3^-	1.9×10^8	–
4-PhO	H	-0.5	N_3^-	1.1×10^8	–
4-MeO	H	-0.7	OH^-	2.0×10^7	9.1×10^5
			N_3^-	7.5×10^7	–
H	4-CF_3	0.8	OH^-	1.9×10^8	7.5×10^6
			N_3^-	1.1×10^9	–
H	3-CF_3	0.5	N_3^-	8.1×10^8	–
H	3-Cl	0.4	OH^-	1.4×10^8	4.3×10^6
			N_3^-	7.1×10^8	–

Table 4.40: Continued

X	Y	*E*	Nucleophile	k_{exp}, L mol^{-1} s^{-1}	k_{calc}, L mol^{-1} s^{-1}
H	4-Cl	0.3	OH^-	1.0×10^8	2.5×10^6
			N_3^-	5.3×10^8	–
H	3-Me	-0.2	N_3^-	2.2×10^8	1.8×10^6
H	4-PhO	-0.3	N_3^-	1.8×10^8	–
H	4-Me	-0.4	OH^-	6.1×10^7	1.4×10^6
			N_3^-	2.0×10^8	–
H	4-MeO	-0.5	OH^-	4.7×10^7	1.2×10^6
			N_3^-	1.2×10^8	–
H	*i*-Pr	-2.3	$OH^{-\,a}$	5.2×10^6	9.6×10^4
			$N_3^{-\,a}$	3.9×10^6	–

[a] In water

4.19 Nitrenium ions

Recently, many kinetic investigations with nitrenium ions have been performed because of their suspected carcinogenicity.[75] Nitrenium ions may exist in singlet and triplet states, but in most cases, the ground state of arylnitrenium ions is a singlet.[75] While n-nucleophiles, as water, attack nitrenium ions at a ring carbon, carbon nucleophiles, as guanine, attack the nitrogen of arylnitrenium ions (Scheme 4.18). In order to compare nitrenium ion reactivities with carbocation reactivities, Tables 4.40-4.43 include only data which refer to attack at carbon centers.

Scheme 4.18

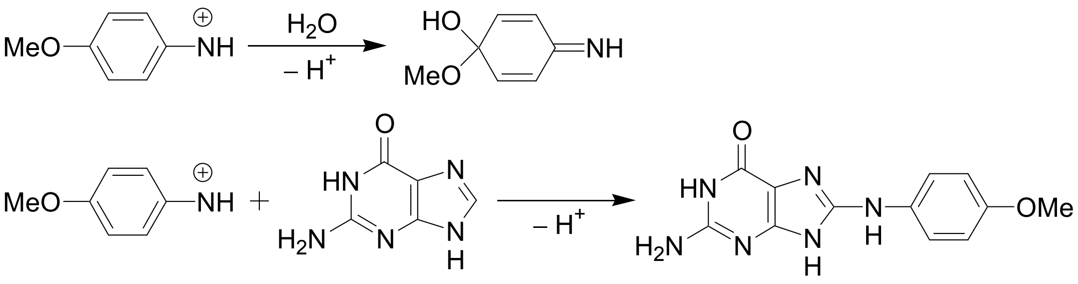

The stilbene substituted nitrenium ions may be considered as imino quinone methide substituted carbenium ions (see right resonance structure in Scheme 4.19). They react with water in analogy to arylallyl cations, which allow us to compare their electrophilicities with those of ordinary carbenium ions.

Scheme 4.19

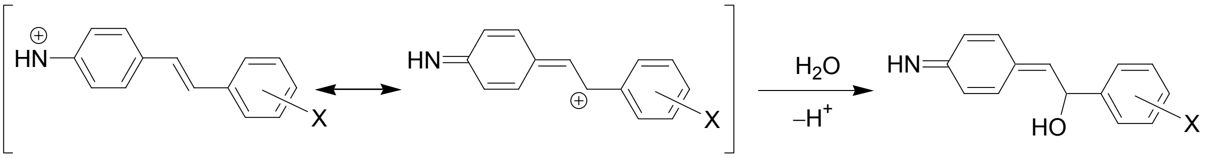

Table 4.40: Rate constants for the reactions of stilbene substituted nitrenium ions with solvents at 20°C, $I = 0.5$ ($NaClO_4$) and electrophilicity parameters derived therefrom.

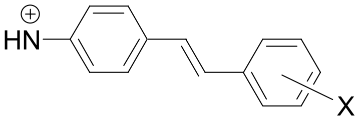

X	E	Solvent [a]	N_1	s	k_{exp}, s^{-1}	Method [b]	Ref.
4-Br	2.6	80W20AN	5.04	0.89	6.5×10^6	LF	30
H	2.6	80W20AN	5.04	0.89	6.3×10^6	LF	30
3-Me	2.4	80W20AN	5.04	0.89	4.6×10^6	LF	30
4-Me	1.9	80W20AN	5.04	0.89	1.5×10^6	LF	30
4-NMeAc	1.4	80W20AN	5.04	0.89	5.6×10^5	LF	30
4-MeO	0.3	80W20AN	5.04	0.89	6.1×10^4	LF	30

[a] Mixtures of solvents are given as (v/v), solvents: W = water, AN = acetonitrile.
[b] LF = laser flash photolysis.

Comparison with the E parameters of benzhydrylium ions indicates that the electron donating effect of an imino quinone methide substituent is comparable to that of a 4-methoxyphenyl group (Scheme 4.20).

Scheme 4.20

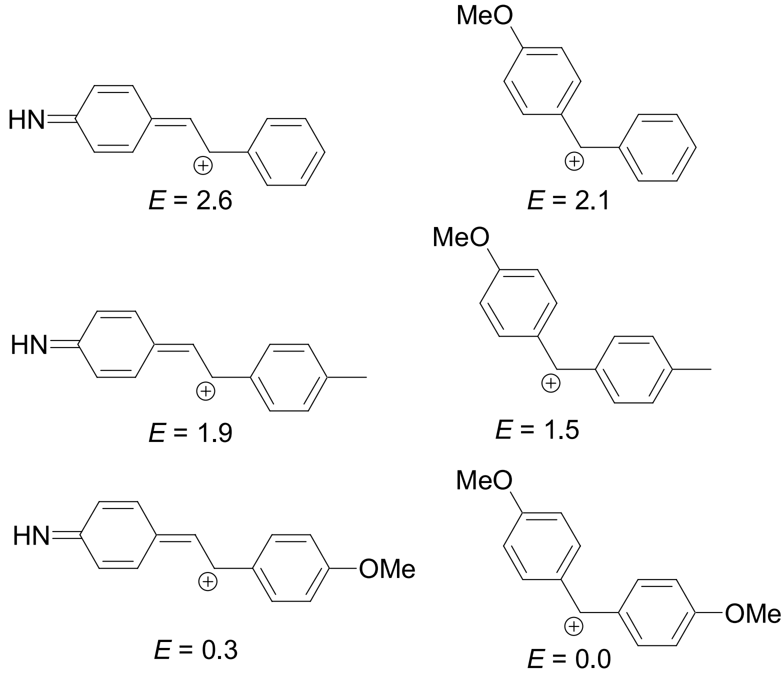

The reason for the low quality of the Hammett correlation in Figure 4.22 is not clear.

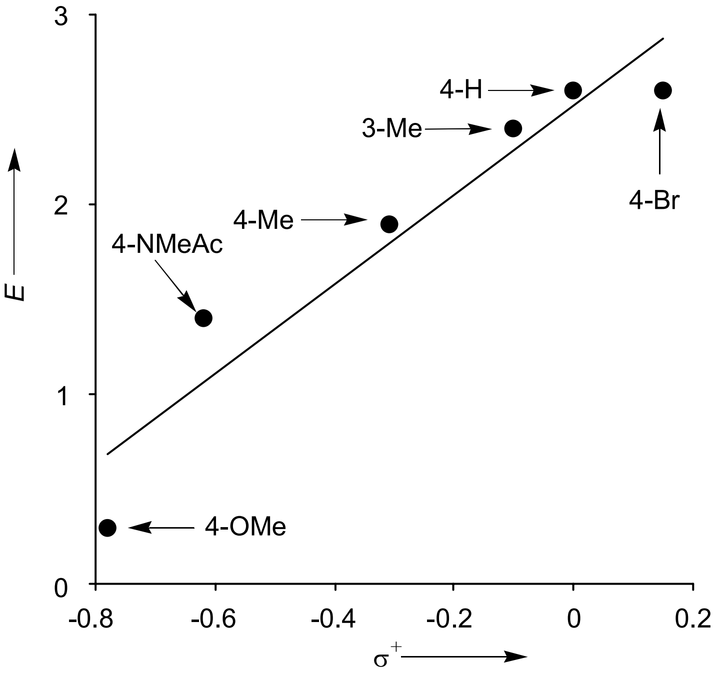

Figure 4.16: Correlation of the electrophilicity parameters E of ArCH=CHC$_6$H$_4$–NH$^+$ with the Hammett σ$^+$-parameters.[14a] $E = 2.35\sigma^+ + 2.52$, n = 6, R^2 = 0.909.

Table 4.41 shows that replacement of hydrogen at the nitrenium-nitrogen by an acetyl group causes a slight increase of electrophilicity by 0.4 units in *E*.

Table 4.41: Rate constants for the reactions of stilbene substituted *N*-acylnitrenium ions with solvents at 20°C, *I* = 0.5 ($NaClO_4$) and electrophilicity parameters derived therefrom.

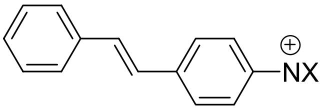

X	*E*	Solvent [a]	N_1	*s*	k_{exp}, s^{-1}	k_{calc}, s^{-1}	$\Delta^2 \log k$	Method [b]	Ref.
Ac	3.0	60W40AN[c]	5.05	0.90	2.6×10^{7}	1.7×10^{7}	3.9×10^{-2}	LF	30
		95W5AN[d]	5.16	0.91	1.6×10^{7}	2.5×10^{7}	3.8×10^{-2}	LF	30
H	2.6	80W20AN	5.04	0.89	6.3×10^{6}	6.3×10^{6}		LF	30

[a] Mixtures of solvents are given as (v/v), solvents: W = water, AN = acetonitrile. [b] LF = laser flash photolysis. [c] N_1 and *s* parameters of 67W33AN were used for calculation. [d] N_1 and *s* parameters of 91W9AN were used for calculation.

As shown in Scheme 4.21, water generally attacks aryl nitrenium ions in para-position, also if this is substituted, which is the case in most systems investigated (Table 4.42).

Scheme 4.21

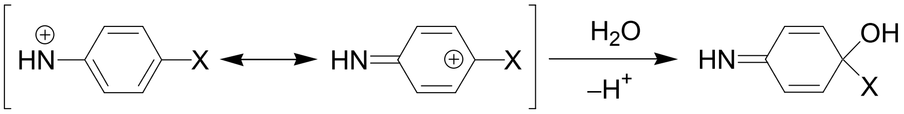

Table 4.42: Rate constants for the reactions of arylnitrenium ions with solvents and electrophilicity parameters derived therefrom.

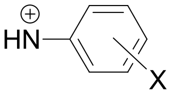

X	*E*	Solvent [a]	N_1	*s*	*T*, °C	*I*, [b]	k_{exp}, s^{-1}	k_{calc}, s^{-1}	$\Delta^2 \log k$	Method [c]	Ref.
2,6-Me$_2$	4.7	W	5.20	0.89	25	1.0	7.0×10^{8}	7.0×10^{8}		Br,Cl	76
4-PhO	3.0	W	5.20	0.89	20	–	1.9×10^{7}	1.9×10^{7}		LF	77
4-(4-NMe$_2$C$_6$H$_4$O)	2.8	W	5.20	0.89	20	–	1.4×10^{7}	1.4×10^{7}		LF	77
4-MeO	2.0	W	5.20	0.89	20	–	2.7×10^{6}	2.7×10^{6}		LF	77
		W	*5.20*	*0.89*	*20*	*0.5*	*1.9×10^{6}*	*2.7×10^{6}*		*Azide*	*78*
4-EtO	1.8	W	5.20	0.89	20	–	1.8×10^{6}	1.8×10^{6}		LF	77
		W	*5.20*	*0.89*	*20*	0.5	*1.2×10^{6}*	*1.8×10^{6}*		*Azide*	*78*
Ph	1.7	80W20AN	5.04	0.89	20	1.0	1.1×10^{6}	1.0×10^{6}	2.4×10^{-4}	LF	79
		95W5AN[d]	5.16	0.91	20	0.5	1.8×10^{6}	1.9×10^{6}	2.3×10^{-4}	LF	80
		95W5AN[d]	*5.16*	*0.91*	*20*	*0.5*	*1.7×10^{6}*	*1.8×10^{6}*	*7.5×10^{-4}*	*Azide*	*81*
4-*i*-PrO	1.4	W	5.20	0.89	20	–	8.0×10^{5}	8.0×10^{5}		LF	77
4-MeO-2,3-benzo	1.3	90W10AN	5.16	0.91	20	–	7.4×10^{5}	7.4×10^{5}		LF	77
4-*t*-BuO	1.3	W	5.20	0.89	20	–	6.4×10^{5}	6.4×10^{5}		LF	77
4-(2-Fluorenyl)	-0.3	80W20AN	5.04	0.89	20	1.0	1.3×10^{4}	1.7×10^{4}	1.2×10^{-2}	LF	79
		95W5AN[d]	5.16	0.91	20	0.5	3.4×10^{4}	2.7×10^{4}	1.1×10^{-2}	LF	80
		*95W5A*N[d]	*5.16*	*0.91*	*20*	0.5	*8.1×10^{4}*	*2.7×10^{4}*	*1.1×10^{-2}*	*Azide*	*82*
4-NMeAc	-2.6	W	5.20	0.89	?	–	2.2×10^{2}	2.2×10^{2}		LF	83
4-(4-NH$_2$C$_6$H$_4$)	-7.4	W	5.20	0.89	20	–	1.0×10^{-2}	1.0×10^{-2}		LF	84
4-(4-NMe$_2$C$_6$H$_4$)	-8.0	W	5.20	0.89	20	–	3.1×10^{-3}	3.1×10^{-3}		LF	84

[a] Mixtures of solvents are given as (v/v), solvents: W = water, AN = acetonitrile. [b] Ionic strength maintained with NaClO$_4$. [c] LF = laser flash photolysis; Azide = azide clock, Br, Cl = Br¯ or Cl¯ clock. [d] N_1 and *s* parameters of 91W9AN were used for calculation.

While 4-alkoxyphenyl substituted nitrenium ions have electrophilicity parameters between 1 and 2, 4-(4-aminophenyl)phenylnitrenium ions are considerably less electrophilic due to the strong resonance stabilization shown in Scheme 4.22.

Scheme 4.22

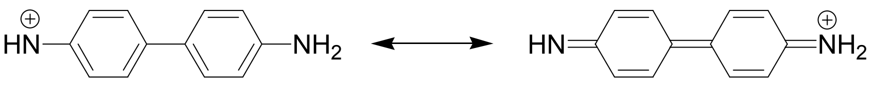

As discussed for the stilbene substituted nitrenium ions (Table 4.41), also in aryl substituted nitrenium ions, the replacement of the NH group by an NAc group causes only a slight increase of electrophilicity by 0.5 to 1 units in *E* (Tables 4.42 and 4.43).

Table 4.43: Rate constants for the reactions of *N*-acyl-arylnitrenium ions with solvents at 20°C and electrophilicity parameters derived therefrom.

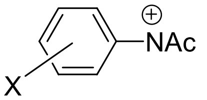

X	*E*	Solvent [a]	N_1	*s*	*I*, [b]	k_{exp}, s^{-1}	k_{calc}, s^{-1}	$\Delta^2 \log k$	Method [c]	Ref.
4-Cl	4.0	95W5AN[d]	5.16	0.91	0.5	2.1×10^8	2.1×10^8		Azide	82
Ph	2.6	80W20AN	5.04	0.89	1.0	3.4×10^6	6.6×10^6	8.1×10^{-2}	LF	79
		95W5AN[d]	5.16	0.91	0.5	5.9×10^6	1.2×10^7	9.5×10^{-2}	LF	80
		*95W5A*N[d]	*5.16*	*0.91*	0.5	*4.9×10^6*	*1.2×10^7*		*Azide*	*81*
		W	5.20	0.89	–	1.1×10^7	9.1×10^6	6.8×10^{-3}	LF	43
		T	1.23	0.92	–	1.1×10^4	3.5×10^3	2.5×10^{-1}	LF	43
4-EtO	2.5	95W5AN[d]	5.16	0.91	0.5	9.1×10^6	9.1×10^6		Azide	82
4-(2-Fluorenyl)	0.3	80W20AN	5.04	0.89	1.0	4.4×10^4	5.8×10^4	1.4×10^{-2}	LF	79
		95W5AN[d]	5.16	0.91	0.5	7.7×10^4	9.5×10^4	8.2×10^{-3}	LF	80
		W	5.20	0.89	–	1.3×10^5	8.0×10^4	4.4×10^{-2}	LF	43

[a] Mixtures of solvents are given as (v/v), solvents: W = water, T = trifluoroethanol, AN = acetonitrile. [b] Ionic strength maintained with $NaClO_4$. [c] LF = laser flash photolysis; Azide = azide clock. [d] N_1 and *s* parameters of 91W9AN were used for calculation.

Table 4.43 shows that the experimental rate constants for the reactions of nitrenium ions with hydroxide ion and *n*-butylamine can be calculated with an accuracy of factor 3, using eq. 4.1 and the electrophilicity parameters of nitrenium ions listed in Table 4.42.

Table 4.43: The reactions of 4-$ArC_6H_4NH^+$ with hydroxide ions and *n*-$BuNH_2$ in water at 20°C.

Ar	*E*	Nucleophile	*N*	*s*	k_{exp}, L mol^{-1} s^{-1}	k_{calc}, L mol^{-1} s^{-1}
Ph	1.7	*n*-$BuNH_2$ [a]	13.33	0.56	1.3×10^{8} [b]	2.6×10^{8}
2-fluorenyl	-0.3	*n*-$BuNH_2$ [a]	13.33	0.56	6.4×10^{7} [b]	2.0×10^{7}
4-$H_2NC_6H_4$	-7.4	OH^-	10.47	0.61	3.1×10^{2} [c]	7.2×10^{1}
4-$Me_2NC_6H_4$	-8.0	OH^-	10.47	0.61	8.6×10^{1} [c]	3.2×10^{1}

[a] N_1 and *s* parameters of *n*-$PrNH_2$ were used for calculation. [b] From ref. 75c in 20% aqueous acetonitrile, at $I = 0.1$ ($NaClO_4$). [c] Ref. 84.

The reaction of the 4-biphenylnitrenium ion with ethyl vinyl ether is 10^3 times faster than calculated by eq. 4.1 from $E = 1.7$ and the reactivity parameters for ethyl vinyl ether ($N = 3.92$, $s = 0.9$).[62] Possibly this reaction, which finally yields an indol derivative, as illustrated in Scheme 4.23, proceeds via a concerted [3+2] cycloaddition, which may account for the high reaction rate. Initial attack of the vinyl ethers at nitrogen and successive cyclization has been excluded by the regioselectivity of the reaction with 1-ethoxypropene.[75b]

Scheme 4.23

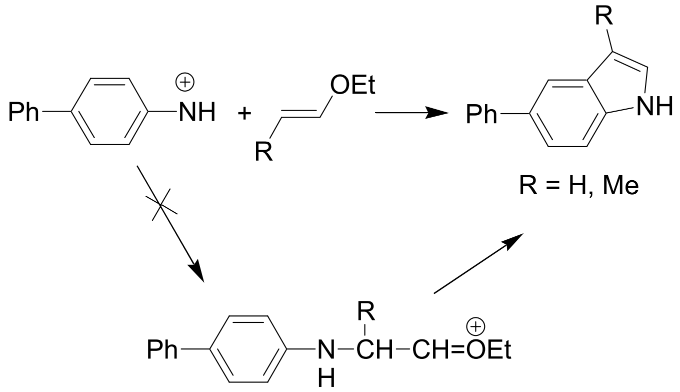

4.20 Determination of the nucleophilicity of 1,1,1,3,3,3-hexafluoro-2-propanol (HFIP)

Because of its high ionizing power and low nucleophilicity 1,1,1,3,3,3-hexafluoro-2-propanol (HFIP) has often been used as a solvent in solvolysis studies[85] and in by laser flash photolytic investigations of reaction with reactive carbocations (benzyl cations,[6,7] dialkyl carbenium ions[86]).

So far, I have not been able to determine the nucleophilicity parameters N_1 and s for HFIP by the procedure described in Chapter 3. When using the stopped-flow apparatus, problems arose because of leaking syringes, which caused a mixing of the solutions prior to the actual experiment. The laser flash investigations of the reaction of the 4-methylbenzhydrylium ion with hexafluoro-2-propanol, were probably carried out with moist solvent and shall not be reported here. An approximate value N_1 [$(CF_3)_2CHOH$] ≈ -2.4 can be derived, however, from the carbocation electrophilicities derived in earlier sections of this chapter assuming a value of $s = 0.9$, as for other alcohols. Using these nucleophilicity parameters, the eleven rate constants listed in Table 4.44 can be reproduced with a standard deviation of factor 3.7, which corroborates the reliability of the E, N_1, and s values employed for this analysis.

Table 4.44: Determination of nucleophilicity parameter of HFIP.

Cation	E	N_1	s	k_{exp}, s^{-1}	k_{calc}, s^{-1}	Ref.
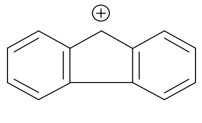	8.4	-2.4	0.9	4.0×10^4	2.7×10^5	87
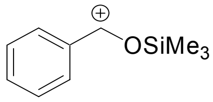	6.4			1.0×10^4	4.2×10^3	53
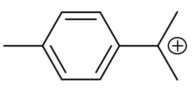	6.4			6.0×10^2	4.2×10^3	6
Ph_2CH^+	5.90			5.0×10^3	1.5×10^3	53
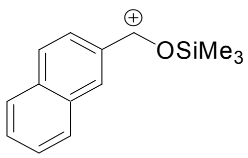	5.9			1.0×10^3	1.5×10^3	53
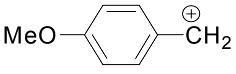	5.9			3.0×10^2	1.5×10^3	6

Table 4.44: Continued

Cation	E	N_1	s	k_{exp}, s^{-1}	k_{calc}, s^{-1}	Ref.
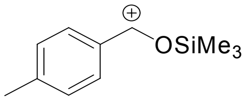	5.6			7.0×10^3	8.1×10^2	53
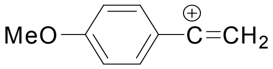	5.4			3.0×10^2	5.3×10^2	6
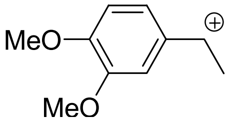	4.8			2.0×10^2	1.5×10^2	6
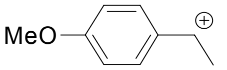	4.4			2.0×10^2	6.7×10^1	6
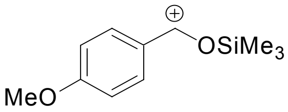	4.5			1.0×10^2	8.3×10^1	53

The summary of solvent nucleophilicities in Table 4.45 shows the tremendous differences of the nucleophilicities of solvents.

Table 4.45: The comparison of nucleophilicity parameters of water and alcohols.

Alcohol	N_1	s
MeOH	7.54	0.92
EtOH	7.44	0.90
H_2O	5.20	0.89
CF_3CH_2OH	1.23	0.92
$(CF_3)_2CHOH$	-2.4	0.9

4.21 References

(1) Mayr, H.; Bug, T.; Gotta, M. F.; Hering, N.; Irrgang, B.; Janker, B.; Kempf, B.; Loos, R.; Ofial, A. R.; Remennikov, G.; Schimmel, H. *J. Am. Chem. Soc.* **2001**, *123*, 9500–9512.

(2) (a) Roth, M.; Mayr, H. *Angew. Chem.* **1995**, *107*, 2428–2430; *Angew. Chem., Int. Ed. Engl.* **1995**, *34*, 2250–2252. (b) See ref. 80.

(3) Gotta, M. *Dissertation*, Ludwig-Maximilians-Universität München, 2000.

(4) Richard, J. P.; Rothenberg, M. E.; Jencks, W. P. *J. Am. Chem. Soc.* **1984**, *106*, 1361–1372.

(5) Richard, J. P.; Tsuji, Y. *J. Am. Chem. Soc.* **2000**, *122*, 3963–3964.

(6) Cozens, F. L.; Kanagasabapathy, V. M.; McClelland, R. A.; Steenken, Steen. *Can. J. Chem.* **1999**, *77*, 2069–2082.

(7) McClelland, R. A.; Chan, C.; Cozens, F.; Modro, A.; Steenken, S. *Angew. Chem.* **1991**, *103*, 1389–1391; *Angew. Chem., Int. Ed. Engl.* **1991**, *30*, 1337–1339.

(8) McClelland, R. A; Kanagasabapathy, V. M.; Steenken, S. *J. Am. Chem. Soc.* **1988**, *110*, 6913–6914.

(9) McClelland, R. A; Cozens, F.; Steenken, S. *Tetrahedron Lett.* **1990**, *31*, 2821–2824.

(10) McClelland, R. A.; Cozens, F. L.; Steenken, S.; Amyes, T. L.; Richard, J. P. *J. Chem. Soc., Perkin Trans. 2* **1993**, 1717–1722.

(11) Richard, J. P. *J. Am. Chem. Soc.* **1986**, *110*, 6819–6820.

(12) Amyes, T. L.; Stevens, I. W.; Richard, J. P. *J. Org. Chem.* **1993**, *58*, 6057–6066.

(13) Chiang, Y.; Kresge, A. J.; Zhu, Y. *J. Am. Chem. Soc.* **2002**, *124*, 717–722.

(14) (a) Taylor, R. *Electrophilic Aromatic Substitution*; Wiley: Chichester, 1990 (b) Exner, O. *Correlation Analysis of Chemical Data*; Plenum Press: New York, 1988.

(15) Amyes, T. L.; Richard, J. P.; Novak, M. *J. Am. Chem. Soc.* **1992**, *114*, 8032–8041.

(16) Amyes, T. L.; Mizerski, T. W.; Richard, J. P. *Can. J. Chem.* **1999**, *77*, 922–933.

(17) Amyes, T. L.; Richard, J. P. *J. Am. Chem. Soc.* **1990**, *112*, 9507–9512.

(18) Schepp, N. P.; Wirz, J. *J. Am. Chem. Soc.* **1994**, *116*, 11749–11753.

(19) Richard, J. P.; Amyes, T. L.; Bei, L.; Stubblefield, V. *J. Am. Chem. Soc.* **1990**, *112*, 9513–9519.

(20) Kirmse, W.; Krzossa, B.; Steenken, S. *J. Am. Chem. Soc.* **1996**, *118*, 7473–7477.

(21) McClelland, R. A.; Licence, V. E.; Richard, J. P.; Williams, K. B.; Lin, S.-S. *Can. J. Chem.* **1998**, *76*, 1910–1915.

(22) Creary, X.; Zhu, C.; Jiang, Z. *J. Am. Chem. Soc.* **1996**, *118*, 12331–12338.

(23) Richard, J. P. *J. Am. Chem. Soc.* **1989**, *111*, 1455–1465.

(24) Richard, J. P.; Amyes, T. L.; Stevens, I. W. *Tetrahedron Lett.* **1991**, *32*, 4255–4258.

(25) Richard, J. P.; Lin, S.-S.; Buccigross, J. M.; Amyes, T. L. *J. Am. Chem. Soc.* **1996**, *118*, 12603–12613.

(26) Lee, I.; Chung D. S.; Jung, J. H. *Tetrahedron* **1994**, *50*, 7981–7986.

(27) Richard, J. P.; Amyes, T. L.; Toteva, M. M. *Acc. Chem. Res.* **2001**, *34*, 981–988.

(28) Richard, J. P. *Tetrahedron* **1995**, *51*, 1535–1573.

(29) Olah, G. A.; Spear, R. J. *J. Am. Chem. Soc.* **1975**, *97*, 1539–1546.

(30) Bose, R.; Ahmad, A. R.; Dicks, A. P.; Novak, M.; Kayser, K. J.; McClelland, R. A. *J. Chem. Soc., Perkin. Trans. 2* **1999**, 1591–1599.

(31) Nekipelova, T. D.; Kurkovskaya, L. N.; Levina, I. I. *Russ. Chem. Bull.* **2002**, *51,* 2055–2058.

(32) Kirmse, W.; Krzossa, B.; Steenken, S. *Tetrahedron Lett.* **1996**, *38*, 1197–2000.

(33) Chiang, Y.; Kresge, A. J.; Zhu, Y. *J. Am. Chem. Soc.* **2002**, *124*, 6349–6356.

(34) Pirinccioglu, N.; Thibblin, A. *J. Am. Chem. Soc.* **1998**, *120*, 6512–6517.

(35) McCormack, A. C.; McDonnell, C. M.; More O'Ferrall, R. A.; O'Donoghue, A. C.; Nagaraja Rao, S. *J. Am. Chem. Soc.* **2002**, *124*, 8575–8583.

(36) Richard, J. P.; Amyes, T. L.; Vontor, T. *J. Am. Chem. Soc.* **1992**, *114*, 5626–5634.

(37) Abe, M.; Adam, W. Heidenfelder, T.; Nau, W. M.; and Zhang, X. *J. Am. Chem. Soc.* **2000**, *122*, 2019–2026.

(38) McClelland, R. A.; Banait, N.; Steenken, S. *J. Am. Chem. Soc.* **1989**, *111*, 2929–2935.

(39) Okuyama, T.; Ueno, K.; Morishima, Y.; Kamachi, M.; Fueno, T. *Chem. Lett.* **1990**, *19*, 1129–1132.

(40) Fichtner, C. *Dissertation*, Ludwig-Maximilians-Universität München, 2001.

(41) Minegishi, S.; Mayr, H. *J. Am. Chem. Soc.* **2003**, *125*, 286–295.

(42) Alonso, E. O.; Johnston, L. J.; Scaiano, J. C.; Toscano, V. G. *Can. J. Chem.* **1992**, *70*, 1784–1794.

(43) Davidse, P. A.; Kahley, M. J.; McClelland, R. A.; Novak, M. *J. Am. Chem. Soc.* **1994**, *116*, 4513–4514.

(44) (a) Pham, T. V.; McClelland, R. A. *Can. J. Chem.* **2001**, *79*, 1887–1897. (b) *J. Chem. Soc., Perkin Trans. 2*, **2001**, 2235–2236. McClelland, R. A.; Moriarty, M. M.; Chevalier, J. M.

(45) Pirinccioglu, N.; Jia, Z. S.; Thibblin, A. *J. Chem. Soc., Perkin Trans. 2*, **2001**, 2271–2275.

(46) Hilinski, E., unpublished result shown in McClelland, R. A. *Tetrahedron* **1996**, *52*, 6823–6858.

(47) Lew, C S. Q.; Wong, D. F.; Johnston, L. J.; Bertone, M.; Hopkinson, A. C.; Lee-Ruff, E. *J. Org. Chem.* **1996**, *61*, 6805–6808.

(48) Cozens, F. L.; Mathivanan, N.; McClelland, R. A.; Steenken, S. *J. Chem. Soc., Perkin. Trans. 2* **1992**, 2083–2090.

(49) (a) Kobayashi, S.; Kitamura, T.; Taniguchi, H.; Schnabel, W. *Chem. Lett.* **1983**, *12*, 1117–1120. (b) Kobayashi, S.; Schnabel, W. *Z. Naturforsch. B* **1992**, *47*, 1319–1323. (c) Kobayashi, S.; Hori, Y.; Hasako, T.; Koga, K.; Yamataka, H. *J. Org. Chem.* **1996**, *61*, 5274–5279.

(50) Verbeek, J.-M.; Stapper, M.; Krijnen, E, S.; van Loon, J.-D.; Lodder, G.; Steenken, S. *J. Phys. Chem.* **1994**, *98*, 9526–9536.

(51) Amyes, T. L.; Jencks, W. P. *J. Am. Chem. Soc.* **1989**, *111*, 7888–7900.

(52) Jagannadham, V.; Amyes, T. L.; Richard, J. P. *J. Am. Chem. Soc.* **1993**, *115*, 8465–8466.

(53) Kirmse, W.; Guth, M.; Steenken, S. *J. Am. Chem. Soc.* **1996**, *118*, 10838–10849.

(54) Amyes, T. L.; Richard, J. P. *J. Chem. Soc., Chem. Commun.* **1991**, 200–202.

(55) Burfeindt, J.; Patz, M.; Müller, M.; Mayr, H. *J. Am. Chem. Soc.* **1998**, *120*, 3629–3634.

(56) Young, P. R.; Jencks, W. P. *J. Am. Chem. Soc.* **1977**, *99*, 8238–8248.

(57) McClelland, R. A.; Ahmad, M. *J. Am. Chem. Soc.* **1978**, *100*, 7031–7036.

(58) McClelland, R. A.; Steenken, S. *J. Am. Chem. Soc.* **1988**, *110*, 5860–5866.

(59) Steenken, S.; McClelland, R. A. *J. Am. Chem. Soc.* **1989**, *111*, 4967–4973.

(60) Okuyama, T. *Acc. Chem. Res.* **1986**, *19*, 370–376.

(61) Steenken, S.; Buschek, J.; McClelland, R. A. *J. Am. Chem. Soc.* **1986**, *108*, 2808–2813.

(62) Mayr, H.; Kempf, B.; Ofial, A. R. *Acc. Chem. Res.* **2003**, *36*, 66–77.

(63) Okuyama, T.; Haga, N.; Takane, S.; Ueno, K.; Fueno, T. *Bull. Chem. Soc. Jpn.* **1991**, *64*, 2751–2756.

(64) (a) Lemieux, R. U.; Koto, S. *Tetrahedron* **1974**, *30*, 1933–1944. (b) Schleyer, P. v. R.; Jemmis, E. D.; Spitznagel, G. W. *J. Am. Chem. Soc.* **1985**, *107*, 6393–6394.

(65) (a) Okuyama, T. *J. Am. Chem. Soc.* **1984**, *106,* 7134–7139. (b) Okuyama, T.; Toyoda, M.; Fueno, T. *Can. J. Chem.* **1986**, *64*, 1116–1123.

(66) Okuyama, T.; Fujiwara, W.; Fueno, T. *J. Am. Chem. Soc.* **1984**, *106,* 657–662.

(67) Eldin, S.; Jencks, W. P. *J. Am. Chem. Soc.* **1995**, *117*, 4851–4857.

(68) Eldin, S.; Digits, J. A.; Huang, S.-T.; Jencks, W. P. *J. Am. Chem. Soc.* **1995**, *117*, 6631–6632.

(69) Dalby, K. N.; Jencks, W. P. *J. Am. Chem. Soc.* **1997**, *119*, 7271–7280.

(70) Gaebert, G.; Siegner, C.; Mattay, J.; Toubartz, M.; Steenken, S. *J. Chem. Soc., Perkin Trans. 2* **1998**, 2735–2740.

(71) Tokuyasu, T.; Mayr, H. Unpublished results.

(72) Amyes, T. L.; Richard, J. P.; Novak, M. *J. Am. Chem. Soc.* **1995**, *117*, 5198–5205.

(73) Henninger, J. *Dissertation*, Ludwig-Maximilians-Universität München, 1999.

(74) Ruane, P. H.; Ahmed, A. R.; McClelland, R. A. *J. Chem. Soc., Perkin Trans. 2* **2002**, 312–317.

(75) (a) Gassman, P. G. *Acc. Chem. Res.* **1970**, *3*, 26–33. (b) McClelland, R. A.; Kahley, M. J.; Davidse, P. A. *J. Phys. Org. Chem.* **1996**, *9*, 355–360. (c) McClelland, R. A.; Gadosy, T. A.; Ren, D. *Can. J. Chem.* **1998**, *76*, 1327–1337. (d) Falvey, D. E. *J. Phys. Org. Chem.* **1999**, *12*, 589–596. (e) Benigni, R.; Giuliani, A.; Franke, R.; Gruska, A. *Chem. Rev.* **2000**, *100*, 3697–3714.

(76) Fishbein, J. C.; McClelland, R. A. *Can. J. Chem.* **1996**, *74*, 1321–1328.

(77) Ramlall, P.; McClelland, R. A. *J. Chem. Soc., Perkin Trans. 2* **1999**, 225–232.

(78) Sukhai, P.; McClelland, R. A. *J. Chem. Soc., Perkin Trans. 2* **1996**, 1529–1530.

(79) McClelland, R. A.; Kahley, M. J.; Davidse, P. A.; Hadzialic, G. *J. Am. Chem. Soc.* **1996**, *118,* 4794–4803.

(80) McClelland, R. A.; Davidse, P. A.; Hadzialic, G. *J. Am. Chem. Soc.* **1995**, *117*, 4173–4174.

(81) Novak, M.; Kahley, M. J.; Eiger, E.; Helmick, J. S.; Peters, H. E. *J. Am. Chem. Soc.* **1993**, *115*, 9453–9460.

(82) Novak, M.; Kahley, M. J.; Lin, J.; Kennedy, S. A.; James, T. G. *J. Org. Chem.* **1995**, *60*, 8294–8304.

(83) Ruane, P. H.; McClelland, R. A. *Can. J. Chem.* **2001**, *79*, 1875–1880.

(84) McClelland, R. A.; Ren, D.; D'Sa, R.; Ahmed, A. R. *Can. J. Chem.* **2000**, *78*, 1178–1185.

(85) (a) Sunko, D. E.; Szele, I. *Tetrahedron Lett.* **1972**, *13*, 3617–3620. (b) Schadt, F. L.; Schleyer, P. v. R.; Bentley, T. W. *Tetrahedron Lett.* **1974**, *15*, 2335–2338. (c) Bentley, T. W.; Schleyer, P. v. R. *J. Am. Chem. Soc.* **1976**, *98*, 7658–7666. (d) Schadt, F. L.; Bentley, T. W.; Schleyer, P. v. R. *J. Am. Chem. Soc.* **1976**, *98*, 7667–7675.

(e) Bentley, T. W.; Bowen, C. T.; Parker, W.; Watt, C. I. F. *J. Am. Chem. Soc.* **1979**, *101*, 2486–2488. (f) Bentley, T. W.; Bowen, C. T.; Morten, D. H.; Schleyer, P. v. R. *J. Am. Chem. Soc.* **1981**, *103*, 5466–5475. (g) Apeloig, Y.; Stanger, A. *J. Am. Chem. Soc.* **1987**, *109*, 272–273. (h) Dietze, P. E.; Hariri, R.; Khattak, J. *J. Org. Chem.* **1989**, *54*, 3317–3320. (i) Lee, I.; Lee, W. H.; Lee, H. W.; Lee, B. C. *J. Chem. Soc.,* *Perkin Trans. 2* **1991**, 785–791. (j) Kevill, D. N.; Abduljaber, M. H. *J. Chem. Soc., Perkin Trans. 2* **1995**, 1985–1989. (k) Williams, K. B.; Richard, J. P. *J. Phys. Org. Chem.* **1998**, *11*, 701–706. (l) Takeuchi, K.; Okazaki, T.; Kitagawa, T.; Ushino, T.; Ueda, K.; Endo, T.; Notario, R. *J. Org. Chem.* **2001**, *66*, 2034–2043.

(86) Pezacki, J. P.; Shukla, D.; Lusztyk, J.; Warkentin, J. *J. Am. Chem. Soc.* **1999**, *121,* 6589–6598.

(87) McClelland, R. A.; Mathivanan, N.; Steenken, S. *J. Am. Chem. Soc.* **1990**, *112*, 4857–4861.

5. Complete energy profiles for S_N1 solvolyses

5.1 Introduction

Ingold's differentiation of bimolecular (S_N2) and unimolecular nucleophilic substitutions (S_N1) marks the beginning of the mechanistic period of Organic Chemistry.[1] Since then, countless investigations on the rates and products of S_N1 reactions have been performed. A considerable part of our knowledge on the relationships between structure and reactivity of carbocations (R^+), the intermediates of these reactions, has been derived from solvolysis studies[2–5] (eq.5.1).

$$\mathrm{RX} \underset{k_{-1}}{\overset{k_1}{\rightleftharpoons}} \mathrm{R^+ + X^-} \xrightarrow[\mathrm{SolvOH}]{k_{\mathrm{SolvOH}}} \mathrm{ROSolv} \qquad (5.1)$$

Investigations of salt effects, equilibration of labeled oxygen during the solvolysis of 4-nitrobenzoates and 4-toluenesulfonates, allylic rearrangements, and racemization of optically active substrates provided information on the relative magnitudes of k_{SolvOH} and k_{-1}. These experiments have demonstrated the existence of different types of ion pairs along with the free ions formulated in eq. 5.1.

In this chapter, we will replace the qualitative solvolysis schemes, so far employed, by quantitative energy profiles.

The last of the three rate constants in eq. 5.1 (k_{SolvOH}) has been determined in Chapter 3 or can be calculated from the solvent nucleophilicities N_1 and s given in Chapter 3 and the carbocation electrophilicities E given in Chapter 4.

If solvent nucleophilicity is sufficiently high, all solvolytically generated carbocations (eq. 5.1) will be trapped by the solvent, and the measured solvolysis rate constants are equivalent to k_1 of eq. 5.1. In collaboration with a Croatian group, we have developed a general approach for predicting k_1 of eq. 5.1 as described in the appendix.

As shown for the solvolysis reactions of benzhydryl derivates in 90 % aqueous acetone (Figure 5.1), we can thus directly compare the rates of ionization of benzhydryl derivatives (k_1) and the rates of reactions of the corresponding carbocations with water (k_{SolvOH}) in the same reaction medium.

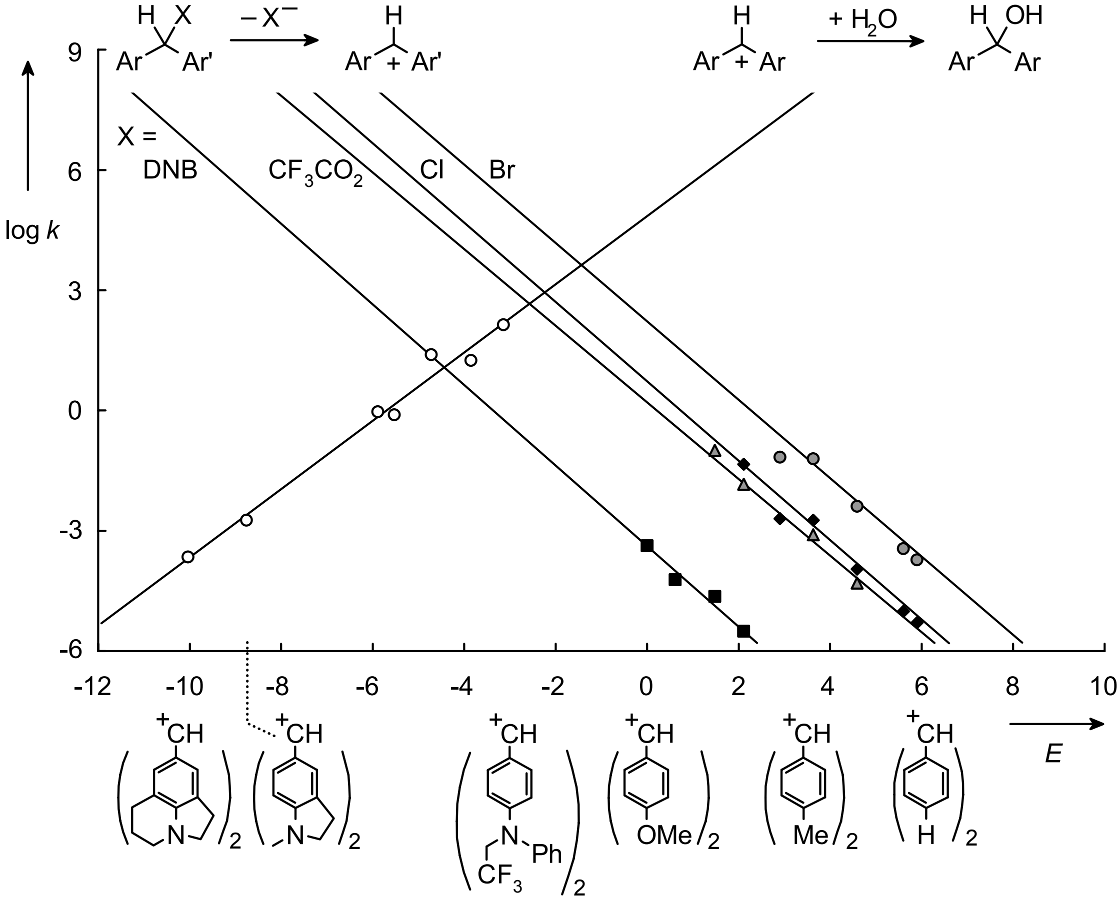

Figure 5.1: First-order rate constants for the ionization (25 °C) and solvent combination (20 °C) of benzhydrylium derivatives in 90 % aqueous acetone (v/v); DNB = 3,5-dinitrobenzoate.

With this information, the rate constants for the reactions of carbocations with X^-, k_{-1}, are the only missing rate constants of eq. 5.1. In this chapter, we will report on the kinetics of the reactions of benzhydrylium ions with halide ions in solvents previously used for the studies of solvolysis reactions.

5.2 Kinetics of the reactions of halide anions with benzhydrylium ions

The reactions of benzhydrylium ions with halide anions in alcoholic solvents were measured by the laser flash photolysis method. Benzhydrylium ions were generated from 4-cyanophenolates or acetates in aqueous or alcoholic solution in the presence of tetrabutylammonium halides. In the most cases, the decays of the benzhydrylium absorbances followed single exponentials from which pseudo-first-order rate constants ($k_{1\Psi}$) were derived. As expressed by eq. 5.2, the pseudo-first-order rate constants $k_{1\Psi}$ include a second-order term for the reactions of the carbocations with halide ions and a first-order term for the reactions of the carbocations with the solvents.

$$k_{1\Psi} = k_{-1}[X^-] + k_{SolvOH} \qquad (5.2)$$

As illustrated in Figure 5.2, the second-order rate constants k_{-1} were obtained as the slopes of the plots of $k_{1\Psi}$ versus the concentrations of the halide anions, while the intercepts correspond to the reactions with the solvent.

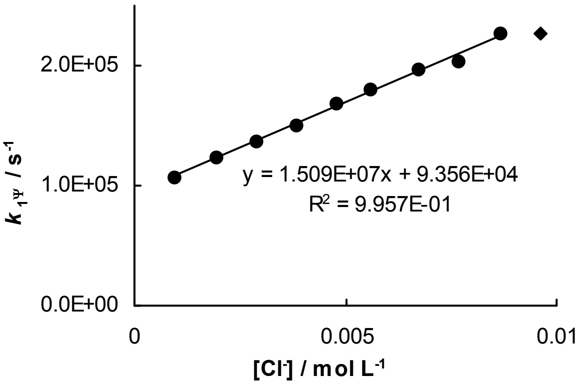

Figure 5.2: Linear correlation of the pseudo-first-order rate constants of the reactions $(ani)_2CH^+$ with Cl^- in 50/50 (v/v) water/acetonitrile with the concentration of tetrabutylammonium chloride.

However, the situation shown in Figure 5.2 is not found in all cases. Sometimes, the pseudo-first-order rate constants do not correlate linearly with the concentrations of the halide anions. At higher halide concentrations, the curves are flattening, probably because of ion-pairing. In such cases, only the linear parts of the correlations in the low concentration range were evaluated to obtain second-order rate constants for the reactions of benzhydrylium ions with halide anions. The results of the kinetics are shown in Table 5.2 and the details of kinetics are described in the experimental section.

In some cases, the decay of the absorption did not follow a single exponential curve because the benzhydryl halides are partially ionic under the reaction conditions. If this is the case, part of the carbocations will be consumed by halide anions in fast reversible reactions, and the remaining carbocations will react with solvents to give alcohols or ethers in slower consecutive reactions (eqs. 5.3 and 5.4).

$$\mathrm{Ar_2CH^+ + X^-} \xrightleftharpoons{\text{fast}} \mathrm{Ar_2CHX} \tag{5.3}$$

$$\mathrm{Ar_2CH^+ + SolvOH} \xrightarrow{\text{slow}} \mathrm{Ar_2CHOSolv} \tag{5.4}$$

To analyze such kinetics, a double-exponential curve (eq. 5.5) was fitted to the observed decay of the absorption, and eq. 5.6 was used to obtain the rate constants for the combination of benzhydrylium ions with anions (eq. 5.6 and Figure 5.3).

$$[A] = A_1[\exp(-r_1 t)] + A_2[\exp(-r_2 t)] \tag{5.5}$$

$$r_1 + r_2 = k_{-1}[\mathrm{X}^-] + k_{\mathrm{SolvOH}} + k_1 \tag{5.6}$$

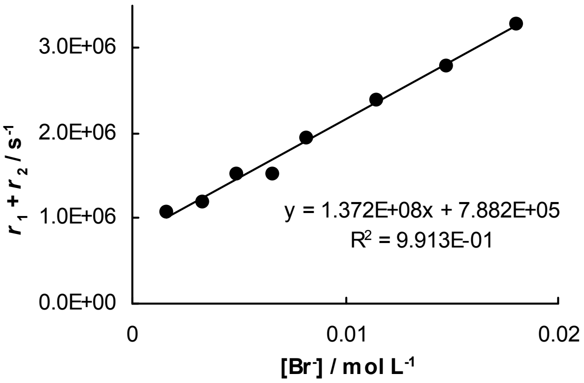

Figure 5.3: Linear correlation of (r_1 + r_2) for the reaction of $(\mathrm{ani})_2\mathrm{CH}^+$ with Br^- with $[\mathrm{Br}^-]$ in 50/50 (v/v) ethanol/water.

According to eq. 5.6, the sum $k_{\mathrm{SolvOH}} + k_1$ is obtained as the intercept of the correlation of $r_1 + r_2$ versus $[\mathrm{X}^-]$, as illustrated in Figure 5.3. However, an accurate value of the ionization rate constant (k_1) can only be obtained by subtracting the known rate constant for the reaction with solvent (k_{SolvOH}) from the intercept (r_1 + r_2), if the two rate constants are of similar magnitude or if the ionizations of the benzhydryl halides are much faster than the reactions of the carbocations with solvents. Thus, approximate values of the ionization constants k_1 could only be derived for few systems in Table 5.1.

These rate constants are in the same order of magnitude as k_1 values estimated from solvent ionizing power and the correlation described in the appendix.

Table 5.1: Rate constants for the reactions of (ani)$_2$CHX in different solvents (20°C).

Ar$_2$CHX	Solvent [a]	$k_{\mathrm{SolvOH}} + k_1$,[b] s^{-1}	k_{SolvOH}, s^{-1}	k_1, s^{-1}	k_1 (estimated), s^{-1}
(ani)$_2$CHCl	80W20AN	1.23×10^5	1.0×10^5	2.3×10^4	8×10^5 [c]
(ani)$_2$CHBr	50E50W	7.88×10^5	4.96×10^5	2.92×10^5	5×10^6 [d]
(ani)$_2$CHBr	50W50AN	1.81×10^5	1.04×10^5	7.7×10^4	

[a] Mixtures of solvents are given as (v/v), solvents: E = ethanol, W = water, AN = acetonitrile. [b] Intercept according to eq. 5.6 (or Figure 5.3). [c] From the sum of log k_1((ani)$_2$CHCl) in 80% aqueous ethanol = 2.1×10^3 s^{-1} and Y_{OTs} (80W20AN) = 2.55 interpolated from 20 and 25 w% of aqueous acetonitrile.[6] [d] From the sum of log k_1((ani)$_2$CHBr) in 80% aqueous ethanol = 7.5×10^4 s^{-1} and Y_{Cl} (50E50W) = 2.02.[6]

In all the other cases, only rate constants for the combinations of halide anions with benzhydrylium ions were derived from these experiments (Table 5.2).

Table 5.2: Kinetics of the reactions of anions with benzhydrylium ions at 20 ºC.

Ar$_2$CH$^+$	Solvent [a]	k_{SolvOH},[b] s^{-1}	$k_{-1}(\mathrm{Cl}^-)$, L mol^{-1} s^{-1}	$k_{-1}(\mathrm{Br}^-)$, L mol^{-1} s^{-1}
(ani)$_2$CH$^+$	M	8.6×10^6	5.33×10^7	5.31×10^8
	50M50AN	2.33×10^6	3.02×10^8	1.63×10^9
	E	5.5×10^6	6.99×10^8	2.75×10^9
	50E50AN	1.41×10^6	1.71×10^9	4.32×10^9
	80E20W	1.51×10^6	6.05×10^7	4.84×10^8
	50E50W	4.96×10^5	1.20×10^7	1.37×10^8
	80W20AN	1.0×10^5	3.23×10^6	
	50W50AN	1.04×10^5	1.51×10^7	1.86×10^8
	20W80AN	9.82×10^4	9.53×10^7	7.02×10^8
(ani)(tol)CH$^+$	80E20W	7.88×10^6	5.01×10^8	
	50E50W	3.86×10^6	1.26×10^8	8.26×10^8
	W	7.8×10^5	9.24×10^6 [c]	8.24×10^7 [c]
	80W20AN	8.2×10^5	2.41×10^7 [c]	1.53×10^8 [c]

Table 5.2: Continued

Ar_2CH^+	Solvent[a]	k_{SolvOH},[b] s^{-1}	$k_{-1}(Cl^-)$, $L\ mol^{-1}\ s^{-1}$	$k_{-1}(Br^-)$, $L\ mol^{-1}\ s^{-1}$
$(ani)(tol)CH^+$	60W40AN		4.82×10^{7} [c]	3.72×10^{8} [c]
	50W50AN	8.55×10^{5}	1.01×10^{8}	5.37×10^{8} [c]
	40W60AN		1.27×10^{8} [c]	8.11×10^{8} [c]
	20W80AN	8.29×10^{5}	5.29×10^{8} [c]	2.52×10^{9} [c]
	10W90AN	6.81×10^{5}	2.26×10^{9} [c]	6.58×10^{9} [c]
	5W95AN		6.36×10^{9} [c]	1.16×10^{10} [c]
	3W97AN		1.11×10^{10} [c]	1.66×10^{10} [c]
	AN		2.44×10^{10} [c]	2.59×10^{10} [c]
$(ani)PhCH^+$	50E50W	7.91×10^{6}	6.19×10^{8}	1.19×10^{9}
	W	1.9×10^{6}	2.16×10^{7} [c]	2.41×10^{8} [c]
	80W20AN	2.0×10^{6}	5.22×10^{7} [c]	4.37×10^{8} [c]
	60W40AN		1.18×10^{8} [c]	6.15×10^{8} [c]
	50W50AN	1.84×10^{6}	2.64×10^{8}	9.29×10^{8} [c]
	40W60AN		2.26×10^{8} [c]	1.21×10^{9} [c]
	30W70AN			1.65×10^{9} [c]
	20W80AN	1.87×10^{6}	1.02×10^{9} [c]	3.40×10^{9} [c]
	15W85AN			4.50×10^{9} [c]
	10W90AN	1.83×10^{6}	3.33×10^{9} [c]	7.02×10^{9} [c]
	5W95AN		8.38×10^{9} [c]	1.34×10^{10} [c]
	3W97AN		1.21×10^{10} [c]	1.84×10^{10} [c]
	AN		2.20×10^{10} [c]	2.73×10^{10} [c]
	T	1.2×10^{3}	2.60×10^{7}	1.92×10^{8}
$(tol)_2CH^+$	T	2.4×10^{4}	2.53×10^{8}	1.76×10^{9}
$(tol)PhCH^+$	T	2.7×10^{5}	1.07×10^{9}	3.89×10^{9}
	H		3.47×10^{7}	-
Ph_2CH^+	T	3.2×10^{6}	1.9×10^{9} [d]	6.5×10^{9} [d]
	H	5×10^{3} [e]	6.12×10^{8}	2.55×10^{9}

[a] Mixtures of solvents are given as (v/v), solvents: M = methanol, E = ethanol, W = water, AN = acetonitrile, T = trifluoroethanol, H = hexafluoro-2-propanol. [b] From Chapter 3. [c] From ref. 7b. [d] From ref. 7a. [e] From ref. 8.

5.3 Nucleophilicity parameters for halide anions.

In the preceding chapters, rate constants of the reactions of nucleophiles with benzhydrylium ions (reference electrophiles) have been employed to determine the nucleophile-specific parameters N and s as defined by eq. 5.6.[9] It was emphasized, however, that only second-order rate constants $k < 10^8$ L mol^{-1}s^{-1} should be used for the calculation of nucleophilicity parameters because at higher values of k, deviations from the linear correlation (eq. 5.6) occur.[9-11]

$$\log k(20°\mathrm{C}) = s(N + E) \tag{5.6}$$

As shown in Figure 5.4, nucleophilicity parameters N and s could be calculated for the chloride ion in 80 % water / 20 % acetonitrile, because all three rate constants were below 10^8 L mol^{-1}s^{-1} and correlated linearly with the electrophilicity parameters E.

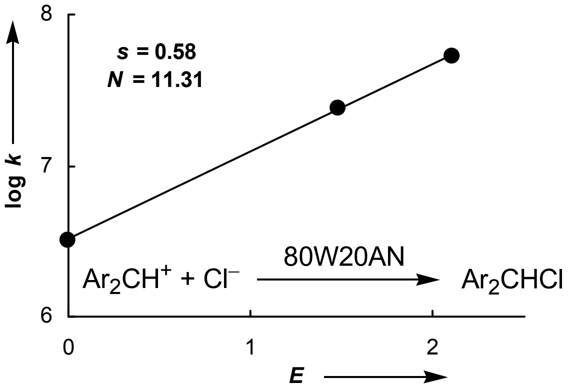

Figure 5.4: Plot of the rate constants for the reactions of benzhydrylium ions with chloride ions in 80/20 (v/v) water/acetonitrile versus the corresponding electrophilicity parameters.

The slope parameter $s = 0.58$ derived from Figure 5.4 is similar to that of other anions in aqueous solution[12] and can, therefore, be assumed to be the same also for chloride and for bromide in the solvents and solvent mixtures listed in Table 5.2. With this assumption, it was possible to calculate N parameters also for Cl^- and Br^- in such solvents, where only one or two rate constants below 10^8 L mol^{-1}s^{-1} were available. Table 5.3 shows that the N parameters thus determined also give reasonable agreement with observed rate constants in the range $10^8 – 10^9$ L mol^{-1}s^{-1}. For that reason, lower limits of *N* parameters have also been calculated for systems where only rate constants between (1-5) × 10^8 L $mol^{-1}s^{-1}$ were available.

Table 5.3: Nucleophilicity parameters *N* for chloride and bromide ions in various solvents (for $s = 0.58$)

Anion/solvent [a]	*N*	Ar_2CH^+	k_{obs}, L $mol^{-1}s^{-1}$	k_{calc}, L $mol^{-1}s^{-1}$
Cl^-/M	13.3	$(ani)_2CH^+$	5.33×10^7	identical
Cl^-/50M50AN	≥ 14.6	$(ani)_2CH^+$	3.03×10^8	identical
Cl^-/80E20W	13.4	$(ani)_2CH^+$	6.05×10^7	identical
		$(ani)(tol)CH^+$	5.01×10^8	4.3×10^8
Cl^-/50E50W	12.2	$(ani)_2CH^+$	1.20×10^7	identical
		$(ani)(tol)CH^+$	1.26×10^8	8.6×10^7
		$(ani)PhCH^+$	6.19×10^8	2.0×10^8
Cl^-/W	10.5	$(ani)(tol)CH^+$	9.24×10^6	identical
		$(ani)PhCH^+$	2.16×10^7	2.1×10^7
Cl^-/60W40AN	11.8	$(ani)(tol)CH^+$	4.82×10^7	identical
		$(ani)PhCH^+$	1.18×10^8	1.17×10^8
Cl^-/50W50AN	12.4	$(ani)_2CH^+$	1.51×10^7	identical
		$(ani)(tol)CH^+$	1.01×10^8	1.1×10^8
		$(ani)PhCH^+$	2.64×10^8	2.6×10^8
Cl^-/40W60AN	≥ 12.5	$(ani)(tol)CH^+$	1.27×10^8	identical
		$(ani)PhCH^+$	2.26×10^8	$\geq 3.0 \times 10^8$
Cl^-/20W80AN	13.8	$(ani)_2CH^+$	9.53×10^7	identical
		$(ani)(tol)CH^+$	5.29×10^8	7.3×10^8
		$(ani)PhCH^+$	1.02×10^9	1.7×10^9
Cl^-/AN	17.2	$(dpa)_2CH^+$ [b]	1.8×10^7	identical
		$(mfa)_2CH^+$ [b]	1.6×10^8	5.5×10^7
		$(pfa)_2CH^+$ [b]	9.7×10^8	1.4×10^8
		$(fur)_2CH^+$ [b]	9.4×10^9	1.5×10^9
		$(ani)_2CH^+$ [b]	1.5×10^{10}	9.5×10^9
Cl^-/T	10.7	$(ani)PhCH^+$	2.60×10^7	identical

Table 5.3: Continued

Anion/solvent [a]	N	Ar_2CH^+	k_{obs}, L $mol^{-1}s^{-1}$	k_{calc}, L $mol^{-1}s^{-1}$
Cl^-/T	10.7	$(tol)_2CH^+$	2.53×10^8	2.0×10^8
		$(tol)PhCH^+$	1.07×10^9	7.4×10^8
		Ph_2CH^+	1.9×10^9	4.2×10^9
Cl^-/H	8.4	$(tol)PhCH^+$	3.47×10^7	identical
		Ph_2CH^+	6.12×10^8	2.0×10^8
Br^-/80E20W	≥ 15.0	$(ani)_2CH^+$	4.84×10^8	identical
Br^-/50E50W	≥ 14.0	$(ani)_2CH^+$	1.37×10^8	identical
		$(ani)(tol)CH^+$	8.26×10^8	$\geq 9.5 \times 10^8$
		$(ani)PhCH^+$	1.19×10^9	$\geq 2.2 \times 10^9$
Br^-/W	12.2	$(ani)(tol)CH^+$	8.24×10^7	identical
		$(ani)PhCH^+$	2.41×10^8	2.0×10^8
Br^-/80W20AN	≥ 12.6	$(ani)(tol)CH^+$	1.53×10^8	identical
		$(ani)PhCH^+$	4.37×10^8	$\geq 3.4 \times 10^8$
Br^-/60W40AN	≥ 13.3	$(ani)(tol)CH^+$	3.72×10^8	identical
		$(ani)PhCH^+$	6.15×10^8	$\geq 8.7 \times 10^8$
Br^-/50W50AN	≥ 14.3	$(ani)_2CH^+$	1.86×10^8	identical
		$(ani)(tol)CH^+$	5.37×10^8	$\geq 1.4 \times 10^9$
		$(ani)PhCH^+$	9.29×10^8	$\geq 3.3 \times 10^9$
Br^-/T	≥ 12.2	$(ani)PhCH^+$	1.92×10^8	identical
		$(tol)_2CH^+$	1.76×10^9	$\geq 1.5 \times 10^9$
		$(tol)PhCH^+$	3.89×10^9	$\geq 5.4 \times 10^9$
		Ph_2CH^+	6.5×10^9	$\geq 3.1 \times 10^{10}$

[a] Mixtures of solvents are given as (v/v), solvents: M = methanol, E = ethanol, W = water, AN = acetonitrile, T = trifluoroethanol, H = hexafluoro-2-propanol. [b] From Ref. 13.

McClelland has already demonstrated the increase of nucleophilicities of halide anions in aqueous acetonitrile mixtures with decreasing amount of water.[7b] By using different reference electrophiles, we can now show that chloride nucleophilicities decrease in the order of AN (17.2) > E (≈ 15) > M (13.3) > T (10.7) ≥ W (10.5) > H (8.4).

With the *N* parameters thus derived, we can compare nucleophilicities of halide ions with those of other nucleophiles. Figure 5.5 shows that in water the nucleophilicities of chloride ion and of hydroxide are closely similar, while that of bromide is bigger. This ordering contrasts the relative magnitudes of N_+ parameters [Cl^-: 1.2, Br^-: 2.2 vs. OH^-: 4.75] derived by Richard from nucleophilic additions to the quinone methide 4-[bis(trifluoromethyl)methylene]cyclohexa-2,5-dienone.[14] The reason for this strong deviation is presently not clear.

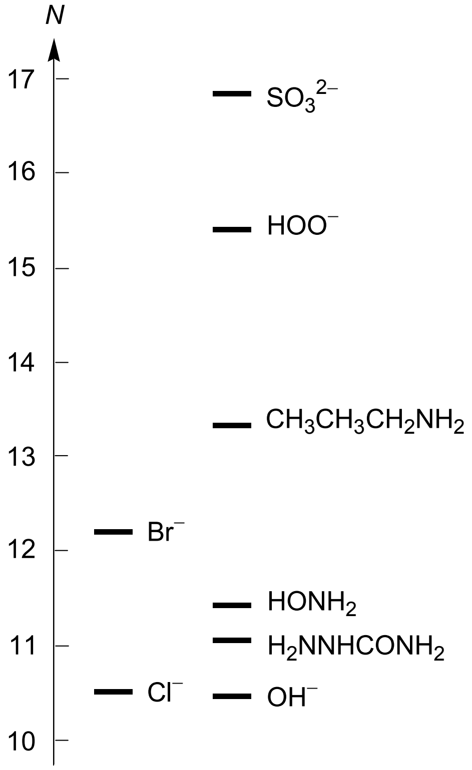

Figure 5.5: Comparison of the reactivities of anionic and neutral n-nucleophiles in water.[12]

When the *N* parameters for Cl^- and Br^- presented in this work are combined with the previously published *E* parameter of the tritylium ion (*E* = 0.51),[12] rate constants for the reaction of the tritylium ion with Cl^- and Br^- in water are calculated, which are approximately one order of magnitude higher than McClelland's experimental data[15] (Table 5.4).

Table 5.4: Comparison of calculated and experimental rate constants (L $mol^{-1}s^{-1}$) for the reaction of Cl^{-} and Br^{-} with Ph_3C^+ ($E = 0.51$) in aqueous acetonitrile.

Hal^{-}	N/s (60W40AN)	k_{calc}	k_{obs} (67W33AN) [a]
Cl^{-}	11.8/0.58	1.4×10^7	2.2×10^6
Br^{-}	≥ 13.3/0.58	$\geq 1.0 \times 10^8$	5×10^6 [b]

[a] Ref. 15. [b] $[Br^{-}] = 0.1\text{-}0.3$ (KBr).

With N_+ values differing by 3.5 units for Cl^{-} and OH^{-}, as derived by Richard, one cannot explain McClelland's observation that OH^{-} (5.2×10^6 L $mol^{-1}s^{-1}$), Cl^{-} (2.2×10^6 L $mol^{-1}s^{-1}$), and Br^{-} (5×10^6 L $mol^{-1}s^{-1}$) possess similar reactivities toward Ph_3C^+ in 67/33 (v/v) water/acetonitrile.

As previously demonstrated by McClelland,[7b] the nucleophilicity of bromide is generally bigger than that of chloride. The nucleophilicities of both anions increase in acetonitrile/water mixtures as the water content decreases (Figure 5.6).

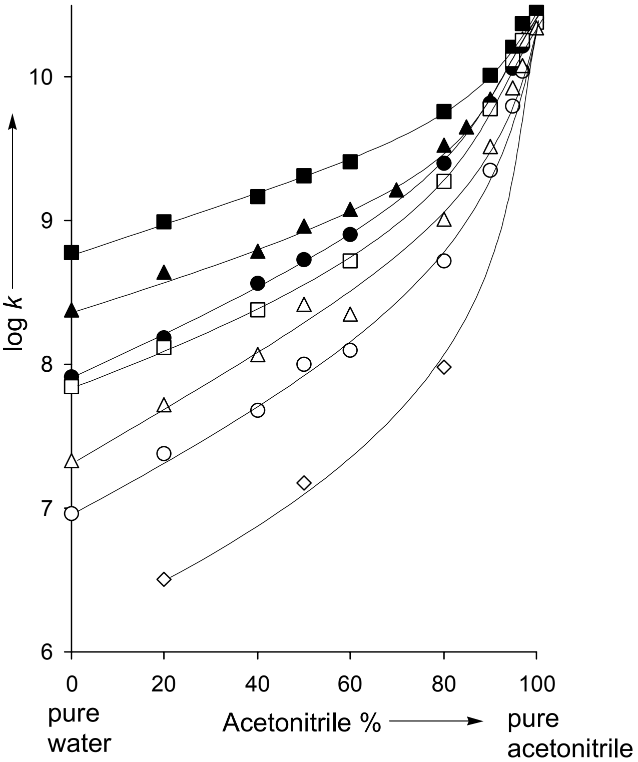

Figure 5.6: Variations in rate constants for the combinations of bromide anion and chloride anion with benzhydrylium ions in aqueous acetonitrile; ◊ $(ani)_2CH^+ + Cl^{-}$, ○ $(ani)(tol)CH^+ + Cl^{-}$, Δ $(ani)PhCH^+ + Cl^{-}$, □ $(4\text{-}MeOC_6H_4)(4\text{-}F_3CC_6H_4)CH^+ + Cl^{-}$, ● $(ani)(tol)CH^+ + Br^{-}$, ▲ $(ani)PhCH^+ + Br^{-}$, ■ $(4\text{-}MeOC_6H_4)(4\text{-}F_3CC_6H_4)CH^+ + Br^{-}$; rate constants from Table 5.2.

The nucleophilicity of halides strongly depends on the solvent. In Figure 5.7 rates of carbocation-chloride combinations (represented by *N*) are correlated with solvent ionizing power. The good correlation shows that the same interactions between solvent and anions are responsible for the ionization of RCl and for the combination of R^+ with Cl^-.

From the unity slopes of Figures 5.7 and 5.8 one can derive that variation of solvents affects ionization in opposite sense and to a greater extent than ion combination, since *N* is converted into log *k* by multiplication with $s = 0.58$ (see above), while *Y* is converted into log *k* by multiplication with $m \approx 0.9$.[16]

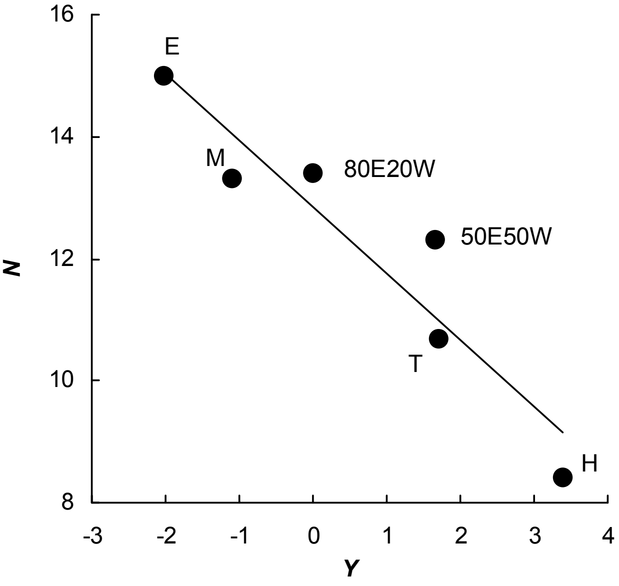

Figure 5.7: Correlation of *N*-parameters of Cl^- in several solvents with solvent ionizing power Y^6 (derived from *t*-butyl chloride solvolysis) of the solvents. $N = -1.09Y + 12.8$, $n = 7$, $R^2 = 0.887$.

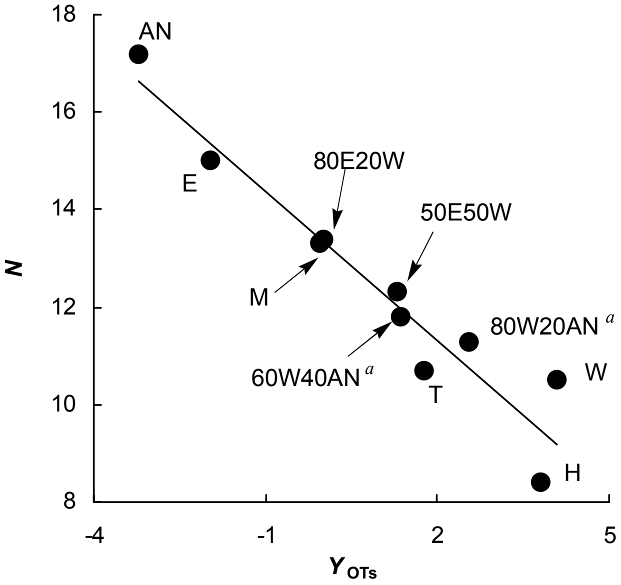

Figure 5.8: Correlation of *N*-parameters of Cl^- in several solvents with solvent ionizing power Y_{OTs} [6] (derived from 1- or 2-adamantyl tosylates solvolyses) of the solvents. [a] Interpolated values from ref. 6. $N = -1.02Y_{OTs} + 13.4$, $n = 10$, $R^2 = 0.920$.

The smaller slope of the correlation in Figure 5.9 indicates that solvent variation affects the combination of chloride anions with benzhydrylium ions to similar extent but in opposite sense than the ionization of adamantly chloride.

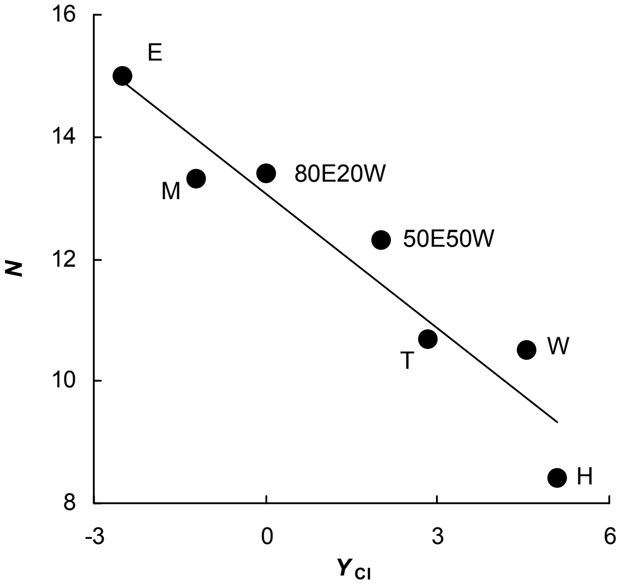

Figure 5.9: Correlation of *N*-parameters of Cl^- in several solvents with solvent ionizing power Y_{Cl} [6] (derived from 1-adamantyl chloride solvolysis) of the solvents. $N = -0.74Y_{Cl} + 13.1$, $n = 7$, $R^2 = 0.911$.

Kamlet, Taft, and coworkers derived the hydrogen bonding ability of solvents from the solvatochromism of 4-nitroaniline, *N*,*N*-dimethyl-4-nitroaniline, 4-nitroanisol, and 2,6-diphenyl-4-(2,4,6-triphenyl-1-pyridinio)phenolate (Reichardt's dye).[17] The analysis of the spectral data yielded hydrogen bond donor acidity (α), hydrogen bond acceptor basicity (β), and nonspecific solvent polarity (π*). Table 5.5 and Figure 5.10 show that the hydrogen bond donor ability is the crucial interaction that controls the reactivity of halide anions in different solvents.

Table 5.5: α, β, and π* parameters for solvents

Solvent [a]	α	β	π*
Acetonitrile [b]	0.19	0.31	0.75
20W80AN [c]	0.82		
50W50AN [c]	0.90		
60W40AN [c]	0.95		
80W20AN [c]	1.08		
Ethanol [b]	0.83	(0.77)	0.54
50E50W [c]	0.94		1.01
80E20W [c]	0.90		0.79
Methanol [b]	0.93	(0.62)	0.60
Water [b]	1.17	0.18	1.09
Trifluoroethanol [b]	1.51	0.00	0.73
Hexafluoro-2-propanol [b]	1.96	0.00	0.65

[a] Mixtures of solvents are given as (v/v), solvents: M = methanol, E = ethanol, W = water, AN = acetonitrile, T = trifluoroethanol, H = hexafluoro-2-propanol. [b] From ref. 17. [c] From ref. 18.

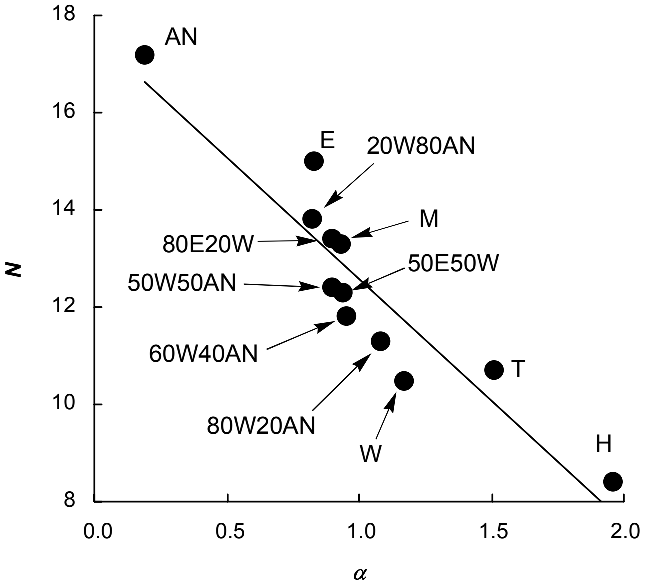

Figure 5.10: Correlation of *N*-parameters of Cl^- in several solvents with hydrogen bond donor acidity α[17,18] of the solvents. $N = -5.02\alpha + 17.6$, $n = 12$, $R^2 = 0.859$.

From Figure 5.6 one can derive that in reactions with carbocations, the bromide anion is generally a stronger nucleophile than the chloride anion, in aprotic[13] as well as in protic solvents. While the same reactivity order of halide anions has been found for S_N2 reactions (Scheme 5.1) in protic solvents,[19] in aprotic solvents as well as in the gas-phase, Cl^- was found to be a more reactive nucleophile than Br^- in S_N2 reactions.[19] The reason for the deviating behavior under the conditions of this work is presently not clear.

Scheme 5.1

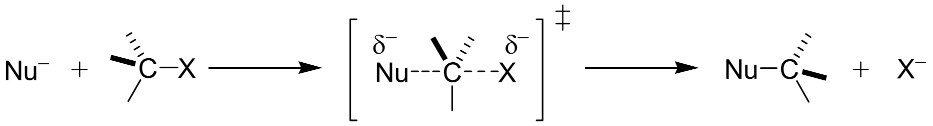

Figure 5.11 compares rate constants of the reactions of benzhydrylium ions with bromide and chloride in different solvents with the nucleophilicities of the corresponding solvents.

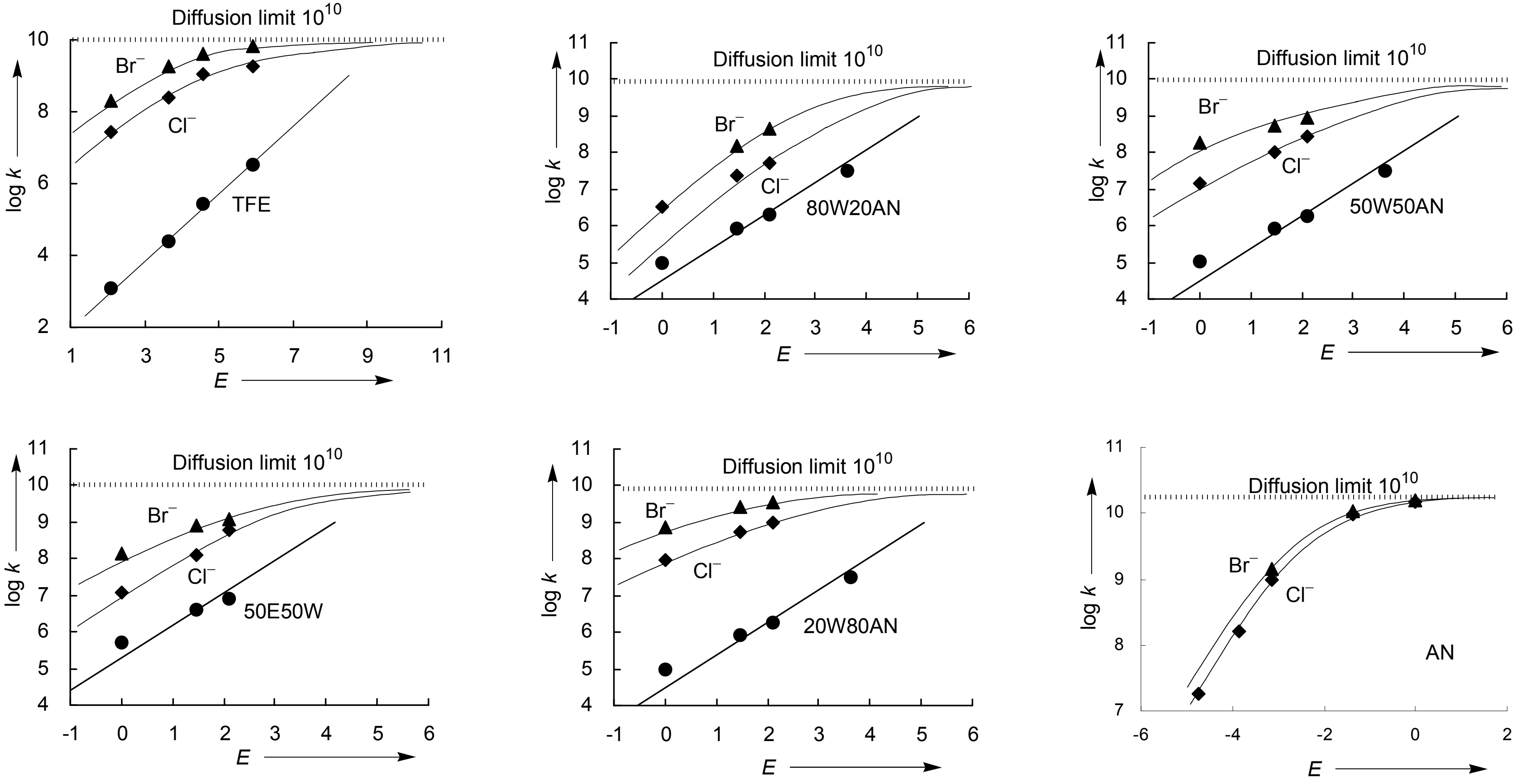

Figure 5.11: Comparison of the second-order rate constants of the reactions of benzhydrylium ions (characterized by their electrophilicities *E*) with Cl⁻ and Br⁻ in different solvents with the first-order rate constants of the reactions with the solvents.

It is obvious that the correlation lines for chloride and bromide, which refer to second-order rate constants, are generally above those for the corresponding solvents, which correspond to first-order rate constants. One can see that chloride reaches diffusion control in trifluoroethanol at $E > 7$, in 20 % and 50 % aqueous acetonitrile at $E > 5$, in 50 % aqueous ethanol and in 80 % aqueous acetonitrile at $E > 4$, and in acetonitrile at $E > 0$. For bromide, diffusion limit is reached with weaker electrophiles, e.g., in trifluoroethanol at $E > 5$, in 20 % and 50 % aqueous acetonitrile as well as in 50 % aqueous ethanol at $E > 4$, in 80 % aqueous acetonitrile at $E > 3$, and in acetonitrile at $E > -1$.

5.4 Complete energy profiles for S_N1 solvolyses

In order to decide whether a solvolytically generated carbocation preferentially reacts with solvent to yield the product or reacts with the leaving group to regenerate the starting material, i.e., whether a common ion effect can be expected, the second-order rate constants for the combination with halide anions have to be multiplied with the concentrations [Hal^-]. If one neglects the change of the medium due to the presence of salts (the ionization constants k_1 generally increase by a factors of less than 16, when 0.1 mol L^{-1} of inert salt is present)[20] the relative heights of the lines in Figures 5.12 and 5.13 directly reflect the probability of the different events. Thus, $(mor)_2CH^+$ ($E = -5.53$) will not combine with chloride in 80 % aqueous ethanol at any chloride concentration, because $k_1 > k_{-1}[Cl^-]$. The benzhydrylium ion will react with the solvent (half-life 0.07 s) to give the product.

Solvolysis of $(ani)_2CHCl$ ($E = 0$) in 80 % aqueous ethanol will generate the carbocation in a first-order reaction ($k_1 = 10^3$ s^{-1}). The carbocation cannot accumulate, however, because both, the reactions with Cl^- and with solvent, are faster than the ionization. While at [Cl^-] = 10^{-2} mol L^{-1}, the reactions with Cl^- and with solvent will be of similar rate, recombination with Cl^- will be faster at [Cl^-] = 1 mol L^{-1}, and the reaction with the solvent will be faster at [Cl^-] < 10^{-2} mol L^{-1}.

Carbocations with $E > 6$ will be short-lived intermediates, and external nucleophiles will not be able to compete with the solvent. Only at high local concentrations of chloride ions (equivalent to ion-pairs) does recombination have a chance.

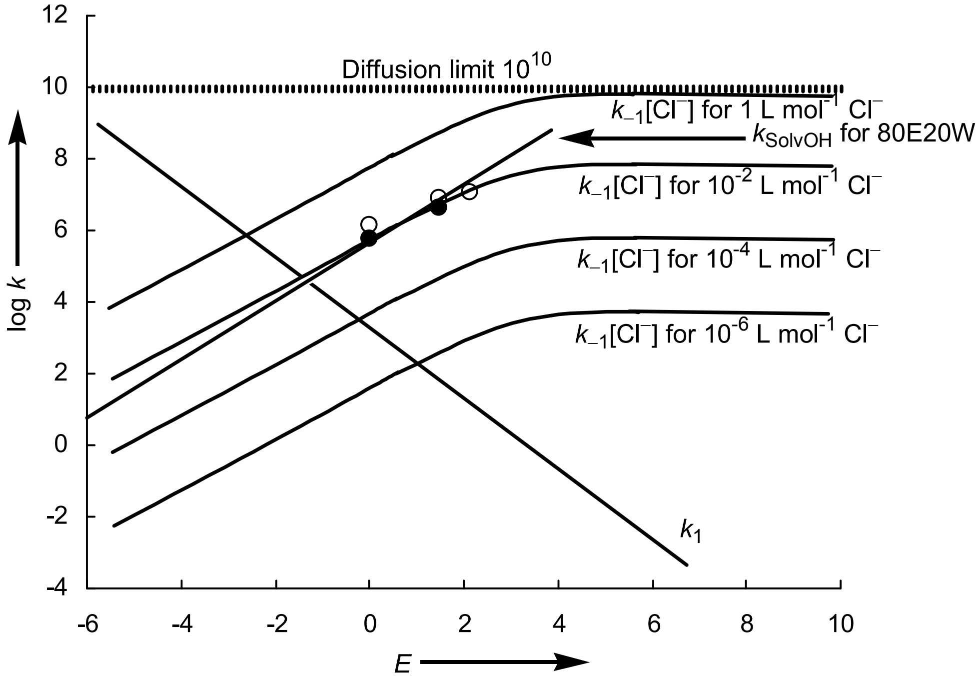

Figure 5.12: Rate constants for the different steps in the solvolysis of various benzhydryl chlorides in 80 % aqueous ethanol at 20 °C for the reactions of benzhydrylium ions with solvent and Cl^-, at 25 °C for ionization. ○: Reactions of benzhydryl cations with 80E20W, ●: Reactions of benzhydryl cations with chloride anion (10^{-2} mol L^{-1}) in 80E20W.

The situation is different in the less nucleophilic solvent trifluoroethanol (Figure 5.13). While $(mor)_2CH^+$ ($E = -5.53$) again does not combine with chloride, even at high halide concentrations, the benzhydrylium chloride $(ani)_2CHCl$ now ionizes faster than the carbocation $(ani)_2CH^+$ ($E = 0$) will react with the solvent.

Even the combination with Cl^- will be slower (unless $[Cl^-] \geq 1$ mol L^{-1}) than ionization; as a consequence the carbocation $(ani)_2CH^+$ will accumulate during the reaction before it is trapped by the solvent. In accord with this analysis, the decay of laser flash photolytically generated $(ani)_2CH^+$ was not accelerated when 0.2 mol L^{-1} Bu_4N^+ Cl^- was added to the solutions. Benzhydrylium chlorides with $E > 2$ show the well-known reactivity pattern of solvolysis reactions, i.e., slow ionization followed by fast combination with the solvent. Large common ion depressions can be expected for trifluoroethanolysis of benzhydryl chloride of $2 < E < 8$, and only at $E > 10$ will combination with external chloride anions (1 mol L^{-1}) be negligible.

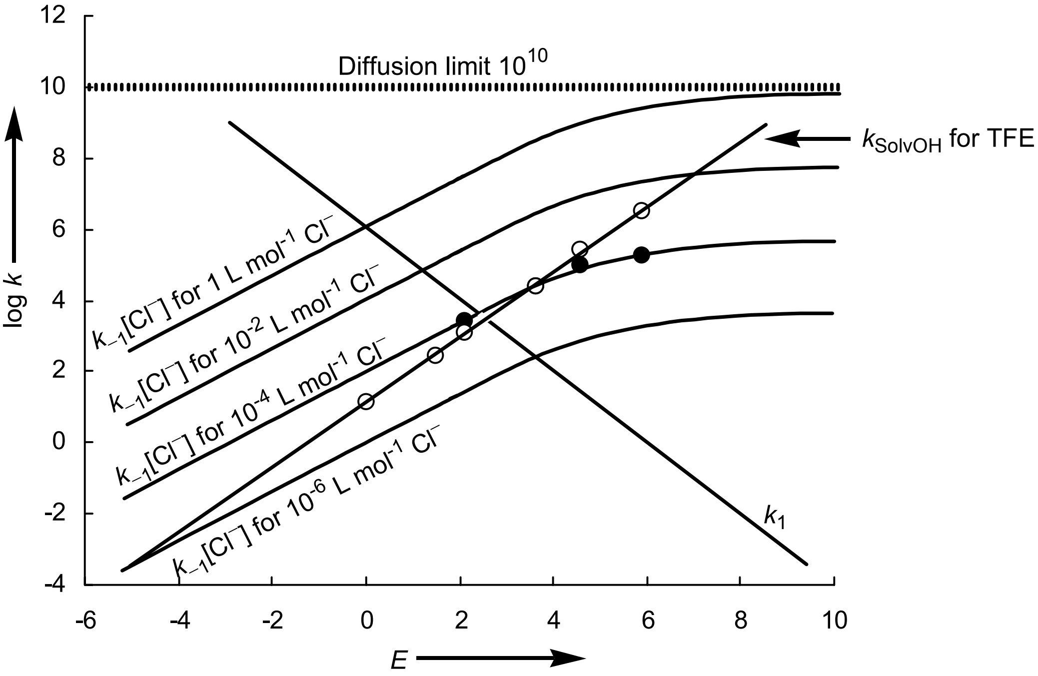

Figure 5.13: Rate constants for the different steps in the solvolysis of various benzhydryl chlorides in trifluoroethanol at 20 °C for the reactions of benzhydrylium ions with solvent and Cl^-, at 25 °C for ionization. ○: Reactions of benzhydryl cations with TFE, ●: Reactions of benzhydryl cations with chloride anion (10^{-4} mol L^{-1}) in TFE.

Figures 5.14 and 5.15 translate this information into free energy profiles. In 80% aqueous ethanol, for example, solvolysis of the $(tol)_2CHCl$ proceeds with formation of a small equilibrium concentration of $(tol)_2CH^+$. Though ion combination will be preferred in the presence of external Cl^- (> 0.1 mol L^{-1}), the reaction with the solvent will also be very fast ($k_{SolvOH} \approx 10^8$ s^{-1}). Since the ionization of this substrate is already very fast ($\tau_{1/2}$ = 0.9 s), most investigated solvolysis reactions are slower, and therefore, follow the typical pattern, slow ionization followed by fast trapping by the solvent, often diffusion controlled.

A similar behavior, but with much higher reversibility of the ionization step is expected for the dimethoxy substituted benzhydryl chloride $(ani)_2CHCl$ in 80% aqueous ethanol. Ionization cannot be observed directly because dissolution of $(ani)_2CHCl$ in 80% aqueous ethanol cannot be achieved on the ms time scale; in contrast the rates of reactions of $(ani)_2CH^+$ with chloride anions and the solvent can directly be observed with photolytically generated carbocations.

Because of unfavorable thermodynamics, $(mor)_2CH^+$ will not combine with Cl^- in aqueous ethanol, and the left part of this energy profile refers to extrapolated values.

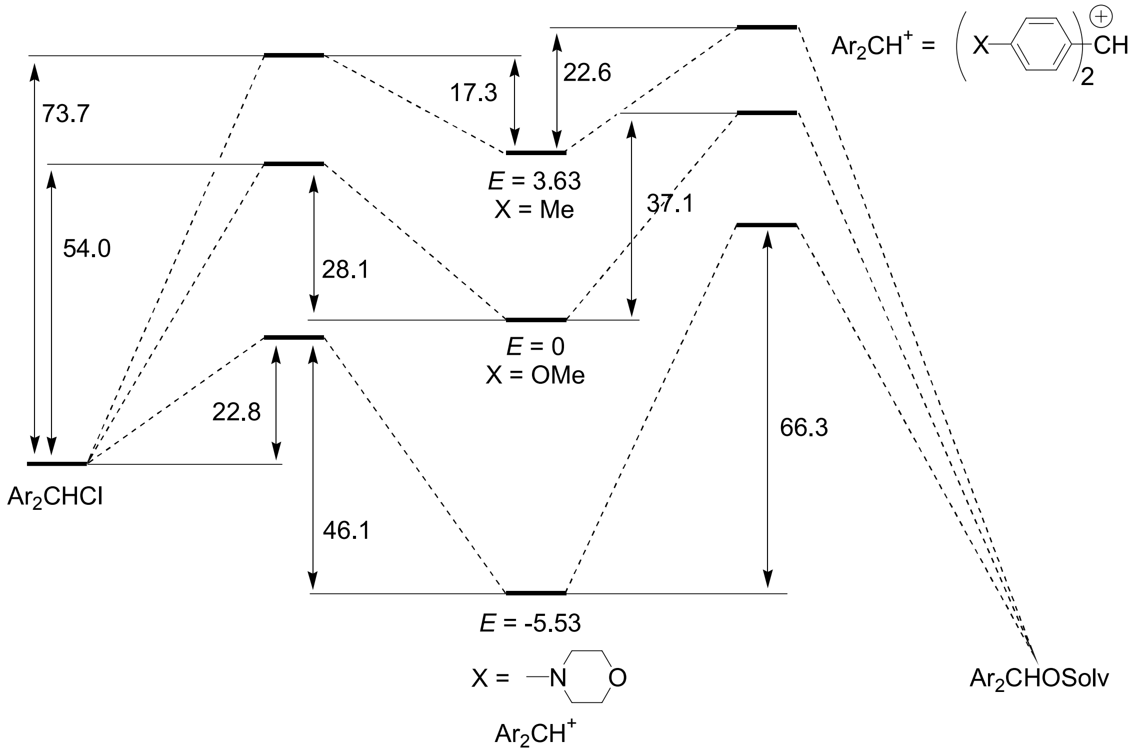

Figure 5.14: Free energy profiles for the solvolysis of various benzhydryl chlorides in 80 % aqueous ethanol at 20 °C for the reactions of benzhydrylium ions with solvent and Cl^-, at 25 °C for ionization. Unit is kJ mol^{-1}.

The free energy profiles in Figure 5.15 differ from those in Figure 5.14 in the sense that the ions are generally lower in the energy compared to the corresponding covalent benzhydryl chlorides, particularly because of the solvation of the anions. The higher walls around the ionic materials are due to the better hydrogen bond stabilization of the chloride (left wall) and the lower nucleophilicity of trifluoroethanol compared to aqueous ethanol (right wall).

It should be noted that in trifluoroethanol the ionized $(ani)_2CH^+Cl$ is only slightly higher in free energy than the covalent material, i.e., at low concentrations of chloride anions, the ionization equilibrium will favor the ionic forms.

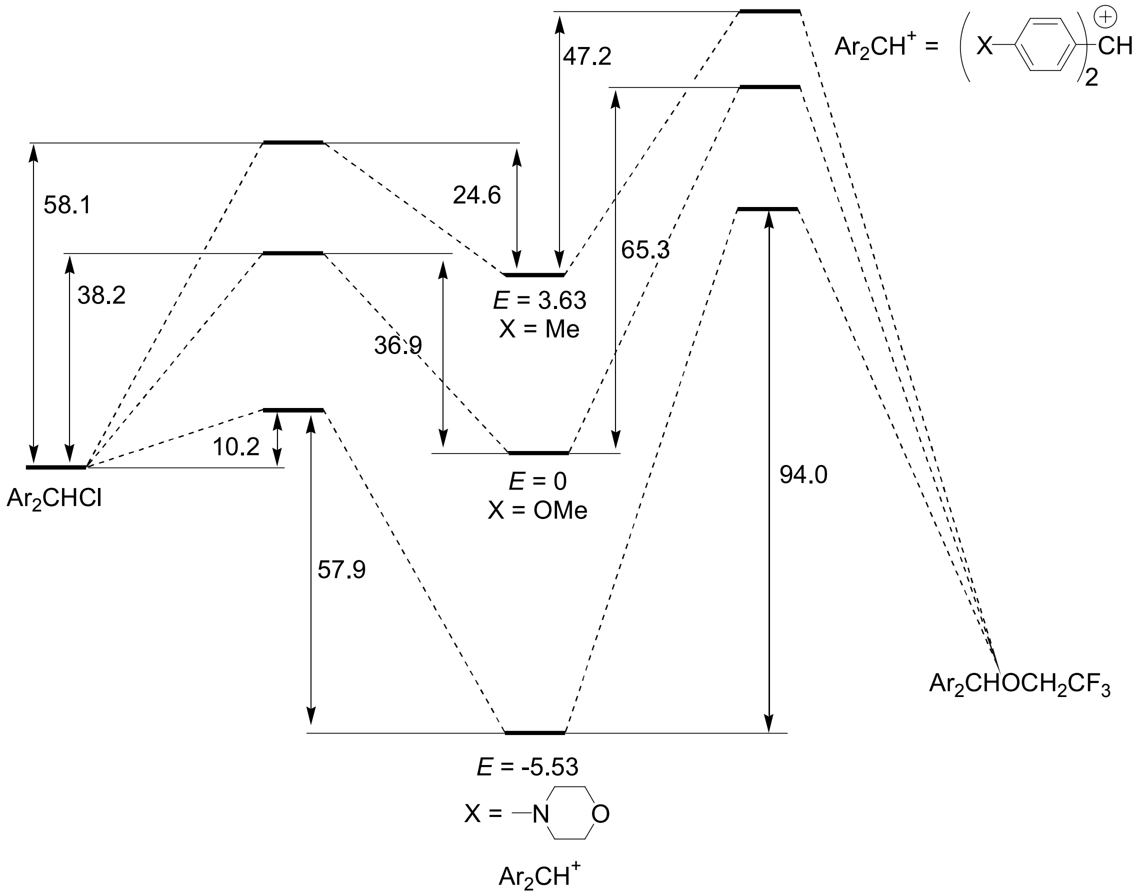

Figure 5.15: Free energy profiles for the solvolysis of various benzhydryl chlorides in TFE at 20 °C for the reactions of benzhydrylium ions with solvent and Cl^-, at 25 °C for ionization. Unit is kJ mol^{-1}. N_f for Cl^- in TFE was assumed as 6.1 from the rate constant of Ph_2CHCl in 97/3 (w/w) TFE/Water (1.05 s^{-1})[21] with $s_f = 1$.

The next section shows an experimental verification of this analysis.

5.5 Direct observation of the two distinct steps in an S_N1 reaction

(as published by H. Mayr and S. Minegishi in *Angew. Chem.* **2002**, *114*, 4674–4676; *Angew. Chem. Int. Ed.* **2002**, *41*, 4493–4495.)

In agreement with earlier conclusions from solvolysis studies,[6,16] the rates of decay of laser-flash photolytically generated carbocations in 2,2,2-trifluoroethanol (TFE) revealed this alcohol as a weakly nucleophilic solvent (Chapter 3). Accordingly, we have now found a first-order rate constant of 12.7 ± 0.4 s^{-1} for the decay of $(ani)_2CHBF_4$, in 91/9 (v/v) TFE/acetonitrile (CH_3CN) at 20 °C, corresponding to a half-life of 60 ms (Table 5.6, entry 1). This rate constant is only slightly reduced in the presence of a common ion salt (Table 5.6, entry 2) and remains almost constant as the TFE/CH_3CN ratio is reduced from 91/9 to 20/80 (v/v) (Table 3.1, entries 3–5). Entries 6 and 7 in Table 5.6 indicate that the presence of 0.5 M $NaClO_4$ or $LiClO_4$ does not affect the rate of the reaction of $(ani)_2CH^+$ with TFE.[22]

Table 5.6: Kinetics of the reaction of bis(4-methoxyphenyl)carbenium tetrafluoroborate ($(ani)_2CHBF_4$) in TFE/CH_3CN solutions at 20 ºC.

Entry	TFE/CH_3CN [a]	Additive	k_{TFE} [b] [s^{-1}]
1	91/9		12.7 [c]
2	91/9	Bu_4NCl (0.01 L mol^{-1})	10.3
3	80/20		13.5
4	60/40		13.1
5	20/80		10.0
6	20/80	$NaClO_4$ (0.5 L mol^{-1})	10.0
7	20/80	$LiClO_4$ (0.5 L mol^{-1})	10.4

[a] Solvent ratio in v/v. [b] Reactions were monitored at 500 nm. [c] Four independent experiments gave a standard deviation of ± 0.4.

The ethanolysis rate constant of chloro-bis(4-methoxyphenyl)methane ($(ani)_2CHCl$) (the rate of the S_N1 reaction in ethanol), has previously been determined as $k = 57$ s^{-1} at 25 °C, a million times higher than the ethanolysis rate constant of the parent chloro-diphenylmethane (5.34×10^{-5} s^{-1}).[23] Since chloro-diphenylmethane, on the other hand, was reported to undergo solvolysis in 97/3 (w/w) TFE/water with $k = 1.05$ s^{-1},[21] we extrapolated an S_N1 reactivity of $(ani)_2CHCl$ in 97/3 (w/w) TFE/water of 57 s^{-1} × (1.05 / 5.34×10^{-5}) = 1.1×10^6 s^{-1}

The ionization of $(ani)_2CHCl$ in TFE was thus expected to be 10^5 times faster than the reaction of $(ani)_2CH^+$ with this solvent. Since intermediates, which are produced faster than they are consumed, enrich during a reaction sequence, we were prompted by these considerations to search for the intermediate carbocation $(ani)_2CH^+$ during the trifluoroethanolysis of $(ani)_2CHCl$ (eq. 5.7).

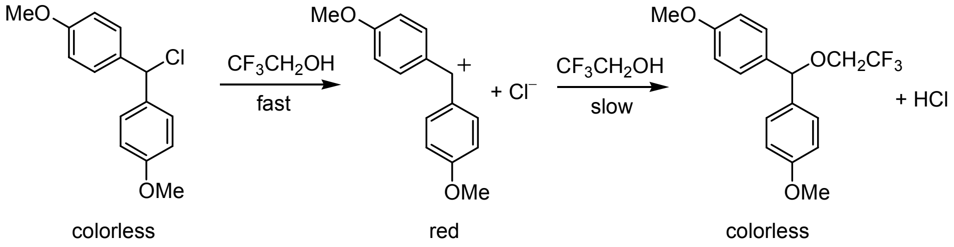

(5.7)

Immediately after mixing the colorless solution of $(ani)_2CHCl$ in CH_3CN with the tenfold volume of TFE (dried by distillation over $CaSO_4$) in a stopped-flow apparatus, the well-known[24] UV-Vis spectrum of the cation $(ani)_2CH^+$ with an absorption maximum at λ = 500 nm was observable (Figure 5.16). This spectrum is almost identical to that obtained for $(ani)_2CH^+$ in pure acetonitrile (λ_{max} = 500 nm).[24]

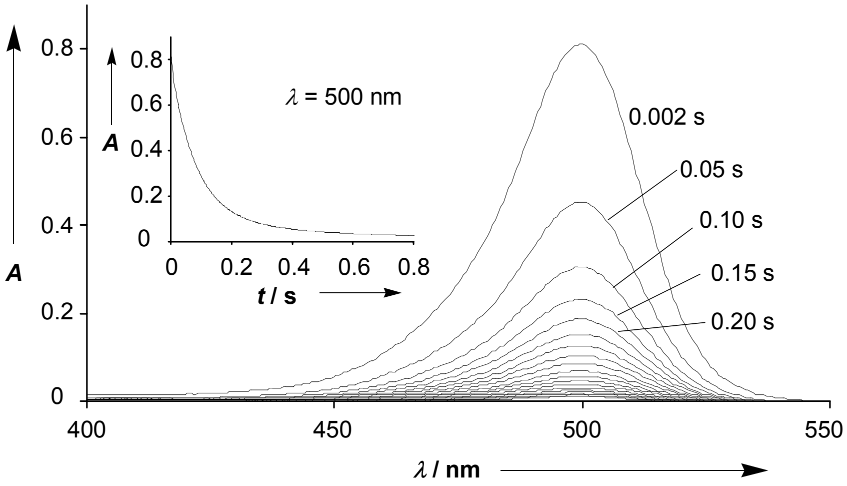

Figure 5.16: Decay of the absorbance (*A*) of the bis(4-methoxyphenyl)carbenium ion ($(ani)_2CH^+$) generated from chloro-bis(4-methoxyphenyl)methane ($(ani)_2CHCl$) in 91/9 (v/v) TFE/CH_3CN at 20 °C.

From the molar absorption coefficient (log $\varepsilon = 5.10$),[24] one can derive that 80% of $(ani)_2CHCl$ (8.5×10^{-6} M) are observable as the cation $(ani)_2CH^+$ immediately after mixing. This band disappeared with a first-order rate constant of 11.4 s^{-1} (Figure 5.7), i.e., a similar rate as previously observed (Table 5.6) for the reaction of $(ani)_2CHBF_4$ with TFE under the same conditions.

Only small changes of the rate of the first-order decay were observable, when the TFE/CH_3CN ratio was reduced from 91/9 to 50/50 (Table 5.7, entries 1 and 6–9). Addition of tetra-*n*-butylammonium chloride (Bu_4NCl) caused a slight decrease of the rate of the carbocation decay (Table 5.7, entries 1–5). In the presence of 10^{-2} M Bu_4NCl, a hypsochromic shift of $\Delta\lambda = 1$ nm and a decrease of the intensity of the absorption band by 35% was observed. In all cases, the maximum of the carbocation absorption (A_{max}) was detected immediately after mixing, in accord with the high ionization rate constants of $(ani)_2CHCl$ estimated above.

Attempts to slow down the ionization reaction to measurable rates by employing TFE/CH_3CN mixtures with a smaller solvent ionizing power than pure TFE[6] were not successful. While the maximal absorbance was still observed immediately after mixing, even in 30/70 (v/v) TFE/CH_3CN (Table 5.7, entry 11), the absorbance was considerably smaller than in solutions with a high TFE/CH_3CN ratio, indicating that under these conditions the ionization equilibrium (first step in eq. 5.7) was shifted towards the covalent diaryl chloromethane $(ani)_2CHCl$. Because of incomplete ionization, the carbocation consumption did not show an exponential decay in the cases with small absorbance, and the rate constants of entries 10, 11, and 13 in Table 5.7 have to be considered as approximations.

Formation as well as decay of the carbocation $(ani)_2CH^+$ was observable, however, in 20/80 (v/v) TFE/CH_3CN which contained 1.0 M of $LiClO_4$[22] (Figure 5.17).

Table 5.7: Kinetics of the solvolysis of chloro-bis(4-methoxyphenyl)methane ($(ani)_2CHCl$) in TFE/CH_3CN solutions at 20 ºC.

Entry	$[(ani)_2CHCl]_0$, L mol^{-1}	TFE/CH_3CN [a]	Additive	A_{max} [b]	k_i, s^{-1}	k_{TFE}, s^{-1}
1	8.51×10^{-6}	91/9		0.81	fast	11.4
2	8.51×10^{-6}	91/9	Bu_4NCl (5×10^{-4} L mol^{-1})	0.83	fast	11.1
3	8.51×10^{-6}	91/9	Bu_4NCl (1×10^{-3} L mol^{-1})	0.81	fast	11.0
4	8.51×10^{-6}	91/9	Bu_4NCl (5×10^{-3} L mol^{-1})	0.68	fast	10.6
5	8.51×10^{-6}	91/9	Bu_4NCl (1×10^{-2} L mol^{-1})	0.54 [c]	fast	10.6
6	7.44×10^{-6}	80/20		0.67	fast	14.1
7	7.44×10^{-6}	70/30		0.61	fast	14.8
8	7.44×10^{-6}	60/40		0.55	fast	13.2
9	7.44×10^{-6}	50/50		0.50	fast	12.4
10	7.44×10^{-6}	40/60		0.37	fast	(6.47) [d]
11	7.44×10^{-6}	30/70		0.20	— [e]	(3.80) [d]
12	1.10×10^{-5}	30/70	$LiClO_4$ (1.0 L mol^{-1})	0.64	7×10^2	12.7
13	7.44×10^{-6}	20/80		0.10	— [e]	(2.66) [d]
14	7.44×10^{-6}	20/80	$NaClO_4$ (1.0 L mol^{-1})	0.26	3×10^2	10.1
15	1.10×10^{-5}	20/80	$LiClO_4$ (1.0 L mol^{-1})	0.52	5×10^2	10.4

[a] Solvent ratio in v/v. [b] Absorbance at $\lambda_{max} = 500$. [c] $\lambda_{max} = 499$ nm. [d] The rate constant (k_{TFE}) has to be considered as approximation. The carbocation consumption did not show an exponential decay with small absorbance because of incomplete ionization. [e] The rate constant of ionization (k_i) was not determined because of too small increase of absorbance in cation formation step.

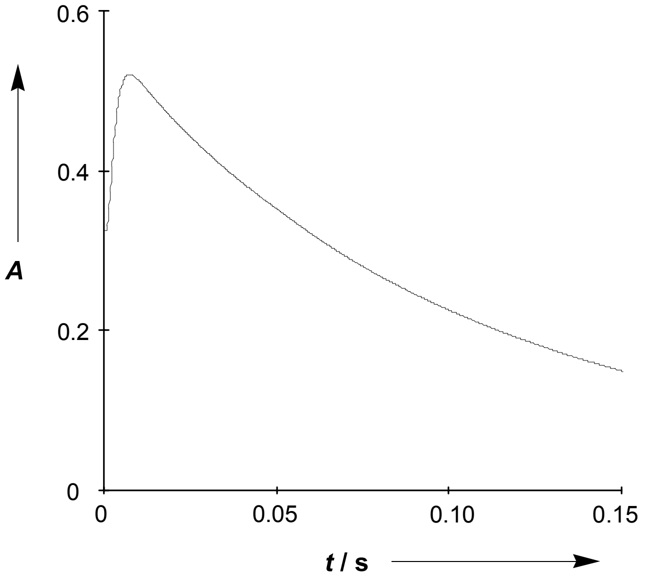

Figure 5.17: Generation and decay of the bis(4-methoxyphenyl)carbenium ion ($(ani)_2CH^+$) observed after dissolving chloro-bis(4-methoxyphenyl)methane ($(ani)_2CHCl$) in 20/80 (v/v) TFE/CH_3CN containing 1.0 M of $LiClO_4$.

At the maximum of the carbocation concentration, i.e., 7 milliseconds after mixing, 40% of the initial $(ani)_2CHCl$ was observable as the benzhydryl cation $(ani)_2CH^+$. The carbocation, which was formed with a rate constant (k_i) of 5×10^2 s^{-1} was consumed with a rate constant (k_{TFE}) of 10.4 s^{-1} under these conditions (Table 5.7, entry 15). Analogously, formation and consumption of $(ani)_2CH^+$ was observable in other TFE/CH_3CN mixtures containing alkali perchlorates[22] (Table 5.7, entries 12 and 14).

The solvolysis of (ani)(pop)CHCl and (ani)(tol)CHCl were also examined in TFE/CH_3CN mixtures As expected, (ani)(pop)CHCl gave the corresponding benzhydrylium ion in TFE-acetonitrile mixtures (Table 5.8), but the absorption of a benzhydrylium ion was not observed in any of these mixtures during the solvolysis of (ani)(tol)CHCl. The rate constant for the reaction of $(ani)(pop)CH^+$ with TFE is two times faster than calculated (k_{calc} = 49 s^{-1}). Analogous deviations of phenylamino- substituted benzhydrylium ions have previously been observed in other polar solvents (water, alcohols, and acetonitrile).[13,25]

Table 5.8: Kinetics of the solvolysis of (ani)(pop)CHCl in TFE/CH_3CN solutions at 20 ºC.

Ar_2CHCl	$[Ar_2CHCl]_0$ L mol^{-1}	TFE/CH_3CN [a]	k_{TFE}, L mol^{-1}
(ani)(pop)CHCl	8.37×10^{-6}	91/9	1.2×10^2
	8.37×10^{-6}	80/20	1.1×10^2
	8.37×10^{-6}	70/30	1.1×10^2
	8.37×10^{-6}	60/40	4.9×10^1 [b]
	8.37×10^{-6}	50/50	4.3×10^1 [b]

[a] Solvent ratio in v/v. [b] The rate constant (k_{TFE}) has to be considered as approximation. The carbocation consumption did not show an exponential decay with small absorbance because of incomplete ionization.

The direct observation of the carbocationic intermediate demonstrated in this experiment is certainly not a singular case. Increasing stabilization of the carbocation and decreasing solvent nucleophilicity transform the generally accepted energy profiles of S_N1 reactions with carbocations as short-lived intermediates (Figure 5.18, upper graph) into energy profiles which imply the buildup of significant concentrations of the intermediate carbocations (Figure 5.18, lower graph).

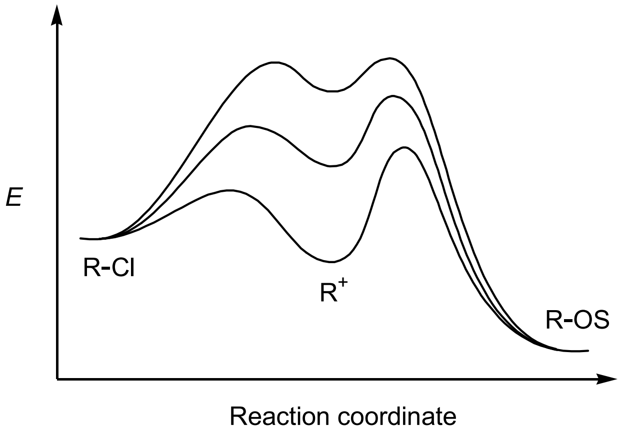

Figure 5.18: Schematic energy profiles for solvolytic displacement reactions in TFE. Upper graph: Slow ionization (conventional S_N1). Lower graph: Rate determining carbocation-nucleophile combination with directly observable intermediate. – Ion-pairing and proton transfer steps neglected.

The occurrence of such scenarios can easily be predicted from available ionization and combination rate constants as demonstrated in this report. Since ionization and nucleophile addition must be uncoupled when the intermediate is observable, the investigation of such reaction cascades may open a new era in the study of solvolytic displacement reactions. As salt and solvent effects on the two steps of the reaction can now be studied separately, many ambiguities in the earlier interpretations of the mechanisms of solvolytic displacement reactions can be resolved.

5.6 References

(1) (a) Ingold, C. K.; Rothstein, E. *J. Chem. Soc.* **1928**, 1217–1221 (b) Ingold, C. K. *Structure and Mechanism in Organic Chemistry, 2nd Ed.,* Cornell Univ. Press, Ithaca, New York, **1969**.

(2) *Carbonium Ions, Vol. 1–5,* (Eds.: Olah, G. A.; Schleyer, P. v. R.), Interscience, New York, **1968–1976**.

(3) Vogel, P. *Carbocation Chemistry* Elsevier, Amsterdam, **1985**.

(4) (a) Creary, X. *Advances in Carbocation Chemistry, Vol. 1,* JAI Press, Greenwich, CT, **1989** (b) Coxon, J. M. *Advances in Carbocation Chemistry, Vol. 2,* JAI Press, Greenwich, CT, **1995**.

(5) (a) Cox, R. A. *Carbocations* in *Organic Reaction Mechanisms* (Eds.: Knipe, A. C.; Watts, W. E.), Wiley, Chichester, **1985–2001** (b) Streitwieser, A. Jr. *Solvolytic Displacement Reactions*, McGraw-Hill, New York, **1962**.

(6) Bentley, T. W.; Llewellyn, G. *Prog. Phys. Org. Chem.* **1990**, *17*, 121–159.

(7) (a) Faria, J. L.; McClelland, R. A.; Steenken, S. *Chem. Eur. J.* **1998**, *4*, 1275–1280. (b) Pham, T. V.; McClelland, R. A. *Can. J. Chem.* **2001**, *79*, 1887–1897.

(8) Kirmse, W.; Guth, M.; Steenken, S. *J. Am. Chem. Soc.* **1996**, *118*, 10838–10849.

(9) Mayr, H.; Bug, T.; Gotta, M. F.; Hering, N.; Irrgang, B.; Janker, B.; Kempf, B.; Loos, R.; Ofial, A. R.; Remennikov, G.; Schimmel, H. *J. Am. Chem. Soc.* **2001**, *123*, 9500–9512.

(10) Roth, M.; Mayr, H. *Angew. Chem.* **1995**, *107*, 2428–2430; *Angew. Chem., Int. Ed. Engl.* **1995**, *34*, 2250–2252.

(11) Mayr, H.; Kuhn, O.; Gotta, M. F.; Patz, M. *J. Phys. Org. Chem.* **1998**, *11*, 642–654.

(12) Minegishi, S.; Mayr, H. *J. Am. Chem. Soc.* **2003**, *125*, 286–295.

(13) Loos, R. *Dissertation*, Ludwig-Maximilians-Universität München, 2003.

(14) Richard, J. P.; Toteva, M. M.; Crugeiras, J. *J. Am. Chem. Soc.* **2000**, *122*, 1664–1674.

(15) McClelland, R. A.; Banait, N.; Steenken, S. *J. Am. Chem. Soc.* **1986**, *108*, 7023–7027.

(16) Kevill, D. N. *Advances in Quantitative Structure-Property Relationships*; Charton, M. Ed., JAI Press, Greenwich, CT, **1996**, Vol. 1, pp 81–115.

(17) (a) Kamlet, M.; Taft, R. W. J. *J. Am. Chem. Soc.* **1976**, *98*, 377–383. (b) Taft, R. W.; Kamlet, M. J. *J. Am. Chem. Soc.* **1976**, *98*, 2886–2894. (c) Kamlet, M.; Abboud, J.-L. M.; Abraham, M. H.; Taft, R. W. J. *J. Org. Chem.* **1983**, *48*, 2877–2887.

(18) Park, J. H.; Jang, M. D.; Kim, D. S.; Carr, P. W. *J. Chromatogr.* **1990**, *513*, 107–116.

(19) (a) Parker; A. J. *Chem. Rev.* **1969**, *69*, 1–32. (b) Reichardt, C. *Solvents and Solvent Effects in Organic Chemistry*; VCH, Weinheim, 1988.

(20) see, ref. 22, p266.

(21) Bunton, C. A.; Mhala, M. M.; Moffatt, J. R. *J. Org. Chem.* **1984**, *49*, 3639–3641.

(22) Raber, D. J.; Harris, J. M.; Schleyer, P. v. R. in *Ions and Ion Pairs in Organic Reactions, Vol. 2* (Ed.: M. Szwarc), John Wiley & Sons, Inc., New York, **1974**.

(23) Schade, C.; Mayr, H. *Tetrahedron* **1988**, *44*, 5761–5770.

(24) Bartl, J.; Steenken, S.; Mayr, H.; McClelland, R. A. *J. Am. Chem. Soc.* **1990**, *112*, 6918–6928.

(25) See Chapter 3 and Appendix.

6. Miscellaneous kinetics experiments

6.1 Unique reactivity of 1,4-diazabicyclo[2.2.2]octane (DABCO).

6.1.1 Introduction

While the pK_{HA} value of 1,4-diazabicyclo[2.2.2]octane (DABCO) is somewhat smaller (pK_{HA} = 8.8)[1a] than that of acyclic trialkylamines (pK_{HA} = 10-11),[1b] its nucleophilicity is comparable to primary or secondary amines.[2] For that reason it has been used as a nucleophilic catalyst in several organic reactions.[3]

In the Baylis–Hillman reaction, for example, DABCO first attacks at an alkene, which is activated by an electron withdrawing group (EWG), to give a zwitterion that undergoes nucleophilic attack at a carbonyl or imino group.[4] Elimination of DABCO in the last step yields an allyl alcohol or allyl amine as shown in Scheme 6.1.

Scheme 6.1

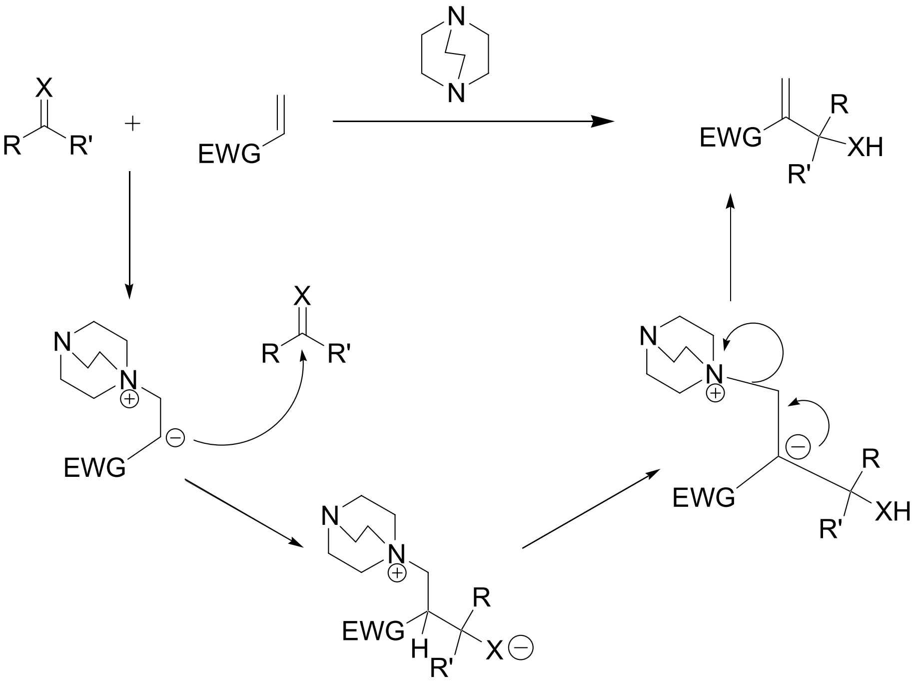

6.1.2 Reaction of benzhydrylium ions with DABCO

Ritchie measured the rate constants of the reactions of stabilized trityl cations with water in the presence of DABCO.[5] The acceleration of these reactions by DABCO has been explained by general base catalysis. In the case of more reactive carbocations the addition of water to the carbocation is irreversible, and the observed rate constants are not affected when the concentration of DABCO buffer is changed (Chapter 3). The observed rate constant for the reaction of $(dma)_2CH^+$ with water decreased when the concentration of DABCO buffer increased (Figure 6.1). This effect may be explained by the partial reversible combination of DABCO with $(dma)_2CH^+$ as described below (eqs 6.1-6.5).

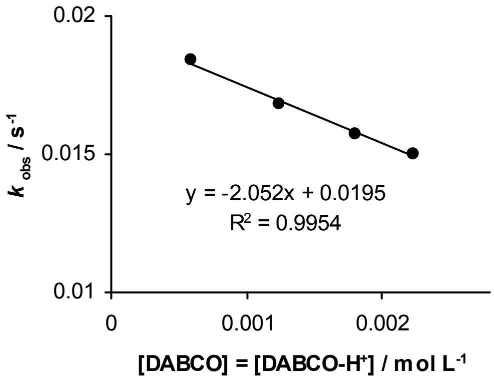

Figure 6.1: Relationship between observed rate constants and concentration of DABCO-DABCO-H^+ (1:1).

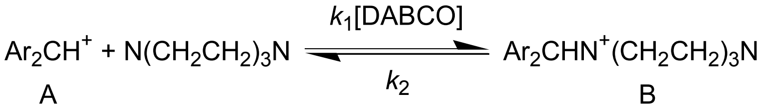

$$\underset{A}{Ar_2CH^+} + N(CH_2CH_2)_3N \underset{k_2}{\overset{k_1[DABCO]}{\rightleftharpoons}} \underset{B}{Ar_2CHN^+(CH_2CH_2)_3N} \qquad (6.1)$$

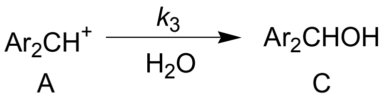

$$\underset{A}{Ar_2CH^+} \xrightarrow[H_2O]{k_3} \underset{C}{Ar_2CHOH} \qquad (6.2)$$

When DABCO is used in high excess, its concentration can be considered being constant, and the differentiated equations 6.3-6.5 can be written.

$$d[A]/dt = -(k_1[DABCO] + k_3)[A] + k_2[B] \qquad (6.3)$$
$$d[B]/dt = k_1[DABCO][A] - k_2[B] \qquad (6.4)$$
$$d[C]/dt = k_3[A] \qquad (6.5)$$

When A and DABCO yield B in a fast and reversible step, and the final product is formed slowly (k_1[DABCO] + k_2 >> k_3), [B]/[A] = k_1[DABCO]/k_2.[6] Differentiation with respect to time yields,

$$d[B]/dt = (k_1[DABCO]/k_2)d[A]/dt \qquad (6.6)$$

Further we differentiate the mass balance equation,

$$[A] + [B] + [C] = [A]_0 \qquad (6.7)$$

with respect to time,

$$0 = d[A]/dt + d[B]/dt + d[C]/dt \qquad (6.8)$$

The combination of eqs 6.6 and 6.8 leads to

$$\{1 + (k_1[\text{DABCO}]/k_2)\}d[A]/dt = -d[C]/dt \qquad (6.9)$$

Substituting this equation into eq. 6.5 gives,

$$d[A]/dt = -k_3[A]/ \{1 + (k_1[\text{DABCO}]/k_2)\} \qquad (6.10)$$
$$= -k_2k_3[A]/(k_1[\text{DABCO}] + k_2)$$

therefore,

$$k_{\text{obs}} = k_2k_3 / (k_1[\text{DABCO}] + k_2) \qquad (6.11)$$

With the rate constant for the reaction of $(\text{dma})_2\text{CH}^+$ with water from Chapter 3 ($k_3 = 2.06 \times 10^{-2}$ s^{-1}) an equilibrium constant of $K = 1.8 \times 10^2$ L mol^{-1} is calculated for the reaction of $(\text{dma})_2\text{CH}^+$ with DABCO. Accordingly, an equilibrium constant of $K = 1.7 \times 10^2$ L mol^{-1} for the reaction of $(\text{dma})_2\text{CH}^+$ with DABCO in 9% aqueous acetonitrile was obtained from the initial absorption in stopped-flow experiments.

In the stopped-flow measurement the combination of $(\text{dma})_2\text{CH}^+$ with DABCO could not be measured because this reaction is faster than the mixing process. It was observed, however, that the initial absorption of $(\text{dma})_2\text{CH}^+$ got lower with increasing concentration of the DABCO buffer (91/9 (v/v) water/acetonitrile). From the mixing-time of the stopped-flow instrument, we can derive first-order rate constant > 1000 s^{-1} for the reaction of $(\text{dma})_2\text{CH}^+$ with DABCO (10^{-3} mol L^{-1}), corresponding to a second-order rate constant > 10^6 L mol^{-1} s^{-1}.

The second-order rate constants for the reactions of $(dma)_2CH^+$ with several nucleophiles are shown in Table 6.1. If DABCO has the typical s parameter for n-nucleophiles ($s = 0.6$, Chapter 2), its nucleophilicity parameter must be $N > 17$ (in water), larger than for most other nucleophiles in water (Table 2.4).

Table 6.1: Second-order rate constants and equilibrium constants for the reaction of $(dma)_2CH^+$ with nucleophiles

Nucleophile (Solvent)	k_2(20 °C), L $mol^{-1}s^{-1}$	K(20 °C), L mol^{-1}
DABCO (Water)	$> 10^6$	1.8×10^2
Ph_3P (CH_2Cl_2)[a]	5.21×10^4	1.26×10^5
DMAP (CH_2Cl_2)[b]	6.56×10^5	4.31×10^7
OH^- (Water)[c]	1.31×10^2	2.5×10^8[d]
n-$PrNH_2$ (Water)	3.12×10^3[c]	
n-$PrNH_2$ (DMSO)	3.59×10^5[e]	
Morpholine (DMSO)	4.57×10^6[e]	

[a] From ref. 7. [b] DMAP = (4-dimethylamino)pyridine, From ref. 7. [c] From Chapter 2. [d] Calculated from pK_{R+} of $(dma)_2CH^+$ (5.61).[8] [e] Calculated from N and s parameters (see Chapter 2).

From the first entry in Table 6.1 the heterolysis rate constant of $(dma)_2CHN^+(CH_2CH_2)_3N$ in water is estimated $> 6 \times 10^3$ s^{-1}. From the nucleofugalities of bromide, chloride, trifluoroacetate, and 3,5-dinitrobenzoate in different solvents (Appendix), one can calculate the heterolysis rates of various substrates $(dma)_2CHX$ and compare them with the heterolysis rates of the corresponding DABCO adduct (Table 6.2).

Table 6.2: Comparison of nucleofugality of leaving groups for $(dma)_2CH^+$

Nucleofuge	Solvent	Calculated heterolysis rate (s^{-1})[a]
DABCO	Water	$> 6\times 10^3$[b]
Bromide	90/10 (v/v) acetone/water	1.3×10^9
Chloride	90/10 (v/v) acetone/water	4.7×10^7
Trifluoroacetate	90/10 (v/v) acetone/water	1.7×10^7
3,5-Dinitrobenzoate	90/10 (v/v) acetone/water	4.6×10^3

[a] Calculated from eq. 3 in Appendix. E_f of $(dma)_2CH^+$ is estimated from $E_f \approx -E$. [b] This work.

In agreement with these interpretations, $(\text{mor})_2\text{CH}^+$ was consumed completely within 1 ms, the mixing-time in the stopped-flow instrument when combined with 50/50 (v/v) water/acetonitrile in the presence of DABCO buffer.

McClelland reported the reaction of DABCO with tritylium ions (E = 0.5)[9] in 67/33 (v/v) water/acetonitrile. The second-order rate constant (7.7×10^5 L mol^{-1} s^{-1})[10] is rather slow compared to that observed with benzhydrylium ions, which can again be interpreted as a steric effect.

6.1.3 Conclusion

DABCO has a high nucleophilicity comparable to primary and secondary amines. This property is the reason for DABCO being often the most favorable catalyst in the Baylis-Hillman reaction. Laser flash photolysis should be used to exactly investigate the nucleophilicity and carbon basicity (or nucleofugality) of DABCO, and to quantify the height of the intrinsic barrier.

6.2 Electrophilicity and nucleophilicity of Grignard reagents

6.2.1 Introduction

About a century ago Grignard synthesized the first organomagnesium compounds.[11] Since then Grignard reagents have become one of the most important reagents in organic chemistry.[12] While their synthetic applications have been extensively developed, relatively few investigations on the properties of Grignard reagents have so far been reported.[12,13]

Relative reactivities of Grignard reagents toward carbonyl compounds have been determined.[14] It is well-understood that Grignard reagents behave both as nucleophiles attacking the carbonyl carbon and as Lewis acids, activating the carbonyl group by coordination of magnesium to the carbonyl oxygen. There are some examples where the function of the Grignard reagent as a Lewis acid can be separated from its function as a nucleophile (Scheme 6.1).[15]

Scheme 6.1

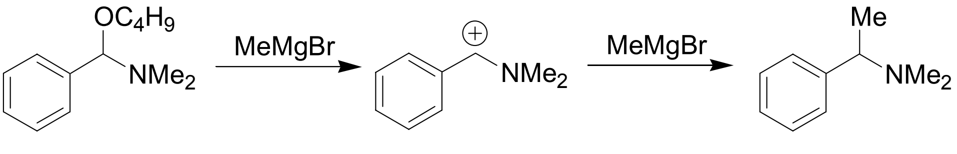

Thus in the reaction of an amino ether with a Grignard reagent, the initial step is the formation of carbocationic intermediate which reacts with the alkyl group of Grignard reagents in a successive reaction (Scheme 6.1). We have now investigated the reactions of benzhydrylium phenoxide with methyl magnesium bromide, expecting that the intermediate carbocation might directly be observable (Scheme 6.2).

Scheme 6.2

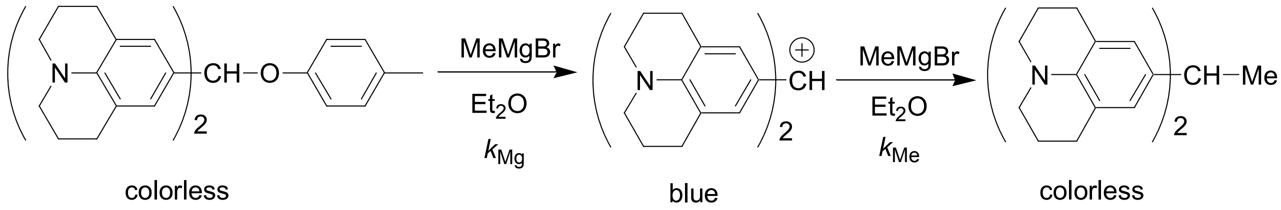

6.2.2 Kinetic method

Because of the high sensitivity of Grignard reagents to moisture, all glassware was dried in an oven at 70 ºC for at least 3h. Syringes and needles were kept under vacuum over P_2O_5. All operations were done under nitrogen or argon atmosphere. Grignard reagents were generally used in concentrations below 0.04 mol L^{-1} since at higher concentration associates are formed.[12] The final concentrations of the solution of MeMgBr were calculated from the dilution factor (factor of 10-300) of the original stock solutions whose concentrations were titrated by 2-hydroxybenzaldehyde phenylhydrazone as described in ref 16 (Scheme 6.3).

Scheme 6.3

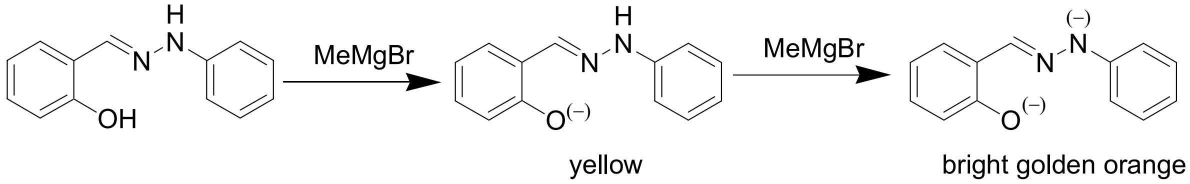

6.2.3 Direct observation of the two steps of the reaction of methyl magnesium bromide with $(jul)_2CHOTol$.

One syringe of the stopped-flow instrument was filled with an etheral solution of $(jul)_2CHOTol$, and the second syringe contained the dilute MeMgBr solution. After mixing of the two solutions rise and decay of the absorbances at 635 nm was monitored (Figure 6.2). This is the absorption maximum of the intermediate generated in this experiment. It is in between λ_{max} of $(jul)_2CH^+BF_4^-$ in CH_2Cl_2 (λ_{max} = 642 nm) and λ_{max} of this salt in diethyl ether containing 0.5% CH_2Cl_2 (λ_{max} = 628 nm). The counter ion of the benzhydrylium ion generated in this way is unknown. Since $[TolOMgMe_2]^-$ or $[TolOMgMeBr]^-$ are expected to be highly reactive species, we assume $[TolOMgBr_2]^-$ or bromide ion to be the counter ion.

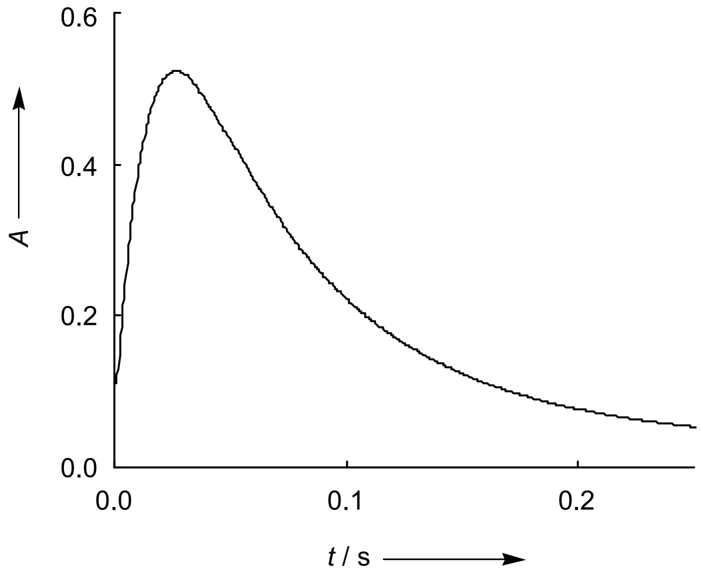

Figure 6.2: Direct observation of the generation and the consumption of $(jul)_2CH^+$ in the reaction of $(jul)_2CHOTol$ with MeMgBr in Et_2O.

6.2.4 Evaluation of the kinetic experiment.

Double-exponential fitting of the absorbance of $(jul)_2CH^+$ yielded the ionization rate and the rate of disappearance of the carbocation. Figures 6.3 and 6.4 show that both the rates of ionization rate and of the consumption of $(jul)_2CH^+$ correlate linearly with the concentration of MeMgBr.

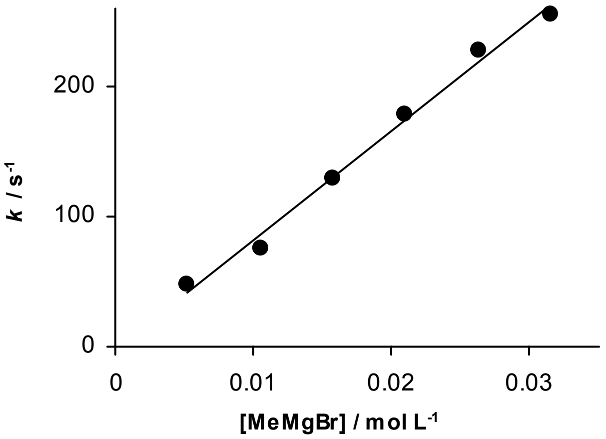

Figure 6.3: Correlation of the generation of $(jul)_2CH^+$ with the concentration of MeMgBr.

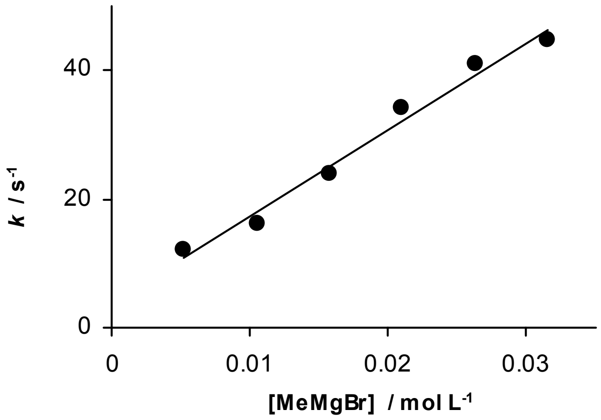

Figure 6.4: Correlation of the consumption of $(jul)_2CH^+$ with the concentration of MeMgBr.

From these correlations the second-order rate constants for ionization and consumption are obtained as 8.4×10^3 and 1.3×10^3 L mol^{-1} s^{-1}, respectively. Because of the uncertainty of the concentration of MeMgBr these rate constants are not very accurate, but rate constants obtained in different experiments agreed within a factor of 2 for both ionization and disappearance of the benzhydryl cations.

The observed rate constants of both ionization and cation consumption show linear correlations with concentrations of MeMgBr. In the range of low concentration of Grignard reagents, there is no aggregation between MeMgBr. Therefore, the Schlenk equilibrium is rather simple and the ratio of [MeMgBr] and $[MgMe_2]$ is constant (eqs. 6.12 and 6.13).[13a]

$$MgMe_2 + MgBr_2 \rightleftharpoons 2MeMgBr \qquad (6.12)$$

$$K = [MeMgBr]^2 / [MgMe_2][MgBr_2] = \{[MgMeBr] / [MgMe_2]\}^2 \qquad (6.13)$$

From this study the second-order rate constant of the reaction for $(jul)_2CH^+$ with MeMgBr in Et_2O was obtained. It is, therefore, possible to compare the reactivity of MeMgBr with the reactivities of other nucleophiles (Scheme 6.4).

Scheme 6.4: Relative reactivity of nucleophiles toward $(jul)_2CH^+$ based on MeMgBr in Et_2O. Solvent is given in parenthesis.

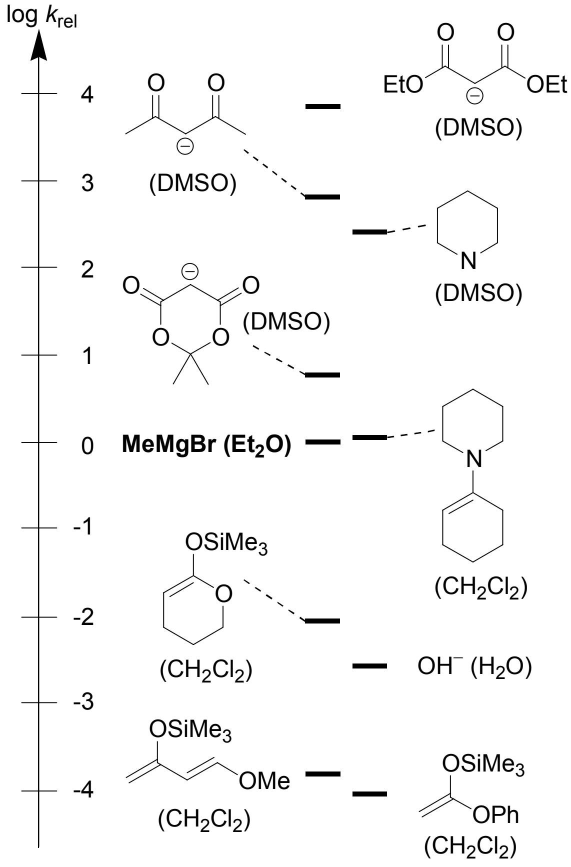

A molecular interpretation of these rate constants is problematic, however, because in all experiments more than 1000 equivalents of Grignard reagent were used. From the Schlenk equilibrium constant of ca. 400[13a] one can derive that each of the concentrations [$MgMe_2$], [$MgBr_2$], and [MeMgBr] would remain constant during the reaction which inhibits more detailed analysis. For that reason, the position of methyl magnesium bromide among other nucleophiles in Scheme 6.4 may strongly be affected by concentration.

Though detailed investigations are needed to draw safe conclusions, it has been shown that benzhydrylium ions can in principle be used for studying nucleophilicities of Grignard reagents.

6.3 References

(1) (a) Paoletti, P.; Stern, J. H.; Vacca, H. *J. Phys. Chem.* **1965**, *69*, 3759–3762. (b) Smith, M. B.; March, J. *Advanced Organic Chemistry*, 5th ed.; Wiley: New York, 2001, p 330.

(2) Ritchie, C. D. *J. Am. Chem. Soc.* **1975**, *97*, 1170–1179.

(3) (a) Huang, B.-S.; Parish, E. J.; Miles, D. H. *J. Org. Chem.* **1974,** *39,* 2647–2648. (b) Linn, J. A.; McLean, E. W.; Kelly, J. L. *J. Chem. Soc., Chem. Commun.* **1994**, 913–914. (c) Uozumi, Y.; Arii, T.; Watanabe, T. *J. Org. Chem.* **2001,** *66,* 5272–5274 (d) Shieh, W.-C.; Dell, S.; Bach, A.; Repic, O.; Blacklock, T. J. *J. Org. Chem.* **2003,** *68,* 1954–1957

(4) (a) Basavaiah, D.; Rao, P. D.; Hyma, R. S. *Tetrahedron* **1996**, *52*, 8001–8062. (b) Basavaiah, D.; Rao, A. J.; Satyanarayana, T. *Chem. Rev.* **2003**, *103*, 811–891.

(5) (a) Ritchie, C. D. *J. Am. Chem. Soc.* **1972**, *94*, 3275–3276. (b) Ritchie, C. D.; Wright, D. J.; Huang, D.-S.; Kamego, A. A. *J. Am. Chem. Soc.* **1975**, *97*, 1163–1170.

(6) Schmid, R.; Sapunov, V. N. *Monographs in Modern Chemistry, Vol. 14: Non-Formal Kinetics in Search for Chemical Reaction Pathways*; VCH, Weinheim, Germany, 1982, p. 20.

(7) Kempf, B. *Dissertation*, Ludwig-Maximilians-Universität München, 2003.

(8) Deno, N. C.; Jaruzelski, J. J.; Schriesheim, A. *J. Am. Chem. Soc.* **1955**, *77*, 3044–3051.

(9) Minegishi, S.; Mayr, H. *J. Am. Chem. Soc.* **2003**, *125*, 286–295.

(10) McClelland, R. A.; Banait, N.; Steenken, S. *J. Am. Chem. Soc.* **1986**, *108*, 7023–7027.

(11) Grignard, V. *Ann. Chim. Phys.* **1901**, *24*, 433-490.

(12) *Grignard Reagents: New Developments* (Ed.: Richey, H. G., Jr.), Wiley, Chichester, 2000.

(13) (a) Ashby, E. C.; Laemmle, J.; Neumann, H. M. *Acc. Chem. Res.* **1974**, *7*, 272–280. (b) Garst, J. F. *Acc. Chem. Res.* **1991**, *24*, 95–97. (c) Walling, C. *Acc. Chem. Res.* **1991**, *24*, 255–256.

(14) (a) Oki, M.; Hirota, M.; Satonaka, H.; Hagiwara, T. *Tetrahedron Lett.* **1967**, *8*, 1785–1788. (b) Biller, J.; Smith, S. G. *J. Am. Chem. Soc.* **1968**, *90*, 4108–4116. (c) Felkin, H.; Frajerman, C. *Tetrahedron Lett.* **1970**, *11*, 1045–1048. (d) Felkin, H.; Kaeseberg, C. *Tetrahedron Lett.* **1970**, *11*, 4587–4590. (e) Ashby, E. C.; Laemmle, J.; Neumann, H. M. *J. Am. Chem. Soc.* **1972**, *94*, 5421–5434. (f) Holm, T. *Acta Chem. Scand.* **1973**, *27*, 1552–1556. (g) Holm, T. *Acta Chem. Scand., Ser. B* **1988**, *42*, 685–689. (h) Holm, T. *J. Org. Chem.* **2000**, *65,* 1188–1192.

(15) Stewart, A. T. Jr.; Hauser, C. R.; *J. Am. Chem. Soc.* **1955**, *77*, 1098–1103.

(16) Love, B. E.; Jones, E. G. *J. Org. Chem.* **1999,** *64,* 3755–3756.

7 Experimental section

7.1 General conditions

Kinetic measurements: The rates of slow reactions ($\tau_{1/2}$ > 10 s) were determined by using a J&M TIDAS diode array spectrophotometer which was controlled by Labcontrol Spectacle software and connected to a Hellma 661.502-QX quartz Suprasil immersion probe (5 mm light path) via fiber optic cables and standard SMA connectors. The temperature of solutions during all kinetic studies was kept at 20 °C (± 0.2 °C) by using a circulating bath thermostat and monitored with a thermo-couple probe that was inserted into the reaction mixture.

Hi-Tech SF-61DX2 stopped-flow spectrophotometer systems (controlled by Hi-Tech KinetAsyst2 software) were used for the investigation of rapid reactions of benzhydrylium ions with nucleophiles ($\tau_{1/2}$ < 10 s at 20 °C). For the stopped-flow measurements, syringe volume ratios of 1/1 and 10/1 were employed.

The rates of rapid reactions ($\tau_{1/2}$ < 1 ms) were determined with laser flash photolytically generated benzhydrylium ions which were obtained from diarylmethyl 4-cyanophenolates or diarylmethyl acetates. Irradiation by laser flash in a quartz cell was carried out with a Continuum PL9010 Nd:YAG laser flash apparatus (λ = 266 nm; power/puls ca. 50 mJ), and an Osram XBO 150W xenon lamp was used as a light source for the detection in the UV–vis region.

Analytical data: NMR data were recorded on a Varian Mercury 200 (200 MHz), Burker ARX 300, or NNM-A500 (500 MHz). Chemical shifts are reported as a δ-scale in ppm relative to tetramethylsilane (δ_H: 0.00, δ_C: 0.00) or relative to the resonance of the deuterated solvent: $CDCl_3$ (δ_H: 7.24, δ_C: 77.0), CD_2Cl_2 (δ_H: 5.32, δ_C: 53.1). Coupling constants are reported in Hz. For the characterization of the observed signal multiplicities the following abbreviations were applied: s (singlet), d (dublet), t (triplet), q (quartet), m (multiplet). Mass spectra were measured with a Finnigan MAT 95 Q or JMS-HX110A.

Chromatography: Thin layer chromatography (TLC) was performed using aluminum plates coated with SiO_2 (Merck 60, F-254) or Al_2O_3 (Merck 60, F-254). The chromatograms were viewed under UV light. Column chromatography was performed using SiO_2 (Merck) or Al_2O_3 (Fluka, type 507 neutral). GPC (JAI LC-908) was used for purification for some cases.

Solvents: Water was distilled and passed through a Milli-Q water purification system. Alternatively HPLC grade water was distilled before use. Methanol and ethanol were distilled over CaH_2. 2,2,2-Trifluoroethanol was stored over molecular sieves (3Å) and distilled over $CaSO_4$. 1,1,1,3,3,3-Hexafluoro-2-propanol was dried over molecular sieves (4Å) and distilled over $CaSO_4$. Dimethyl sulfoxide (DMSO, Fluka, puriss., stored over molecular sieve, $H_2O \leq 0.01\%$) was used without further purification. Acetonitrile was dried with molecular sieves (3Å) or distilled over diphenylketene. Diethyl ether (Merck, 99.5%) was dried over molecular sieves (4Å), distilled over sodium diphenyl ketyl and immediately used or degassed with nitrogen and kept over molecular sieves (4Å) in a dark bottle and used within 2 days. Dichloromethane (Merck, puriss.) was vigorously stirred over concentrated H_2SO_4 to remove traces of olefins (72 h), then washed with water, 5% aqueous K_2CO_3 solution, and water. After drying over $CaCl_2$, the solvent was freshly distilled from CaH_2.

Chemicals: The following chemicals were purchased: Potassium hydroxide standard solution (Aldrich, 0.5073 M or 0.4921 M), 2,2,2-trifluoroethylamine (Acros, 99.5%), semicarbazide hydrochloride (Fluka, 99.5%), hydroxylamine hydrochloride (Fluka, > 99%), glycine ethyl ester hydrochloride (Fluka, > 99%), sodium sulfite (Fluka, > 98%), sodium azide (Fluka, 99.5%), sodium acetate (Fluka, 99.9%), 30% aqueous hydrogen peroxide (Merck), phenol (Merck, > 99.5%), *p*-nitrophenol (Aldrich, 99+%), *n*-propylamine (Acros, 99+%), morpholine (Acros, 99+%), *N*-methylmorpholine (Acros, 99%), piperidine (Acros, 99+%), diazabicyclo[2.2.2]octane (Acros, 97%), benzenesulfonic acid (Fluka, 98%), sodium tetrafluoroborate (Acros, 98%), sodium perchrolate (Acros, 99+%), lithium perchlorate (Aldrich, 99%), tetrabutylammonium chloride (Fluka, > 99% or Tokyo Kasei, > 98%) tetrabutylammonium bromide (Tokyo Kasei, > 99%), potassium thiocyanate (Nakalai, > 99.5%), methyl magnesium bromide in ether (3 M, Aldrich). The following chemicals were taken from the working supply or prepared as previously described: Benzhydrylium ions,[1] benzhydryl chlorides,[2,3] and benzhydrols.[1-3]

7.2 How constant are Ritchie's "constant selectivity relationships"?– a general reactivity scale for n-, π-, and σ-nucleophiles

Water-acetonitrile Mixtures: Dabco (839 mg, 7.48 × 10^{-3} mol) and 460 µL of aq. HBF_4 (50 w%, 3.74 × 10^{-3} mol) were dissolved in 10 mL of water. 50 µL of this solution was added to 24.72 g of water in a thermostat with stirring. $(thq)_2CH^+BF_4^-$ (8.7 mg, 2.22 × 10^{-5} mol) was dissolved in 10 ml of CH_3CN (c = 2.22 × 10^{-3} mol L^{-1}). 100 µL of the carbocation salt solution was added to the buffered water, and the reaction was followed photometrically (conventional UV-Vis spectroscopy: J&M) at 620 nm. After reaction, the pH-value of the solution was measured. The concentration of free Dabco was obtained from the pH and pK_a (8.8)[4] of conjugated acid of Dabco. Observed rate constants did not change with increasing concentrations of Dabco. The first-order rate constant (k_1) was calculated as the average of observed pseudo-first-order rate constants. (Run 245.1)

$(thq)_2CH^+$+ water in 99.6/0.4 (v/v) H_2O/CH_3CN (J&M, detection at 620 nm)

No.	T, °C	$[(thq)_2CH^+]_0$, mol L^{-1}	$[Dabco]_{free}$, mol L^{-1}	conversion, %	$k_{1\Psi}$, s^{-1}
245.1	20.0	8.92 × 10^{-6}	6.92 × 10^{-4}	80	2.26 × 10^{-3}
245.2	20.0	8.81 × 10^{-6}	1.37 × 10^{-3}	94	2.21 × 10^{-3}
245.3	20.0	8.79 × 10^{-6}	1.94 × 10^{-3}	94	2.23 × 10^{-3}
245.4	20.0	8.87 × 10^{-6}	2.58 × 10^{-3}	92	2.11 × 10^{-3}
245.5	20.0	8.85 × 10^{-6}	3.26 × 10^{-3}	95	2.19 × 10^{-3}

k_1 = 2.20 × 10^{-3} s^{-1}

$(pyr)_2CH^+$+ water in 99.6/0.4 (v/v) H_2O/CH_3CN (J&M, detection at 610 nm)

No.	T, °C	$[(pyr)_2CH^+]_0$, mol L^{-1}	$[Dabco]_{free}$, mol L^{-1}	pH	conversion, %	$k_{1\Psi}$, s^{-1}
246.1	20.0	2.36 × 10^{-6}	6.66 × 10^{-4}	8.70	95	5.54 × 10^{-3}
246.2	20.0	2.35 × 10^{-6}	1.30 × 10^{-3}	8.68	95	5.52 × 10^{-3}
246.3	20.0	2.35 × 10^{-6}	2.04 × 10^{-3}	8.72	69	5.62 × 10^{-3}
246.4	20.0	2.35 × 10^{-6}	2.69 × 10^{-3}	8.71	84	5.63 × 10^{-3}
246.5	20.0	2.35 × 10^{-6}	3.35 × 10^{-3}	8.71	67	5.55 × 10^{-3}

k_1 = 5.57 × 10^{-3} s^{-1}

$(mor)_2CH^+$+ water in 50/50 (v/v) H_2O/CH_3CN) (Stopped-flow, detection at 610 nm)

$(mor)_2CH^+BF_4^-$ (13.3 mg, 3.13 × 10^{-5} mol) was dissolved in 10 mL of CH_3CN (c = 3.13 × 10^{-3} mol L^{-1}). 160 µL of this solution was dissolved in 20 of mL CH_3CN (c = 2.50 × 10^{-5} mol L^{-1}). In the stopped-flow instrument equal volumes of the electrophile in CH_3CN solution and water were mixed to give the final concentrations listed in the table. The reactions were followed photometrically at λ = 610 nm. The mixing of pure water and CH_3CN was also monitored and the absorbances determined at different times were subtracted to eliminate the effect of mixing. The listed rate constants are averaged of 5 experiments.

Ar_2CH^+ in 50/50 (v/v) H_2O/CH_3CN 50W50AN (Stopped-flow)

No.	Cation	$[Ar_2CH^+]_0$, mol L^{-1}	Detection, nm	k_{obs}, s^{-1}
247	$(mor)_2CH^+$	1.25×10^{-6}	610	3.31×10^{-1}
249	$(mfa)_2CH^+$	1.40×10^{-6}	585	3.78

OH^- (KOH) in water

$(lil)_2CH^+BF_4^-$ (34.3 mg, 8.24×10^{-5} mol) was dissolved in 10 ml of CH_3CN (c = 8.24×10^{-3} mol L^{-1}). 60 μL of CH_3CN and 40 μL of the carbocation solution were added to 24.55 g of water in a thermostat with stirring to give a 1.33×10^{-5} mol L^{-1} solution (CH_3CN = 0.4% v/v). Potassium hydroxide was purchased as an aqueous standard solution. 50 μL of this solution (0.5073 mol L^{-1}) was added, and the reactions were followed photometrically at 630 nm. A plot of $k_{1\Psi}$ versus concentration of OH^- yields a straight line, the slope of which corresponds to the second order rate constant. (Run 205.1)

$(lil)_2CH^+$+ OH^- in 99.6/0.4 (v/v) H_2O/CH_3CN (J&M, detection at 630 nm)

No.	T, °C	$[(lil)_2CH^+]_0$, mol L^{-1}	$[OH^-]_0$, mol L^{-1}	conversion, %	$k_{1\Psi}$, s^{-1}
205.1	20.0	1.33×10^{-5}	1.03×10^{-3}	94	2.66×10^{-3}
205.2	20.0	1.33×10^{-5}	2.05×10^{-3}	92	4.87×10^{-3}
205.3	20.0	1.33×10^{-5}	3.06×10^{-3}	96	7.18×10^{-3}
205.4	20.0	1.32×10^{-5}	4.05×10^{-3}	95	9.17×10^{-3}

$k_2 = 2.16$ L $mol^{-1}s^{-1}$

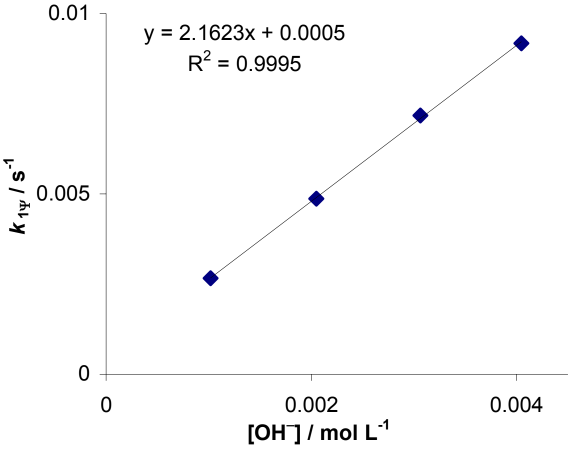

(lil)$_2$CH$^+$+ OH$^-$ in 99.6/0.4 (v/v) H$_2$O/CH$_3$CN, I = 0.005 (J&M, detection at 630 nm)

No.	T, °C	[(lil)$_2$CH$^+$]$_0$, mol L^{-1}	[OH$^-$]$_0$, mol L^{-1}	[NaBF$_4$], mol L^{-1}	conversion, %	$k_{1\Psi}$, s^{-1}
239.1	20.0	1.18×10^{-5}	1.01×10^{-3}	3.99×10^{-3}	94	1.76×10^{-3}
239.2	20.0	1.18×10^{-5}	2.03×10^{-3}	2.97×10^{-3}	95	3.97×10^{-3}
239.3	20.0	1.18×10^{-5}	3.04×10^{-3}	1.96×10^{-3}	77	6.06×10^{-3}
239.4	20.0	1.18×10^{-5}	4.05×10^{-3}	9.50×10^{-4}	79	8.62×10^{-3}

k_2 = 2.24 L mol^{-1}s^{-1}

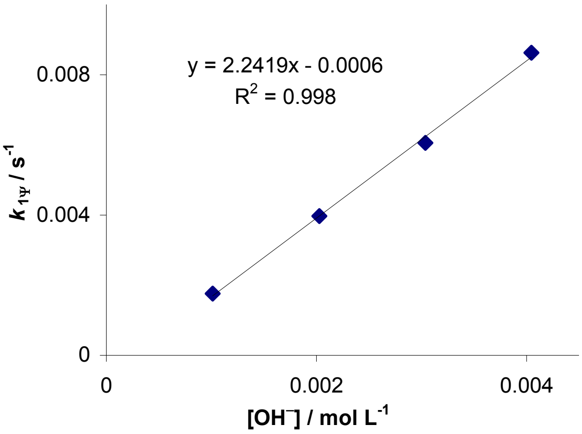

(lil)$_2$CH$^+$+ OH$^-$ in 99.6/0.4 (v/v) H$_2$O/CH$_3$CN, I = 0.01 (J&M, detection at 630 nm)

No.	T, °C	[(lil)$_2$CH$^+$]$_0$, mol L^{-1}	[OH$^-$]$_0$, mol L^{-1}	[NaBF$_4$], mol L^{-1}	conversion, %	$k_{1\Psi}$, s^{-1}
240.1	20.0	9.29×10^{-6}	9.97×10^{-4}	9.00×10^{-3}	96	1.96×10^{-3}
240.2	20.0	9.28×10^{-6}	1.99×10^{-3}	8.01×10^{-3}	95	3.96×10^{-3}
240.3	20.0	1.16×10^{-5}	2.99×10^{-3}	7.01×10^{-3}	97	5.90×10^{-3}
240.4	20.0	9.29×10^{-6}	3.99×10^{-3}	6.01×10^{-3}	94	7.71×10^{-3}

k_2 = 1.93 L mol^{-1}s^{-1}

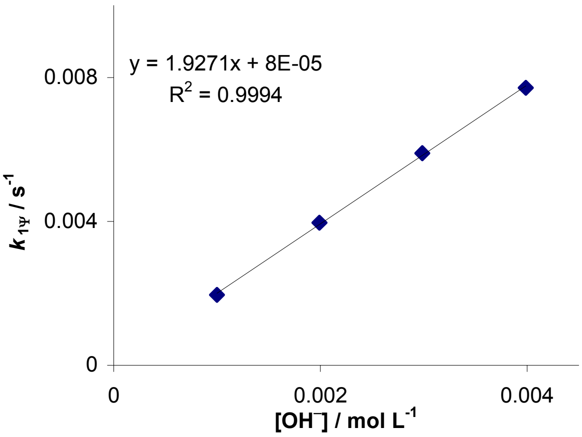

(lil)$_2$CH$^+$+ OH$^-$ in 99.6/0.4 (v/v) H_2O/CH_3CN, I = 0.05 (J&M, detection at 630 nm)

No.	T, °C	[(lil)$_2$CH$^+$]$_0$, mol L^{-1}	[OH$^-$]$_0$, mol L^{-1}	[NaBF$_4$], mol L^{-1}	conversion, %	$k_{1\Psi}$, s^{-1}
241.1	20.0	9.44×10^{-6}	2.03×10^{-3}	4.80×10^{-2}	87	2.28×10^{-3}
241.2	20.0	9.44×10^{-6}	3.01×10^{-3}	4.70×10^{-2}	81	3.77×10^{-3}
241.3	20.0	9.16×10^{-6}	3.93×10^{-3}	4.61×10^{-2}	89	4.45×10^{-3}
241.4	20.0	9.27×10^{-6}	5.97×10^{-3}	4.40×10^{-2}	89	6.62×10^{-3}
241.5	20.0	9.22×10^{-6}	7.92×10^{-3}	4.21×10^{-2}	83	9.48×10^{-3}

k_2 = 1.18 L mol^{-1}s^{-1}

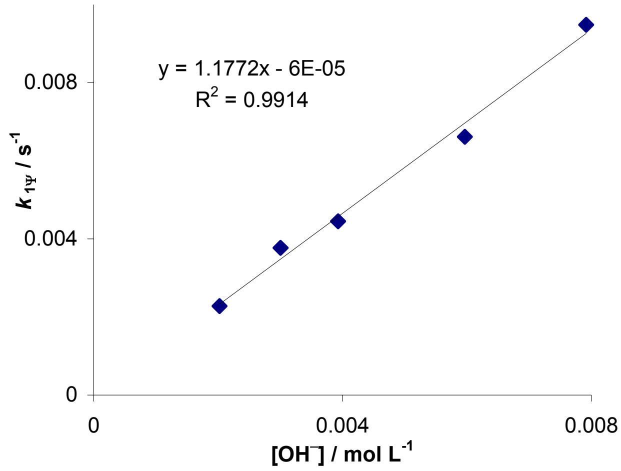

(lil)$_2$CH$^+$+ OH$^-$ in 95/5 (v/v) H_2O/CH_3CN (J&M, detection at 630 nm)

No.	T, °C	[(lil)$_2$CH$^+$]$_0$, mol L^{-1}	[OH$^-$]$_0$, mol L^{-1}	conversion, %	$k_{1\Psi}$, s^{-1}
204.1	20.0	1.27×10^{-5}	9.80×10^{-4}	94	2.30×10^{-3}
204.2	20.0	1.27×10^{-5}	1.96×10^{-3}	95	4.05×10^{-3}
204.3	20.0	1.27×10^{-5}	2.93×10^{-3}	98	5.88×10^{-3}
204.4	20.0	1.23×10^{-5}	3.78×10^{-3}	97	7.63×10^{-3}

k_2 = 1.90 L mol^{-1}s^{-1}

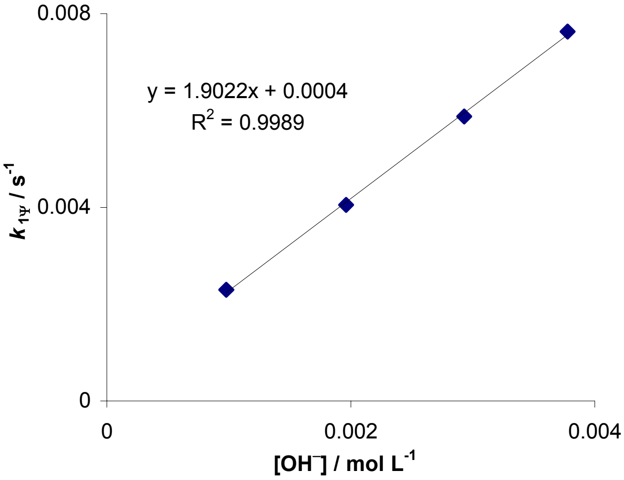

$(lil)_2CH^+$ + OH^- in 91/9 (v/v) H_2O/CH_3CN (J&M, detection at 630 nm)

No.	T, °C	$[(lil)_2CH^+]_0$, mol L^{-1}	$[OH^-]_0$, mol L^{-1}	conversion, %	$k_{1\Psi}$, s^{-1}
201.1	20.0	2.89×10^{-5}	1.06×10^{-3}	97	2.04×10^{-3}
201.2	20.0	2.83×10^{-5}	2.08×10^{-3}	97	3.71×10^{-3}
201.3	20.0	1.63×10^{-5}	4.98×10^{-3}	95	8.50×10^{-3}

$k_2 = 1.65$ L $mol^{-1}s^{-1}$

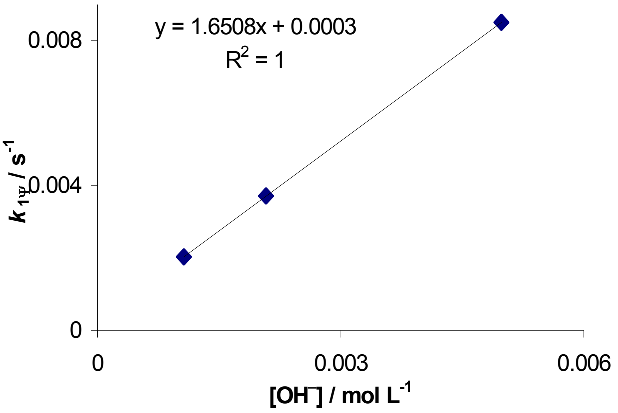

$(lil)_2CH^+$ + OH^- in 75/25 (v/v) H_2O/CH_3CN (J&M, detection at 635 nm)

No.	T, °C	$[(lil)_2CH^+]_0$, mol L^{-1}	$[OH^-]_0$, mol L^{-1}	conversion, %	$k_{1\Psi}$, s^{-1}
206.1	20.0	1.21×10^{-5}	9.29×10^{-4}	94	1.16×10^{-3}
206.2	20.0	1.31×10^{-5}	2.01×10^{-3}	98	2.32×10^{-3}
206.3	20.0	1.34×10^{-5}	3.10×10^{-3}	95	3.43×10^{-3}
206.4	20.0	1.33×10^{-5}	4.09×10^{-3}	97	4.47×10^{-3}

$k_2 = 1.05$ L $mol^{-1}s^{-1}$

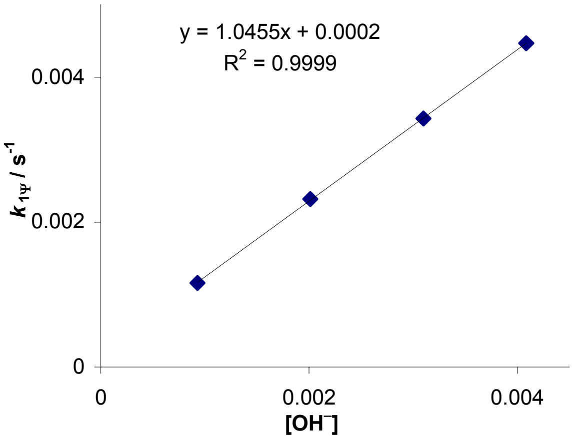

$(lil)_2CH^+$ + OH^- in 50/50 (v/v) H_2O/CH_3CN (J&M, detection at 635 nm)

No.	*T*, °C	$[(lil)_2CH^+]_0$, mol L^{-1}	$[OH^-]_0$, mol L^{-1}	conversion, %	$k_{1\Psi}$, s^{-1}
202.1	20.0	9.80×10^{-6}	1.01×10^{-3}	94	1.16×10^{-3}
202.2	20.0	9.77×10^{-6}	2.01×10^{-3}	98	2.28×10^{-3}
202.3	20.0	9.77×10^{-6}	3.01×10^{-3}	95	3.23×10^{-3}
202.4	20.0	9.77×10^{-6}	4.01×10^{-3}	97	4.22×10^{-3}

$k_2 = 1.01$ L mol^{-1}s^{-1}

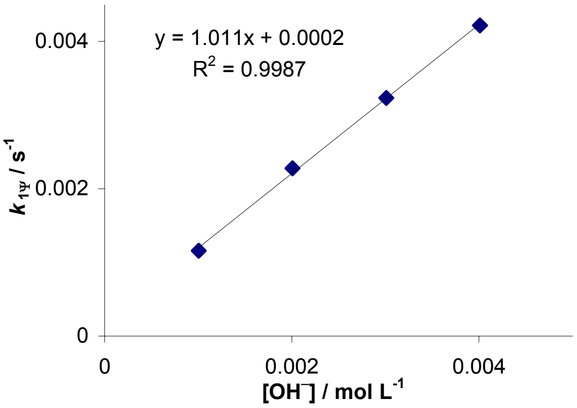

$(lil)_2CH^+$ + OH^- in 25/75 (v/v) H_2O/CH_3CN (J&M, detection at 635 nm)

No.	*T*, °C	$[(lil)_2CH^+]_0$, mol L^{-1}	$[OH^-]_0$, mol L^{-1}	conversion, %	$k_{1\Psi}$, s^{-1}
203.1	20.0	1.31×10^{-5}	1.01×10^{-3}	96	3.24×10^{-3}
203.2	20.0	1.30×10^{-5}	2.00×10^{-3}	96	6.18×10^{-3}
203.3	20.0	1.29×10^{-5}	2.97×10^{-3}	96	8.62×10^{-3}
203.4	20.0	1.28×10^{-5}	3.93×10^{-3}	97	1.16×10^{-2}

$k_2 = 2.81$ L mol^{-1}s^{-1}

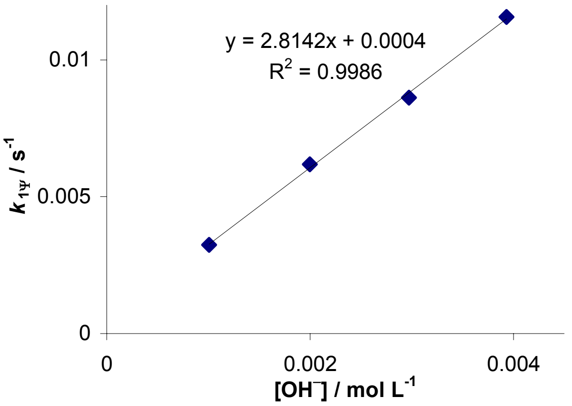

$(lil)_2CH^+$ + OH^- in 15/85 (v/v) H_2O/CH_3CN (J&M, detection at 635 nm)

No.	*T*, °C	$[(lil)_2CH^+]_0$, mol L^{-1}	$[OH^-]_0$, mol L^{-1}	conversion, %	$k_{1\Psi}$, s^{-1}
212.1	20.0	9.55×10^{-6}	9.80×10^{-4}	97	1.20×10^{-2}
212.2	20.0	9.41×10^{-6}	1.93×10^{-3}	97	2.30×10^{-2}
212.3	20.0	9.20×10^{-6}	2.83×10^{-3}	92	3.17×10^{-2}
212.4	20.0	9.49×10^{-6}	3.89×10^{-3}	99	4.49×10^{-2}

$k_2 = 1.12 \times 10^1$ L $mol^{-1}s^{-1}$

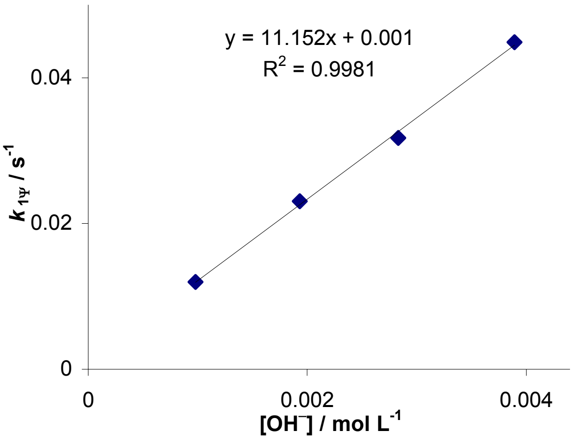

$(jul)_2CH^+$ + OH^- in 99.6/0.4 (v/v) H_2O/CH_3CN (J&M, detection at 640 nm)

No.	*T*, °C	$[(jul)_2CH^+]_0$, mol L^{-1}	$[OH^-]_0$, mol L^{-1}	conversion, %	$k_{1\Psi}$, s^{-1}
215.1	20.0	1.35×10^{-5}	5.40×10^{-4}	94	2.09×10^{-3}
215.2	19.9	1.33×10^{-5}	1.07×10^{-3}	91	3.83×10^{-3}
215.3	20.0	1.33×10^{-5}	1.60×10^{-3}	94	5.84×10^{-3}
215.4	20.0	1.33×10^{-5}	1.97×10^{-3}	96	6.95×10^{-3}

$k_2 = 3.44$ L $mol^{-1}s^{-1}$

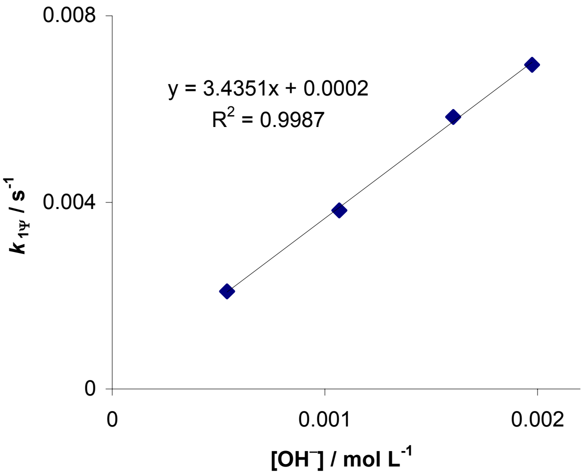

$(ind)_2CH^+ + OH^-$ in 99.6/0.4 (v/v) H_2O/CH_3CN (J&M, detection at 615 nm)

No.	T, °C	$[(ind)_2CH^+]_0$, mol L^{-1}	$[OH^-]_0$, mol L^{-1}	conversion, %	$k_{1\Psi}$, s^{-1}
207.1	20.0	1.41×10^{-5}	5.01×10^{-4}	97	6.91×10^{-3}
207.2	20.0	1.38×10^{-5}	1.02×10^{-3}	98	1.24×10^{-2}
207.3	20.0	1.38×10^{-5}	1.56×10^{-3}	98	1.83×10^{-2}
207.4	20.0	1.38×10^{-5}	2.05×10^{-3}	99	2.35×10^{-2}

$k_2 = 1.08 \times 10^1$ L mol^{-1}s^{-1}

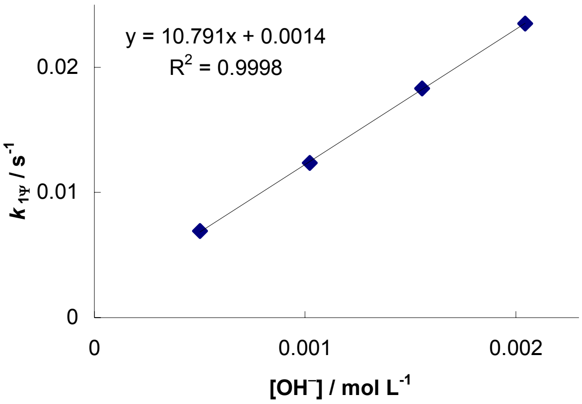

$(ind)_2CH^+ + OH^-$ in 50/50 (v/v) H_2O/CH_3CN (J&M, detection at 615 nm)

No.	T, °C	$[(ind)_2CH^+]_0$, mol L^{-1}	$[OH^-]_0$, mol L^{-1}	conversion, %	$k_{1\Psi}$, s^{-1}
251.1	20.0	8.84×10^{-6}	9.96×10^{-4}	98	8.58×10^{-3}
251.2	20.0	8.82×10^{-6}	1.99×10^{-3}	98	1.71×10^{-2}
251.3	20.1	8.88×10^{-6}	3.00×10^{-3}	97	2.65×10^{-2}
251.4	20.1	8.77×10^{-6}	3.95×10^{-3}	97	3.36×10^{-2}

$k_2 = 8.56$ L mol^{-1}s^{-1}

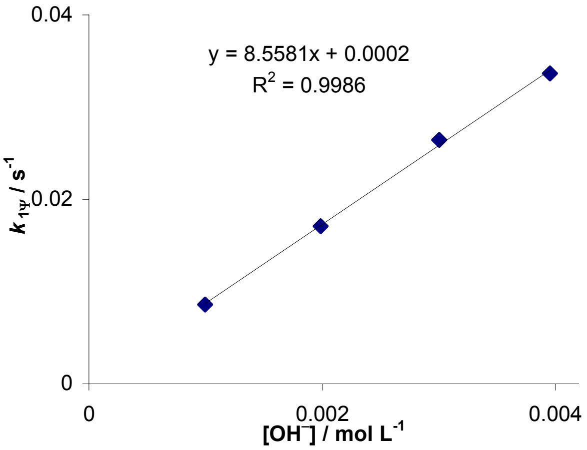

$(pyr)_2CH^+ + OH^-$ in 99.6/0.4 (v/v) H_2O/CH_3CN (Stopped-flow, detection at 610 nm)

No.	T, °C	$[(pyr)_2CH^+]_0$, mol L^{-1}	$[OH^-]_0$, mol L^{-1}	$k_{1\Psi}$, s^{-1}
209.1	20.0	1.65×10^{-5}	1.02×10^{-3}	5.99×10^{-2}
209.2	20.0	1.65×10^{-5}	2.03×10^{-3}	1.08×10^{-1}
209.3	20.0	1.65×10^{-5}	3.04×10^{-3}	1.60×10^{-1}
209.4	20.0	1.65×10^{-5}	4.06×10^{-3}	2.07×10^{-1}

$k_2 = 4.85 \times 10^1$ L mol^{-1}s^{-1}

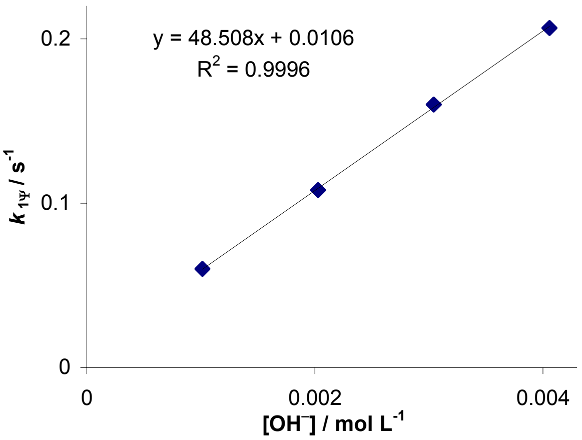

$(dma)_2CH^+$ + OH^- in 99.6/0.4 (v/v) H_2O/CH_3CN (Stopped-flow, detection at 605 nm), stabilization by toluenesulfonic acid

$(dma)_2CH^+BF_4^-$ (21.9 mg, 6.44 × 10^{-5} mol) was dissolved in 10 mL of CH_3CN (c = 6.44 × 10^{-3} mol L^{-1}). 160 μL of this solution and 16 μL of toluenesulfonic acid aqueous solution (c = 3.13 × 10^{-5} mol L^{-1}) were dissolved in 20 mL of water ($(dma)_2CH^+$: c = 5.15 × 10^{-5} mol L^{-1}, acid: c = 2.00 × 10^{-5} mol L^{-1}). 40 μL of KOH solution (c = 0.5073 mol L^{-1}) was diluted with water to give 10 mL (c = 2.03 × 10^{-3} mol L^{-1}). In the stopped-flow instrument, equal volumes of the electrophile and nucleophile solutions were mixed to give the final concentrations listed in the table. The reactions were followed photometrically at λ = 605 nm. A plot of $k_{1\Psi}$ versus the non-corrected concentration of hydroxide ion yields a straight line, the slope of which corresponds to the second order rate constant. (Run 210.1)

No.	T, °C	$[(dma)_2CH^+]_0$, mol L^{-1}	$[OH^-]_0$, mol L^{-1}	$k_{1\Psi}$, s^{-1}
210.1	20.0	2.58 × 10^{-5}	1.02 × 10^{-3}	1.71 × 10^{-1}
210.2	20.0	2.58 × 10^{-5}	2.03 × 10^{-3}	3.16 × 10^{-1}
210.3	20.0	2.58 × 10^{-5}	3.04 × 10^{-3}	4.45 × 10^{-1}
210.4	20.0	2.58 × 10^{-5}	4.06 × 10^{-3}	5.80 × 10^{-1}
210.5	20.0	2.58 × 10^{-5}	5.07 × 10^{-3}	7.03 × 10^{-1}

k_2 = 1.31 × 10^2 L $mol^{-1}s^{-1}$

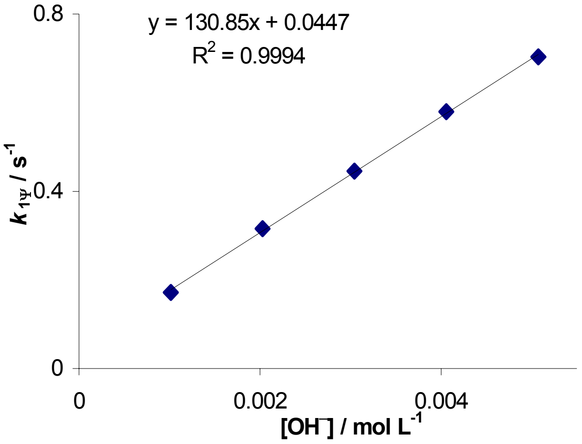

$(dma)_2CH^+$ + OH^- in 50/50 (v/v) H_2O/CH_3CN (Stopped-flow, detection at 605 nm)

$(dma)_2CH^+$ BF_4^- (10.4 mg, 3.06×10^{-5} mol) was dissolved in 10 mL of CH_3CN (c = 3.06×10^{-3} mol L^{-1}). 100 μL of this solution was dissolved in 10 mL of CH_3CN (c = 3.05×10^{-5} mol L^{-1}). 40 μL of KOH solution (c = 0.5073 mol L^{-1}) was diluted with water to 10 mL (c = 2.03×10^{-3} mol L^{-1}). In the stopped-flow instrument, equal volumes of the electrophile and nucleophile solutions were mixed to give the final concentrations listed in the table. The reactions were followed photometrically at λ = 605 nm. The mixing of pure water and CH_3CN was also monitored and the absorbances determined at different times were subtracted to eliminate the effect of mixing. A plot of $k_{1\Psi}$ versus the concentration of hydroxide ion yields a straight line, the slope of which corresponds to the second order rate constant. (Run 253.1)

No.	T, °C	$[(dma)_2CH^+]_0$, mol L^{-1}	$[OH^-]_0$, mol L^{-1}	$k_{1\Psi}$, s^{-1}
253.1	20.0	1.53×10^{-5}	1.02×10^{-3}	1.54×10^{-1}
253.2	20.0	1.53×10^{-5}	2.03×10^{-3}	2.68×10^{-1}
253.3	20.0	1.53×10^{-5}	3.04×10^{-3}	3.68×10^{-1}
253.4	20.0	1.53×10^{-5}	4.06×10^{-3}	4.53×10^{-1}

$k_2 = 9.83 \times 10^1$ L $mol^{-1}s^{-1}$

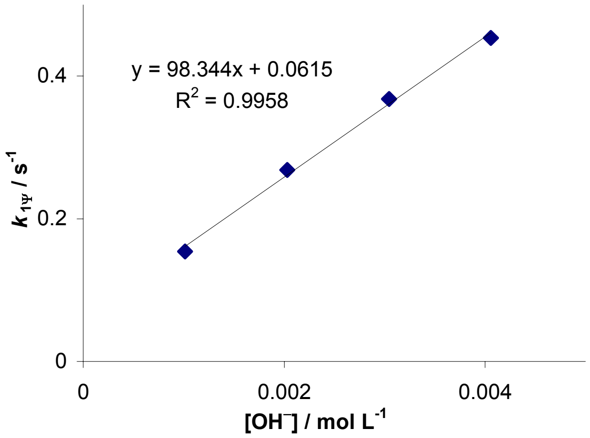

$(mor)_2CH^+$+ OH^- in 50/50 (v/v) H_2O/CH_3CN (Stopped-flow, detection at 610 nm)

No.	T, °C	$[(mor)_2CH^+]_0$, mol L^{-1}	$[OH^-]_0$, mol L^{-1}	$k_{1\Psi}$, s^{-1}
254.1	19.9	1.57×10^{-5}	1.27×10^{-3}	2.25
254.2	19.9	1.57×10^{-5}	2.54×10^{-3}	3.61
254.3	20.0	1.57×10^{-5}	3.80×10^{-3}	5.18
254.4	20.0	1.57×10^{-5}	5.07×10^{-3}	6.22

$k_2 = 1.06 \times 10^3$ L $mol^{-1}s^{-1}$

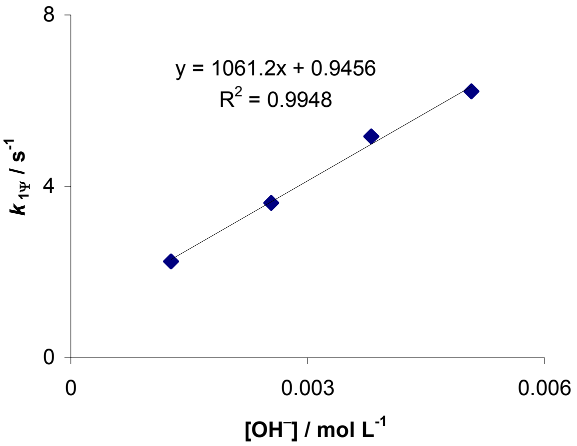

$(mfa)_2CH^+$+ OH^- in 50/50 (v/v) H_2O/CH_3CN (Stopped-flow, detection at 585 nm)

No.	T, °C	$[(mfa)_2CH^+]_0$, mol L^{-1}	$[OH^-]_0$, mol L^{-1}	$k_{1\Psi}$, s^{-1}
255.1	20.0	8.77×10^{-6}	7.61×10^{-4}	8.91
255.2	20.0	8.77×10^{-6}	1.52×10^{-3}	13.5
255.3	20.0	8.77×10^{-6}	2.28×10^{-3}	18.4
255.4	20.0	8.77×10^{-6}	3.04×10^{-3}	23.7
255.5	20.0	8.77×10^{-6}	3.81×10^{-3}	29.2

$k_2 = 6.67 \times 10^3$ L $mol^{-1}s^{-1}$

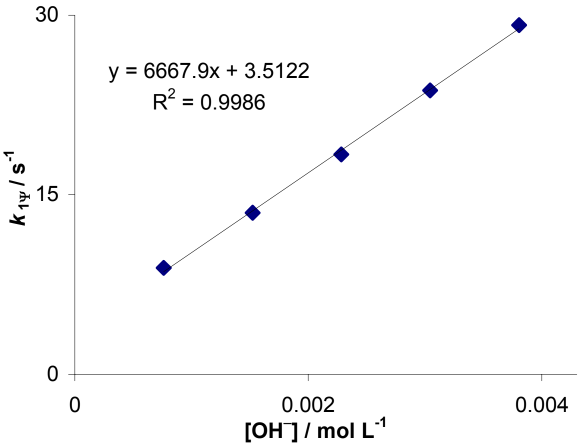

Semicarbazide ($H_2NNHCONH_2$) in water

$(lil)_2CH^+BF_4^-$ (13.4 mg, 3.22×10^{-5} mol) was dissolved in 10 mL of trifluoroethanol (c = 3.22×10^{-3} mol L^{-1}). 100 μL of this solution was added to 24.56 g of water in a thermostat with stirring. Semicarbazide hydrochloride (386.5 mg, 3.47×10^{-3} mol) was mixed with 7.04 mL of 0.4921 mol L^{-1} KOH aq (3.47×10^{-3} mol), and filled up to 10 mL with water (c = 3.47×10^{-1} mol L^{-1}). 18 μL of the semicarbazide solution was added to the solution of $(lil)_2CH^+BF_4^-$ and the consumption of the carbocation was followed photometrically at 630 nm.

The reaction of semicarbazide with $(lil)_2CH^+$ in water reached an equilibrium, and the rate constants were derived as described in ref. 5. k_+ and k_- are the rate constants of the forward and the backward reactions, respectively.

$$Ar_2CH^+ + Nu \underset{k_-}{\overset{k_+}{\rightleftharpoons}} P$$

Replacing Ar_2CH^+ by E and k_+[Nu] by $k_{1\Psi}$ (pseudo-first-order rate constant for large [Nu]) yields,

$$-d[E]/dt = k_{1\Psi}[E] - k_-[P] \tag{7.1}$$

at equilibrium,

$$k_{1\Psi}[E]_{eq} = k_-[P]_{eq} = k_-[E]_0 - [E]_{eq} \tag{7.2}$$

then,

$$[E]_{eq} = k_-[E]_0/(k_{1\Psi} + k_-) \tag{7.3}$$

from eq. 7.1,

$$-d[E]/dt = k_{1\Psi}[E] - k_-([E]_0 - [E]) = (k_{1\Psi} + k_-)\{[E]- k_-[E]_0/(k_{1\Psi} + k_-)\} \tag{7.4}$$

from 7.3 and 7.4,

$$d[E]/dt = -(k_{1\Psi} + k_-)([E] - [E]_{eq}) \tag{7.5}$$

eq. 7.5 is integrated,

$$\ln\{([E] - [E]_{eq})/([E]_0 - [E]_{eq})\} = -(k_{1\Psi} + k_-)\, t. \tag{7.6}$$

Therefore, a graph of $\ln([E] - [E]_{eq})$ versus t gives a straight line of the slope $-(k_{1\Psi} + k_-)$. Combination with eq. 7.2 yields $k_{1\Psi}$.

$(lil)_2CH^+$ + semicarbazide in 99.6/0.4 (v/v) H_2O/TFE [a] (J&M, detection at 630 nm)

No.	*T*, °C	$[(lil)_2CH^+]_0$, mol L^{-1}	$[semicarbazide]_0$, mol L^{-1}	A_0	A_{eq}	$k_{1\Psi}$, s^{-1}
110.1	20.0	1.29×10^{-5}	2.50×10^{-4}	0.652	0.413	9.67×10^{-4}
110.2	20.0	1.31×10^{-5}	5.22×10^{-4}	0.707	0.317	1.66×10^{-3}
113.1	20.0	1.29×10^{-5}	7.74×10^{-4}	0.672	0.266	2.71×10^{-3}
113.2	20.0	1.31×10^{-5}	1.05×10^{-3}	0.700	0.195	3.76×10^{-3}
110.3	20.1	1.29×10^{-5}	1.39×10^{-3}	0.659	0.0632	4.59×10^{-3}

a) All reactions reached equilibria.

$k_2 = 3.32$ L $mol^{-1}s^{-1}$

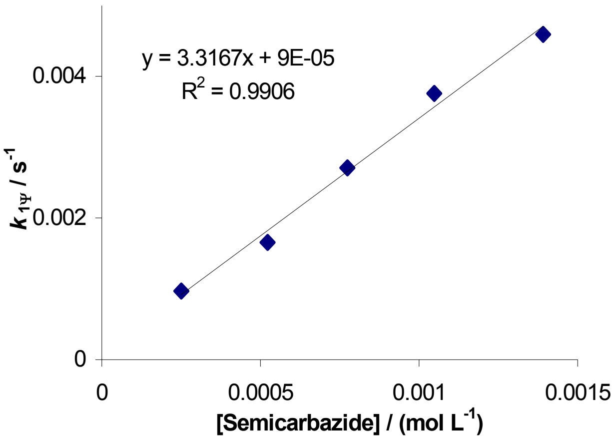

$(thq)_2CH^+$ + semicarbazide in 99.6/0.4 (v/v) H_2O/TFE (J&M, detection at 620 nm)

No.	*T*, °C	$[(thq)_2CH^+]_0$, mol L^{-1}	$[semicarbazide]_0$, mol L^{-1}	conversion, %	$k_{1\Psi}$, s^{-1}
146.1	19.9	9.08×10^{-6}	9.96×10^{-4}	96	3.10×10^{-2}
146.2	19.9	9.04×10^{-6}	1.98×10^{-3}	91	6.05×10^{-2}
146.3	19.9	8.99×10^{-6}	2.96×10^{-3}	96	8.83×10^{-2}
146.4	20.0	8.94×10^{-5}	3.72×10^{-3}	82	1.09×10^{-1}

$k_2 = 2.86 \times 10^1$ L $mol^{-1}s^{-1}$

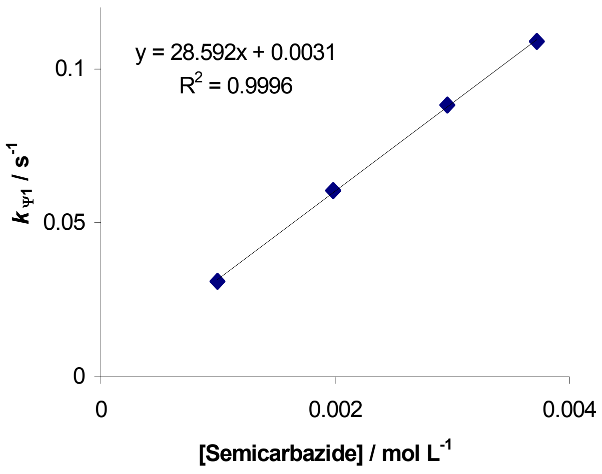

$(pyr)_2CH^+$ + semicarbazide in 99.6/0.4 (v/v) H_2O/TFE (J&M, detection at 610 nm)

No.	T, °C	$[(pyr)_2CH^+]_0$, mol L^{-1}	[semicarbazide]$_0$, mol L^{-1}	conversion, %	$k_{1\Psi}$, s^{-1}
145.1	20.0	9.07×10^{-6}	9.95×10^{-4}	97	5.54×10^{-2}
145.2	20.0	8.95×10^{-6}	1.96×10^{-3}	98	1.08×10^{-1}
145.3	20.0	8.94×10^{-6}	2.94×10^{-3}	95	1.61×10^{-1}
145.4	20.0	8.89×10^{-6}	3.71×10^{-3}	99	2.07×10^{-1}

$k_2 = 5.56 \times 10^1$ L $mol^{-1}s^{-1}$

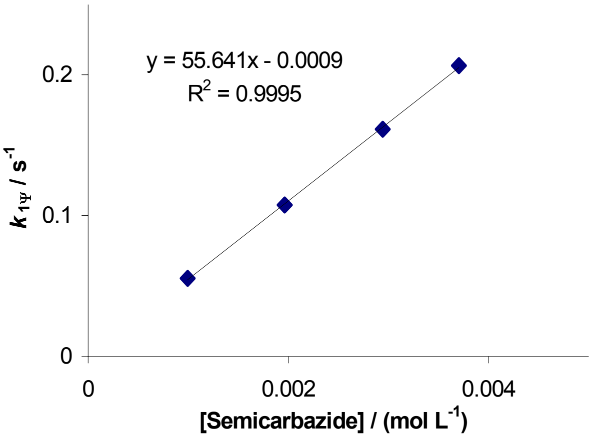

$(dma)_2CH^+$ + semicarbazide in 99.6/0.4 (v/v) H_2O/TFE (J&M, detection at 605 nm)

No.	T, °C	$[(dma)_2CH^+]_0$, mol L^{-1}	[semicarbazide]$_0$, mol L^{-1}	conversion, %	$k_{1\Psi}$, s^{-1}
139.1	20.0	1.44×10^{-5}	1.19×10^{-3}	93	1.66×10^{-1}
139.2	20.1	1.44×10^{-5}	1.98×10^{-3}	92	2.61×10^{-1}
139.3	20.0	1.45×10^{-5}	2.79×10^{-3}	89	3.35×10^{-1}
139.4	20.0	1.45×10^{-5}	3.60×10^{-3}	92	4.63×10^{-1}

$k_2 = 1.20 \times 10^2$ L $mol^{-1}s^{-1}$

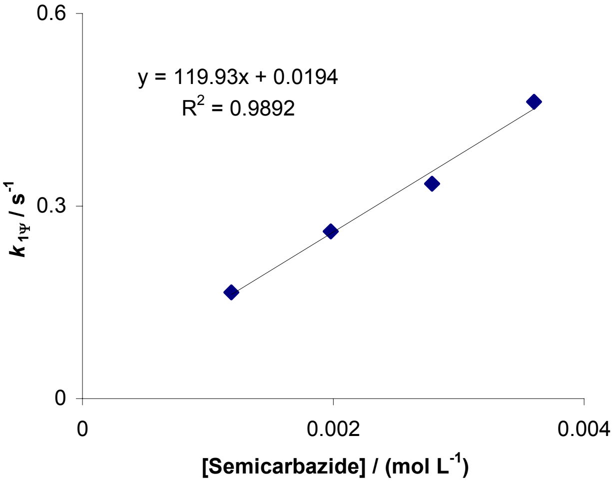

$(dma)_2CH^+$ + semicarbazide in 99.6/0.4 (v/v) H_2O/ CH_3CN (J&M, detection at 605 nm)

No.	*T*, °C	$[(dma)_2CH^+]_0$, mol L^{-1}	$[semicarbazide]_0$, mol L^{-1}	conversion, %	$k_{1\Psi}$, s^{-1}
139.1	20.0	4.04×10^{-6}	4.10×10^{-4}	83	7.83×10^{-2}
139.2	20.0	4.03×10^{-6}	8.19×10^{-4}	80	1.27×10^{-1}
139.3	20.0	3.96×10^{-6}	1.21×10^{-3}	89	1.69×10^{-1}
139.4	20.0	4.03×10^{-6}	1.64×10^{-3}	87	2.28×10^{-1}

$k_2 = 1.20 \times 10^2$ L $mol^{-1}s^{-1}$

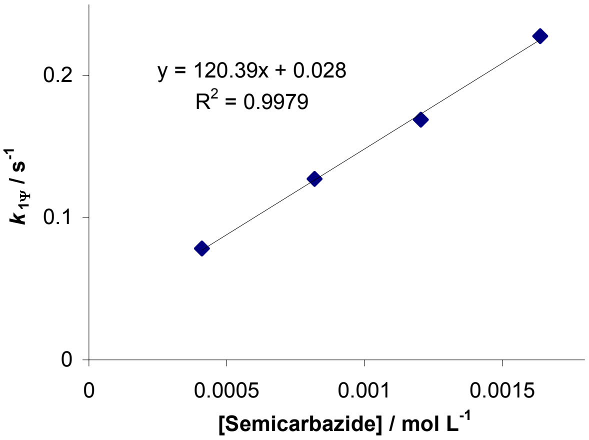

Hydroxylamine ($HONH_2$) in water

$(lil)_2CH^+BF_4^-$ (13.8 mg, 3.32 × 10^{-5} mol) was dissolved in 10 ml of CH_3CN (c = 3.32 × 10^{-3} mol L^{-1}). 100 µL of the solution was added to 24.66 g of water in a thermostat with stirring to give a 1.34 × 10^{-5} mol L^{-1} solution (TFE = 0.4% v/v). Hydroxylamine hydrochloride (292 mg, 4.21 × 10^{-3} mol) was dissolved in 8.28 mL of aqueous KOH (0.5073 mol L^{-1}), then the solution was filled up to 10 mL with water (4.20 × 10^{-1} mol L^{-1}). 16 µL of this solution was added, and the reactions were followed photometrically at 630 nm. A plot of $k_{1\Psi}$ versus concentration of $HONH_2$ yields a straight line, the slope of which corresponds to the second order rate constant. (Run 177.1)

$(lil)_2CH^+$ + $HONH_2$ in 99.6/0.4 (v/v) H_2O/TFE (J&M, detection at 630 nm)

No.	T, °C	$[(lil)_2CH^+]_0$, mol L^{-1}	$[HONH_2]_0$, mol L^{-1}	conversion, %	$k_{1\Psi}$, s^{-1}
177.1	20.0	1.34 × 10^{-5}	2.71 × 10^{-4}	67	2.26 × 10^{-3}
177.2	20.1	1.34 × 10^{-5}	5.44 × 10^{-4}	66	3.77 × 10^{-3}
177.3	20.0	1.34 × 10^{-5}	8.13 × 10^{-4}	77	5.65 × 10^{-3}
177.4	20.0	1.34 × 10^{-5}	1.08 × 10^{-3}	90	7.57 × 10^{-3}
177.5	19.9	1.31 × 10^{-5}	1.33 × 10^{-3}	91	9.10 × 10^{-3}

k_2 = 6.59 L $mol^{-1}s^{-1}$

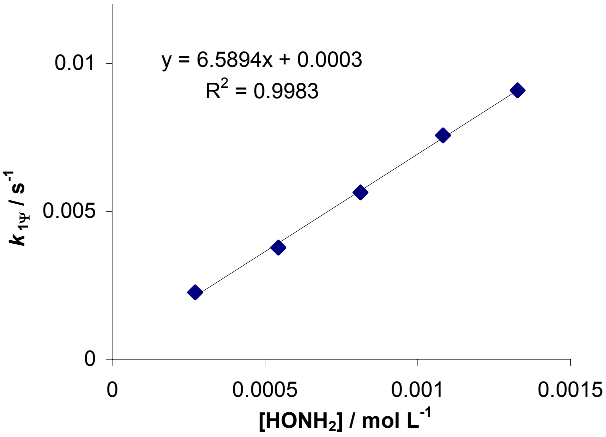

$(lil)_2CH^+$ + $HONH_2$ in 99.6/0.4 (v/v) H_2O/CH_3CN (J&M, detection at 630 nm)

No.	*T*, °C	$[(lil)_2CH^+]_0$, mol L^{-1}	$[HONH_2]_0$, mol L^{-1}	conversion, %	$k_{1\Psi}$, s^{-1}
214.1	20.0	1.33×10^{-5}	5.12×10^{-4}	52	3.54×10^{-3}
214.2	20.1	1.34×10^{-5}	1.03×10^{-3}	65	7.18×10^{-3}
214.3	20.0	1.29×10^{-5}	1.49×10^{-3}	67	1.00×10^{-2}
214.4	20.0	1.33×10^{-5}	2.04×10^{-3}	74	1.33×10^{-2}

$k_2 = 6.37$ L mol^{-1}s^{-1}

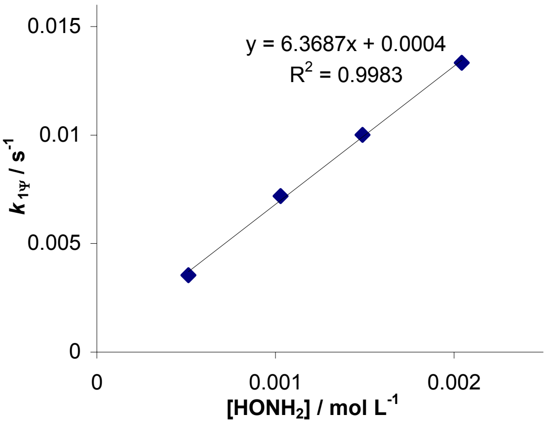

$(jul)_2CH^+$ + $HONH_2$ in 99.6/0.4 (v/v) H_2O/TFE (J&M, detection at 630 nm)

No.	*T*, °C	$[(jul)_2CH^+]_0$, mol L^{-1}	$[HONH_2]_0$, mol L^{-1}	conversion, %	$k_{1\Psi}$, s^{-1}
179.1	20.0	8.41×10^{-6}	6.11×10^{-4}	86	5.90×10^{-3}
179.2	20.0	8.44×10^{-6}	1.23×10^{-3}	56	1.06×10^{-2}
179.3	20.0	8.45×10^{-6}	1.84×10^{-3}	84	1.69×10^{-2}
179.4	20.0	8.42×10^{-6}	2.45×10^{-3}	82	2.27×10^{-2}
179.5	20.0	8.40×10^{-6}	3.05×10^{-3}	60	2.91×10^{-2}

$k_2 = 9.58$ L mol^{-1}s^{-1}

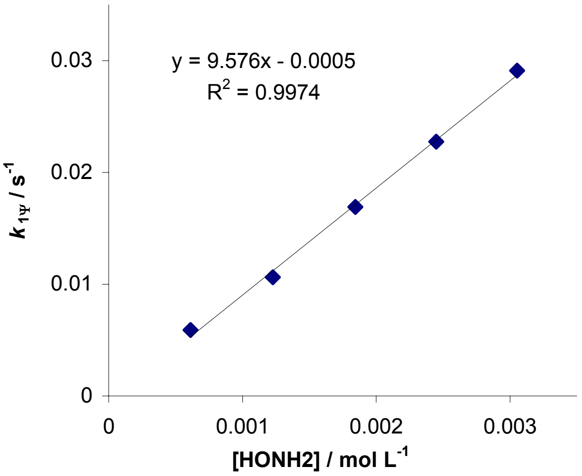

$(ind)_2CH^+$ + $HONH_2$ in 99.6/0.4 (v/v) H_2O/TFE (J&M, detection at 615 nm)

No.	T, °C	$[(ind)_2CH^+]_0$, mol L^{-1}	$[HONH_2]_0$, mol L^{-1}	conversion, %	$k_{1\Psi}$, s^{-1}
178.1	19.9	2.52×10^{-5}	5.08×10^{-4}	77	1.68×10^{-2}
178.2	20.0	2.52×10^{-5}	1.02×10^{-3}	74	3.17×10^{-2}
178.3	20.0	2.52×10^{-5}	1.52×10^{-3}	88	4.73×10^{-2}
178.4	20.0	2.52×10^{-5}	2.03×10^{-3}	93	6.14×10^{-2}
178.5	20.0	2.52×10^{-5}	2.54×10^{-3}	91	7.63×10^{-2}

$k_2 = 2.94 \times 10^1$ L $mol^{-1}s^{-1}$

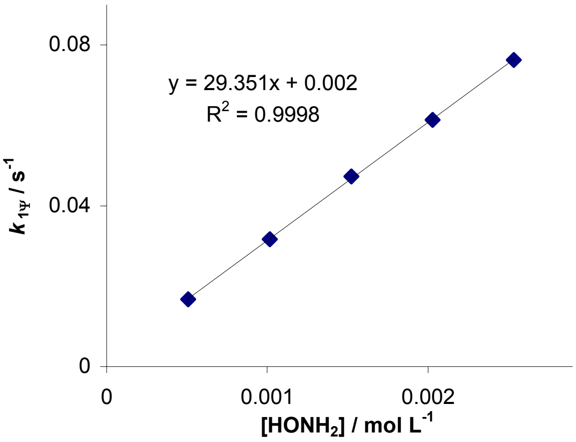

$(pyr)_2CH^+$ + $HONH_2$ in 99.6/0.4 (v/v) H_2O/TFE (Stopped-flow, detection at 610 nm)

No.	T, °C	$[(pyr)_2CH^+]_0$, mol L^{-1}	$[HONH_2]_0$, mol L^{-1}	$k_{1\Psi}$, s^{-1}
180.1	20.1	5.10×10^{-6}	1.02×10^{-3}	9.38×10^{-2}
180.2	20.1	5.10×10^{-6}	2.03×10^{-3}	2.26×10^{-1}
180.3	20.1	5.10×10^{-6}	3.04×10^{-3}	3.50×10^{-1}
180.4	20.1	5.10×10^{-6}	4.06×10^{-3}	4.71×10^{-1}

$k_2 = 1.24 \times 10^2$ L $mol^{-1}s^{-1}$

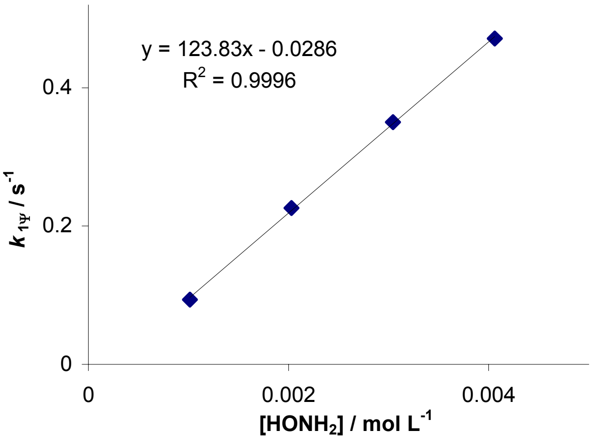

$(dma)_2CH^+$+ $HONH_2$ in 99.6/0.4 (v/v) H_2O/TFE (Stopped-flow, detection at 605 nm)

No.	*T*, °C	$[(dma)_2CH^+]_0$, mol L^{-1}	$[HONH_2]_0$, mol L^{-1}	$k_{1\Psi}$, s^{-1}
183.1	20.1	1.62×10^{-5}	5.07×10^{-4}	1.03×10^{-1}
183.2	20.1	1.62×10^{-5}	1.02×10^{-3}	2.07×10^{-1}
183.3	20.1	1.62×10^{-5}	1.52×10^{-3}	3.64×10^{-1}
183.4	20.1	1.62×10^{-5}	2.03×10^{-3}	4.42×10^{-1}
183.5	20.1	1.62×10^{-5}	2.54×10^{-3}	6.25×10^{-1}

$k_2 = 2.52 \times 10^2$ L $mol^{-1}s^{-1}$

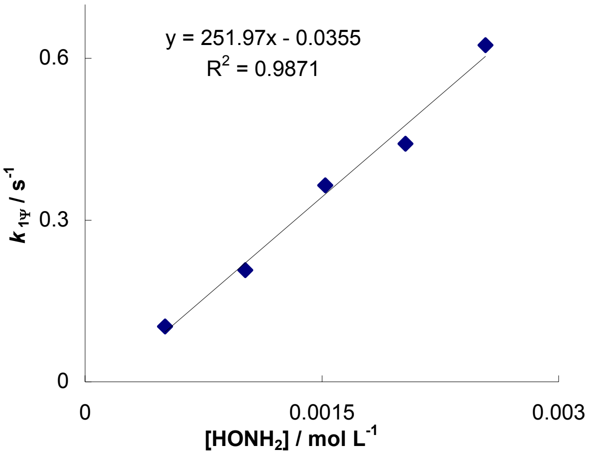

Trifluoroethylamine ($CF_3CH_2NH_2$) in DMSO

$(lil)_2CH^+BF_4^-$ (41.6 mg, 9.99 × 10^{-5} mol) was dissolved in 10 mL of DMSO (c = 9.99 × 10^{-3} mol L^{-1}). 25 µL of this solution was added to 27.33 g of DMSO (24.85 mL) in a thermostat with stirring to give a 1.00 × 10^{-5} mol L^{-1} solution. Trifluoroethylamine (396 mg, 4.00 × 10^{-3} mol) was dissolved in 10 mL of DMSO (c = 0.400mol L^{-1}). 50 µL of the amine solution was added to the carbocation solution and the consumption of the carbocation was followed at 640 nm. A plot of $k_{1\Psi}$ versus concentration of trifluoroethylamine yields a straight line, the slope of which corresponds to the second order rate constant. (Run 43.4)

$(lil)_2CH^+$ + trifluoroethylamine in DMSO (J&M, detection at 640 nm)

No.	T, °C	$[(lil)_2CH^+]_0$, mol L^{-1}	[trifluoroethylamine]$_0$, mol L^{-1}	conversion, %	$k_{1\Psi}$, s^{-1}
43.1	20.0	1.01 × 10^{-5}	3.22 × 10^{-4}	86	6.71 × 10^{-3}
43.2	20.0	1.01 × 10^{-5}	4.84 × 10^{-4}	94	1.01 × 10^{-2}
43.3	20.0	1.02 × 10^{-5}	6.50 × 10^{-4}	97	1.39 × 10^{-2}
43.4	20.0	1.00 × 10^{-5}	8.03 × 10^{-4}	97	1.76 × 10^{-2}

$k_2 = 2.26 \times 10^1$ L $mol^{-1}s^{-1}$

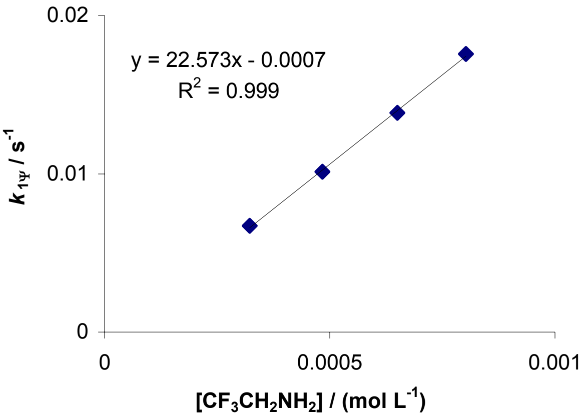

$(ind)_2CH^+$ + trifluoroethylamine in DMSO (J&M, detection at 630 nm)

No.	T, °C	$[(ind)_2CH^+]_0$, mol L^{-1}	[trifluoroethylamine]$_0$, mol L^{-1}	conversion, %	$k_{1\Psi}$, s^{-1}
52.1	20.0	1.58×10^{-5}	3.17×10^{-4}	98	4.27×10^{-2}
52.2	20.0	1.58×10^{-5}	6.31×10^{-4}	98	9.03×10^{-2}
52.3	20.0	1.58×10^{-5}	9.48×10^{-4}	99	1.38×10^{-1}
52.4	20.0	1.57×10^{-5}	1.26×10^{-3}	98	1.78×10^{-1}

$k_2 = 1.44 \times 10^2$ L mol^{-1}s^{-1}

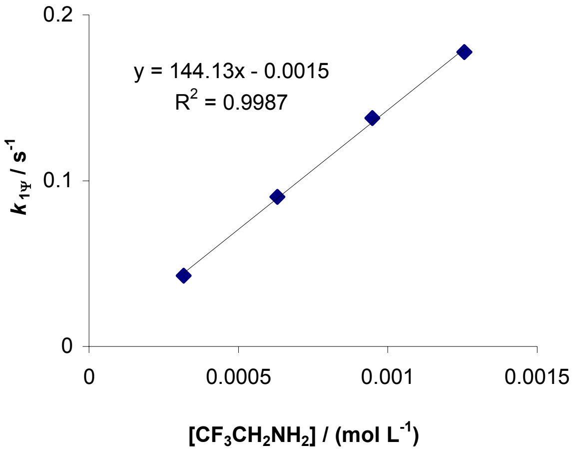

$(dma)_2CH^+$ + trifluoroethylamine in DMSO (stopped flow, detection at 615 nm)

No.	T, °C	$[(dma)_2CH^+]_0$, mol L^{-1}	[trifluoroethylamine]$_0$, mol L^{-1}	$k_{1\Psi}$, s^{-1}
158.1	20.0	2.49×10^{-5}	5.19×10^{-4}	1.49
158.2	20.0	2.49×10^{-5}	1.04×10^{-3}	3.08
158.3	20.1	2.49×10^{-5}	1.56×10^{-3}	4.81
158.4	20.0	2.49×10^{-5}	2.07×10^{-3}	6.25

$k_2 = 3.09 \times 10^3$ L mol^{-1}s^{-1}

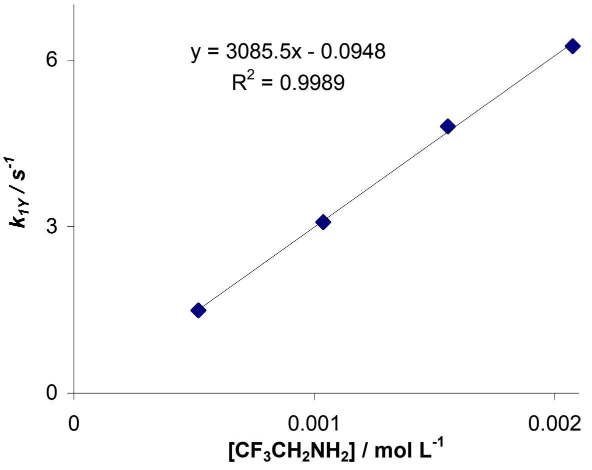

$(mor)_2CH^+$ + trifluoroethylamine in DMSO (stopped flow, detection at 620 nm)

No.	T, °C	$[(mor)_2CH^+]_0$, mol L^{-1}	$[\text{trifluoroethylamine}]_0$, mol L^{-1}	$k_{1\Psi}$, s^{-1}
157.1	20.1	2.54×10^{-5}	5.02×10^{-4}	8.54
157.2	20.0	2.54×10^{-5}	1.00×10^{-3}	1.64×10^{1}
157.3	20.1	2.54×10^{-5}	1.51×10^{-3}	2.48×10^{1}
157.4	20.1	2.54×10^{-5}	2.01×10^{-3}	3.33×10^{1}

$k_2 = 1.65 \times 10^4$ L mol^{-1}s^{-1}

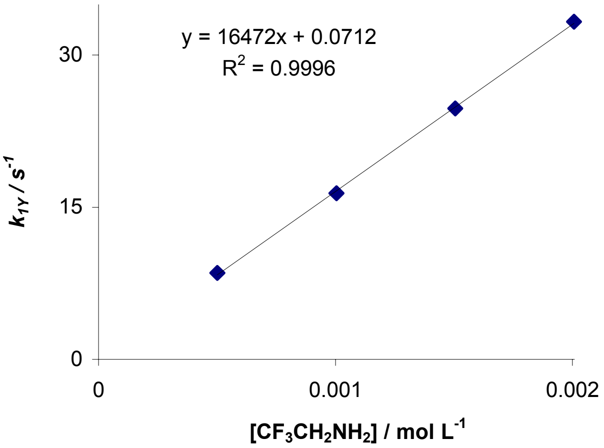

Trifluoroethoxide ($CF_3CH_2O^-$) in water

$(lil)_2CH^+BF_4^-$ (13.4 mg, 3.22×10^{-5} mol) was dissolved in 10 ml of trifluoroethanol (c = 3.22×10^{-3} mol L^{-1}). 100 µL of the solution was added to 24.56 g of water in a thermostat with stirring to give a 1.30×10^{-5} mol L^{-1} solution. Potassium hydroxide was purchased as an aqueous standard solution. 100 µL of this solution (0.4921 mol L^{-1}) was added, and the reactions were followed photometrically at 630 nm. The concentration of $CF_3CH_2O^-$ was calculated from $pK_a = 12.4$ [6] for CF_3CH_2OH. Because of the low concentrations of the acids and bases involved, the usually employed approximations for calculations of buffer solutions are not applicable, and all concentrations in the formula $K_b = [CF_3CH_2OH][OH^-]/[CF_3CH_2O^-]$ have to be considered explicitly. A plot of $k_{2,CF_3CH_2O^-}[CF_3CH_2O^-]_{eff}$ versus concentration of $[CF_3CH_2O^-]_{eff}$ yields a straight line, the slope of which corresponds to the second order rate constant. (Run 97.6)

$(lil)_2CH^+ + CF_3CH_2O^-$ in 99.6/0.4 (v/v) H_2O/TFE (J&M, detection at 630 nm)

No.	T, °C	$[(lil)_2CH^+]_0$, mol L^{-1}	$[CF_3CH_2OH]_0$, mol L^{-1}	$[OH^-]_0$, mol L^{-1}	conversion, %	$k_{1\Psi,obs}$, s^{-1}
97.1	20.1	1.30×10^{-5}	5.61×10^{-2}	2.58×10^{-4}	79	7.68×10^{-3}
97.2	20.1	1.27×10^{-5}	5.48×10^{-2}	5.04×10^{-4}	83	1.47×10^{-2}
97.3	20.0	1.29×10^{-5}	5.66×10^{-2}	7.38×10^{-4}	84	2.04×10^{-2}
97.4	20.0	1.29×10^{-5}	5.55×10^{-2}	1.02×10^{-3}	88	2.91×10^{-2}
97.5	20.0	1.31×10^{-5}	5.64×10^{-2}	1.56×10^{-3}	75	3.93×10^{-2}
97.6	20.0	1.30×10^{-5}	5.62×10^{-2}	1.99×10^{-3}	86	5.56×10^{-2}

No.	$[OH^-]_{eff}$, mol L^{-1}	$[CF_3CH_2O^-]_{eff}$, mol L^{-1}	$k_{2,OH^-}[OH^-]$, s^{-1}	$k_{2,CF_3CH_2O^-}[CF_3CH_2O^-]_{eff}$, s^{-1}
97.1	8.00×10^{-5}	1.78×10^{-4}	1.73×10^{-4}	7.51×10^{-3}
97.2	1.59×10^{-4}	3.45×10^{-4}	3.44×10^{-4}	1.44×10^{-2}
97.3	2.40×10^{-4}	5.27×10^{-4}	5.20×10^{-4}	1.98×10^{-2}
97.4	3.21×10^{-4}	7.01×10^{-4}	6.94×10^{-4}	2.84×10^{-2}
97.5	4.86×10^{-4}	1.07×10^{-3}	1.05×10^{-3}	3.82×10^{-2}
97.6	6.25×10^{-4}	1.36×10^{-3}	1.35×10^{-3}	5.43×10^{-2}

$k_2 = 3.79 \times 10^1$ L $mol^{-1}s^{-1}$

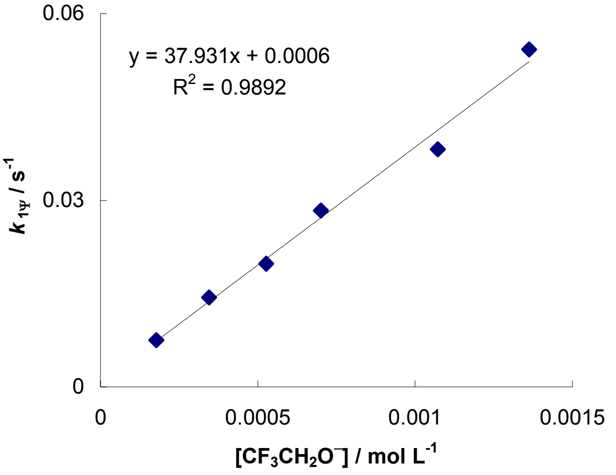

$(jul)_2CH^+$ + $CF_3CH_2O^-$ in 99.6/0.4 (v/v) H_2O/TFE (J&M, detection at 630 nm)

No.	T, °C	$[(jul)_2CH^+]_0$, mol L^{-1}	$[CF_3CH_2OH]_0$, mol L^{-1}	$[OH^-]_0$, mol L^{-1}	conversion, %	$k_{1\Psi,obs}$, s^{-1}
100.1	19.9	1.45×10^{-5}	5.64×10^{-2}	5.79×10^{-4}	93	2.74×10^{-2}
100.2	20.1	1.45×10^{-5}	5.63×10^{-2}	1.16×10^{-3}	91	4.94×10^{-2}
100.3	20.0	1.43×10^{-5}	5.54×10^{-2}	1.71×10^{-3}	97	8.20×10^{-2}
100.4	19.9	1.44×10^{-5}	5.59×10^{-2}	2.27×10^{-3}	96	1.10×10^{-1}
100.5	20.1	1.43×10^{-5}	5.56×10^{-2}	2.85×10^{-3}	87	1.36×10^{-1}

No.	$[OH^-]_{eff}$, mol L^{-1}	$[CF_3CH_2O^-]_{eff}$, mol L^{-1}	$k_{2,OH^-}[OH^-]$, s^{-1}	$k_{2,CF_3CH_2O^-}[CF_3CH_2O^-]_{eff}$, s^{-1}
100.1	1.79×10^{-4}	3.99×10^{-4}	6.16×10^{-4}	2.68×10^{-2}
100.2	3.60×10^{-4}	7.96×10^{-4}	1.24×10^{-3}	4.81×10^{-2}
100.3	5.40×10^{-4}	1.17×10^{-3}	1.86×10^{-3}	8.02×10^{-2}
100.4	7.19×10^{-4}	1.55×10^{-3}	2.47×10^{-3}	1.07×10^{-1}
100.5	9.10×10^{-4}	1.94×10^{-3}	3.13×10^{-3}	1.33×10^{-1}

$k_2 = 7.06 \times 10^1$ L mol^{-1}s^{-1}

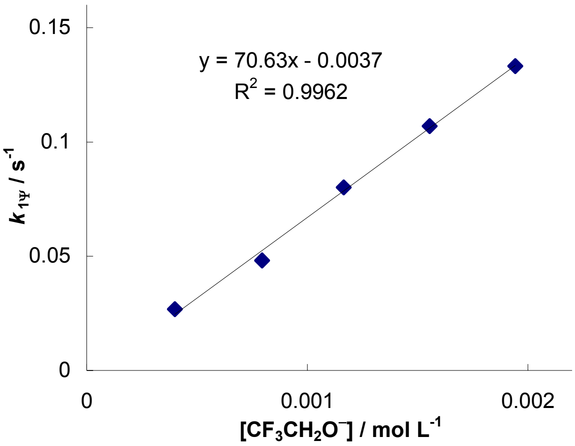

$(thq)_2CH^+ + CF_3CH_2O^-$ in 99.6/0.4 (v/v) H_2O/TFE (J&M, detection at 620 nm)

No.	T, °C	$[(thq)_2CH^+]_0$, mol L^{-1}	$[CF_3CH_2OH]_0$, mol L^{-1}	$[OH^-]_0$, mol L^{-1}	conversion, %	$k_{1\Psi,\mathrm{obs}}$, s^{-1}
106.1	20.0	8.41×10^{-6}	5.59×10^{-2}	1.69×10^{-4}	77	4.90×10^{-2}
106.2	20.0	8.48×10^{-6}	5.64×10^{-2}	3.41×10^{-4}	85	1.05×10^{-1}
106.3	20.0	8.45×10^{-6}	5.62×10^{-2}	4.97×10^{-4}	88	1.50×10^{-1}
106.4	20.0	8.40×10^{-6}	5.59×10^{-2}	6.72×10^{-4}	83	2.04×10^{-1}

No.	$[OH^-]_{\mathrm{eff}}$, mol L^{-1}	$[CF_3CH_2O^-]_{\mathrm{eff}}$, mol L^{-1}	$k_{2,OH^-}[OH^-]$,[a] s^{-1}	$k_{2,CF_3CH_2O^-}[CF_3CH_2O^-]_{\mathrm{eff}}$, s^{-1}
106.1	5.25×10^{-5}	1.17×10^{-4}	1.24×10^{-3}	4.78×10^{-2}
106.2	1.05×10^{-4}	2.36×10^{-4}	2.48×10^{-3}	1.03×10^{-1}
106.3	1.54×10^{-4}	3.43×10^{-4}	3.64×10^{-3}	1.46×10^{-1}
106.4	2.10×10^{-4}	4.62×10^{-4}	4.94×10^{-3}	1.99×10^{-1}

[a] k_{2,OH^-} was calculated from $E = -8.22$ for $(thq)_2CH^+$ and N, $s = 10.47, 0.61$ for OH^-.

$k_2 = 4.35 \times 10^2$ L $mol^{-1}s^{-1}$

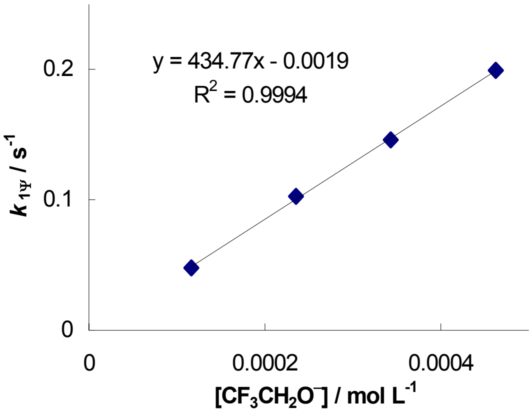

$(dma)_2CH^+ + CF_3CH_2O^-$ in 99.6/0.4 (v/v) H_2O/TFE (Stopped-flow, detection at 605 nm)

No.	T, °C	$[(dma)_2CH^+]_0$, mol L^{-1}	$[CF_3CH_2OH]_0$, mol L^{-1}	$[OH^-]_0$, mol L^{-1}	$k_{1\Psi,obs}$, s^{-1}
114.1	20.0	2.05×10^{-5}	5.56×10^{-2}	4.05×10^{-4}	6.46×10^{-1}
114.2	20.0	$2.05 \times 10^{-}$	5.56×10^{-2}	8.15×10^{-4}	1.30
114.3	20.0	$2.05 \times 10^{-}$	5.56×10^{-2}	1.23×10^{-3}	1.93
114.4	20.0	$2.05 \times 10^{-}$	5.56×10^{-2}	1.63×10^{-3}	2.48

No.	$[OH^-]_{eff}$, mol L^{-1}	$[CF_3CH_2O^-]_{eff}$, mol L^{-1}	$k_{2,OH^-}[OH^-]$, s^{-1}	$k_{2,CF_3CH_2O^-}[CF_3CH_2O^-]_{eff}$, s^{-1}
114.1	1.27×10^{-4}	2.79×10^{-4}	1.66×10^{-2}	6.29×10^{-1}
114.2	2.56×10^{-4}	5.60×10^{-4}	3.34×10^{-2}	1.26
114.3	3.85×10^{-4}	8.40×10^{-4}	5.04×10^{-2}	1.88
114.4	5.15×10^{-4}	1.12×10^{-3}	6.73×10^{-2}	2.42

$k_2 = 2.14 \times 10^3$ L $mol^{-1}s^{-1}$

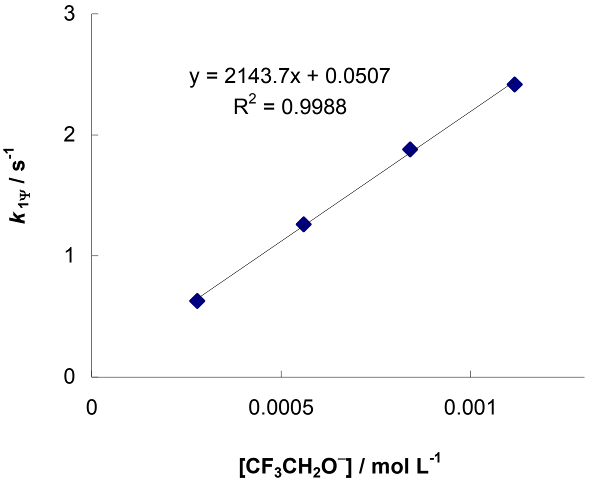

n-Propylamine (n-PrNH$_2$) in water

$(\text{lil})_2\text{CH}^+\text{BF}_4^-$ (12.3 mg, 2.95×10^{-5} mol) was dissolved in 10 ml of CH_3CN (c = 2.95×10^{-3} mol L^{-1}). 100 µL of this solution and 60 µL of CH_3CN were dissolved in 20 mL of water (c = 1.48×10^{-5} mol L^{-1}, CH_3CN 0.8 volume %). n-PrNH$_2$ (508 mg, 8.59×10^{-3} mol) was dissolved in 10 mL of water (c = 0.859 mol L^{-1}). 30 µL of the solution was dissolved in 10 mL of water (c = 2.58×10^{-3} mol L^{-1}). In the stopped-flow instrument equal volumes of the electrophile and nucleophile solutions were mixed to give the concentrations listed in the table. The course of the reactions was followed at 630 nm. The concentration of n-PrNH$_2$ of free base form was calculated from K_b of n-PrNH$_2$ (pK_a of conjugated acid = 10.7).[7] Because of the low concentrations of the acids and bases involved, the usually employed approximations for calculations of buffer solutions are not applicable, and all concentrations in the formula $K_b = [n\text{-PrNH}_3^+][\text{OH}^-]/[n\text{-PrNH}_2]$ have to be considered explicitly. A plot of $k_{2,n\text{-PrNH}_2}[n\text{-PrNH}_2]_{\text{eff}}$ versus concentration of $[n\text{-PrNH}_2]_{\text{eff}}$ yields a straight line, the slope of which corresponds to the second order rate constant. (Run 227.1)

$(\text{lil})_2\text{CH}^+$ + n-PrNH$_2$ in 99.6/0.4 (v/v) H_2O/CH_3CN (Stopped-flow, detection at 630 nm)

No.	T, °C	$[(\text{lil})_2\text{CH}^+]_0$, mol L^{-1}	$[n\text{-PrNH}_2]_0$, mol L^{-1}	$k_{1\Psi,\text{obs}}$, s^{-1}
227.1	20.0	7.39×10^{-6}	1.29×10^{-3}	5.63×10^{-2}
227.2	20.0	7.39×10^{-6}	2.15×10^{-3}	1.05×10^{-1}
227.3	20.0	7.39×10^{-6}	3.01×10^{-3}	1.59×10^{-1}
227.4	20.1	7.39×10^{-6}	4.30×10^{-3}	2.39×10^{-1}
227.5	20.0	7.39×10^{-6}	5.16×10^{-3}	3.02×10^{-1}

No.	$[\text{OH}^-]$, mol L^{-1}	$[n\text{-PrNH}_2]_{\text{eff}}$, mol L^{-1}	$k_{2,\text{OH}^-}[\text{OH}^-]$, s^{-1}	$k_{2,n\text{-PrNH}_2}[n\text{-PrNH}_2]_{\text{eff}}$, s^{-1}
227.1	5.96×10^{-4}	6.93×10^{-4}	1.30×10^{-3}	5.50×10^{-2}
227.2	8.24×10^{-4}	1.32×10^{-3}	1.78×10^{-3}	1.03×10^{-1}
227.3	1.01×10^{-3}	2.00×10^{-3}	2.19×10^{-3}	1.57×10^{-1}
227.4	1.25×10^{-3}	3.05×10^{-3}	2.70×10^{-3}	2.36×10^{-1}
227.5	1.39×10^{-3}	3.77×10^{-3}	3.01×10^{-3}	2.99×10^{-1}

$k_2 = 7.89 \times 10^1$ L mol^{-1}s^{-1}

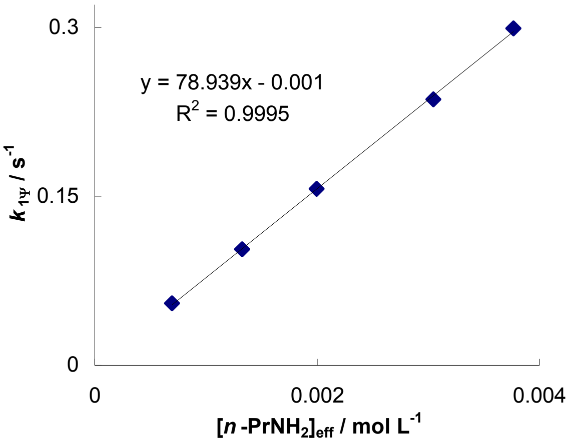

$(ind)_2CH^+$ + n-$PrNH_2$ in 99.6/0.4 (v/v) H_2O/CH_3CN (Stopped-flow, detection at 615 nm)

No.	T, °C	$[(ind)_2CH^+]_0$, mol L^{-1}	$[n\text{-}PrNH_2]_0$, mol L^{-1}	$k_{1\Psi,obs}$, s^{-1}
223.1	20.1	2.06×10^{-5}	2.04×10^{-3}	3.88×10^{-1}
223.2	20.1	2.06×10^{-5}	4.08×10^{-3}	8.82×10^{-1}
223.3	20.1	2.06×10^{-5}	6.11×10^{-3}	1.44
223.4	20.1	2.06×10^{-5}	8.15×10^{-3}	1.99
223.5	20.1	2.06×10^{-5}	1.02×10^{-2}	2.51

No.	$[OH^-]$, mol L^{-1}	$[n\text{-}PrNH_2]_{eff}$, mol L^{-1}	$k_{2,OH^-}[OH^-]$, s^{-1}	$k_{2,n\text{-}PrNH_2}[n\text{-}PrNH_2]_{eff}$, s^{-1}
223.1	7.97×10^{-4}	1.24×10^{-3}	8.61×10^{-3}	3.79×10^{-2}
223.2	1.21×10^{-3}	2.86×10^{-3}	1.31×10^{-2}	8.69×10^{-1}
223.3	1.53×10^{-3}	4.58×10^{-3}	1.65×10^{-2}	1.42
223.4	1.80×10^{-3}	6.35×10^{-3}	1.95×10^{-2}	1.97
223.5	2.04×10^{-3}	8.14×10^{-3}	2.21×10^{-2}	2.49

$k_2 = 3.07 \times 10^2$ L $mol^{-1}s^{-1}$

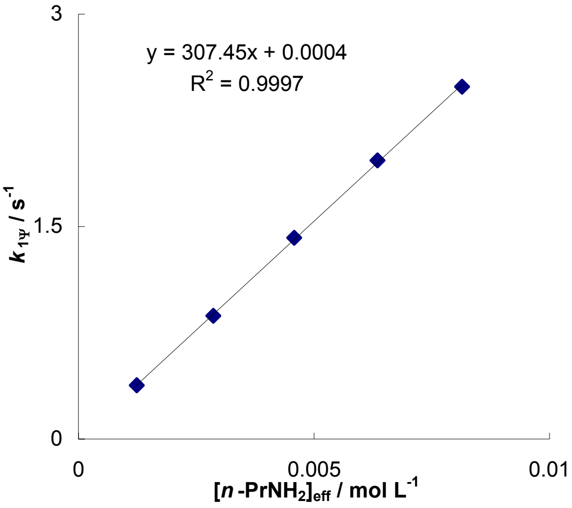

$(pyr)_2CH^+$ + n-$PrNH_2$ in 99.6/0.4 (v/v) H_2O/CH_3CN (Stopped-flow, detection at 610 nm)

No.	T, °C	$[(pyr)_2CH^+]_0$, mol L^{-1}	$[n\text{-}PrNH_2]_0$, mol L^{-1}	$k_{1\Psi,obs}$, s^{-1}
222.1	20.0	8.26×10^{-6}	9.20×10^{-4}	5.95×10^{-1}
222.2	20.0	8.26×10^{-6}	1.84×10^{-3}	1.31
222.3	20.0	8.26×10^{-6}	3.07×10^{-3}	2.46
222.4	20.0	8.26×10^{-6}	3.99×10^{-3}	3.44
222.5	20.0	8.26×10^{-6}	4.91×10^{-2}	4.46

No.	$[OH^-]$, mol L^{-1}	$[n\text{-}PrNH_2]_{eff}$, mol L^{-1}	$k_{2,OH^-}[OH^-]$, s^{-1}	$k_{2,n\text{-}PrNH_2}[n\text{-}PrNH_2]_{eff}$, s^{-1}
222.1	4.77×10^{-4}	4.44×10^{-4}	2.31×10^{-2}	5.71×10^{-1}
222.2	7.49×10^{-4}	1.09×10^{-3}	3.63×10^{-2}	1.27
222.3	1.02×10^{-3}	2.04×10^{-3}	4.97×10^{-2}	2.41
222.4	1.20×10^{-3}	2.79×10^{-3}	5.80×10^{-2}	3.38
222.5	1.35×10^{-3}	3.56×10^{-3}	6.55×10^{-2}	4.40

$k_2 = 1.23 \times 10^3$ L $mol^{-1}s^{-1}$

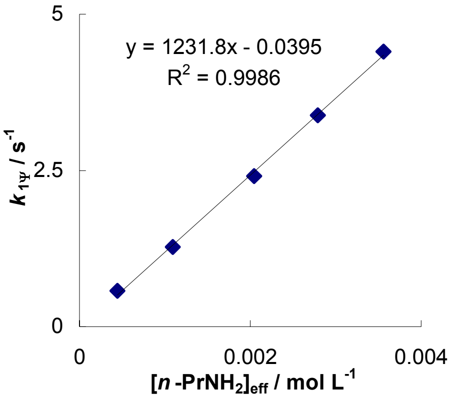

$(dma)_2CH^+$ + *n*-$PrNH_2$ in 99.6/0.4 (v/v) H_2O/CH_3CN (Stopped-flow, detection at 605 nm) stabilized by toluenesulfonic acid (6.26 × 10^{-6} mol L^{-1})

No.	T, °C	$[(dma)_2CH^+]_0$, mol L^{-1}	$[n\text{-}PrNH_2]_0$, mol L^{-1}	$k_{1\Psi,obs}$, s^{-1}
224.1	20.1	2.00×10^{-5}	2.04×10^{-3}	4.13
224.2	20.1	2.00×10^{-5}	4.08×10^{-3}	9.21
224.3	20.1	2.00×10^{-5}	6.11×10^{-3}	1.47×10^{1}
224.4	20.1	2.00×10^{-5}	8.15×10^{-3}	2.00×10^{1}
224.5	20.1	2.00×10^{-5}	1.02×10^{-2}	2.59×10^{1}

No.	$[OH^-]$, mol L^{-1}	$[n\text{-}PrNH_2]_{eff}$, mol L^{-1}	$k_{2,OH^-}[OH^-]$, s^{-1}	$k_{2,n\text{-}PrNH_2}[n\text{-}PrNH_2]_{eff}$, s^{-1}
224.1	7.97×10^{-4}	1.24×10^{-3}	1.04×10^{-1}	4.03
224.2	1.21×10^{-3}	2.86×10^{-3}	1.59×10^{-1}	9.05
224.3	1.53×10^{-3}	4.58×10^{-3}	2.01×10^{-1}	1.45×10^{1}
224.4	1.80×10^{-3}	6.35×10^{-3}	2.36×10^{-1}	1.97×10^{1}
224.5	2.04×10^{-3}	8.14×10^{-3}	2.67×10^{-1}	2.56×10^{1}

$k_2 = 3.12 \times 10^3$ L $mol^{-1}s^{-1}$

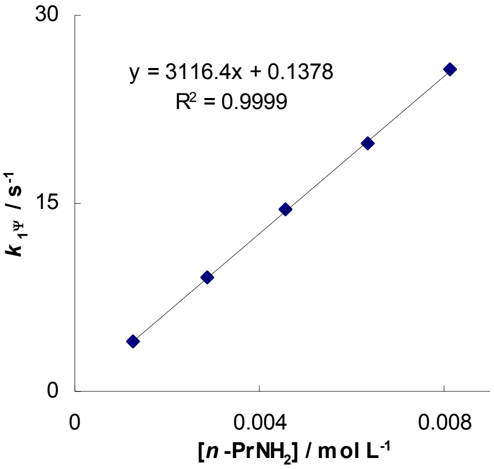

$(mor)_2CH^+$ + n-$PrNH_2$ in 91/9 (v/v) H_2O/CH_3CN (Stopped-flow, detection at 610 nm)

No.	T, °C	$[(mor)_2CH^+]_0$, mol L^{-1}	$[n\text{-}PrNH_2]_0$, mol L^{-1}	$k_{1\Psi,obs}$, s^{-1}
432.1	19.9	8.78×10^{-6}	1.87×10^{-3}	3.55×10^{1}
432.2	20.0	8.78×10^{-6}	3.74×10^{-3}	7.50×10^{1}
432.3	20.1	8.78×10^{-6}	5.61×10^{-3}	1.10×10^{2}
432.4	20.1	8.78×10^{-6}	7.48×10^{-3}	1.45×10^{2}
432.5	20.0	8.78×10^{-6}	9.35×10^{-3}	1.94×10^{2}

No.	$[OH^-]$, mol L^{-1}	$[n\text{-}PrNH_2]_{eff}$, mol L^{-1}	$k_{2,OH^-}[OH^-]$,[a] s^{-1}	$k_{2,n\text{-}PrNH_2}[n\text{-}PrNH_2]_{eff}$, s^{-1}
432.1	7.56×10^{-4}	1.11×10^{-3}	7.78×10^{-1}	3.47×10^{1}
432.2	1.15×10^{-3}	2.59×10^{-3}	1.19	7.38×10^{1}
432.3	1.46×10^{-3}	4.15×10^{-3}	1.50	1.09×10^{2}
432.4	1.72×10^{-3}	5.76×10^{-3}	1.77	1.44×10^{2}
432.5	1.95×10^{-3}	7.40×10^{-3}	2.01	1.92×10^{2}

[a] k_{2,OH^-} was calculated from E = -5.53 for $(mor)_2CH^+$ and N, s = 10.47, 0.61 for OH^-.

$k_2 = 2.44 \times 10^4$ L $mol^{-1}s^{-1}$

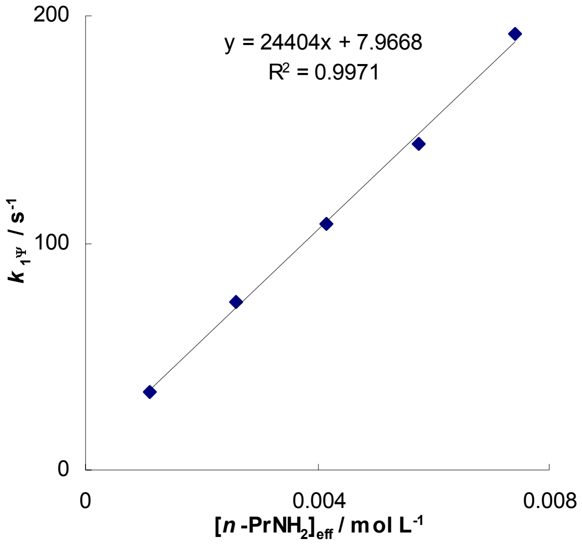

$(mfa)_2CH^+$ + n-$PrNH_2$ in 91/9 (v/v) H_2O/CH_3CN (Stopped-flow, detection at 585 nm)

No.	T, °C	$[(mfa)_2CH^+]_0$, mol L^{-1}	$[n\text{-}PrNH_2]_0$, mol L^{-1}	$k_{1\Psi,obs}$, s^{-1}
436.1	20.0	8.78×10^{-6}	3.69×10^{-4}	5.41×10^{1}
436.2	20.0	8.78×10^{-6}	4.21×10^{-4}	5.65×10^{1}
436.3	20.0	8.78×10^{-6}	5.26×10^{-4}	6.83×10^{1}
436.4	20.0	8.78×10^{-6}	5.53×10^{-4}	7.26×10^{1}
436.5	20.0	8.78×10^{-6}	9.22×10^{-4}	1.18×10^{2}
436.6	20.0	8.78×10^{-6}	1.11×10^{-3}	1.38×10^{2}

No.	$[OH^-]$, mol L^{-1}	$[n\text{-}PrNH_2]_{eff}$, mol L^{-1}	$k_{2,OH^-}[OH^-]$,[a] s^{-1}	$k_{2,n\text{-}PrNH_2}[n\text{-}PrNH_2]_{eff}$, s^{-1}
436.1	2.49×10^{-4}	1.20×10^{-4}	2.71	5.14×10^{1}
436.2	2.74×10^{-4}	1.47×10^{-4}	2.99	5.35×10^{1}
436.3	3.23×10^{-4}	2.03×10^{-4}	3.52	6.48×10^{1}
436.4	3.35×10^{-4}	2.19×10^{-4}	3.65	6.89×10^{1}
436.5	4.78×10^{-4}	4.45×10^{-4}	5.21	1.13×10^{2}
436.6	5.39×10^{-4}	5.67×10^{-4}	5.88	1.32×10^{2}

[a] k_{2,OH^-} was calculated from E = -3.85 for $(mor)_2CH^+$ and N, s = 10.47, 0.61 for OH^-.

$k_2 = 1.87 \times 10^5$ L $mol^{-1}s^{-1}$

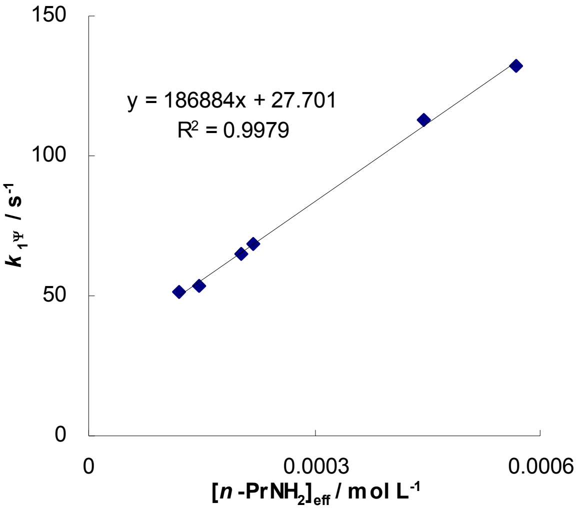

Glycine ethyl ester ($H_2NCH_2CO_2Et$) in DMSO

Glycine ethyl ester[8] (221 mg, 2.15×10^{-3} mol) was diluted to 10 mL with DMSO (c = 2.15×10^{-1} mol L^{-1}). 47 µL of the solution were diluted to 10 mL (c = 1.01×10^{-3} mol L^{-1}). $(jul)_2CH^+BF_4^-$ (22.3 mg, 5.02×10^{-5} mol) was dissolved in 25 mL of DMSO (c = 2.01×10^{-3} mol L^{-1}). 249 µL of this solution was diluted to 10 mL with DMSO (c = 5.00×10^{-5} mol L^{-1}). In the stopped-flow instrument equal volumes of electrophile and nucleophile solutions were mixed to give the final concentrations listed in the tables. The reactions were followed at 640 nm. A plot of $k_{1\Psi}$ versus concentration of glycine ethyl ester yields a straight line, the slope of which corresponds to the second order rate constant. (Run 88.1)

$(lil)_2CH^+$ + glycine ethyl ester in DMSO (Conventional UV-vis spectrophotometer, detection at 640 nm)

No.	T, °C	$[(lil)_2CH^+]_0$, mol L^{-1}	[glycine ethyl ester]$_0$, mol L^{-1}	$k_{1\Psi}$, s^{-1}
75.1	19.9	1.97×10^{-6}	1.57×10^{-4}	1.21×10^{-1}
75.2	20.0	1.97×10^{-6}	1.15×10^{-4}	8.21×10^{-2}
75.3	20.0	2.47×10^{-6}	9.82×10^{-5}	7.15×10^{-2}
75.4	20.0	2.47×10^{-6}	4.93×10^{-5}	3.65×10^{-2}

$k_2 = 7.78 \times 10^2$ L $mol^{-1}s^{-1}$

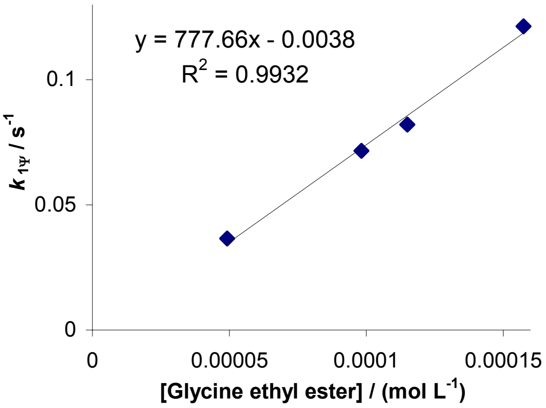

$(jul)_2CH^+$ + glycine ethyl ester in DMSO (Stopped-flow, detection at 640 nm)

No.	T, °C	$[(jul)_2CH^+]_0$, mol L^{-1}	[glycine ethyl ester]$_0$, mol L^{-1}	$k_{1\Psi}$, s^{-1}
88.1	20.0	2.50×10^{-5}	5.04×10^{-4}	1.02
88.2	20.0	2.50×10^{-5}	9.97×10^{-4}	2.03
88.3	20.0	2.50×10^{-5}	1.50×10^{-3}	3.07
88.4	20.0	2.50×10^{-5}	1.99×10^{-3}	4.08

$k_2 = 2.05 \times 10^3$ L mol^{-1}s^{-1}

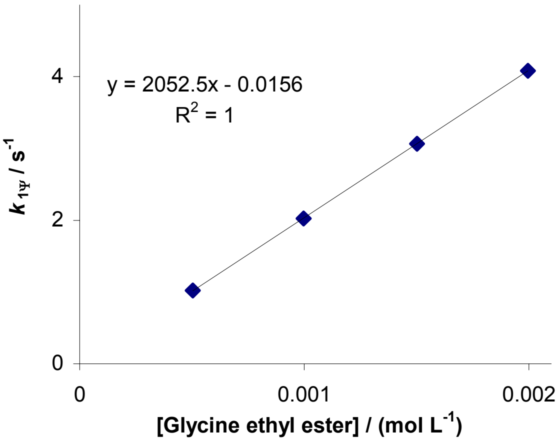

$(ind)_2CH^+$ + glycine ethyl ester in DMSO (Stopped-flow, detection at 630 nm)

No.	T, °C	$[(ind)_2CH^+]_0$, mol L^{-1}	[glycine ethyl ester]$_0$, mol L^{-1}	$k_{1\Psi}$, s^{-1}
89.1	20.0	2.50×10^{-5}	5.05×10^{-4}	1.89
89.2	20.0	2.50×10^{-5}	9.98×10^{-4}	3.84
89.3	19.9	2.50×10^{-5}	1.50×10^{-3}	5.88
89.4	20.0	2.50×10^{-5}	2.00×10^{-3}	7.83

$k_2 = 3.99 \times 10^3$ L mol^{-1}s^{-1}

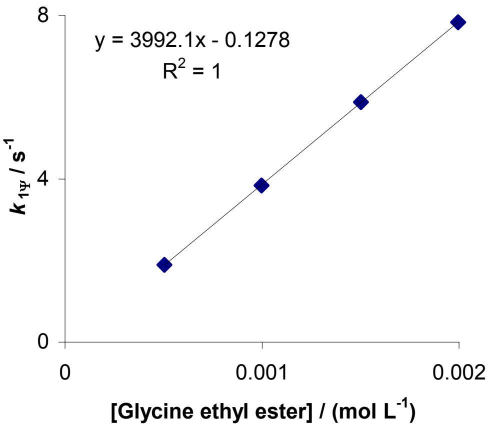

$(thq)_2CH^+$ + glycine ethyl ester in DMSO (Stopped-flow, detection at 630 nm)

No.	*T*, °C	$[(thq)_2CH^+]_0$, mol L^{-1}	[glycine ethyl ester]$_0$, mol L^{-1}	$k_{1\Psi}$, s^{-1}
92.1	20.0	2.50×10^{-5}	4.97×10^{-4}	6.37
92.2	20.0	2.50×10^{-5}	9.94×10^{-4}	12.9
92.3	19.9	2.50×10^{-5}	1.50×10^{-3}	19.9
92.4	20.0	2.50×10^{-5}	2.00×10^{-3}	26.3

$k_2 = 1.33 \times 10^4$ L mol^{-1}s^{-1}

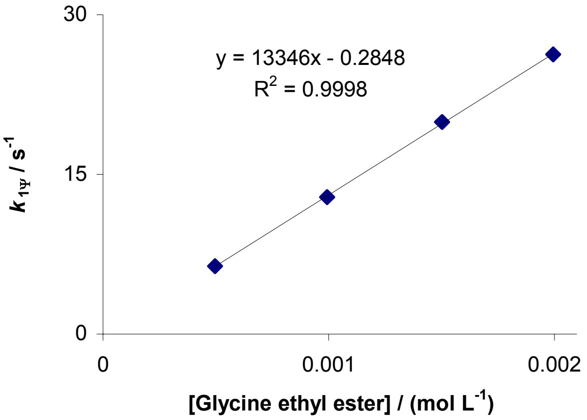

$(dma)_2CH^+$ + glycine ethyl ester in DMSO (Stopped-flow, detection at 630 nm)

No.	*T*, °C	$[(dma)_2CH^+]_0$, mol L^{-1}	[glycine ethyl ester]$_0$, mol L^{-1}	$k_{1\Psi}$, s^{-1}
225.1	20.0	1.01×10^{-5}	5.51×10^{-4}	4.65×10^{1}
225.2	20.0	1.01×10^{-5}	1.10×10^{-3}	9.67×10^{1}
225.3	20.0	1.01×10^{-5}	1.65×10^{-3}	1.40×10^{2}
225.4	20.0	1.01×10^{-5}	2.21×10^{-3}	1.87×10^{2}

$k_2 = 8.43 \times 10^4$ L mol^{-1}s^{-1}

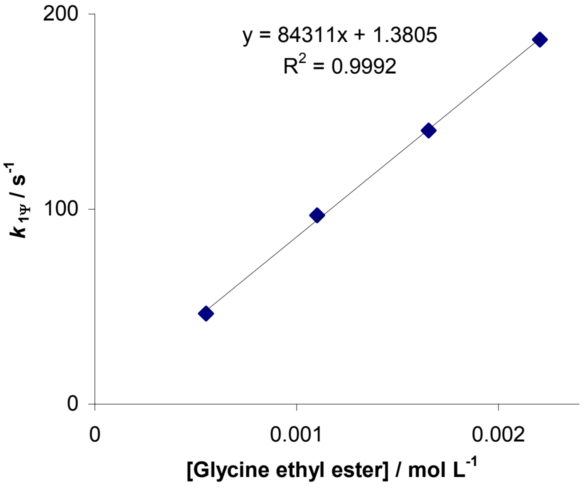

HOO^- in water

$(lil)_2CH^+BF_4^-$ (12.3 mg, 2.95 × 10^{-5} mol) was dissolved in 10 ml of CH_3CN (c = 2.95 × 10^{-3} mol L^{-1}). 40 µL of this solution and 120 µL of CH_3CN were dissolved in 20 mL of water (c = 5.91 × 10^{-6} mol L^{-1}, CH_3CN 0.8 volume %). 10 µL of aq. H_2O_2 (2.45 × 10^{-1} mol L^{-1}) and 400 µL of aq. KOH (5.07 × 10^{-1} mol L^{-1}) were dissolved in 10 mL of water (c = 2.45 × 10^{-4} mol L^{-1}). In the stopped-flow instrument equal volumes of the electrophile and nucleophile solutions were mixed to give the concentrations listed in the table. The course of the reactions was followed at 630 nm. The concentration of HOO^- was calculated from pK_a of H_2O_2 (11.8).[9] A plot of $k_{2,HOO}$-$[HOO^-]_{eff}$ versus concentration of $[HOO^-]_{eff}$ yields a straight line, the slope of which corresponds to the second order rate constant. (Run 226.1)

$(lil)_2CH^+$ + HOO^- in 99.6/0.4 (v/v) H_2O/CH_3CN (Stopped-flow, detection at 630 nm)

No.	T, °C	$[(lil)_2CH^+]_0$, mol L^{-1}	$[H_2O_2]_0$, mol L^{-1}	$k_{1\Psi,obs}$, s^{-1}
226.1	20.0	2.95 × 10^{-6}	1.23 × 10^{-4}	9.40 × 10^{-2}
226.2	20.0	2.95 × 10^{-6}	2.45 × 10^{-4}	1.60 × 10^{-1}
226.3	20.0	2.95 × 10^{-6}	3.68 × 10^{-4}	2.41 × 10^{-1}
226.4	20.0	2.95 × 10^{-6}	4.90 × 10^{-4}	3.03 × 10^{-1}
226.5	20.0	2.95 × 10^{-6}	6.13 × 10^{-4}	3.79 × 10^{-1}

No.	$[OH^-]$, mol L^{-1}	$[HOO^-]_{eff}$, mol L^{-1}	$k_{2,OH}$-$[OH^-]$, s^{-1}	$k_{2,HOO}$-$[HOO^-]_{eff}$, s^{-1}
226.1	1.02 × 10^{-2}	7.56 × 10^{-5}	2.19 × 10^{-2}	7.21 × 10^{-2}
226.2	1.02 × 10^{-2}	1.51 × 10^{-4}	2.19 × 10^{-2}	1.39 × 10^{-1}
226.3	1.02 × 10^{-2}	2.27 × 10^{-4}	2.19 × 10^{-2}	2.20 × 10^{-1}
226.4	1.02 × 10^{-2}	3.02 × 10^{-4}	2.19 × 10^{-2}	2.81 × 10^{-1}
226.5	1.02 × 10^{-2}	3.79 × 10^{-4}	2.19 × 10^{-2}	3.57 × 10^{-1}

k_2 = 9.43 × 10^2 L $mol^{-1}s^{-1}$

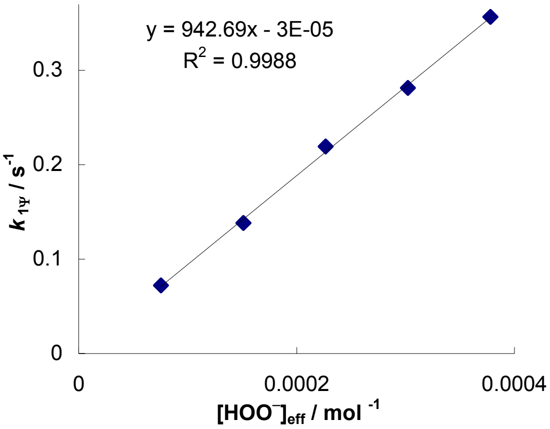

$(ind)_2CH^+$ + HOO^- in 99.6/0.4 (v/v) H_2O/CH_3CN (Stopped-flow, detection at 615 nm)

No.	T, °C	$[(ind)_2CH^+]_0$, mol L^{-1}	$[H_2O_2]_0$, mol L^{-1}	$k_{1\Psi,obs}$, s^{-1}
228.1	20.0	1.07×10^{-5}	2.07×10^{-4}	6.65×10^{-1}
228.2	20.0	1.07×10^{-5}	3.11×10^{-4}	9.50×10^{-1}
228.3	20.0	1.07×10^{-5}	4.14×10^{-4}	1.21
228.4	20.0	1.07×10^{-5}	5.18×10^{-4}	1.48

No.	$[OH^-]$, mol L^{-1}	$[HOO^-]_{eff}$, mol L^{-1}	$k_{2,OH}$-$[OH^-]$, s^{-1}	$k_{2,HOO}$-$[HOO^-]_{eff}$, s^{-1}
228.1	1.02×10^{-2}	1.28×10^{-4}	1.10×10^{-1}	5.55×10^{-1}
228.2	1.02×10^{-2}	1.92×10^{-4}	1.10×10^{-1}	8.41×10^{-1}
228.3	1.02×10^{-2}	2.56×10^{-4}	1.10×10^{-1}	1.10
228.4	1.02×10^{-2}	3.19×10^{-4}	1.10×10^{-1}	1.37

$k_2 = 4.22 \times 10^3$ L $mol^{-1}s^{-1}$

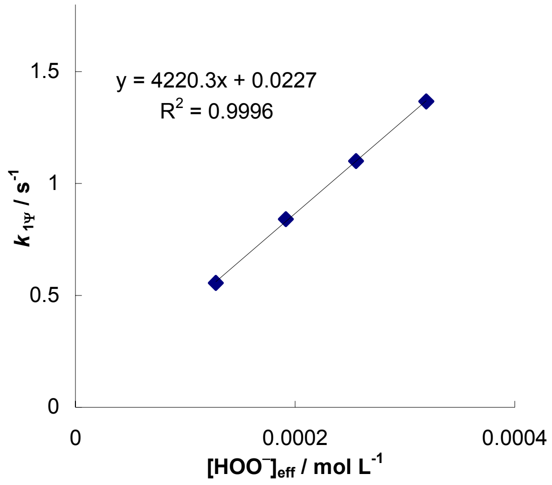

$(dma)_2CH^+$ + HOO^- in 99.6/0.4 (v/v) H_2O/CH_3CN (Stopped-flow, detection at 605 nm) stabilized by toluenesulfonic acid (6.26 × 10^{-6} mol L^{-1})

No.	T, °C	$[(dma)_2CH^+]_0$, mol L^{-1}	$[H_2O_2]_0$, mol L^{-1}	$k_{1\Psi,obs}$, s^{-1}
230.1	20.0	2.00×10^{-5}	9.45×10^{-5}	3.93
230.2	20.0	2.00×10^{-5}	1.97×10^{-4}	6.79
230.3	20.0	2.00×10^{-5}	3.03×10^{-4}	9.29
230.4	20.0	2.00×10^{-5}	4.02×10^{-4}	1.21×10^{1}

No.	$[OH^-]$, mol L^{-1}	$[HOO^-]_{eff}$, mol L^{-1}	$k_{2,OH}$-$[OH^-]$, s^{-1}	$k_{2,HOO}$-$[HOO^-]_{eff}$, s^{-1}
230.1	1.02×10^{-2}	6.07×10^{-5}	1.33	2.60
230.2	1.02×10^{-2}	1.21×10^{-4}	1.33	5.46
230.3	1.02×10^{-2}	1.87×10^{-4}	1.33	7.97
230.4	1.02×10^{-2}	2.48×10^{-4}	1.33	1.08×10^{1}

$k_2 = 4.31 \times 10^4$ L $mol^{-1}s^{-1}$

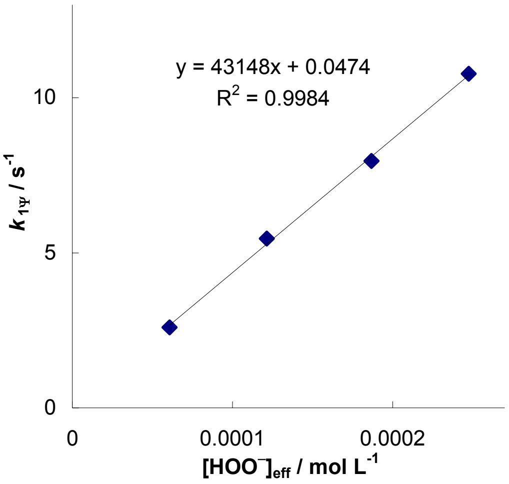

n-PrNH$_2$ in DMSO

(lil)$_2$CH$^+$ + n-PrNH$_2$ in DMSO (Stopped-flow, detection at 640 nm)

No.	T, °C	[(lil)$_2$CH$^+$]$_0$, mol L^{-1}	[n-PrNH$_2$]$_0$, mol L^{-1}	$k_{1\Psi}$, s^{-1}
RL1.1	20.0	1.12×10^{-5}	2.17×10^{-4}	8.08×10^{-1}
RL1.2	20.0	1.12×10^{-5}	4.34×10^{-4}	1.65
RL1.3	20.0	1.12×10^{-5}	6.50×10^{-4}	2.48
RL1.4	20.0	1.12×10^{-5}	8.67×10^{-4}	3.37

$k_2 = 3.93 \times 10^3$ L mol^{-1}s^{-1}

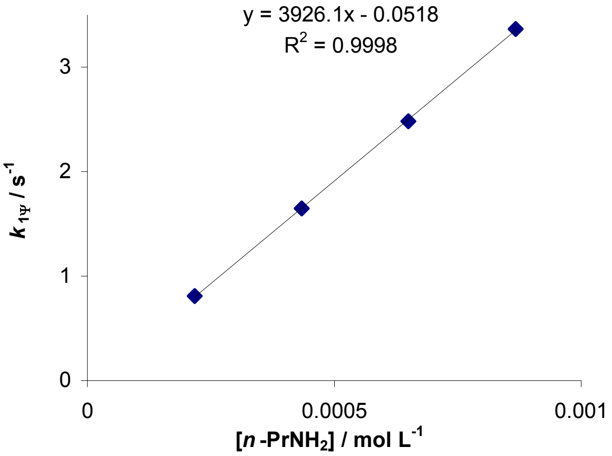

(jul)$_2$CH$^+$ + n-PrNH$_2$ in DMSO (Stopped-flow, detection at 640 nm)

No.	T, °C	[(jul)$_2$CH$^+$]$_0$, mol L^{-1}	[n-PrNH$_2$]$_0$, mol L^{-1}	$k_{1\Psi}$, s^{-1}
RL2.1	20.0	1.00×10^{-5}	2.14×10^{-4}	2.10×10^{1}
RL2.2	20.0	1.00×10^{-5}	4.28×10^{-4}	4.41×10^{1}
RL2.3	20.0	1.00×10^{-5}	6.43×10^{-4}	6.83×10^{1}
RL2.4	20.0	1.00×10^{-5}	8.57×10^{-4}	9.29×10^{1}

$k_2 = 1.12 \times 10^4$ L mol^{-1}s^{-1}

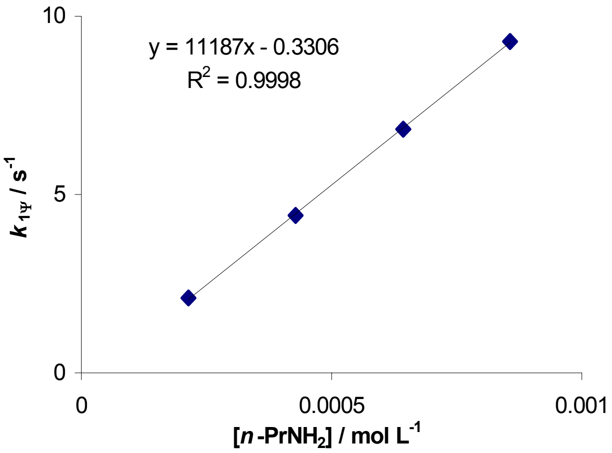

$(ind)_2CH^+$ + n-PrNH$_2$ in DMSO (Stopped-flow, detection at 625 nm)

No.	T, °C	$[(ind)_2CH^+]_o$, mol L^{-1}	$[n\text{-PrNH}_2]_o$, mol L^{-1}	$k_{1\Psi}$, s^{-1}
RL3.1	20.0	1.00×10^{-5}	2.17×10^{-4}	4.31
RL3.2	20.0	1.00×10^{-5}	4.34×10^{-4}	8.76
RL3.3	20.0	1.00×10^{-5}	6.50×10^{-4}	1.31×10^{1}
RL3.4	20.0	1.00×10^{-5}	8.67×10^{-4}	1.78×10^{1}

$k_2 = 2.06 \times 10^4$ L mol^{-1}s^{-1}

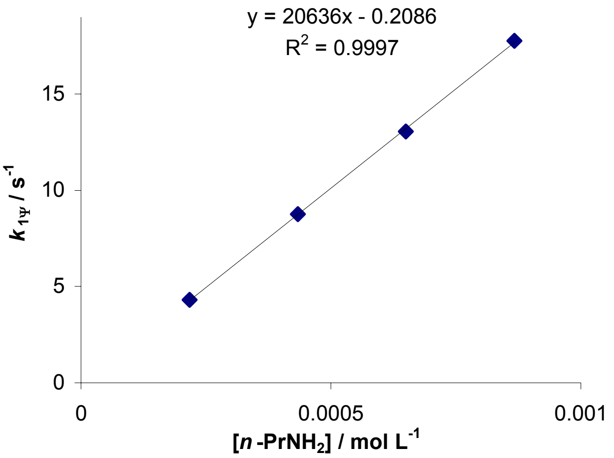

$(thq)_2CH^+$ + n-PrNH$_2$ in DMSO (Stopped-flow, detection at 630 nm)

No.	T, °C	$[(thq)_2CH^+]_o$, mol L^{-1}	$[n\text{-PrNH}_2]_o$, mol L^{-1}	$k_{1\Psi}$, s^{-1}
RL4.1	20.0	1.12×10^{-5}	2.14×10^{-4}	1.29×10^{1}
RL4.2	20.0	1.12×10^{-5}	4.28×10^{-4}	2.70×10^{1}
RL4.3	20.0	1.12×10^{-5}	6.43×10^{-4}	4.14×10^{1}
RL4.4	20.0	1.12×10^{-5}	8.57×10^{-4}	5.53×10^{1}

$k_2 = 6.61 \times 10^4$ L mol^{-1}s^{-1}

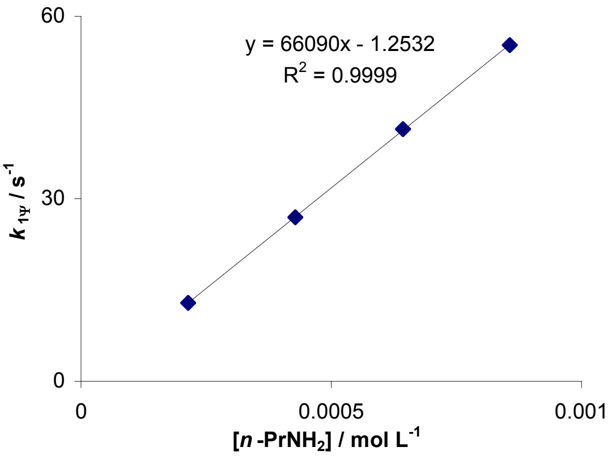

SO_3^{2-} (Na_2SO_3) in water

$(lil)_2CH^+BF_4^-$ (13.8 mg, 3.32 × 10^{-5} mol) was dissolved in 10 ml of TFE (c = 3.32 × 10^{-3} mol L^{-1}). 160 µL of the solution was dissolved in 20 mL of water (c = 2.65 × 10^{-5} mol L^{-1}). Na_2SO_3 (236 mg, 1.87 × 10^{-3} mol) was dissolved in 10 mL of water (c = 1.87 × 10^{-1} mol L^{-1}). 20 µL of the solution and 10 µL of aqueous hydroquinone solution (c = 2.38 × 10^{-2} mol L^{-1}) were dissolved in 10 mL of water (SO_3^{2-}: c = 3.74 × 10^{-4} mol L^{-1}, hydroquinone: c = 2.38 × 10^{-5} mol L^{-1}). In the stopped-flow instrument equal volumes of the electrophile and nucleophile solutions were mixed to give the final concentrations listed in the table. The reactions were followed photometrically at λ = 630 nm. A plot of $k_{1\Psi}$ versus the concentration of sulfite ion yields a straight line, the slope of which corresponds to the second order rate constant. (Run 167.1)

$(lil)_2CH^+$+ SO_3^{2-} in 99.6/0.4 (v/v) H_2O/TFE (Stopped-flow, detection at 630 nm)

No.	T, °C	$[(lil)_2CH^+]_0$, mol L^{-1}	$[SO_3^{2-}]_0$, mol L^{-1}	[Hydroquinone] mol L^{-1}	$k_{1\Psi}$, s^{-1}
167.1	20.1	1.33 × 10^{-5}	1.87 × 10^{-4}	1.19 × 10^{-5}	1.54
167.2	20.1	1.33 × 10^{-5}	3.74 × 10^{-4}	1.19 × 10^{-5}	2.95
167.3	20.1	1.33 × 10^{-5}	5.61 × 10^{-4}	1.19 × 10^{-5}	4.56
167.4	20.1	1.33 × 10^{-5}	7.48 × 10^{-4}	1.19 × 10^{-5}	5.81

k_2 = 7.72 × 10^3 L $mol^{-1}s^{-1}$

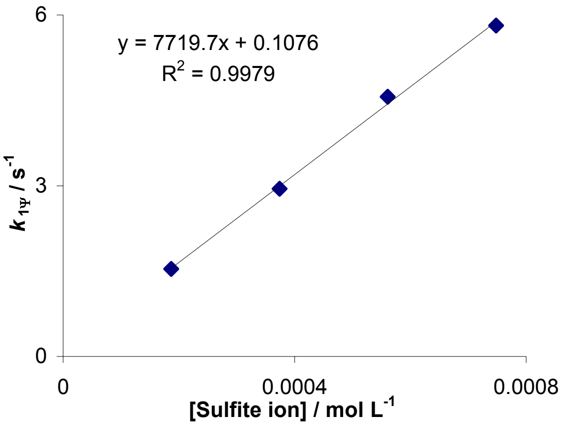

$(lil)_2CH^+$+ SO_3^{2-} in 99.6/0.4 (v/v) H_2O/CH_3CN (Stopped-flow, detection at 630 nm)

No.	T, °C	$[(lil)_2CH^+]_0$, mol L^{-1}	$[SO_3^{2-}]_0$, mol L^{-1}	[Hydroquinone] mol L^{-1}	$k_{1\Psi}$, s^{-1}
218.1	20.0	7.09×10^{-6}	1.88×10^{-4}	1.14×10^{-5}	1.63
218.2	20.1	7.09×10^{-6}	2.82×10^{-4}	1.14×10^{-5}	2.37
218.3	20.1	7.09×10^{-6}	3.77×10^{-4}	1.14×10^{-5}	3.15
218.4	20.0	7.09×10^{-6}	4.71×10^{-4}	1.14×10^{-5}	3.87
218.5	20.0	7.09×10^{-6}	9.41×10^{-4}	1.14×10^{-5}	7.30

$k_2 = 7.50 \times 10^3$ L $mol^{-1}s^{-1}$

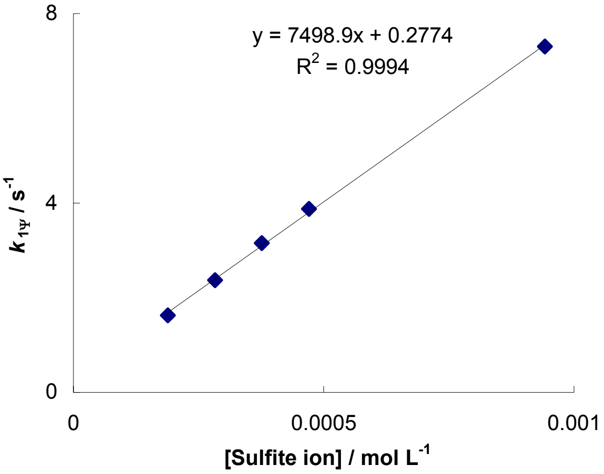

$(jul)_2CH^+$+ SO_3^{2-} in 99.6/0.4 (v/v) H_2O/TFE (Stopped-flow, detection at 630 nm)

No.	T, °C	$[(jul)_2CH^+]_0$, mol L^{-1}	$[SO_3^{2-}]_0$, mol L^{-1}	[Hydroquinone] mol L^{-1}	$k_{1\Psi}$, s^{-1}
174.1	20.1	8.37×10^{-6}	1.10×10^{-4}	1.01×10^{-5}	1.18
174.2	20.2	8.37×10^{-6}	2.21×10^{-4}	1.01×10^{-5}	2.28
174.3	20.1	8.37×10^{-6}	3.31×10^{-4}	1.01×10^{-5}	3.80
174.4	20.1	8.37×10^{-6}	4.41×10^{-4}	1.01×10^{-5}	5.14
174.4	20.1	8.37×10^{-6}	5.52×10^{-4}	1.01×10^{-5}	6.38

$k_2 = 1.20 \times 10^4$ L $mol^{-1}s^{-1}$

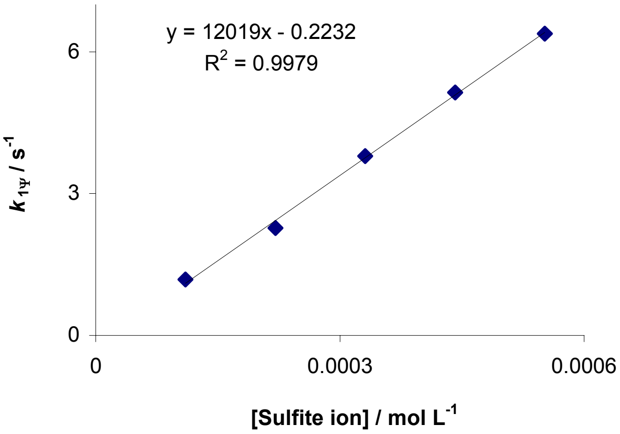

$(ind)_2CH^+ + SO_3^{2-}$ in 99.6/0.4 (v/v) H_2O/TFE (Stopped-flow, detection at 615 nm)

No.	T, °C	$[(ind)_2CH^+]_0$, mol L^{-1}	$[SO_3^{2-}]_0$, mol L^{-1}	[Hydroquinone] mol L^{-1}	$k_{1\Psi}$, s^{-1}
168.1	20.1	7.83×10^{-6}	2.34×10^{-4}	1.19×10^{-5}	9.17
168.2	20.1	7.83×10^{-6}	4.67×10^{-4}	1.19×10^{-5}	1.87×10^{1}
168.3	20.1	7.83×10^{-6}	7.01×10^{-4}	1.19×10^{-5}	2.73×10^{1}
168.4	20.1	7.83×10^{-6}	9.35×10^{-4}	1.19×10^{-5}	3.62×10^{1}

$k_2 = 3.83 \times 10^4$ L $mol^{-1}s^{-1}$

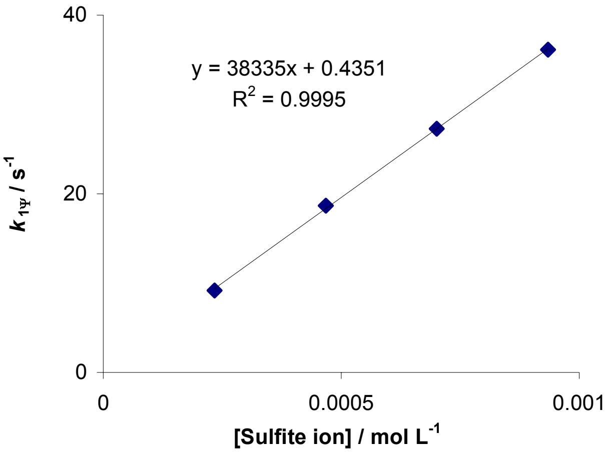

$(thq)_2CH^+ + SO_3^{2-}$ in H_2O–TFE 99.6/0.4 (v/v) H_2O/TFE (Stopped-flow, detection at 620 nm)

No.	T, °C	$[(thq)_2CH^+]_0$, mol L^{-1}	$[SO_3^{2-}]_0$, mol L^{-1}	[Hydroquinone] mol L^{-1}	$k_{1\Psi}$, s^{-1}
166.1	20.1	6.45×10^{-6}	2.34×10^{-4}	1.19×10^{-5}	5.87
166.2	20.2	6.45×10^{-6}	4.67×10^{-4}	1.19×10^{-5}	1.21×10^{1}
166.3	20.1	6.45×10^{-6}	7.01×10^{-4}	1.19×10^{-5}	1.87×10^{1}
166.4	20.2	6.45×10^{-6}	9.35×10^{-4}	1.19×10^{-5}	2.57×10^{1}

$k_2 = 7.06 \times 10^4$ L $mol^{-1}s^{-1}$

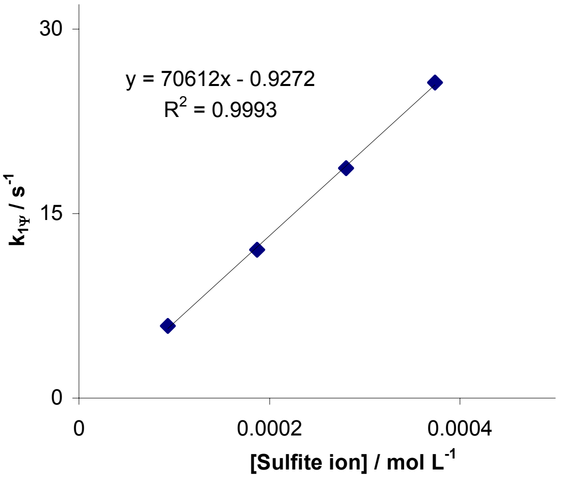

$(pyr)_2CH^+ + SO_3^{2-}$ in 99.6/0.4 (v/v) H_2O/TFE (Stopped-flow, detection at 610 nm)

No.	T, °C	$[(pyr)_2CH^+]_0$, mol L^{-1}	$[SO_3^{2-}]_0$, mol L^{-1}	[Hydroquinone] mol L^{-1}	$k_{1\Psi}$, s^{-1}
171.1	20.0	1.59×10^{-6}	2.07×10^{-5}	1.10×10^{-5}	2.46
171.2	20.1	1.59×10^{-6}	4.15×10^{-5}	1.10×10^{-5}	5.90
171.3	20.0	1.59×10^{-6}	6.22×10^{-5}	1.10×10^{-5}	8.39
171.4	20.0	1.59×10^{-6}	8.30×10^{-5}	1.10×10^{-5}	1.20×10^{1}

$k_2 = 1.50 \times 10^5$ L $mol^{-1}s^{-1}$

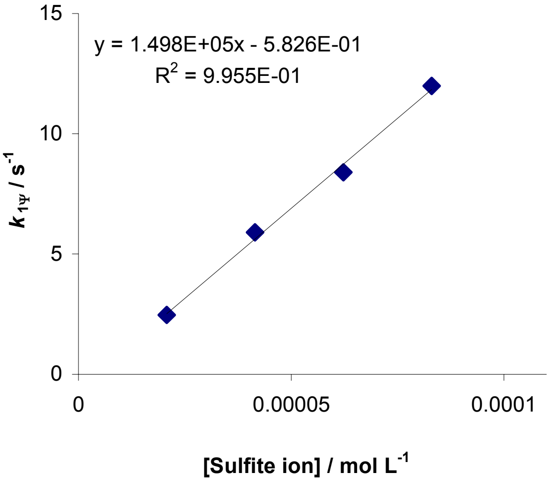

Morpholine in DMSO

Morpholine (167 mg, 1.92 × 10^{-3} mol) was diluted to 50 mL with DMSO (c = 3.84 × 10^{-2} mol L^{-1}). 52 μL of the solution were diluted to 10 mL (c = 2.00 × 10^{-4} mol L^{-1} respectively). $(thq)_2CH^+BF_4^-$ (26.9 mg, 6.86 × 10^{-5} mol) was dissolved in 10 mL of DMSO (c = 6.86 × 10^{-3} mol L^{-1}). 73 μL of the solution was diluted to 50 mL with DMSO (c = 1.00 × 10^{-5} mol L^{-1}). In the stopped-flow instrument equal volumes of the electrophile and nucleophile solutions were mixed to give the concentrations listed in the tables. The course of the reactions was followed at 630 nm. A plot of $k_{1\Psi}$ versus concentration of morpholine yields a straight line, the slope of which corresponds to the second order rate constant. (Run 96.1)

$(lil)_2CH^+$ + morpholine in DMSO (Stopped-flow, detection at 640 nm)

No.	T, °C	$[(lil)_2CH^+]_0$, mol L^{-1}	$[morpholine]_0$, mol L^{-1}	$k_{1\Psi}$, s^{-1}
63.1	20.0	2.49 × 10^{-5}	5.05 × 10^{-4}	2.26 × 10^{1}
63.2	20.0	2.49 × 10^{-5}	9.95 × 10^{-4}	4.52 × 10^{1}
63.3	20.0	2.49 × 10^{-5}	1.50 × 10^{-3}	6.91 × 10^{1}
63.4	19.9	2.49 × 10^{-5}	2.00 × 10^{-3}	9.16 × 10^{1}

k_2 = 4.62 × 10^{4} L $mol^{-1}s^{-1}$

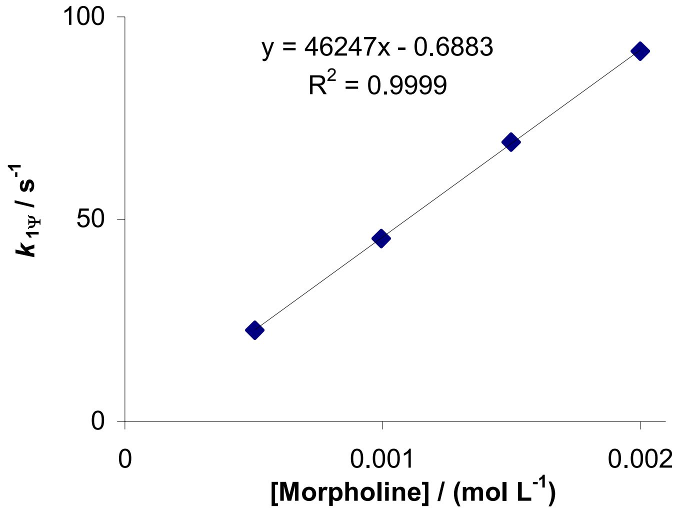

$(jul)_2CH^+$ + morpholine in DMSO (Stopped-flow, detection at 640 nm)

No.	T, °C	$[(jul)_2CH^+]_0$, mol L^{-1}	$[morpholine]_0$, mol L^{-1}	$k_{1\Psi}$, s^{-1}
93.1	20.0	2.50×10^{-5}	4.91×10^{-4}	5.87×10^{1}
93.2	*20.0*	2.50×10^{-5}	9.81×10^{-4}	9.36×10^{1} a)
93.3	20.0	2.50×10^{-5}	1.47×10^{-3}	1.70×10^{2}
93.4	20.0	2.50×10^{-5}	1.96×10^{-3}	2.31×10^{2}

a) This value was not used for the calculation of k_2.

$k_2 = 1.17 \times 10^5$ L mol^{-1}s^{-1}

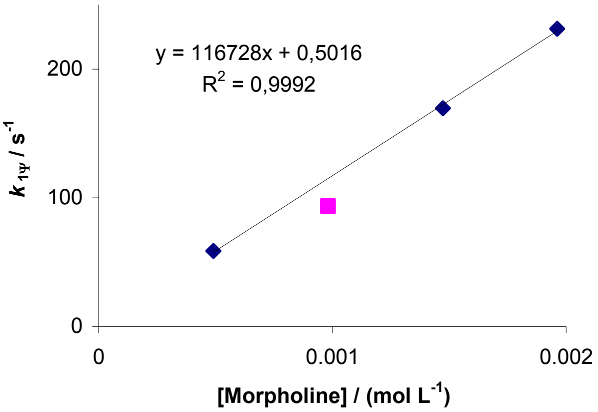

$(ind)_2CH^+$ + morpholine in DMSO (Stopped-flow, detection at 630 nm)

No.	T, °C	$[(ind)_2CH^+]_0$, mol L^{-1}	$[morpholine]_0$, mol L^{-1}	$k_{1\Psi}$, s^{-1}
64.1	20.0	2.48×10^{-5}	4.98×10^{-4}	6.98×10^{1}
64.2	20.0	2.48×10^{-5}	9.95×10^{-4}	1.02×10^{2}
64.3	20.0	2.48×10^{-5}	1.51×10^{-3}	2.31×10^{2}
64.4	20.0	2.48×10^{-5}	2.01×10^{-3}	3.03×10^{2}

$k_2 = 3.23 \times 10^5$ L mol^{-1}s^{-1}

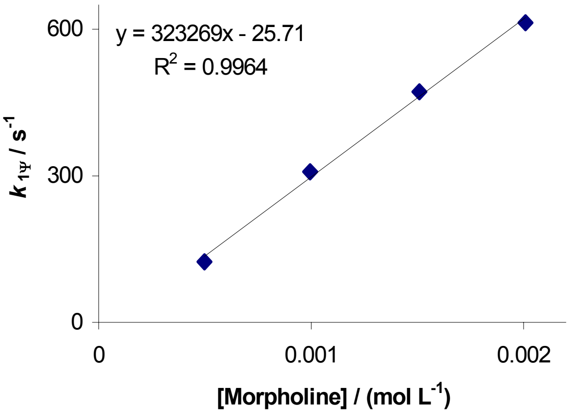

$(thq)_2CH^+$ + morpholine in DMSO (Stopped-flow, detection at 630 nm)

No.	T, °C	$[(thq)_2CH^+]_0$, mol L^{-1}	$[morpholine]_0$, mol L^{-1}	$k_{1\Psi}$, s^{-1}
96.1	20.0	5.01×10^{-6}	9.98×10^{-5}	6.98×10^{1}
96.2	20.0	5.01×10^{-6}	1.50×10^{-4}	1.02×10^{2}
96.3	20.0	5.01×10^{-6}	2.99×10^{-4}	2.31×10^{2}
96.4	20.0	5.01×10^{-6}	3.99×10^{-4}	3.03×10^{2}

$k_2 = 7.94 \times 10^5$ L $mol^{-1}s^{-1}$

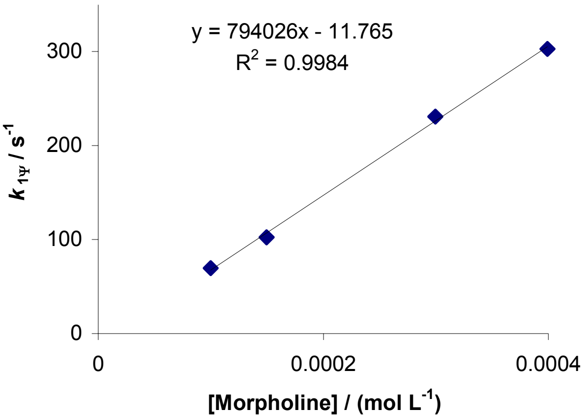

Piperidine in DMSO

Piperidine (212 mg, 2.48 × 10^{-3} mol) was diluted to 10 mL with DMSO (c = 0.248 mol L^{-1}). 40 µL of the solution were diluted with DMSO to 10 mL (c = 9.92 × 10^{-4}). $(lil)_2CH^+BF_4^-$ (24.7 mg, 5.93 × 10^{-5} mol) was dissolved in 10 mL of DMSO (c = 5.93 × 10^{-3} mol L^{-1}). 84 µL of the solution was diluted to 10 ml with DMSO to give a 4.98 × 10^{-5} mol L^{-1} solution. In the stopped-flow instrument the same volume of electrophile and nucleophile solution were mixed to give the final concentrations listed in the tables. The reactions were followed photometrically at λ = 640 nm. A plot of $k_{1\Psi}$ versus concentration of piperidine yields a straight line, the slope of which corresponds to the second order rate constant. (Run 62.1)

$(lil)_2CH^+$ + piperidine in DMSO (Stopped-flow, detection at 640 nm)

No.	T, °C	$[(lil)_2CH^+]_0$, mol L^{-1}	$[piperidine]_0$, mol L^{-1}	$k_{1\Psi}$, s^{-1}
62.1	20.0	2.49 × 10^{-5}	4.96 × 10^{-4}	5.62 × 10^{1}
62.2	20.0	2.49 × 10^{-5}	9.95 × 10^{-4}	1.13 × 10^{2}
62.3	20.0	2.49 × 10^{-5}	1.51 × 10^{-3}	1.74 × 10^{2}
62.4	20.0	2.49 × 10^{-5}	2.00 × 10^{-3}	2.24 × 10^{2}

$k_2 = 1.13 \times 10^5$ L $mol^{-1}s^{-1}$

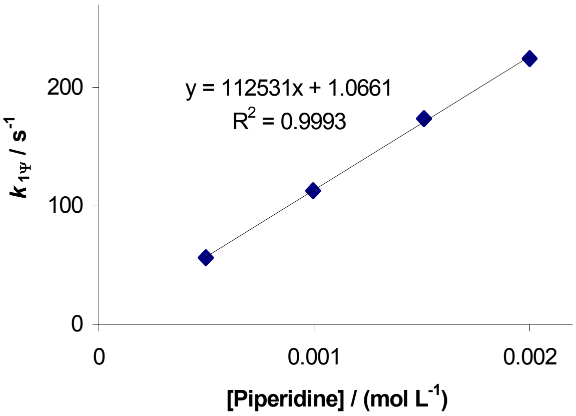

$(jul)_2CH^+$ + piperidine in DMSO (Stopped-flow, detection at 640 nm)

No.	T, °C	$[(jul)_2CH^+]_0$, mol L^{-1}	$[piperidine]_0$, mol L^{-1}	$k_{1\Psi}$, s^{-1}
65.1	20.0	2.49×10^{-5}	5.00×10^{-4}	1.53×10^{2}
65.2	20.0	2.49×10^{-5}	1.01×10^{-3}	3.25×10^{2}
65.3	20.0	2.49×10^{-5}	1.51×10^{-3}	4.70×10^{2}
65.4	19.9	2.49×10^{-5}	2.00×10^{-3}	6.35×10^{2}

$k_2 = 3.19 \times 10^5$ L mol^{-1}s^{-1}

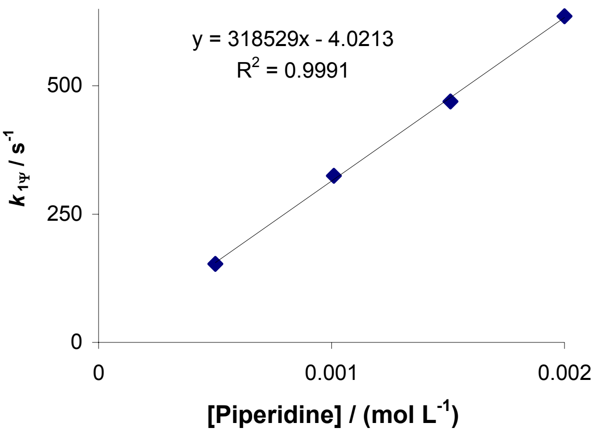

$(ind)_2CH^+$ + piperidine in DMSO (Stopped-flow, detection at 630 nm)

No.	T, °C	$[(ind)_2CH^+]_0$, mol L^{-1}	$[piperidine]_0$, mol L^{-1}	$k_{1\Psi}$, s^{-1}
60.1	20.0	2.51×10^{-5}	2.50×10^{-4}	1.49×10^{2}
60.2	20.0	2.51×10^{-5}	5.00×10^{-4}	3.21×10^{2}
60.3	20.0	2.51×10^{-5}	7.50×10^{-4}	4.98×10^{2}
60.4	20.0	2.51×10^{-5}	1.00×10^{-3}	7.02×10^{2}
60.5	20.1	2.50×10^{-5}	1.25×10^{-3}	8.24×10^{2}
60.6	20.1	2.50×10^{-5}	1.50×10^{-3}	9.73×10^{2}

$k_2 = 6.67 \times 10^5$ L mol^{-1}s^{-1}

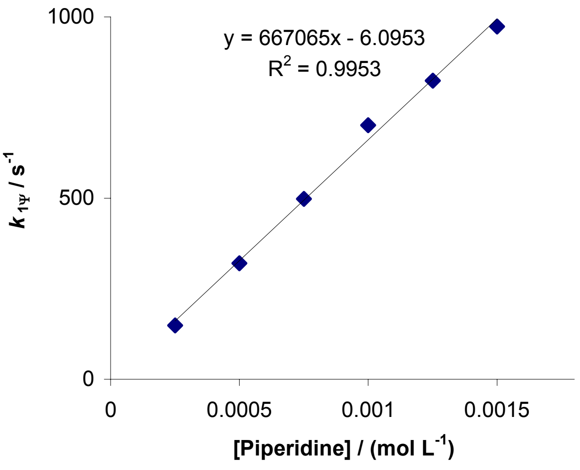

$(thq)_2CH^+$ + piperidine in DMSO (Stopped-flow, detection at 630 nm)

No.	T, °C	$[(thq)_2CH^+]_0$, mol L^{-1}	$[piperidine]_0$, mol L^{-1}	$k_{1\Psi}$, s^{-1}
91.1	20.0	4.99×10^{-6}	7.01×10^{-5}	1.45×10^{2}
91.2	20.0	4.99×10^{-6}	1.37×10^{-4}	2.99×10^{2}
91.3	19.9	4.99×10^{-6}	2.09×10^{-4}	4.98×10^{2}
91.4	20.0	4.99×10^{-6}	2.77×10^{-4}	6.58×10^{2}

$k_2 = 2.51 \times 10^6$ L $mol^{-1}s^{-1}$

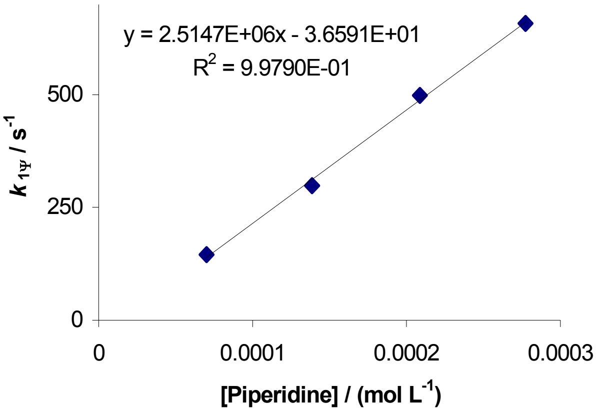

$^{-}SCH_2CO_2^{-}$ in water

$HSCH_2CO_2Na$ (114 mg, 1.00 × 10^{-3} mol) was dissolved in water (10 mL, c = 1.00 × 10^{-1} mol L^{-1}). 100 µL of the solution and 20, 40, 100, 140, 220, 320, 420, 520, or 620 µL of 0.5073 mol L^{-1} aqueous KOH were dissolved in water (Run 192.1–9). $(lil)_2CH^+BF_4^-$ (13.8 mg, 3.32 × 10^{-5} mol) was dissolved in 10 mL of water (c = 3.32 × 10^{-3} mol L^{-1}). 40 µL of the solution and 40 µL of TFE were diluted to 10 ml with water to give a 9.94 × 10^{-5} mol L^{-1} solution. In the stopped-flow instrument the same volume of electrophile and nucleophile solution were mixed to give the final concentrations listed in the tables. The observed rate constants were equal when the concentrations of OH^{-} were 3.54 × 10^{-3} – 1.06 × 10^{-2} mol L^{-1}. Under these conditions $HSCH_2CO_2^{-}$ is completely converted into $^{-}SCH_2CO_2^{-}$ by OH^{-}. In a second series of experiments the reactions were monitored in presence of constant concentration of $[OH^{-}]_0$ (5.57 × 10^{-3} mol L^{-1}) and variable $[HSCH_2CO_2^{-}]_o$ < 5.00 × 10^{-4} mol L^{-1} (Run 192.10–13). The reactions were followed photometrically at λ = 630 nm. A plot of $k_{1\Psi}$ versus concentration of $^{-}SCH_2CO_2^{-}$ yields a straight line, the slope of which corresponds to the second order rate constant. The almost-zero intercept indicates that the reaction $CF_3CH_2O^{-}$ is negligible under these conditions.

$(lil)_2CH^+$+ $^{-}SCH_2CO_2^{-}$ in 99.6/0.4 (v/v) H_2O/TFE (Stopped-flow, detection at 630 nm)

No.	T, °C	$[(lil)_2CH^+]_0$, mol L^{-1}	$[HSCH_2CO_2^{-}]_0$, mol L^{-1}	$[OH^{-}]_0$, mol L^{-1}	$k_{1\Psi}$, s^{-1}
192.1	20.0	4.97 × 10^{-6}	5.00 × 10^{-4}	5.00 × 10^{-4}	5.60 × 10^{1}
192.2	20.0	4.97 × 10^{-6}	5.00 × 10^{-4}	1.01 × 10^{-3}	9.06 × 10^{1}
192.3	20.0	4.97 × 10^{-6}	5.00 × 10^{-4}	2.53 × 10^{-3}	1.30 × 10^{2}
192.4	20.0	4.97 × 10^{-6}	5.00 × 10^{-4}	3.54 × 10^{-3}	1.45 × 10^{2}
192.5	20.0	4.97 × 10^{-6}	5.00 × 10^{-4}	5.57 × 10^{-3}	1.45 × 10^{2}
192.6	19.9	4.97 × 10^{-6}	5.00 × 10^{-4}	8.11 × 10^{-3}	1.46 × 10^{2}
192.7	19.9	4.97 × 10^{-6}	5.00 × 10^{-4}	1.06 × 10^{-2}	1.45 × 10^{2}
192.8	19.9	4.97 × 10^{-6}	5.00 × 10^{-4}	1.32 × 10^{-2}	1.38 × 10^{2}
192.9	20.0	4.97 × 10^{-6}	5.00 × 10^{-4}	1.57 × 10^{-2}	1.34 × 10^{2}
192.10	19.9	4.97 × 10^{-6}	1.00 × 10^{-4}	5.57 × 10^{-3}	2.81 × 10^{1}
192.11	20.0	4.97 × 10^{-6}	2.00 × 10^{-4}	5.57 × 10^{-3}	6.06 × 10^{1}
192.12	20.0	4.97 × 10^{-6}	3.00 × 10^{-4}	5.57 × 10^{-3}	8.56 × 10^{1}
192.13	20.0	4.97 × 10^{-6}	4.00 × 10^{-4}	5.57 × 10^{-3}	1.14 × 10^{2}

$k_2 = 2.88 \times 10^5$ L mol^{-1}s^{-1}

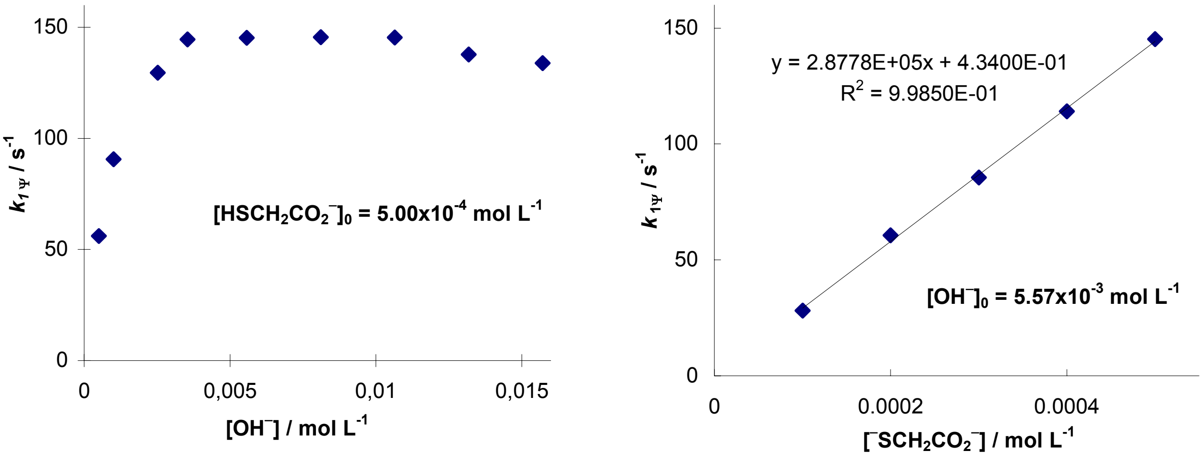

$(lil)_2CH^+$ + $^-SCH_2CO_2^-$ in 99.6/0.4 (v/v) H_2O/CH_3CN (Stopped-flow, detection at 630 nm)

No.	T, °C	$[(lil)_2CH^+]_0$, mol L^{-1}	$[HSCH_2CO_2^-]_0$, mol L^{-1}	$[OH^-]_0$, mol L^{-1}	$k_{1\Psi}$, s^{-1}
220.1	20.0	2.95×10^{-6}	1.32×10^{-4}	5.07×10^{-3}	4.38×10^{1}
220.2	20.0	2.95×10^{-6}	2.64×10^{-4}	5.07×10^{-3}	8.55×10^{1}
220.3	20.0	2.95×10^{-6}	3.96×10^{-4}	5.07×10^{-3}	1.26×10^{2}
220.4	20.0	2.95×10^{-6}	5.28×10^{-4}	5.07×10^{-3}	1.66×10^{2}

$k_2 = 3.09 \times 10^5$ L mol^{-1}s^{-1}

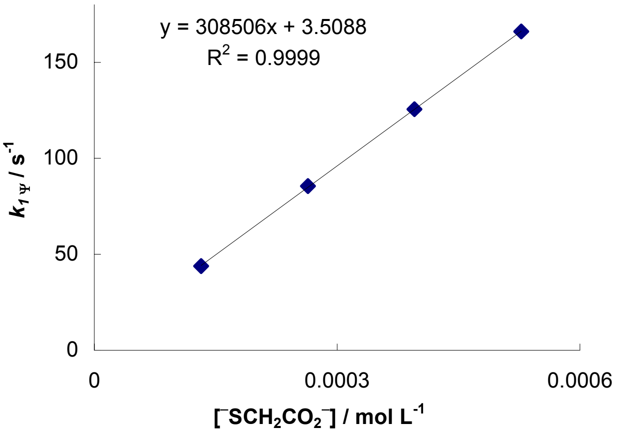

$(jul)_2CH^+ + {}^-SCH_2CO_2^-$ in 99.6/0.4 (v/v) H_2O/TFE (Stopped-flow, detection at 630 nm)

No.	T, °C	$[(jul)_2CH^+]_0$, mol L^{-1}	$[HSCH_2CO_2^-]_0$, mol L^{-1}	$[OH^-]_0$, mol L^{-1}	$k_{1\Psi}$, s^{-1}
196.1	20.0	4.66×10^{-6}	8.26×10^{-5}	5.57×10^{-3}	3.76×10^{1}
196.2	20.0	4.66×10^{-6}	1.65×10^{-4}	5.57×10^{-3}	7.16×10^{1}
196.3	20.0	4.66×10^{-6}	2.48×10^{-4}	5.57×10^{-3}	9.99×10^{1}
196.4	20.0	4.66×10^{-6}	3.31×10^{-4}	5.57×10^{-3}	1.26×10^{2}
196.5	20.0	4.66×10^{-6}	4.13×10^{-4}	5.57×10^{-3}	1.58×10^{2}

$k_2 = 3.87 \times 10^5$ L mol^{-1}s^{-1}

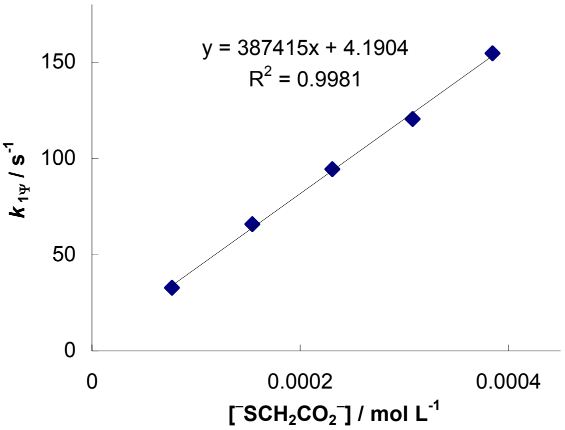

$(ind)_2CH^+ + {}^-SCH_2CO_2^-$ in 99.6/0.4 (v/v) H_2O/TFE (Stopped-flow, detection at 615 nm)

No.	T, °C	$[(ind)_2CH^+]_0$, mol L^{-1}	$[HSCH_2CO_2^-]_0$, mol L^{-1}	$[OH^-]_0$, mol L^{-1}	$k_{1\Psi}$, s^{-1}
194.1	20.0	3.13×10^{-6}	4.54×10^{-5}	5.57×10^{-3}	5.08×10^{1}
194.2	20.0	3.13×10^{-6}	9.08×10^{-5}	5.57×10^{-3}	9.43×10^{1}
194.3	20.0	3.13×10^{-6}	1.36×10^{-4}	5.57×10^{-3}	1.42×10^{2}
194.4	20.0	3.13×10^{-6}	1.82×10^{-4}	5.57×10^{-3}	1.81×10^{2}

$k_2 = 9.67 \times 10^5$ L mol^{-1}s^{-1}

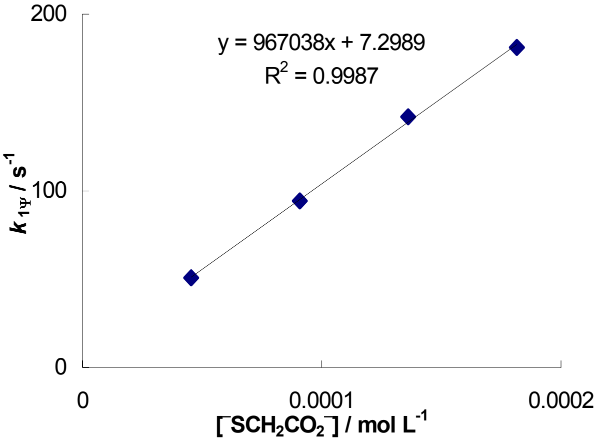

$(thq)_2CH^+$ + $^-SCH_2CO_2^-$ in 99.6/0.4 (v/v) H_2O/TFE (Stopped-flow, detection at 620 nm)

No.	T, °C	$[(thq)_2CH^+]_0$, mol L^{-1}	$[HSCH_2CO_2^-]_0$, mol L^{-1}	$[OH^-]_0$, mol L^{-1}	$k_{1\Psi}$, s^{-1}
195.1	20.0	1.61×10^{-6}	3.90×10^{-5}	5.23×10^{-3}	5.50×10^{1}
195.2	20.0	1.61×10^{-6}	7.80×10^{-5}	5.23×10^{-3}	1.21×10^{2}
195.3	20.0	1.61×10^{-6}	1.17×10^{-4}	5.23×10^{-3}	1.82×10^{2}
195.4	20.0	1.61×10^{-6}	1.56×10^{-4}	5.23×10^{-3}	2.43×10^{2}

$k_2 = 1.61 \times 10^6$ L $mol^{-1}s^{-1}$

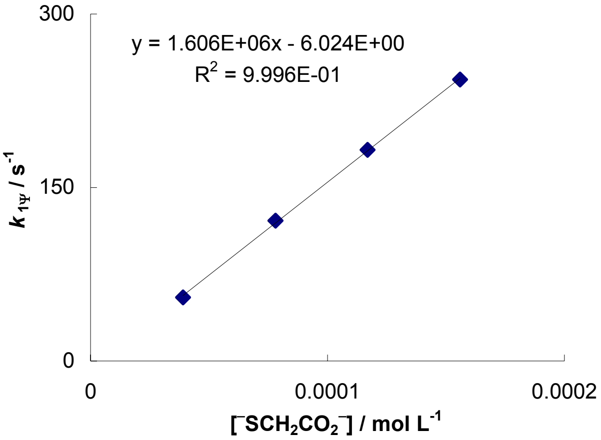

Azide ion (NaN_3) in DMSO

Sodium azide (12.1 mg, 1.86 × 10^{-4} mol) was dissolved in 10 mL of DMSO (c = 1.86 × 10^{-2} mol L^{-1}). 24 µL of this solution was diluted with DMSO to 10 mL (c = 5.09 × 10^{-5} mol L^{-1}). $(lil)_2CH^+BF_4^-$ (4.8 mg, 1.15 × 10^{-5} mol) was dissolved in 10 mL of DMSO (c = 1.15 × 10^{-3} mol L^{-1}). 90 µL of this solution was diluted to 20 mL with DMSO (c = 5.19 × 10^{-6} mol L^{-1}). In the stopped-flow instrument equal volumes of the electrophile and nucleophile solutions were mixed to yield the concentrations listed in the tables. The consumption of the carbocations was followed at 640 nm. The absorption did not disappear completely since the reactions reached equilibria. Second-order rate constant was obtained as shown in the section of semicarbazide (Run 124.1).

$(lil)_2CH^+$ + azide ion in DMSO (stopped flow, detection at 640 nm) [a]

No.	T, °C	$[(lil)_2CH^+]_0$, mol L^{-1}	[azide ion]$_0$, mol L^{-1}	$k_{1\Psi}$, s^{-1}	K, L mol^{-1}
124.1	20.0	2.59 × 10^{-6}	2.55 × 10^{-5}	3.64 × 10^{1}	7.3 × 10^{4}
124.2	20.0	2.59 × 10^{-6}	5.20 × 10^{-5}	7.88 × 10^{1}	7.5 × 10^{4}
124.3	20.0	2.59 × 10^{-6}	7.75 × 10^{-5}	1.21 × 10^{2}	7.1 × 10^{4}
124.4	20.0	2.59 × 10^{-6}	1.04 × 10^{-4}	1.67 × 10^{2}	6.9 × 10^{4}

[a] All reaction reached equilibria.

k_2 = 1.68 × 10^6 L $mol^{-1}s^{-1}$

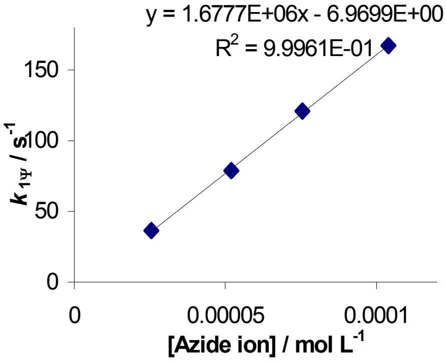

$(jul)_2CH^+$ + azide ion in DMSO (stopped flow, detection at 640 nm)

No.	T, °C	$[(jul)_2CH^+]_0$, mol L^{-1}	[azide ion]$_0$, mol L^{-1}	$k_{1\Psi}$, s^{-1}
123.1	20.0	2.50 × 10^{-6}	2.51 × 10^{-5}	> 40
123.2	20.0	2.50 × 10^{-6}	5.03 × 10^{-5}	> 80
123.3	20.0	2.50 × 10^{-6}	7.54 × 10^{-5}	> 120
123.4	20.0	2.50 × 10^{-6}	9.96 × 10^{-5}	> 160

k_2 > 2 × 10^6 L $mol^{-1}s^{-1}$

Product from $(dma)_2CH^+$ with $CF_3CH_2O^-$ in water: A solution of $(dma)_2CH^+BF_4^-$ (200 mg, 0.588 mmol) in 10 mL of CH_3CN was added to a mixture of trifluoroethanol (TFE, 2 mL) and aqueous KOH (0.491 M, 1.4 mL) in 500 mL of water. After stirring at room temperature for 30 min, the organic layer was extracted with four 100-mL portions of CH_2Cl_2. The combined organic layers were washed with water and dried with $MgSO_4$. Then the solvent was evaporated to give 117 mg of a 7:1 mixture of $(dma)_2CHOCH_2CF_3$ and $((dma)_2CH)_2O$ (according to ^1H NMR) as a pale blue solid.

7.3 Solvent nucleophilicity

7.3.1 Synthesis of benzhydrylium ion precursors[10]

Synthesis of 4-[bis(4-methoxyphenyl)methoxy]benzonitrile

The mixture of chloro-bis(4-methoxyphenyl)methane (1.40 g, 5.33 mmol) and sodium 4-cyanophenoxide (0.79 g, 5.6 mmol) in acetonitrile (100 mL) was stirred at room temperature for 3h. After CH_2Cl_2 was added, the organic layr was washed with water (4 × 100 mL), dried with $MgSO_4$, filtered, and evaporated. The product was separated by silica gel column chromatography with hexane/AcOEt, and recrystallized from hexane/CH_2Cl_2 to give colorless crystals (0.92 g, 2.7 mmol, 51%). ^{1}H NMR (300 MHz, $CDCl_3$): δ = 3.79 (s, 6H, OMe), 6.19 (s, 1H, Ar_2CH), 6.88 (d, 4H, J = 8.6 Hz, ArH), 6.98 (d, 2H, J = 8.9 Hz, ArH), 7.27 (d, 4H, J = 8.6 Hz, ArH), 7.50 (d, 2H, J = 8.9 Hz, ArH); ^{13}C NMR (75 MHz, $CDCl_3$): δ = 55.2 (ArO$\underline{Me}$), 88.8 ($Ar_2\underline{C}H$), 104.1 (Ar), 116.7 (CN), 119.2 (Ar), 128.1 (Ar), 132.3 (Ar), 133.9 (Ar), 159.4 (Ar), 161.4 (Ar), HRMS: m/z 345.1365 (calc), 345.1370 (found).

Synthesis of 4-[(4-methyl-4'-methoxy-diphenyl)methoxy]benzonitrile

The mixture of chloro-(4-methyl-4'-methoxy-diphenyl)methane (1.39 g, 5.63 mmol) and sodium 4-cyanophenoxide (1.11 g, 7.87 mmol) in THF (110 mL) was refluxed for 3 days. After ether (150 mL) was added, the etheral solution was washed water (4 × 100 mL), dried with $MgSO_4$, filtered, and evaporated. The product was separated by silica gel column chromatography with hexane/AcOEt and by GPC ($CHCl_3$) to give a colorless oil (0.68g, 2.37 mmol, 42%). ^{1}H NMR (500 MHz, $CDCl_3$): δ = 2.30 (s, 3H, Me), 3.78 (s, 3H, OMe), 6.20 (s, 1H, Ar_2CH), 6.88 (d, 2H, J = 8.8 Hz, ArH), 6.98 (d, 2H, J = 9.0 Hz, ArH), 7.16 (d, 2H, J = 8.0 Hz, ArH), 7.24-7.31 (4H, ArH), 7.50 (d, 2H, J = 9.0 Hz, ArH); ^{13}C NMR (125 MHz, $CDCl_3$): δ = 21.1 (Ar$\underline{Me}$), 55.3 (ArO$\underline{Me}$), 81.7 ($Ar_2\underline{C}H$), 104.0 (Ar), 114.1 (Ar), 116.7 (CN), 119.2 (Ar), 126.6 (Ar), 128.2 (Ar), 129.5 (Ar), 132.3 (Ar), 133.9 (Ar), 137.3 (Ar), 137.9 (Ar), 159.4 (Ar), 161.4 (Ar). HRMS: m/z 329.1416 (calc), 329.1426 (found).

Synthesis of 4-[(4-methoxydiphenyl)methoxy]benzonitrile

The mixture of chloro-(4-methoxydiphenyl)methane (2.02 g, 8.68 mmol) and sodium 4-cyanophenoxide (1.84 g, 13.0 mmol) in THF (110 mL) was refluxed for 3 days. After ether (200 mL) was added, the etheral solution was washed with cold 0.1 M NaOH (150 mL) and 10% aqueous NaCl (4 × 100 mL), dried with $MgSO_4$, filtered, and evaporated. The product was separated by silica gel column chromatography with hexane/AcOEt and recrystallized from hexane/ether to give colorless crystals (1.54 g, 4.9 mmol, 56%). ^{1}H NMR (500 MHz, CDCl$_3$): δ = 3.79 (s, 3H, OMe), 6.22 (s, 1H, Ar$_2$CH), 6.88 (d, 2H, *J* = 9.0 Hz, ArH), 6.99 (d, 2H, *J* = 8.5 Hz, ArH), 7.28-7.37 (7H, ArH), 7.51 (d, 2H, *J* = 9.0 Hz, ArH); ^{13}C NMR (125 MHz, CDCl$_3$): δ = 55.3 (ArO$\underline{\text{Me}}$), 81.8 (Ar$_2\underline{\text{C}}$H), 104.2 (Ar), 114.2 (Ar), 116.7 (CN), 119.2 (Ar), 126.6 (Ar), 128.1 (Ar), 128.3 (Ar), 128.8 (Ar), 132.1 (Ar), 133.9 (Ar), 140.2 (Ar), 159.5 (Ar), 161.3 (Ar). HRMS: *m/z* 316.1338 (calc), 316.1258 (found).

Synthesis of 4-[bis(4-methylphenyl)methoxy]benzonitrile

The mixture of chloro-bis(4-methylphenyl)methane (2.01 g, 8.71 mmol) and sodium 4-cyanophenoxide (2.44 g, 17.3 mmol) in THF (230 mL) was refluxed for 3 days. After ether (200 mL) was added, the etheral solution was washed with cold 0.1 M NaOH (150 mL) and 10% NaCl (4 × 100 mL), dried with MgSO$_4$, filtered, and evaporated. The product was recrystallized from hexane/CH$_2$Cl$_2$ to give colorless crystals (1.30 g, 4.56 mmol, 62%). ^{1}H NMR (300 MHz, CDCl$_3$): δ = 2.31 (s, 6H, Me), 6.20 (s, 1H, Ar$_2$CH), 6.98 (d, 2H, *J* = 9.0 Hz, ArH), 7.15 (d, 4H, *J* = 8.0 Hz, ArH), 7.25 (d, 4H, *J* = 8.0 Hz, ArH), 7.49 (d, 2H, *J* = 9.0 Hz, ArH); ^{13}C NMR (75 MHz, CDCl$_3$): δ = 21.1 (Ar$\underline{\text{Me}}$), 81.9 (Ar$_2\underline{\text{C}}$H), 104.1 (Ar), 116.7 (CN), 119.2 (Ar), 126.7 (Ar), 129.5 (Ar), 133.9 (Ar), 137.2 (Ar), 137.9 (Ar), 161.4 (Ar), HRMS: *m/z* 313.1467 (calc), 313.1470 (found).

Synthesis of 4-[(4-methyldiphenyl)methoxy]benzonitrile

The mixture of chloro-(4-methyldiphenyl)methane (1.78 g, 8.26 mmol) and sodium 4-cyanophenoxide (1.41 g, 10.0 mmol) in acetonitrile (100 mL) was refluxed for 19h. After ether (200 mL) was added, the etheral solution was washed with water (4 × 100 mL), dried with MgSO$_4$, filtered, and evaporated. The product was separated by silica gel column chromatography with hexane/AcOEt and recrystallized from hexane/ether to give colorless crystals (1.20 g, 3.8 mmol, 46%). ^{1}H NMR (300 MHz, CDCl$_3$): δ = 2.33 (s, 3H, Me), 6.22 (s, 1H, Ar$_2$CH), 6.99 (d, 2H, *J* = 8.9 Hz, ArH), 7.16 (d, 2H, *J* = 8.0 Hz, ArH), 7.25-7.37 (7H, ArH), 7.50 (d, 2H, *J* = 8.9 Hz, ArH); ^{13}C NMR (75 MHz, CDCl$_3$): δ = 21.1 (Ar$\underline{\text{Me}}$), 82.0 (Ar$_2\underline{\text{C}}$H), 104.2 (Ar), 116.7 (CN), 119.1 (Ar), 126.7 (Ar), 126.8 (Ar), 128.1 (Ar), 128.8 (Ar), 129.5 (Ar), 133.9 (Ar), 137.1 (Ar), 138.1 (Ar), 140.2 (Ar), 161.4 (Ar). HRMS: *m/z* 300.1388 (calc), 300.1385 (found).

Synthesis of 4-[(diphenyl)methoxy]benzonitrile

The mixture of chloro-(diphenyl)methane (1.50 g, 7.40 mmol) and sodium 4-cyanophenoxide (2.46 g, 17.4 mmol) in acetonitrile (75 mL) was refluxed for 11 h. After ether (100 mL) was added, the etheral solution was washed with water (4 × 100 mL), dried with $MgSO_4$, filtered, and evaporated. The product was recrystallized from hexane/CH_2Cl_2 to give colorless crystals (1.30 g, 4.56 mmol, 62%). ^{1}H NMR (300 MHz, $CDCl_3$): δ = 6.25 (s, 1H, Ar_2CH), 7.00 (d, 2H, J = 9.0 Hz, ArH), 7.27-7.41 (10H, ArH), 7.51 (d, 2H, J = 9.0 Hz, ArH); ^{13}C NMR (75 MHz, $CDCl_3$): δ = 82.1 ($Ar_2\underline{C}H$), 104.3 (Ar), 116.7 (CN), 119.1 (Ar), 126.8 (Ar), 128.2 (Ar), 128.8 (Ar), 133.9 (Ar), 140.0 (Ar), 161.3 (Ar), HRMS: *m/z* 286.1232 (calc), 286.1228 (found).

Synthesis of bis(4-methoxyphenyl)methyl acetate

Acetyl chloride (0.99g, 12.6 mmol) was added dropwise to bis(4-methoxyphenyl)methanol (1.00 g, 4.09 mmol) in pyridine (60 mL) at room temperature, and the mixture was stirred for 24 h. After quenching with water (50 mL), the product was extracted with three portions of ether (60 mL). The combined ether layers were washed with saturated aqueous $NaHCO_3$ (60 mL), dried with $MgSO_4$, filtered, and the solvent was removed in the rotary evaporator. The product was purified by GPC ($CHCl_3$) to give a pale yellow oil (0.68g, 2.37 mmol, 58%). ^{1}H NMR (500 MHz, $CDCl_3$): δ = 2.13 (s, 3H, Ac), 3.78 (s, 6H, OMe), 6.82 (s, 1H, Ar_2CH), 6.86 (d, 4H, J = 8.5 Hz, ArH), 7.24 (d, 4H, J = 8.5 Hz, ArH); ^{13}C NMR ($CDCl_3$, 126 MHz): δ = 21.3 (C(O)$\underline{\mathrm{Me}}$), 55.2 (OMe), 76.2 ($Ar_2\underline{C}H$), 113.8 (Ar), 128.4 (Ar), 132.6 (Ar), 159.2 (Ar), 170.1 (C=O).

Synthesis of (4-methyl-4'-methoxydiphenyl)methyl acetate

Acetyl chloride (0.83g, 11 mmol) was added dropwise to (4-methyl-4'-methoxydiphenyl)methanol (0.75 g, 3.3 mmol) in pyridine (50 mL) at room temperature, and the mixture was stirred for 14 h. After quenching with water (100 mL), the product was extracted with three portions of CH_2Cl_2 (50 mL). The combined CH_2Cl_2 layers were washed with saturated aqueous $NaHCO_3$ (50 mL), dried with $MgSO_4$, filtered, and the solvent was removed by rotary evaporator. The product was purified by silica gel column chromatography with hexane/AcOEt to give colorless crystals (0.71g, 2.6 mmol, 79%). ^{1}H NMR (500 MHz, $CDCl_3$): δ = 2.13 (s, 3H, Ac), 2.33 (s, 3H, Me), 3.78 (s, 3H, OMe), 6.82 (s, 1H, Ar_2CH), 6.85 (d, 2H, J = 8.5 Hz, ArH), 7.14 (d, 2H, J = 9.0 Hz, ArH), 7.20-7.26 (m, 4H, ArH); ^{13}C NMR ($CDCl_3$, 126 MHz): δ = 21.1, 21.3 (ArMe, C(O)$\underline{\mathrm{Me}}$), 55.3 (OMe), 76.5 ($Ar_2\underline{C}H$), 113.8 (Ar), 126.9 (Ar), 128.6 (Ar), 129.1 (Ar), 132.6 (Ar), 137.5 (2C, Ar), 159.2 (Ar), 170.1 (C=O).

Synthesis of bis(2,3-dihydrobenzofuran-5-yl)methylium tetrafluoroborate $(fur)_2CH^+BF_4^-$.

$(fur)_2CHOH$ (0.87 g, 3.2 mmol) was dissolved in a mixture of 50 mL of dry ether and 2.2 mL (17 mmol) of propionic anhydride. A 54% ether solution of $HBF_4{\cdot}OEt_2$ (1.34 g, 8.24 mmol) was added. The mixture was stirred at room temperature for 1 h and cooled in an ice bath for 20 min. The precipitate was filtered off under nitrogen and washed successively with cold, dry ether and cold, dry pentane. The residue was dried in vacuo to yield 0.79 g of a deep-violet powder (2.3 mmol, 72%). ^{1}H NMR (300 MHz, CD_2Cl_2): δ = 3.49 (t, *J* = 8.6 Hz, 4 H), 5.01 (t, *J* = 8.6 Hz, 4 H), 7.18 (d, *J* = 8.7 Hz, 2 H), 8.12 (d, *J* = 8.7 Hz, 2 H), 8.27 (s, 2 H), 8.72 (s, 1 H, $Ar_2\underline{C}H$). ^{13}C NMR (100.6 MHz, CD_2Cl_2): δ = 27.5 ($OCH_2\underline{C}H_2$), 76.3 ($O\underline{C}H_2CH_2$), 113.5 (Ar), 129.9 (Ar), 134.0 (Ar), 136.3 (Ar), 146.6 (Ar), 175.2, 175.5 (Ar, $Ar_2\underline{C}H$).[14]

7.3.2 Details of the kinetic experiments of reactions of benzhydrylium ions with solvents

Water

$(dma)_2CH^+$ in water with phosphate buffer at pH 8.0 (J&M, detection at 605 nm)

No.	$[(dma)_2CH^+]_0$, mol L^{-1}	$[phosphate]_{total}$, mol L^{-1}	k_{obs}, s^{-1}	conversion, %
552-1	1.17×10^{-5}	5.14×10^{-3}	2.01×10^{-2}	98
552-2	1.23×10^{-5}	1.09×10^{-2}	2.13×10^{-2}	99
552-3	1.22×10^{-5}	1.61×10^{-2}	2.03×10^{-2}	98

$k = 2.06 \times 10^{-2}$ s^{-1}

Ar_2CH^+ in water (Laser flash photolysis)

No.	Cation	Precursor [a]	$[Precursor]_0$, mol L^{-1}	Detection, nm	k_{obs}, s^{-1}
F172-1	$(ani)_2CH^+$	$(ani)_2CHOAc$	1.59×10^{-4}	500	9.44×10^4

[a] OAc = acetate

91W9AN

$(thq)_2CH^+$ in 91W9AN with DABCO-DABCOH$^+$ (1:1) buffer (J&M, detection at 620 nm)

No.	$[(thq)_2CH^+]_0$, mol L^{-1}	[DABCO],[a] mol L^{-1}	k_{obs}, s^{-1}	conversion, %
313-1	8.24×10^{-6}	2.59×10^{-3}	1.68×10^{-3}	98
313-2	8.41×10^{-6}	5.29×10^{-3}	1.67×10^{-3}	98
313-3	8.03×10^{-6}	7.57×10^{-3}	1.64×10^{-3}	96
313-4	7.96×10^{-6}	1.00×10^{-2}	1.67×10^{-3}	94
313-5	8.18×10^{-6}	1.29×10^{-2}	1.65×10^{-3}	96

$k = 1.66 \times 10^{-3}$ s^{-1}

[a] [DABCO] = [DABCO-H$^+$]

$(pyr)_2CH^+$ in 91W9AN with DABCO-DABCOH$^+$ (1:1) buffer (J&M, detection at 620 nm)

No.	$[(pyr)_2CH^+]_0$, mol L^{-1}	[DABCO],[a] mol L^{-1}	k_{obs}, s^{-1}	conversion, %
365-1	3.82×10^{-6}	2.17×10^{-3}	4.35×10^{-3}	93
365-2	3.41×10^{-6}	3.87×10^{-3}	4.25×10^{-3}	94
365-3	3.39×10^{-6}	5.77×10^{-3}	4.36×10^{-3}	92
365-4	3.32×10^{-6}	7.53×10^{-3}	4.19×10^{-3}	97

$k = 4.29 \times 10^{-3}$ s^{-1}

[a] [DABCO] = [DABCO-H$^+$]

Ar_2CH^+ in 91W9AN (Stopped-flow)

No.	Cation	$[Ar_2CH^+]_0$, mol L^{-1}	Detection, nm	k_{obs}, s^{-1}
333-1	$(mpa)_2CH^+$	1.05×10^{-5}	610	3.31×10^{-1}
309-1	$(mor)_2CH^+$	5.72×10^{-6}	610	6.73×10^{-1}
309-2	*$(dpa)_2CH^+$*	*3.00×10^{-6}*	*660*	*1.39×10^{2}*
309-3	$(mfa)_2CH^+$	4.12×10^{-6}	585	4.39
309-4	$(pfa)_2CH^+$	7.22×10^{-6}	590	9.36×10^{1}

Ar_2CH^+ in 91W9AN (Laser flash photolysis)

No.	Cation	Precursor [a]	$[Precursor]_0$, mol L^{-1}	Detection, nm	k_{obs}, s^{-1}
F152-1	$(ani)_2CH^+$	$(ani)_2CHOAc$	1.59×10^{-4}	500	9.55×10^{4}
F151-6	$(ani)(tol)CH^+$	(ani)(tol)CHOAc	1.52×10^{-4}	480	7.99×10^{5}

[a] OAc = acetate

80W20AN

$(thq)_2CH^+$ in 80W20AN with DABCO-DABCOH$^+$ (1:1) buffer (J&M, detection at 620 nm)

No.	$[(thq)_2CH^+]_0$, mol L^{-1}	[DABCO],[a] mol L^{-1}	k_{obs}, s^{-1}	conversion, %
359-1	4.87×10^{-6}	1.19×10^{-3}	1.26×10^{-3}	96
359-2	4.74×10^{-6}	2.30×10^{-3}	1.21×10^{-3}	94
359-3	4.67×10^{-6}	3.41×10^{-3}	1.23×10^{-3}	97

$k = 1.23 \times 10^{-3}$ s^{-1}

[a] [DABCO] = [DABCO-H$^+$]

$(pyr)_2CH^+$ in 80W20AN with DABCO-DABCOH$^+$ (1:1) buffer (J&M, detection at 610 nm)

No.	$[(pyr)_2CH^+]_0$, mol L^{-1}	[DABCO],[a] mol L^{-1}	k_{obs}, s^{-1}	conversion, %
364-1	3.87×10^{-6}	2.47×10^{-3}	3.86×10^{-3}	90
364-2	3.84×10^{-6}	4.90×10^{-3}	3.76×10^{-3}	98
364-3	3.84×10^{-6}	7.35×10^{-3}	3.74×10^{-3}	97
364-4	3.86×10^{-6}	9.85×10^{-3}	3.72×10^{-3}	97

$k = 3.77 \times 10^{-3}$ s^{-1}

[a] [DABCO] = [DABCO-H$^+$]

Ar_2CH^+ in 80W20AN (Stopped-flow)

No.	Cation	$[Ar_2CH^+]_0$, mol L^{-1}	Detection, nm	k_{obs}, s^{-1}
333-2	$(mpa)_2CH^+$	1.05×10^{-5}	610	2.84×10^{-1}
309-5	$(mor)_2CH^+$	5.72×10^{-6}	610	4.93×10^{-1}
309-6	*$(dpa)_2CH^+$*	*3.00×10^{-6}*	*660*	*3.06×10^{1}*
309-7	$(mfa)_2CH^+$	4.12×10^{-6}	585	3.98
309-8	$(pfa)_2CH^+$	7.22×10^{-6}	590	4.93×10^{1}

67W33AN

$(thq)_2CH^+$ in 67W33AN with DABCO-DABCOH$^+$ (1:1) buffer (J&M, detection at 620 nm)

No.	$[(thq)_2CH^+]_0$, mol L^{-1}	[DABCO],[a] mol L^{-1}	k_{obs}, s^{-1}	conversion, %
361-1	4.60×10^{-6}	1.12×10^{-3}	1.17×10^{-3}	93
361-2	5.74×10^{-6}	2.80×10^{-3}	1.16×10^{-3}	96
361-3	5.30×10^{-6}	3.87×10^{-3}	1.17×10^{-3}	96

$k = 1.17 \times 10^{-3}$ s^{-1}

[a] [DABCO] = [DABCO-H$^+$]

$(pyr)_2CH^+$ in 67W33AN with DABCO-DABCOH$^+$ (1:1) buffer (J&M, detection at 610 nm)

No.	$[(pyr)_2CH^+]_0$, mol L^{-1}	[DABCO],[a] mol L^{-1}	k_{obs}, s^{-1}	conversion, %
366-1	4.61×10^{-6}	2.62×10^{-3}	4.23×10^{-3}	95
366-2	3.93×10^{-6}	4.45×10^{-3}	4.04×10^{-3}	95
366-3	4.15×10^{-6}	7.05×10^{-3}	4.00×10^{-3}	93
366-4	3.76×10^{-6}	8.52×10^{-3}	3.93×10^{-3}	93

$k = 4.05 \times 10^{-3}$ s^{-1}

[a] [DABCO] = [DABCO-H$^+$]

Ar_2CH^+ in 67W33AN (Stopped-flow)

No.	Cation	$[Ar_2CH^+]_0$, mol L^{-1}	Detection, nm	k_{obs}, s^{-1}
333-3	$(mpa)_2CH^+$	1.05×10^{-5}	610	2.83×10^{-1}
309-9	$(mor)_2CH^+$	5.72×10^{-6}	610	4.13×10^{-1}
309-10	*$(dpa)_2CH^+$*	*3.00×10^{-6}*	*660*	*7.20*
309-11	$(mfa)_2CH^+$	4.12×10^{-6}	585	4.47
309-12	$(pfa)_2CH^+$	7.22×10^{-6}	590	4.96×10^{1}

50W50AN

$(thq)_2CH^+$ in 50W50AN with DABCO-DABCOH$^+$ (1:1) buffer (J&M, detection at 620 nm)

No.	$[(thq)_2CH^+]_0$, mol L^{-1}	[DABCO],[a] mol L^{-1}	k_{obs}, s^{-1}	conversion, %
311-1	6.84×10^{-6}	9.44×10^{-4}	1.24×10^{-3}	93
311-2	8.57×10^{-6}	2.37×10^{-3}	1.22×10^{-3}	97
311-3	8.06×10^{-6}	3.33×10^{-3}	1.21×10^{-3}	74
311-4	7.84×10^{-6}	4.33×10^{-3}	1.22×10^{-3}	93
311-5	8.39×10^{-6}	5.79×10^{-3}	1.22×10^{-3}	97

$k = 1.22 \times 10^{-3}$ s^{-1}

[a] [DABCO] = [DABCO-H$^+$]

$(pyr)_2CH^+$ in 50W50AN with DABCO-DABCOH$^+$ (1:1) buffer (J&M, detection at 610 nm)

No.	$[(pyr)_2CH^+]_0$, mol L^{-1}	[DABCO],[a] mol L^{-1}	k_{obs}, s^{-1}	conversion, %
248-1	2.32×10^{-6}	1.18×10^{-3}	4.36×10^{-3}	94
	2.31×10^{-6}	2.95×10^{-3}	4.37×10^{-3}	95
	2.33×10^{-6}	3.57×10^{-3}	4.27×10^{-3}	94
	2.31×10^{-6}	4.72×10^{-3}	4.31×10^{-3}	94
	2.29×10^{-6}	5.85×10^{-3}	4.34×10^{-3}	96

$k = 4.33 \times 10^{-3}$ s^{-1}

[a] [DABCO] = [DABCO-H$^+$]

Ar_2CH^+ in 50W50AN (Stopped-flow)

No.	Cation	$[Ar_2CH^+]_0$, mol L^{-1}	Detection, nm	k_{obs}, s^{-1}
397-1	$(mpa)_2CH^+$	5.85×10^{-6}	610	2.52×10^{-1}
397-2	$(dpa)_2CH^+$	1.07×10^{-5}	660	4.44
397-3	$(pfa)_2CH^+$	7.06×10^{-6}	590	3.62×10^{1}

Ar_2CH^+ in 50W50AN (Laser flash photolysis)

No.	Cation	Precursor [a]	$[\text{Precursor}]_0$, mol L^{-1}	Detection, nm	k_{obs}, s^{-1}
F5-4	$(ani)_2CH^+$	$(ani)_2CHOAr'$	1.18×10^{-4}	500	1.01×10^{5}
F47-4	$(ani)(tol)CH^+$	(ani)(tol)CHOAr'	1.38×10^{-4}	480	8.55×10^{5}
F19-4	$(ani)PhCH^+$	(ani)PhCHOAr'	1.29×10^{-4}	455	1.84×10^{6}
F9-1	$(tol)_2CH^+$	$(tol)_2CHOAr'$	1.95×10^{-4}	460	3.28×10^{7}

[a] OAr' = 4-cyanophenoxide

33W67AN

$(thq)_2CH^+$ in 33W67AN with DABCO-DABCOH$^+$ (1:1) buffer (J&M, detection at 620 nm)

No.	$[(thq)_2CH^+]_0$, mol L^{-1}	[DABCO]],[a] mol L^{-1}	k_{obs}, s^{-1}	conversion, %
475-1	1.12×10^{-5}	8.65×10^{-4}	1.24×10^{-3}	84
475-2	1.13×10^{-5}	2.52×10^{-3}	1.30×10^{-3}	89
475-3	1.09×10^{-5}	4.33×10^{-3}	1.30×10^{-3}	89

$k = 1.28 \times 10^{-3}$ s^{-1}

[a] [DABCO] = [DABCO-H$^+$]

Ar_2CH^+ in 33W67AN (Stopped-flow)

No.	Cation	$[Ar_2CH^+]_0$, mol L^{-1}	Detection, nm	k_{obs}, s^{-1}
394-1	$(mpa)_2CH^+$	5.85×10^{-6}	610	2.24×10^{-1}
394-2	$(mor)_2CH^+$	7.82×10^{-6}	610	2.85×10^{-1}
394-3	$(dpa)_2CH^+$	1.07×10^{-5}	660	4.12
394-4	$(mfa)_2CH^+$	8.50×10^{-6}	585	3.58
394-5	$(pfa)_2CH^+$	7.06×10^{-6}	590	3.39×10^{1}

Ar_2CH^+ in 33W67AN (Laser flash photolysis)

No.	Cation	Precursor [a]	$[Precursor]_0$, mol L^{-1}	Detection, nm	k_{obs}, s^{-1}
F5-3	$(ani)_2CH^+$	$(ani)_2CHOAr'$	1.18×10^{-4}	500	1.01×10^{5}
F47-3	$(ani)(tol)CH^+$	(ani)(tol)CHOAr'	1.38×10^{-4}	480	8.95×10^{5}
F19-3	$(ani)PhCH^+$	(ani)PhCHOAr'	1.29×10^{-4}	455	2.31×10^{6}
F9-2	$(tol)_2CH^+$	$(tol)_2CHOAr'$	1.95×10^{-4}	460	3.47×10^{7}

[a] OAr' = 4-cyanophenoxide

20W80AN

Ar_2CH^+ in 20W80AN (Stopped-flow)

No.	Cation	$[Ar_2CH^+]_0$, mol L^{-1}	Detection, nm	k_{obs}, s^{-1}
395-1	$(mpa)_2CH^+$	5.85×10^{-6}	610	2.17×10^{-1}
395-2	$(mor)_2CH^+$	7.82×10^{-6}	610	2.51×10^{-1}
395-3	$(dpa)_2CH^+$	1.07×10^{-5}	660	3.97
395-4	$(mfa)_2CH^+$	8.50×10^{-6}	585	3.62
395-5	$(pfa)_2CH^+$	7.06×10^{-6}	590	3.32×10^{1}

Ar$_2$CH$^+$ in 20W80AN (Laser flash photolysis)

No.	Cation	Precursor [a]	[Precursor]$_0$, mol L^{-1}	Detection, nm	k_{obs}, s^{-1}
F5-2	(ani)$_2$CH$^+$	(ani)$_2$CHOAr'	1.18×10^{-4}	500	9.82×10^{4}
F47-2	(ani)(tol)CH$^+$	(ani)(tol)CHOAr'	1.38×10^{-4}	480	8.29×10^{5}
F19-2	(ani)PhCH$^+$	(ani)PhCHOAr'	1.29×10^{-4}	455	1.87×10^{6}
F9-3	(tol)$_2$CH$^+$	(tol)$_2$CHOAr'	1.95×10^{-4}	460	3.06×10^{7}

[a] OAr' = 4-cyanophenoxide

10W90AN

Ar$_2$CH$^+$ in 10W90AN (Stopped-flow)

No.	Cation	[Ar$_2$CH$^+$]$_0$, mol L^{-1}	Detection, nm	k_{obs}, s^{-1}
396-1	(mpa)$_2$CH$^+$	5.85×10^{-6}	610	8.08×10^{-2}
396-2	(mor)$_2$CH$^+$	7.82×10^{-6}	610	8.08×10^{-2}
396-3	(dpa)$_2$CH$^+$	1.07×10^{-5}	660	1.56
396-4	(mfa)$_2$CH$^+$	8.50×10^{-6}	585	1.57
396-5	(pfa)$_2$CH$^+$	7.06×10^{-6}	590	1.42×10^{1}
448-1	(fur)$_2$CH$^+$	3.11×10^{-5}	520	7.11×10^{2}

Ar$_2$CH$^+$ in 10W90AN (Laser flash photolysis)

No.	Cation	Precursor [a]	[Precursor]$_0$, mol L^{-1}	Detection, nm	k_{obs}, s^{-1}
F148-1	(ani)$_2$CH$^+$	(ani)$_2$CHOAc	1.59×10^{-4}	500	9.87×10^{4}
F47-1	(ani)(tol)CH$^+$	(ani)(tol)CHOAr'	1.38×10^{-4}	480	6.81×10^{5}
F28-1	(ani)PhCH$^+$	(ani)PhCHOAr'	2.03×10^{-4}	455	1.83×10^{6}
F9-4	(tol)$_2$CH$^+$	(tol)$_2$CHOAr'	1.95×10^{-4}	460	2.37×10^{7}

[a] OAr' = 4-cyanophenoxide

Ethanol-Water Mixtures

90E10W

(lil)$_2$CH$^+$ in 90E10W (J&M, detection at 630 nm)

No.	[(lil)$_2$CH$^+$]$_0$, mol L^{-1}	k_{obs}, s^{-1}	conversion, %
484-1	8.75×10^{-6}	3.08×10^{-3}	95
484-2	7.89×10^{-6}	3.15×10^{-3}	94
484-3	7.17×10^{-6}	2.87×10^{-3}	98

$k = 3.03 \times 10^{-3}$ s^{-1}

(ind)$_2$CH$^+$ in 90E10W (J&M, detection at 615 nm)

No.	[(ind)$_2$CH$^+$]$_0$, mol L^{-1}	k_{obs}, s^{-1}	conversion, %
483-1	8.01×10^{-6}	2.85×10^{-2}	98
483-2	8.87×10^{-6}	2.75×10^{-2}	99
483-3	7.45×10^{-6}	2.74×10^{-2}	97

$k = 2.78 \times 10^{-3}$ s^{-1}

Ar$_2$CH$^+$ in 90E10W (Stopped-flow)

No.	Cation	[Ar$_2$CH$^+$]$_0$, mol L^{-1}	Detection, nm	k_{obs}, s^{-1}
524-1	(pyr)$_2$CH$^+$	5.11×10^{-6}	610	3.02×10^{-1}
532-1	(dma)$_2$CH$^+$	1.84×10^{-5}	605	8.33×10^{-1}

Ar$_2$CH$^+$ in 90E10W (Laser flash photolysis)

No.	Cation	Precursor [a]	[Precursor]$_0$, mol L^{-1}	Detection, nm	k_{obs}, s^{-1}
F43-1	(ani)$_2$CH$^+$	(ani)$_2$CHOAr'	1.99×10^{-4}	500	2.53×10^{6}
F55-1	(ani)(tol)CH$^+$	(ani)(tol)CHOAr'	1.38×10^{-4}	480	9.47×10^{6}
F147-5	*(ani)PhCH*$^+$	*(ani)PhCHOAr'*	1.36×10^{-4}	*455*	7.04×10^{6}

[a] OAr' = 4-cyanophenoxide

80E20W

(lil)$_2$CH$^+$ in 80E20W (J&M, detection at 630 nm)

No.	[(lil)$_2$CH$^+$]$_0$, mol L^{-1}	k_{obs}, s^{-1}	conversion, %
476-1	8.22×10^{-6}	1.60×10^{-3}	95
476-2	8.14×10^{-6}	1.69×10^{-3}	94
476-3	8.42×10^{-6}	1.65×10^{-3}	98

$k = 1.65 \times 10^{-3}$ s^{-1}

(ind)$_2$CH$^+$ in 80E20W (J&M, detection at 615 nm)

No.	[(ind)$_2$CH$^+$]$_0$, mol L^{-1}	k_{obs}, s^{-1}	conversion, %
477-1	8.55×10^{-6}	1.50×10^{-2}	96
477-2	8.73×10^{-6}	1.43×10^{-2}	96
477-3	8.37×10^{-6}	1.41×10^{-2}	97

$k = 1.45 \times 10^{-2}$ s^{-1}

Ar$_2$CH$^+$ in 80E20W (Stopped-flow)

No.	Cation	[Ar$_2$CH$^+$]$_0$, mol L^{-1}	Detection, nm	k_{obs}, s^{-1}
524-2	(pyr)$_2$CH$^+$	5.11×10^{-6}	610	1.40×10^{-1}
532-2	(dma)$_2$CH$^+$	1.84×10^{-5}	605	4.05×10^{-1}

Ar$_2$CH$^+$ in 80E20W (Laser flash photolysis)

No.	Cation	Precursor [a]	[Precursor]$_0$, mol L^{-1}	Detection, nm	k_{obs}, s^{-1}
F43-2	(ani)$_2$CH$^+$	(ani)$_2$CHOAr'	1.99×10^{-4}	500	1.51×10^{6}
F55-2	(ani)(tol)CH$^+$	(ani)(tol)CHOAr'	1.38×10^{-4}	480	7.88×10^{6}
F147-4	(ani)PhCH$^+$	(ani)PhCHOAr'	1.36×10^{-4}	455	1.22×10^{7}

[a] OAr' = 4-cyanophenoxide

60E40W

(lil)$_2$CH$^+$ in 60E40W (J&M, detection at 630 nm)

No.	[(lil)$_2$CH$^+$]$_0$, mol L^{-1}	k_{obs}, s^{-1}	conversion, %
491-1	8.08×10^{-6}	7.13×10^{-4}	92
491-2	8.07×10^{-6}	7.26×10^{-4}	89
491-3	7.51×10^{-6}	7.18×10^{-4}	94
491-4	8.15×10^{-6}	7.07×10^{-4}	93

$k = 7.16 \times 10^{-4}$ s^{-1}

(ind)$_2$CH$^+$ in 60E40W (J&M, detection at 615 nm)

No.	[(ind)$_2$CH$^+$]$_0$, mol L^{-1}	k_{obs}, s^{-1}	conversion, %
490-1	7.91×10^{-6}	5.67×10^{-4}	95
490-2	6.73×10^{-6}	6.04×10^{-4}	91
490-3	8.08×10^{-6}	5.83×10^{-4}	93

$k = 5.84 \times 10^{-3}$ s^{-1}

Ar$_2$CH$^+$ in 60E40W (Stopped-flow)

No.	Cation	[Ar$_2$CH$^+$]$_0$, mol L^{-1}	Detection, nm	k_{obs}, s^{-1}
524-3	(pyr)$_2$CH$^+$	5.11×10^{-6}	610	5.28×10^{-2}
532-3	(dma)$_2$CH$^+$	1.84×10^{-5}	605	1.70×10^{-1}

Ar$_2$CH$^+$ in 60E40W (Laser flash photolysis)

No.	Cation	Precursor [a]	[Precursor]$_0$, mol L^{-1}	Detection, nm	k_{obs}, s^{-1}
F43-3	(ani)$_2$CH$^+$	(ani)$_2$CHOAr'	1.99×10^{-4}	500	7.13×10^{5}
F55-3	(ani)(tol)CH$^+$	(ani)(tol)CHOAr'	1.38×10^{-4}	480	6.55×10^{6}
F147-2	(ani)PhCH$^+$	(ani)PhCHOAr'	1.36×10^{-4}	455	1.06×10^{7}

[a] OAr' = 4-cyanophenoxide

50E50W

(ind)$_2$CH$^+$ in 50E50W (J&M, detection at 615 nm)

No.	[(ind)$_2$CH$^+$]$_0$, mol L^{-1}	k_{obs}, s^{-1}	conversion, %
487-1	4.15×10^{-6}	3.54×10^{-3}	91
487-2	3.92×10^{-6}	3.97×10^{-3}	93
487-3	6.88×10^{-6}	4.05×10^{-3}	95
479-3	8.31×10^{-6}	3.80×10^{-3}	97

$k = 3.84 \times 10^{-3}$ s^{-1}

$(dma)_2CH^+$ in 50E50W (J&M, detection at 605 nm)

No.	$[(dma)_2CH^+]_0$, mol L^{-1}	k_{obs}, s^{-1}	conversion, %
526-1	6.27×10^{-6}	7.64×10^{-2}	92
526-2	5.91×10^{-6}	7.31×10^{-2}	90
526-3	6.08×10^{-6}	7.33×10^{-2}	88

$k = 7.43 \times 10^{-2}$ s^{-1}

Ar_2CH^+ in 50E50W (Laser flash photolysis)

No.	Cation	Precursor [a]	$[\text{Precursor}]_0$, mol L^{-1}	Detection, nm	k_{obs}, s^{-1}
F43-4	$(ani)_2CH^+$	$(ani)_2CHOAr'$	1.99×10^{-4}	500	4.96×10^{6}
F55-4	$(ani)(tol)CH^+$	(ani)(tol)CHOAr'	1.38×10^{-4}	480	3.86×10^{6}
F147-1	$(ani)PhCH^+$	(ani)PhCHOAr'	1.36×10^{-4}	455	7.91×10^{6}

[a] OAr' = 4-cyanophenoxide

40E60W

$(ind)_2CH^+$ in 40E60W in presence of DABCO buffer (J&M, detection at 615 nm)

No.	$[(ind)_2CH^+]_0$, mol L^{-1}	$[\text{DABCO}]_{free}$, mol L^{-1}	$[\text{DABCO-H}^+]$, mol L^{-1}	k_{obs}, s^{-1}	conversion, %
535-1	7.28×10^{-6}	7.88×10^{-4}	4.59×10^{-4}	2.63×10^{-3}	93
535-2	7.25×10^{-6}	1.31×10^{-3}	4.57×10^{-4}	2.59×10^{-3}	95
535-3	7.06×10^{-6}	1.78×10^{-3}	4.46×10^{-4}	2.62×10^{-3}	93

$k = 2.61 \times 10^{-3}$ s^{-1}

$(dma)_2CH^+$ in 40E60W (J&M, detection at 605 nm)

No.	$[(dma)_2CH^+]_0$, mol L^{-1}	k_{obs}, s^{-1}	conversion, %
527-1	6.39×10^{-6}	6.42×10^{-2}	85
527-2	6.19×10^{-6}	5.05×10^{-2}	84
527-3	6.34×10^{-6}	6.00×10^{-2}	85
543-1	1.11×10^{-5}	5.58×10^{-2}	99
543-2	1.07×10^{-5}	5.67×10^{-2}	96
543-3	1.02×10^{-5}	5.56×10^{-2}	91

$k = 5.71 \times 10^{-2}$ s^{-1}

Ar_2CH^+ in 40E60W (Laser flash photolysis)

No.	Cation	Precursor [a]	$[\text{Precursor}]_0$, mol L^{-1}	Detection, nm	k_{obs}, s^{-1}
F43-5	$(ani)_2CH^+$	$(ani)_2CHOAr'$	1.99×10^{-4}	500	3.68×10^{5}
F55-5	$(ani)(tol)CH^+$	(ani)(tol)CHOAr'	1.38×10^{-4}	480	3.38×10^{6}
F147-3	$(ani)PhCH^+$	(ani)PhCHOAr'	1.36×10^{-4}	455	6.62×10^{6}

[a] OAr' = 4-cyanophenoxide

20E80W

$(thq)_2CH^+$ in 20E80W in presence of DABCO buffer (J&M, detection at 620 nm)

No.	$[(thq)_2CH^+]_0$, mol L^{-1}	$[DABCO]_{free}$, mol L^{-1}	$[DABCO\text{-}H^+]$, mol L^{-1}	k_{obs}, s^{-1}	conversion, %
531-1	9.81×10^{-6}	6.66×10^{-4}	2.33×10^{-4}	2.76×10^{-3}	97
531-2	9.63×10^{-6}	1.31×10^{-3}	2.30×10^{-4}	2.96×10^{-3}	98
531-3	9.68×10^{-6}	1.97×10^{-3}	2.30×10^{-4}	3.00×10^{-3}	98

$k = 2.91 \times 10^{-3}$ s^{-1}

Ar_2CH^+ in 20E80W (Laser flash photolysis)

No.	Cation	Precursor [a]	$[Precursor]_0$, mol L^{-1}	Detection, nm	k_{obs}, s^{-1}
F43-6	$(ani)_2CH^+$	$(ani)_2CHOAr'$	3.99×10^{-5}	500	2.20×10^{5}
F55-6	$(ani)(tol)CH^+$	(ani)(tol)CHOAr'	5.52×10^{-5}	480	2.72×10^{6}

[a] OAr' = 4-cyanophenoxide

10E90W

$(thq)_2CH^+$ in 10E90W in presence of DABCO buffer (J&M, detection at 620 nm)

No.	$[(thq)_2CH^+]_0$, mol L^{-1}	$[DABCO]_{free}$, mol L^{-1}	$[DABCO\text{-}H^+]$, mol L^{-1}	k_{obs}, s^{-1}	conversion, %
533-1	9.95×10^{-6}	8.10×10^{-4}	4.72×10^{-4}	2.39×10^{-3}	92
533-2	9.99×10^{-6}	1.36×10^{-3}	4.74×10^{-4}	2.36×10^{-3}	95
533-3	9.95×10^{-6}	1.81×10^{-3}	4.53×10^{-4}	2.54×10^{-3}	94

$k = 2.43 \times 10^{-3}$ s^{-1}

Ar_2CH^+ in 10E90W at 20 °C (Laser flash photolysis)

No.	Cation	Precursor [a]	$[Precursor]_0$, mol L^{-1}	Detection, nm	k_{obs}, s^{-1}
F152-2	$(ani)_2CH^+$	$(ani)_2CHOAc$	1.59×10^{-4}	500	1.38×10^{5}
F152-5	$(ani)(tol)CH^+$	(ani)(tol)CHOAc	1.52×10^{-4}	480	9.54×10^{5}

[a] OAc = acetate

Trifluoroethanol-Water Mixtures

90T10W

Ar_2CH^+ in 90T10W at 20 °C (Stopped-flow)

No.	Cation	$[Ar_2CH^+]_0$, mol L^{-1}	Detection, nm	k_{obs}, s^{-1}
525-1	$(dpa)_2CH^+$	1.22×10^{-5}	660	3.76×10^{-2}
525-2	$(mfa)_2CH^+$	1.12×10^{-5}	585	1.23×10^{-1}
525-3	$(pfa)_2CH^+$	2.10×10^{-5}	590	3.01×10^{-1}

Ar_2CH^+ in 90T10W at 20 °C (Laser flash photolysis)

No.	Cation	Precursor [a]	[Precursor]$_0$, mol L^{-1}	Detection, nm	k_{obs}, s^{-1}
F142-1	(ani)$_2$CH$^+$	(ani)$_2$CHOAc	1.59×10^{-4}	500	6.50×10^{2}
F151-1	(ani)(tol)CH$^+$	(ani)(tol)CHOAc	1.52×10^{-4}	480	1.28×10^{4}
F24-1	(ani)PhCH$^+$	(ani)PhCHOAr'	2.03×10^{-4}	455	4.01×10^{4}
F11-1	(tol)$_2$CH$^+$	(tol)$_2$CHOAr'	9.44×10^{-5}	460	4.32×10^{5}
F62-1	(tol)PhCH$^+$	(tol)PhCHOAr'	9.44×10^{-5}	450	2.45×10^{6}

[a] OAr' = 4-cyanophenoxide, OAc = acetate

80T20W

Ar_2CH^+ in 80T20W at 20 °C (Stopped-flow)

No.	Cation	[Ar$_2$CH$^+$]$_0$, mol L^{-1}	Detection, nm	k_{obs}, s^{-1}
525-4	(dpa)$_2$CH$^+$	1.22×10^{-5}	660	6.59×10^{-2}
525-5	(mfa)$_2$CH$^+$	1.12×10^{-5}	585	1.53×10^{-1}
525-6	(pfa)$_2$CH$^+$	2.10×10^{-5}	590	5.55×10^{-1}

Ar_2CH^+ in 80T20W at 20 °C (Laser flash photolysis)

No.	Cation	Precursor [a]	[Precursor]$_0$, mol L^{-1}	Detection, nm	k_{obs}, s^{-1}
F142-2	(ani)$_2$CH$^+$	(ani)$_2$CHOAc	1.59×10^{-4}	500	2.55×10^{3}
F151-2	(ani)(tol)CH$^+$	(ani)(tol)CHOAc	1.52×10^{-4}	480	2.35×10^{4}
F24-2	(ani)PhCH$^+$	(ani)PhCHOAr'	2.03×10^{-4}	455	3.45×10^{4}
F11-2	(tol)$_2$CH$^+$	(tol)$_2$CHOAr'	9.44×10^{-5}	460	9.11×10^{5}
F62-2	(tol)PhCH$^+$	(tol)PhCHOAr'	9.44×10^{-5}	450	4.19×10^{6}

[a] OAr' = 4-cyanophenoxide, OAc = acetate

60T40W

Ar_2CH^+ in 60T40W at 20 °C (Stopped-flow)

No.	Cation	[Ar$_2$CH$^+$]$_0$, mol L^{-1}	Detection, nm	k_{obs}, s^{-1}
525-7	(dpa)$_2$CH$^+$	1.22×10^{-5}	660	7.96×10^{-2}
525-8	(mfa)$_2$CH$^+$	1.12×10^{-5}	585	1.90×10^{-1}
525-9	(pfa)$_2$CH$^+$	2.10×10^{-5}	590	9.37×10^{-1}

Ar_2CH^+ in 60T40W at 20 °C (Laser flash photolysis)

No.	Cation	Precursor [a]	[Precursor]$_0$, mol L^{-1}	Detection, nm	k_{obs}, s^{-1}
F142-3	(ani)$_2$CH$^+$	(ani)$_2$CHOAc	1.59×10^{-4}	500	6.04×10^{3}
F53-3	(ani)(tol)CH$^+$	(ani)(tol)CHOAr'	1.38×10^{-4}	480	5.46×10^{4}
F151-3		(ani)(tol)CHOAc	1.52×10^{-4}	480	5.23×10^{4}
F24-3	(ani)PhCH$^+$	(ani)PhCHOAr'	2.03×10^{-4}	455	1.27×10^{5}
F11-6	(tol)$_2$CH$^+$	(tol)$_2$CHOAr'	9.44×10^{-5}	460	1.24×10^{6}
F62-3	(tol)PhCH$^+$	(tol)PhCHOAr'	9.44×10^{-5}	450	6.95×10^{6}

[a] OAr' = 4-cyanophenoxide, OAc = acetate

50T50W

Ar_2CH^+ in 50T50W at 20 °C (Stopped-flow)

No.	Cation	$[Ar_2CH^+]_0$, mol L^{-1}	Detection, nm	k_{obs}, s^{-1}
525-10	$(dpa)_2CH^+$	1.22×10^{-5}	660	1.12×10^{-1}
525-11	$(mfa)_2CH^+$	1.12×10^{-5}	585	2.57×10^{-1}
525-12	$(pfa)_2CH^+$	2.10×10^{-5}	590	1.34

Ar_2CH^+ in 50T50W at 20 °C (Laser flash photolysis)

No.	Cation	Precursor [a]	$[\text{Precursor}]_0$, mol L^{-1}	Detection, nm	k_{obs}, s^{-1}
F142-4	$(ani)_2CH^+$	$(ani)_2CHOAc$	1.59×10^{-4}	500	7.03×10^{3}
F53-4	$(ani)(tol)CH^+$	(ani)(tol)CHOAr'	1.38×10^{-4}	480	7.11×10^{4}
F24-4	$(ani)PhCH^+$	(ani)PhCHOAr'	2.03×10^{-4}	455	1.66×10^{5}
F11-4	$(tol)_2CH^+$	$(tol)_2CHOAr'$	9.44×10^{-5}	460	1.39×10^{6}
F62-4	$(tol)PhCH^+$	(tol)PhCHOAr'	9.44×10^{-5}	450	8.20×10^{6}

[a] OAr' = 4-cyanophenoxide, OAc = acetate

40T60W

Ar_2CH^+ in 40T60W at 20 °C (Stopped-flow)

No.	Cation	$[Ar_2CH^+]_0$, mol L^{-1}	Detection, nm	k_{obs}, s^{-1}
525-13	$(mor)_2CH^+$	8.80×10^{-6}	610	4.79×10^{-2}
525-14	$(dpa)_2CH^+$	1.22×10^{-5}	660	1.20×10^{-1}
525-15	$(mfa)_2CH^+$	1.12×10^{-5}	585	3.27×10^{-1}
525-16	$(pfa)_2CH^+$	2.10×10^{-5}	590	1.79

Ar_2CH^+ in 40T60W at 20 °C (Laser flash photolysis)

No.	Cation	Precursor [a]	$[\text{Precursor}]_0$, mol L^{-1}	Detection, nm	k_{obs}, s^{-1}
F142-5	$(ani)_2CH^+$	$(ani)_2CHOAc$	1.59×10^{-4}	500	9.95×10^{3}
F53-5	$(ani)(tol)CH^+$	(ani)(tol)CHOAr'	1.38×10^{-4}	480	1.02×10^{5}
F24-5	$(ani)PhCH^+$	(ani)PhCHOAr'	2.03×10^{-4}	455	2.26×10^{5}
F11-7	$(tol)_2CH^+$	$(tol)_2CHOAr'$	9.44×10^{-5}	460	1.41×10^{6}
F146-1	$(tol)PhCH^+$	(tol)PhCHOAr'	9.48×10^{-5}	450	1.07×10^{7}

[a] OAr' = 4-cyanophenoxide, OAc = acetate

20T80W

Ar_2CH^+ in 20T80W at 20 °C (Stopped-flow)

No.	Cation	$[Ar_2CH^+]_0$, mol L^{-1}	Detection, nm	k_{obs}, s^{-1}
525-17	$(mor)_2CH^+$	8.80×10^{-6}	610	2.69×10^{-1}
525-18	$(dpa)_2CH^+$	1.22×10^{-5}	660	*a*
525-19	$(mfa)_2CH^+$	1.12×10^{-5}	585	1.48
525-20	$(pfa)_2CH^+$	2.10×10^{-5}	590	*a*

[a] non-single exponemtial curve.

Ar_2CH^+ in 20T80W at 20 °C (Laser flash photolysis)

No.	Cation	Precursor [a]	[Precursor]$_0$, mol L^{-1}	Detection, nm	k_{obs}, s^{-1}
F142-6	$(ani)_2CH^+$	$(ani)_2CHOAc$	1.59×10^{-4}	500	4.05×10^{4}
F53-6	$(ani)(tol)CH^+$	(ani)(tol)CHOAr'	1.38×10^{-4}	480	3.31×10^{5}
F24-6	$(ani)PhCH^+$	(ani)PhCHOAr'	7.68×10^{-5}	455	1.20×10^{6}
F164-5	$(tol)_2CH^+$	$(tol)_2CHOAr'$	7.60×10^{-5}	460	5.57×10^{6}
F146-2	$(tol)PhCH^+$	(tol)PhCHOAr'	9.48×10^{-5}	450	1.92×10^{7}

[a] OAr' = 4-cyanophenoxide, OAc = acetate

10T90W

Ar_2CH^+ in 10T90W at 20 °C (Stopped-flow)

No.	Cation	$[Ar_2CH^+]_0$, mol L^{-1}	Detection, nm	k_{obs}, s^{-1}
525-21	$(mor)_2CH^+$	8.80×10^{-6}	610	7.09×10^{-1}
525-22	$(dpa)_2CH^+$	1.22×10^{-5}	660	*a*
525-23	$(mfa)_2CH^+$	1.12×10^{-5}	585	3.80
525-24	$(pfa)_2CH^+$	2.10×10^{-5}	590	*a*

[a] non-single exponemtial curve.

Ar_2CH^+ in 10T90W at 20 °C (Laser flash photolysis)

No.	Cation	Precursor [a]	[Precursor]$_0$, mol L^{-1}	Detection, nm	k_{obs}, s^{-1}
F142-7	$(ani)_2CH^+$	$(ani)_2CHOAc$	1.59×10^{-4}	500	7.95×10^{4}
F151-4	$(ani)(tol)CH^+$	(ani)(tol)CHOAc	1.38×10^{-4}	480	5.78×10^{5}
F146-4	$(ani)PhCH^+$	(ani)PhCHOAr'	1.01×10^{-4}	455	2.59×10^{6}

[a] OAr' = 4-cyanophenoxide, OAc = acetate

Ethanol-Acetonitrile Mixtures

Ethanol

$(lil)_2CH^+$ in ethanol at 20 °C (J&M, detection at 630 nm)

No.	$[(lil)_2CH^+]_0$, mol L^{-1}	k_{obs}, s^{-1}	conversion, %
280-1	4.15×10^{-6}	5.69×10^{-3}	98
280-2	4.07×10^{-6}	5.67×10^{-3}	98
280-3	4.13×10^{-6}	5.58×10^{-3}	99
280-4	4.00×10^{-6}	5.85×10^{-3}	97

$k = 5.70 \times 10^{-3}$ s^{-1}

$(jul)_2CH^+$ in ethanol at 20 °C (J&M, detection at 635 nm)

No.	$[(jul)_2CH^+]_0$, mol L^{-1}	k_{obs}, s^{-1}	conversion, %
319-1	1.14×10^{-5}	1.51×10^{-2}	99
319-2	1.13×10^{-5}	1.51×10^{-2}	99
319-3	1.12×10^{-5}	1.53×10^{-2}	98
319-4	1.14×10^{-5}	1.53×10^{-2}	99

$k = 1.52 \times 10^{-2}$ s^{-1}

$(ind)_2CH^+$ in ethanol at 20 °C (J&M, detection at 615 nm)

No.	$[(ind)_2CH^+]_0$, mol L^{-1}	k_{obs}, s^{-1}	conversion, %
283-1	1.00×10^{-5}	5.79×10^{-2}	98
283-2	1.03×10^{-5}	5.68×10^{-2}	98
283-3	1.04×10^{-5}	5.91×10^{-2}	99
283-4	1.06×10^{-5}	5.64×10^{-2}	97

$k = 5.75 \times 10^{-2}\ s^{-1}$

$(thq)_2CH^+$ in ethanol at 20 °C (J&M, detection at 620 nm)

No.	$[(thq)_2CH^+]_0$, mol L^{-1}	k_{obs}, s^{-1}	conversion, %
289-1	8.75×10^{-6}	1.62×10^{-1}	96
289-2	8.70×10^{-6}	1.64×10^{-1}	96
289-3	8.88×10^{-6}	1.64×10^{-1}	96
289-4	8.70×10^{-6}	1.64×10^{-1}	96
289-5	8.70×10^{-6}	1.64×10^{-1}	96

$k = 1.63 \times 10^{-1}\ s^{-1}$

Ar_2CH^+ in ethanol at 20 °C (Laser flash photolysis)

No.	Cation	Precursor [a]	$[Precursor]_0$, mol L^{-1}	Detection, nm	k_{obs}, s^{-1}
F51-1	*(ani)(tol)CH*$^+$	*(ani)(tol)CHOAr'*	1.38×10^{-4}	*480*	8.68×10^{6}
F22-8	*(ani)PhCH*$^+$	*(ani)PhCHOAr'*	1.92×10^{-4}	*455*	9.56×10^{6}

[a] OAr' = 4-cyanophenoxide

91E9AN

$(lil)_2CH^+$ in 91E9AN at 20 °C (J&M, detection at 630 nm)

No.	$[(lil)_2CH^+]_0$, mol L^{-1}	k_{obs}, s^{-1}	conversion, %
420-1	8.15×10^{-6}	3.52×10^{-3}	99
420-2	7.82×10^{-6}	3.52×10^{-3}	98
420-3	7.23×10^{-6}	3.53×10^{-3}	98

$k = 3.52 \times 10^{-3}\ s^{-1}$

$(ind)_2CH^+$ in 91E9AN at 20 °C (J&M, detection at 615 nm)

No.	$[(lil)_2CH^+]_0$, mol L^{-1}	k_{obs}, s^{-1}	conversion, %
415-1	7.38×10^{-6}	3.80×10^{-2}	97
415-2	6.48×10^{-6}	3.78×10^{-2}	95
415-3	7.09×10^{-6}	3.86×10^{-2}	96

$k = 3.82 \times 10^{-2}\ s^{-1}$

Ar$_2$CH$^+$ in 91E9AN at 20 °C (Stopped-flow)

No.	Cation	[Ar$_2$CH$^+$]$_0$, mol L^{-1}	Detection, nm	k_{obs}, s^{-1}
325-1	(pyr)$_2$CH$^+$	2.60×10^{-6}	610	2.72×10^{-1}
325-2	(dma)$_2$CH$^+$	7.38×10^{-6}	605	9.24×10^{-1}
325-3	(mpa)$_2$CH$^+$	5.72×10^{-6}	610	1.45×10^{1}
325-4	(mor)$_2$CH$^+$	6.76×10^{-6}	610	1.38×10^{1}
325-5	(dpa)$_2$CH$^+$	3.00×10^{-6}	660	2.60×10^{2}
325-6	(mfa)$_2$CH$^+$	4.12×10^{-6}	585	2.55×10^{2}

Ar$_2$CH$^+$ in 91E9AN at 20 °C (Laser flash photolysis)

No.	Cation	Precursor [a]	[Precursor]$_0$, mol L^{-1}	Detection, nm	k_{obs}, s^{-1}
F15-7	(ani)$_2$CH$^+$	(ani)$_2$CHOAr'	1.35×10^{-4}	500	4.33×10^{6}
F51-2	*(ani)(tol)CH*$^+$	*(ani)(tol)CHOAr'*	1.38×10^{-4}	*480*	1.05×10^{7}
F22-7	*(ani)PhCH*$^+$	*(ani)PhCHOAr'*	1.92×10^{-4}	*455*	9.04×10^{6}

[a] OAr' = 4-cyanophenoxide

80E20A

(lil)$_2$CH$^+$ in 80E20AN at 20 °C (J&M, detection at 630 nm)

No.	[(lil)$_2$CH$^+$]$_0$, mol L^{-1}	k_{obs}, s^{-1}	conversion, %
419-1	8.74×10^{-6}	2.12×10^{-3}	99
419-2	8.26×10^{-6}	2.13×10^{-3}	97
419-3	7.75×10^{-6}	2.09×10^{-3}	97

$k = 2.12 \times 10^{-3}$ s^{-1}

(ind)$_2$CH$^+$ in 80E20AN at 20 °C (J&M, detection at 615 nm)

No.	[(ind)$_2$CH$^+$]$_0$, mol L^{-1}	k_{obs}, s^{-1}	conversion, %
422-1	8.04×10^{-6}	2.43×10^{-2}	93
422-2	8.46×10^{-6}	2.40×10^{-2}	96
422-3	8.54×10^{-6}	2.38×10^{-2}	96

$k = 2.40 \times 10^{-2}$ s^{-1}

Ar$_2$CH$^+$ in 80E20AN at 20 °C (Stopped-flow)

No.	Cation	[Ar$_2$CH$^+$]$_0$, mol L^{-1}	Detection, nm	k_{obs}, s^{-1}
328-1	(pyr)$_2$CH$^+$	2.60×10^{-6}	610	2.27×10^{-1}
328-2	(dma)$_2$CH$^+$	7.38×10^{-6}	605	6.78×10^{-1}
328-3	(mpa)$_2$CH$^+$	5.72×10^{-6}	610	1.14×10^{1}
328-4	(mor)$_2$CH$^+$	6.76×10^{-6}	610	1.07×10^{1}
328-5	(dpa)$_2$CH$^+$	3.00×10^{-6}	660	2.22×10^{2}
328-6	(mfa)$_2$CH$^+$	4.12×10^{-6}	585	2.07×10^{2}

Ar_2CH^+ in 80E20AN at 20 °C (Laser flash photolysis)

No.	Cation	Precursor [a]	$[Precursor]_0$, mol L^{-1}	Detection, nm	k_{obs}, s^{-1}
F15-6	$(ani)_2CH^+$	$(ani)_2CHOAr'$	2.95×10^{-4}	500	3.02×10^{6}
F51-3	*$(ani)(tol)CH^+$*	*(ani)(tol)CHOAr'*	*1.38×10^{-4}*	*480*	*1.08×10^{7}*
F22-6	*$(ani)PhCH^+$*	*(ani)PhCHOAr'*	*1.92×10^{-4}*	*455*	*8.98×10^{6}*

[a] OAr' = 4-cyanophenoxide

67E33AN

$(lil)_2CH^+$ in 67E33AN at 20 °C (J&M, detection at 630 nm)

No.	$[(lil)_2CH^+]_0$, mol L^{-1}	k_{obs}, s^{-1}	conversion, %
417-1	9.16×10^{-6}	1.27×10^{-3}	98
417-2	8.31×10^{-6}	1.25×10^{-3}	99
417-3	8.34×10^{-6}	1.27×10^{-3}	98

$k = 1.26 \times 10^{-3}$ s^{-1}

$(ind)_2CH^+$ in 67E33AN at 20 °C (J&M, detection at 615 nm)

No.	$[(ind)_2CH^+]_0$, mol L^{-1}	k_{obs}, s^{-1}	conversion, %
413-1	6.80×10^{-6}	1.43×10^{-2}	98
413-2	6.77×10^{-6}	1.47×10^{-2}	96
413-3	6.86×10^{-6}	1.48×10^{-2}	97

$k = 1.46 \times 10^{-2}$ s^{-1}

Ar_2CH^+ in 67E33AN at 20 °C (Stopped-flow)

No.	Cation	$[Ar_2CH^+]_0$, mol L^{-1}	Detection, nm	k_{obs}, s^{-1}
327-1	$(pyr)_2CH^+$	2.60×10^{-6}	610	1.39×10^{-1}
327-2	$(dma)_2CH^+$	7.38×10^{-6}	605	4.51×10^{-1}
327-3	$(mpa)_2CH^+$	5.72×10^{-6}	610	7.92
327-4	$(mor)_2CH^+$	6.76×10^{-6}	610	7.60
327-5	$(dpa)_2CH^+$	3.00×10^{-6}	660	1.65×10^{2}
327-6	$(mfa)_2CH^+$	4.12×10^{-6}	585	1.53×10^{2}

Ar_2CH^+ in 67E33AN at 20 °C (Laser flash photolysis)

No.	Cation	Precursor [a]	$[Precursor]_0$, mol L^{-1}	Detection, nm	k_{obs}, s^{-1}
F15-5	$(ani)_2CH^+$	$(ani)_2CHOAr'$	2.95×10^{-4}	500	2.30×10^{6}
F51-4	$(ani)(tol)CH^+$	(ani)(tol)CHOAr'	1.38×10^{-4}	480	1.23×10^{7}
F22-5	*$(ani)PhCH^+$*	*(ani)PhCHOAr'*	*1.92×10^{-4}*	*455*	*1.07×10^{7}*

[a] OAr' = 4-cyanophenoxide

50E50AN

(lil)$_2$CH$^+$ in 50E50AN at 20 °C (J&M, detection at 630 nm)

No.	[(lil)$_2$CH$^+$]$_0$, mol L^{-1}	k_{obs}, s^{-1}	conversion, %
281-1	3.97×10^{-6}	6.72×10^{-4}	98
281-2	3.95×10^{-6}	6.62×10^{-4}	95
281-3	3.95×10^{-6}	6.64×10^{-4}	99
281-4	3.98×10^{-6}	6.60×10^{-4}	99

$k = 6.65 \times 10^{-4}$ s^{-1}

(ind)$_2$CH$^+$ in 50E50AN at 20 °C (J&M, detection at 615 nm)

No.	[(ind)$_2$CH$^+$]$_0$, mol L^{-1}	k_{obs}, s^{-1}	conversion, %
282-1	5.06×10^{-6}	7.99×10^{-3}	91
282-2	1.01×10^{-5}	7.93×10^{-3}	93
282-3	1.01×10^{-5}	7.98×10^{-3}	93
282-4	1.02×10^{-5}	7.91×10^{-3}	93

$k = 7.95 \times 10^{-3}$ s^{-1}

Ar$_2$CH$^+$ in 50E50AN at 20 °C (Stopped-flow)

No.	Cation	[Ar$_2$CH$^+$]$_0$, mol L^{-1}	Detection, nm	k_{obs}, s^{-1}
280-1	(thq)$_2$CH$^+$	5.42×10^{-6}	615	2.32×10^{-2}
280-2	(pyr)$_2$CH$^+$	3.89×10^{-6}	610	7.04×10^{-2}
280-3	(dma)$_2$CH$^+$	4.06×10^{-6}	605	2.46×10^{-1}
280-4	(mpa)$_2$CH$^+$	1.24×10^{-5}	610	2.49
280-5	(dpa)$_2$CH$^+$	8.50×10^{-6}	660	5.39×10^{1}
280-6	(mfa)$_2$CH$^+$	1.75×10^{-5}	585	5.23×10^{1}
280-7	(pfa)$_2$CH$^+$	2.45×10^{-6}	590	4.05×10^{2}

Ar$_2$CH$^+$ in 50E50AN at 20 °C (Laser flash photolysis)

No.	Cation	Precursor [a]	[Precursor]$_0$, mol L^{-1}	Detection, nm	k_{obs}, s^{-1}
F15-4	(ani)$_2$CH$^+$	(ani)$_2$CHOAr'	2.95×10^{-4}	500	1.41×10^{6}
F51-5	(ani)(tol)CH$^+$	(ani)(tol)CHOAr'	1.38×10^{-4}	480	1.21×10^{7}
F22-4	*(ani)PhCH$^+$*	*(ani)PhCHOAr'*	*1.92×10^{-4}*	*455*	*1.10×10^{7}*

[a] OAr' = 4-cyanophenoxide

33E67AN

(ind)$_2$CH$^+$ in 33E67AN at 20 °C (J&M, detection at 630 nm)

No.	[(ind)$_2$CH$^+$]$_0$, mol L^{-1}	k_{obs}, s^{-1}	conversion, %
412-1	6.75×10^{-6}	3.97×10^{-3}	95
412-2	7.00×10^{-6}	3.99×10^{-3}	96
412-3	6.74×10^{-6}	3.93×10^{-3}	99

$k = 3.97 \times 10^{-3}$ s^{-1}

$(pyr)_2CH^+$ in 33E67AN at 20 °C (J&M, detection at 615 nm)

No.	$[(pyr)_2CH^+]_0$, mol L^{-1}	k_{obs}, s^{-1}	conversion, %
421-1	4.06×10^{-6}	3.70×10^{-2}	92
421-2	4.44×10^{-6}	3.63×10^{-2}	96
421-3	4.81×10^{-6}	3.68×10^{-2}	95

$k = 3.67 \times 10^{-2}$ s^{-1}

Ar_2CH^+ in 33E67AN at 20 °C (Stopped-flow)

No.	Cation	$[Ar_2CH^+]_0$, mol L^{-1}	Detection, nm	k_{obs}, s^{-1}
411-1	$(dma)_2CH^+$	6.83×10^{-6}	605	1.40×10^{-1}
411-2	$(mpa)_2CH^+$	1.47×10^{-5}	610	1.63
411-3	$(mor)_2CH^+$	1.97×10^{-5}	610	1.68
411-4	$(dpa)_2CH^+$	9.67×10^{-6}	660	4.03×10^{1}
411-5	$(mfa)_2CH^+$	2.42×10^{-6}	585	4.05×10^{1}
411-6	$(pfa)_2CH^+$	1.77×10^{-5}	590	3.11×10^{2}

Ar_2CH^+ in 33E67AN at 20 °C (Laser flash photolysis)

No.	Cation	Precursor [a]	$[Precursor]_0$, mol L^{-1}	Detection, nm	k_{obs}, s^{-1}
F15-3	$(ani)_2CH^+$	$(ani)_2CHOAr'$	2.95×10^{-4}	500	8.77×10^{5}
F51-6	$(ani)(tol)CH^+$	(ani)(tol)CHOAr'	1.38×10^{-4}	480	8.48×10^{6}
F22-3	$(ani)PhCH^+$	(ani)PhCHOAr'	1.92×10^{-4}	455	1.18×10^{7}

[a] OAr' = 4-cyanophenoxide

20E80AN

$(ind)_2CH^+$ in 20E80AN at 20 °C (J&M, detection at 615 nm)

No.	$[(ind)_2CH^+]_0$, mol L^{-1}	k_{obs}, s^{-1}	conversion, %
414-1	6.82×10^{-6}	2.37×10^{-3}	58
414-2	6.48×10^{-6}	2.26×10^{-3}	67
414-3	6.50×10^{-6}	2.33×10^{-3}	60

$k = 2.32 \times 10^{-3}$ s^{-1}

$(pyr)_2CH^+$ in 20E80AN at 20 °C (J&M, detection at 610 nm)

No.	$[(pyr)_2CH^+]_0$, mol L^{-1}	k_{obs}, s^{-1}	conversion, %
418-1	5.03×10^{-6}	1.80×10^{-2}	78
418-2	4.73×10^{-6}	1.78×10^{-3}	84
418-3	4.47×10^{-6}	1.77×10^{-3}	81

$k = 1.78 \times 10^{-2}$ s^{-1}

Ar_2CH^+ in 20E80AN at 20 °C (Stopped-flow)

No.	Cation	$[Ar_2CH^+]_0$, mol L^{-1}	Detection, nm	k_{obs}, s^{-1}
411-7	$(mpa)_2CH^+$	1.47×10^{-5}	610	9.54×10^{-1}
411-8	$(mor)_2CH^+$	1.97×10^{-5}	610	9.05×10^{-1}
411-9	$(dpa)_2CH^+$	9.67×10^{-6}	660	2.18×10^{1}
411-10	$(mfa)_2CH^+$	2.42×10^{-6}	585	2.24×10^{1}
411-11	$(pfa)_2CH^+$	1.77×10^{-5}	590	1.72×10^{2}

Ar_2CH^+ in 20E80AN at 20 °C (Laser flash photolysis)

No.	Cation	Precursor [a]	$[Precursor]_0$, mol L^{-1}	Detection, nm	k_{obs}, s^{-1}
F15-2	$(ani)_2CH^+$	$(ani)_2CHOAr'$	2.95×10^{-4}	500	5.33×10^{5}
F51-7	$(ani)(tol)CH^+$	(ani)(tol)CHOAr'	1.38×10^{-4}	480	5.99×10^{6}
F22-2	$(ani)PhCH^+$	(ani)PhCHOAr'	1.92×10^{-4}	455	9.41×10^{6}

[a] OAr' = 4-cyanophenoxide

10E90AN

Ar_2CH^+ in 10E90AN at 20 °C (Stopped-flow)

No.	Cation	$[Ar_2CH^+]_0$, mol L^{-1}	Detection, nm	k_{obs}, s^{-1}
442-1	$(mpa)_2CH^+$	3.66×10^{-6}	610	2.87×10^{-1}
442-2	$(mor)_2CH^+$	3.06×10^{-6}	610	2.96×10^{-1}
442-3	$(dpa)_2CH^+$	1.61×10^{-5}	660	7.28
442-4	$(mfa)_2CH^+$	8.78×10^{-6}	585	7.07
442-5	$(pfa)_2CH^+$	1.06×10^{-5}	590	5.86×10^{1}

Ar_2CH^+ in 10E90AN at 20 °C (Laser flash photolysis)

No.	Cation	Precursor [a]	$[Precursor]_0$, mol L^{-1}	Detection, nm	k_{obs}, s^{-1}
F15-1	$(ani)_2CH^+$	$(ani)_2CHOAr'$	2.95×10^{-4}	500	3.06×10^{5}
F51-8	$(ani)(tol)CH^+$	(ani)(tol)CHOAr'	1.38×10^{-4}	480	2.44×10^{6}
F22-1	$(ani)PhCH^+$	(ani)PhCHOAr'	1.92×10^{-4}	455	4.80×10^{6}

[a] OAr' = 4-cyanophenoxide

Methanol-Acetonitrile Mixtures

MeOH

$(lil)_2CH^+$ in methanol at 20 °C (J&M, detection at 630 nm)

No.	$[(lil)_2CH^+]_0$, mol L^{-1}	k_{obs}, s^{-1}	conversion, %
257-1	7.06×10^{-6}	6.39×10^{-3}	99
257-2	8.65×10^{-6}	6.10×10^{-3}	98
257-3	7.83×10^{-6}	6.30×10^{-3}	99
257-4	9.40×10^{-6}	6.10×10^{-3}	96

$k = 6.23 \times 10^{-3}\ s^{-1}$

(ind)$_2$CH$^+$ in methanol at 20 °C (J&M, detection at 615 nm)

No.	[(ind)$_2$CH$^+$]$_0$, mol L^{-1}	k_{obs}, s^{-1}	conversion, %
259-1	6.54×10^{-6}	6.09×10^{-2}	99
259-2	5.65×10^{-6}	5.79×10^{-2}	96
259-3	5.81×10^{-6}	6.15×10^{-2}	97
259-4	5.99×10^{-6}	5.99×10^{-2}	97

$k = 6.00 \times 10^{-2}$ s^{-1}

Ar$_2$CH$^+$ in methanol at 20 °C (Laser flash photolysis)

No.	Cation	Precursor [a]	[Precursor]$_0$, mol L^{-1}	Detection, nm	k_{obs}, s^{-1}
F49-1	*(ani)(tol)CH*$^+$	*(ani)(tol)CHOAr'*	*1.38×10^{-4}*	*480*	*1.33×10^{7}*
F121-1	*(ani)PhCH*$^+$	*(ani)PhCHOAr'*	*2.13×10^{-4}*	*455*	*1.15×10^{7}*

[a] OAr' = 4-cyanophenoxide

91M9AN

(lil)$_2$CH$^+$ in 91M9AN at 20 °C (J&M, detection at 630 nm)

No.	[(lil)$_2$CH$^+$]$_0$, mol L^{-1}	k_{obs}, s^{-1}	conversion, %
299-1	4.37×10^{-6}	6.41×10^{-3}	96
299-2	4.43×10^{-6}	6.20×10^{-3}	94
299-3	4.34×10^{-6}	6.10×10^{-3}	98
299-4	4.41×10^{-6}	6.11×10^{-3}	97
299-5	4.24×10^{-6}	5.88×10^{-3}	97

$k = 6.14 \times 10^{-3}$ s^{-1}

Ar$_2$CH$^+$ in 91M9AN at 20 °C (Stopped-flow)

No.	Cation	[Ar$_2$CH$^+$]$_0$, mol L^{-1}	Detection, nm	k_{obs}, s^{-1}
308-1	(thq)$_2$CH$^+$	5.92×10^{-6}	620	2.17×10^{-1}
305-2	(pyr)$_2$CH$^+$	4.24×10^{-6}	610	9.32×10^{-1}
305-3	(dma)$_2$CH$^+$	7.38×10^{-6}	605	2.31
305-1	(mpa)$_2$CH$^+$	6.76×10^{-6}	610	2.79×10^{1}
305-4	(mor)$_2$CH$^+$	5.72×10^{-6}	610	2.65×10^{1}
308-2	(dpa)$_2$CH$^+$	3.00×10^{-6}	660	3.60×10^{2}
308-3	(mfa)$_2$CH$^+$	4.12×10^{-6}	585	4.02×10^{2}

Ar$_2$CH$^+$ in 91M9AN at 20 °C (Laser flash photolysis)

No.	Cation	Precursor [a]	[Precursor]$_0$, mol L^{-1}	Detection, nm	k_{obs}, s^{-1}
F13-8	(ani)$_2$CH$^+$	(ani)$_2$CHOAr'	1.18×10^{-4}	500	4.95×10^{6}
F49-2	*(ani)(tol)CH*$^+$	*(ani)(tol)CHOAr'*	*1.38×10^{-4}*	*480*	*1.39×10^{7}*
F121-2	*(ani)PhCH*$^+$	*(ani)PhCHOAr'*	*2.13×10^{-4}*	*455*	*9.88×10^{6}*

[a] OAr' = 4-cyanophenoxide

80M20AN

(lil)$_2$CH$^+$ in 80M20AN at 20 °C (J&M, detection at 630 nm)

No.	[(lil)$_2$CH$^+$]$_0$, mol L^{-1}	k_{obs}, s^{-1}	conversion, %
341-1	4.35×10^{-6}	3.52×10^{-3}	89
341-2	4.65×10^{-6}	3.41×10^{-3}	96
341-3	4.57×10^{-6}	3.63×10^{-3}	91
341-4	4.57×10^{-6}	3.39×10^{-3}	93

$k = 3.49 \times 10^{-3}$ s^{-1}

Ar$_2$CH$^+$ in 80M20AN at 20 °C (Stopped-flow)

No.	Cation	[Ar$_2$CH$^+$]$_0$, mol L^{-1}	Detection, nm	k_{obs}, s^{-1}
306-1	(pyr)$_2$CH$^+$	4.24×10^{-6}	610	4.64×10^{-1}
306-2	(dma)$_2$CH$^+$	7.38×10^{-6}	605	1.30
306-3	(mpa)$_2$CH$^+$	6.76×10^{-6}	610	1.85×10^{1}
306-4	(mor)$_2$CH$^+$	5.72×10^{-6}	610	1.82×10^{1}
308-4	(dpa)$_2$CH$^+$	3.00×10^{-6}	660	2.89×10^{2}
308-5	(mfa)$_2$CH$^+$	4.12×10^{-6}	585	3.11×10^{2}

Ar$_2$CH$^+$ in 80M20AN at 20 °C (Laser flash photolysis)

No.	Cation	Precursor [a]	[Precursor]$_0$, mol L^{-1}	Detection, nm	k_{obs}, s^{-1}
F13-7	(ani)$_2$CH$^+$	(ani)$_2$CHOAr'	1.18×10^{-4}	500	4.12×10^{6}
F49-3	*(ani)(tol)CH$^+$*	*(ani)(tol)CHOAr'*	1.38×10^{-4}	*480*	1.20×10^{7}
F121-3	*(ani)PhCH$^+$*	*(ani)PhCHOAr'*	2.13×10^{-4}	*455*	8.55×10^{6}

[a] OAr' = 4-cyanophenoxide

67M33AN

(lil)$_2$CH$^+$ in 67M33AN at 20 °C (J&M, detection at 630 nm)

No.	[(lil)$_2$CH$^+$]$_0$, mol L^{-1}	k_{obs}, s^{-1}	conversion, %
261-1	1.03×10^{-5}	2.00×10^{-3}	96
261-2	9.93×10^{-6}	1.96×10^{-3}	98
261-3	1.03×10^{-5}	2.03×10^{-3}	98
261-4	9.77×10^{-6}	2.00×10^{-3}	97

$k = 1.99 \times 10^{-3}$ s^{-1}

Ar$_2$CH$^+$ in 67M33AN at 20 °C (Stopped-flow)

No.	Cation	[Ar$_2$CH$^+$]$_0$, mol L^{-1}	Detection, nm	k_{obs}, s^{-1}
307-1	(pyr)$_2$CH$^+$	4.24×10^{-6}	610	3.27×10^{-1}
307-2	(dma)$_2$CH$^+$	7.38×10^{-6}	605	8.82×10^{-1}
307-3	(mpa)$_2$CH$^+$	6.76×10^{-6}	610	1.32×10^{1}
307-4	(mor)$_2$CH$^+$	5.72×10^{-6}	610	1.28×10^{1}
308-6	(dpa)$_2$CH$^+$	3.00×10^{-6}	660	2.23×10^{2}
308-7	(mfa)$_2$CH$^+$	4.12×10^{-6}	585	2.42×10^{2}

Ar_2CH^+ in 67M33AN at 20 °C (Laser flash photolysis)

No.	Cation	Precursor [a]	[Precursor]$_0$, mol L^{-1}	Detection, nm	k_{obs}, s^{-1}
F13-6	(ani)$_2$CH$^+$	(ani)$_2$CHOAr'	1.18×10^{-4}	500	3.48×10^{6}
F49-4	*(ani)(tol)CH*$^+$	*(ani)(tol)CHOAr'*	*1.38×10^{-4}*	*480*	*1.24×10^{7}*
F121-4	*(ani)PhCH*$^+$	*(ani)PhCHOAr'*	*2.13×10^{-4}*	*455*	*8.87×10^{6}*

[a] OAr' = 4-cyanophenoxide

50M50AN

(lil)$_2$CH$^+$ in 50M50AN at 20 °C (J&M, detection at 630 nm)

No.	[(lil)$_2$CH$^+$]$_0$, mol L^{-1}	k_{obs}, s^{-1}	conversion, %
262-1	6.13×10^{-6}	1.16×10^{-3}	98
262-2	5.77×10^{-6}	1.18×10^{-3}	97
262-3	5.88×10^{-6}	1.17×10^{-3}	98
262-4	5.55×10^{-6}	1.17×10^{-3}	98

$k = 1.17 \times 10^{-3}$ s^{-1}

(ind)$_2$CH$^+$ in 50M50AN at 20 °C (J&M, detection at 615 nm)

No.	[(ind)$_2$CH$^+$]$_0$, mol L^{-1}	k_{obs}, s^{-1}	conversion, %
264-1	7.84×10^{-6}	1.34×10^{-2}	99
264-2	7.36×10^{-6}	1.35×10^{-2}	99
264-3	7.14×10^{-6}	1.33×10^{-2}	99
264-4	6.83×10^{-6}	1.33×10^{-2}	99

$k = 1.34 \times 10^{-2}$ s^{-1}

Ar_2CH^+ in 50M50AN at 20 °C (Stopped-flow)

No.	Cation	[Ar$_2$CH$^+$]$_0$, mol L^{-1}	Detection, nm	k_{obs}, s^{-1}
266-1	(dma)$_2$CH$^+$	3.16×10^{-6}	605	4.36×10^{-1}
266-2	(mpa)$_2$CH$^+$	6.25×10^{-6}	610	4.81
266-3	(dpa)$_2$CH$^+$	6.37×10^{-6}	660	9.52×10^{1}
266-4	(mfa)$_2$CH$^+$	3.59×10^{-6}	585	1.22×10^{2}

Ar_2CH^+ in 50M50AN at 20 °C (Laser flash photolysis)

No.	Cation	Precursor [a]	[Precursor]$_0$, mol L^{-1}	Detection, nm	k_{obs}, s^{-1}
F13-5	(ani)$_2$CH$^+$	(ani)$_2$CHOAr'	1.18×10^{-4}	500	2.33×10^{6}
F49-5	(ani)(tol)CH$^+$	(ani)(tol)CHOAr'	1.38×10^{-4}	480	1.47×10^{7}
F121-5	*(ani)PhCH*$^+$	*(ani)PhCHOAr'*	*2.13×10^{-4}*	*455*	*9.16×10^{6}*

[a] OAr' = 4-cyanophenoxide

33M67AN

(lil)$_2$CH$^+$ in 33M67AN at 20 °C (J&M, detection at 630 nm)

No.	[(lil)$_2$CH$^+$]$_0$, mol L^{-1}	k_{obs}, s^{-1}	conversion, %
369-1	4.46×10^{-6}	5.75×10^{-4}	98
369-2	4.81×10^{-6}	6.22×10^{-4}	97
369-3	4.41×10^{-6}	5.90×10^{-4}	96

$k = 5.96 \times 10^{-4}$ s^{-1}

$(ind)_2CH^+$ in 33M67AN at 20 °C (J&M, detection at 615 nm)

No.	$[(ind)_2CH^+]_0$, mol L^{-1}	k_{obs}, s^{-1}	conversion, %
378-1	6.78×10^{-6}	5.77×10^{-3}	99
378-2	6.80×10^{-6}	5.85×10^{-3}	96
378-3	6.83×10^{-6}	5.77×10^{-3}	96

$k = 5.80 \times 10^{-3}$ s^{-1}

Ar_2CH^+ in 33M67AN at 20 °C (Stopped-flow)

No.	Cation	$[Ar_2CH^+]_0$, mol L^{-1}	Detection, nm	k_{obs}, s^{-1}
391-1	$(dma)_2CH^+$	1.22×10^{-5}	605	2.62×10^{-1}
391-2	$(mpa)_2CH^+$	4.79×10^{-6}	610	3.85
391-3	$(mor)_2CH^+$	7.04×10^{-6}	610	3.51
391-4	$(dpa)_2CH^+$	9.67×10^{-6}	660	8.87×10^{1}
391-5	$(mfa)_2CH^+$	1.06×10^{-5}	585	8.46×10^{1}
391-6	$(pfa)_2CH^+$	6.36×10^{-6}	590	4.85×10^{2}

Ar_2CH^+ in 33M67AN at 20 °C (Laser flash photolysis)

No.	Cation	Precursor [a]	$[Precursor]_0$, mol L^{-1}	Detection, nm	k_{obs}, s^{-1}
F13-4	$(ani)_2CH^+$	$(ani)_2CHOAr'$	1.18×10^{-4}	500	1.54×10^{6}
F49-6	$(ani)(tol)CH^+$	$(ani)(tol)CHOAr'$	1.38×10^{-4}	480	1.33×10^{7}
F21-3	*$(ani)PhCH^+$*	*$(ani)PhCHOAr'$*	*1.92×10^{-4}*	*455*	*1.00×10^{7}*

[a] OAr' = 4-cyanophenoxide

20M80AN

$(ind)_2CH^+$ in 20M80AN at 20 °C (J&M, detection at 615 nm)

No.	$[(ind)_2CH^+]_0$, mol L^{-1}	k_{obs}, s^{-1}	conversion, %
371-1	6.44×10^{-6}	3.08×10^{-3}	93
371-2	6.56×10^{-6}	3.08×10^{-3}	97
371-3	6.54×10^{-6}	3.12×10^{-3}	98

$k = 3.09 \times 10^{-3}$ s^{-1}

$(thq)_2CH^+$ in 20M80AN at 20 °C (J&M, detection at 620 nm)

No.	$[(thq)_2CH^+]_0$, mol L^{-1}	k_{obs}, s^{-1}	conversion, %
377-1	5.08×10^{-6}	6.54×10^{-3}	95
377-2	4.87×10^{-6}	6.71×10^{-3}	95
377-3	5.01×10^{-6}	6.41×10^{-3}	91

$k = 6.55 \times 10^{-3}$ s^{-1}

Ar_2CH^+ in 20M80AN at 20 °C (Stopped-flow)

No.	Cation	$[Ar_2CH^+]_0$, mol L^{-1}	Detection, nm	k_{obs}, s^{-1}
392-1	$(dma)_2CH^+$	1.22×10^{-5}	605	1.22×10^{-1}
392-2	$(mpa)_2CH^+$	4.79×10^{-6}	610	2.15
392-3	$(mor)_2CH^+$	7.04×10^{-6}	610	1.96
392-4	$(dpa)_2CH^+$	9.67×10^{-6}	660	5.43×10^{1}
392-5	$(mfa)_2CH^+$	1.06×10^{-5}	585	4.81×10^{1}
392-6	$(pfa)_2CH^+$	6.36×10^{-6}	590	3.58×10^{2}

Ar_2CH^+ in 20M80AN at 20 °C (Laser flash photolysis)

No.	Cation	Precursor [a]	[Precursor]$_0$, mol L^{-1}	Detection, nm	k_{obs}, s^{-1}
F13-2	(ani)$_2$CH$^+$	(ani)$_2$CHOAr'	1.18×10^{-4}	500	8.58×10^{5}
F49-7	(ani)(tol)CH$^+$	(ani)(tol)CHOAr'	1.38×10^{-4}	480	9.91×10^{6}
F21-2	*(ani)PhCH$^+$*	*(ani)PhCHOAr'*	*1.92×10^{-4}*	*455*	*1.07×10^{7}*

[a] OAr' = 4-cyanophenoxide

10M90AN

$(ind)_2CH^+$ in 10M90AN at 20 °C (J&M, detection at 615 nm)

No.	[(ind)$_2$CH$^+$]$_0$, mol L^{-1}	k_{obs}, s^{-1}	conversion, %
374-1	6.61×10^{-6}	8.47×10^{-4}	94
374-2	5.56×10^{-6}	7.46×10^{-4}	91
374-3	6.06×10^{-6}	7.24×10^{-4}	94

$k = 7.72 \times 10^{-4}$ s^{-1}

$(pyr)_2CH^+$ in 10M90AN at 20 °C (J&M, detection at 610 nm)

No.	[(pyr)$_2$CH$^+$]$_0$, mol L^{-1}	k_{obs}, s^{-1}	conversion, %
376-1	3.60×10^{-6}	7.15×10^{-3}	88
376-2	3.55×10^{-6}	6.93×10^{-3}	93
376-3	3.46×10^{-6}	7.14×10^{-3}	82

$k = 7.07 \times 10^{-3}$ s^{-1}

$(dma)_2CH^+$ in 10M90AN at 20 °C (J&M, detection at 605 nm)

No.	[(dma)$_2$CH$^+$]$_0$, mol L^{-1}	k_{obs}, s^{-1}	conversion, %
385-1	1.15×10^{-5}	4.25×10^{-2}	89
385-2	1.14×10^{-5}	3.60×10^{-2}	86
416-1	2.60×10^{-5}	3.24×10^{-2}	98
416-2	2.18×10^{-5}	3.80×10^{-2}	93
416-3	1.90×10^{-5}	4.37×10^{-2}	86
416-4	2.38×10^{-5}	4.10×10^{-2}	84
416-5	2.17×10^{-5}	4.13×10^{-2}	84

$k = 3.93 \times 10^{-2}$ s^{-1}

Ar_2CH^+ in 10M90AN at 20 °C (Stopped-flow)

No.	Cation	[Ar$_2$CH$^+$]$_0$, mol L^{-1}	Detection, nm	k_{obs}, s^{-1}
393-1	(mpa)$_2$CH$^+$	4.79×10^{-6}	610	7.21×10^{-1}
393-2	(mor)$_2$CH$^+$	7.04×10^{-6}	610	6.83×10^{-1}
393-3	(dpa)$_2$CH$^+$	9.67×10^{-6}	660	1.78×10^{1}
393-4	(mfa)$_2$CH$^+$	1.06×10^{-5}	585	1.64×10^{1}
393-5	(pfa)$_2$CH$^+$	6.36×10^{-6}	590	1.60×10^{2}

Ar_2CH^+ in 10M90AN at 20 °C (Laser flash photolysis)

No.	Cation	Precursor [a]	[Precursor]$_0$, mol L^{-1}	Detection, nm	k_{obs}, s^{-1}
F148-1	(ani)$_2$CH$^+$	(ani)$_2$CHOAr'	1.66×10^{-4}	500	4.20×10^{5}
F49-8	(ani)(tol)CH$^+$	(ani)(tol)CHOAr'	1.38×10^{-4}	480	6.22×10^{6}
F21-1	*(ani)PhCH$^+$*	*(ani)PhCHOAr'*	*1.92×10^{-4}*	*455*	*7.47×10^{6}*

[a] OAr' = 4-cyanophenoxide

Water-Acetone Mixtures:

20W80A

Ar_2CH^+ in 20W80A at 20 °C (Stopped-flow)

No.	Cation	$[Ar_2CH^+]_0$, mol L^{-1}	Detection, nm	k_{obs}, s^{-1}
575-5	$(mpa)_2CH^+$	4.09×10^{-5}	590	1.90×10^{2}
575-4	$(mor)_2CH^+$	1.71×10^{-5}	585	1.90×10^{1}
575-3	$(dpa)_2CH^+$	7.73×10^{-6}	660	3.07×10^{1}
575-2	$(mfa)_2CH^+$	8.36×10^{-6}	610	9.34×10^{-1}
575-1	$(pfa)_2CH^+$	9.26×10^{-6}	610	1.20

$(ind)_2CH^+$ in 20W80A in the presence of *N*-methylmorpholine (J&M, detection at 615 nm)

No.	$[(ind)_2CH^+]_0$, mol L^{-1}	[*N*-methylmorpholine], mol L^{-1}	k_{obs}, s^{-1}
713-1	1.39×10^{-5}	2.33×10^{-4}	2.06×10^{-3}
713-2	1.40×10^{-5}	4.70×10^{-4}	2.10×10^{-3}
713-3	1.41×10^{-5}	7.10×10^{-4}	2.08×10^{-3}
			$k = 2.08 \times 10^{-3}$ s^{-1}

$(lil)_2CH^+$ in 20W80A in the presence of sodium acetate (J&M, detection at 630 nm)

No.	$[(lil)_2CH^+]_0$, mol L^{-1}	[NaOAc], mol L^{-1}	k_{obs}, s^{-1}
715-2	1.18×10^{-5}	2.88×10^{-4}	1.99×10^{-4}
715-1	1.15×10^{-5}	5.64×10^{-4}	2.17×10^{-4}
709-1	7.06×10^{-6}	1.01×10^{-3}	2.31×10^{-4}
			$k = 1.89 \times 10^{-4}$ s^{-1}

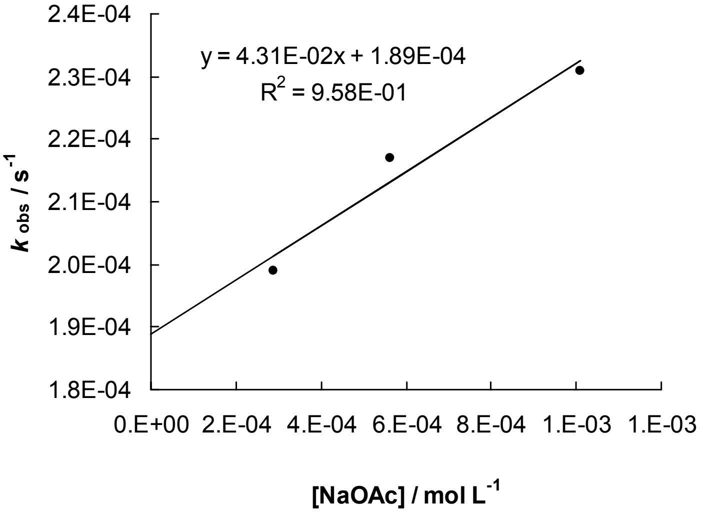

10W90A

Ar_2CH^+ in 10W90A at 20 °C (Stopped-flow)

No.	Cation	$[Ar_2CH^+]_0$, mol L^{-1}	Detection, nm	k_{obs}, s^{-1}
575-10	$(mpa)_2CH^+$	4.09×10^{-5}	590	1.37×10^{2}
575-9	$(mor)_2CH^+$	1.71×10^{-5}	585	1.78×10^{1}
575-8	$(dpa)_2CH^+$	7.73×10^{-6}	660	2.47×10^{1}
575-7	$(mfa)_2CH^+$	8.36×10^{-6}	610	7.75×10^{-1}
575-6	$(pfa)_2CH^+$	9.26×10^{-6}	610	9.40×10^{-1}

$(ind)_2CH^+$ in 10W90A in the presence of *N*-methylmorpholine (J&M, detection at 615 nm)

No.	$[(ind)_2CH^+]_0$, mol L^{-1}	[*N*-methylmorpholine], mol L^{-1}	k_{obs}, s^{-1}
712-1	1.34×10^{-5}	2.82×10^{-3}	1.84×10^{-3}
712-2	1.38×10^{-5}	5.80×10^{-3}	1.80×10^{-3}
712-3	1.39×10^{-5}	8.75×10^{-3}	1.87×10^{-3}
			$k = 1.84 \times 10^{-3}$ s^{-1}

$(lil)_2CH^+$ in 10W90A in the presence of sodium acetate (J&M, detection at 630 nm)

No.	$[(lil)_2CH^+]_0$, mol L^{-1}	[NaOAc], mol L^{-1}	k_{obs}, s^{-1}
711-1	7.21×10^{-6}	3.45×10^{-4}	2.44×10^{-4}
714-1	1.16×10^{-5}	5.69×10^{-4}	2.59×10^{-4}
714-2	1.19×10^{-5}	8.70×10^{-4}	2.79×10^{-4}
			$k = 2.21 \times 10^{-4}$ s^{-1}

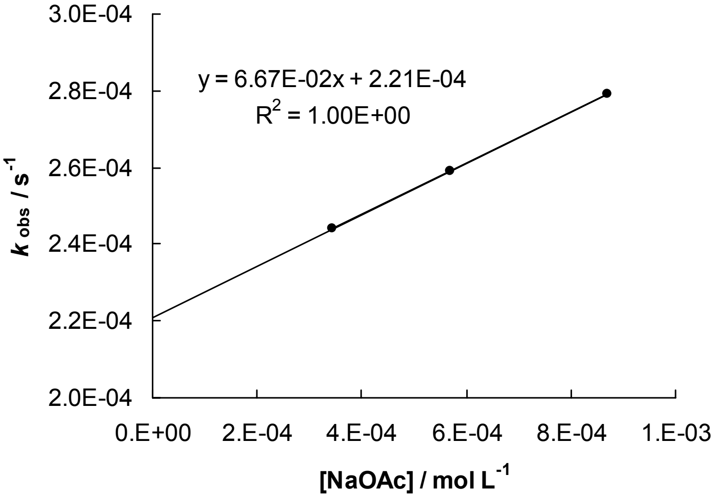

7.4. Complete energy profiles for S_N1 solvolyses

7.4.1 Introduction of eqs 5.5 and 5.6[10,11]

$$\mathrm{A} \underset{k_2}{\overset{k_1}{\rightleftharpoons}} \mathrm{B} \qquad (7.7)$$

$$\mathrm{A} \xrightarrow{k_3} \mathrm{C} \qquad (7.8)$$

In the parallel two first-order reactions in which one step is reversible (eqs. 7.7 and 7.8), the set of differential equations is given by

$$d[\mathrm{A}]/dt = -(k_1 + k_3)[\mathrm{A}] + k_2[\mathrm{B}] \qquad (7.9)$$

$$d[\mathrm{B}]/dt = k_1[\mathrm{A}] - k_2[\mathrm{B}] \qquad (7.10)$$

$$d[\mathrm{C}]/dt = k_3[\mathrm{A}] \qquad (7.11)$$

$$[\mathrm{A}] + [\mathrm{B}] + [\mathrm{C}] = [\mathrm{A}]_0 \qquad (7.12)$$

Differentiating eq. 7.9 with respect to *t* leads to

$$d^2[\mathrm{A}]/\mathrm{d}t^2 = -(k_1 + k_3)\, d[\mathrm{A}]/dt + k_2\, d[\mathrm{B}]/dt \qquad (7.13)$$

From eqs. 7.9 and 7.10

$$d[\mathrm{B}]/dt = -k_3[\mathrm{A}] - d[\mathrm{A}]/dt \qquad (7.14)$$

Elimination of [B] and d[B]/dt from eqs. 7.13 and 7.14 gives

$$d^2[\mathrm{A}]/\mathrm{d}t^2 + (k_1 + k_2 + k_3)d[\mathrm{A}]/dt + k_2k_3[\mathrm{A}] = 0 \qquad (7.15)$$

The general solution of eq. 7.15 is [12]

$$[A] = A_1[\exp(-r_1\mathrm{t})] + A_2[\exp(-r_2\mathrm{t})] \qquad (5.5)$$

$$r_1, r_2 = 1/2[k_1 + k_2 + k_3 \pm \{(k_1 + k_2 + k_3){}^\wedge 2 - 4k_2k_3)\}{}^\wedge 0.5] \qquad (7.16)$$

Therefore

$$r_1 + r_2 = k_1 + k_2 + k_3 \qquad (7.17)$$

$$r_1 + r_2 = k_{2,\mathrm{X}^-}[\mathrm{X}^-] + k_{\mathrm{SOH}} + k_{\mathrm{ionization}} \qquad (5.6)$$

7.4.2 Kinetics of halide anions with benzhydrylium ions.

Chloride ion ($n\mathrm{Bu_4N^+Cl^-}$)

$(\mathrm{ani})_2\mathrm{CH}^+$ from $(\mathrm{ani})_2\mathrm{CHOAr} + \mathrm{Cl}^-$ in methanol at 20°C (laser flash, detection at 500 nm).[a]

No.	[Precursor]$_0$, mol L^{-1}	[Cl$^-$] mol L^{-1}	k_{obs}, s^{-1}
F-63-1	1.99×10^{-4}	1.67×10^{-3}	6.34×10^{6}
F-63-2	1.99×10^{-4}	3.33×10^{-3}	6.61×10^{6}
F-63-3	1.99×10^{-4}	5.00×10^{-3}	6.50×10^{6}
F-63-4	1.99×10^{-4}	6.67×10^{-3}	6.72×10^{6}
F-63-5	1.99×10^{-4}	8.34×10^{-3}	6.62×10^{6}
F-63-6	1.99×10^{-4}	1.00×10^{-2}	7.38×10^{6}
F-63-7	1.99×10^{-4}	2.00×10^{-3}	7.40×10^{6}
F-63-8	1.99×10^{-4}	3.00×10^{-3}	7.85×10^{6}
F-63-9	1.99×10^{-4}	3.59×10^{-3}	8.15×10^{6}
F-63-10	1.99×10^{-4}	4.00×10^{-3}	8.59×10^{6}
F-63-11	1.99×10^{-4}	4.28×10^{-3}	8.69×10^{6}

[a] OAr = 4-cyanophenoxide

$k_2 = 5.33 \times 10^{7}$ L mol^{-1}s^{-1}

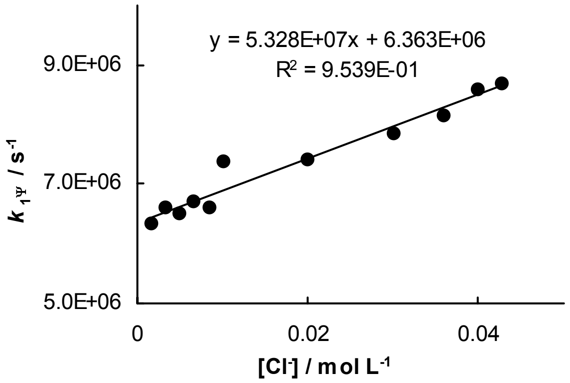

$(ani)_2CH^+$ from $(ani)_2CHOAr + Cl^-$ in ethanol at 20°C (laser flash, detection at 500 nm).[a]

No.	$[Precursor]_0$, mol L^{-1}	$[Cl^-]$ mol L^{-1}	k_{obs}, s^{-1}
F73-1	1.99×10^{-4}	8.85×10^{-4}	6.48×10^{6}
F73-2	1.99×10^{-4}	3.01×10^{-3}	8.26×10^{6}
F73-3	1.99×10^{-4}	4.96×10^{-3}	9.74×10^{6}
F73-4	1.99×10^{-4}	7.08×10^{-3}	1.08×10^{7}
F73-5	1.99×10^{-4}	8.85×10^{-3}	1.22×10^{7}
F73-6	*1.99×10^{-4}*	*1.20×10^{-2}*	*1.22×10^{7}*
F73-7	*1.99×10^{-4}*	*1.50×10^{-2}*	*1.24×10^{7}*
F73-8	*1.99×10^{-4}*	*1.77×10^{-2}*	*1.38×10^{7}*

[a] OAr = 4-cyanophenoxide

$k_2 = 6.99 \times 10^8$ L $mol^{-1}s^{-1}$

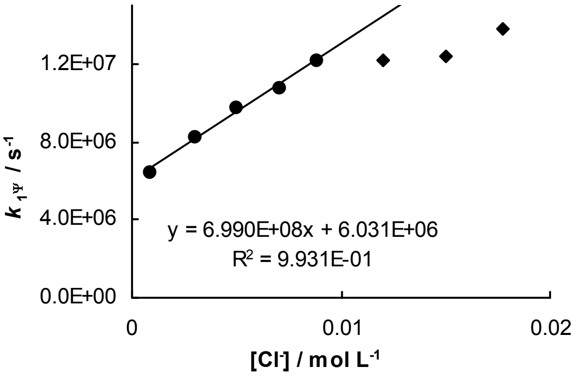

$(ani)_2CH^+$ from $(ani)_2CHOAr + Cl^-$ in 80E20W at 20°C (laser flash, detection at 500 nm).[a]

No.	$[Precursor]_0$, mol L^{-1}	$[Cl^-]$ mol L^{-1}	k_{obs}, s^{-1}
F76-1	1.99×10^{-4}	5.57×10^{-3}	1.94×10^{6}
F76-2	1.99×10^{-4}	1.05×10^{-2}	2.19×10^{6}
F76-3	1.99×10^{-4}	1.55×10^{-2}	2.52×10^{6}
F76-4	1.99×10^{-4}	2.11×10^{-2}	2.70×10^{6}
F76-5	1.99×10^{-4}	2.60×10^{-2}	2.89×10^{6}
F76-6	1.99×10^{-4}	3.10×10^{-2}	3.44×10^{6}
F76-7	1.99×10^{-4}	3.72×10^{-2}	3.93×10^{6}
F76-8	*1.99×10^{-4}*	*4.34×10^{-2}*	*3.85×10^{6}*
F76-9	*1.99×10^{-4}*	*5.97×10^{-2}*	*3.82×10^{6}*
F76-10	*1.99×10^{-4}*	*8.01×10^{-2}*	*4.09×10^{6}*

[a] OAr = 4-cyanophenoxide

$k_2 = 6.05 \times 10^7$ L $mol^{-1}s^{-1}$

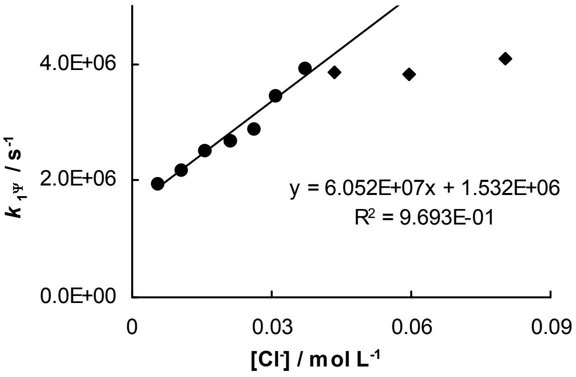

$(\text{ani})_2\text{CH}^+$ from $(\text{ani})_2\text{CHOAc} + \text{Cl}^-$ in 20W80AN at 20°C (laser flash, detection at 500 nm).[a]

No.	[Precursor]$_0$, mol L^{-1}	[Cl$^-$] mol L^{-1}	k_{obs}, s^{-1}
F168-1	1.59×10^{-4}	2.33×10^{-3}	3.45×10^{5}
F168-2	1.59×10^{-4}	3.26×10^{-3}	4.32×10^{5}
F168-3	1.59×10^{-4}	4.65×10^{-3}	5.53×10^{5}
F168-4	1.59×10^{-4}	6.98×10^{-3}	7.73×10^{5}
F168-5	1.59×10^{-4}	7.91×10^{-3}	9.05×10^{5}
F168-6	1.59×10^{-4}	9.30×10^{-3}	9.92×10^{5}
F168-7	1.59×10^{-4}	$\mathit{1.16} \times 10^{-2}$	$\mathit{1.03 \times 10^{6}}$

[a] OAc = acetate

$k_2 = 9.53 \times 10^{7}$ L $\text{mol}^{-1}\text{s}^{-1}$

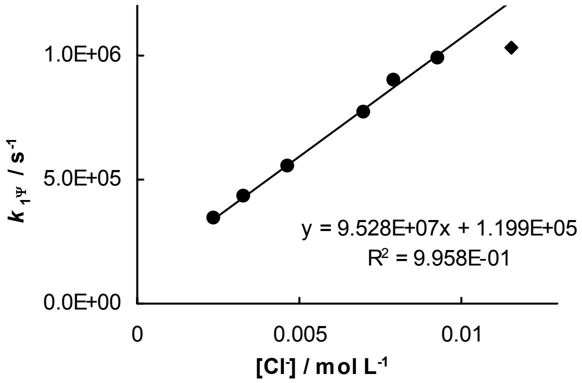

$(\text{ani})_2\text{CH}^+$ from $(\text{ani})_2\text{CHOAc} + \text{Cl}^-$ in 50W50E at 20°C (laser flash, detection at 500 nm).[a]

No.	[Precursor]$_0$, mol L^{-1}	[Cl$^-$] mol L^{-1}	k_{obs}, s^{-1}
F161-1	1.59×10^{-4}	2.03×10^{-3}	4.86×10^{5}
F161-2	1.59×10^{-4}	4.07×10^{-3}	5.34×10^{5}
F161-3	1.59×10^{-4}	6.10×10^{-3}	5.33×10^{5}
F161-4	1.59×10^{-4}	8.14×10^{-3}	5.42×10^{5}
F161-5	1.59×10^{-4}	1.02×10^{-2}	5.99×10^{5}
F161-6	1.59×10^{-4}	1.53×10^{-2}	6.60×10^{5}
F161-7	1.59×10^{-4}	1.86×10^{-2}	6.69×10^{5}
F161-8	1.59×10^{-4}	2.03×10^{-2}	7.25×10^{5}
F161-9	1.59×10^{-4}	2.54×10^{-2}	7.68×10^{5}

[a] OAc = acetate

$k_2 = 1.20 \times 10^{7}$ L $\text{mol}^{-1}\text{s}^{-1}$

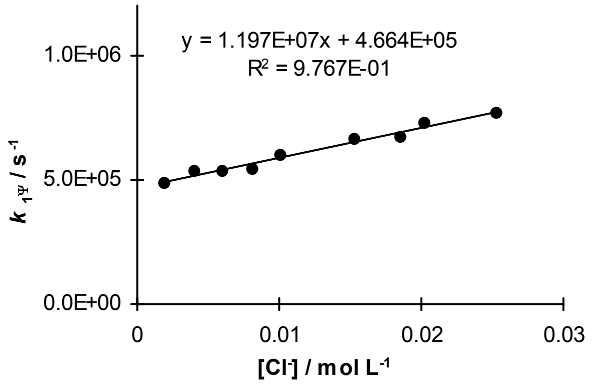

(ani)$_2$CH$^+$ from (ani)$_2$CHOAc + Cl$^-$ in 50M50AN at 20°C (laser flash, detection at 500 nm).[a]

No.	[Precursor]$_0$, mol L^{-1}	[Cl$^-$] mol L^{-1}	k_{obs}, s^{-1}
F154-1	1.59×10^{-4}	9.62×10^{-4}	2.42×10^{6}
F154-2	1.59×10^{-4}	1.92×10^{-3}	2.75×10^{6}
F154-3	1.59×10^{-4}	2.89×10^{-3}	3.01×10^{6}
F154-4	1.59×10^{-4}	3.85×10^{-3}	3.40×10^{6}
F154-5	1.59×10^{-4}	4.81×10^{-3}	3.55×10^{6}

[a] OAc = acetate.

$k_2 = 3.02 \times 10^8$ L mol^{-1}s^{-1}

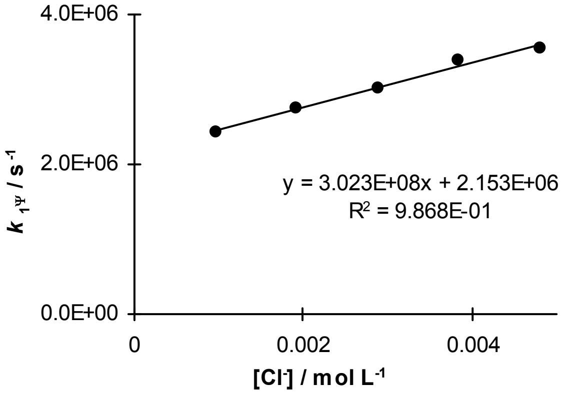

(ani)$_2$CH$^+$ from (ani)$_2$CHOAc + Cl$^-$ in 50E50AN at 20°C (laser flash, detection at 500 nm).[a]

No.	[Precursor]$_0$, mol L^{-1}	[Cl$^-$] mol L^{-1}	k_{obs}, s^{-1}
F153-1	1.59×10^{-4}	1.60×10^{-4}	1.46×10^{6}
F153-2	1.59×10^{-4}	3.21×10^{-4}	1.65×10^{6}
F153-3	1.59×10^{-4}	4.81×10^{-4}	1.98×10^{6}
F153-4	1.59×10^{-4}	6.41×10^{-4}	2.22×10^{6}
F153-5	1.59×10^{-4}	8.02×10^{-4}	2.55×10^{6}

[a] OAc = acetate.

$k_2 = 1.71 \times 10^9$ L mol^{-1}s^{-1}

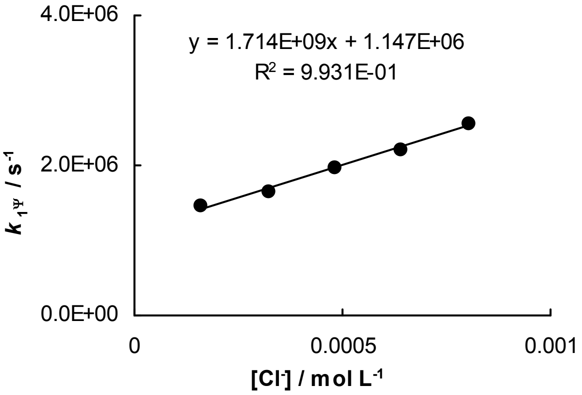

$(ani)_2CH^+$ from $(ani)_2CHOAr + Cl^-$ in 80W20AN at 20°C (laser flash, detection at 500 nm).[a]

No.	$[Precursor]_0$, mol L^{-1}	$[Cl^-]$ mol L^{-1}	$r_1 + r_2$ s^{-1}
F174-1	1.59×10^{-4}	8.09×10^{-3}	1.57×10^{5}
F174-2	1.59×10^{-4}	1.01×10^{-2}	1.62×10^{5}
F174-3	1.59×10^{-4}	2.43×10^{-2}	2.25×10^{5}
F174-4	1.59×10^{-4}	3.24×10^{-2}	2.41×10^{5}

[a] OAr = 4-cyanophenoxide

$k_2 = 3.23 \times 10^6$ L $mol^{-1}s^{-1s}$

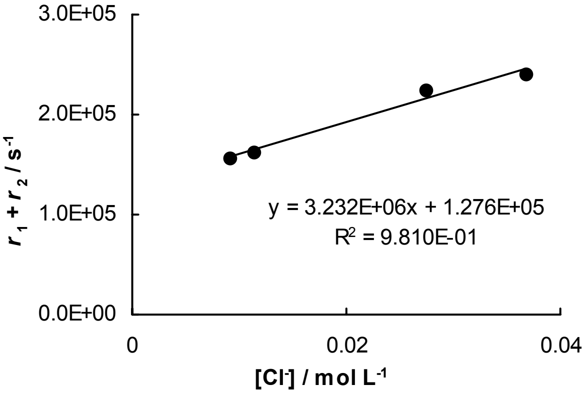

$(ani)_2CH^+$ from $(ani)_2CHOAc + Cl^-$ in 50W50AN at 20°C (laser flash, detection at 500 nm).[a]

No.	$[Precursor]_0$, mol L^{-1}	$[Cl^-]$ mol L^{-1}	k_{obs}, s^{-1}
F155-1	1.59×10^{-4}	9.62×10^{-4}	1.07×10^{5}
F155-2	1.59×10^{-4}	1.92×10^{-3}	1.24×10^{5}
F155-3	1.59×10^{-4}	2.89×10^{-3}	1.36×10^{5}
F155-4	1.59×10^{-4}	3.85×10^{-3}	1.50×10^{5}
F155-5	1.59×10^{-4}	4.81×10^{-3}	1.68×10^{5}
F155-6	1.59×10^{-4}	5.57×10^{-3}	1.80×10^{5}
F155-7	1.59×10^{-4}	6.73×10^{-3}	1.97×10^{5}
F155-8	1.59×10^{-4}	7.69×10^{-3}	2.04×10^{5}
F155-9	1.59×10^{-4}	8.66×10^{-3}	2.26×10^{5}
F155-10	1.59×10^{-4}	9.62×10^{-3}	2.25×10^{5}

[a] OAc = acetate.

$k_2 = 1.51 \times 10^7$ L $mol^{-1}s^{-1}$

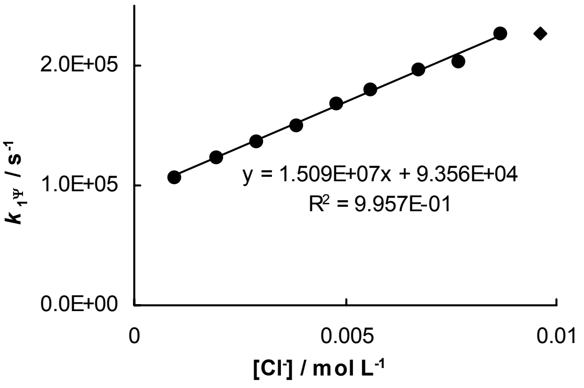

(ani)(tol)CH$^+$ from (ani)(tol)CHOAr + Cl$^-$ in 80E20W at 20°C (laser flash, detection at 480 nm).[a]

No.	[Precursor]$_0$, mol L^{-1}	[Cl$^-$] mol L^{-1}	k_{obs}, s^{-1}
F118-1	2.00×10^{-4}	2.14×10^{-3}	8.94×10^{6}
F118-2	2.00×10^{-4}	4.28×10^{-3}	1.03×10^{7}
F118-3	2.00×10^{-4}	6.42×10^{-3}	1.09×10^{7}
F118-4	2.00×10^{-4}	8.55×10^{-3}	1.21×10^{7}
F118-5	2.00×10^{-4}	1.07×10^{-2}	1.34×10^{7}

[a] OAr = 4-cyanophenoxide

$k_2 = 5.01 \times 10^8$ L mol^{-1}s^{-1}

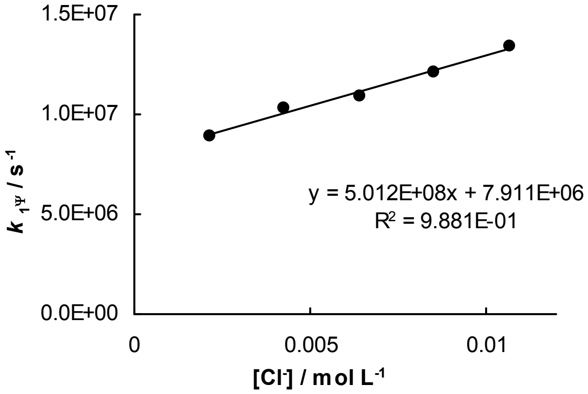

(ani)(tol)CH$^+$ from (ani)(tol)CHOAc + Cl$^-$ in 50W50AN at 20°C (laser flash, detection at 480 nm).[a]

No.	[Precursor]$_0$, mol L^{-1}	[Cl$^-$] mol L^{-1}	k_{obs}, s^{-1}
F169-1	1.50×10^{-4}	9.30×10^{-4}	9.31×10^{5}
F169-2	1.50×10^{-4}	1.86×10^{-3}	1.07×10^{6}
F169-3	1.50×10^{-4}	2.79×10^{-3}	1.18×10^{6}
F169-4	1.50×10^{-4}	3.72×10^{-3}	1.25×10^{6}
F169-5	1.50×10^{-4}	4.65×10^{-3}	1.31×10^{6}
F169-6	1.50×10^{-4}	7.91×10^{-3}	1.54×10^{6}
F169-7	1.50×10^{-4}	1.02×10^{-2}	1.93×10^{6}
F169-8	1.50×10^{-4}	1.49×10^{-2}	2.38×10^{6}

[a] OAc = 4-cyanophenoxide

$k_2 = 1.01 \times 10^8$ L mol^{-1}s^{-1}

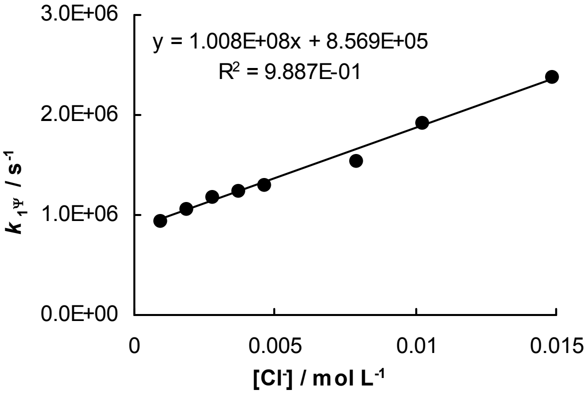

(ani)(tol)CH$^+$ from (ani)(tol)CHOAc + Cl$^-$ in 50E50W at 20°C (laser flash, detection at 480 nm).[a]

No.	[Precursor]$_0$, mol L^{-1}	[Cl$^-$] mol L^{-1}	k_{obs}, s^{-1}
F163-1	1.51×10^{-4}	3.39×10^{-3}	3.14×10^{6}
F163-2	1.51×10^{-4}	6.78×10^{-3}	3.51×10^{6}
F163-3	1.51×10^{-4}	1.02×10^{-2}	3.97×10^{6}
F163-4	1.51×10^{-4}	1.36×10^{-2}	4.49×10^{6}
F163-5	1.51×10^{-4}	1.70×10^{-2}	4.80×10^{6}

[a] OAr = acetate

$k_2 = 1.26 \times 10^8$ L mol^{-1}s^{-1}

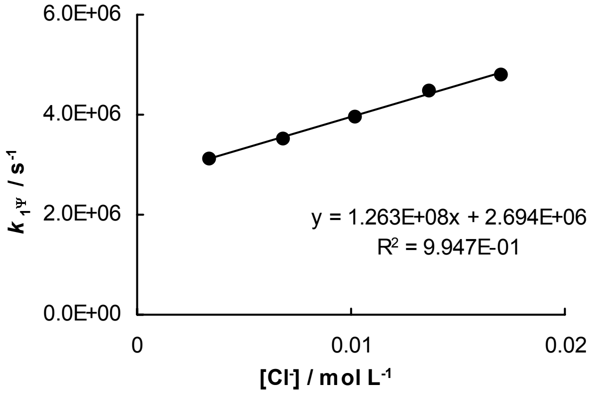

(ani)PhCH$^+$ from (ani)PhCHOAr + Cl$^-$ in 50E50W at 20°C (laser flash, detection at 460 nm).[a]

No.	[Precursor]$_0$, mol L^{-1}	[Cl$^-$] mol L^{-1}	k_{obs}, s^{-1}
F164-1	1.36×10^{-4}	6.78×10^{-4}	7.82×10^{6}
F164-2	1.36×10^{-4}	1.36×10^{-3}	7.98×10^{6}
F164-3	1.36×10^{-4}	2.03×10^{-3}	8.77×10^{6}
F164-4	1.36×10^{-4}	2.71×10^{-3}	8.72×10^{6}
F164-5	1.36×10^{-4}	3.39×10^{-3}	9.41×10^{6}
F164-6	1.36×10^{-4}	4.07×10^{-3}	9.91×10^{6}

[a] OAr = 4-cyanophenoxide

$k_2 = 6.19 \times 10^8$ L mol^{-1}s^{-1}

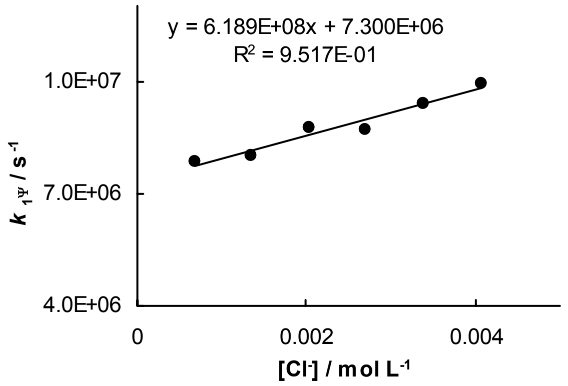

(ani)PhCH$^+$ from (ani)PhCHOAr + Cl$^-$ in 50W50AN at 20°C (laser flash, detection at 460 nm).[a]

No.	[Precursor]$_0$, mol L^{-1}	[Cl$^-$] mol L^{-1}	k_{obs}, s^{-1}
F170-1	1.36×10^{-4}	4.65×10^{-4}	2.13×10^{6}
F170-2	1.36×10^{-4}	9.30×10^{-4}	2.35×10^{6}
F170-3	1.36×10^{-4}	2.33×10^{-3}	2.75×10^{6}
F170-4	1.36×10^{-4}	3.26×10^{-3}	2.95×10^{6}
F170-5	1.36×10^{-4}	4.65×10^{-3}	3.26×10^{6}
F170-6	*1.36×10^{-4}*	*6.98×10^{-3}*	*3.42×10^{6}*
F170-7	*1.36×10^{-4}*	*9.30×10^{-3}*	*3.76×10^{6}*
F170-8	*1.36×10^{-4}*	*1.16×10^{-2}*	*4.26×10^{6}*
F170-9	*1.36×10^{-4}*	*1.40×10^{-2}*	*4.44×10^{6}*

[a] OAr = 4-cyanophenoxide

$k_2 = 2.64 \times 10^{8}$ L mol^{-1}s^{-1}

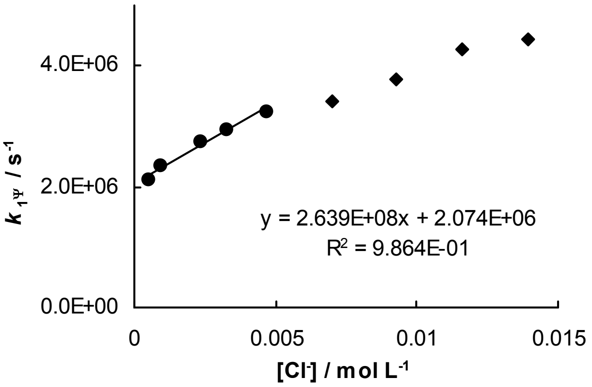

(ani)PhCH$^+$ from (ani)PhCHOAr + Cl$^-$ in TFE at 20°C (laser flash, detection at 460 nm).[a]

No.	[Precursor]$_0$, mol L^{-1}	[Cl$^-$] mol L^{-1}	k_{obs}, s^{-1}
F90-1	1.78×10^{-4}	2.15×10^{-3}	1.19×10^{5}
F90-2	1.78×10^{-4}	3.94×10^{-3}	1.71×10^{5}
F90-3	1.78×10^{-4}	6.09×10^{-3}	2.33×10^{5}
F90-4	1.78×10^{-4}	7.88×10^{-3}	2.72×10^{5}
F90-5	1.78×10^{-4}	1.00×10^{-2}	3.24×10^{5}

[a] OAr = 4-cyanophenoxide

$k_2 = 2.60 \times 10^{7}$ L mol^{-1}s^{-1}

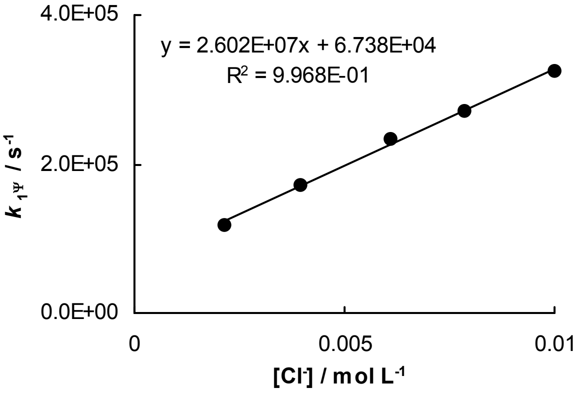

$(tol)_2CH^+$ from $(tol)_2CHOAr + Cl^-$ in TFE at 20°C (laser flash, detection at 460 nm).[a]

No.	$[Precursor]_0$, mol L^{-1}	$[Cl^-]$ mol L^{-1}	k_{obs}, s^{-1}
F84-1	9.44×10^{-5}	1.31×10^{-3}	7.40×10^{5}
F84-2	9.44×10^{-5}	2.61×10^{-3}	1.06×10^{6}
F84-3	9.44×10^{-5}	3.92×10^{-3}	1.41×10^{6}
F84-4	9.44×10^{-5}	5.23×10^{-3}	1.73×10^{6}
F84-5	9.44×10^{-5}	6.54×10^{-3}	2.06×10^{6}

[a] OAr = 4-cyanophenoxide

$k_2 = 2.53 \times 10^8$ L $mol^{-1}s^{-1}$

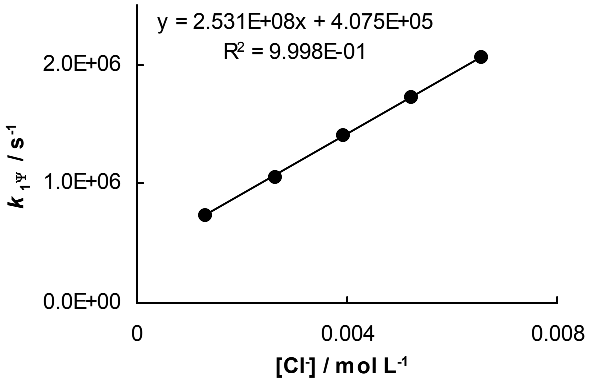

$(tol)PhCH^+$ from $(tol)PhCHOAr + Cl^-$ in TFE at 20°C (laser flash, detection at 450 nm).[a]

No.	$[Precursor]_0$, mol L^{-1}	$[Cl^-]$ mol L^{-1}	k_{obs}, s^{-1}
F92-1	1.74×10^{-4}	7.16×10^{-4}	1.59×10^{6}
F92-2	1.74×10^{-4}	1.59×10^{-3}	2.83×10^{6}
F92-3	1.74×10^{-4}	1.07×10^{-3}	2.08×10^{6}
F92-4	1.74×10^{-4}	2.51×10^{-3}	3.51×10^{6}
F92-5	1.74×10^{-4}	3.04×10^{-3}	3.82×10^{6}
F92-6	1.74×10^{-4}	3.58×10^{-3}	4.80×10^{6}
F92-7	1.74×10^{-4}	4.30×10^{-3}	5.64×10^{6}

[a] OAr = 4-cyanophenoxide

$k_2 = 1.07 \times 10^9$ L $mol^{-1}s^{-1}$

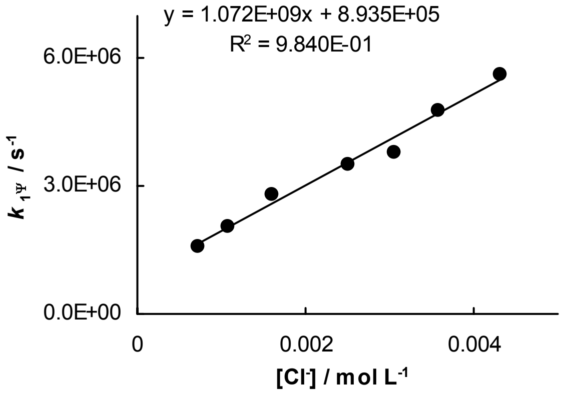

(tol)PhCH$^+$ from (tol)PhCHOAr + Cl$^-$ in HFIP at 20°C (laser flash, detection at 455 nm).[a]

No.	[Precursor]$_0$, mol L^{-1}	[Cl$^-$] mol L^{-1}	k_{obs}, s^{-1}
F139-1	2.88×10^{-4}	2.23×10^{-3}	1.52×10^{5}
F139-2	2.88×10^{-4}	4.46×10^{-3}	2.32×10^{5}
F139-3	2.88×10^{-4}	8.92×10^{-3}	3.85×10^{5}
F139-4	*2.88×10^{-4}*	*1.12×10^{-2}*	*4.30×10^{5}*
F139-5	*2.88×10^{-4}*	*1.20×10^{-2}*	*4.16×10^{5}*
F139-6	*2.88×10^{-4}*	*1.34×10^{-2}*	*4.30×10^{5}*
F139-7	*2.88×10^{-4}*	*2.68×10^{-2}*	*6.53×10^{5}*

[a] OAr = 4-cyanophenoxide

$k_2 = 3.47 \times 10^{7}$ L mol^{-1}s^{-1}

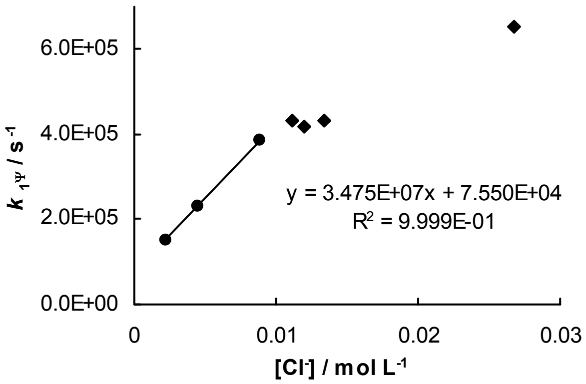

Ph$_2$CH$^+$ from Ph$_2$CHOAr + Cl$^-$ in HFIP at 20°C (laser flash, detection at 440 nm).[a]

No.	[Precursor]$_0$, mol L^{-1}	[Cl$^-$] mol L^{-1}	k_{obs}, s^{-1}
F138-1	2.23×10^{-4}	2.47×10^{-4}	2.67×10^{5}
F138-2	2.23×10^{-4}	4.94×10^{-4}	4.27×10^{5}
F138-3	2.23×10^{-4}	7.42×10^{-4}	5.67×10^{5}
F138-4	2.23×10^{-4}	9.89×10^{-4}	7.08×10^{5}
F138-5	2.23×10^{-4}	1.24×10^{-3}	8.85×10^{5}
F138-6	*2.23×10^{-4}*	*2.47×10^{-3}*	*1.36×10^{6}*
F138-7	*2.23×10^{-4}*	*3.71×10^{-3}*	*1.88×10^{6}*
F138-8	*2.23×10^{-4}*	*4.94×10^{-3}*	*2.18×10^{6}*
F138-9	*2.23×10^{-4}*	*6.18×10^{-3}*	*2.26×10^{6}*

[a] OAr = 4-cyanophenoxide

$k_2 = 6.12 \times 10^{8}$ L mol^{-1}s^{-1}

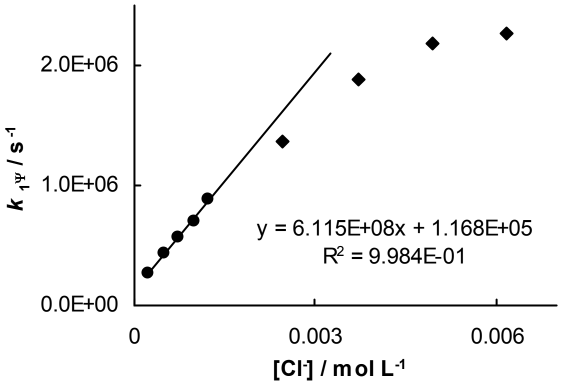

Bromide ion ($n\mathrm{Bu_4N^+Br^-}$)

$(\mathrm{ani})_2\mathrm{CH^+}$ from $(\mathrm{ani})_2\mathrm{CHOAr} + \mathrm{Br^-}$ in methanol at 20°C (laser flash, detection at 500 nm).[a]

No.	[Precursor]$_0$, mol L^{-1}	[Br$^-$] mol L^{-1}	k_{obs}, s^{-1}
F67-1	1.99×10^{-4}	1.09×10^{-3}	6.75×10^{6}
F67-2	1.99×10^{-4}	2.03×10^{-3}	8.28×10^{6}
F67-3	1.99×10^{-4}	3.60×10^{-3}	8.88×10^{6}
F67-4	1.99×10^{-4}	5.00×10^{-3}	8.67×10^{6}
F67-5	1.99×10^{-4}	6.57×10^{-3}	1.08×10^{7}
F67-6	1.99×10^{-4}	7.82×10^{-3}	1.14×10^{7}
F67-7	1.99×10^{-4}	1.02×10^{-2}	1.18×10^{7}
F67-8	1.99×10^{-4}	1.33×10^{-2}	1.43×10^{7}
F67-9	1.99×10^{-4}	1.56×10^{-2}	1.55×10^{7}
F67-10	1.99×10^{-4}	1.80×10^{-2}	1.58×10^{7}
F67-11	1.99×10^{-4}	2.03×10^{-2}	1.74×10^{7}

[a] OAr = 4-cyanophenoxide

$k_2 = 5.31 \times 10^{8}$ L mol^{-1}s^{-1}

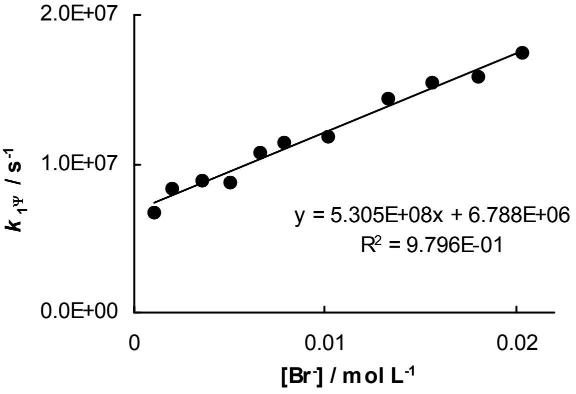

$(\mathrm{ani})_2\mathrm{CH^+}$ from $(\mathrm{ani})_2\mathrm{CHOAr} + \mathrm{Br^-}$ in ethanol at 20°C (laser flash, detection at 500 nm).[a]

No.	[Precursor]$_0$, mol L^{-1}	[Br$^-$] mol L^{-1}	k_{obs}, s^{-1}
F71-1	1.99×10^{-4}	8.91×10^{-4}	7.94×10^{6}
F71-2	1.99×10^{-4}	1.78×10^{-3}	1.22×10^{7}
F71-3	1.99×10^{-4}	2.67×10^{-3}	1.51×10^{7}
F71-4	1.99×10^{-4}	2.23×10^{-3}	1.33×10^{7}
F71-5	1.99×10^{-4}	3.56×10^{-3}	1.65×10^{7}
F71-6	1.99×10^{-4}	4.45×10^{-3}	1.83×10^{7}
F71-7	1.99×10^{-4}	5.34×10^{-3}	2.23×10^{7}
F71-8	1.99×10^{-4}	6.68×10^{-3}	2.45×10^{7}

[a] OAr = 4-cyanophenoxide

$k_2 = 2.75 \times 10^{9}$ L mol^{-1}s^{-1}

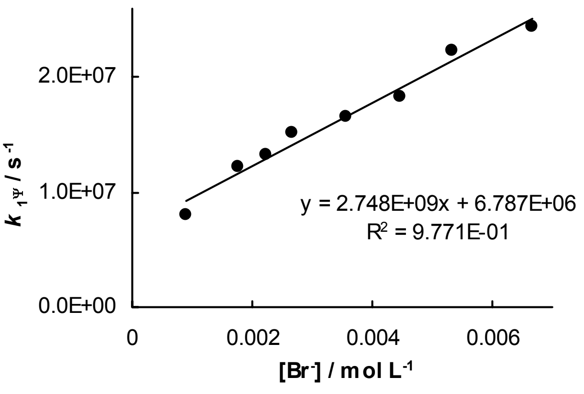

$(ani)_2CH^+$ from $(ani)_2CHOAr + Br^-$ in 80E20W at 20°C (laser flash, detection at 500 nm).[a]

No.	[Precursor]$_0$, mol L^{-1}	[Br$^-$] mol L^{-1}	k_{obs}, s^{-1}
F112-1	1.11×10^{-4}	1.04×10^{-3}	2.21×10^{6}
F112-2	1.11×10^{-4}	2.08×10^{-3}	2.69×10^{6}
F112-3	1.11×10^{-4}	3.12×10^{-3}	3.18×10^{6}
F112-4	1.11×10^{-4}	4.17×10^{-3}	3.48×10^{6}
F112-5	1.11×10^{-4}	5.21×10^{-3}	4.19×10^{6}
F112-6	1.11×10^{-4}	6.25×10^{-3}	4.78×10^{6}

[a] OAr = 4-cyanophenoxide

$k_2 = 4.84 \times 10^8$ L mol^{-1}s^{-1}

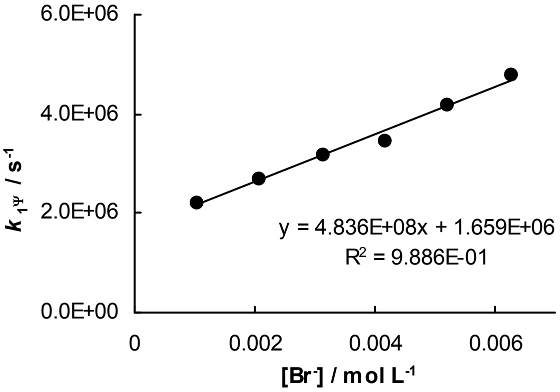

$(ani)_2CH^+$ from $(ani)_2CHOAc + Br^-$ in 50E50W at 20°C (laser flash, detection at 500 nm).[a]

No.	[Precursor]$_0$, mol L^{-1}	[Br$^-$] mol L^{-1}	$r_1 + r_2$ s^{-1}
F165-1	1.59×10^{-4}	1.64×10^{-3}	1.08×10^{6}
F165-2	1.59×10^{-4}	3.27×10^{-3}	1.21×10^{6}
F165-3	1.59×10^{-4}	4.91×10^{-3}	1.52×10^{6}
F165-4	1.59×10^{-4}	6.55×10^{-3}	1.52×10^{6}
F165-5	1.59×10^{-4}	8.19×10^{-3}	1.94×10^{6}
F165-6	1.59×10^{-4}	1.15×10^{-2}	2.39×10^{6}
F165-7	1.59×10^{-4}	1.47×10^{-2}	2.79×10^{6}
F165-8	1.59×10^{-4}	1.80×10^{-2}	3.28×10^{6}

[a] OAr = acetate

$k_2 = 1.37 \times 10^8$ L mol^{-1}s^{-1}

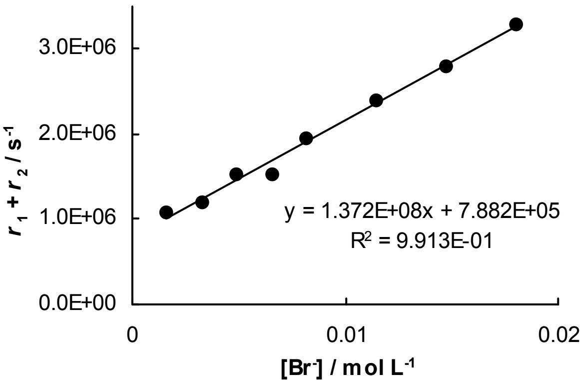

$(ani)_2CH^+$ from $(ani)_2CHOAc$ + Br^- in 50M50AN at 20°C (laser flash, detection at 500 nm).[a]

No.	$[Precursor]_0$, mol L^{-1}	$[Br^-]$ mol L^{-1}	k_{obs}, s^{-1}
F159-1	1.59×10^{-4}	2.70×10^{-4}	2.87×10^{6}
F159-2	1.59×10^{-4}	5.40×10^{-4}	3.14×10^{6}
F159-3	1.59×10^{-4}	8.10×10^{-4}	3.69×10^{6}
F159-4	1.59×10^{-4}	1.08×10^{-3}	4.06×10^{6}
F159-5	1.59×10^{-4}	1.35×10^{-3}	4.61×10^{6}

[a] OAc = acetate

$k_2 = 1.63 \times 10^9$ L $mol^{-1}s^{-1}$

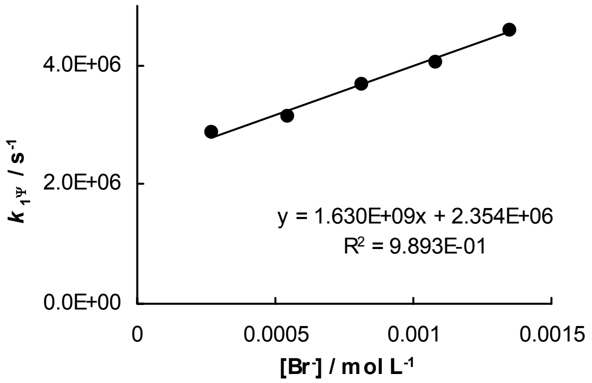

$(ani)_2CH^+$ from $(ani)_2CHOAc$ + Br^- in 50E50AN at 20°C (laser flash, detection at 500 nm).[a]

No.	$[Precursor]_0$, mol L^{-1}	$[Br^-]$ mol L^{-1}	k_{obs}, s^{-1}
F158-1	1.59×10^{-4}	1.35×10^{-4}	1.87×10^{6}
F158-2	1.59×10^{-4}	2.70×10^{-4}	3.04×10^{6}
F158-3	1.59×10^{-4}	4.05×10^{-4}	3.46×10^{6}
F158-4	1.59×10^{-4}	5.40×10^{-4}	3.58×10^{6}
F158-5	1.59×10^{-4}	6.75×10^{-4}	4.43×10^{6}
F158-6	1.59×10^{-4}	8.10×10^{-4}	5.09×10^{6}

[a] OAc = acetate

$k_2 = 4.32 \times 10^9$ L $mol^{-1}s^{-1}$

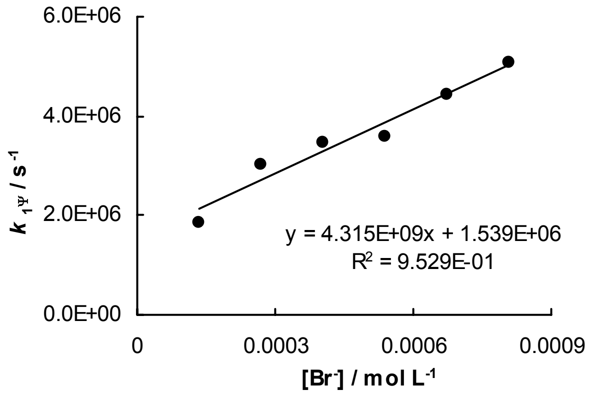

$(ani)_2CH^+$ from $(ani)_2CHOAc + Br^-$ in 50W50AN at 20°C (laser flash, detection at 500 nm).[a]

No.	$[Precursor]_0$, mol L^{-1}	$[Br^-]$ mol L^{-1}	$r_1 + r_2$ s^{-1}
F171-1	1.59×10^{-4}	1.70×10^{-3}	5.51×10^{5}
F171-2	1.59×10^{-4}	3.40×10^{-3}	7.09×10^{5}
F171-3	1.59×10^{-4}	5.09×10^{-3}	1.07×10^{6}
F171-4	1.59×10^{-4}	6.79×10^{-3}	1.55×10^{6}
F171-5	1.59×10^{-4}	1.02×10^{-2}	2.15×10^{6}
F171-6	1.59×10^{-4}	1.36×10^{-2}	2.65×10^{6}

[a] OAc = acetate

$k_2 = 1.86 \times 10^8$ L $mol^{-1}s^{-1}$

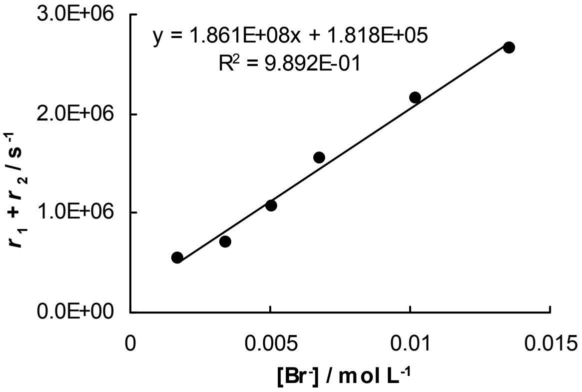

$(ani)_2CH^+$ from $(ani)_2CHOAc + Br^-$ in 20W80AN at 20°C (laser flash, detection at 500 nm).[a]

No.	$[Precursor]_0$, mol L^{-1}	$[Br^-]$ mol L^{-1}	k_{obs}, s^{-1}
F160-1	1.59×10^{-4}	2.70×10^{-4}	3.13×10^{5}
F160-2	1.59×10^{-4}	5.40×10^{-4}	5.29×10^{5}
F160-3	1.59×10^{-4}	8.10×10^{-4}	7.71×10^{5}
F160-4	1.59×10^{-4}	1.08×10^{-3}	8.89×10^{5}
F160-5	1.59×10^{-4}	1.35×10^{-3}	1.08×10^{6}

[a] OAc = acetate

$k_2 = 7.02 \times 10^8$ L $mol^{-1}s^{-1}$

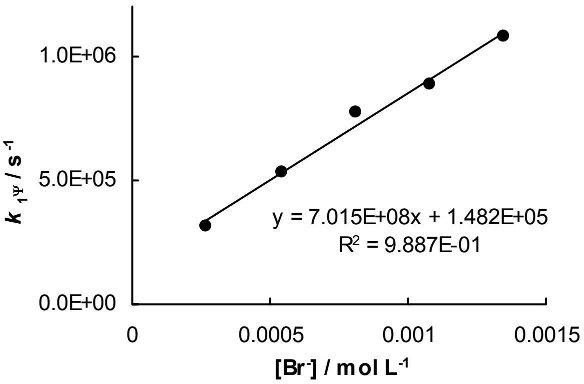

(ani)(tol)CH$^+$ from (ani)(tol)CHOAc + Br$^-$ in 50E50W at 20°C (laser flash, detection at 480 nm).[a]

No.	[Precursor]$_0$, mol L^{-1}	[Br$^-$] mol L^{-1}	k_{obs}, s^{-1}
F166-1	1.51×10^{-4}	9.82×10^{-4}	3.79×10^{6}
F166-2	1.51×10^{-4}	1.96×10^{-3}	5.05×10^{6}
F166-3	1.51×10^{-4}	2.95×10^{-3}	5.71×10^{6}
F166-4	1.51×10^{-4}	3.93×10^{-3}	6.59×10^{6}
F166-5	1.51×10^{-4}	4.91×10^{-3}	7.08×10^{6}

[a] OAc = acetate

$k_2 = 8.26 \times 10^8$ L mol^{-1}s^{-1}

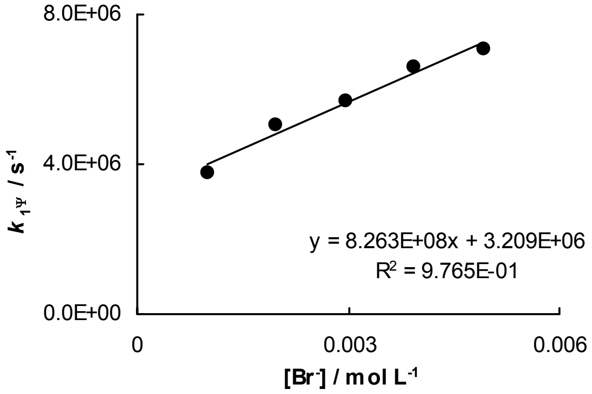

(ani)PhCH$^+$ from (ani)PhCHOAr + Br$^-$ in 50E50W at 20°C (laser flash, detection at 460 nm).[a]

No.	[Precursor]$_0$, mol L^{-1}	[Br$^-$] mol L^{-1}	k_{obs}, s^{-1}
F167-1	1.36×10^{-4}	6.55×10^{-4}	7.82×10^{6}
F167-2	1.36×10^{-4}	1.31×10^{-3}	8.56×10^{6}
F167-3	1.36×10^{-4}	1.96×10^{-3}	9.16×10^{6}
F167-4	1.36×10^{-4}	2.62×10^{-3}	9.72×10^{6}
F167-5	1.36×10^{-4}	3.27×10^{-3}	1.08×10^{7}
F167-6	1.36×10^{-4}	3.93×10^{-3}	1.18×10^{7}

[a] OAr = 4-cyanophenoxide

$k_2 = 1.19 \times 10^9$ L mol^{-1}s^{-1}

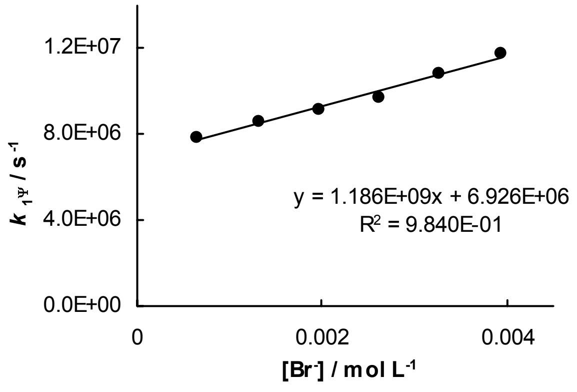

(ani)PhCH$^+$ from (ani)PhCHOAr + Br$^-$ in TFE at 20°C (laser flash, detection at 460 nm).[a]

No.	[Precursor]$_0$, mol L^{-1}	[Br$^-$] mol L^{-1}	k_{obs}, s^{-1}
F105-1	1.78×10^{-4}	1.94×10^{-3}	6.55×10^{5}
F105-2	1.78×10^{-4}	2.91×10^{-3}	8.98×10^{5}
F105-3	1.78×10^{-4}	3.87×10^{-3}	1.13×10^{6}
F105-4	1.78×10^{-4}	4.84×10^{-3}	1.30×10^{6}
F105-5	1.78×10^{-4}	7.75×10^{-3}	1.73×10^{6}
F105-6	1.78×10^{-4}	9.69×10^{-3}	2.23×10^{6}

[a] OAr = 4-cyanophenoxide

$k_2 = 1.92 \times 10^8$ L mol^{-1}s^{-1}

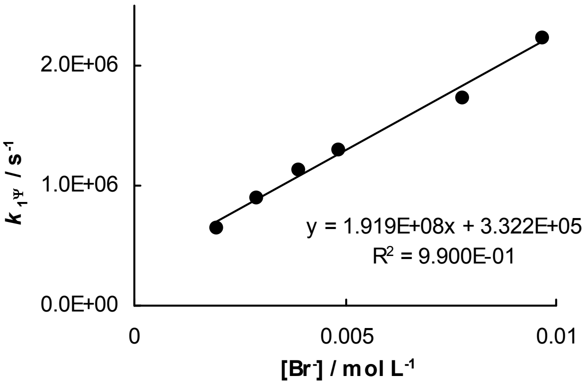

(tol)$_2$CH$^+$ from (tol)$_2$CHOAr + Br$^-$ in TFE at 20°C (laser flash, detection at 460 nm).[a]

No.	[Precursor]$_0$, mol L^{-1}	[Br$^-$] mol L^{-1}	k_{obs}, s^{-1}
F103-1	9.44×10^{-5}	1.94×10^{-4}	6.15×10^{5}
F103-2	9.44×10^{-5}	3.87×10^{-4}	1.05×10^{6}
F103-3	9.44×10^{-5}	5.81×10^{-4}	1.46×10^{6}
F103-4	9.44×10^{-5}	7.75×10^{-4}	1.82×10^{6}
F103-5	9.44×10^{-5}	9.69×10^{-4}	2.23×10^{6}
F85-1	9.44×10^{-5}	1.07×10^{-3}	2.42×10^{6}
F85-2	9.44×10^{-5}	1.61×10^{-3}	3.41×10^{6}
F85-3	9.44×10^{-5}	2.14×10^{-3}	4.42×10^{6}
F85-4	9.44×10^{-5}	2.68×10^{-3}	4.98×10^{6}
F85-5	9.44×10^{-5}	3.21×10^{-3}	6.02×10^{6}
F85-6	9.44×10^{-5}	3.75×10^{-3}	7.04×10^{6}
F85-7	*9.44×10^{-5}*	*4.28×10^{-3}*	*7.17×10^{6}*
F85-8	*9.44×10^{-5}*	*5.36×10^{-3}*	*8.42×10^{6}*
F103-6	*9.44×10^{-5}*	*7.75×10^{-3}*	*1.21×10^{7}*
F103-7	*9.44×10^{-5}*	*9.69×10^{-3}*	*1.43×10^{7}*

[a] OAr = 4-cyanophenoxide

$k_2 = 1.76 \times 10^9$ L mol^{-1}s^{-1}

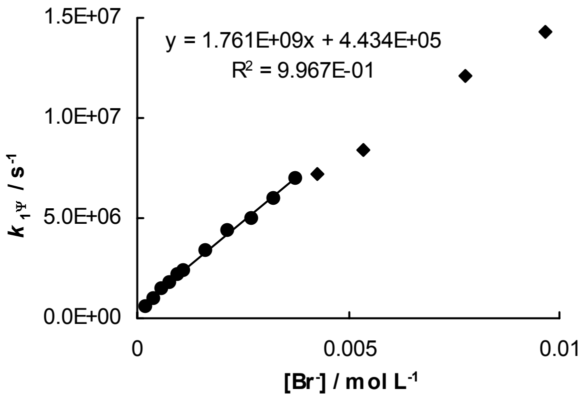

(tol)PhCH$^+$ from (tol)PhCHOAr + Br$^-$ in TFE at 20°C (laser flash, detection at 450 nm).[a]

No.	[Precursor]$_0$, mol L^{-1}	[Br$^-$] mol L^{-1}	k_{obs}, s^{-1}
F107-1	1.74×10^{-4}	1.94×10^{-4}	1.28×10^{6}
F107-2	1.74×10^{-4}	3.87×10^{-4}	2.16×10^{6}
F107-3	1.74×10^{-4}	5.81×10^{-4}	2.94×10^{6}
F107-4	1.74×10^{-4}	7.75×10^{-4}	3.51×10^{6}
F107-5	1.74×10^{-4}	9.69×10^{-4}	4.44×10^{6}
F107-6	1.74×10^{-4}	1.36×10^{-3}	5.89×10^{6}
F107-7	1.74×10^{-4}	1.94×10^{-3}	8.13×10^{6}

[a] OAr = 4-cyanophenoxide

$k_2 = 3.89 \times 10^9$ L mol^{-1}s^{-1}

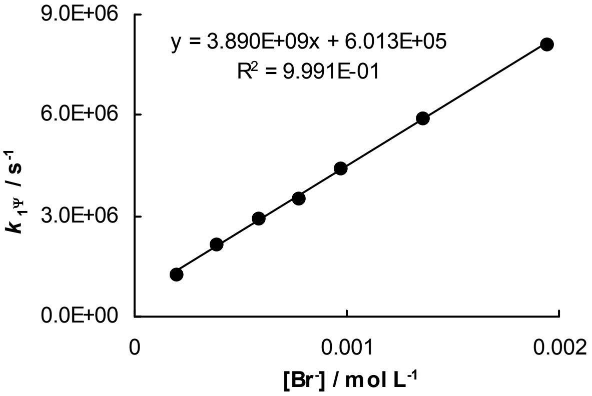

Ph_2CH^+ from Ph_2CHOAr + Br^- in HFIP at 20°C (laser flash, detection at 440 nm).[a]

No.	[Precursor]$_0$, mol L^{-1}	[Br^-] mol L^{-1}	k_{obs}, s^{-1}
F140-1	2.23×10^{-4}	2.30×10^{-4}	8.27×10^{5}
F140-2	2.23×10^{-4}	4.59×10^{-4}	1.62×10^{6}
F140-3	2.23×10^{-4}	6.89×10^{-4}	2.16×10^{6}
F140-4	2.23×10^{-4}	9.18×10^{-4}	2.46×10^{6}
F140-5	2.23×10^{-4}	1.15×10^{-3}	3.04×10^{6}
F140-6	2.23×10^{-4}	2.07×10^{-3}	5.66×10^{6}
F140-7	*2.23×10^{-4}*	*3.90×10^{-3}*	*7.43×10^{6}*
F140-8	*2.23×10^{-4}*	*5.97×10^{-3}*	*1.02×10^{7}*
F140-9	*2.23×10^{-4}*	*8.04×10^{-3}*	*1.28×10^{7}*
F140-10	*2.23×10^{-4}*	*9.87×10^{-3}*	*1.36×10^{7}*
F140-11	*2.23×10^{-4}*	*1.15×10^{-2}*	*1.55×10^{7}*

[a] OAr = 4-cyanophenoxide

$k_2 = 2.55 \times 10^9$ L mol^{-1}s^{-1}

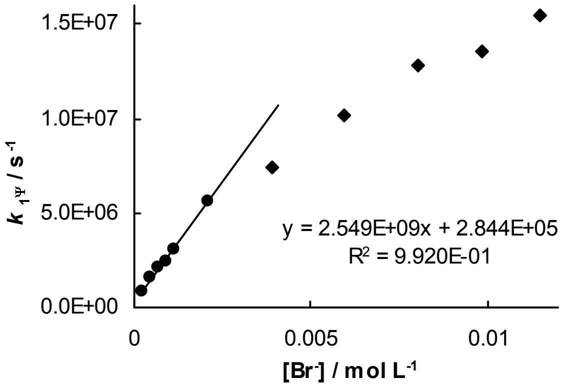

7.4.3 First direct observation of the two distinct steps in an S_N1 reaction

Bis(4,4-methoxyphenyl)methyl tetrafluoroborate $(ani)_2CH^+BF_4^-$.[15]

$(ani)_2CHOH$ (2.47g, 10.1 mmol) was dissolved in a mixture of 50 mL of dry ether and 6.5 mL (50 mmol) of propionic anhydride. A 54% ether solution of $HBF_4{\cdot}OEt_2$ (3.55 g, 26.5 mmol) was added. The mixture was stirred at room temperature for 20 min and cooled in an ice bath for 10 min. The precipitate was filtered off under nitrogen and washed successively with cold, dry ether and cold, dry pentane. The residue was dried in vacuo to yield 1.75 g of a red powder (5.57 mmol, 55%). ^1H NMR (200 MHz, CD_2Cl_2): $\delta = 4.16$ (s, 6 H), 7.32 (d, $J = 9.1$ Hz, 4 H), 8.35 (d, $J = 9.1$ Hz, 4 H), 9.00 (s, 1 H);[16] ^{13}C NMR (100.6 MHz, CD_2Cl_2): $\delta = 57.\ 6$ (ArO$\underline{Me}$), 118.3 (Ar), 129.4 (Ar), 144.7 (Ar), 174.0 (Ar), 178.8 (Ar$\underline{C}$HAr).[16]

Kinetics of Ar_2CHBF_4 in TFE-CH_3CN mixtures.

$(ani)_2CH^+$ in TFE-CH_3CN mixtures (Stopped-flow) at 20 ºC.

No.	$[(ani)_2CHBF_4]_0$ mol L^{-1}	TFE/CH_3CN [a]	Additive mol L^{-1}	k_{TFE} [b], s^{-1}
384-1	9.64×10^{-6}	91/9		12.7
388-1	8.55×10^{-6}	91/9	Bu_4NCl (0.01 L mol^{-1})	10.3
384-2	9.64×10^{-6}	80/20		13.5
384-3	9.64×10^{-6}	60/40		13.1
384-4	9.64×10^{-6}	20/80		10.0
385-1	1.10×10^{-5}	20/80	$NaClO_4$ (0.5 L mol^{-1})	10.0
385-2	1.10×10^{-5}	20/80	$LiClO_4$ (0.5 L mol^{-1})	10.4

[a] Solvent ratio in v/v. [b] Reactions were monitored at 500 nm.

Solvolysis of $(\text{ani})_2\text{CHCl}$ in TFE/CH_3CN solutions at 20 ºC.

No.	$[(\text{ani})_2\text{CHCl}]_0$ L mol^{-1}	TFE/CH_3CN [a]	Additive (L mol^{-1})	A_{max} [b]	k_{i}, s^{-1}	k_{TFE}, s^{-1}
380-1	8.51×10^{-6}	91/9		0.81	fast	11.4
380-2	8.51×10^{-6}	91/9	Bu_4NCl (5×10^{-4} L mol^{-1})	0.83	fast	11.1
380-3	8.51×10^{-6}	91/9	Bu_4NCl (1×10^{-3} L mol^{-1})	0.81	fast	11.0
380-4	8.51×10^{-6}	91/9	Bu_4NCl (5×10^{-3} L mol^{-1})	0.68	fast	10.6
380-5	8.51×10^{-6}	91/9	Bu_4NCl (1×10^{-2} L mol^{-1})	0.54 [c]	fast	10.6
368-1	7.44×10^{-6}	80/20		0.67	fast	14.1
368-2	7.44×10^{-6}	70/30		0.61	fast	14.8
368-3	7.44×10^{-6}	60/40		0.55	fast	13.2
368-4	7.44×10^{-6}	50/50		0.50	fast	12.4
368-5	7.44×10^{-6}	40/60		0.37	fast	(6.47) [d]
368-6	7.44×10^{-6}	30/70		0.20	— [e]	(3.80) [d]
398-1	1.10×10^{-5}	30/70	$LiClO_4$ (1.0 L mol^{-1})	0.64	7×10^2	12.7
368-7	7.44×10^{-6}	20/80		0.10	— [e]	(2.66) [d]
372-1	7.44×10^{-6}	20/80	$NaClO_4$ (1.0 L mol^{-1})	0.26	3×10^2	10.1
381-1	1.10×10^{-5}	20/80	$LiClO_4$ (1.0 L mol^{-1})	0.52	5×10^2	10.4

[a] Solvent ratio in v/v. [b] Absorbance at $\lambda_{\text{max}} = 500$. [c] $\lambda_{\text{max}} = 499$ nm. [d] The rate constant (k_{TFE}) has to be considered as approximation. The carbocation consumption did not show an exponential decay with small absorbance because of incomplete ionization. [e] The rate constant of ionization (k_{i}) was not determined because of too small increase of absorbance in cation formation step.

Solvolysis of Ar_2CHCl in TFE/CH_3CN solutions at 20 ºC.

No.	Ar_2CHCl	$[Ar_2CHCl]_0$ L mol^{-1}	TFE/CH_3CN [a]	Detection, nm	k_{TFE}, s^{-1}
423-1	(ani)(pop)CHCl	8.37×10^{-6}	91/9	500	1.2×10^2
423-2		8.37×10^{-6}	80/20	500	1.1×10^2
423-3		8.37×10^{-6}	70/30	500	1.1×10^2
423-4		8.37×10^{-6}	60/40	500	4.9×10^1 [b]
423-5		8.37×10^{-6}	50/50	500	4.3×10^1 [b]
373-5	(ani)(tol)CHCl	7.89×10^{-6}	91/9	480	— [c]

[a] Solvent ratio in v/v. [b] The rate constant (k_{TFE}) has to be considered as approximation. The carbocation consumption did not show an exponential decay with small absorbance because of incomplete ionization. [c] No absorption was observed.

7.5 Unique Reactivity of 1,4-diazabicyclo[2.2.2]octane (DABCO).

$(dma)_2CH^+$ + DABCO in 99.6/0.4 (v/v) water/acetonitrile at 20°C (J&M, detection at 605 nm).

No.	$[(dma)_2CHBF_4]_0$, mol L^{-1}	$[DABCO]^a$ mol L^{-1}	k_{obs}, s^{-1}	K, L mol^{-1}
318-1	1.09×10^{-5}	5.90×10^{-4}	1.84×10^{-2}	2.1×10^{2}
318-2	1.09×10^{-5}	1.24×10^{-3}	1.68×10^{-2}	1.8×10^{2}
318-3	1.09×10^{-5}	1.81×10^{-3}	1.57×10^{-2}	1.7×10^{2}
318-4	1.09×10^{-5}	2.24×10^{-3}	1.50×10^{-2}	1.7×10^{2}
			$K =$	1.8×10^{2}

[a] DABCO-$DABCOH^+$ (1:1)

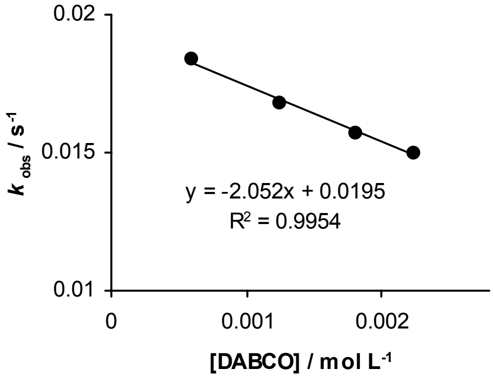

$(dma)_2CH^+$ + DABCO in 91/9 (v/v) water/acetonitrile at 20°C (Stopped-flow, detection at 605 nm).

No.	$[(dma)_2CHBF_4]_0$, mol L^{-1}	$[DABCO]^a$ mol L^{-1}	A_0	K, L mol^{-1}
562-1	7.43×10^{-6}	0	0.83	—
562-2	7.43×10^{-6}	1.76×10^{-3}	0.62	1.9×10^{2}
562-3	7.43×10^{-6}	3.53×10^{-3}	0.51	1.8×10^{2}
562-4	7.43×10^{-6}	5.29×10^{-3}	0.41	1.9×10^{2}
562-5	7.43×10^{-6}	7.05×10^{-3}	0.39	1.6×10^{2}
562-6	7.43×10^{-6}	9.10×10^{-3}	0.37	1.4×10^{2}
			$K =$	1.7×10^{2}

[a] DABCO-$DABCOH^+$ (1:1)

$(mor)_2CH^+$ + DABCO in 50/50 (v/v) water/acetonitrile at 20°C (Stopped-flow, detection at 610 nm).

No.	$[(mor)_2CHBF_4]_0$, Mol L^{-1}	$[DABCO]^a$ mol L^{-1}
247-1	1.25×10^{-5}	4.98×10^{-4}
247-2	1.25×10^{-5}	9.96×10^{-4}
247-3	1.25×10^{-5}	1.49×10^{-3}
247-4	1.25×10^{-5}	1.99×10^{-3}
247-5	1.25×10^{-5}	2.49×10^{-3}

[a] DABCO-$DABCOH^+$ (1:1).

No absorption in all runs.

7.6 Electrophilicity and nucleophilicity of Grignard reagent

Bis(julolidin-9-yl)methyl 4-methylphenolate:

Sodium 4-methylphenolate (88 mg, 0.68 mmol) in 3.2 mL of Et_2O/EtOH (4/1) was added to $(jul)_2CHBF_4$ (300 mg, 0.68 mmol) in ether (10 mL), and stirred 5 min at room temperature. The reaction mixture was filtered and evaporated. The residue was recrystallized from hexane/Et_2O to give colorless crystals (0.11 g, 0.25 mmol, 38%). ^{1}H NMR (300 MHz, CD_2Cl_2): δ = 1.88-1.96 (m, 8H), 2.24 (s, 3H, Me), 2.70 (t, J = 6.4, 8H), 3.10 (t, J = 5.6, 8H), 5.82 (s, 1H, $Ar_2C\underline{H}$), 6.74 (s, 2H, Ar), 6.81 (d, 2H, J = 8.4 Hz, ArH), 7.00 (d, 2H, J = 8.4 Hz, ArH); ^{13}C NMR (75.5 MHz, CD_2Cl_2): δ = 19.8 (Me), 21.9 ($-CH_2-$), 27.5 ($-CH_2-$), 49.7 ($-CH_2-$), 81.6 ($Ar\underline{C}HAr$), 115.5 (Ar), 121.1 (Ar), 124.9 (Ar), 128.9 (Ar), 129.2 (Ar), 129.3 (Ar), 141.9 (Ar), 156.2 (Ar).

Kinetics of bis(julolidin-9-yl)methyl 4-methylphenolate ($(jul)_2CHOTol$) with methylmagnesium bromide in diethyl ether at 20°C (Stopped-flow, detection at 635nm).

No.	$[(jul)_2CHOTol]_0$, mol L^{-1}	[MeMgBr] mol L^{-1}	k_{Mg}, L mol^{-1} s^{-1}	k_{Me}, L mol^{-1} s^{-1}
602-1	5.43×10^{-6}	5.25×10^{-3}	4.70×10^{2}	1.20×10^{1}
602-2	5.43×10^{-6}	1.05×10^{-2}	7.53×10^{2}	1.63×10^{1}
602-3	5.43×10^{-6}	1.58×10^{-2}	1.29×10^{2}	2.40×10^{1}
602-4	5.43×10^{-6}	2.10×10^{-2}	1.79×10^{2}	3.42×10^{1}
602-5	5.43×10^{-6}	2.63×10^{-2}	2.27×10^{2}	4.10×10^{1}
602-6	5.43×10^{-6}	3.15×10^{-2}	2.56×10^{2}	4.48×10^{1}

Kinetics of bis(julolidin-9-yl)methyl 4-methylphenolate ($(jul)_2CHOTol$) with methylmagnesium bromide in diethyl ether at 20°C (Stopped-flow, detection at 635nm).

No.	$[(jul)_2CHOTol]_0$, mol L^{-1}	[MeMgBr] mol L^{-1}	k_{Mg}, L mol^{-1} s^{-1}	k_{Me}, L mol^{-1} s^{-1}
689-1	5.2×10^{-6}	4.08×10^{-3}	5.82×10^{1}	1.35×10^{1}
689-2	5.2×10^{-6}	8.16×10^{-3}	7.41×10^{1}	1.53×10^{1}
689-3	5.2×10^{-6}	1.22×10^{-2}	1.00×10^{2}	1.63×10^{1}
689-4	5.2×10^{-6}	1.63×10^{-2}	1.07×10^{2}	2.30×10^{1}
689-5	5.2×10^{-6}	2.04×10^{-2}	1.51×10^{2}	3.01×10^{1}

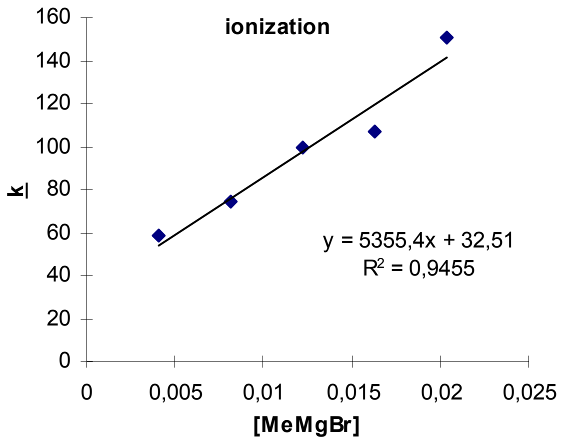

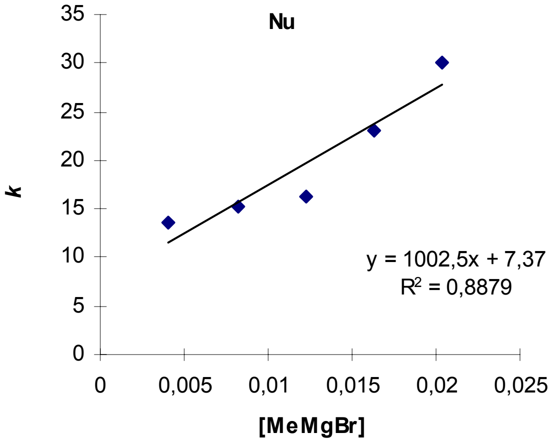

Kinetics of bis(julolidin-9-yl)methyl 4-methylphenolate ($(jul)_2CHOTol$) with methylmagnesium bromide in diethyl ether at 20°C (Stopped-flow, detection at 635nm).

No.	$[(jul)_2CHOTol]_0$, mol L^{-1}	[MeMgBr] mol L^{-1}	k_{Mg}, L mol^{-1} s^{-1}	k_{Me}, L mol^{-1} s^{-1}
690-1	6.0×10^{-6}	7.73×10^{-3}	3.47×10^{1}	9.17
690-2	6.0×10^{-6}	1.03×10^{-2}	5.46×10^{1}	1.61×10^{1}
690-3	6.0×10^{-6}	1.29×10^{-2}	$6.4.3 \times 10^{1}$	2.06×10^{1}
690-4	6.0×10^{-6}	1.55×10^{-2}	8.18×10^{1}	2.45×10^{1}
690-5	6.0×10^{-6}	1.80×10^{-2}	9.58×10^{1}	2.93×10^{1}
690-6	6.0×10^{-6}	2.06×10^{-2}	1.12×10^{2}	3.50×10^{1}
690-7	6.0×10^{-6}	2.32×10^{-2}	1.36×10^{2}	4.08×10^{1}

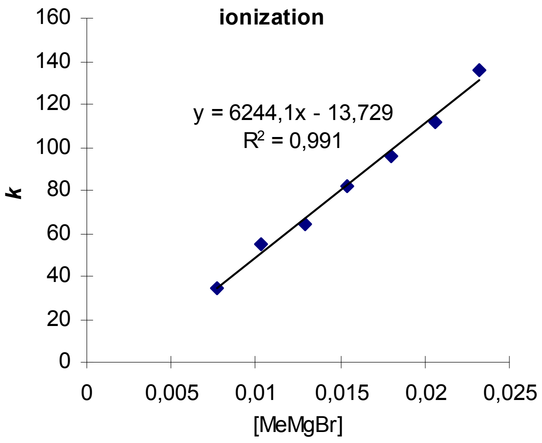

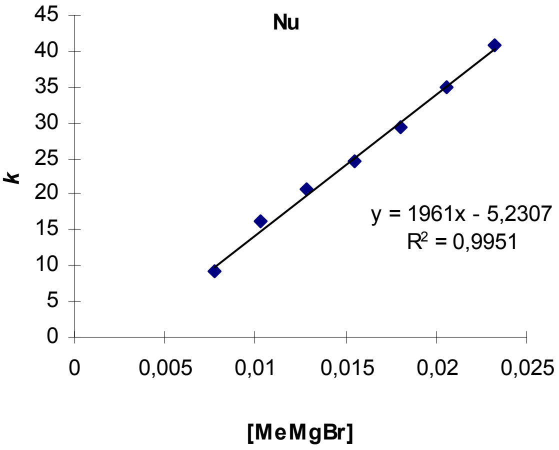

Kinetics of bis(julolidin-9-yl)methyl 4-methylphenolate ((jul)$_2$CHOTol) with methylmagnesium bromide in diethyl ether at 20°C (Stopped-flow, detection at 635nm).

No.	[(jul)$_2$CHOTol]$_0$, mol L^{-1}	[MeMgBr] mol L^{-1}	k_{Mg}, L mol^{-1} s^{-1}	k_{Me}, L mol^{-1} s^{-1}
702-1	5.0×10^{-6}	5.74×10^{-3}	4.25×10^{1}	7.60
702-2	5.0×10^{-6}	1.44×10^{-2}	8.83×10^{1}	1.67×10^{1}
702-3	5.0×10^{-6}	1.87×10^{-2}	1.10×10^{2}	2.11×10^{1}
702-4	5.0×10^{-6}	2.30×10^{-2}	1.25×10^{2}	2.60×10^{1}
702-5	5.0×10^{-6}	2.87×10^{-2}	1.53×10^{2}	3.00×10^{1}

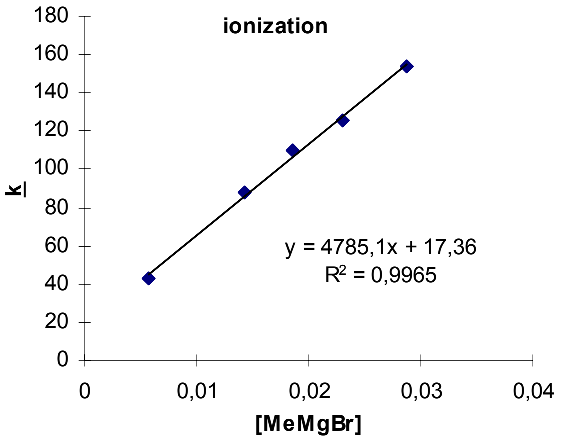

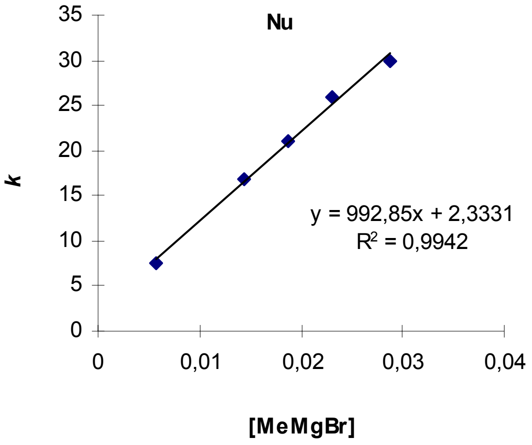

7.7 References

(1) Mayr, H.; Bug, T.; Gotta, M. F.; Hering, N.; Irrgang, B.; Janker, B.; Kempf, B.; Loos, R.; Ofial, A. R.; Remennikov, G.; Schimmel, H. *J. Am. Chem. Soc.* **2001**, *123*, 9500–9512.

(2) Schneider, R.; Mayr, H.; Plesch, P. H. *Ber. Bunsenges. Phys. Chem.* **1987**, *91,* 1369–1374.

(3) Funke, M.-A. Dissertation, Technische Hochschule Darmstadt, 1997.

(4) Paoletti, P.; Stern, J. H.; Vacca, H. *J. Phys. Chem.* **1965**, *69*, 3759–3762.

(5) Schmid, R.; Sapunov, V. N. *Monographs in Modern Chemistry, Vol. 14: Non-Formal Kinetics in Search for Chemical Reaction Pathways*; VCH, Weinheim, Germany, 1982, p.20.

(6) Ritchie, C. D. *Can. J. Chem.* **1986**, *64*, 2239–2250

(7) Evans, A. G.; Hamann, S. D. *Trans. Faraday Soc.* **1951**, *47,* 34–40.

(8) Kane-Maguire, L. A. P.; Kanitz, R.; Jones, P.; Williams, P. A. *J. Organomet. Chem.* **1994**, *464*, 203–213.

(9) Evans, M. G.; Uri, N. *Trans. Faraday. Soc.* **1949**, *45*, 224–230.

(10) (a) McClelland, R. A.; Kanagasabapathy, V. M.; Banait, N. S.; Steenken, S. *J. Am. Chem. Soc.* **1989**, *111*, 3966–3972. (b) Pham, T. V.; McClelland, R. A. *Can. J. Chem.* **2001**, *79*, 1887–1897.

(11) Chiang, Y.; Kresge, A. J.; Zhu, Y. *J. Am. Chem. Soc.* **2002**, *124*, 6349–6356.

(12) Hammett, L. P. *Physical Organic Chemistry: Reaction Rates, Equilibria, and Mechanisms*, 2nd ed.; McGraw-Hill: New York, 1970.

(13) Ceccon, G.; Giacometti, G.; Venzo, A.; Paolucci, D.; Benozzi, D *J. Organomet. Chem.* **1980**, *185*, 231–239.

(14) Kelly, D. P.; Jenkins, M. J. *J. Org. Chem.* **1984**, *49*, 409–413.

(15) Arnett, E. M.; Amarnath, K.; Harvey, N. G.; Cheng, J. *J. Am. Chem. Soc.* **1990**, *112*, 346–355.

(16) Ohwada, T.; Shudo, K. *J. Org. Chem.* **1989**, *54*, 5227–5237.

Appendix: Autopsy of S_N1 Reactions

(Denegri, B.; Minegishi, S.; Kronja, O.; Mayr, H. *Angew. Chem.* 2004 in print.)

Solvolysis reactions, which follow the S_N1 (or $D_N + A_N$)[1] mechanism, are usually considered to proceed via slow ionization and fast consecutive trapping of the intermediate carbocation [Eq. (1)].[2]

$$\text{R-X} \underset{k_{-1}}{\overset{k_1}{\rightleftharpoons}} \text{R}^+ + \text{X}^- \xrightarrow[k_2]{+\text{ SolvOH}} \text{R-OSolv} + \text{HX} \qquad (1)$$

Salt effects have been investigated to determine the reversibility of the ionization step.[2] While Ingold had already noted that the relative rates of the two steps may be reversed in the case of highly stabilized carbocations (S_N2C^+),[3] we have recently reported the first example of a solvolysis reaction, where the rates of both steps can directly be measured.[4] We now report that fast ionization and slow reaction of the carbocation with the solvent is typical for a large variety of S_N1 solvolyses. Since we succeeded to separately study the two steps of Equation (1), we can now define the borders between conventional S_N1 mechanisms and those with inverse rate profiles.

Equation (2) has previously been demonstrated to be suitable for describing the rates of the reactions of carbocations R^+ with π-, σ-, and n-nucleophiles.[5–9]

Carbocation nucleophile combinations:

$$\log k(20\ °\text{C}) = s\,(N + E) \qquad (2)$$

where s, N = nucleophile specific parameters and E = electrophile specific parameter

In view of the tremendous scope of Equation (2) for describing electrophile nucleophile combinations, we have examined whether an analogous approach might be used for describing heterolysis reactions. We now suggest Equation (3) which is not only mathematically analogous to Equation (2):[10]

Heterolysis reactions:

$$\log k(25\ °\text{C}) = s_f\,(N_f + E_f) \qquad (3)$$

where s_f, N_f = nucleofuge specific parameters and E_f = electrofuge specific parameter

The nucleofuge specific parameters N_f and s_f [Eq. (3)] refer to combinations of leaving groups and solvents in the same way as the nucleophile specific parameters N and s [Eq. (2)] for anions and amines which have been defined with respect to a certain solvent.[8] Electrofugality E_f, like electrophilicity E, is characterized by a single parameter. Furthermore, the same benzhydrylium ions (Scheme 1), which have previously been employed as reference electrophiles[6] are now employed as reference electrofuges which allow us to relate the scales of electrophilicity and electrofugality with each other.[11–13]

Scheme 1: Benzydrylium ions that are used as reference electrofuges and electrophiles.

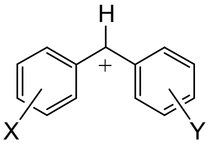

1 - **24**

Table S1 in the Supporting Information summarizes first-order solvolysis rate constants of benzhydryl bromides, chlorides, trifluoroacetates, and 3,5-dinitrobenzoates in 80% aqueous ethanol, 100% ethanol, 80% aqueous acetone, and 90% aqueous acetone, which were either determined in this work or collected from the literature. These data were subjected to a least-squares fit on the basis of Equation (3)[14] by using the predefined parameters $E_f[(4\text{-MeO-}C_6H_4)_2CH^+)] = 0$ and $s_f(Cl^-/100\%\ EtOH) = 1$. Figure 1 shows 10 of the 16 correlation lines (four leaving groups in four solvents) and reveals the applicability of Equation (3) for correlating heterolysis rate constants.

According to Table 1, the nucleofugality parameters obtained by this regression analysis range over 8 orders of magnitude, from $N_f = -3.4$ for 3,5-dinitrobenzoate in 90% aqueous acetone to $N_f = 4.7$ for bromide in 80% aqueous ethanol. While all slope parameters (of chlorides, bromides and 3,5-dinitrobenzoates) are close to 1.0, the slope parameter s_f for trifluoroacetate is somewhat smaller in all solvents, indicating a slightly smaller carbocation character of the activated complexes of trifluoroacetate solvolysis.

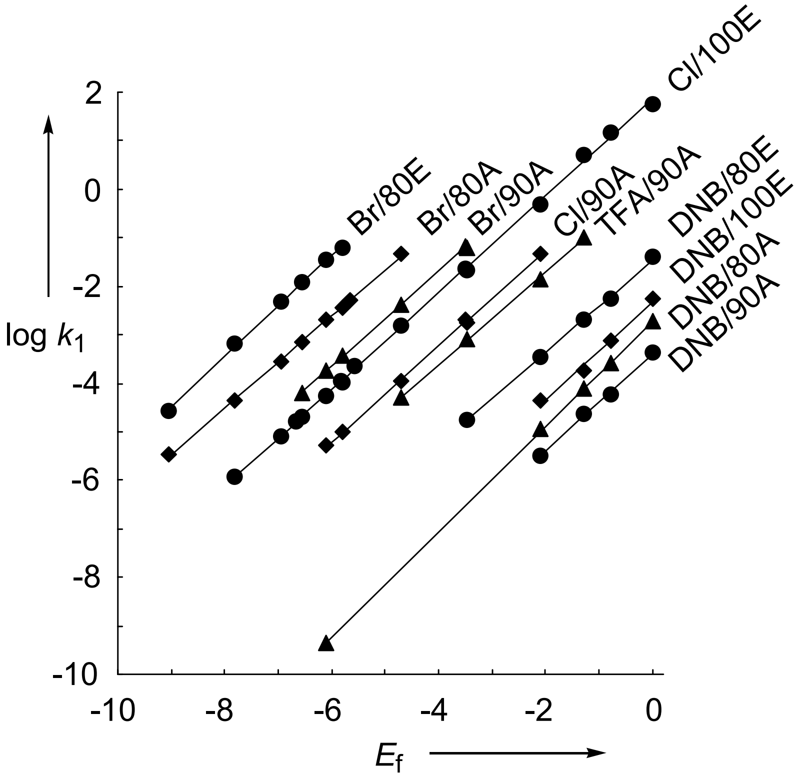

Figure 1. Plot of log k(25°C) vs. the electrofugality parameters E_f for the solvolysis reactions of substituted benzhydrylium substrates (TFA = trifluoroacetate, DNB = 3,5-dinitrobenzoate). Only 10 of the 16 linear correlations evaluated are shown to avoid overlapping correlation lines. Mixtures of solvents are given as (v/v), solvents: A = acetone, E = ethanol, 80E is for 80% ethanol/20 % water etc.

Table 1. Nucleofugality parameters (N_f / s_f)[a] for four leaving groups in four solvents.

Solvent[b]	Bromide	Chloride	TFA[c]	DNB[d]
80E20W	4.69 / 1.04	3.36 / 0.99	1.45 / 0.81	–1.53 / 0.95
100E	3.09 / 0.96	1.87 / 1.00	0.32 / 0.87	–2.28 / 1.02
80A20W	3.26 / 0.95	1.95 / 1.01	0.54 / 0.85	–2.49 / 1.09
90A10W	2.27 / 0.98	0.73 / 0.99	0.22 / 0.96	–3.36 / 1.01

[a] As defined by Equation (3). [b] Mixtures of solvents are given as (v/v), solvents: W = water, A = acetone, E = ethanol. [b] TFA = trifluoroacetate. [c] DNB = 3,5-dinitrobenzoate.

The comparison of the electrofugality parameters E_f with the electrophilicity parameters E (Table 2) shows that in most cases $E_\mathrm{f} \approx -E$, but that the 4-phenoxy and 4,4'-dichloro substituted benzhydrylium ions **6** and **15** are poorer electrofuges than expected on the basis of their electrophilicities (see also Figure 2). The reasons for these deviations are presently not clear. While an inverse relationship between E and E_f was expected, the slope of –1 is accidental due to the choice of the predefined slope parameters for nucleophiles (s = 1.0 for 2-methyl-1-pentene)[5, 6a] and nucleofuges (s_f = 1.0 for Cl in 100% EtOH, see above).

Table 2. Electrofugality (E_f) and electrophilicity (E) parameters of benzhydrylium ions **1**–**17**.

Benzhydrylium Ion			E_f[a]	E[b]
	X =	Y =		
1	4-OCH_3	4-OCH_3	0.00[c]	0.00[c]
2	4-OCH_3	4-OC_6H_5	–0.79	0.61
3	4-OCH_3	4-CH_3	–1.27	1.48
4	4-OCH_3	H	–2.10	2.11
5	4-CH_3	4-CH_3	–3.48	3.63
6	4-OC_6H_5	H	–3.49	2.90
7	4-CH_3	H	–4.71	4.59
8	3,5-$(CH_3)_2$	H	–5.56	—
9	4-OC_6H_5	4-NO_2	–5.66	—
10	4-F	H	–5.81	5.60
11	3-CH_3	H	–5.83	—
12	H	H	–6.09	5.90
13	4-Cl	H	–6.55	—
14	4-Br	H	–6.67	—
15	4-Cl	4-Cl	–6.95	6.02
16	3-Cl	H	–7.80	—
17	4-NO_2	H	–9.05	—

[a] As defined by Equation (3). [b] As defined by Equation (2), from ref. [6]. [c] By definition, see text.

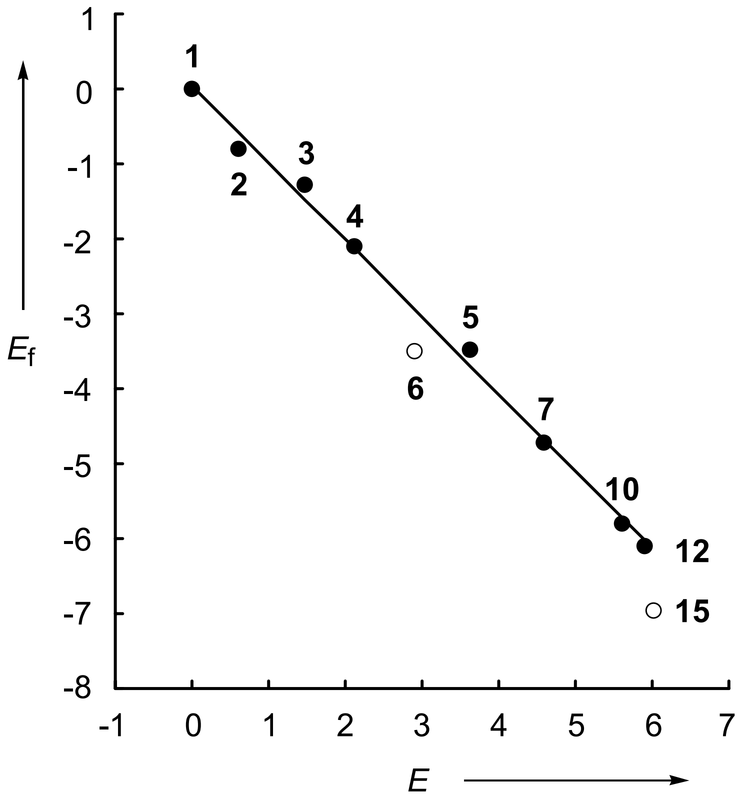

Figure 2. Linear correlation of electrofugality parameters E_f with the electrophilicity parameters E ($E_f = -1.03E + 0.05$, $n = 8$, $r^2 = 0.9962$; electrofuges **6** and **15** not considered for the correlation).

In order to determine the rate constants k_2 of Equation (1), we have measured the decay of the UV-Vis absorbances of the stable tetrafluoroborates of the benzhydrylium ions **18**–**24** in aqueous acetone (Table 3) using the methodology described previously.[8b]

The linear correlation in Figure 3 shows that the reactions of carbocations with solvents can also be described by Equation (2), in accord with Ritchie's work[15] and previous investigations of this group.[8b] It is thus possible to calculate N and s parameters for solvents as listed in Table 4. Though these parameters have been derived from reactions with benzhydrylium ions, they can also be employed for calculating the reaction rates of other types of carbocations (see chapter 4).

Table 3. First-order rate constants k_2 (s^{-1}) for the reactions of the benzhydrylium ions **18**–**24** with the solvent at 20 °C.

Benzhydrylium Ions		E[a]	k_2 / s^{-1}	
	X =Y =		80A20W[b]	90A10W[b]
18	4-NPh(CH_2CF_3)	–3.14	1.90×10^{2}	1.37×10^{2}
19	4-NMe(CH_2CF_3)	–3.85	1.90×10^{1}	1.78×10^{1}
20	4-NPh_2	–4.72	3.07×10^{1}	2.47×10^{1}
21	4-(N-morpholino)	–5.53	9.34×10^{-1}	7.75×10^{-1}
22	4-NPhMe	–5.89	1.20	9.40×10^{-1}
23	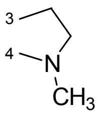	–8.76	2.08×10^{-3}	1.84×10^{-3}
24	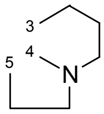	–10.04	1.89×10^{-4}	2.21×10^{-4}

[a] As defined by Equation (2), from ref. [6]. [b] Mixtures of solvents are given as (v/v), solvents: W = water, A = acetone.

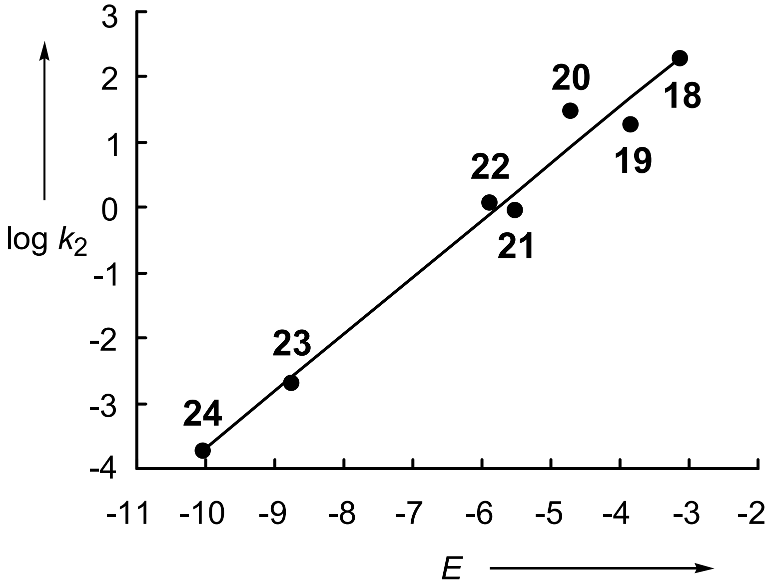

Figure 3. Linear correlation of the first-order rate constants log k_2(20 °C) of the reactions of benzhydrylium cations with 80% aqueous acetone (v/v) versus the electrophilicity parameters E of the corresponding benzhydrylium ions (log $k = 0.87E + 5.03$, $n = 7$, $r^2 = 0.9806$).

Table 4. Nucleophilicity parameters N and s for four solvents, frequently used for kinetic investigations of solvolysis reactions.

Solvent[a]	N[b]	s[b]
90A10W	5.70	0.85
80A20W	5.77	0.87
80E20W	6.68[c]	0.85[c]
100E	7.44[c]	0.90[c]

[a] Mixtures of solvents are given as (v/v), solvents: W = water, A = acetone, E = ethanol. [b] As defined by Equation (2). [c] From ref. [16].

Because of the inverse relationship $E_f \approx -E$ shown in Table 2 and Figure 2, one can use the electrophilicity scale E as a common abscissa for plotting rate constants for electrophile-nucleophile combinations as well as for the reverse reactions (heterolyses). The four almost parallel lines from bottom right to top left in Figure 4 indicate the leaving group abilities Br^- > Cl^- > $CF_3CO_2^-$ > 3,5-dinitrobenzoate (DNB) in 90% aqueous acetone. The ionization rates increase from right to left as the stabilization of the carbocations increases. In contrast, the rate constants for the reactions of carbocations with water increase from left to right as the stabilization of the carbocations decreases. If we neglect ion-pair return and the fact that the combination rates refer to 20 °C while the ionization rates refer to 25 °C, the pseudo-first order rate constants depicted in Figure 4 are directly comparable with each other. Since the rate constants for ionization and trapping by the solvent are identical at the point of intersection, conventional S_N1 reactions (slow ionization, fast solvent trapping) are found on the right of the intersections, while S_N1 reactions with inverse rate profiles (fast ionization, slow solvent trapping) are found on the left. With the approximations $k_{20°C} \approx k_{25°C}$, $E_f \approx -E$, and s, $s_f \approx 1$, Equations (2) and (3) can be combined to yield a rough estimate for the point of intersection at $E = (N_f - N)/2$.

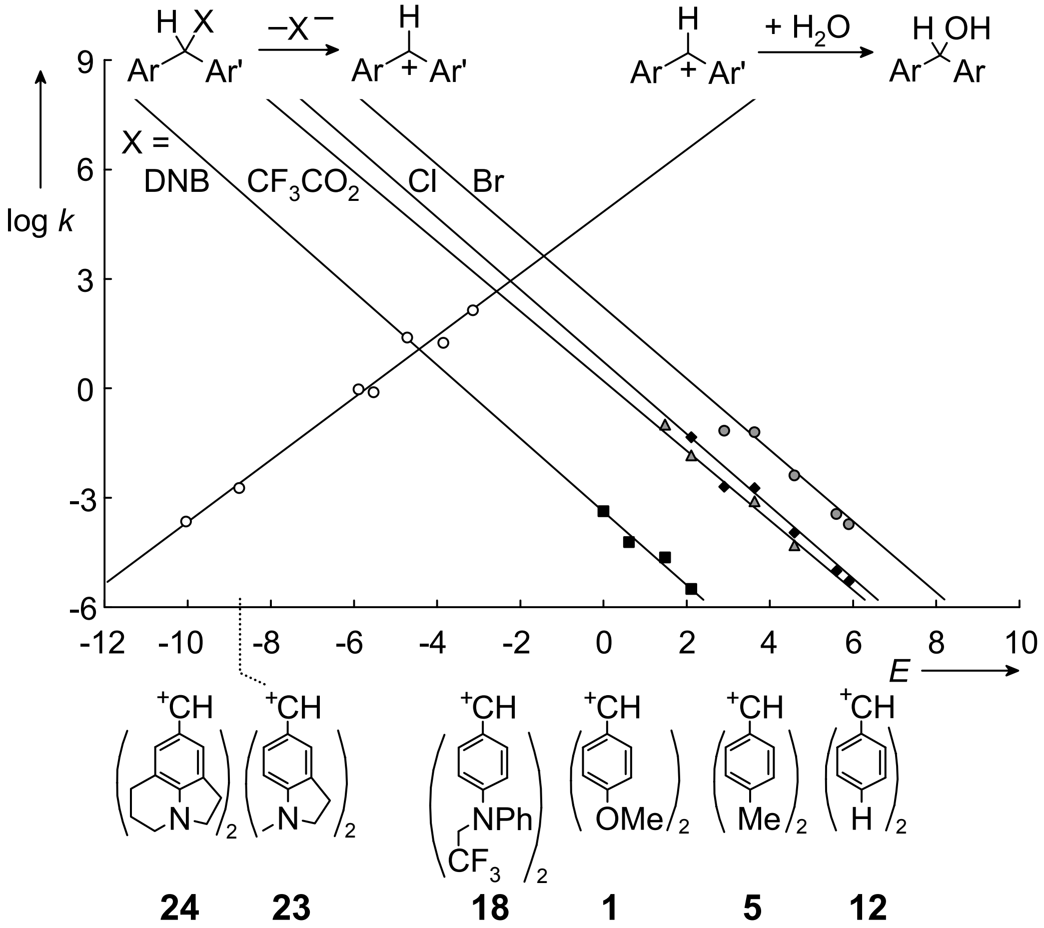

Figure 4. First-order rate constants for the ionization (25 °C) and solvent combination (20 °C) of benzhydrylium derivatives in 90 % aqueous acetone (v/v); DNB = 3,5-dinitrobenzoate. Abscissa: Electrophilicity parameters *E* of benzhydrylium ions.

It is obvious from this formula as well as from Figure 4, that accumulation of carbocationic intermediates must be expected in numerous solvolysis reactions, even with moderately stabilized carbocations, if solvents of low nucleophilicity (*N*) and systems with high nucleofugality (N_f) are employed. Figure 4 shows, for example, that alkyl bromide solvolyses in 90% aqueous acetone will proceed with accumulation of the intermediate carbocations if $E < -2$. In solvents of lower nucleophilicity,[16] this border is shifted towards less stabilized carbocations. Accordingly, the 4,4'-dimethoxy substituted benzhydryl cation **1** has UV-Vis spectroscopically been observed during the trifluoroethanolysis of the benzhydryl chloride **1**-Cl.[4] More solvent nucleophilicity parameters as well as nucleofugality parameters are needed to generally predict the borderline between the two mechanistic alternatives.

References and notes

[1] R. D. Guthrie, W. P. Jencks, *Acc. Chem. Res.* **1989**, *22*, 343–349; **1990**, *23*, 270.

[2] a) A. Streitwieser, Jr., *Solvolytic Displacement Reactions*, McGraw-Hill, New York, **1962**; b) *Carbonium Ions*, Vol. 1–5 (Eds.: G. A. Olah, P. v. R. Schleyer), Interscience, New York, **1968–1976**; c) P. Vogel, *Carbocation Chemistry*, Elsevier, Amsterdam, **1985**; d) X. Creary, *Advances in Carbocation Chemistry*, Vol. 1, JAI Press, Greenwich, CT, **1989**; e) J. M. Coxon, *Advances in Carbocation Chemistry*, Vol. 2, JAI Press, Greenwich, CT, **1995**; f) D. J. Raber, J. M. Harris, P. v. R. Schleyer in *Ions and Ion Pairs in Organic Reactions*, Vol. 2 (Ed.: M. Szwarc), Wiley, New York, **1974**, pp. 247–374.

[3] E. Gelles, E. D. Hughes, C. K. Ingold, *J. Chem. Soc.* **1954**, 2918–2929.

[4] H. Mayr, S. Minegishi, *Angew. Chem.* **2002**, *114*, 4674–4676; *Angew. Chem. Int. Ed.* **2002**, *41*, 4493–4495.

[5] H. Mayr, M. Patz, *Angew. Chem.* **1994**, *106*, 990–1010; *Angew. Chem. Int. Ed. Engl.* **1994**, *33*, 938–957;

[6] a) H. Mayr, T. Bug, M. F. Gotta, N. Hering, B. Irrgang, B. Janker, B. Kempf, R. Loos, A. R. Ofial, G. Remennikov, H. Schimmel, *J. Am. Chem. Soc.* **2001**, *123*, 9500–9512; b) H. Mayr, B. Kempf, A. R. Ofial, *Acc. Chem. Res.* **2003**, *36*, 66–77.

[7] a) B. Kempf, N. Hampel, A. R. Ofial, H. Mayr, *Chem. Eur. J.* **2003**, *9*, 2209–2218; b) T. Bug, M. Hartnagel, C. Schlierf, H. Mayr, *Chem. Eur. J.* **2003**, *9*, 4068–4076.

[8] a) R. Lucius, R. Loos, H. Mayr, *Angew. Chem.* **2002**, *114*, 97–102; *Angew. Chem. Int. Ed.* **2002**, *41*, 91–95; b) S. Minegishi, H. Mayr, *J. Am. Chem. Soc.* **2003**, *125*, 286–295; c) T. Bug, H. Mayr, *J. Am. Chem. Soc.* **2003**, *125*, 12980–12986; d) R. Loos, S. Kobayashi, H. Mayr, *J. Am. Chem. Soc.* **2003**, *125*, 14126–14132.

[9] H. Mayr, G. Lang, A. R. Ofial, *J. Am. Chem. Soc.* **2002**, *124*, 4076–4083.

[10] Since most reported rate constants on electrophile nucleophile combinations refer to 20 °C while those of solvolysis reactions usually refer to 25 °C, it was necessary to use different temperatures for Equations (2) and (3).

[11] Because s_f as well as N_f are nucleofuge specific parameters, one might ask the question, why Equation (3) is used instead of the mathematically equivalent expression $\log k = N_f' + s_f E_f$, with $N_f' = s_f N_f$, in analogy to most common linear free energy relationships (ref. [12]). We have repeatedly discussed for Equation (2), that it is this special term, with N as the negative intercept *on the abscissa* (E-axis), which renders nucleophilicity parameters N that are of immediate use for practicing chemists (refs.

[5, 13]). While the intersections of the correlation lines with the abscissa (log $k = 0$) are always within or close to the experimental range, intersections with the ordinate (E or $E_f = 0$) will often be far outside of the experimental range. When the intercepts on the ordinate N' or N_f' are considered, even qualitative comparisons of compounds with large differences in reactivity are only possible in combination with the corresponding slope parameters. In contrast, nucleophilicity N as well as nucleofugality N_f, the intercepts on the abscissa, can *always* be qualitatively discussed without consideration of the slopes s or s_f.

[12] A. Williams, *Free Energy Relationships in Organic and Bioorganic Chemistry*, The Royal Society of Chemistry, Cambridge, **2003**, and refs quoted therein.

[13] a) H. Mayr, M. Patz, M. F. Gotta, A. R. Ofial, *Pure Appl. Chem.* **1998**, *70*, 1993–2000; b) H. Mayr, O. Kuhn, M. F. Gotta, M. Patz, *J. Phys. Org. Chem.* **1998**, *11*, 642–654.

[14] Parameters E_f, N_f, and s_f have been calculated by minimizing $\Sigma\Delta^2$, where $\Delta^2 = (\log k_1 - \log k_1^{\text{calc}})^2 = (\log k_1 - s_f(N_f + E_f))^2$ using the program "*What'sBest!* 4.0 Commercial" by Lindo Systems Inc.

[15] a) C. D. Ritchie, *Acc. Chem. Res.* **1972**, *5*, 348–354; b) C. D. Ritchie, *Can. J. Chem.* **1986**, *64*, 2239–2250.

[16] a) D. N. Kevill in *Advances in Quantitative Structure-Property Relationships*, Vol. 1 (Ed.: M. Charton), JAI Press, Greenwich, CT, **1996**, pp. 81–115. b) R. A. McClelland, *Tetrahedron* **1996**, *52*, 6823–6858.

Curriculum vitae

Personal data

Name: Shinya Minegishi
Date of birth: 29.10.1975
Place of birth: Saitama (Japan)
Family status: Single

Education

4/82 – 3/88	Kawamoto Minami Elementary School
4/88 – 3/91	Kawamoto Junior High School
4/91 – 3/94	Kumagaya High School
4/95 – 3/99	Kyoto University, Faculty of Engineering, Industrial Chemistry
4/99 – 3/01	Master course at Kyoto University, Graduate School of Engineering at Takeuchi group under the direction of Professor Dr. K. Takeuchi and Associate Professor Dr. T. Kitagawa: “Reactivity of Carbocations toward Rearrangement and Bond Formation”
(6/00 – 1/01)	Ludwig-Maximilians-Universität, the Department Chemie, under the direction of Professor Dr. H. Mayr.
4/01 – 3/04	Doctor course at Ludwig-Maximilians-Universität München, Department Chemie under the guidance of Professor Dr. H. Mayr: “Reactivity Selectivity Relationships in Reactions of Carbocations with Nucleophiles”

Professional Career

4/01 –3/04	Wissenschaftlicher Mitarbeiter at Department Chemie, Ludwig-Maximilians-Universität München.